Bieke Soen

Bieke Soen

GHENT UNIVERSITY

VIB-UGENT CENTER FOR INFLAMMATION RESEARCH

CRIG
CANCER RESEARCH INSTITUTE GHENT

Zeb1 and Zeb2: master regulators of mononuclear phagocyte development and homeostasis

Zeb1 and Zeb2 : master regulators of mononuclear phagocyte development and homeostasis

Bieke Soen

Thesis submitted in partial fulfilment of the requirements for the degree of

"**Doctor of Science: Biotechnology**"

Promotors: Prof. Dr. Geert Berx and Prof. Dr. Charlotte Scott

Academic year 2017-2018

Bieke Soen was supported by a personal PhD fellowship at the Research Foundation Flanders (FWO).

Gerealiseerd met behulp van een onderzoeksbeurs van het Fonds Wetenschappelijk Onderzoek Vlaanderen (FWO).

Cover design: Niels Vandamme.

Zeb1 and Zeb2 : master regulators of mononuclear phagocyte development and homeostasis

Bieke Soen

Molecular and Cellular Oncology Lab
Department of Biomedical Molecular Biology, Ghent University
Cancer Research Institute Ghent (CRIG)
VIB-UGent Center for Inflammation Research

Examination Committee:

Chair	Prof. Dr. Rudi Beyaert [1]
Secretary	Prof. Dr. Geert van Loo [1]
Promotors	Prof. Dr. Geert Berx [1,2]
	Prof. Dr. Charlotte Scott [1]
Examination Board	Prof. Dr. Tessa Kerre [3]
	Prof. Dr. William Winston Agace [4,5]
	Dr. Steven Goossens [1,2,6]
	Prof. Dr. Bart Lambrecht [7]
	Prof. Dr. Georges Leclercq [3]
	Prof. Dr. Tom Taghon [3]

[1] Department of Biomedical Molecular Biology, Ghent University, Belgium
VIB-UGent Center for Inflammation Research, Belgium
[2] Cancer Research Institute Ghent, Belgium
[3] Department of Clinical Chemistry, Microbiology and Immunology, Ghent University, Belgium
[4] Department of Experimental Medical Science, Lund University, Sweden
[5] Division of Immunology and Vaccinology, Technical University of Denmark, Denmark
[6] Department of Pediatrics and Genetics, Ghent University, Belgium
[7] Department of Internal Medicine, Ghent University, Belgium
VIB-UGent Center for Inflammation Research, Belgium

Summary

Zeb1 and Zeb2 are two highly homologous transcription factors (TFs) that are mainly known for their role in epithelial-mesenchymal transition (EMT). EMT is a multistep process important during embryonic development and is aberrantly activated by tumor cells in order to disseminate and form distant metastasis. However, in recent years it has become clear that Zeb proteins do not solely function as EMT-TFs, but are also crucial for the homeostasis of several lineages of the hematopoietic system. Zeb2 has been shown to play a role in NK cell maturation and $CD8^+$ T cell terminal differentiation, while Zeb1 is involved in early T cell development. The main objective of this thesis was to further unravel the role of Zeb proteins in the hematopoietic system, specifically focusing on dendritic cells (DCs) and macrophages.

First we identified a crucial role for Zeb2 in dendritic cell development. DCs are divided into two main classes: plasmacytoid DCs (pDCs) and conventional DCs (cDCs), which are further subdivided in cDC1s and cDC2s. We found that Zeb2 regulates pDC commitment from the pre-pDC stage onward by directly repressing Id2, a TF important in pDC development. Additionally, we showed that Zeb2 acts as a cDC subset fate switch, with its absence skewing the cDCs toward the cDC1 lineage and its overexpression skewing the cDCs towards the cDC2 lineage. The mechanism behind this Zeb2 controlled fate switch again involved direct repression of Id2. Secondly, we discovered a role for Zeb1 in splenic mononuclear phagocytes. Loss of Zeb1 expression specifically in cDC1s not only resulted in a reduction of splenic cDC1s, but also in a reduction of splenic macrophages, an increase in CD103 expression in the remaining splenic cDC1s and a loss of definition between $ESAM^+$ and $ESAM^-$ splenic cDC2s. Work is ongoing to determine how Zeb1 in splenic cDC1s is governing the homeostasis of other splenic mononuclear phagocytes. Finally, we identified that high mRNA expression of TF Zeb2 is a conserved feature across murine tissue-resident macrophages and the removal of Zeb2 from fully differentiated macrophages in lung, spleen, colon and liver results in an altered phenotype and eventually leads to their disappearance. In conclusion, we found that Zeb1 and Zeb2 are master regulators of mononuclear phagocyte development and homeostasis.

Having shown a physiological role for Zeb1 and Zeb2 in dendritic cells and macrophages, it is not a surprise that genetic events changing the levels of Zeb proteins can have serious consequences and lead to the development of lymphomas and leukemias. As such it was previously shown that both Zeb1 and Zeb2 act as oncogenes in acute myeloid leukemia. Additionally, recurrent deleterious mutations in the *Zeb2* gene locus suggest a role for Zeb2 as tumor suppressor in a rare leukemia called blastic plasmacytoid dendritic cell neoplasm (BPDCN), a disease that is believed to originate in pDC precursors. Currently the outcome for BPDCN patients is very poor and an appropriate clinically relevant mouse model would aid in the development of better targeted therapies. Therefore, we attempted to model the disease by simultaneously deleting Zeb2 and tumor suppressor p53 from dendritic cells. Although the mice developed a hematopoietic malignancy, unfortunately the disease did not resemble human BPDCN and thus further research is needed to develop a clinically relevant mouse model for this disease.

Samenvatting

Zeb1 en Zeb2 zijn twee homologe transcriptiefactoren die voornamelijk gekend zijn voor hun rol in epitheliale-mesenchymale transitie of EMT. EMT is een moleculair proces dat belangrijk is tijdens embryonale ontwikkeling. Daarnaast wordt het EMT-proces misbruikt door kankercellen om zich los te maken van de primaire tumor om uit te zaaien en secundaire tumoren te vormen. De laatste jaren is echter duidelijk geworden dat Zeb-eiwitten niet alleen functioneren als EMT-inducerende transcriptiefactoren, maar ook cruciaal zijn voor de homeostase van verschillende hematopoëtische cellen. Zo werd aangetoond dat Zeb2 een rol speelt in de maturatie van Natural-Killer cellen (NK cellen) en de terminale differentiatie van $CD8^+$ T-cellen. Voor Zeb1 werd dan weer aangetoond dat het betrokken is in de vroege ontwikkeling van T-cellen in de thymus. Het verder ontrafelen van de rol die Zeb-eiwitten vervullen in het hematopoëtisch systeem, meer specifiek in dendritisch cellen en macrofagen, was dan ook het hoofddoel van deze thesis.

In eerste instantie hebben we vastgesteld dat Zeb2 een cruciale rol heeft tijdens de ontwikkeling van dendritisch cellen (DCs). DCs worden ingedeeld in drie subgroepen, namelijk plasmacytoide DCs (pDCs), type 1 conventionele DCs (cDC1s) en type 2 conventionele DCs (cDC2s). Experimenteel werk in deze thesis heeft aangetoond dat Zeb2 de ontwikkeling van pDCs reguleert en dit door de transcriptie te verhinderen van Id2, een transcriptiefactor belangrijk in pDC-ontwikkeling. Bovendien hebben we aangetoond dat Zeb2 functioneert als een schakelaar in cDC-ontwikkeling. Het is namelijk zo dat in de afwezigheid van Zeb2 de cDC-ontwikkeling wordt gestuurd in de richting van de cDC1s, terwijl aanwezigheid van Zeb2 de cDC-ontwikkeling in de richting van de cDC2s stuurt. Ook hier is de directe repressie van Id2 door Zeb2 in betrokken. In tweede instantie hebben we ontdekt dat Zeb1 een rol speelt in de homeostase van mononucleaire fagocyten in de milt. Verlies van Zeb1 expressie specifiek in cDC1s resulteerde niet alleen in de reductie van de cDC1 populatie in de milt, maar tevens in een milt-specifieke reductie van de macrofaag-populatie, een toename van CD103 expressie in de overgebleven cDC1s en een onscherpe aflijning tussen $ESAM^+$ en $ESAM^-$ cDC2s. Verder onderzoek is lopende om te bepalen hoe het gebrek aan Zeb1 expressie in cDC1s ook andere mononucleaire fagocyten in de milt

kan beïnvloeden. Tot slot hebben we vastgesteld dat Zeb2 ook een belangrijke rol vervult in macrofagen. Hoge mRNA expressie van transcriptiefactor Zeb2 is een algemene karakteristiek van macrofagen in verschillende weefsels in de muis. Bovendien leidt het verwijderen van Zeb2 expressie in gedifferentieerde macrofagen in de long, milt, dikke darm en lever tot een gewijzigd fenotype en het uiteindelijke verlies van de macrofagen. Alles samengenomen hebben we aangetoond dat Zeb1 en Zeb2 de ontwikkeling en homeostase van mononucleaire fagocyten reguleren.

Zeb1 en Zeb2 hebben duidelijk een fysiologisch functie in dendritische cellen en macrofagen. Het is dan ook geen verrassing dat genetische wijzigingen die resulteren in verhoogde of verlaagde eiwitniveaus van Zeb1 of Zeb2 geassocieerd worden met de ontwikkeling van lymfomen en verschillende leukemie subtypes. Zo werd reeds aangetoond dat zowel Zeb1 als Zeb2 kunnen fungeren als oncogen in acute myeloïde leukemie. Daarenboven werden terugkerende mutaties in het *Zeb2* gen geïdentificeerd in patiënten die leiden aan blastair plasmacytoïd dendritisch cel neoplasma (BPDCN), een zeldzame leukemie waarvan wordt gedacht dat ze ontstaat in pDC-precursoren. Momenteel zijn de overlevingskansen van BPDCN-patiënten zeer laag en de ontwikkeling van een geschikt klinisch relevant muismodel zou de ontwikkeling van betere therapieën ten goede komen. Daarom hebben wij in deze thesis geprobeerd om de ziekte na te bootsen in muizen door simultaan expressie van Zeb2 en tumorsuppresorgen p53 uit te schakelen in dendritische cellen. De muizen ontwikkelden inderdaad een hematopoëtische kanker, maar deze was echter verschillend van de humane ziekte BPDCN. Verder onderzoek naar een geschikt klinisch muismodel voor deze zeldzame, maar dodelijk leukemie is dus vereist.

Table of contents

List of abbreviations

A

ALL	Acute lymphoblastic leukemia
AM	Alveolar macrophage
AML	Acute myeloid leukemia
APC	Antigen presenting cell
ATLL	Adult T cell leukemia/lymphoma

B

B-ALL	B cell acute lymphoblastic leukemia
bHLH	Basic helix-loop-helix
BM	Bone marrow
Bmp	Bone morphogenetic protein
BPDCN	Blastic plasmacytoid dendritic cell neoplasm

C

Cbfβ	Core-binding factor subunit beta
cDC	Conventional/classical dendritic cell
CDP	Common dendritic cell precursor
ChIP	Chromatin immunoprecipitation
CHOP	Cyclophosphamide, vincristine, prednisone and doxorubicin
CID	Ctbp interaction domain
CLP	Common lymphoid progenitor
cMoP	Common monocyte progenitor
CMP	Common myeloid progenitor
Crtam	Cytotoxic and regulatory T cell molecule
CSC	Cancer stem cell
Ctbp	C-terminal binding protein
CTL	Cytotoxic T lymphocyte
CTCL	Cutaneous T cell lymphoma
CZF	C-terminal zinc finger cluster

D

δEf1	Delta-crystallin enhancer binding factor 1
DC	Dendritic cell
DLBCL	Diffuse large B cell lymphoma
DN	Double negative
DP	Double positive

E

EBV	Epstein-Barr virus
EDTA	Ethylene-diamine-tetra-acetic acid
EMP	Erythro-myeloid progenitor
EMT	Epithelial-mesenchymal transition
Epcam	Epithelial cell adhesion molecule
ETP	Early T cell precursor
ETS	E26 transform-specific

F

FACS	Fluorescence activated cell sorting
FC	Fold change
FcεRI	Fc fragment of IgE receptor I
FCS	Fetal calf serum
Flt3(L)	Fms-like tyrosine kinase 3 (ligand)

G

GM-Csf or Csf2	Granulocyte-macrophage colony-stimulating factor
GMP	Granulocyte-monocyte progenitor

H

HCV	Hepatitis C virus
HD	Homeodomain
Hdac1	Histone deacetylase 1
HPC	Hematopoietic progenitor cell
HSC	Hematopoietic stem cell
HTLV-1	Human T-lymphotropic virus -1

I

Id2	Inhibitor of DNA binding 2
IEL	Intraepithelial lymphocyte
IFN	Interferon
IL	Interleukin
ILN	Inguinal lymph node
IRES	Internal ribosome entry site
Irf4/8	Interferon regulatory factor 4/8

K

KC	Kupffer cell
KO	Knockout

L

LT-HSC	Long-term hematopoietic stem cell
LC	Langerhans cell
LN	Lymph node

M

MC	Monocyte-derived cell
MCL	Mantle cell lymphoma
M-Csf or Csf1	Macrophage colony-stimulating factor
MDP	Monocyte-dendritic cell precursor
MedLN	Mediastinal lymph node
MEP	Megakaryocytic erythroid progenitor
MF	Mycosis fungoides
MFs	Macrophages
Mhc	Major histocompatibility complex
MLN	Mesenteric lymph node
MMP	Matrix metalloproteinase
MPP	Multipotent progenitor
MPS	Mononuclear phagocyte system
MZ	Marginal zone

N

NIM	Nurd interacting motif
NK cell	Natural killer cell
NSCLC	Non-small cell lung cancer
Nurd	Nucleosome remodeling and deacetylase
NZF	N-terminal zinc finger cluster

O

OVA	Ovalbumin

P

PAMP	Pathogen associated molecular pattern
PBS	Phosphate Buffered Saline

pDC	Plasmacytoid dendritic cell
PDGFRB	Platelet-derived growth factor receptor B
PFA	Paraformaldehyde
PRR	Pattern recognition receptor

R

RBC	Red blood cell
R-Smads	Receptor-regulated Smads
RT	Room temperature
RT-qPCR	Real-time quantitative polymerase chain reaction

S

SBD	Smad binding domain
Seq	Sequencing
SI	Small intestine
SILP	Small intestine lamina propria
Sip1	Smad interacting protein 1
Sirpα	Signal regulatory protein alpha
Smad	Mothers against decapentaplegic homolog
SP	Single positive
SRE	Smad responsive element
SS	Sézary syndrome

T

T-ALL	T cell acute lymphoblastic leukemia
TCR	T cell receptor
TE	Terminal effector
TF	Transcription factor
Tgfβ	Transforming growth factor beta
Th	T helper cell
Tlr	Toll-like receptor
Treg	Regulatory T cell

W

WT	Wild type

X

Xcr1	X-C Motif chemokine receptor 1

Z

Zeb1/2	Zinc finger E-box-binding homeobox 1/2
Zfh-1/2	Zinc finger homeodomain -1/2

Part 1
General Introduction

I. Zeb family of proteins originally seen as EMT-TFs

I.1 Discovery

Zeb (Zinc finger E-box-binding homeobox) proteins were discovered in *Drosophila melanogaster* and termed Zfh-1 (Zinc finger homeodomain -1) and Zfh-2, now called respectively Zeb1 and Zeb2[1]. Later on Zeb1 was described in different organisms with different names: AREB6 or ZEB in human, δEf1 (Delta-crystallin enhancer binding factor 1) in chicken, Bzp in hamster and Zag-1 in *Caenorhabditis elegans*[2–7]. Zeb2 was first picked up for its ability to bind Smad (Mothers against decapentaplegic homolog) proteins and was first called Sip1 (Smad interacting protein 1)[8]. Zebs were the first proteins described in which two types of DNA binding motifs exist side-by-side, namely a homeodomain (HD) and different zinc finger clusters[1]. The high degree of homology between both transcription factors (TFs) is likely a consequence of gene duplication coinciding with the origin of vertebrate life[9].

Analysis of expression patterns in *Drosophila* embryos already suggested a role for both proteins in neurogenesis and additional functions for Zeb1 in mesoderm development[10]. The following years it became clear that Zebs function in many different tissues and cell types. mRNA expression of human *ZEB1* is abundant in heart and skeletal muscle, moderate in brain and lung and low in liver, kidney and pancreas[2]. In mice, *Zeb1* expression was confirmed in pancreas, pituitary gland and central nervous system[4]. Next to that a function for Zeb1 was suggested in T cells and B cells[5,11], in different aspects of embryogenesis[3,7,12] and terminal differentiation of neurons[7]. Determining the function of Zeb2 was initially based on the finding that deleterious mutations in the gene or full deletions of the locus cause Hirschsprung disease, which is characterized by a lack of enteric nerves in parts of the intestine[13–16]. Patients with Mowat-Wilson syndrome carrying heterozygous *ZEB2* mutations often suffer from Hirschsprung disease, next to mental retardation, facial malformation, epilepsy and congenital heart disease. This clue for ZEB2 functionality in the nervous system was confirmed when mRNA expression was found in developing human embryos in neural crest derived cells, central nervous system and muscle[17].

I.2 Structure: different domains and their function

Initially, it was the protein structure of Zeb1 that was described by different research groups in several organisms. They all reported the presence of seven zinc finger motifs organised in two widely separated zinc finger clusters and a homeodomain in the middle of the protein[2–4,18]. Both Zeb1 and Zeb2 contain this C-terminal (CZF) and N-terminal zinc finger cluster (NZF), which have a high sequence homology and are conserved between both Zebs[19] (Figure 1). The presence of the zinc fingers enables the proteins to bind to regulatory sequences in the DNA in order to exert their function as transcription factors[2]. As such it was shown that Zeb1 binds to the enhancer sequence of *delta 1-crystallin* in order to repress transcription of this gene during lens development in chicken[3]. The repressive function of Zeb proteins is executed through the specific binding of the CZF to 5'-CACCT sequences in different promoters. This particular sequence is included in the E2-box sequence 5'-CACCTG, which is the binding site for transcriptional activators of the basic helix-loop-helix (bHLH) family. In that way Zebs compete for the binding to E2-box sequences with other transcriptional regulators[5,8,12,18]. The optimal binding site for the NZF was determined as 5'-GTCACCTGT or 5'-TGCACCTGT[18]. Zeb proteins show the highest affinity for binding when a bipartite 5'-CACCT and 5'-CACCTG sequence is present. The orientation and spacing between the two E-boxes can vary and experiments suggested that binding of one of the zinc finger clusters to the first E-box and binding of the other cluster to the second E-box stabilizes the monomeric DNA-protein interaction[19].

Although it was already clear that Zeb proteins are able to repress transcription by binding promoter regions of genes, it were Postigo and Dean who discovered how the repressor function is established. They localized the repressor domain of Zeb1 to the central region of the protein where they identified a PLDLS amino acid sequence, a typical binding site for the Ctbp (C-terminal binding protein) corepressor (Figure 1). Two additional Ctbp-like sites were found in the cDNA sequence and all three sites participate in the repressive function of Zeb1 through binding with the Ctbp proteins at the promoter regions of repressed genes[20]. Later, a model was proposed in which Zeb1 cooperates with Ctbp2 and histone deacetylase 1 (Hdac1) in order to form a repressor complex[21,22].

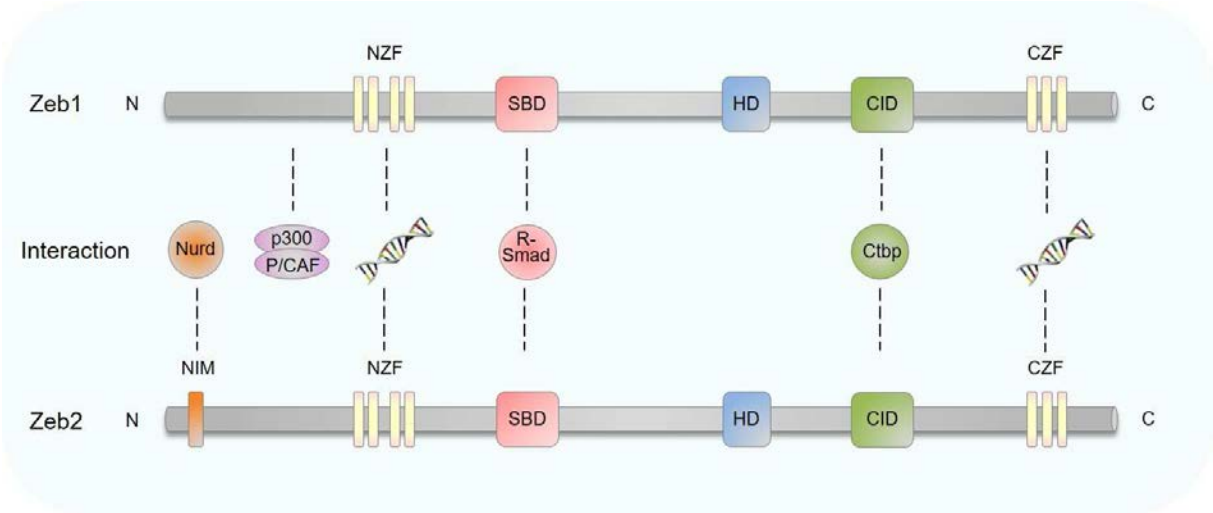

Figure 1 | Zeb1 and Zeb2 protein domains and their interaction partners. NIM: Nurd Interacting Motif – interaction with Nurd (Nucleosome remodelling and deacetylase) complex, N-terminal region of Zeb1 – interaction with p300 or P/CAF, NZF: N-terminal zinc finger cluster – interaction with DNA, SBD: Smad binding domain – interaction with R-Smads, HD: Homeodomain - no interaction shown, CID: Ctbp interaction domain – interaction with Ctbp (C-terminal binding protein), CZF: C-terminal zinc finger cluster – interaction with DNA. (Based on De Smedt *et al.*, 2017 for Zeb1 and Akay *et al.*, 2017 for Zeb2; Encyclopedia of Signaling Molecules, 2nd edition)

Zebs not only have the ability to bind to DNA and regulate transcription, they are also involved in protein-protein interactions for which they possess other domains (Figure 1). The ability to interact with Smad proteins was discovered by Verschueren and colleagues. A yeast two hybrid screen for interaction with the MH2 domain of Smad led to the identification of Zeb2. The domain responsible for the interaction is called the Smad binding domain (SBD) and is located in between the NZF and the HD. In mammalian cells, Zeb2 only interacts with the MH2 domain of activated full length receptor-regulated Smads (R-Smads)[8] which links Zeb2 with Tgfβ (Transforming growth factor beta) signalling, as ligation of Tgfβ to its receptors generates phosphorylated R-Smads[23]. Initially the minimal binding motif of the SBD was identified as a 51 amino acid long stretch, but later redefined to be as short as 14 amino acids. This short SBD stretch was modelled as part of an α-helix that may fit in the hydrophobic pocket within the MH2 domain of activated Smad proteins[8,24]. Zeb1 contains a domain downstream of its NZF which shows high homology with the SBD of Zeb2 and is conserved across species. Although both binding Smads through a similar domain, the Zeb proteins have an opposite effect on Tgfβ and Bmp (Bone morphogenetic protein) mediated transcription. Zeb1 synergizes with Smad proteins to

activate transcription, while Zeb2 inhibits Tgfβ/Bmp-mediated transcription[25]. It is the different recruitment of coactivators and corepressors that explains this opposition. The N-terminal region of Zeb1 interacts with p300 and P/CAF to assemble a Zeb1-Smad activation complex. The interaction with p300 provides transcriptional synergy, but it is the recruitment of P/CAF that switches Zeb1 from a repressor to an activator through the displacement of Ctbp1 from the Ctbp interaction domain (CID) of Zeb1[26]. Later, others demonstrated that, depending on the experimental context, Zeb1 and Zeb2 are equally potent to bind p300 and P/CAF[27]. This suggests that other mechanisms and/or cofactors are contributing to the differential Zeb1/2-specific effects on Smad-mediated transcription.

Finally, Zeb2 contains a Nurd interacting motif (NIM) in its N-terminal domain[28] (Figure 1). The Nurd (nucleosome remodelling and deacetylase) complex is involved in chromatin remodelling and plays a key role in transcriptional repression[29,30]. Importance of the ZEB2-NURD interaction became apparent from a Mowat-Wilson syndrome patient, in which the NIM was substituted with an unrelated sequence rendering the transcription factor unable to recruit the NURD complex and so causing the disease[28]. Later on the relevance of the Nurd interaction was also highlighted in murine Schwann cell differentiation and remyelination. Here it was found that Zeb2 controls maturation of these cells by recruiting Hdac1/2-Nurd complexes thereby inhibiting a Notch-Hey2 signalling pathway[31]. As such the Zeb2-Nurd interaction was proven to be important in several neuropathies caused by mutations in the NIM motif.

Based on the extensive and continuously growing list of interaction partners and putative downstream targets, one can expect that Zebs have very pleiotropic functions, which largely depend on the cellular context. Indeed, the chromatin status and the presence/absence of tissue-specific interaction partners strongly influences their role as a transcriptional repressor/activator. This can, to some extent, explain why in some cell types Zebs play complementary or synergistic roles, while in others seemingly opposite roles.

I.3 Zebs as EMT-TFs

Zeb proteins are primarily known as inducers of epithelial-mesenchymal transition (EMT), and thus called EMT-TFs. EMT is a process during which polarized epithelial cells undergo a molecular switch to become motile mesenchymal cells that have lost polarity[32]. EMT is important during embryonic development, wound healing and cancer progression[33] (Figure 2). The main hallmark of EMT is the loss of E-cadherin expression. Zebs are able to repress *E-cadherin* transcription by directly binding to the E-box sequences in the *E-cadherin* promoter[34–36]. Additionally, Zeb2 was shown to directly downregulate gene expression of epithelial tight junction, desmosomal and gap junction proteins like Occludin, Zonula occludens 3, Plakophilin 2 and Connexin 26[37,38]. On the other hand upregulation of mesenchymal markers, like Vimentin, has also been associated with high expression of Zeb proteins[39,40].

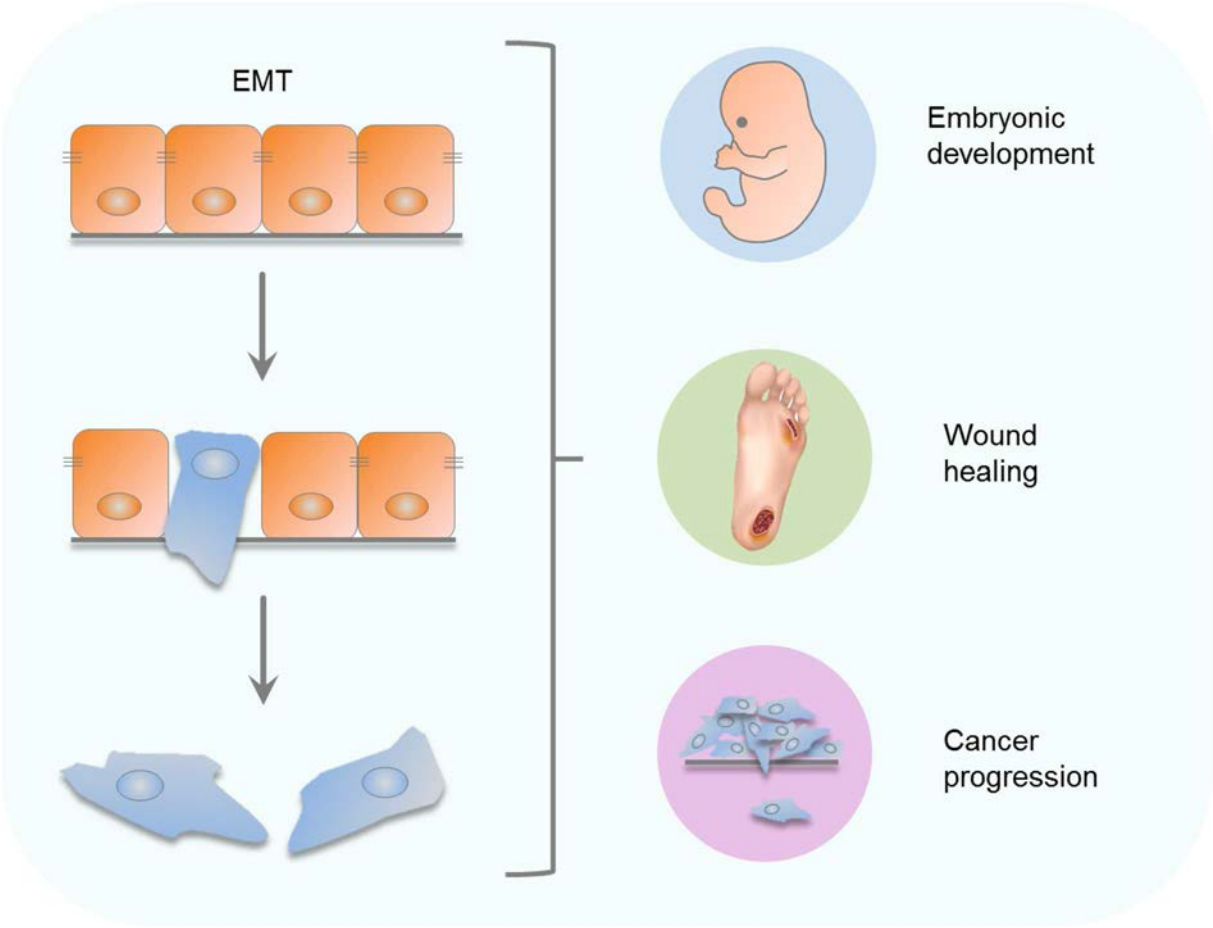

Figure 2 | Importance of EMT in embryonic development, wound healing and cancer progression. During EMT (Epithelial-mesenchymal transition) epithelial cells lose their adhesive capacities and gain mesenchymal properties. EMT is of importance for embryonic development, wound healing and cancer progression leading to metastasis.

At different stages of embryogenesis (e.g. gastrulation, formation of the neural crest, morphogenesis of heart, muscles and skeletal structures) cells temporarily need to acquire the ability to migrate. This temporal motility is governed by EMT and therefore by EMT-TFs like Zeb1/2[32]. As such Zeb2 was found to be highly expressed in embryos in developing peripheral and central nervous system, muscle and neural crest derived cells[41,17]. Evidence for a physiological role for ZEB2 in embryonic development is found in Mowat-Wilson syndrome patients as described above (see I.1 Discovery). More proof was found when Higashi and colleagues created a CRE-mediated conditional Zeb2 knockout (KO) mouse. They demonstrated that full KO of Zeb2 leads to embryonic lethality between E9.5 and E10.5[42]. Zeb1 on the other hand was detected in murine embryonic nervous system progenitors, notochord, somites and neural crest derivatives[43,44]. In accordance to this Zeb1 null mice are perinatally lethal, exhibiting different skeletal defects including craniofacial abnormalities of neural crest origin[44].

Although EMT is essential during embryonic development, the program can also be aberrantly activated by cancer cells. EMT endows tumor cells to disseminate from the primary tumor in order to form distant metastasis, the biggest cause of death in cancer patients[45]. Keeping this in mind, it is not a surprise that high expression of ZEB proteins has been associated with aggressiveness and poor outcome in different types of carcinomas. Typically, ZEB1 and ZEB2 are not expressed in the centre or in well differentiated regions of the tumor, but are upregulated at dedifferentiated and invading sites[46]. For example, high ZEB2 expression and consequently low E-CADHERIN levels have been correlated with bad outcome of ovarian and breast carcinoma and with adverse overall survival of oral squamous cell carcinoma[47,48]. Another mechanism by which ZEB2 facilitates the invasion of carcinoma cells is the downregulation of matrix metalloproteinases (MMPs)[49]. ZEB1 was correlated with high VIMENTIN/low E-CADHERIN expression in non-small cell lung cancer (NSCLC) and inhibition of cell polarity genes like *LGL2* in metastatic colorectal tumors[40,50,51].

EMT not only facilitates invasion of cancer cells, it also renders them with stem cell properties and thus creating so called cancer stem cells (CSCs)[57,58]. CSCs or tumor-initiating cells have the potential to self-renew and form secondary tumors when transplanted into immune deficient or syngeneic mice. As Zebs, in combination with a negative feedback loop with the miR-200 family, control EMT, they are very likely

involved in managing this stem cell state[54]. Zeb1 for instance, was found to inhibit members of the miR-200 family that repress known stem cell factors including Sox2, Klf4 and Bmi1. Therefore EMT-associated upregulation of Zeb1 leads to increased expression of these stem cell factors[55]. ZEB1 is also implicated in a self-enforcing feedback loop with stem cell marker CD44, in which ZEB1-induced repression of ESRP1 controls alternative splicing of CD44[56].

Often CSCs are resistant to certain drugs and form the basis of disease relapse. Acquisition of stemness through the EMT program has been linked with therapy resistance in cancer patients[57–59]. For several drugs it was shown that ZEB proteins play a role in this process. In NSCLC ZEB1 driven EMT is interrelated with resistance to tyrosine kinase inhibitors[60,61] and the miR-200/ZEB loop with resistance to the angiokinase inhibitor nintedanib[62]. ZEB1 driven EMT is also responsible for the existence of docetaxel resistant CSCs in castration resistant prostate cancer[58] and the cause of resistance to gemcitabine, 5-FU and cisplatin in pancreatic cancer cell lines[63]. MiR-200b regulated ZEB2 in turn is associated with multi-drug resistance in small cell lung cancer[64]. As such ZEBs can act as important regulators of therapy resistance in cancer patients.

To conclude, the roles of ZEB proteins in solid tumor progression have been extensively documented. Therefore, ZEB expression levels and the expression of their targets could be used in the clinic as prognostic markers for solid tumor aggressiveness and poor patient outcome.

II. Emerging role for Zeb proteins in immune system development and homeostasis

Although originally discovered as transcription factors in EMT, it is becoming more and more evident that Zeb proteins also have physiological functions during hematopoiesis and in mature hematopoietic cells. Before going deeper into detail concerning the different immune cell lineages, we will have a general look at mRNA expression levels of *Zeb1* and *Zeb2* at different stages of murine hematopoiesis (Figure 3).

Both *Zeb1* and *Zeb2* are expressed at moderate levels in early hematopoietic precursors, but upon further development it seems that *Zeb1* and *Zeb2* mRNA levels are mostly mutually exclusive (Figure 3). Remarkably, the decision to develop along the lymphoid or myeloid lineage is marked with expression of respectively *Zeb1* (common lymphoid progenitor; CLP) and *Zeb2* (common myeloid progenitor; CMP). For the T cell lineage, which develops mostly in the thymus, *Zeb1* is highly expressed in mature single positive T cells (T-CD4 and T-CD8) and upon activation *Zeb2* is expressed, whereas *Zeb1* is downregulated. High expression of *Zeb1* and low expression of *Zeb2* is seen in mature B cells, granulocytes and erythrocytes, while opposite high expression of *Zeb2* and low expression of *Zeb1* is typical for NK cells, macrophages and monocytes (Figure 3). On the next pages a more detailed overview will be given on what has already been elucidated so far, starting with the importance for Zebs more early in murine immune cell development, followed by their function in terminally differentiated and mature cells.

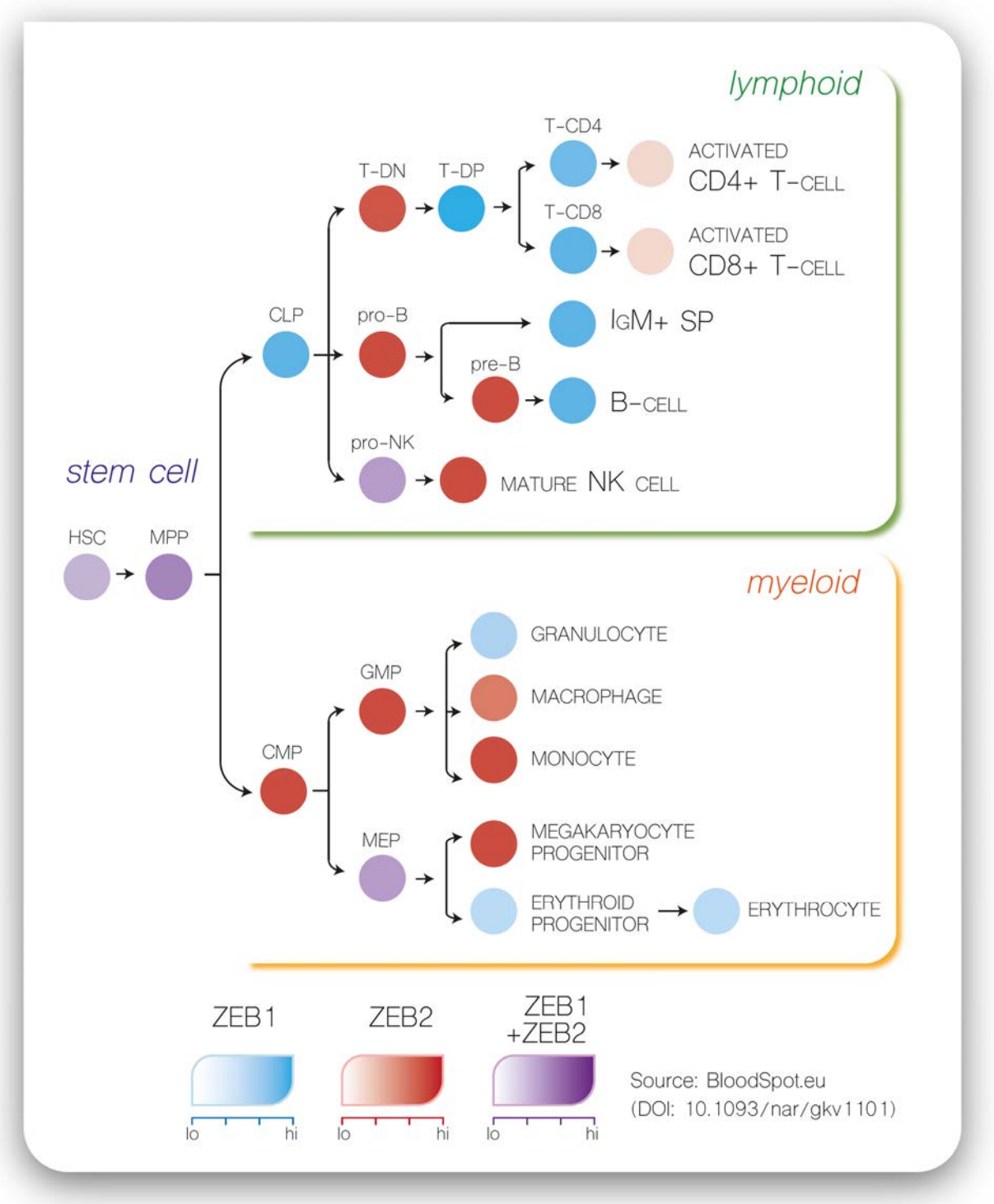

Figure 3 | *Zeb1* and *Zeb2* mRNA levels are mostly mutually exclusive during murine hematopoietic differentiation. The figure is based on expression data available via http://servers.binf.ku.dk/bloodspot/ and shows micro-array data from murine samples. HSC: Hematopoietic stem cell, MPP: Multipotent progenitor, CMP: Common myeloid progenitor**,** GMP: Granulocyte-monocyte progenitor, MEP: Megakaryocytic erythroid progenitor, CLP: Common lymphoid progenitor, T-DN: T cell $CD4^{-}CD8^{-}$ double negative, T-DP: T cell $CD4^{+}CD8^{+}$ double positive, T-CD4: T cell $CD4^{+}$ single positive, T-CD8: T cell $CD8^{+}$ single positive, pro-B: Pro B cell, pre-B: Pre B cell, IgM^{+} SP: IgM positive side population, pro-NK: Natural killer cell progenitor, NK cell: Natural killer cell.

II.1 Zeb2 is essential in embryonic HSC/HPC differentiation and controls adult hematopoietic differentiation

Zeb proteins are mainly known for their role in EMT, which is essential for many developmental processes during embryogenesis. One such process is the formation of hematopoietic stem cells (HSCs) from the hemogenic endothelium through an EMT-like program. In mice it has been shown that Zeb2 is dispensable for the initial formation of HSCs, but is essential in early HSC and hematopoietic progenitor cell (HPC) differentiation[65]. Next to that Zeb2 is involved in downregulation of genes associated with adhesion, e.g. *β1-integrin*, and hence crucial for mobilization of HSCs/HPCs from the fetal liver to the bone marrow (BM)[65]. Zeb2 not only plays a role early in embryonic HSC differentiation, but also controls murine adult hematopoietic differentiation. Inducible loss of Zeb2 in adult BM leads to the accumulation of precursor cells due to inefficient commitment to differentiation and maturation programs. For instance commitment into the B cell lineage and terminal differentiation of megakaryocytes and erythrocytes are dependent on Zeb2[66].

II.2 Zeb1 in early T cell development

T cells develop from HSCs present in fetal liver and in BM during adult life. After homing to the thymus, cells undergo several developmental stages before leaving the thymus as mature T cells in order to function in peripheral organs. The different stages in the thymus can be recognized through the expression of several cell surface markers. The first four stages are characterized by a lack of CD4 and CD8 and are the so called double negative (DN) stages. DN1 can be defined by $CD44^{+}CD25^{-}cKit^{+}$, DN2 by $CD44^{+}CD25^{+}cKit^{+}$, DN3 by $CD44^{-}CD25^{+}cKit^{-}$ and the DN4 stage by $CD44^{-}CD25^{-}cKit^{-}$ surface marker expression. Starting from the DN2 stage onward, developing T cells undergo rearrangements in their T cell receptor (TCR) genes and start to express CD3, a TCR coreceptor molecule, and in that way proceed to a $CD4^{+}CD8^{+}$ (DP) stage. In the next step cells pass through a positive and negative selection. Positive selection is based on a weak interaction of the TCR with self-peptide-Mhc (Major histocompatibility complex) complexes and protects thymocytes from ‘death-by-neglect’, while negative

selection eliminates T cells responding to self-antigen with high affinity by inducing apoptosis. These selections leads to a single positive (SP) stage with both $CD4^+CD8^-$ and $CD4^-CD8^+$ T cells, which are able to leave the thymus and move into peripheral tissues[67].

Two different mouse models have highlighted a possible role for Zeb1 in early T cell development. The first model, called ΔC-fin, contains a mutation which leads to a truncated protein lacking the CZF of Zeb1[68]. The other mouse model is called the cellophane mouse, in which a T to A transversion was identified in the seventh exon of Zeb1 leading to a premature stop codon and the expression of a protein also lacking the CZF[69]. In both models small, hypocellular thymi with a poor distinction between medulla and cortex were observed in homozygous mutant mice. For the ΔC-fin mice a reduction in number of thymocytes was reported down to 1% of the number in wild type (WT) mice. In both models the proportions of the different developmental stages were investigated in the thymus. Thymi of homozygous mutant mice showed a lower proportion of DP thymocytes and expanded populations of the DN and SP stages. The group working with the ΔC-fin mice looked deeper into the thymus populations with flow cytometry analysis and showed that it was specifically the $CD44^+CD25^+cKit^+$ DN2 population that was depleted. In addition to a defect in T cell development, the cellophane mice also showed a reduced natural killer (NK) cell population in the spleen together with a lack of a discrete population of marginal zone (MZ) B cells. Splenic B cells of cellophane mice also proliferate poorly in response to B cell receptor dependent stimuli. All together we can conclude that Zeb1 likely plays an important role in early T cell development in the thymus[68,69].

Next to this developmental function, Zeb1 is also important in repressing several genes in mature T cells. As such Zeb1 represses *Crtam* (cytotoxic and regulatory T cell molecule) transcription in non-stimulated and stimulated T cells[70]. The EMT-TF also negatively regulates CD4 expression by competing with transcriptional activators E12 and Heb at the *CD4* gene promoter site[71]. Furthermore Zeb1 cooperates with Ctbp2 and Hdac1 in order to repress *IL-2*, a cytokine expressed after T cell activation and important in proliferation and homeostasis of the activated cells[22].

II.3 Zeb1 and Zeb2 are involved in a counterregulatory network that regulates the fate of CD8$^+$ T cells

Mature T cells can be subdivided into two major subsets on the basis of CD4 and CD8 surface expression. CD4$^+$ or T helper (Th) cells owe their name to the fact that they assist other cells during immune responses. Th cells help the maturation of B cells into plasma cells or memory B cells and the activation of macrophages or cytotoxic T lymphocytes (CTLs). This last type of T cells is characterized by the expression of CD8 and is important in immunity against intracellular pathogens like viruses. When an intracellular infection is detected CD8$^+$ T cells proliferate and differentiate into a heterogeneous population of effector T cells, which are able to destroy infected cells. About 90% of the antigen-specific effector cells are short-lived and terminally differentiated (TE). They can be distinguished through a Klrg1^{hi}CD127^{lo} surface expression. Klrg1^{lo}CD127^{hi} expression marks the minority of CD8$^+$ T cells after infection. These cells are long-lived multipotent memory precursors that facilitate a quick expansion of antigen-specific T cells upon secondary infection[72,73].

Zeb2 was found to be important in regulating CTL differentiation as a response to infection in mice. *Zeb2* mRNA is, amongst T cells, almost exclusively detected in Klrg1^{hi}CD127^{lo} TE cells following infection. In these effector cells Zeb2 expression is directly induced by T-bet, another transcription factor shown to promote Klrg1^{hi} effector cell differentiation. Zeb2 and T-bet cooperate to induce the expression of genes correlated with terminal differentiation and to repress the expression of the memory precursor program. Zeb2 and T-bet probably coordinately bind to the loci of several memory precursor genes. On those sites Zeb2 may prevent T-bet binding and subsequent T-bet dependent gene activation and/or directly repress transcription[74,75]. Furthermore, maturation of memory CD8$^+$ T cells after viral infection is associated with Tgfβ induced expression of *Zeb1*, whereas both Tgfβ and the miR-200 family members selectively inhibit Zeb2 during this process. As such it was shown that Zeb1 is critical for memory T cell survival and function, protective recall response and the formation of central memory T cells[76]. In conclusion, Zeb1, Zeb2, Tgfβ and the miR-200 family members are involved in a counterregulatory network that regulates the fate of CD8$^+$ T cells following viral infection[74–76].

II.4 Zeb2 is important for NK cell maturation

Natural killer (NK) cells are lymphocytes which recognize cells that are infected with an intracellular pathogen. They are able to kill the affected cells through the release of granules containing cytotoxic perforin and granzymes. NK cells are also important in cancer immunosurveillance, where they can distinguish malignant cells from healthy cells[77]. NK cells develop in the BM and after commitment they undergo maturation, during which they lose the capacity to proliferate and gain the ability to egress from the BM[77,78]. Three maturation stages can be identified on the basis of surface markers CD11b and CD27: $CD11b^{-}CD27^{+}$ ($CD11b^{-}$), $CD11b^{+}CD27^{+}$ (DP) and $CD11b^{+}CD27^{-}$ ($CD27^{-}$)[79,80].

It was shown that Zeb2 has an important role in the terminal maturation of NK cells[81]. During NK cell maturation cells gradually express higher *Zeb2* mRNA levels. Mice with a loss of Zeb2 expression specifically in the NK cell lineage display an accumulation of NK cells in the BM and a decrease in the blood and peripheral organs. The mice virtually lack the mature $CD27^{-}$ population in all organs. On the other hand Zeb2 overexpression promoted NK cell maturation. Next to its role in maturation, Zeb2 is also essential for the survival of mature NK cells and the egression of these cells from the BM. Mice with NK cell specific Zeb2 knockout had a comparable phenotype with mice in which NK cells lack T-bet, a transcription factor known to be important in NK cell maturation, and van Helden *et al.* demonstrated that Zeb2 controls NK cell maturation acting downstream of T-bet. T-bet levels increase during the maturation process and this leads to the induction of Zeb2. In mature NK cells, T-bet and Zeb2 control the expression of the same genes. In that way the T-bet/Zeb2 regulatory axis irreversibly induces terminal maturation in the NK cell lineage[81].

II.5 A function for Zeb2 in mast cell activation?

Mast cells originate from progenitors in the bone marrow and undergo final maturation once they arrive at their destination, which is made up by epithelial and mucosal tissues throughout the body. These myeloid cells are best known for their involvement in the pathophysiology of many diseases like allergy, asthma and a range of different

malignancies, but they also function under homeostatic conditions in vasodilatation, angiogenesis and the innate and adaptive immune responses. Mast cells are activated through the aggregation of IgE receptors (FcεRI) on the cell surface after contact with antigen-IgE complexes. A phosphorylation mediated signaling transduction eventually leads to degranulation of preformed granules and the *de novo* synthesis of inflammatory mediators[82].

One study suggests a role for Zeb2 in regulating signaling in mast cells. Reduced Zeb2 expression in an *in vitro* model for mast cell function resulted in a decreased expression of FcεRI and several other proteins involved in the signaling cascade following activation. Additionally, the phosphorylation of several transducers in this pathway was reduced. Eventually this led to a decrease in mast cell degranulation and cytokine release after FcεRI-mediated activation. Lowering Zeb2 expression also led to a block in cell cycle progression. Taken together, Zeb2 seems to control the expression of signaling molecules thereby regulating both early and late events in mast cell activation[83]. Experiments with *in vivo* models are necessary to validate these findings.

II.6 Zebs in the mononuclear phagocyte system?

The term 'mononuclear phagocyte system' (MPS) was first introduced by Van Furth during the late 1960s[84]. Initially the MPS was comprised of monocytes, macrophages and their BM precursors[84], but later on also dendritic cells (DCs), consisting of plasmacytoid DCs (pDCs) and conventional DCs (cDCs) were included[85]. Although not a lot of research has focused on Zeb proteins in the MPS, we can find some evidence in literature that Zeb1 and Zeb2 could be important in mononuclear phagocytes.

First, a possible role for both ZEB1 and ZEB2 was identified in human Langerhans cells (LCs), a type of macrophages present in the skin epidermis. LCs are specialized to recognize foreign proteins present in the epidermis, after which they migrate through the dermis into the skin draining lymph nodes (LNs) in order to initiate a specific immune response[86]. In the epidermis LCs are present in an immature status characterized by the expression of several epithelial adhesion molecules like E-Cadherin, Claudin-1 and Zonula occludens 3. Through these epithelial features LCs are able to form cell-cell contacts with epidermal keratinocytes and hence a crucial

step in LC migration is the downregulation of E-cadherin. This downregulation of adhesion is accompanied with the induction of mesenchymal markers like MMPs and certain integrins, but also N-cadherin. Konradi *et al.* showed with a human *in vitro* LC maturation system that the E-CADHERIN to N-CADHERIN switch goes hand in hand with an increased expression and nuclear localization of ZEB1 and ZEB2. The study provides a first hint on how Zeb proteins and EMT might facilitate LC mobilization and migration[87]. As the conclusions of Konradi *et al.* are based on *in vitro* work only, relevance of the results will have to be confirmed in *in vivo* settings.

Additionally, Zeb2 has recently been identified in several genome-wide microarray and RNA-sequencing transcriptional analyses as potentially involved in cDC development[88–90]. Conventional DCs are further subdivided into cDC1s and cDC2s based on their ontogeny and function[91] and Zeb2 was found to be specifically associated with cDC2 development. The transcription factor was found to be expressed in pre-cDC2s and cDC2s[88,90], while being down-regulated in pre-cDC1s and cDC1s[89]. Furthermore, Zeb2 was found to be part of the pre-macrophage core profile[92]. Also, Cortés and colleagues showed that tumor associated macrophages depend on Zeb1 for their cancer-promoting capacities[93]. As most of the data on Zebs in the MPS presented here, is circumvential or based on *in vitro* experiments, the role of Zebs in mononuclear phagocytes remains unclear. As such, the main objective of this thesis will be to elucidate the role of Zeb proteins specifically in dendritic cells and macrophages and therefore the next part of this introduction will discuss these two cell types in detail.

III. Dendritic cells

Dendritic cells or DCs were discovered by Steinman and Kohn in 1973. After dissociation of mouse spleen and adherence of the single cells to plastic or glass, they noticed a cell that had a different morphology than that of earlier described cell types. Dendritic cells are characterized by a large nucleus and owe their name to their long cytoplasmic projections that continuously elongate, retract and reorientate themselves[94]. A few years later it was found that DCs express high levels of MhcII, an antigen presenting peptide, on their surface and are capable of inducing specific T lymphocyte proliferation much more efficiently than other antigen presenting cells (APCs) discovered so far [95]. Today, we know that the key function of DCs is to sample antigen in peripheral organs, followed by their migration to the draining LNs and presentation of the antigen to specific T cells. As such DCs form the crucial link between the innate and adaptive arms of the immune system[96].

III.1 Dendritic cell subsets and their function

Dendritic cells are rare hematopoietic cells that reside in almost all tissues of the body. They are subdivided into two main classes: plasmacytoid DCs (pDCs) and conventional or classical DCs (cDCs)[96].

Plasmacytoid DCs

Morphologically, pDCs resemble plasma cells and when activated they present a dendritic appearance. Their main function is the capacity to produce large amounts of type 1 interferon (IFN) upon stimulation with viral infections or certain Toll-like receptor (Tlr) ligands[97–99]. pDCs do not express MhcII and therefore are, compared to cDCs, inefficient at presenting antigen at steady state[100]. However, upon stimulation they can gain expression of MhcII and present antigen to $CD4^+$ T cells and depending on the context this results in either $CD4^+$ T cell activation or tolerance[100–102]. Murine pDCs express the DC marker CD11c (but at lower levels than cDCs), CD45R (B220), SiglecH and Bst2 on their cell surface[103–106]. Several cytokines are able to promote pDC

development: fms-like tyrosine kinase 3 ligand (Flt3L), macrophage colony-stimulating factor (M-Csf or Csf1), thrombopoietin and interleukin-7 (IL-7)[107–110].

Conventional or classical DCs

The term conventional or classical DC was first introduced by Steinman and refers to short-lived cells with a stellate morphology that have the capacity to migrate and stimulate naive T cells[111]. cDCs are seen as the professional APCs of the immune system. They form the bridge between the innate and adaptive immune response by sampling antigen after which they migrate to draining LNs in order to present antigenic peptides on MhcI and MhcII to naive T cells[96]. Depending on the co-stimulatory molecules on the surface and the cytokines produced by the cDCs, the T cells will proliferate and polarize in either antigen specific effector T cells or regulatory T cells (Tregs). Subsequently, the activated T cells will home to the tissue where the antigen was originally sampled by the cDC, and further orchestrate the immune response[96,112]. Murine cDCs are dependent on Flt3L for their development[113,114] and are typically identified through the high expression of both surface markers CD11c and MhcII[96]. cDCs can be divided into two main subtypes, which have been termed cDC1s and cDC2s by Guilliams *et al*[91]. cDC1s are characterized by Xcr1 (X-C motif chemokine receptor 1) expression, CD8α expression in the spleen and CD24 or CD103 expression in the periphery. They are specialists in cross-presentation of antigen to $CD8^+$ T cells and hence in defence against intracellular pathogens. cDC2s express CD172a (Signal regulatory protein alpha or Sirpα) and usually CD11b and function primarily to present antigen to $CD4^+$ T cells thereby protecting against extracellular pathogens[96,111]. However, as CD172a is also expressed by LCs, other macrophages and certain monocyte-derived cells[115] and CD11c expression can be downregulated on cDCs[116], we must be careful when identifying cDC subsets using expression of these surface markers. Therefore, further analysis of cDC populations in this thesis will be based on a recently published flow cytometry approach developed by Guilliams *et al.* This method allows to correctly identify cDCs across different tissues based on their expression of CD11c and CD26, without contamination by $F4/80^+CD64^+$ macrophages[115].

III.2 Dendritic cell development

All DCs start their development from an HSC in the BM (Figure 4). HSCs give rise to progeny thereby progressively losing self-renewal capacity and gaining a further degree of commitment to specific immune cell lineages. Unravelling the complexity of DC development started with the discovery of the common myeloid progenitor or CMP. This CMP gives rise to all myeloid lineages (which comprises monocytes, DCs, granulocytes, platelets and erythrocytes), but has lost the ability to develop into lymphoid cells (T and B lymphocytes)[117]. The next milestone was the identification of the monocyte-DC precursor or MDP which lacks granulocyte, platelet and erythrocyte potential, but can generate monocytes, macrophages and dendritic cells[118]. MDPs further commit into a common dendritic cell precursor (CDP)[119] capable of generating pDCs and cDCs[120,121]. Further differentiation of the CDP results in either a pre-pDC[122] or a pre-cDC[119]. Pre-pDCs develop into full mature pDCs within the BM, while pre-cDCs migrate out of the BM to reach full maturity in peripheral tissues either as cDC1s or cDC2s. Recent advances in single cell analyses revealed that there exists heterogeneity in the pre-cDC population. In the BM and the spleen pre-cDCs can be found which are pre-committed to the cDC1- or cDC2-lineage and they were termed respectively pre-cDC1s and pre-cDC2s[89,90] (Figure 4).

III.3 Growth factors and cytokines in dendritic cell development

The main cytokine regulating DC development is Flt3L. Ligation of Flt3L to its receptor fms-like tyrosine kinase 3 (Flt3) on the cell surface of DCs, results in downstream signalling mediated by Stat3 and the Pi3k/mTor pathway[123,124]. The importance of the Flt3L-Flt3 interaction in DC development is supported by *in vivo* studies influencing both Flt3L levels or expression and functioning of its receptor. As such Flt3L-treatment or the induction of Flt3L with a tetracyclin-inducible system in mice led to increased DC numbers[125–127], while mice deficient for Flt3L showed a reduction in all DC populations[114]. On the other hand Flt3 negative BM progenitors are unable to differentiate into pDCs and cDCs *in vitro*[128] and mice treated with a Flt3 tyrosine kinase

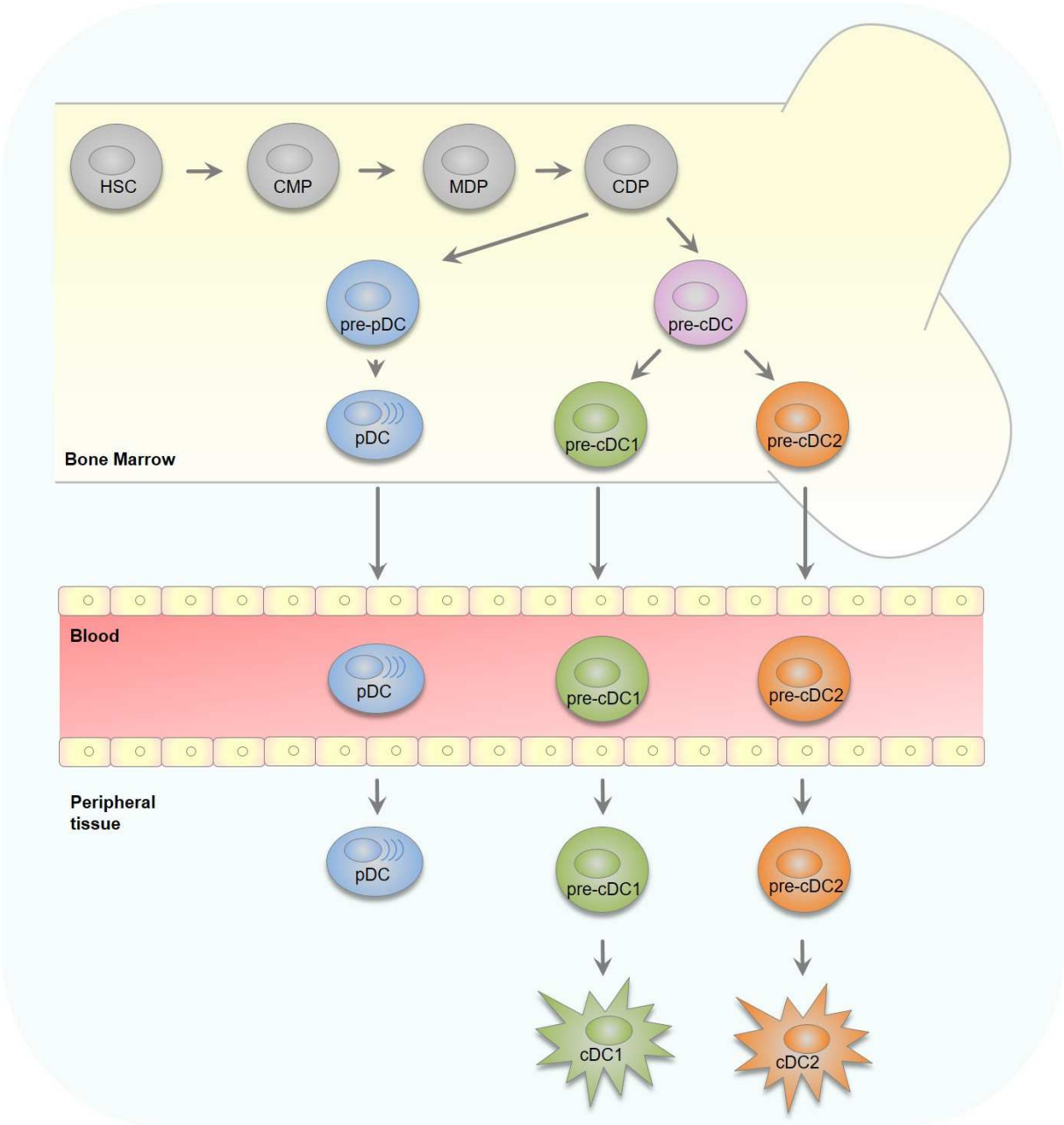

Figure 4 | Development of the different dendritic cell subsets. In the bone marrow hematopoietic stem cells (HSCs) subsequently develop into common myeloid progenitors (CMP), monocyte-DC precursors (MDP) and common DC precursors (CDP). CDPs further develop into pre-pDCs which give rise to mature pDCs in the bone marrow. pDCs will start circulating in the blood in order to seed peripheral tissues. The CDP also develops into the pre-cDC population which contains cells that are already pre-committed to the cDC1- and cDC2-lineage, the pre-cDC1s and pre-cDC2s respectively. Pre-cDC1s and pre-cDC2s will leave the bone marrow and enter peripheral tissues through the blood circulation, where they finally mature into cDC1s and cDC2s.

inhibitor are deficient for all DC subsets[129]. Moreover, only Flt3-expressing BM precursors are capable of developing into DCs[130]. As culturing BM in the presence of Flt3L generates pDCs, cDC1s and cDC2s[89], it is a widely used tool to investigate DC

development. *In vitro* generation of BM-derived cells using granulocyte-macrophage colony-stimulating factor (GM-Csf or Csf2) as a growth factor is also used in DC research, however these cultures only generate cDCs and macrophages, but not pDCs[131]. It was shown that Csf2 is involved in the homeostasis and survival of non-lymphoid tissue CD103$^+$ cDC1s and intestinal lamina propria CD103$^+$ cDC2s[132,133]. Furthermore, addition of Csf2 to Flt3L BM-cultures increased the production of CD103$^+$ cDC1s, a population generated in low amounts in cultures containing Flt3L alone[134]. However, Edelson *et al.* suggested that Csf2 signalling simply induces the expression of CD103 in cDC1s[135] and hence the precise contribution of this growth factor to DC development remains unclear. Finally, few studies reported on a possible role for M-Csf or Csf1 in regulating DC development. As such it was shown that BM cultured in the presence of Csf1 generates pDCs and cDCs[108] and that a Csf1 receptor reporter mouse contained labelled pDC and cDC populations[108,136].

III.4 Transcription factors in dendritic cell development and homeostasis

Several transcription factors were proven to be important in the generation of all DC lineages. Core-binding factor subunit beta (Cbfβ) is essential early in DC lineage commitment. This TF is crucial for the development of the MDP in the BM and subsequently all DC subsets in the periphery[137]. Another general DC protein is Ikaros, as mice homozygous for a dominant negative form of this TF lack all DCs and the developmental requirement for Ikaros is cell intrinsic[138]. It was also shown that Ikaros controls pDC differentiation and regulates terminal DC maturation and their capacity to induce a Th1 response[139,140]. A requirement for ETS (E26 transform-specific) family member Pu.1 in DC development was already highlighted in 2000[141,142], but only a decade later Carotta and colleagues were able to resolve the mechanism behind this dependency. They identified that Pu.1 controls the expression of the Flt3L cytokine receptor in a dose-dependent matter[143]. Another protein controlling Flt3 expression, but also IL-7R expression, is Bcl11a. As such Bcl11a is required for the development of all DCs[144,145]. Moreover, Gfi1 has a cell autonomous and non-redundant role in dendritic cell development. Gfi$^{-/-}$ mice show a global reduction in DCs and Gfi$^{-/-}$ hematopoietic progenitor cells are unable to develop into DCs, but instead differentiate into macrophages. In addition, Gfi was also shown to be important in DC maturation

and activation[146]. Mechanistically this could be ascribed to a decrease in Stat3, a TF important in DC development through its central role in Flt3L signalling[147].

pDC specific TFs

The main TF regulating pDC development is E2-2. This member of the bHLH family of TFs is highly and preferentially expressed in human and mouse pDCs and its deletion leads to abrogated pDC development[148]. E2-2 not only functions during pDC development, but is also important in maintaining pDC cell fate, as deleting E2-2 in mature pDCs skews their gene expression towards a cDC-like signature[149]. It was shown that, together with helix-loop-helix protein Id2 (Inhibitor of DNA binding 2), E2-2 is important at balancing pDC versus cDC commitment. Compared to Id2 expression during pDC development, cDC commitment is accompanied by increased expression of Id2. This increased Id2 expression during cDC development leads to increased formation of Id2/E2-2 complexes, which inhibits E2-2 to dimerize and perform its function as a transcriptional regulator[150]. Furthermore, E2-2 directly activates the expression of two other transcription factors important in the pDC lineage, namely Spi-b and Interferon regulatory factor 8 (Irf8)[148]. Spi-b is an ETS TF important in pDC development and functioning[151]. It is found to be exclusively expressed in the pDC lineage and its knockdown inhibits pDC development[152]. Spi-b acts through controlling survival of pDCs and pDC progenitors by directly upregulating the anti-apoptotic protein Bcl2a1[153]. The first clue that Irf8 is important for pDCs came from the observation that Irf8 KO mice lack the pDC population[154,155]. Later on it was confirmed that Irf8 contributes to pDC development by regulating Flt3L-mediated differentiation[156] and in 2014 Amit and colleagues stated that Irf8 governs the establishment and maintenance of pDC-specific enhancer states and gene expression[157]. However, recently it has been proven that Irf8 is not intrinsically required for pDC development, but is required for proper functioning of the cells. Sichien *et al.* showed that loss of Irf8 expression in pDCs affects their ability to produce type I IFNs and their capacity to activate and induce proliferation of $CD4^+$ T cells[158].

cDC specific TFs

The expression of zinc finger transcription factor Zbtb46 (zDC) is, among mononuclear phagocytes, restricted to pre-cDCs and cDCs and therefore useful as a marker for cDCs versus pDCs and macrophages[159,160]. Zbtb46 is additionally expressed by some vascular endothelium, at low levels in the megakaryocyte-erythroid progenitor (MEP)[159] and in Langerhans cells[161]. Zbtb46 is a TLR-responsive protein that helps in the prevention of cDC maturation during steady state conditions[162]. Although it is a marker for cDC commitment, it is not required for cDC development[159,162]. Nevertheless, its discovery as a cDC specific TF will help in the development of tools to study DC functions, such as the recently developed zDC-DTR[160] and zDC-CRE[163] mice.

cDC1 specific TFs

Next to general DC TFs, also specific TFs for cDC1 commitment and terminal selection were identified. One such TF, already discovered in 2003, is Id2. Mice lacking Id2 expression show a reduction in splenic cDC1s[164,165]. It was suggested that Id2 expression in cDC1s is induced by Tgfβ[164]. Later on it was confirmed that Id2 is actually expressed in all cDC subsets, but is expressed at the highest level by the cDC1 lineage[166]. A second cDC1 specific TF is Batf3. Deletion of Batf3 ablates cDC1 development in lymphoid tissues[167] and Batf3 KO mice also lack cDC1s in peripheral non-lymphoid tissues[135]. Batf3 already determines cDC1 fate at the level of the pre-cDC1 by maintaining auto-activation of Irf8, which is important at different steps of cDC1 development[89]. Irf8 is not only crucial for the generation of the pre-cDC1 out of the CDP, but also for the further commitment of the pre-cDC1s towards mature cDC1s[89,168]. Additionally, it has been shown that Irf8 functions as a terminal selector in mature cDC1s, as it is crucial to maintain the cDC1 identity throughout its lifespan[158]. Probably acting in the same network as previously mentioned TFs, is basic leucine zipper Nfil3. Nfil3 KO mice show a selective defect in cDC1 development and pre-cDCs from these mice have a reduced expression of Batf3, suggesting that Nfil3 acts upstream of Batf3[169]. Although all four TFs presented so far have their role in the cDC1 lineage, not all of them are strictly required. As such it was shown that forced expression of Id2 and/or Batf3 in BM from Irf8$^{-/-}$ mice is not sufficient to induce cDC1

development[170]. Furthermore, experiments with short-term BM reconstitution showed that expansion of cDC1s upon viral infection takes place in the absence of Id2, Nfil3 and Batf3, but not in the absence of Irf8[171]. Based on these studies it was suggested that Irf8 acts upstream of Batf3 and Id2 in the cDC1 developmental program[170], but how the different TFs are exactly intertwined needs to be determined.

cDC2 specific TFs

A number of transcription factors were shown to be important in terminal differentiation and survival of cDC2s, but so far those determining early cDC2 lineage commitment have not been identified. While Irf8 expression is specific for cDC1s, another interferon regulatory factor, namely Irf4 is expressed by cDC2s. Although initially thought to be required for cDC2 generation[156,172], it has since been shown that Irf4 does not function during the development of the cDC2 lineage. Rather, it seems that Irf4 plays a role in survival or function of terminally differentiated cDC2s or is only required by certain subsets of cDC2s. As such, Persson *et al.* identified how intestinal $CD103^+$ cDC2s, but not their $CD103^-$ counterparts, are dependent on Irf4 for their survival[173]. Furthermore, Bajaña and colleagues showed how Irf4 is required by $CD24^+$, but not $CD24^-$ cDC2s in the lung and by $CD4^+$, but not $CD4^-$ cDC2s in the spleen[168]. Additionally, Irf4 is essential for the migration of cDC2s from peripheral tissues to draining LNs[168,173,174] and for the priming of Th responses[175], such as the Th2 response in house dust mite driven asthma[176]. Meanwhile others identified that DC specific Notch2 deletion revealed a cDC2 subset specifically requiring this protein. The mice showed an ablation of $Esam^{hi}$ cDC2s in the spleen and a loss of $CD103^+$ cDC2s in the lamina propria of the intestine[177,178]. The deficiency for Notch2 in DCs resulted in a reduced capacity to induce a Th17 response and an impaired IL-23 production following *Citrobacter rodentium* infection[177]. Also Klf4 seems to be an important TF for cDC2s, as deletion of this protein leads to a reduction of cDC2s in all lymphoid and peripheral tissues. As for Notch2, not all cDC2s are affected, pointing to the presence of Klf4-dependent cDC2 subpopulations[179]. As such it was shown that in the skin dermis and the lung it are respectively the $CD11b^-$ cDC2s and the $CD24^+MgI2^+$ cDC2s that require Klf4[179]. Mice with a deficiency for Klf4 in DCs are susceptible to *Schistosoma mansoni* helminth infection and protected against house dust mite allergy induced asthma, due to a defective Th2 response[179]. Next to these more recent reports on Notch2, Klf4 and

Irf4, two other TFs were reported much earlier. Mice that are knockout for Irf2 have a selective defect in cDC2s, though this was only evaluated in the spleen[180]. Additionally, the results are based on full KO mice and further research to a possible role for Irf2 in cDC2s across tissues using a DC specific KO is required. Also the finding that cDC2s may depend on TF Relb, needs more detailed research. Again this study only showed dependency in the spleen and used mice with a mutation in the *Relb* gene, of which it is not clear if this leads to lack of expression or the expression of a dominant negative form of the Relb protein[181].

IV. Macrophages

Macrophages were first discovered by Metchnikoff in 1883. He described how phagocytic cells in frogs are not only important in host defense against pathogens, but are also able to eliminate degenerating or dying cells in the tissue[182,183]. Later on macrophages were classified based on morphology, function, kinetics and origin into the 'mononuclear phagocyte system' (MPS)[184], comprising monocytes, macrophages and DCs[85]. Originally the MPS also included BM promonocytes, which were at the time believed to be the sole progenitors of monocytes and macrophages[185]. In recent years however it has become clear that the diversity in tissue macrophages is originating from a multi-layered developmental process that takes place in the developing embryo and the post-natal BM[186].

IV.1 Macrophages and their functions

Macrophages can be found in all tissues throughout the adult body and in each tissue they have a unique name. Macrophages localised in the brain are called microglial cells, while in the liver they are named after the person who identified them and termed Kupffer cells. The names of splenic and lung-residing macrophages depend on the specific niche in which they reside. As such we find red pulp macrophages and marginal zone macrophages in the spleen and alveolar and interstitial macrophages in the lung[187,188]. Langerhans cells or LCs are skin residing phagocytes[189] and although LCs share many features with cDCs, it was suggested to classify them as macrophages based on their ontogeny[91]. This last subset of macrophages will be discussed in a separate paragraph (IV.5).

In mice, tissue-resident macrophages are typically expressing the following surface markers: Csf1R which is the receptor for M-Csf or Csf1, integrin CD11b, Fcγ receptor 1 (CD64), MerTK and F4/80[189]. In some tissues they also express CD11c and MhcII, two markers used to delineate dendritic cells. Moreover, some cDC2s also express the macrophage marker F4/80. In order to avoid inclusion of cDC2s in the macrophage gate, it was recently suggested to always define macrophages as $F4/80^{+}CD64^{+}$ when

using flow cytometric analysis. Additionally, this accurate identification of macrophages avoids contamination of $CD11c^{+}MhcII^{+}$ DCs[115].

Macrophages have a range of diverse functions in immune defense and tissue homeostasis. The phagocytic cells not only help clearing infections by enhanced phagocytosis of pathogens which have been opsonized by antibodies or complement factors, they are also able to recognize pathogens in order to initiate host defense. For this macrophages are equipped with pattern recognition receptors (PRRs) on their cell surface or in their cytoplasm, which allows them to interact with so called pathogen associated molecular patterns or PAMPs[190]. Interaction of PRRs with microbial pathogens induces the expression of pro-inflammatory cytokines and chemokines, which results in the influx of inflammatory leukocytes among which are neutrophils and monocytes[187]. However, in order to avoid excessive or permanent damage in an inflamed tissue, it is important to also resolve inflammation and return to a normal tissue homeostasis. Macrophages also function during this resolution and the restoration of equilibrium after injury in many tissues[191–196]. The process mostly starts with efferocytosis, which is the phagocytosis of apoptotic inflammatory cells, like neutrophils, by macrophages[197,198]. Following efferocytosis, resident and recruited monocyte-derived macrophages shift from a pro-inflammatory to an anti-inflammatory state, promoting resolution of inflammation and tissue repair[191–196].

Macrophages clearly assist to restore tissue balance after injury and inflammation, but also during steady state they are responsible for maintaining tissue homeostasis, and in some instances they even support the development of a tissue. In the lung for instance, alveolar macrophages (AMs) are responsible for phagocytosis of dust, senescent cells and allergens[191]. Next to that AMs contribute to catabolism of surfactants in the lung. Absence of AMs leads to accumulation of surfactants in the air spaces and eventually to pulmonary alveolar proteinosis[199,200]. Additionally, Kupffer cells were shown to support iron[201] and lipid[200,202] metabolism in hepatocytes. Also splenic red pulp macrophages are implicated in the recycling of heme-associated iron[203,204]. In the gastro-intestinal tract, macrophages are not only responsible for removal of senescent and dying cells, but also support the integrity of the epithelial barrier[205,206]. BM-resident macrophages are essential for the development of red blood cells (RBCs) and also at the end of their lifetime senescent RBCs are again cleared by tissue residing macrophages[207]. As a final example of tissue-specific accessory

macrophage functions, microglia have been shown to contribute to synaptic maturation in developing brain [208].

IV.2 Macrophage development

For decades it was believed that all tissue-resident macrophages develop from circulating monocytes. The idea was that blood monocytes originate from BM progenitor cells or promonocytes, migrate into the different tissues and further give rise to tissue-resident macrophages[209,210]. However, more recently it was shown that tissue-resident macrophages already develop in the embryo alongside their tissue and are able to maintain their pool during adult life without influx from adult blood monocytes[211]. Yolk sac macrophages and fetal liver monocytes are the embryonic macrophage precursors that colonize the tissues before birth[212]. Yolk sac macrophages develop from erythro-myeloid progenitors (EMPs) that develop during primitive hematopoiesis from yolk-sac blood islands and yolk-sac hemogenic endothelium[212,213]. For the development of fetal liver monocytes, there are currently two hypotheses. The first hypothesis is that late yolk sac EMPs home to the fetal liver, where they expand and further differentiate into fetal liver monocytes[214]. In the second hypothesis pre-hematopoietic stem cells (pre-HSCs) produced in the aorta-gonad-mesonephros home to the fetal liver, where they subsequently develop in fetal liver HSCs, which in turn give rise to fetal liver monocytes[215] (Figure 5) .

Fetal liver monocytes will next colonize all tissues in the embryo, except for the brain, proliferate and develop into macrophages (Figure 5). Indeed, brain resident macrophages or microglia solely develop from yolk sac progenitors[213,216–218] and this is probably due to the closure of the blood-brain barrier before fetal liver monocytes can colonize the embryonic brain[215]. Whether yolk sac macrophages also contribute to other adult tissue-resident macrophages than microglia remains matter of debate. While Schulz *et al.* suggest that most tissue-resident macrophages are derived from yolk sac progenitors[217], others showed contribution of fetal liver monocytes to tissue-resident macrophages in the lung alveolar space, liver, spleen, peritoneal cavity and heart[211,212,219,220]. Besides a population of tissue-resident macrophages that maintains itself through local proliferation, tissues often contain a subpopulation of macrophages

that are derived from adult circulating monocytes. Monocytes start their development in the BM from an HSC subsequently differentiating into a CMP, MDP and common monocyte progenitor (cMoP) to ultimately start circulating in the blood as a monocyte[118,221,222] (Figure 5). The precise contribution of adult blood monocytes to the macrophage pool is tissue-dependent and was among others shown for cardiac macrophages[223,224], dermal macrophages in the skin[225], intestinal macrophages[226], Kupffer cells[227] and pancreas-resident macrophages[228]. In some tissues the proliferation rate of the embryonic-derived macrophages declines and with age the relative contribution of blood monocytes to the macrophage pool increases. This is for instance the case for cardiac macrophages and the macrophage population in the intestinal mucosa[223,226].

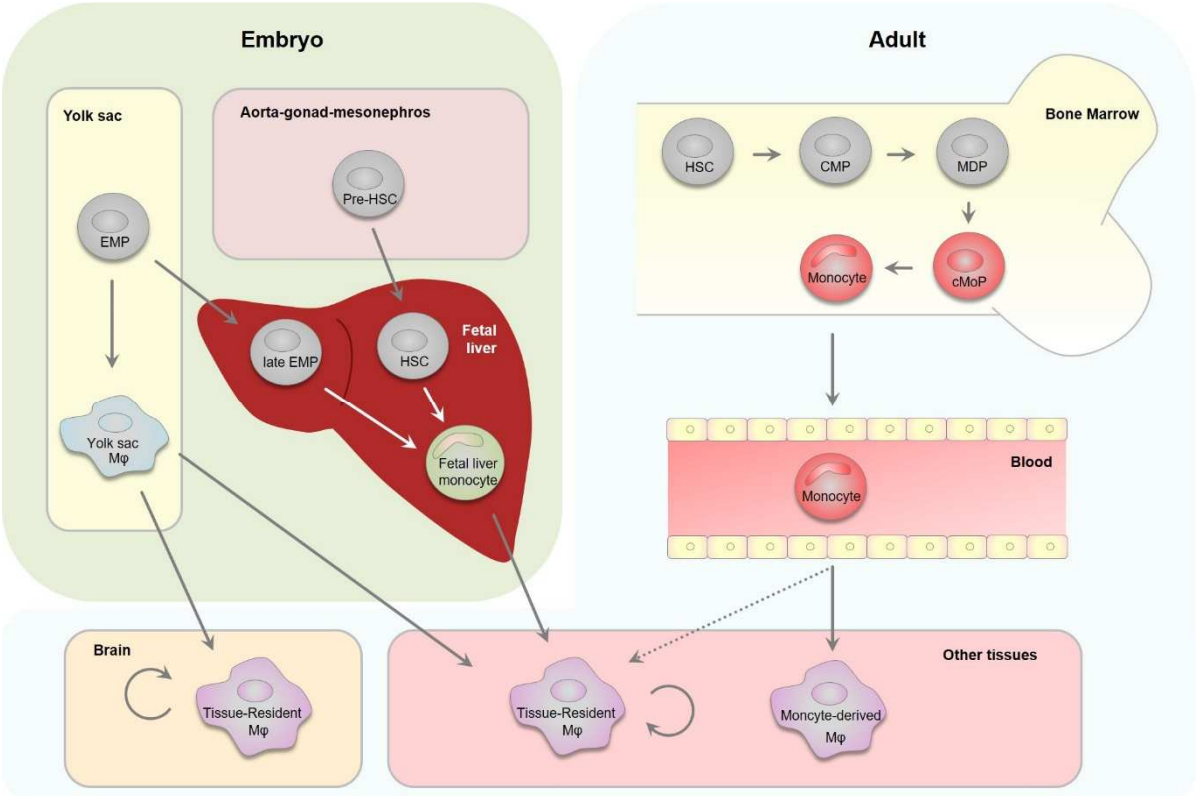

Figure 5 | Development of tissue-resident macrophages. During primitive hematopoiesis in the embryonic yolk sac the erythro-myeloid progenitor (EMP) differentiates into a yolk sac macrophage (Mφ), which will colonize the brain and other tissues before birth, where they develop into tissue-resident macrophages that maintain themselves in the adult tissue through local proliferation. Fetal liver monocytes arise from late EMPs or pre-hematopoietic stem cells (pre-HSCs) that migrate to the fetal liver from the yolk sac or aorta-gonad-mesonephros respectively. Fetal liver monocytes will seed all embryonic tissues, except the brain, were they proliferate and differentiate into tissue-resident Mφ that self-maintain throughout adult life. Hematopoietic stem cells in the adult bone marrow subsequently develop into common myeloid progenitors (CMP), monocyte-dendritic cell precursors (MDP), common monocyte progenitors (cMoP) and ultimately into monocytes that start circulating in the blood. Monocytes will enter adult tissues where they will further develop into monocyte-derived macrophages. Monocytes are also able to develop into self-renewing tissue-resident macrophages.

IV.3 Growth factors and cytokines in macrophage development

Several cytokines or growth factors have been shown to regulate macrophage numbers and their function. M-Csf or Csf1 is commonly used to generate macrophages from BM *in vitro*. Its role was discovered through the use of the Csf1$^{op/op}$ mice, which carry a mutation in the coding region of the *Csf1* gene[229]. These mice show a reduced number of macrophages in different tissues, like bone, liver, spleen and kidney[230,231]. Csf1 is expressed by different cell types among which are endothelial cells and osteoblasts[232,233]. The cytokine functions through its receptor Csf1R[234] and upon ligand-receptor binding, autophosphorylation is followed by a cascade of intracellular signals to further regulate survival and homeostasis of the cell[235]. Csf1 typically induces an immunosuppressive polarization of the macrophage, just like IL-34 which signals through the same Csf1R[236]. However, IL-34 is less efficient in stimulating receptor phosphorylation and subsequent macrophage proliferation, due to a lower affinity of the receptor for IL-34 compared to Csf1[237]. IL-34 specifically regulates the differentiation of LCs and microglial cells, coinciding with its expression in skin keratinocytes and neurons in the brain[238,239]. In contrast to Csf1 and IL-34, Csf2 (or GM-Csf) causes a polarization of the macrophage to a pro-inflammatory state[240]. This is in accordance with elevated levels of Csf2 in inflammatory and auto-immune diseases, where it is produced by a variety of cell types[241,242].

IV.4 Transcription factors regulating macrophage development and identity

Despite being derived from a limited number of progenitors (yolk sac macrophages, fetal monocytes and blood monocytes), gene expression among tissue-resident macrophages is immensely heterogeneous[243,244]. This tissue-specific expression allows tissue-resident macrophages to perform their tissue-specific functions and it implies that macrophages are highly influenced by the micro-environment in which they reside[245]. It was suggested that local signals induce the expression of tissue-specific TFs that regulate the development, function and identity of tissue-resident macrophages. Bach1 for instance was shown to play a role in splenic red pulp macrophages. In monocytes, Bach1 is a transcriptional repressor of Spi-c, a protein

that is required for the development of splenic red pulp macrophages. A typical feature of the splenic tissue environment is the presence of heme, derived from senescent RBCs. This heme induces the degradation of Bach1 and subsequently the expression of Spi-c, allowing macrophage development[203]. Another tissue-specific signal that regulates tissue-resident macrophages is retinoic acid. It induces expression of TF Gata6 in peritoneal macrophages and in that way controls their localization and functional polarization[246]. Looking at the lung environment, it seems that Csf2 induces expression of nuclear receptor Pparγ in fetal monocytes. Functioning as a TF, Pparγ regulates perinatal development of AMs and governs the specific identity of these cells[247]. C/Ebpβ also plays a role in the generation of AMs, as mice deficient for this TF lack AMs as well as functional large peritoneal macrophages[248]. It is likely that the tissue-specific TFs mentioned here cooperate with the more general factor Pu.1. Upon binding to the DNA, Pu.1 controls nucleosome remodelling and H3K4 mono-methylation and is thus able to change the chromatin landscape and determine gene expression[244,249]. It has been proposed that all macrophages have a common enhancer repertoire, but that the tissue-specific TFs, which are induced by signals in the local environment, collaborate with Pu.1 to establish tissue-specific enhancers[250]. This would explain the immense differences in gene expression between different tissue-resident macrophage populations.

Recently, research focused on the heterogeneity of macrophages from one tissue to another, but factors that govern macrophage identity across tissues remain unknown. Gautier *et al.* explored gene expression across multiple tissue-resident macrophages and found that only a small core of a few hundred genes were selectively expressed by macrophages compared to DCs. TFs predicted to regulate this core macrophage signature are Tcfe3, C/Ebpα, Creg-1 and Bach1[243]. However, the gene signature in this study was only based on four different tissue-resident macrophages and most of the genes were not shared among all four macrophage populations. More recently, Geissmann and colleagues defined a set of genes that is differentially expressed during the differentiation from EMP to macrophage[92]. One TF identified in this core macrophage program was Zeb2 and therefore investigating the role of this TF in the macrophage lineage is one of the aims of this thesis.

IV.5 Langerhans cells

Langerhans cells or LCs are mononuclear phagocytes that reside in the skin epidermis, where they sample antigen. Upon activation they migrate through the dermis to skin draining LNs in order to prime $CD4^+$ T cells[86]. LCs display a lot of DC-like features, such as their stellate morphology, surface expression of CD11c and MhcII and the ability to migrate and present antigen[150,251]. Therefore they were previously considered to be dendritic cells, but based on recent advances in the ontogeny-research on LCs, it was decided to classify them as macrophages[91]. Indeed, LCs develop from yolk sac macrophages and fetal liver monocytes in the embryo and maintain themselves through local proliferation in the adult skin[217,252,253]. Additionally, LCs do not depend on the DC-associated growth factor Flt3L, but on the macrophage-associated factors Csf1 and IL-34[238,239,254]. Interestingly, a recent study combined lineage-tracing of macrophages and dendritic cells, respectively based on *Mafb* and *Zbtb46*[161]. As LCs were marked by both system, this re-enforced the finding that LCs share features of both DCs and macrophages.

Several transcription factors are of importance for the development of LCs. As such $Runx3^{-/-}$ mice completely lack LCs in their skin epidermis[255]. Mechanistically, Runx3 is part of the Tgfβ-signalling pathway and LCs require autocrine and paracrine Tgfβ for their differentiation[256,257]. Furthermore, Irf2 and Id2 are implicated in LC development, as both Irf2 and Id2 KO mice showed reduced numbers of LCs[164,180].

IV.6 Monocyte-derived cells with macrophage- and DC-features

During inflammation high numbers of monocytes are recruited to the affected tissue, were they further mature into monocyte-derived cells (MCs) that show both DC-like and macrophage-like features[215]. MCs exert many functions during inflammation, such as migration to the draining LNs, antigen-presentation and clearance of pathogens[258,259]. MCs showing pre-dominantly DC-associated features, such as their morphology, migration to draining LNs and expression of typical cDC markers (CD11c, MhcII, CD80 and CD86), are often referred to as moDCs[260–262]. Human moDCs can be cultured starting from blood or BM monocytes, when supplemented with CSF2 and

IL-4[263]. These *in vitro* derived moDCs are routinely used in human DC-based immunotherapy against cancer[264]. On the other hand, MCs showing more macrophage-like characteristics, for instance expression of F4/80, are often referred to as moMφs[192,194–196]. However, moDCs and moMφs often display surface markers and functions related to DCs and macrophages. Moreover, a recent lineage-tracing study demonstrated that the so-called moDCs lack expression of the DC-associated *Zbtb46*, but do express the macrophage-related *Mafb*[161]. MoDCs and moMφs probably represent the same highly plastic population that arises from monocytes during inflammatory settings and therefore it was suggested to no longer make a distinction and refer to them as MCs[215].

V. Leukemia: when ZEB proteins are out of balance in the immune system

As discussed above, Zeb proteins have a physiological role in a range of different immune cells. Considering this, it is not a surprise that genetic events changing the levels of Zeb proteins can have serious consequences and lead to the development of lymphomas and leukemias. One aim of this thesis was to contribute to the development of mouse models that allow to study the role of Zeb proteins in leukemia and can eventually be used to develop better therapies. Thus, here I will summarise what is known on how ZEBs function as tumor suppressors or oncogenes in hematological malignancies (Table 1). In several types of malignancies originating in the T cell lineage, ZEB1 acts as a tumor suppressor. ZEB2 on the other hand has been described as an oncogene in ETP-ALL, an immature form of T cell acute lymphoblastic leukemia (T-ALL). For some B cell malignancies ZEB1 was shown to be oncogenic, while in other B cell malignancies ZEB2 acts as a tumor suppressor. Additionally, both ZEBs have been associated with oncogenic function in acute myeloid leukemia (AML), while ZEB2 might act as a tumor suppressor in blastic plasmacytoid dendritic cell neoplasm (BPDCN), a rare malignancy believed to originate from pDC precursors.

Table 1 | ZEBs as oncogenes or tumor suppressors of leukemia. Table showing the known and suggestive oncogenic and tumor suppressive roles for ZEB1 and ZEB2 in various leukemias.

ZEB1	
Tumor suppressor	**Oncogene**
T cell malignancies • CTLL: cutaneous T-cell lymphoblastic lymphoma/leukemia • ATLL: adult T-cell lymphoblastic leukemia	Acute myeloid leukemia B cell malignancies • (gastric) diffuse large B-cell lymphoma • Mantle cell lymphoma EBV-related malignancies
ZEB2	
Tumor suppressor	**Oncogene**
Blastic plasmacytoid dendritic cell neoplasm B cell malignancies • HCV-related lymphoma • B-ALL	Acute myeloid leukemia T cell malignancies • ETP/immature-ALL

V.1 ZEBs have opposing roles in T cell malignancies

ZEB2 acts as an oncogene in immature T cell lymphoblastic leukemia

T cell acute lymphoblastic leukemia or T-ALL is an aggressive hematological cancer of thymic T cell progenitors that gradually accumulate epigenetic and genetic changes, leading to a block in differentiation, increased survival and proliferative expansion of a malignant clone[265,266]. Over the last decade, the prognosis of T-ALL has gradually improved with the introduction of intensified chemotherapy for young patients. However, the outcome of T-ALL patients with primary resistant or relapsed disease remains poor[267].

One subgroup of T-ALL can be identified by a gene expression signature similar to that of an early T cell precursor (ETP), the most early T cell lineage progenitor that resides in the thymus[268]. Patients with ETP-ALL suffer from the most aggressive form of T-ALL and have the worst prognosis[269]. Goossens *et al.* identified a rare but recurrent translocation involving *ZEB2* and *BCL11B* in immature/ETP-ALL, suggesting a role for ZEB2 in the disease. It was hypothesized that this translocation retains ZEB2 expression during T cell commitment, leading to a differentiation block and leukemic transformation[270]. Hematopoietic-specific Zeb2 overexpression in the mouse was sufficient to spontaneously develop T-ALL with an immature expression profile and profound similarities to the human disease. Overexpression of Zeb2 resulted in increased expression of the IL-7 receptor (IL7R) and aberrant activation of the IL7R-Jak/Stat signalling pathway. Additionally, Zeb2 overexpression was associated with the acquisition of enhanced leukemia stem cell properties[270]. Furthermore, mouse and human ETP-ALLs characterized by increased Zeb2 levels, were shown to be highly dependent on lysine-specific demethylase Kdm1a activity for their survival. It was demonstrated that disruption of the ZEB2-KDM1A protein interaction or inhibition of KDM1A activity itself, should be considered as a novel therapeutic strategy for ETP-ALL patients in which ZEB2 acts as a driving oncogene[271].

ZEB1 acts as a tumor suppressor in T cell malignancies

In contrast to ZEB2, ZEB1 seems to act as a tumor suppressor in T cell derived hematological neoplasms. First, ZEB1 was identified as an essential downstream mediator of the LMO2 oncogene in T-ALL[272]. During T-cell development LMO2 expression can be detected in early T cell progenitors, but is downregulated from the DN stage on[273]. Aberrant overexpression leads to an arrest in development and can be considered as an oncogenic event in T-ALL[274]. Two observations were suggestive of a link between Lmo2 and Zeb1 in T-ALL. First KO of Zeb1 and overexpression of Lmo2 in mice cause a similar arrest in T cell development and both mouse models spontaneously develop T cell lymphoma/leukemia with a median onset of six months[68,274]. Secondly, an inversely correlated expression pattern of both genes was detected in samples from leukemia patients. LMO2 inhibits ZEB1 activity in two ways: it inhibits ZEB1 transcription and it binds to the NZF of ZEB1 preventing ZEB1 to perform its positive regulatory activity on its target genes[272]. Through this mechanism, ZEB1 can be considered as a tumor suppressor in T-ALL.

Expression analysis of genes mapped within a common breakpoint cluster in the 10p11.2 region of adult T cell leukemia/lymphoma patients (ATLL), suggested that ZEB1 may act as a tumor suppressor in this T cell malignancy[275]. ATLL is caused by infection with the human T-lymphotropic virus-1 (HTLV-1), which is for instance endemic in certain regions of Japan[276]. People typically get infected around birth and about 5% of them develop ATLL with a latency period that can be as long as fifty years, which suggests the need of extra tumorigenic events[277]. Phenotypic analysis revealed that around 80% of patients show a malignant expansion of CD4 SP T lymphocytes. The other phenotypes (CD8 SP, DN and DP) are approximately equally distributed among the rest of the patients[278]. Most ATLL cell lines and primary cells display low mRNA expression levels of *ZEB1*, as a consequence of either chromosomal translocations with heterozygous deletion, intragenic mutations or epigenetic dysregulation[275]. Further confirmation came from the ΔC-fin mouse expressing a truncated form of Zeb1 lacking the C-terminal zinc fingers[68]. 84% of these mice develop T cell leukemia/lymphoma with a median onset of six months and a dominant phenotype of CD4 SP T cells, similar to the human disease[275]. Mechanistically, low ZEB1 levels may result in resistance to TGFβ1 mediated growth arrest. Binding of TGFβ1 to its receptor activates its kinase activity, leading to phosphorylation of

receptor-associated SMAD proteins. These phospho-SMADs accumulate in the nucleus as dimers, and in conjunction with other transcription factors, like ZEB1 and ZEB2, they bind regulatory elements within their target gene promoters[23,25,279]. As an example, TGFβ1 stimulation induces cell cycle arrest in various tumor cell types via the direct upregulation of the cyclin dependent kinase inhibitor p21[280]. ATLL cells with low ZEB1 levels appear to be resistant to these anti-proliferative effects of TGFβ1 and overexpression of ZEB1 restored the TGFβ1-mediated growth suppression in these cells, associated with increased p21 expression. In more detail, ZEB1 expression, and its direct binding to the phospho-SMAD3 complex, was demonstrated to be essential for the recruitment of this complex to the SMAD-response element (SRE) within the p21 promoter[281].

Furthermore, aberrant ZEB1 expression has been linked to two types of cutaneous T cell lymphoma (CTCL): Mycosis fungoides (MF) and Sézary syndrome (SS). MF and SS are two types of mature T cell neoplasms with a CD4 SP phenotype[282]. MF arises due to a clonal expansion of skin-homing $CD4^+$ T cells. SS can arise *de novo*, but is mostly identified in patients already suffering from MF and can be considered as the leukemic variant of MF. Three diagnostic criteria are used for SS: erythroderma, lymphadenopathy and circulating $CD4^+$ T cells with convoluted nuclei (also called Sézary cells)[283]. Several genetic alterations targeting *ZEB1* have been reported in both forms of CTCL, including translocations, mutations and both heterozygous and homozygous deletions[284–288]. Mishra *et al.* also reported on the involvement of ZEB1 in the pathogenic role of IL-15 signalling in CTCL. CTCL patients overexpressing IL-15 show a reduced binding of ZEB1 due to hypermethylation of the ZEB1 binding sites in the IL-15 promoter. As such ZEB1 is no longer capable of repressing IL-15[289]. All together these loss of function alterations of *ZEB1* suggest that the transcription factor acts as a tumor suppressor in cutaneous T cell lymphoma.

V.2 ZEBs in B cell malignancies

Altered ZEB1 expression and mutations have been associated with two types of B cell malignancies, namely mantle cell lymphoma (MCL) and diffuse large B cell lymphoma (DLBCL), while deleterious alterations in the *ZEB2* locus have been associated with B cell acute lymphoblastic leukemia (B-ALL).

ZEB1 acts as an oncogene in MCL

MCL is an infrequent subtype of non-Hodgkin B cell lymphoma with a high response rate to chemotherapy, but the majority of patients relapses[290,291]. The genetic characteristic for MCL is the translocation of cyclin D1 to the Ig heavy chain enhancer resulting in overexpression of cyclin D1. This genetic event occurs at the pre-B stage, but the tumor is composed of mature B lymphocytes[290,291]. Half of MCLs display constitutive active Wnt-signalling, with nuclear localization of β-catenin and concomitant high expression of ZEB1. Downregulation of *ZEB1* expression in MCL cell lines reduced their tumor growth capacity in mouse xenograft models. Furthermore, the cell lines with reduced *ZEB1* expression were more sensitive to chemotherapeutics, associated with a differential expression of drug influx and efflux transporters and genes involved in cell survival and apoptosis[292]. Therefore, this study suggests that ZEB1 could serve as a potential predictive biomarker and putative therapeutic target in MCL.

ZEB1 acts as an oncogene in DLBCL

DLBCL is the most common type of adult non-Hodgkin lymphoma[282]. Standard therapy consists of cyclophosphamide, vincristine, prednisone and doxorubicin (CHOP), combined with the anti-CD20 monoclonal antibody rituximab[293,294]. ZEB1 can be considered as an oncogene in DLBCL for several reasons. First, strong nuclear immunohistochemical staining for ZEB1 was associated with an adverse 3-year overall survival of DLBCL patients, compared to those with no or weak nuclear ZEB1 staining[295]. Secondly, higher levels of the miR-200 family, a micro-RNA family known to negatively regulate *ZEB1* mRNA levels, results in less aggressive behaviour of the disease[296]. *Helicobacter pylori* positive gastric DLBCLs, which typically show lower

ZEB1 expression, have less lymph node metastasis, better response to chemotherapy and are less aggressive[296]. This last subgroup is also characterized by higher expression levels of *BCL6*, a known predictor of better prognosis in DLBCL[297] and a direct target of ZEB1[298]. Combined, these expression data suggest that ZEB1 may act as an oncogene in this type of non-Hodgkin lymphoma.

ZEB2 acts as a tumor suppressor in B cell malignancies

Interestingly, loss and not gain of 2q22.3, the genomic region spanning the *ZEB2* locus, has been recurrently observed in B cell lymphoma patients[299]. In addition, rare but recurrent *ZEB2* point mutations were found in B-ALL[300], the most common childhood malignancy that initiates in the BM with oncogenic transformation of B cell progenitors. Depending on the cell of origin, several subtypes of B-ALL can be identified: early pre-B-ALL or pro-B-ALL, pre-B-ALL, common B-ALL and mature B-ALL[301]. Interestingly, in all five reported B-ALL patients with a mutant *ZEB2* locus, a single amino acid change affected the C-terminal zinc fingers of the TF[300]. Zhou and colleagues also reported a *ZEB2-PDGFRB* translocation in one B-ALL patient. In this translocation event, the C-terminal zinc finger cluster of *ZEB2* is missing and in frame fused to the catalytic domain of the platelet-derived growth factor receptor B (*PDGFRB*)[302]. However, no additional data is available whether this chimeric protein is expressed, functional and whether it contributes to the disease progression. The notion that ZEB2, or a mutant version, may play an important role in the initiation and/or progression of B-ALL is further supported by the observed high occurrence of viral insertions at the *Zeb2* locus in two independent retroviral mutagenesis screens using mouse models that are predisposed to spontaneously develop B-ALL, the Calm-af10 transgenic and the heterozygote Pax5$^{-/+}$ mice[303,304]. Nonetheless, no information is available whether these viral integrations result in loss or gain of Zeb2 function.

Combining the mutation data of the human patients and the mutagenesis screenings in the B-ALL mouse models, we hypothesize that Zeb2 acts as a tumor suppressor in B cell malignancies, in contrast to Zeb1, which seems to act as an oncogene. More research with conditional Zeb1/2 gain or loss of function mouse models, using a B cell restricted CRE line, will be necessary to further test this hypothesis.

V.3 ZEBs in myeloid malignancies

ZEBs act as oncogenes in AML

Acute myeloid leukemia or AML is a clinically and genetically heterogeneous malignancy, characterized by an uncontrolled accumulation of immature myeloid cells in the BM and the blood of the patient. This accumulation of blast cells, and the cytokines they produce, interfere with normal hematopoiesis which leads to a general deficiency of hematopoietic cells. The main diagnostic criterion for AML is the presence of 20% or more of such blast cells in the blood and/or BM[305,306]. It's a rare, but aggressive disease with a median onset age of 65 years and occurring more in men than in women[305]. Despite rapid advances in the field, including new drug targets and increased understanding of the biology, current treatment for AML still leads to relapse in patients. Allogeneic transplant remains the best chance for cure in patients with intermediate or high risk disease[306].

One recurrent translocation associated with extra-medullary disease (such as chloroma or central nervous system involvement), relapse and poor survival of AML is the t(9;11)(p22;q23) rearrangement leading to the MLL-AF9 fusion. Recently, a conditional mouse model was used to address the role of the cellular origin of MLL-AF9^{+} AML. Activation of Mll-af9 in long-term hematopoietic stem cells (LT-HSCs) induces a particularly invasive and chemoresistant disease[307]. Strikingly, about 10-20% of human AMLs express a very similar gene signature like LT-HSC-derived Mll-af9 AMLs in mice, which is characterized by expression of high *Zeb1* mRNA levels. Chromatin immunoprecipitation (ChIP) experiments suggested that *Zeb1* is a direct target of the Mll-af9 fusion. Interestingly, knockdown of *Zeb1* expression compromised the invasive behaviour of Mll-af9 AML cells *in vitro* and *in vivo*. Notably, LT-HSC-derived Mll-af9 AML cells also displayed increased expression of many genes regulating migration and invasion, an thus showing at least at the transcriptional level some similarities to that of solid cancer cells undergoing EMT[307].

In addition to involvement of ZEB1, increasing evidence also suggests an important role for ZEB2 in AML development. In 2015 one AML patient was found with tumor cells carrying a similar t(2;14)(q22;q23) translocation as earlier identified in ETP-ALL, resulting in a ZEB2-BCL11B fusion[270,308]. In the resulting ZEB2-BCL11B fusion

transcript, the first 19 amino acids of BCL11B are replaced by the first 24 amino acids of ZEB2. As all functional domains of BCL11B are retained in this fusion product and the inverse BCL11B-ZEB2 transcript could not be detected, the authors concluded that the principal result of this translocation is aberrant expression of BCL11B controlled by the *ZEB2* promoter/enhancer[308]. Interestingly, other genetic events driving BCL11B overexpression have been reported in AML, further reinforcing the putative oncogenic role of BCL11B in the myeloid lineage[309]. These observations are in sharp contrast with the proposed role of BCL11B in T-ALL as a tumor suppressor[317]. This contradiction suggests that a similar genetic aberration, t(2;14)(q22;q23), can drive leukemic transformation both in the myeloid and the lymphoid lineage. In the case of AML, BCL11B overexpression most probably drives malignant transformation, whereas retained ZEB2 expression during T cell commitment is most probably the oncogenic driver in the case of ETP-ALL[270]. More recent experiments showed that ZEB2 expression is essential for maintenance of leukemic growth of AML[311,312]. Furthermore, using an *in vitro* genome-wide shRNA screening method followed by an *in vivo* secondary screen using a murine AML model driven by the expression of a Mll-af9 fusion, *Zeb2* was identified as an essential gene for AML progression. Further molecular analysis demonstrated that Zeb2 represses transcription of genes important in myeloid differentiation. Consequently, Zeb2 depletion in AML cells will force differentiation of the leukemic cells[311]. The notion that AML cells depend on sustained ZEB2 expression was recently confirmed by a large-scale deep RNAi screen that unravelled cancer dependencies in an extensive series of human tumor cell lines, including AML[313].

Is ZEB2 a tumor suppressor in BPDCN?

Blastic plasmacytoid dendritic cell neoplasm or BPDCN is a rare and aggressive disorder which is believed to originate from pDC-precursors[314–316]. The malignancy is currently classified as a myeloid neoplasm[317]. Patients typically show skin lesions and later on involvement of BM, LNs and peripheral blood. Treatment with chemotherapy often leads to relapse and currently allogeneic stem cell transplantation gives the best improvement on survival. BPDCN occurs mostly in elderly patients with a median age of onset above 60 years[318].

One study showed a possible role for ZEB2 in the disease. The researchers performed whole exome sequencing on material of three patients followed by a targeted next-generation sequencing of 38 selected genes in 25 other tumors. This revealed that the *ZEB2* locus is mutated in 16% of cases. Two frameshift mutations and one mutation causing a single amino acid change were identified[319]. These deleterious changes in the *ZEB2* gene could be the first clue for a possible tumor suppressive role for the TF in BPDCN and in this thesis we will use this finding in an attempt to model the disease in mice. Currently, there is no standardized therapeutical approach for BPDCN patients and we believe that a preclinical mouse model could be helpful for developing better targeted therapies, eventually leading in better outcome for patients.

V.4 ZEBs in pathogen-induced hematologic malignancies

Altered expression of ZEB1 has been associated with few pathogen-induced leukemia subtypes, like *Helicobacter pylori* positive gastric DLBCLs[296], HTLV-1 related ATLL[275] and Epstein-Barr virus (EBV) associated lymphomas[320]. EBV is a human herpesvirus that was first isolated from a cultured Burkitt's lymphoma cell line. It has been estimated that more than 90% of the world's population is carrying the virus, usually through a first asymptomatic infection during childhood. EBV has been linked to many types of malignancies including several epithelial cancers and some B cell malignancies like Burkitt's and Hodgkin's lymphoma. EBV can infect epithelial cells and B cells, either causing a lytic infection with active production of viral particles and killing of the host cell, or a latent infection which is maintained stably in the host cell[320,321]. Breaking through the latency and activating the lytic cycle of the virus could be used as a therapy for EBV infected malignancies. It has been shown that ZEB1 is important in regulating this latent-lytic switch. The switch can be initiated by expression of the viral immediate-early *Bzlf1* gene. This gene codes for the DNA-binding protein Zta, a transactivator of viral genes for lytic replication[321]. The *Bzlf1* gene has two promoters, the proximal Zp which is most active and a more distal Rp. It was shown in B lymphocytes that ZEB1 binds to the Zp promoter to actively repress its transcription[322]. More specifically, ZEB1 binds to two consensus ZEB binding sites in the Zp promoter through both the

N-terminal and C-terminal zinc finger domains[323]. Breaking through the latency by inhibiting ZEB1 could be a potential mechanism to achieve a switch to the lytic phase of infection and possibly leading to dead of the virally infected malignant cells.

As mentioned before, Zeb2 expression is essential for differentiation, maturation and/or function of NK cells and $CD8^+$ T cells, two types of immune cells involved in antiviral host defense[74,75,81]. Interestingly, recurrent deletions of the *ZEB2* locus are significantly enriched in Hepatitis C virus (HCV)-related non-Hodgkin's lymphoma patients. Furthermore, viral integrations at the *Zeb2* locus are sufficient to induce leukemia in mice haplo-sufficient for Pax5[304]. This mouse model spontaneously develops B-ALL only in a conventional animal facility and not under specific pathogen free conditions, suggesting that exposure to infectious agents can act as a trigger for the development of B-ALL. We hypothesize that the expression of Zeb2 is essential for the functionality of the innate and adaptive immune system to efficiently eradicate pathogens, but also infected and (partially) transformed cells from the body, before they can develop into a lymphoma/leukemia. Van Helden and colleagues showed that Zeb2 also plays a pivotal role in the immunosurveillance and clearance of melanoma cells after transplantation in syngeneic mice[81], suggesting our hypothesis could serve as a more common mechanism also outside of hematologic malignancies.

In general, more research is needed to better understand the role of Zeb proteins in immune cells and hence their role in the eradication of pathogens, immunosurveillance of cancer and development of leukemia. Therefore, the main goal of this thesis is to further assess the physiological role of Zebs in dendritic cells and macrophages, two cell types that express Zeb1/2, but where a possible function for these TFs has not yet been investigated.

References

1. Fortini ME, Lai ZC, Rubin GM. The Drosophila zfh-1 and zfh-2 genes encode novel proteins containing both zinc-finger and homeodomain motifs. *Mechanisms of development*. 1991;34(2-3):113–22.
2. Watanabe Y, Kawakami K, Hirayama Y, Nagano K. Transcription factors positively and negatively regulating the Na,K-ATPase alpha 1 subunit gene. *J. Biochem.* 1993;114(6):849–55.
3. Funahashi J, Sekido R, Murai K, Kamachi Y, Kondoh H. Delta-crystallin enhancer binding protein delta EF1 is a zinc finger-homeodomain protein implicated in postgastrulation embryogenesis. *Development*. 1993;119(2):433–46.
4. Franklin AJ, Jetton TL, Shelton KD, Magnuson MA. BZP, a novel serum-responsive zinc finger protein that inhibits gene transcription. *Mol. Cell. Biol.* 1994;14(10):6773–88.
5. Genetta T, Ruezinsky D, Kadesch T. Displacement of an E-box-binding repressor by basic helix-loop-helix proteins: implications for B-cell specificity of the immunoglobulin heavy-chain enhancer. *Mol. Cell. Biol.* 1994;14(9):6153–63.
6. Sekido R, Takagi T, Okanami M, et al. Organization of the gene encoding transcriptional repressor deltaEF1 and cross-species conservation of its domains. *Gene*. 1996;173(2):227–32.
7. Clark SG, Chiu C. C. elegans ZAG-1, a Zn-finger-homeodomain protein, regulates axonal development and neuronal differentiation. *Development*. 2003;130(16):3781–94.
8. Verschueren K, Remacle JE, Collart C, et al. SIP1, a novel zinc finger/homeodomain repressor, interacts with Smad proteins and binds to 5'-CACCT sequences in candidate target genes. *The Journal of biological chemistry*. 1999;274(29):20489–98.
9. Gheldof A, Hulpiau P, van Roy F, De Craene B, Berx G. Evolutionary functional analysis and molecular regulation of the ZEB transcription factors. *Cell. Mol. Life Sci.* 2012;69(15):2527–41.
10. Lai ZC, Fortini ME, Rubin GM. The embryonic expression patterns of zfh-1 and zfh-2, two Drosophila genes encoding novel zinc-finger homeodomain proteins. *Mechanisms of development*. 1991;34(2-3):123–34.
11. Williams TM, Moolten D, Burlein J, et al. Identification of a zinc finger protein that inhibits IL-2 gene expression. *Science (New York, N.Y.)*. 1992;254(5039):1791–4.
12. Sekido R, Murai K, Funahashi J, et al. The delta-crystallin enhancer-binding protein delta EF1 is a repressor of E2-box-mediated gene activation. *Mol. Cell. Biol.* 1994;14(9):5692–700.
13. Wakamatsu N, Yamada Y, Yamada K, et al. Mutations in SIP1, encoding Smad interacting protein-1, cause a form of Hirschsprung disease. *Nature genetics*. 2001;27(4):369–70.
14. Yamada K, Yamada Y, Nomura N, et al. Nonsense and frameshift mutations in ZFHX1B, encoding Smad-interacting protein 1, cause a complex developmental disorder with a great variety of clinical features. *Am. J. Hum. Genet.* 2001;69(6):1178–85.
15. Amiel J, Espinosa-Parrilla Y, Steffann J, et al. Large-scale deletions and SMADIP1 truncating mutations in syndromic Hirschsprung disease with involvement of midline structures. *American journal of human genetics*. 2002;69(6):1370–7.
16. Van de Putte T, Maruhashi M, Francis A, et al. Mice lacking ZFHX1B, the gene that codes for Smad-interacting protein-1, reveal a role for multiple neural crest cell defects in the etiology of Hirschsprung disease-mental retardation syndrome. *American journal of human genetics*. 2003;72(2):465–70.
17. Espinosa-Parrilla Y, Amiel J, Augé J, et al. Expression of the SMADIP1 gene during early human development. *Mechanisms of development*. 2002;114(1-2):187–91.
18. Ikeda K, Kawakami K. DNA binding through distinct domains of zinc-finger-homeodomain protein AREB6 has different effects on gene transcription. *Eur. J. Biochem.* 1995;233(1):73–82.
19. Remacle JE, Kraft H, Lerchner W, et al. New mode of DNA binding of multi-zinc finger transcription factors: deltaEF1 family members bind with two hands to two target sites. *The EMBO journal*. 1999;18(18):5073–84.
20. Postigo AA, Dean DC. Independent repressor domains in ZEB regulate muscle and T-cell differentiation. *Molecular and cellular biology*. 2000;19(12):7961–71.
21. Zhao L-JJ, Kuppuswamy M, Vijayalingam S, Chinnadurai G. Interaction of ZEB and histone deacetylase with the PLDLS-binding cleft region of monomeric C-terminal binding protein 2. *BMC molecular biology*. 2009;10:89.
22. Wang J, Lee S, Teh CE, et al. The transcription repressor, ZEB1, cooperates with CtBP2 and HDAC1 to suppress IL-2 gene activation in T cells. *Int. Immunol.* 2009;21(3):227–35.
23. Javelaud D, Mauviel A. Crosstalk mechanisms between the mitogen-activated protein kinase pathways and Smad signaling

downstream of TGF-beta: implications for carcinogenesis. *Oncogene*. 2005;24(37):5742–50.
24. Conidi A, van den Berghe V, Leslie K, et al. Four amino acids within a tandem QxVx repeat in a predicted extended α-helix of the Smad-binding domain of Sip1 are necessary for binding to activated Smad proteins. *PloS one*. 2013;8(10):e76733.
25. Postigo AA. Opposing functions of ZEB proteins in the regulation of the TGFbeta/BMP signaling pathway. *The EMBO journal*. 2003;22(10):2443–52.
26. Postigo AA, Depp JL, Taylor JJ, Kroll KL. Regulation of Smad signaling through a differential recruitment of coactivators and corepressors by ZEB proteins. *The EMBO journal*. 2003;22(10):2453–62.
27. Van Grunsven LA, Taelman V, Michiels C, et al. deltaEF1 and SIP1 are differentially expressed and have overlapping activities during Xenopus embryogenesis. *Dev. Dyn.* 2006;235(6):1491–500.
28. Verstappen G, van Grunsven LA, Michiels C, et al. Atypical Mowat-Wilson patient confirms the importance of the novel association between ZFHX1B/SIP1 and NuRD corepressor complex. *Human molecular genetics*. 2008;17(8):1175–83.
29. Bowen NJ, Fujita N, Kajita M, Wade PA. Mi-2/NuRD: multiple complexes for many purposes. *Biochimica et biophysica acta*. 2004;1677(1-3):52–7.
30. Xue Y, Wong J, Moreno GT, et al. NURD, a novel complex with both ATP-dependent chromatin-remodeling and histone deacetylase activities. *Molecular cell*. 1999;2(6):851–61.
31. Wu LM, Wang J, Conidi A, et al. Zeb2 recruits HDAC-NuRD to inhibit Notch and controls Schwann cell differentiation and remyelination. *Nature neuroscience*. 2016;19(8):1060–72.
32. Vandewalle C, Van Roy F, Berx G. The role of the ZEB family of transcription factors in development and disease. *Cell. Mol. Life Sci.* 2009;66(5):773–87.
33. Zeisberg M, Neilson EG. Biomarkers for epithelial-mesenchymal transitions. *The Journal of clinical investigation*. 2009;119(6):1429–37.
34. Comijn J, Berx G, Vermassen P, et al. The two-handed E box binding zinc finger protein SIP1 downregulates E-cadherin and induces invasion. *Molecular cell*. 2001;7(6):1267–78.
35. Shirakihara T, Saitoh M, Miyazono K. Differential regulation of epithelial and mesenchymal markers by deltaEF1 proteins in epithelial mesenchymal transition induced by TGF-beta. *Mol. Biol. Cell*. 2007;18(9):3533–44.
36. Eger A, Aigner K, Sonderegger S, et al. DeltaEF1 is a transcriptional repressor of E-cadherin and regulates epithelial plasticity in breast cancer cells. *Oncogene*. 2005;24(14):2375–85.
37. Vandewalle C, Comijn J, De Craene B, et al. SIP1/ZEB2 induces EMT by repressing genes of different epithelial cell-cell junctions. *Nucleic acids research*. 2005;33(20):6566–78.
38. Tatari MN, De Craene B, Soen B, et al. ZEB2-transgene expression in the epidermis compromises the integrity of the epidermal barrier through the repression of different tight junction proteins. *Cell. Mol. Life Sci.* 2014;71(18):3599–609.
39. Bindels S, Mestdagt M, Vandewalle C, et al. Regulation of vimentin by SIP1 in human epithelial breast tumor cells. *Oncogene*. 2006;25(36):4975–85.
40. Takeyama Y, Sato M, Horio M, et al. Knockdown of ZEB1, a master epithelial-to-mesenchymal transition (EMT) gene, suppresses anchorage-independent cell growth of lung cancer cells. *Cancer Lett.* 2010;296(2):216–24.
41. Bassez G, Camand OJ, Cacheux V, et al. Pleiotropic and diverse expression of ZFHX1B gene transcripts during mouse and human development supports the various clinical manifestations of the “Mowat-Wilson” syndrome. *Neurobiol. Dis.* 2004;15(2):240–50.
42. Higashi Y, Maruhashi M, Nelles L, et al. Generation of the floxed allele of the SIP1 (Smad-interacting protein 1) gene for Cre-mediated conditional knockout in the mouse. *Genesis (New York, N.Y. : 2000)*. 2002;32(2):82–4.
43. Darling DS, Stearman RP, Qi Y, Qiu MS, Feller JP. Expression of Zfhep/deltaEF1 protein in palate, neural progenitors, and differentiated neurons. *Gene expression patterns : GEP*. 2003;3(6):709–17.
44. Takagi T, Moribe H, Kondoh H, Higashi Y. DeltaEF1, a zinc finger and homeodomain transcription factor, is required for skeleton patterning in multiple lineages. *Development (Cambridge, England)*. 1998;125(1):21–31.
45. De Craene B, Berx G. Regulatory networks defining EMT during cancer initiation and progression. *Nat. Rev. Cancer*. 2013;13(2):97–110.
46. Sánchez-Tilló E, Liu Y, de Barrios O, et al. EMT-activating transcription factors in cancer: beyond EMT and tumor invasiveness. *Cell. Mol. Life Sci.* 2012;69(20):3429–56.
47. Elloul S, Elstrand MB, Nesland JM, et al. Snail, Slug, and Smad-interacting protein 1 as novel parameters of disease aggressiveness in metastatic ovarian and breast carcinoma. *Cancer*. 2005;103(8):1631–43.
48. Maeda G, Chiba T, Okazaki M, et al. Expression of SIP1 in oral squamous cell carcinomas: implications for E-cadherin expression and tumor progression. *International journal of oncology*. 2006;27(6):1535–41.

49. Miyoshi A, Kitajima Y, Sumi K, et al. Snail and SIP1 increase cancer invasion by upregulating MMP family in hepatocellular carcinoma cells. *Br. J. Cancer*. 2004;90(6):1265–73.
50. Spaderna S, Schmalhofer O, Wahlbuhl M, et al. The transcriptional repressor ZEB1 promotes metastasis and loss of cell polarity in cancer. *Cancer research*. 2008;68(2):537–44.
51. Aigner K, Dampier B, Descovich L, et al. The transcription factor ZEB1 (deltaEF1) promotes tumour cell dedifferentiation by repressing master regulators of epithelial polarity. *Oncogene*. 2007;26(49):6979–88.
52. Mani SA, Guo W, Liao M-JJ, et al. The epithelial-mesenchymal transition generates cells with properties of stem cells. *Cell*. 2008;133(4):704–15.
53. Scheel C, Eaton EN, Li SH, et al. Paracrine and autocrine signals induce and maintain mesenchymal and stem cell states in the breast. *Cell*. 2011;145(6):926–40.
54. Brabletz S, Brabletz T. The ZEB/miR-200 feedback loop--a motor of cellular plasticity in development and cancer? *EMBO Rep.* 2010;11(9):670–7.
55. Wellner U, Schubert J, Burk UC, et al. The EMT-activator ZEB1 promotes tumorigenicity by repressing stemness-inhibiting microRNAs. *Nat. Cell Biol.* 2009;11(12):1487–95.
56. Preca B-TT, Bajdak K, Mock K, et al. A self-enforcing CD44s/ZEB1 feedback loop maintains EMT and stemness properties in cancer cells. *Int. J. Cancer*. 2015;137(11):2566–77.
57. Meidhof S, Brabletz S, Lehmann W, et al. ZEB1-associated drug resistance in cancer cells is reversed by the class I HDAC inhibitor mocetinostat. *EMBO Mol Med*. 2015;7(6):831–47.
58. Hanrahan K, O'Neill A, Prencipe M, et al. The role of epithelial-mesenchymal transition drivers ZEB1 and ZEB2 in mediating docetaxel-resistant prostate cancer. *Mol Oncol*. 2017;11(3):251–265.
59. McConkey DJ, Choi W, Marquis L, et al. Role of epithelial-to-mesenchymal transition (EMT) in drug sensitivity and metastasis in bladder cancer. *Cancer Metastasis Rev.* 2009;28(3-4):335–44.
60. Rastogi I, Rajanna S, Webb A, et al. Mechanism of c-Met and EGFR tyrosine kinase inhibitor resistance through epithelial mesenchymal transition in non-small cell lung cancer. *Biochem. Biophys. Res. Commun.* 2016;477(4):937–944.
61. Yoshida T, Song L, Bai Y, et al. ZEB1 Mediates Acquired Resistance to the Epidermal Growth Factor Receptor-Tyrosine Kinase Inhibitors in Non-Small Cell Lung Cancer. *PLoS ONE*. 2016;11(1):e0147344.
62. Nishijima N, Seike M, Soeno C, et al. miR-200/ZEB axis regulates sensitivity to nintedanib in non-small cell lung cancer cells. *Int. J. Oncol.* 2016;48(3):937–44.
63. Arumugam T, Ramachandran V, Fournier KF, et al. Epithelial to mesenchymal transition contributes to drug resistance in pancreatic cancer. *Cancer Res.* 2009;69(14):5820–8.
64. Fang S, Zeng X, Zhu W, et al. Zinc finger E-box-binding homeobox 2 (ZEB2) regulated by miR-200b contributes to multi-drug resistance of small cell lung cancer. *Exp. Mol. Pathol.* 2014;96(3):438–44.
65. Goossens S, Janzen V, Bartunkova S, et al. The EMT regulator Zeb2/Sip1 is essential for murine embryonic hematopoietic stem/progenitor cell differentiation and mobilization. *Blood*. 2011;117(21):5620–30.
66. Li J, Riedt T, Goossens S, et al. The EMT transcription factor Zeb2 controls adult murine hematopoietic differentiation by regulating cytokine signaling. *Blood*. 2017;129(4):460–472.
67. Labrecque N, Baldwin T, Lesage S. Molecular and genetic parameters defining T-cell clonal selection. *Immunol. Cell Biol.* 2011;89(1):16–26.
68. Higashi Y, Moribe H, Takagi T, et al. Impairment of T cell development in deltaEF1 mutant mice. *The Journal of experimental medicine*. 1997;185(8):1467–79.
69. Arnold CN, Pirie E, Dosenovic P, et al. A forward genetic screen reveals roles for Nfkbid, Zeb1, and Ruvbl2 in humoral immunity. *Proc. Natl. Acad. Sci. U.S.A.* 2012;109(31):12286–93.
70. Rojas-Marquez C, Valle-Rios R, Lopez-Bayghen E, Ortiz-Navarrete V. CRTAM is negatively regulated by ZEB1 in T cells. *Mol. Immunol.* 2015;66(2):290–8.
71. Brabletz T, Jung A, Hlubek F, et al. Negative regulation of CD4 expression in T cells by the transcriptional repressor ZEB. *Int. Immunol.* 1999;11(10):1701–8.
72. Joshi NS, Cui W, Chandele A, et al. Inflammation directs memory precursor and short-lived effector CD8(+) T cell fates via the graded expression of T-bet transcription factor. *Immunity*. 2007;27(2):281–95.
73. Kaech SM, Cui W. Transcriptional control of effector and memory CD8+ T cell differentiation. *Nat. Rev. Immunol.* 2012;12(11):749–61.
74. Dominguez CX, Amezquita RA, Guan T, et al. The transcription factors ZEB2 and T-bet cooperate to program cytotoxic T cell terminal differentiation in response to LCMV viral infection. *J. Exp. Med.* 2015;212(12):2041–56.
75. Omilusik KD, Best JA, Yu B, et al. Transcriptional repressor ZEB2 promotes

terminal differentiation of CD8+ effector and memory T cell populations during infection. *J. Exp. Med.* 2015;212(12):2027–39.
76. Guan T, Dominguez CX, Amezquita RA, et al. ZEB1, ZEB2, and the miR-200 family form a counterregulatory network to regulate CD8+T cell fates. *J. Exp. Med.* 2018;215(4):1153–1168.
77. Huntington ND, Vosshenrich CA, Di Santo JP. Developmental pathways that generate natural-killer-cell diversity in mice and humans. *Nat. Rev. Immunol.* 2007;7(9):703–14.
78. Kim S, Iizuka K, Kang H-SPS, et al. In vivo developmental stages in murine natural killer cell maturation. *Nat. Immunol.* 2002;3(6):523–8.
79. Hayakawa Y, Smyth MJ. CD27 dissects mature NK cells into two subsets with distinct responsiveness and migratory capacity. *Journal of immunology (Baltimore, Md.: 1950)*. 2006;176(3):1517–24.
80. Huntington ND, Tabarias H, Fairfax K, et al. NK cell maturation and peripheral homeostasis is associated with KLRG1 up-regulation. *Journal of immunology (Baltimore, Md.: 1950)*. 2007;178(8):4764–70.
81. Van Helden MJ, Goossens S, Daussy C, et al. Terminal NK cell maturation is controlled by concerted actions of T-bet and Zeb2 and is essential for melanoma rejection. *J. Exp. Med.* 2015;212(12):2015–25.
82. Krystel-Whittemore M, Dileepan KN, Wood JG. Mast Cell: A Multi-Functional Master Cell. *Front Immunol*. 2015;6:620.
83. Barbu EA, Zhang J, Berenstein EH, et al. The transcription factor Zeb2 regulates signaling in mast cells. *J. Immunol.* 2012;188(12):6278–86.
84. Van Furth R, Cohn ZA, Hirsch JG, et al. The mononuclear phagocyte system: a new classification of macrophages, monocytes, and their precursor cells. *Bull. World Health Organ.* 1972;46(6):845–52.
85. Tussiwand R, Gautier EL. Transcriptional Regulation of Mononuclear Phagocyte Development. *Front Immunol*. 2015;6:533.
86. Romani N, Brunner PM, Stingl G. Changing views of the role of Langerhans cells. *J. Invest. Dermatol.* 2012;132(3 Pt 2):872–81.
87. Konradi S, Yasmin N, Haslwanter D, et al. Langerhans cell maturation is accompanied by induction of N-cadherin and the transcriptional regulators of epithelial-mesenchymal transition ZEB1/2. *Eur. J. Immunol.* 2014;44(2):553–60.
88. Miller JC, Brown BD, Shay T, et al. Deciphering the transcriptional network of the dendritic cell lineage. *Nat. Immunol.* 2012;13(9):888–99.
89. Grajales-Reyes GE, Iwata A, Albring J, et al. Batf3 maintains autoactivation of Irf8 for commitment of a CD8α(+) conventional DC clonogenic progenitor. *Nat. Immunol.* 2015;16(7):708–17.
90. Schlitzer A, Sivakamasundari V, Chen J, et al. Identification of cDC1- and cDC2-committed DC progenitors reveals early lineage priming at the common DC progenitor stage in the bone marrow. *Nat. Immunol.* 2015;16(7):718–28.
91. Guilliams M, Ginhoux F, Jakubzick C, et al. Dendritic cells, monocytes and macrophages: a unified nomenclature based on ontogeny. *Nat. Rev. Immunol.* 2014;14(8):571–8.
92. Mass E, Ballesteros I, Farlik M, et al. Specification of tissue-resident macrophages during organogenesis. *Science*. 2016;353(6304):
93. Cortés M, Sanchez-Moral L, de Barrios O, et al. Tumor-associated macrophages (TAMs) depend on ZEB1 for their cancer-promoting roles. *EMBO J.* 2017;36(22):3336–3355.
94. Steinman RM, Cohn ZA. Identification of a novel cell type in peripheral lymphoid organs of mice. I. Morphology, quantitation, tissue distribution. *The Journal of experimental medicine*. 1973;137(5):1142–62.
95. Steinman RM, Witmer MD. Lymphoid dendritic cells are potent stimulators of the primary mixed leukocyte reaction in mice. *Proceedings of the National Academy of Sciences of the United States of America*. 1978;75(10):5132–6.
96. Merad M, Sathe P, Helft J, Miller J, Mortha A. The dendritic cell lineage: ontogeny and function of dendritic cells and their subsets in the steady state and the inflamed setting. *Annu. Rev. Immunol.* 2013;31:563–604.
97. Asselin-Paturel C, Boonstra A, Dalod M, et al. Mouse type I IFN-producing cells are immature APCs with plasmacytoid morphology. *Nat. Immunol.* 2001;2(12):1144–50.
98. Gilliet M, Cao W, Liu Y-JJ. Plasmacytoid dendritic cells: sensing nucleic acids in viral infection and autoimmune diseases. *Nature reviews. Immunology*. 2008;8(8):594–606.
99. Swiecki M, Colonna M. Unraveling the functions of plasmacytoid dendritic cells during viral infections, autoimmunity, and tolerance. *Immunol. Rev.* 2010;234(1):142–62.
100. Naik SH, Corcoran LM, Wu L. Development of murine plasmacytoid dendritic cell subsets. *Immunol. Cell Biol.* 2005;83(5):563–70.
101. Young LJ, Wilson NS, Schnorrer P, et al. Differential MHC class II synthesis and ubiquitination confers distinct antigen-presenting properties on conventional and plasmacytoid dendritic cells. *Nat. Immunol.* 2008;9(11):1244–52.
102. Osorio F, Fuentes C, López MN, Salazar-Onfray F, González FEE. Role of Dendritic Cells in the Induction of Lymphocyte Tolerance. *Front Immunol*. 2015;6:535.
103. O'Keeffe M, Hochrein H, Vremec D, et al. Mouse plasmacytoid cells: long-lived cells,

heterogeneous in surface phenotype and function, that differentiate into CD8(+) dendritic cells only after microbial stimulus. *J. Exp. Med.* 2002;196(10):1307–19.
104. Nakano H, Yanagita M, Gunn MD. CD11c(+)B220(+)Gr-1(+) cells in mouse lymph nodes and spleen display characteristics of plasmacytoid dendritic cells. *J. Exp. Med.* 2001;194(8):1171–8.
105. Blasius AL, Giurisato E, Cella M, et al. Bone marrow stromal cell antigen 2 is a specific marker of type I IFN-producing cells in the naive mouse, but a promiscuous cell surface antigen following IFN stimulation. *J. Immunol.* 2006;177(5):3260–5.
106. Zhang J, Raper A, Sugita N, et al. Characterization of Siglec-H as a novel endocytic receptor expressed on murine plasmacytoid dendritic cell precursors. *Blood*. 2006;107(9):3600–8.
107. Gilliet M, Boonstra A, Paturel C, et al. The development of murine plasmacytoid dendritic cell precursors is differentially regulated by FLT3-ligand and granulocyte/macrophage colony-stimulating factor. *J. Exp. Med.* 2002;195(7):953–8.
108. Fancke B, Suter M, Hochrein H, O'Keeffe M. M-CSF: a novel plasmacytoid and conventional dendritic cell poietin. *Blood*. 2008;111(1):150–9.
109. Chen W, Antonenko S, Sederstrom JM, et al. Thrombopoietin cooperates with FLT3-ligand in the generation of plasmacytoid dendritic cell precursors from human hematopoietic progenitors. *Blood*. 2004;103(7):2547–53.
110. Vogt TK, Link A, Perrin J, Finke D, Luther SA. Novel function for interleukin-7 in dendritic cell development. *Blood*. 2009;113(17):3961–8.
111. Murphy TL, Grajales-Reyes GE, Wu X, et al. Transcriptional Control of Dendritic Cell Development. *Annu. Rev. Immunol.* 2016;34:93–119.
112. Banchereau J, Steinman RM. Dendritic cells and the control of immunity. *Nature*. 1998;392(6673):245–52.
113. Karsunky H, Merad M, Cozzio A, Weissman IL, Manz MG. Flt3 ligand regulates dendritic cell development from Flt3+ lymphoid and myeloid-committed progenitors to Flt3+ dendritic cells in vivo. *J. Exp. Med.* 2003;198(2):305–13.
114. McKenna HJ, Stocking KL, Miller RE, et al. Mice lacking flt3 ligand have deficient hematopoiesis affecting hematopoietic progenitor cells, dendritic cells, and natural killer cells. *Blood*. 2000;95(11):3489–97.
115. Guilliams M, Dutertre C-AA, Scott CL, et al. Unsupervised High-Dimensional Analysis Aligns Dendritic Cells across Tissues and Species. *Immunity*. 2016;45(3):669–684.
116. Osorio F, Tavernier SJ, Hoffmann E, et al. The unfolded-protein-response sensor IRE-1α regulates the function of CD8α+ dendritic cells. *Nat. Immunol.* 2014;15(3):248–57.
117. Akashi K, Traver D, Miyamoto T, Weissman IL. A clonogenic common myeloid progenitor that gives rise to all myeloid lineages. *Nature*. 2000;404(6774):193–7.
118. Fogg DK, Sibon C, Miled C, et al. A clonogenic bone marrow progenitor specific for macrophages and dendritic cells. *Science*. 2006;311(5757):83–87.
119. Liu K, Victora GD, Schwickert TA, et al. In vivo analysis of dendritic cell development and homeostasis. *Science*. 2009;324(5925):392–7.
120. Onai N, Obata-Onai A, Schmid MA, et al. Identification of clonogenic common Flt3+M-CSFR+ plasmacytoid and conventional dendritic cell progenitors in mouse bone marrow. *Nature immunology*. 2007;8(11):1207–16.
121. Naik SH, Sathe P, Park H-YY, et al. Development of plasmacytoid and conventional dendritic cell subtypes from single precursor cells derived in vitro and in vivo. *Nat. Immunol.* 2007;8(11):1217–26.
122. Onai N, Kurabayashi K, Hosoi-Amaike M, et al. A clonogenic progenitor with prominent plasmacytoid dendritic cell developmental potential. *Immunity*. 2013;38(5):943–57.
123. Laouar Y, Welte T, Fu X-YY, Flavell RA. STAT3 is required for Flt3L-dependent dendritic cell differentiation. *Immunity*. 2003;19(6):903–12.
124. Sathaliyawala T, O'Gorman WE, Greter M, et al. Mammalian target of rapamycin controls dendritic cell development downstream of Flt3 ligand signaling. *Immunity*. 2010;33(4):597–606.
125. Waskow C, Liu K, Darrasse-Jèze G, et al. The receptor tyrosine kinase Flt3 is required for dendritic cell development in peripheral lymphoid tissues. *Nat. Immunol.* 2008;9(6):676–83.
126. Maraskovsky E, Brasel K, Teepe M, et al. Dramatic increase in the numbers of functionally mature dendritic cells in Flt3 ligand-treated mice: multiple dendritic cell subpopulations identified. *J. Exp. Med.* 1996;184(5):1953–62.
127. Manfra DJ, Chen S-CC, Jensen KK, et al. Conditional expression of murine Flt3 ligand leads to expansion of multiple dendritic cell subsets in peripheral blood and tissues of transgenic mice. *J. Immunol.* 2003;170(6):2843–52.
128. Onai N, Obata-Onai A, Tussiwand R, Lanzavecchia A, Manz MG. Activation of the Flt3 signal transduction cascade rescues and enhances type I interferon-producing and dendritic cell development. *J. Exp. Med.* 2006;203(1):227–38.
129. Tussiwand R, Onai N, Mazzucchelli L, Manz MG. Inhibition of natural type I IFN-producing and dendritic cell development by a

small molecule receptor tyrosine kinase inhibitor with Flt3 affinity. *J. Immunol.* 2005;175(6):3674–80.
130. D'Amico A, Wu L. The early progenitors of mouse dendritic cells and plasmacytoid predendritic cells are within the bone marrow hemopoietic precursors expressing Flt3. *J. Exp. Med.* 2003;198(2):293–303.
131. Helft J, Böttcher J, Chakravarty P, et al. GM-CSF Mouse Bone Marrow Cultures Comprise a Heterogeneous Population of CD11c(+)MHCII(+) Macrophages and Dendritic Cells. *Immunity*. 2015;42(6):1197–211.
132. Greter M, Helft J, Chow A, et al. GM-CSF controls nonlymphoid tissue dendritic cell homeostasis but is dispensable for the differentiation of inflammatory dendritic cells. *Immunity*. 2012;36(6):1031–46.
133. Bogunovic M, Ginhoux F, Helft J, et al. Origin of the lamina propria dendritic cell network. *Immunity*. 2009;31(3):513–25.
134. Mayer CT, Ghorbani P, Nandan A, et al. Selective and efficient generation of functional Batf3-dependent CD103+ dendritic cells from mouse bone marrow. *Blood*. 2014;124(20):3081–91.
135. Edelson BT, Bradstreet TR, KC W, et al. Batf3-dependent CD11b(low/-) peripheral dendritic cells are GM-CSF-independent and are not required for Th cell priming after subcutaneous immunization. *PLoS ONE*. 2011;6(10):e25660.
136. MacDonald KP, Rowe V, Bofinger HM, et al. The colony-stimulating factor 1 receptor is expressed on dendritic cells during differentiation and regulates their expansion. *J. Immunol.* 2005;175(3):1399–405.
137. Satpathy AT, Briseño CG, Cai X, et al. Runx1 and Cbfβ regulate the development of Flt3+ dendritic cell progenitors and restrict myeloproliferative disorder. *Blood*. 2014;123(19):2968–77.
138. Wu L, Nichogiannopoulou A, Shortman K, Georgopoulos K. Cell-autonomous defects in dendritic cell populations of Ikaros mutant mice point to a developmental relationship with the lymphoid lineage. *Immunity*. 1997;7(4):483–92.
139. Allman D, Dalod M, Asselin-Paturel C, et al. Ikaros is required for plasmacytoid dendritic cell differentiation. *Blood*. 2006;108(13):4025–34.
140. Movassagh M, Laderach D, Galy A. Proteins of the Ikaros family control dendritic cell maturation required to induce optimal Th1 T cell differentiation. *Int. Immunol.* 2004;16(6):867–75.
141. Anderson KL, Perkin H, Surh CD, et al. Transcription factor PU.1 is necessary for development of thymic and myeloid progenitor-derived dendritic cells. *Journal of immunology (Baltimore, Md. : 1950)*. 2000;164(4):1855–61.
142. Guerriero A, Langmuir PB, Spain LM, Scott EW. PU.1 is required for myeloid-derived but not lymphoid-derived dendritic cells. *Blood*. 2000;95(3):879–85.
143. Carotta S, Dakic A, D'Amico A, et al. The transcription factor PU.1 controls dendritic cell development and Flt3 cytokine receptor expression in a dose-dependent manner. *Immunity*. 2010;32(5):628–41.
144. Ippolito GC, Dekker JD, Wang Y-HH, et al. Dendritic cell fate is determined by BCL11A. *Proc. Natl. Acad. Sci. U.S.A.* 2014;111(11):E998–1006.
145. Wu X, Satpathy AT, Kc W, et al. Bcl11a controls Flt3 expression in early hematopoietic progenitors and is required for pDC development in vivo. *PLoS ONE*. 2013;8(5):e64800.
146. Rathinam C, Geffers R, Yücel R, et al. The transcriptional repressor Gfi1 controls STAT3-dependent dendritic cell development and function. *Immunity*. 2005;22(6):717–28.
147. Laouar Y, Welte T, Fu X-YY, Flavell RA. STAT3 is required for Flt3L-dependent dendritic cell differentiation. *Immunity*. 2003;19(6):903–12.
148. Cisse B, Caton ML, Lehner M, et al. Transcription factor E2-2 is an essential and specific regulator of plasmacytoid dendritic cell development. *Cell*. 2008;135(1):37–48.
149. Ghosh HS, Cisse B, Bunin A, Lewis KL, Reizis B. Continuous expression of the transcription factor e2-2 maintains the cell fate of mature plasmacytoid dendritic cells. *Immunity*. 2010;33(6):905–16.
150. Seillet C, Belz GT. Terminal differentiation of dendritic cells. *Adv. Immunol.* 2013;120:185–210.
151. Sasaki I, Hoshino K, Sugiyama T, et al. Spi-B is critical for plasmacytoid dendritic cell function and development. *Blood*. 2012;120(24):4733–43.
152. Schotte R, Nagasawa M, Weijer K, Spits H, Blom B. The ETS transcription factor Spi-B is required for human plasmacytoid dendritic cell development. *J. Exp. Med.* 2004;200(11):1503–9.
153. Karrich JJ, Balzarolo M, Schmidlin H, et al. The transcription factor Spi-B regulates human plasmacytoid dendritic cell survival through direct induction of the antiapoptotic gene BCL2-A1. *Blood*. 2012;119(22):5191–200.
154. Tsujimura H, Tamura T, Ozato K. Cutting edge: IFN consensus sequence binding protein/IFN regulatory factor 8 drives the development of type I IFN-producing plasmacytoid dendritic cells. *Journal of immunology (Baltimore, Md.: 1950)*. 2003;170(3):1131–5.
155. Schiavoni G, Mattei F, Sestili P, et al. ICSBP is essential for the development of mouse type I interferon-producing cells and for the generation and activation of CD8alpha(+)

dendritic cells. *J. Exp. Med.* 2002;196(11):1415–25.
156. Tamura T, Tailor P, Yamaoka K, et al. IFN regulatory factor-4 and -8 govern dendritic cell subset development and their functional diversity. *J. Immunol.* 2005;174(5):2573–81.
157. Bornstein C, Winter D, Barnett-Itzhaki Z, et al. A negative feedback loop of transcription factors specifies alternative dendritic cell chromatin States. *Mol. Cell*. 2014;56(6):749–62.
158. Sichien D, Scott CL, Martens L, et al. IRF8 Transcription Factor Controls Survival and Function of Terminally Differentiated Conventional and Plasmacytoid Dendritic Cells, Respectively. *Immunity*. 2016;45(3):626–640.
159. Satpathy AT, KC W, Albring JCC, et al. Zbtb46 expression distinguishes classical dendritic cells and their committed progenitors from other immune lineages. *J. Exp. Med.* 2012;209(6):1135–52.
160. Meredith MM, Liu K, Darrasse-Jeze G, et al. Expression of the zinc finger transcription factor zDC (Zbtb46, Btbd4) defines the classical dendritic cell lineage. *J. Exp. Med.* 2012;209(6):1153–65.
161. Wu X, Briseño CG, Durai V, et al. Mafb lineage tracing to distinguish macrophages from other immune lineages reveals dual identity of Langerhans cells. *J. Exp. Med.* 2016;213(12):2553–2565.
162. Meredith MM, Liu K, Kamphorst AO, et al. Zinc finger transcription factor zDC is a negative regulator required to prevent activation of classical dendritic cells in the steady state. *J. Exp. Med.* 2012;209(9):1583–93.
163. Loschko J, Rieke GJ, Schreiber HA, et al. Inducible targeting of cDCs and their subsets in vivo. *J. Immunol. Methods*. 2016;434:32–8.
164. Hacker C, Kirsch RD, Ju X-SS, et al. Transcriptional profiling identifies Id2 function in dendritic cell development. *Nat. Immunol.* 2003;4(4):380–6.
165. Kusunoki T, Sugai M, Katakai T, et al. TH2 dominance and defective development of a CD8+ dendritic cell subset in Id2-deficient mice. *J. Allergy Clin. Immunol.* 2003;111(1):136–42.
166. Jackson JT, Hu Y, Liu R, et al. Id2 expression delineates differential checkpoints in the genetic program of CD8α+ and CD103+ dendritic cell lineages. *EMBO J.* 2011;30(13):2690–704.
167. Hildner K, Edelson BT, Purtha WE, et al. Batf3 deficiency reveals a critical role for CD8alpha+ dendritic cells in cytotoxic T cell immunity. *Science*. 2008;322(5904):1097–100.
168. Bajaña S, Turner S, Paul J, Ainsua-Enrich E, Kovats S. IRF4 and IRF8 Act in CD11c+ Cells To Regulate Terminal Differentiation of Lung Tissue Dendritic Cells. *J. Immunol.* 2016;196(4):1666–77.
169. Kashiwada M, Pham N-LL, Pewe LL, Harty JT, Rothman PB. NFIL3/E4BP4 is a key transcription factor for CD8α+ dendritic cell development. *Blood*. 2011;117(23):6193–7.
170. Jaiswal H, Kaushik M, Sougrat R, et al. Batf3 and Id2 have a synergistic effect on Irf8-directed classical CD8α+ dendritic cell development. *J. Immunol.* 2013;191(12):5993–6001.
171. Seillet C, Jackson JT, Markey KA, et al. CD8α+ DCs can be induced in the absence of transcription factors Id2, Nfil3, and Batf3. *Blood*. 2013;121(9):1574–83.
172. Suzuki S, Honma K, Matsuyama T, et al. Critical roles of interferon regulatory factor 4 in CD11bhighCD8alpha- dendritic cell development. *Proc. Natl. Acad. Sci. U.S.A.* 2004;101(24):8981–6.
173. Persson EK, Uronen-Hansson H, Semmrich M, et al. IRF4 transcription-factor-dependent CD103(+)CD11b(+) dendritic cells drive mucosal T helper 17 cell differentiation. *Immunity*. 2013;38(5):958–69.
174. Bajaña S, Roach K, Turner S, Paul J, Kovats S. IRF4 promotes cutaneous dendritic cell migration to lymph nodes during homeostasis and inflammation. *J. Immunol.* 2012;189(7):3368–77.
175. Vander Lugt B, Khan AA, Hackney JA, et al. Transcriptional programming of dendritic cells for enhanced MHC class II antigen presentation. *Nat. Immunol.* 2014;15(2):161–7.
176. Williams JW, Tjota MY, Clay BS, et al. Transcription factor IRF4 drives dendritic cells to promote Th2 differentiation. *Nat Commun*. 2013;4:2990.
177. Lewis KL, Caton ML, Bogunovic M, et al. Notch2 receptor signaling controls functional differentiation of dendritic cells in the spleen and intestine. *Immunity*. 2011;35(5):780–91.
178. Satpathy AT, Briseño CG, Lee JS, et al. Notch2-dependent classical dendritic cells orchestrate intestinal immunity to attaching-and-effacing bacterial pathogens. *Nat. Immunol.* 2013;14(9):937–48.
179. Tussiwand R, Everts B, Grajales-Reyes GE, et al. Klf4 expression in conventional dendritic cells is required for T helper 2 cell responses. *Immunity*. 2015;42(5):916–28.
180. Ichikawa E, Hida S, Omatsu Y, et al. Defective development of splenic and epidermal CD4+ dendritic cells in mice deficient for IFN regulatory factor-2. *Proc. Natl. Acad. Sci. U.S.A.* 2004;101(11):3909–14.
181. Wu L, D'Amico A, Winkel KD, et al. RelB is essential for the development of myeloid-related CD8alpha- dendritic cells but not of lymphoid-related CD8alpha+ dendritic cells. *Immunity*. 1998;9(6):839–47.
182. Merien F. A Journey with Elie Metchnikoff: From Innate Cell Mechanisms in

Infectious Diseases to Quantum Biology. *Front Public Health*. 2016;4:125.
183. METSCHNIKOFF E. Memoirs: Researches on the Intracellular Digestion of Invertebrates. *Journal of Cell Science*. 1884;2(93):89–111.
184. Van Furth R, Cohn ZA, Hirsch JG, et al. The mononuclear phagocyte system: a new classification of macrophages, monocytes, and their precursor cells. *Bulletin of the World Health Organization*. 1972;46(6):845–52.
185. Van Furth R, Cohn ZA. The origin and kinetics of mononuclear phagocytes. *The Journal of experimental medicine*. 1968;128(3):415–35.
186. Geissmann F, Mass E. A stratified myeloid system, the challenge of understanding macrophage diversity. *Semin. Immunol.* 2015;27(6):353–6.
187. Davies LC, Jenkins SJ, Allen JE, Taylor PR. Tissue-resident macrophages. *Nat. Immunol.* 2013;14(10):986–95.
188. Lavin Y, Merad M. Macrophages: gatekeepers of tissue integrity. *Cancer Immunol Res*. 2013;1(4):201–9.
189. Lavin Y, Merad M. Macrophages: gatekeepers of tissue integrity. *Cancer immunology research*. 2013;1(4):201–9.
190. Taylor PR, Martinez-Pomares L, Stacey M, et al. Macrophage receptors and immune recognition. *Annu. Rev. Immunol.* 2005;23:901–44.
191. Aggarwal NR, King LS, D'Alessio FR. Diverse macrophage populations mediate acute lung inflammation and resolution. *Am. J. Physiol. Lung Cell Mol. Physiol.* 2014;306(8):L709–25.
192. Arnold L, Henry A, Poron F, et al. Inflammatory monocytes recruited after skeletal muscle injury switch into antiinflammatory macrophages to support myogenesis. *J. Exp. Med.* 2007;204(5):1057–69.
193. Saclier M, Yacoub-Youssef H, Mackey AL, et al. Differentially activated macrophages orchestrate myogenic precursor cell fate during human skeletal muscle regeneration. *Stem Cells*. 2013;31(2):384–96.
194. Nelson PJ, Rees AJ, Griffin MD, et al. The renal mononuclear phagocytic system. *J. Am. Soc. Nephrol.* 2012;23(2):194–203.
195. Shechter R, Schwartz M. Harnessing monocyte-derived macrophages to control central nervous system pathologies: no longer "if" but "how". *J. Pathol.* 2013;229(2):332–46.
196. Kigerl KA, Gensel JC, Ankeny DP, et al. Identification of two distinct macrophage subsets with divergent effects causing either neurotoxicity or regeneration in the injured mouse spinal cord. *J. Neurosci.* 2009;29(43):13435–44.
197. Martin CJ, Peters KN, Behar SM. Macrophages clean up: efferocytosis and microbial control. *Curr. Opin. Microbiol.* 2014;17:17–23.
198. Bratton DL, Henson PM. Neutrophil clearance: when the party is over, clean-up begins. *Trends Immunol.* 2011;32(8):350–7.
199. Lopez-Rodriguez E, Gay-Jordi G, Mucci A, Lachmann N, Serrano-Mollar A. Lung surfactant metabolism: early in life, early in disease and target in cell therapy. *Cell Tissue Res.* 2017;367(3):721–735.
200. Remmerie A, Scott CL. Macrophages and lipid metabolism. *Cell. Immunol.* 2018;
201. Theurl M, Theurl I, Hochegger K, et al. Kupffer cells modulate iron homeostasis in mice via regulation of hepcidin expression. *J. Mol. Med.* 2008;86(7):825–35.
202. Odegaard JI, Ricardo-Gonzalez RR, Red Eagle A, et al. Alternative M2 activation of Kupffer cells by PPARdelta ameliorates obesity-induced insulin resistance. *Cell Metab.* 2008;7(6):496–507.
203. Haldar M, Kohyama M, So AY, et al. Heme-mediated SPI-C induction promotes monocyte differentiation into iron-recycling macrophages. *Cell*. 2014;156(6):1223–1234.
204. Kovtunovych G, Eckhaus MA, Ghosh MC, Ollivierre-Wilson H, Rouault TA. Dysfunction of the heme recycling system in heme oxygenase 1-deficient mice: effects on macrophage viability and tissue iron distribution. *Blood*. 2010;116(26):6054–62.
205. Cummings RJ, Barbet G, Bongers G, et al. Different tissue phagocytes sample apoptotic cells to direct distinct homeostasis programs. *Nature*. 2016;539(7630):565–569.
206. Grainger JR, Wohlfert EA, Fuss IJ, et al. Inflammatory monocytes regulate pathologic responses to commensals during acute gastrointestinal infection. *Nat. Med.* 2013;19(6):713–21.
207. De Back DZ, Kostova EB, van Kraaij M, van den Berg TK, van Bruggen R. Of macrophages and red blood cells; a complex love story. *Front Physiol*. 2014;5:9.
208. Paolicelli RC, Bolasco G, Pagani F, et al. Synaptic pruning by microglia is necessary for normal brain development. *Science*. 2011;333(6048):1456–8.
209. Van Furth R, Cohn ZA. The origin and kinetics of mononuclear phagocytes. *J. Exp. Med.* 1968;128(3):415–35.
210. Van Furth R, Diesselhoff-Den Dulk MM. The kinetics of promonocytes and monocytes in the bone marrow. *J. Exp. Med.* 1970;132(4):813–28.
211. Yona S, Kim K-WW, Wolf Y, et al. Fate mapping reveals origins and dynamics of monocytes and tissue macrophages under homeostasis. *Immunity*. 2013;38(1):79–91.

212. Ginhoux F, Guilliams M. Tissue-Resident Macrophage Ontogeny and Homeostasis. *Immunity*. 2016;44(3):439–449.
213. McGrath KE, Frame JM, Palis J. Early hematopoiesis and macrophage development. *Semin. Immunol.* 2015;27(6):379–87.
214. Lavin Y, Mortha A, Rahman A, Merad M. Regulation of macrophage development and function in peripheral tissues. *Nat. Rev. Immunol.* 2015;15(12):731–44.
215. Scott CL, Henri S, Guilliams M. Mononuclear phagocytes of the intestine, the skin, and the lung. *Immunol. Rev.* 2014;262(1):9–24.
216. Hoeffel G, Ginhoux F. Ontogeny of Tissue-Resident Macrophages. *Front Immunol*. 2015;6:486.
217. Schulz C, Gomez Perdiguero E, Chorro L, et al. A lineage of myeloid cells independent of Myb and hematopoietic stem cells. *Science*. 2012;336(6077):86–90.
218. Ginhoux F, Greter M, Leboeuf M, et al. Fate mapping analysis reveals that adult microglia derive from primitive macrophages. *Science*. 2010;330(6005):841–5.
219. Hashimoto D, Chow A, Noizat C, et al. Tissue-resident macrophages self-maintain locally throughout adult life with minimal contribution from circulating monocytes. *Immunity*. 2013;38(4):792–804.
220. Guilliams M, De Kleer I, Henri S, et al. Alveolar macrophages develop from fetal monocytes that differentiate into long-lived cells in the first week of life via GM-CSF. *J. Exp. Med.* 2013;210(10):1977–92.
221. Kawamura S, Onai N, Miya F, et al. Identification of a Human Clonogenic Progenitor with Strict Monocyte Differentiation Potential: A Counterpart of Mouse cMoPs. *Immunity*. 2017;46(5):835–848.e4.
222. Hettinger J, Richards DM, Hansson J, et al. Origin of monocytes and macrophages in a committed progenitor. *Nat. Immunol.* 2013;14(8):821–30.
223. Molawi K, Wolf Y, Kandalla PK, et al. Progressive replacement of embryo-derived cardiac macrophages with age. *J. Exp. Med.* 2014;211(11):2151–8.
224. Epelman S, Lavine KJ, Beaudin AE, et al. Embryonic and adult-derived resident cardiac macrophages are maintained through distinct mechanisms at steady state and during inflammation. *Immunity*. 2014;40(1):91–104.
225. Tamoutounour S, Guilliams M, Montanana Sanchis F, et al. Origins and functional specialization of macrophages and of conventional and monocyte-derived dendritic cells in mouse skin. *Immunity*. 2013;39(5):925–38.
226. Bain CC, Bravo-Blas A, Scott CL, et al. Constant replenishment from circulating monocytes maintains the macrophage pool in the intestine of adult mice. *Nat. Immunol.* 2014;15(10):929–937.
227. Scott CL, Zheng F, De Baetselier P, et al. Bone marrow-derived monocytes give rise to self-renewing and fully differentiated Kupffer cells. *Nat Commun*. 2016;7:10321.
228. Calderon B, Carrero JA, Ferris ST, et al. The pancreas anatomy conditions the origin and properties of resident macrophages. *J. Exp. Med.* 2015;212(10):1497–512.
229. Wiktor-Jedrzejczak W, Bartocci A, Ferrante AW, et al. Total absence of colony-stimulating factor 1 in the macrophage-deficient osteopetrotic (op/op) mouse. *Proceedings of the National Academy of Sciences of the United States of America*. 1990;87(12):4828–32.
230. Felix R, Cecchini MG, Hofstetter W, et al. Impairment of macrophage colony-stimulating factor production and lack of resident bone marrow macrophages in the osteopetrotic op/op mouse. *J. Bone Miner. Res.* 1990;5(7):781–9.
231. Cecchini MG, Dominguez MG, Mocci S, et al. Role of colony stimulating factor-1 in the establishment and regulation of tissue macrophages during postnatal development of the mouse. *Development*. 1994;120(6):1357–72.
232. Clinton SK, Underwood R, Hayes L, et al. Macrophage colony-stimulating factor gene expression in vascular cells and in experimental and human atherosclerosis. *Am. J. Pathol.* 1992;140(2):301–16.
233. Elford PR, Felix R, Cecchini M, Trechsel U, Fleisch H. Murine osteoblastlike cells and the osteogenic cell MC3T3-E1 release a macrophage colony-stimulating activity in culture. *Calcif. Tissue Int.* 1987;41(3):151–6.
234. Dai X-MM, Ryan GR, Hapel AJ, et al. Targeted disruption of the mouse colony-stimulating factor 1 receptor gene results in osteopetrosis, mononuclear phagocyte deficiency, increased primitive progenitor cell frequencies, and reproductive defects. *Blood*. 2002;99(1):111–20.
235. Hume DA, MacDonald KP. Therapeutic applications of macrophage colony-stimulating factor-1 (CSF-1) and antagonists of CSF-1 receptor (CSF-1R) signaling. *Blood*. 2012;119(8):1810–20.
236. Foucher ED, Blanchard S, Preisser L, et al. IL-34 induces the differentiation of human monocytes into immunosuppressive macrophages. antagonistic effects of GM-CSF and IFNγ. *PLoS ONE*. 2013;8(2):e56045.
237. Wei S, Nandi S, Chitu V, et al. Functional overlap but differential expression of CSF-1 and IL-34 in their CSF-1 receptor-mediated regulation

of myeloid cells. *J. Leukoc. Biol.* 2010;88(3):495–505.
238. Wang Y, Szretter KJ, Vermi W, et al. IL-34 is a tissue-restricted ligand of CSF1R required for the development of Langerhans cells and microglia. *Nat. Immunol.* 2012;13(8):753–60.
239. Wang Y, Bugatti M, Ulland TK, et al. Nonredundant roles of keratinocyte-derived IL-34 and neutrophil-derived CSF1 in Langerhans cell renewal in the steady state and during inflammation. *Eur. J. Immunol.* 2016;46(3):552–9.
240. Fleetwood AJ, Lawrence T, Hamilton JA, Cook AD. Granulocyte-macrophage colony-stimulating factor (CSF) and macrophage CSF-dependent macrophage phenotypes display differences in cytokine profiles and transcription factor activities: implications for CSF blockade in inflammation. *Journal of immunology (Baltimore, Md. : 1950)*. 2007;178(8):5245–52.
241. Williamson DJ, Begley CG, Vadas MA, Metcalf D. The detection and initial characterization of colony-stimulating factors in synovial fluid. *Clin. Exp. Immunol.* 1988;72(1):67–73.
242. Lukens JR, Barr MJ, Chaplin DD, Chi H, Kanneganti T-DD. Inflammasome-derived IL-1β regulates the production of GM-CSF by CD4(+) T cells and γδ T cells. *J. Immunol.* 2012;188(7):3107–15.
243. Gautier EL, Shay T, Miller J, et al. Gene-expression profiles and transcriptional regulatory pathways that underlie the identity and diversity of mouse tissue macrophages. *Nat. Immunol.* 2012;13(11):1118–28.
244. Heinz S, Benner C, Spann N, et al. Simple combinations of lineage-determining transcription factors prime cis-regulatory elements required for macrophage and B cell identities. *Mol. Cell*. 2010;38(4):576–89.
245. Guilliams M, Scott CL. Does niche competition determine the origin of tissue-resident macrophages? *Nat. Rev. Immunol.* 2017;17(7):451–460.
246. Okabe Y, Medzhitov R. Tissue-specific signals control reversible program of localization and functional polarization of macrophages. *Cell*. 2014;157(4):832–44.
247. Schneider C, Nobs SP, Kurrer M, et al. Induction of the nuclear receptor PPAR-γ by the cytokine GM-CSF is critical for the differentiation of fetal monocytes into alveolar macrophages. *Nat. Immunol.* 2014;15(11):1026–37.
248. Cain DW, O'Koren EG, Kan MJ, et al. Identification of a tissue-specific, C/EBPβ-dependent pathway of differentiation for murine peritoneal macrophages. *J. Immunol.* 2013;191(9):4665–75.
249. Lavin Y, Winter D, Blecher-Gonen R, et al. Tissue-resident macrophage enhancer landscapes are shaped by the local microenvironment. *Cell*. 2014;159(6):1312–26.
250. Gosselin D, Link VM, Romanoski CE, et al. Environment drives selection and function of enhancers controlling tissue-specific macrophage identities. *Cell*. 2014;159(6):1327–40.
251. Kumkate S, Jenkins GR, Paveley RA, Hogg KG, Mountford AP. CD207+ Langerhans cells constitute a minor population of skin-derived antigen-presenting cells in the draining lymph node following exposure to Schistosoma mansoni. *Int. J. Parasitol.* 2007;37(2):209–20.
252. Hoeffel G, Wang Y, Greter M, et al. Adult Langerhans cells derive predominantly from embryonic fetal liver monocytes with a minor contribution of yolk sac-derived macrophages. *J. Exp. Med.* 2012;209(6):1167–81.
253. Merad M, Manz MG, Karsunky H, et al. Langerhans cells renew in the skin throughout life under steady-state conditions. *Nat. Immunol.* 2002;3(12):1135–41.
254. Greter M, Lelios I, Pelczar P, et al. Stroma-derived interleukin-34 controls the development and maintenance of langerhans cells and the maintenance of microglia. *Immunity*. 2012;37(6):1050–1060.
255. Fainaru O, Woolf E, Lotem J, et al. Runx3 regulates mouse TGF-beta-mediated dendritic cell function and its absence results in airway inflammation. *EMBO J.* 2004;23(4):969–79.
256. Borkowski TA, Letterio JJ, Farr AG, Udey MC. A role for endogenous transforming growth factor beta 1 in Langerhans cell biology: the skin of transforming growth factor beta 1 null mice is devoid of epidermal Langerhans cells. *J. Exp. Med.* 1996;184(6):2417–22.
257. Kaplan DH, Li MO, Jenison MC, et al. Autocrine/paracrine TGFbeta1 is required for the development of epidermal Langerhans cells. *J. Exp. Med.* 2007;204(11):2545–52.
258. Plantinga M, Guilliams M, Vanheerswynghels M, et al. Conventional and monocyte-derived CD11b(+) dendritic cells initiate and maintain T helper 2 cell-mediated immunity to house dust mite allergen. *Immunity*. 2013;38(2):322–35.
259. Serbina NV, Salazar-Mather TP, Biron CA, Kuziel WA, Pamer EG. TNF/iNOS-producing dendritic cells mediate innate immune defense against bacterial infection. *Immunity*. 2003;19(1):59–70.
260. León B, López-Bravo M, Ardavín C. Monocyte-derived dendritic cells formed at the infection site control the induction of protective T helper 1 responses against Leishmania. *Immunity*. 2007;26(4):519–31.
261. León B, López-Bravo M, Ardavín C. Monocyte-derived dendritic cells. *Semin. Immunol.* 2005;17(4):313–8.

262. Randolph GJ, Inaba K, Robbiani DF, Steinman RM, Muller WA. Differentiation of phagocytic monocytes into lymph node dendritic cells in vivo. *Immunity*. 1999;11(6):753–61.
263. Sallusto F, Lanzavecchia A. Efficient presentation of soluble antigen by cultured human dendritic cells is maintained by granulocyte/macrophage colony-stimulating factor plus interleukin 4 and downregulated by tumor necrosis factor alpha. *J. Exp. Med.* 1994;179(4):1109–18.
264. Anguille S, Smits EL, Lion E, van Tendeloo VF, Berneman ZN. Clinical use of dendritic cells for cancer therapy. *Lancet Oncol.* 2014;15(7):e257–67.
265. Van Vlierberghe P, Ferrando A. The molecular basis of T cell acute lymphoblastic leukemia. *J. Clin. Invest.* 2012;122(10):3398–406.
266. Durinck K, Goossens S, Peirs S, et al. Novel biological insights in T-cell acute lymphoblastic leukemia. *Exp. Hematol.* 2015;43(8):625–39.
267. Chiaretti S, Gianfelici V, O'Brien SM, Mullighan CG. Advances in the Genetics and Therapy of Acute Lymphoblastic Leukemia. *Am Soc Clin Oncol Educ Book*. 2016;35:e314–22.
268. Meijerink JPP. Genetic rearrangements in relation to immunophenotype and outcome in T-cell acute lymphoblastic leukaemia. *Best Pract Res Clin Haematol*. 2010;23(3):307–18.
269. Coustan-Smith E, Mullighan CG, Onciu M, et al. Early T-cell precursor leukaemia: a subtype of very high-risk acute lymphoblastic leukaemia. *The Lancet. Oncology*. 2009;10(2):147–56.
270. Goossens S, Radaelli E, Blanchet O, et al. ZEB2 drives immature T-cell lymphoblastic leukaemia development via enhanced tumour-initiating potential and IL-7 receptor signalling. *Nat Commun*. 2015;6:5794.
271. Goossens S, Peirs S, Van Loocke W, et al. Oncogenic ZEB2 activation drives sensitivity toward KDM1A inhibition in T-cell acute lymphoblastic leukemia. *Blood*. 2017;129(8):981–990.
272. Sun W, Yang S, Shen W, et al. Identification of DeltaEF1 as a novel target that is negatively regulated by LMO2 in T-cell leukemia. *Eur. J. Haematol.* 2010;85(6):508–19.
273. Pike-Overzet K, de Ridder D, Weerkamp F, et al. Ectopic retroviral expression of LMO2, but not IL2Rgamma, blocks human T-cell development from CD34+ cells: implications for leukemogenesis in gene therapy. *Leukemia*. 2007;21(4):754–63.
274. Larson RC, Fisch P, Larson TA, et al. T cell tumours of disparate phenotype in mice transgenic for Rbtn-2. *Oncogene*. 1995;9(12):3675–81.
275. Hidaka T, Nakahata S, Hatakeyama K, et al. Down-regulation of TCF8 is involved in the leukemogenesis of adult T-cell leukemia/lymphoma. *Blood*. 2008;112(2):383–93.
276. Takatsuki K, Yamaguchi K, Kawano F, et al. Clinical diversity in adult T-cell leukemia-lymphoma. *Cancer research*. 1985;45(9 Suppl):4644s–4645s.
277. Matsuoka M. Human T-cell leukemia virus type I and adult T-cell leukemia. *Oncogene*. 2003;22(33):5131–40.
278. Kamihira S, Sohda H, Atogami S, et al. Phenotypic diversity and prognosis of adult T-cell leukemia. *Leukemia research*. 1992;16(5):435–41.
279. Derynck R, Akhurst RJ, Balmain A. TGF-beta signaling in tumor suppression and cancer progression. *Nat. Genet.* 2001;29(2):117–29.
280. Jahn SC, Law ME, Corsino PE, Law BK. TGF-beta antiproliferative effects in tumor suppression. *Front Biosci (Schol Ed)*. 2012;4:749–66.
281. Nakahata S, Yamazaki S, Nakauchi H, Morishita K. Downregulation of ZEB1 and overexpression of Smad7 contribute to resistance to TGF-beta1-mediated growth suppression in adult T-cell leukemia/lymphoma. *Oncogene*. 2010;29(29):4157–69.
282. Swerdlow SH, Campo E, Pileri SA, et al. The 2016 revision of the World Health Organization classification of lymphoid neoplasms. *Blood*. 2016;127(20):2375–90.
283. Olsen E, Vonderheid E, Pimpinelli N, et al. Revisions to the staging and classification of mycosis fungoides and Sezary syndrome: a proposal of the International Society for Cutaneous Lymphomas (ISCL) and the cutaneous lymphoma task force of the European Organization of Research and Treatment of Cancer (EORTC). *Blood*. 2007;110(6):1713–22.
284. Kiel MJ, Sahasrabuddhe AA, Rolland DC, et al. Genomic analyses reveal recurrent mutations in epigenetic modifiers and the JAK-STAT pathway in Sézary syndrome. *Nat Commun*. 2015;6:8470.
285. Prasad A, Rabionet R, Espinet B, et al. Identification of Gene Mutations and Fusion Genes in Patients with Sézary Syndrome. *J. Invest. Dermatol.* 2016;136(7):1490–1499.
286. Choi J, Goh G, Walradt T, et al. Genomic landscape of cutaneous T cell lymphoma. *Nat. Genet.* 2015;47(9):1011–9.
287. McGirt LY, Jia P, Baerenwald DA, et al. Whole-genome sequencing reveals oncogenic mutations in mycosis fungoides. *Blood*. 2015;126(4):508–19.
288. Wang L, Ni X, Covington KR, et al. Genomic profiling of Sézary syndrome identifies alterations of key T cell signaling and

differentiation genes. *Nat. Genet.* 2015;47(12):1426–34.
289. Mishra A, La Perle K, Kwiatkowski S, et al. Mechanism, Consequences, and Therapeutic Targeting of Abnormal IL15 Signaling in Cutaneous T-cell Lymphoma. *Cancer discovery*. 2016;6(9):986–1005.
290. Jares P, Colomer D, Campo E. Molecular pathogenesis of mantle cell lymphoma. *J. Clin. Invest.* 2012;122(10):3416–23.
291. Kahl BS, Dreyling M, Gordon LI, Quintanilla-Martinez L, Sotomayor EM. Recent advances and future directions in mantle cell lymphoma research: report of the 2016 mantle cell lymphoma consortium workshop. *Leukemia & lymphoma*. 2017;1–12.
292. Sánchez-Tilló E, Fanlo L, Siles L, et al. The EMT activator ZEB1 promotes tumor growth and determines differential response to chemotherapy in mantle cell lymphoma. *Cell Death Differ.* 2014;21(2):247–57.
293. Coiffier B, Lepage E, Briere J, et al. CHOP chemotherapy plus rituximab compared with CHOP alone in elderly patients with diffuse large-B-cell lymphoma. *N. Engl. J. Med.* 2002;346(4):235–42.
294. Pfreundschuh M, Kuhnt E, Trümper L, et al. CHOP-like chemotherapy with or without rituximab in young patients with good-prognosis diffuse large-B-cell lymphoma: 6-year results of an open-label randomised study of the MabThera International Trial (MInT) Group. *Lancet Oncol.* 2011;12(11):1013–22.
295. Lemma S, Karihtala P, Haapasaari K-MM, et al. Biological roles and prognostic values of the epithelial-mesenchymal transition-mediating transcription factors Twist, ZEB1 and Slug in diffuse large B-cell lymphoma. *Histopathology*. 2013;62(2):326–33.
296. Huang W-TT, Kuo S-HH, Cheng A-LL, Lin C-WW. Inhibition of ZEB1 by miR-200 characterizes Helicobacter pylori-positive gastric diffuse large B-cell lymphoma with a less aggressive behavior. *Modern pathology : an official journal of the United States and Canadian Academy of Pathology, Inc*. 2014;27(8):1116–25.
297. Chen Y-WW, Hu X-TT, Liang AC, et al. High BCL6 expression predicts better prognosis, independent of BCL6 translocation status, translocation partner, or BCL6-deregulating mutations, in gastric lymphoma. *Blood*. 2006;108(7):2373–83.
298. Papadopoulou V, Postigo A, Sánchez-Tilló E, Porter AC, Wagner SD. ZEB1 and CtBP form a repressive complex at a distal promoter element of the BCL6 locus. *Biochem. J.* 2010;427(3):541–50.
299. Matteucci C, Bracci M, Barba G, et al. Different genomic imbalances in low- and high-grade HCV-related lymphomas. *Leukemia*. 2008;22(1):219–22.
300. Zhang J, McCastlain K, Yoshihara H, et al. Deregulation of DUX4 and ERG in acute lymphoblastic leukemia. *Nat. Genet.* 2016;48(12):1481–1489.
301. Woo JS, Alberti MO, Tirado CA. Childhood B-acute lymphoblastic leukemia: a genetic update. *Exp Hematol Oncol*. 2014;3:16.
302. Zhou X, Edmonson MN, Wilkinson MR, et al. Exploring genomic alteration in pediatric cancer using ProteinPaint. *Nat. Genet.* 2016;48(1):4–6.
303. Caudell D, Zhang Z, Chung YJ, Aplan PD. Expression of a CALM-AF10 fusion gene leads to Hoxa cluster overexpression and acute leukemia in transgenic mice. *Cancer Res.* 2007;67(17):8022–31.
304. Dang J, Wei L, de Ridder J, et al. PAX5 is a tumor suppressor in mouse mutagenesis models of acute lymphoblastic leukemia. *Blood*. 2015;125(23):3609–17.
305. Deschler B, Lübbert M. Acute myeloid leukemia: epidemiology and etiology. *Cancer*. 2006;107(9):2099–107.
306. Saultz JN, Garzon R. Acute Myeloid Leukemia: A Concise Review. *J Clin Med*. 2016;5(3):
307. Stavropoulou V, Kaspar S, Brault L, et al. MLL-AF9 Expression in Hematopoietic Stem Cells Drives a Highly Invasive AML Expressing EMT-Related Genes Linked to Poor Outcome. *Cancer Cell*. 2016;30(1):43–58.
308. Torkildsen S, Gorunova L, Beiske K, et al. Novel ZEB2-BCL11B Fusion Gene Identified by RNA-Sequencing in Acute Myeloid Leukemia with t(2;14)(q22;q32). *PLoS ONE*. 2015;10(7):e0132736.
309. Abbas S, Sanders MA, Zeilemaker A, et al. Integrated genome-wide genotyping and gene expression profiling reveals BCL11B as a putative oncogene in acute myeloid leukemia with 14q32 aberrations. *Haematologica*. 2014;99(5):848–57.
310. Gutierrez A, Kentsis A, Sanda T, et al. The BCL11B tumor suppressor is mutated across the major molecular subtypes of T-cell acute lymphoblastic leukemia. *Blood*. 2011;118(15):4169–73.
311. Li H, Mar BG, Zhang H, et al. The EMT regulator ZEB2 is a novel dependency of human and murine acute myeloid leukemia. *Blood*. 2017;129(4):497–508.
312. Meyer SE. From EMT to HSC to AML: ZEB2 is a cell fate switch. *Blood*. 2017;129(4):400–401.
313. Tsherniak A, Vazquez F, Montgomery PG, et al. Defining a Cancer Dependency Map. *Cell*. 2017;170(3):564–576.e16.
314. Chaperot L, Bendriss N, Manches O, et al. Identification of a leukemic counterpart of the

plasmacytoid dendritic cells. *Blood*. 2001;97(10):3210–7.
315. Pilichowska ME, Fleming MD, Pinkus JL, Pinkus GS. CD4+/CD56+ hematodermic neoplasm ("blastic natural killer cell lymphoma"): neoplastic cells express the immature dendritic cell marker BDCA-2 and produce interferon. *Am. J. Clin. Pathol.* 2007;128(3):445–53.
316. Petrella T, Comeau MR, Maynadié M, et al. "Agranular CD4+ CD56+ hematodermic neoplasm" (blastic NK-cell lymphoma) originates from a population of CD56+ precursor cells related to plasmacytoid monocytes. *Am. J. Surg. Pathol.* 2002;26(7):852–62.
317. Arber DA, Orazi A, Hasserjian R, et al. The 2016 revision to the World Health Organization classification of myeloid neoplasms and acute leukemia. *Blood*. 2016;127(20):2391–405.
318. Laribi K, Denizon N, Besançon A, et al. Blastic Plasmacytoid Dendritic Cell Neoplasm: From Origin of the Cell to Targeted Therapies. *Biol. Blood Marrow Transplant.* 2016;22(8):1357–1367.
319. Menezes J, Acquadro F, Wiseman M, et al. Exome sequencing reveals novel and recurrent mutations with clinical impact in blastic plasmacytoid dendritic cell neoplasm. *Leukemia*. 2014;28(4):823–9.
320. Rezk SA, Weiss LM. Epstein-Barr virus-associated lymphoproliferative disorders. *Human pathology*. 2007;38(9):1293–304.
321. Countryman, Miller. Activation of expression of latent Epstein-Barr herpesvirus after gene transfer with a small cloned subfragment of heterogeneous viral DNA. *Proceedings of the National Academy of Sciences*. 1985;82(12):4085–4089.
322. Kraus RJ, Perrigoue JG, Mertz JE. ZEB negatively regulates the lytic-switch BZLF1 gene promoter of Epstein-Barr virus. *Journal of virology*. 2003;77(1):199–207.
323. Yu X, Wang Z, Mertz JE. ZEB1 regulates the latent-lytic switch in infection by Epstein-Barr virus. *PLoS Pathog.* 2007;3(12):e194.

Part 2
Aims and outline

Zeb1 and Zeb2 are two highly homologous transcription factors (TFs) that are mainly known for their role in epithelial-mesenchymal transition (EMT), a multistep process during which epithelial cells lose their adhesive capacities and polarity to turn into mesenchymal migratory cells. EMT is important for embryonic development and wound healing, but the process can also be aberrantly activated by solid tumor cells in order to disseminate from the primary tumor and form metastasis in secondary organs[1]. In recent years it has become more and more evident that Zeb proteins cannot solely be considered as EMT-inducing TFs. Both TFs also fulfill physiological functions during hematopoiesis and in mature hematopoietic cells. As such Zeb2 has been shown to play a role in embryonic hematopoietic stem cell differentiation, natural killer cell maturation and $CD8^+$ T cell terminal differentiation[2–6]. Zeb1 on the other hand is involved in early T cell development[7,8]. However, at the start of this thesis little was known on the role of Zeb1 and Zeb2 in the mononuclear phagocyte system (MPS). Therefore the main objective of my PhD was to investigate the importance of Zeb proteins in the cells of the MPS, namely dendritic cells and macrophages.

Although the exact roles of Zebs in the MPS were unknown, there was some evidence in literature that these TFs could be important in dendritic cells and macrophages. As such Zeb2 was identified through several genome-wide microarray and RNA-sequencing transcriptional analyses as potentially being involved in the development of conventional dendritic cells (cDCs)[9–11]. Therefore, we decided to first investigate the role of Zeb2 in dendritic cells using CRE-mediated conditional loss or ectopic expression mouse models. Our findings on this are discussed in **Chapter 1** of the results section, 'The transcription factor Zeb2 regulates development of conventional and plasmacytoid DCs by repressing Id2'. Having identified a role for Zeb2 in the dendritic cell lineage, we next examined if its homolog Zeb1 would function in a similar way. The results of this research are discussed in **Chapter 3** 'Understanding the role of Zeb1 in dendritic cell homeostasis'. Furthermore, during the course of our research Zeb2 was found to be expressed by pre-macrophages and was thus considered a core macrophage gene[12]. Accordingly, we also went on to investigate the importance for Zeb2 in the macrophage lineage in **Chapter 4** 'Zeb2 is essential for macrophage survival'.

Having shown a physiological role for Zeb1 and Zeb2 in dendritic cells and macrophages, it is not a surprise that genetic events changing the levels of Zeb proteins can have serious consequences and lead to the development of lymphomas and leukemias. As such it was previously shown that both Zeb1 and Zeb2 act as oncogenes in acute myeloid leukemia[13–15]. Additionally, recurrent deleterious mutations in the *Zeb2* gene locus suggest a role for Zeb2 as tumor suppressor in a rare leukemia called blastic plasmacytoid dendritic cell neoplasm (BPDCN), a disease that is believed to originate in plasmacytoid DC precursors[16]. Currently the outcome for BPDCN patients is very poor and therefore we attempted to model the disease in mice, based on the loss of Zeb2 expression, as we believe that a clinically relevant mouse model could aid the development of better targeted therapies. Results regarding this last aim of my thesis are discussed in **Chapter 2** of the results section.

References

1. De Craene B, Berx G. Regulatory networks defining EMT during cancer initiation and progression. *Nat. Rev. Cancer*. 2013;13(2):97–110.
2. Goossens S, Janzen V, Bartunkova S, et al. The EMT regulator Zeb2/Sip1 is essential for murine embryonic hematopoietic stem/progenitor cell differentiation and mobilization. *Blood*. 2011;117(21):5620–30.
3. Omilusik KD, Best JA, Yu B, et al. Transcriptional repressor ZEB2 promotes terminal differentiation of CD8+ effector and memory T cell populations during infection. *J. Exp. Med.* 2015;212(12):2027–39.
4. Van Helden MJ, Goossens S, Daussy C, et al. Terminal NK cell maturation is controlled by concerted actions of T-bet and Zeb2 and is essential for melanoma rejection. *J. Exp. Med.* 2015;212(12):2015–25.
5. Li J, Riedt T, Goossens S, et al. The EMT transcription factor Zeb2 controls adult murine hematopoietic differentiation by regulating cytokine signaling. *Blood*. 2017;129(4):460–472.
6. Dominguez CX, Amezquita RA, Guan T, et al. The transcription factors ZEB2 and T-bet cooperate to program cytotoxic T cell terminal differentiation in response to LCMV viral infection. *J. Exp. Med.* 2015;212(12):2041–56.
7. Higashi Y, Moribe H, Takagi T, et al. Impairment of T cell development in deltaEF1 mutant mice. *J. Exp. Med.* 1997;185(8):1467–79.
8. Arnold CN, Pirie E, Dosenovic P, et al. A forward genetic screen reveals roles for Nfkbid, Zeb1, and Ruvbl2 in humoral immunity. *Proc. Natl. Acad. Sci. U.S.A.* 2012;109(31):12286–93.
9. Miller JC, Brown BD, Shay T, et al. Deciphering the transcriptional network of the dendritic cell lineage. *Nat. Immunol.* 2012;13(9):888–99.
10. Grajales-Reyes GE, Iwata A, Albring J, et al. Batf3 maintains autoactivation of Irf8 for commitment of a CD8α(+) conventional DC clonogenic progenitor. *Nat. Immunol.* 2015;16(7):708–17.
11. Schlitzer A, Sivakamasundari V, Chen J, et al. Identification of cDC1- and cDC2-committed DC progenitors reveals early lineage priming at the common DC progenitor stage in the bone marrow. *Nat. Immunol.* 2015;16(7):718–28.
12. Mass E, Ballesteros I, Farlik M, et al. Specification of tissue-resident macrophages during organogenesis. *Science*. 2016;353(6304):
13. Stavropoulou V, Kaspar S, Brault L, et al. MLL-AF9 Expression in Hematopoietic Stem Cells Drives a Highly Invasive AML Expressing EMT-Related Genes Linked to Poor Outcome. *Cancer Cell*. 2016;30(1):43–58.
14. Torkildsen S, Gorunova L, Beiske K, et al. Novel ZEB2-BCL11B Fusion Gene Identified by RNA-Sequencing in Acute Myeloid Leukemia with t(2;14)(q22;q32). *PLoS ONE*. 2015;10(7):e0132736.
15. Li H, Mar BG, Zhang H, et al. The EMT regulator ZEB2 is a novel dependency of human and murine acute myeloid leukemia. *Blood*. 2017;129(4):497–508.
16. Menezes J, Acquadro F, Wiseman M, et al. Exome sequencing reveals novel and recurrent mutations with clinical impact in blastic plasmacytoid dendritic cell neoplasm. *Leukemia*. 2014;28(4):823–9.

Part 3
Results

Chapter 1

The transcription factor Zeb2 regulates development of conventional and plasmacytoid DCs by repressing Id2

Contributions: Bieke Soen and Charlotte Scott performed all experiments, except for the ChIP experiment shown in Figure 12. Bieke Soen and Charlotte Scott performed all data analyses, except for the bio-informatics analyses shown in Figure 8A-B and Figure 11A-B. Nicolas Skrypek performed and analyzed the ChIP experiment shown in Figure 12. Joachim Taminau, Gillian Blancke and Gert Van Isterdael provided technical assistance. Liesbet Martens, Wouter Saelens and Yvan Saeys performed the bio-informatics analyses shown in Figure 8A-B and Figure 11A-B. Bieke Soen, Charlotte Scott, Bart Lambrecht, Martin Guilliams and Geert Berx contributed to the conceptualization and discussion of the project and its experiments. Bieke Soen and Charlotte Scott performed the writing of this chapter.

Adapted from:

Scott CL, **Soen B** *et al*. The transcription factor Zeb2 regulates development of conventional and plasmacytoid DCs by repressing Id2. Journal of Experimental Medicine, 2016, Vol. 213 No. 6 897–911.

Published May 16, 2016

JEM

Brief Definitive Report

The transcription factor Zeb2 regulates development of conventional and plasmacytoid DCs by repressing Id2

Charlotte L. Scott,[1,4,5*] Bieke Soen,[2,5*] Liesbet Martens,[3,4] Nicolas Skrypek,[2,5] Wouter Saelens,[3,4] Joachim Taminau,[2,5] Gillian Blancke,[2,5] Gert Van Isterdael,[1,4] Danny Huylebroeck,[6,7] Jody Haigh,[9] Yvan Saeys,[3,4] Martin Guilliams,[1,5] Bart N. Lambrecht,[1,4,8**] and Geert Berx[2,5**]

[1]Laboratory of Immunoregulation and Mucosal Immunology, [2]Unit of Molecular and Cellular Oncology, and [3]Data Mining and Modeling for Biomedicine, Inflammation Research Center, Vlaams Instituut voor Biotechnologie, 9052 Ghent, Belgium
[4]Department of Respiratory Medicine and [5]Department of Biomedical Molecular Biology, Ghent University, 9000 Ghent, Belgium
[6]Laboratory of Molecular Biology (Celgen), Department of Development and Regeneration, Katholieke Universiteit Leuven, 3000 Leuven, Belgium
[7]Department of Cell Biology and [8]Department of Pulmonary Medicine, Erasmus University Medical Center, 3015 GE Rotterdam, Netherlands
[9]Mammalian Functional Genetics Laboratory, Division of Blood Cancers, Australian Centre for Blood Diseases, Monash University, Melbourne, Victoria 3800, Australia

*C.L. Scott and B. Soen contributed equally to this paper.

**B.N. Lambrecht and G. Berx contributed equally to this paper.

1.1 Abstract

Plasmacytoid dendritic cells (pDCs) develop from pre-pDCs, whereas two lineages of conventional DCs (cDC1s and cDC2s) develop from lineage-committed pre-cDCs. Several transcription factors (TFs) have been implicated in regulating the development of pDCs (E2-2 and Id2) and cDC1s (Irf8, Id2, and Batf3); however, those required for the early commitment of pre-cDCs toward the cDC2 lineage are unknown. Here, we identify the TF zinc finger E box–binding homeobox 2 (Zeb2) to play a crucial role in regulating DC development. Zeb2 was expressed from the pre-pDC and pre-cDC stage onward and highly expressed in mature pDCs and cDC2s. Mice conditionally lacking Zeb2 in $CD11c^+$ cells had a cell-intrinsic reduction in pDCs and cDC2s, coupled with an increase in cDC1s. Conversely, mice in which $CD11c^+$ cells overexpressed Zeb2 displayed a reduction in cDC1s. This was accompanied by altered expression of Id2, which was up-regulated in cDC2s and pDCs from conditional knockout mice. Zeb2 chromatin immunoprecipitation (ChIP) analysis revealed Id2 to be a direct target of Zeb2. Thus, we conclude that Zeb2 regulates commitment to both the cDC2 and pDC lineages through repression of Id2.

1.2 Introduction

DCs reside in almost all tissues in the body, where they function as immune sentinels. DCs can be subdivided into two main groups: pDCs, which are specialized in the production of type I interferons to elicit an antiviral immune response[1,2], and cDCs which are professional antigen-presenting cells. cDCs form the crucial link between the innate and adaptive arms of the immune system by sampling local antigens and subsequently migrating to their draining LNs, where they initiate appropriate responses from T cells[3]. cDCs exist in two main subtypes, which were recently termed cDC1s and cDC2s[4]. cDC1s, expressing Xcr1 (X-C motif chemokine receptor 1) and usually CD103 and/or CD8α, are functionally specialized in cross-presentation of antigens to $CD8^+$ T cells[3,5,6,7,8]. cDC2s express CD172a (signal regulatory protein α or Sirpα) and usually CD11b or CD4 and are functionally specialized in the presentation of antigens to $CD4^+$ T cells[3,5]. As some surface markers typically used to identify cDCs (like CD11c and MhcII) can also be expressed by tissue resident macrophages, there is a risk for macrophage contamination while performing flow cytometric analysis of different DC populations. In order to avoid this, we will make use of a flow cytometry approach recently developed in the lab[9] that allows comprehensive and contamination-free classification of cDCs across tissues in the mouse.

DCs develop in the BM through a series of differentiation intermediates, each with a further degree of commitment to a specific lineage, that see the common myeloid progenitor (CMP) become a macrophage-DC progenitor (MDP) and then a common DC progenitor (CDP), with the penultimate step of differentiation resulting in generation of the pre-pDC and pre-cDCs[3,10–14]. Furthermore, it has recently been shown that pre-cDCs can be further subdivided into pre-cDC1s and pre-cDC2s, which are committed to the cDC1 and cDC2 lineages, respectively[15,16]. Pre-pDCs develop into pDCs in the bone marrow (BM), which then migrate out to the periphery, whereas the pre-cDC subsets first migrate to the periphery and then undergo their final differentiation into cDCs[11,13,15]. The development of pDCs, cDC1s, and cDC2s requires the concerted action of several lineage-determining TFs. The main TF involved in pDC development and maintenance is the basic helix–loop–helix E

protein E2-2[17,18], whereas cDC1s require Irf8, Batf3, and Id2[6,16,19–25]. Notch2, Klf4 and more recently Irf4 have been shown to be required for terminal differentiation into tissue-specific cDC2 subsets, but do not seem to be involved in the early commitment toward the cDC2 lineage in the BM[26–30]. Additionally , Irf4 has also been implicated in the survival of differentiated cDC2s[31], as well as in their migration to the LNs[32–34]. However, the TFs involved in the initial specification and commitment toward the cDC2 lineage have not yet been identified, and much remains unknown regarding how the decision to commit to a specific DC lineage is made[35]. Zinc finger E box–binding homeobox 2 (Zeb2) is a TF primarily associated with epithelial-mesenchymal transition, a process important in embryonic development, wound healing, and cancer progression[36]. However, Zeb2 has also been implicated in the development of the nervous system and is known to be required for normal mouse melanocyte differentiation and embryonic hematopoiesis[37–40]. Although its role in the immune system is largely unknown, Zeb2 has recently been shown to be required for the maturation of NK cells and terminal differentiation of T cells[41–43]. Zeb2 has also been identified in transcriptional analyses as a potential TF involved in DC development[15,16,44]. Here, we use mice either lacking or ectopically expressing Zeb2 in $CD11c^{+}$ cells to examine the effects of manipulating Zeb2 expression in DCs[45,46]. We demonstrate that Zeb2 is required for the development of pDCs and cDC2s *in vivo*, with $CD11c^{CRE}xZeb2^{fl/fl}$ cells being more efficient at generating cDC1s, which is associated with a rise in the expression of E protein inhibitor Id2. Reciprocally increasing the expression of Zeb2 resulted in a decrease in the cDC1 population with an associated increase in cDC2 development. Thus, Zeb2 is a previously uncharacterized key player in the regulation of the decision of DC precursors to commit to a specific DC lineage by mediating Id2 expression.

1.3 Results

High expression of Zeb2 beyond the CDP stage and in subsets of mature DCs

Zeb2 has recently been identified in several genome-wide microarrays and RNA-sequencing transcriptional analyses as a TF associated with cDC2 development and found to be expressed in pre-cDC2s and cDC2s[15,44], but down-regulated in pre-cDC1s and cDC1s[16]. To validate these results and determine at which stages in DC development Zeb2 could play a role, we FACS (Fluorescence activated cell sorting) purified CMPs, MDPs, CDPs, and pre-pDCs from the BM and pDCs, pre-cDC1s, pre-cDC2s, cDC1s and cDC2s from the spleen and performed real-time quantitative PCR (RT-qPCR) analysis for *Zeb2* expression. In agreement with published data[15,16], we found *Zeb2* mRNA expression to be increased in pre-cDC2s and decreased in pre-cDC1s compared with CDPs (Figure 1A). Strikingly, we also found *Zeb2* to be up-regulated in pre-pDCs and pDCs, suggesting a role for this TF in pDCs (Figure 1A). As Zeb2 has recently been implicated in NK cell[41] and T cell development[42,43], we also FACS-purified NK cells and $CD4^+$ and $CD8^+$ T cells as a reference for *Zeb2* expression levels. cDC2s and pDCs expressed lower levels of *Zeb2* than NK cells but higher levels of *Zeb2* than both T cell subsets (Figure 1A).

Splenic pDCs are reduced in $CD11c^{CRE}xZeb2^{fl/fl}$ mice

To examine whether Zeb2 expression has a functional role in cDCs and/or pDCs, we generated mice lacking or ectopically expressing either one or both alleles of *Zeb2* in $CD11c^+$ cells, including pre-cDCs, cDCs, and pDCs, by crossing $CD11c^{CRE}$ mice[47] with $Zeb2^{fl/fl}$ mice[45] or with R26-$Zeb2^{Tg/Tg}$ mice[46] to drive transgenic Zeb2 expression from the Rosa-26 promoter (Figure 1B). Analysis of *Zeb2* mRNA levels in the splenic pDC populations of these mice revealed a slight down-regulation of *Zeb2* in the $CD11c^{CRE}xZeb2^{fl/fl}$ mice ($Zeb2^{-/-}$ mice) and a striking up-regulation of *Zeb2* in the $CD11c^{CRE}$xR26-$Zeb2^{Tg/Tg}$ mice ($Zeb2^{Tg/Tg}$ mice; Figure 1C and Figure S1A-B).

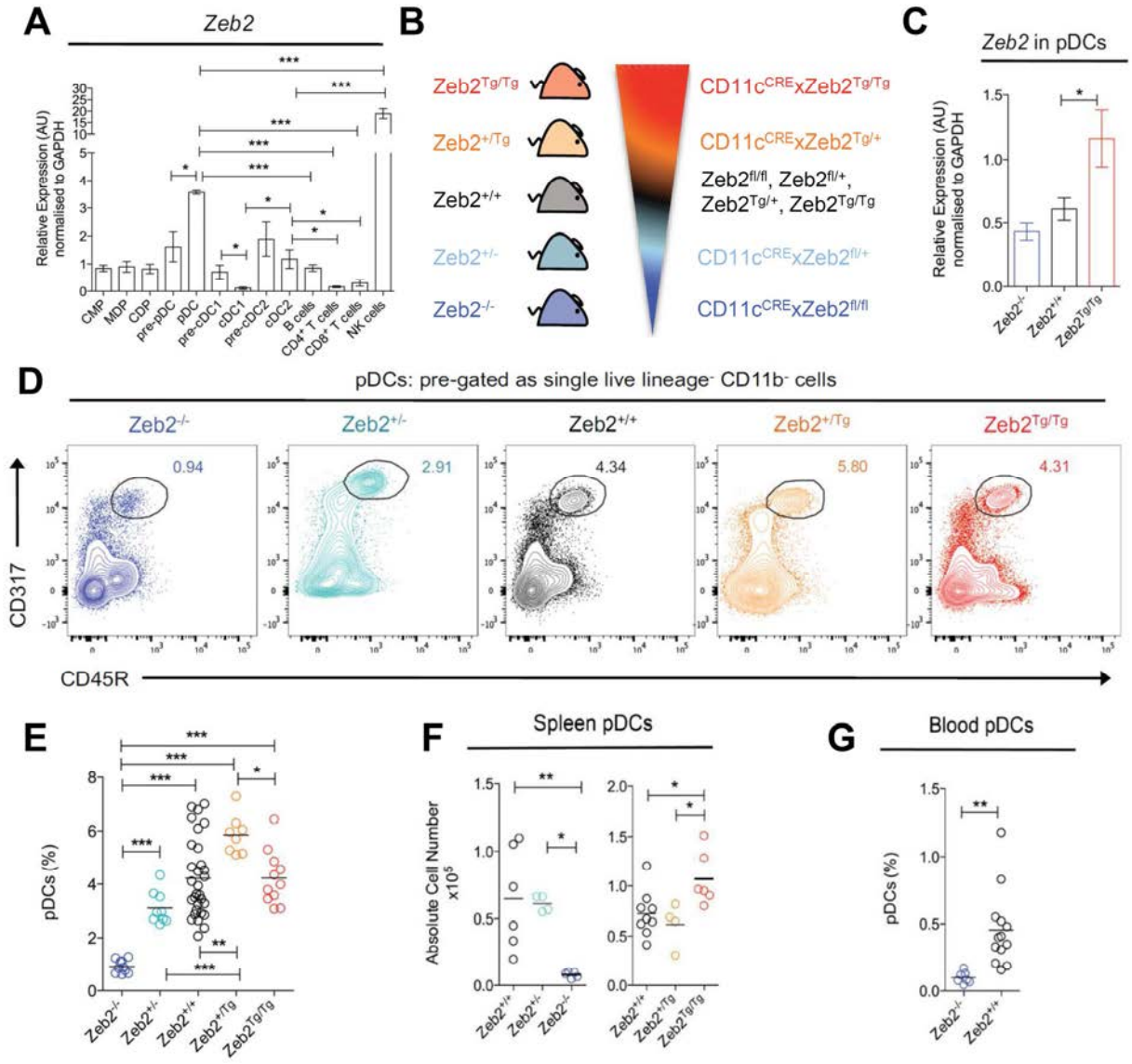

Figure 1 | Zeb2 expression levels regulate pDCs. (A) RT-qPCR for *Zeb2* expression in FACS-purified BM-derived CMPs, MDPs, CDPs, and pre-pDCs and splenic pDCs, pre-cDC1s, pre-cDC2s, cDC1s, cDC2s, $CD4^+$ T cells, $CD8^+$ T cells, and NK cells from WT mice. Results shown are expressed relative to *GAPDH* expression using the $2^{-\Delta\Delta C(t)}$ method with CMP set to 1. Data are pooled from two to three experiments, with at least n = 4 per cell type. Two-way Student's t test was used between indicated groups. (B) Schematic showing range of Zeb2 levels and abbreviations for the transgenic mouse lines used in the study. (C) RT-qPCR for *Zeb2* expression in FACS-purified splenic pDCs from indicated mice. The results shown are expressed relative to *GAPDH* expression using the $2^{-\Delta\Delta C(t)}$ method with $Zeb2^{+/+}$ pDCs set to 1. Data are pooled from two experiments, with at least n = 7 per group. Two-way Student's t test. (D) Representative FACS plots showing identification of $CD317^+CD45R^+$ pDCs in the spleen of indicated mice. Cells were pre-gated as single live $lineage^-CD11b^-$ and were $Ly6C^+MHCII^{int}CD11c^{int}$. Numbers represent proportion of pDCs as a percentage of live $lineage^-CD11b^-$cells. (E) Proportion of splenic pDCs as a percentage of live $lineage^-CD11b^-$ cells in indicated mice. Data are pooled from two experiments with at least n = 8 per group. One-way ANOVA with Bonferroni post-test. (F) Absolute cell number of pDCs in the spleen of indicated mice. Data are representative of at least two experiments where each dot represents one mouse. One-way ANOVA with Bonferroni post-test was used. (G) Proportion of pDCs in the blood of $Zeb2^{+/+}$ and $Zeb2^{-/-}$ mice. Data are pooled from two experiments where each dot represents one mouse. Two-way Student's t test. *, $P < 0.05$; **, $P < 0.01$; ***, $P < 0.001$. Error bars represent SEM. AU, arbitrary units.

Despite the only slight down-regulation of *Zeb2* observed in the remaining pDCs in Zeb2$^{-/-}$ mice, there was a significant reduction in the pDC population in Zeb2$^{-/-}$ mice in the spleen and the blood (Figure 1D-G and Figure S1C), suggesting Zeb2 expression is indeed down-regulated in pDCs. However, loss of only one allele of *Zeb2* (Zeb2$^{+/-}$) had only minimal effects on the pDC population (Figure 1D-F). Increasing expression of Zeb2 in pDCs did not result in any significant changes in the proportion of pDCs, but we did observe an increase in terms of absolute cell numbers (Figure 1D-F).

Splenic cDC2s are reduced in CD11c^{CRE}xZeb2$^{fl/fl}$ mice, whereas splenic cDC1s are reduced in CD11c^{CRE}xR26-Zeb2$^{Tg/Tg}$ mice

Analysis of the cDC populations in the spleens of Zeb2$^{-/-}$ and Zeb2$^{Tg/Tg}$ mice revealed a striking down-regulation of *Zeb2* expression among cDC2s in Zeb2$^{-/-}$ mice and a significant up-regulation of *Zeb2* expression among cDC1s in Zeb2$^{Tg/Tg}$ mice (Figure 2A and Figure S2A-B). Ablation of Zeb2 in cDC1s caused a significant but minor decrease in *Zeb2* expression, likely because WT cDC1 cells do not express Zeb2. There was no significant increase in *Zeb2* levels in cDC2s in Zeb2$^{Tg/Tg}$ mice (Figure 2A). Ablation of Zeb2 expression in CD11c^{+} cells resulted in a reduction in the proportion and absolute number of XCR1^{-}SIRPα^{+} cDC2s (Figure 2B-D and Figure S2C). Somewhat surprisingly, this reduction was coupled with an increase in both the proportion and absolute number of XCR1^{+}SIRPα^{-} cDC1s (Figure 2B-D). Similarly to the pDCs, this reduction in cDC2s was only apparent when both alleles of *Zeb2* were targeted (Figure 2B-D). On the contrary, two alleles of the transgenic *Zeb2* in CD11c^{+} cells led to a decrease in the proportion and number of splenic cDC1s, whereas the cDC2s were unaffected. Once again, we observed that only targeting one allele had limited effects on either subset (Figure 2B-D). Interestingly, the increased expression of Zeb2 in CD11c^{+} cells led to the presence of a new XCR1^{+}SIRPα^{+} population of cDCs in the spleen (Figure 2B-D). These XCR1^{+}SIRPα^{+} (double positive [DP]) cDCs also expressed intermediate levels of CD24, a marker typically associated with cDC1s in the spleen (Figure 2E).

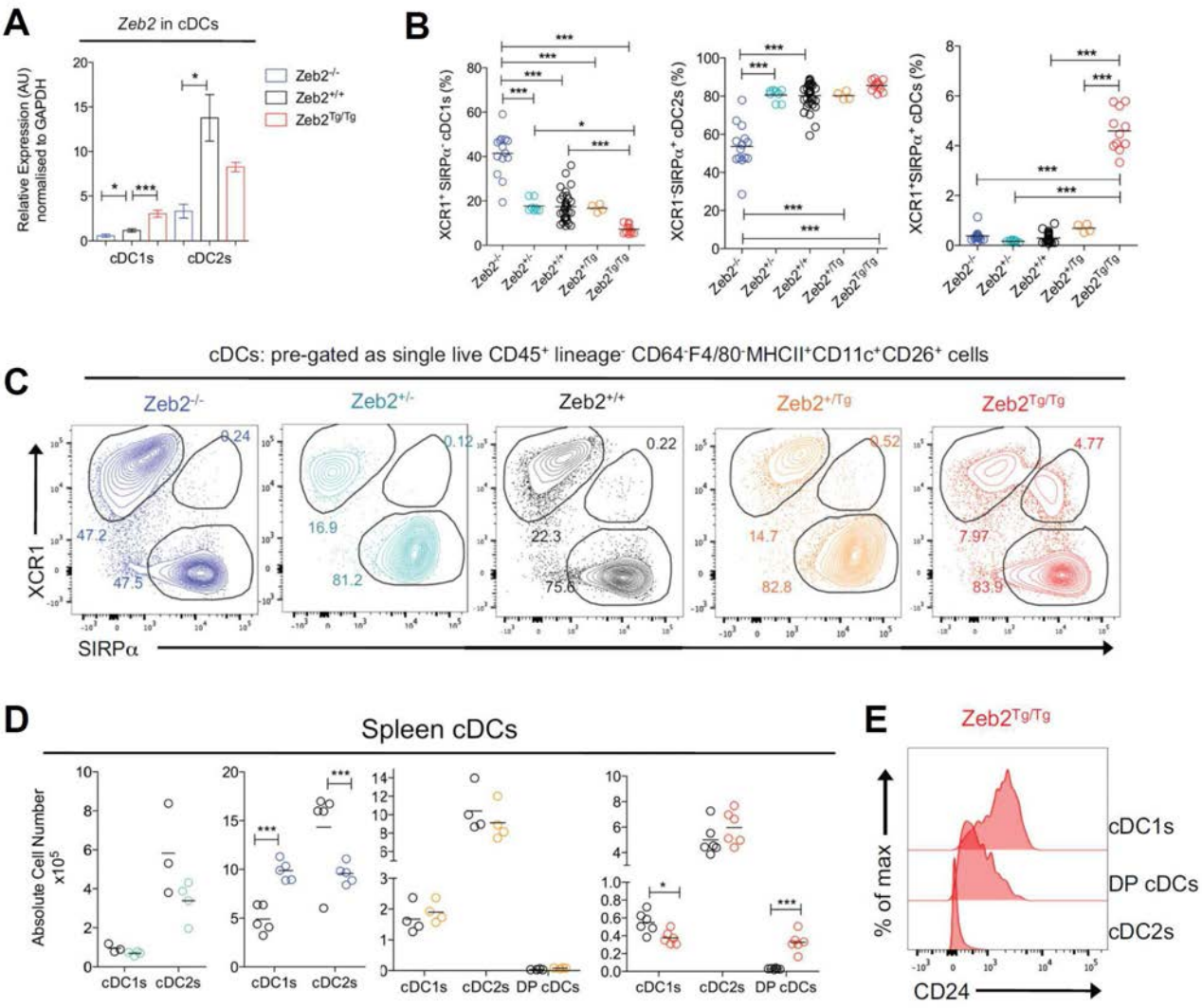

Figure 2 | Zeb2 expression levels regulate cDCs. (A) Splenic cDC1s and cDC2s were FACS-purified from Zeb2$^{+/+}$, Zeb2$^{-/-}$, or Zeb2$^{Tg/Tg}$ mice, and *Zeb2* levels were assessed by RT-qPCR. The results shown are expressed relative to *GAPDH* expression using the $2^{-\Delta\Delta C(t)}$ method with Zeb2$^{+/+}$ cDC1s set to 1. Data are pooled from two to three experiments, with at least n = 7 per group. Two-way Student's t test. (B) Proportion of splenic cDC1s, cDC2s, and DP cDCs as a percentage of total cDCs in indicated mice. Data are pooled from two to three experiments, with at least n = 4 per group. One-way ANOVA with Bonferroni post-test. (C) Representative FACS plots showing identification of XCR1^{+}SIRPα^{-} cDC1s, XCR1^{-}SIRPα^{+} cDC2s, and XCR1^{+}SIRPα^{+} DP cDCs in the spleen of indicated mice. Cells were pre-gated as single live CD45^{+}lineage^{-}CD64^{-}F4/80^{-}MHCII^{+}CD11c^{+}CD26^{+}. Numbers represent proportion of cDC1s, cDC2s, and DP cDCs as a percentage of total cDCs. (D) Absolute cell number of cDC1s, cDC2s, and DP cDCs in the spleen of Zeb2$^{+/+}$ (black) , Zeb2$^{+/-}$ (light blue), Zeb2$^{-/-}$ (dark blue) , Zeb2$^{+/Tg}$ (orange), and Zeb2$^{Tg/Tg}$ (red) mice. Data are representative of at least two experiments where each dot represents one mouse. One-way ANOVA with Bonferroni post-test. (E) Representative histogram showing CD24 expression by splenic cDC1s, cDC2s, and DP cDCs in Zeb2$^{Tg/Tg}$ mice. *, P < 0.05; ***, P < 0.001. Error bars represent SEM. AU, arbitrary units.

Zeb2 expression differentially affects subsets of tissue-resident cDC2s

We next extended our analysis to the liver, lung, and small intestine lamina propria (SILP) to determine whether Zeb2 expression regulates cDCs globally or whether its role is restricted to lymphoid tissues. Analysis of cDC1s and cDC2s on the basis of XCR1 and SIRPα expression in these tissues revealed, similarly to the spleen, an overall increase in cDC1s and decrease in cDC2s in $Zeb2^{-/-}$ mice and an overall decrease in cDC1s in $Zeb2^{Tg/Tg}$ mice (Figure 3 and Figure 4). However, the scale of these differences was tissue dependent. For example, we did not observe any effect of Zeb2 overexpression in the liver (Figure 3A,B and E), whereas the lung cDCs appeared to be extra sensitive to Zeb2 expression levels with effects of Zeb2 loss and overexpression being observed even when only one allele of *Zeb2* was targeted (Figure 3C,D and F). Additionally, a population of $XCR1^{-}SIRP\alpha^{-}$ cDCs was identified in the lungs of the $Zeb2^{-/-}$ and $Zeb2^{+/-}$ mice (Figure 3C). In the SILP, the same trends were observed in terms of total cDC1s and cDC2s as in the other tissues (Figure 4A-B). However, when the cDC2s were further subdivided on the basis of CD103 expression, a marker commonly used to define cDC subsets in the gut[31,48], we found that the two subsets of cDC2s were not equally sensitive to Zeb2 expression. Intriguingly, we found the $CD103^{-}$ cDC2s to be susceptible to the loss of Zeb2 expression, whereas the $CD103^{+}$ cDC2s appeared to be unaffected in $Zeb2^{-/-}$ mice. No effects were seen in either population in $Zeb2^{Tg/Tg}$ mice, with only the cDC1s ($CD103^{+}SIRP\alpha^{-}$) being affected (Figure 4C-E and Figure S3).

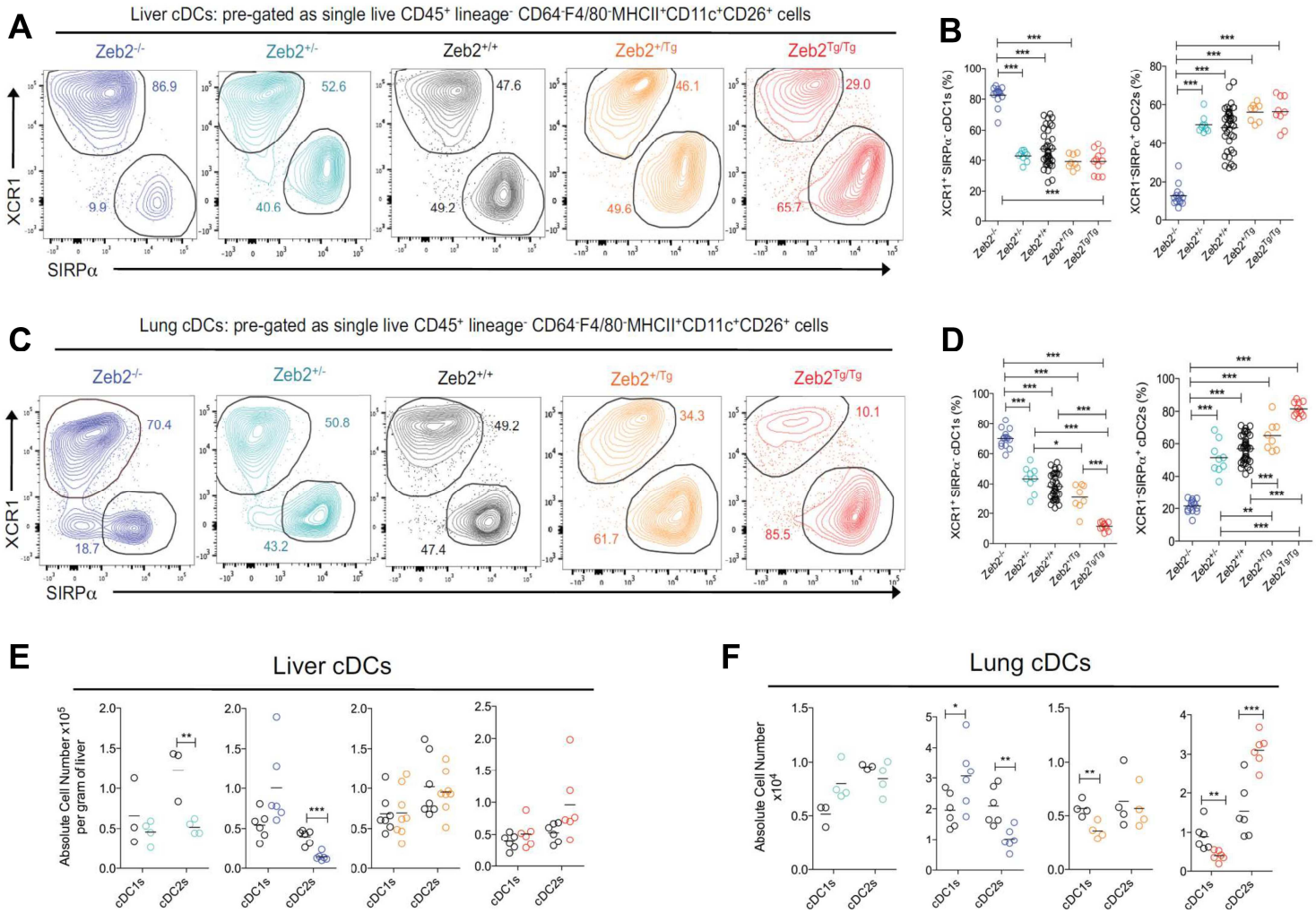

Figure 3 | Zeb2 expression differentially affects subsets of tissue-resident cDC2s. (A and C) Representative FACS plots showing identification of XCR1$^+$SIRPα$^-$ cDC1s and XCR1$^-$SIRPα$^+$ cDC2s in the liver (A) and lung (C) of indicated mice. Cells were pre-gated as single live CD45$^+$lineage$^-$CD64$^-$F4/80$^-$MHCII$^+$CD11c$^+$CD26$^+$. The numbers represent the proportion of cDC1s and cDC2s as a percentage of total cDCs. (B and D) Proportion of liver (B) and lung (D) cDC1s and cDC2s as a percentage of total cDCs in indicated mice. Data are pooled from two to three experiments, with at least n = 7 per group. (E and F) Absolute cell number of cDC1s and cDC2s in liver (E) and lung (F) of indicated mice. Data are representative of two experiments where one dot represents one mouse. *, $P < 0.05$; **, $P < 0.01$; ***, $P < 0.001$. One-way ANOVA with Bonferroni post-test.

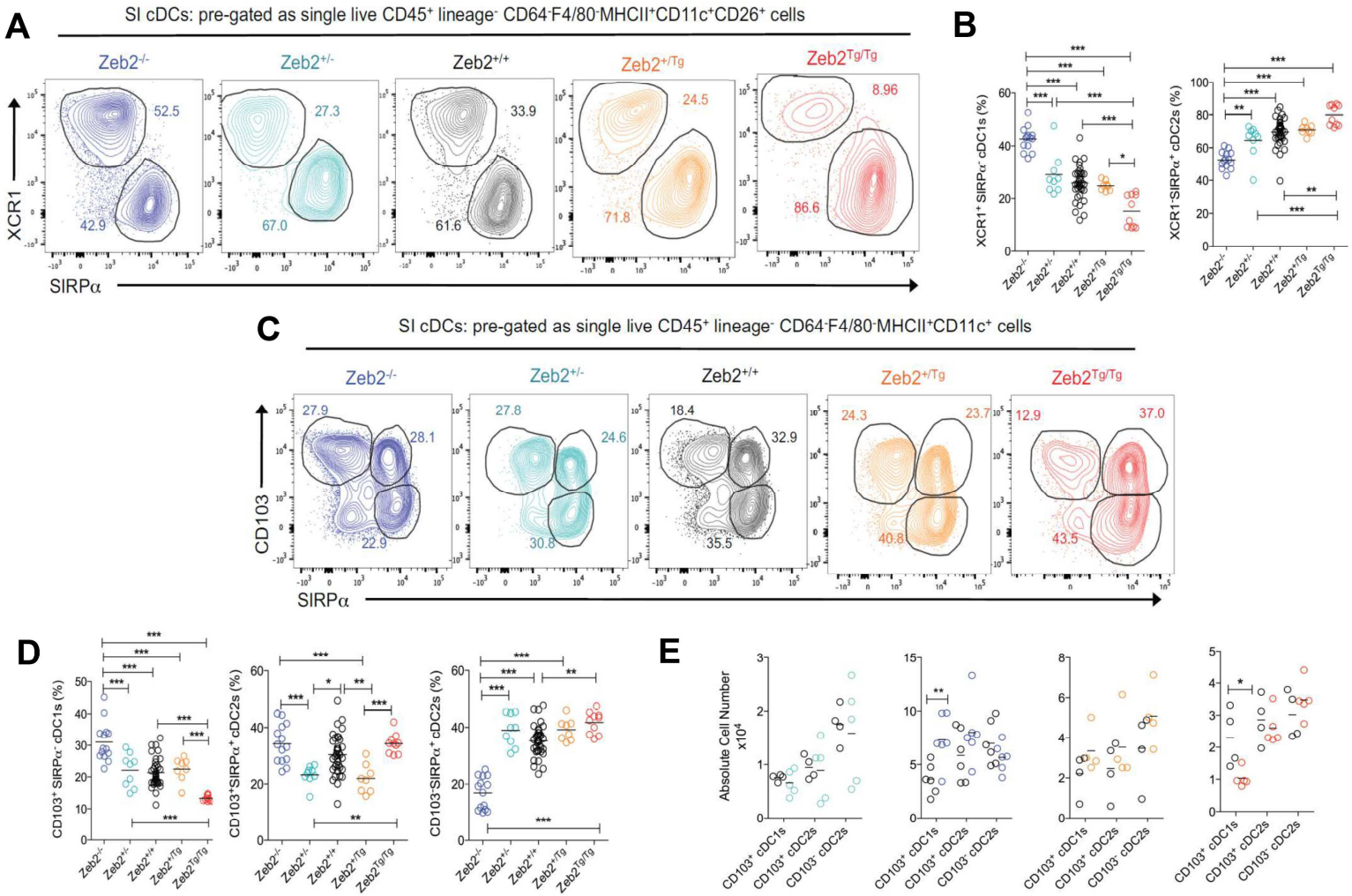

Figure 4 | Zeb2 expression differentially affects subsets of SILP cDCs. (A and C) Representative FACS plots showing identification of XCR1$^+$SIRPα$^-$ cDC1s and XCR1$^-$SIRPα$^+$ cDC2s (A) or CD103$^+$SIRPα$^-$ cDC1s, CD103$^+$SIRPα$^+$ cDC2s and CD103$^-$SIRPα$^+$ cDC2s (C) in the SILP of indicated mice. Cells were pre-gated as single live CD45$^+$lineage$^-$CD64$^-$F4/80$^-$MHCII$^+$CD11c$^+$(CD26$^+$). The numbers represent the proportion of each SILP cDC subset as a percentage of total cDCs. (B and D) Proportion of each SILP cDC subset as a percentage of total cDCs in indicated mice. Data are pooled from two to three experiments, with at least n = 7 per group. (E) Absolute cell number of each SILP subset in indicated mice. Data are representative of two experiments where one dot represents one mouse. *, P < 0.05; **, P < 0.01; ***, P < 0.001. One-way ANOVA with Bonferroni post-test.

DC-intrinsic effects of Zeb2 expression on cDC commitment revealed by competitive BM chimerism

Having shown that Zeb2 expression in CD11c^{+} cells regulates both pDCs and cDCs, we next sought to determine whether these effects were cell intrinsic or caused by immune dysregulation. To this end, we generated competitive BM chimeric mice (Figure 5A), in which CD45.1/CD45.2 WT mice were lethally irradiated and reconstituted with a ~70:30 mix (determined by analysis of neutrophils in the spleen; Figure 5B) of Zeb2$^{fl/fl}$/Zeb2$^{Tg/Tg}$ (Zeb2$^{+/+}$), CD11c^{CRE}xZeb2$^{fl/fl}$ (Zeb2$^{-/-}$), or CD11c^{CRE}xZeb2$^{Tg/Tg}$ (Zeb2$^{Tg/Tg}$) CD45.2^{+} BM and WT CD45.1^{+} BM. 10-12 weeks after reconstitution, the proportions of CD45.2^{+} cells among pDCs in the spleen and cDC1s and cDC2s in the spleen, lung, liver and SILP were analyzed. This analysis revealed that the defect in pDCs in the Zeb2$^{-/-}$ mice was indeed cell intrinsic, with the Zeb2$^{-/-}$ CD45.2^{+} cells dramatically losing the competition with the CD45.1^{+} WT BM to generate pDCs when compared with their Zeb2$^{+/+}$ counterparts (Figure 5C). Consistent with our earlier findings that increasing Zeb2 expression did not alter the pDC population, the WT and Zeb2$^{Tg/Tg}$ BM were equally capable of generating pDCs (Figure 5C). Concurrently, we also found the defect in cDC2 generation in the spleen, lung, and liver and CD103^{-} cDC2 generation in the SILP of Zeb2$^{-/-}$ mice to be cell intrinsic (Figure 5E and Figure 6A-C). Analysis of the cDC1 populations in these tissues also found that the enhanced generation of cDC1s in CD11c^{CRE}xZeb2$^{fl/fl}$ mice was cell intrinsic, as Zeb2$^{-/-}$ CD45.2^{+} BM had a competitive advantage over WT CD45.1^{+} BM in the generation of cDC1s compared with their Zeb2$^{+/+}$ counterparts (Figure 5D and Figure 6A-C). Similarly, we found that the decrease in spleen, lung and SILP cDC1s in CD11c^{CRE}xR26-Zeb2$^{Tg/Tg}$ mice was cell intrinsic (Figure 5D and Figure 6B and 6C), as was the generation of splenic DP cDCs, with these being almost uniformly derived from Zeb2$^{Tg/Tg}$ BM (Figure 5F). However, Zeb2$^{Tg/Tg}$ BM cells did not show a competitive advantage over WT BM in generating cDC2s in the chimeras (Figure 5E and Figure 6A-C). Interestingly, analysis of the CD103^{+} cDC2s in the SILP demonstrated that in addition to having a competitive advantage over WT BM to become cDC1s, Zeb2$^{-/-}$ BM also outcompeted WT BM to generate CD103^{+} cDC2s, whereas WT BM outcompeted Zeb2$^{Tg/Tg}$ BM to become both CD103^{+} cDC1s

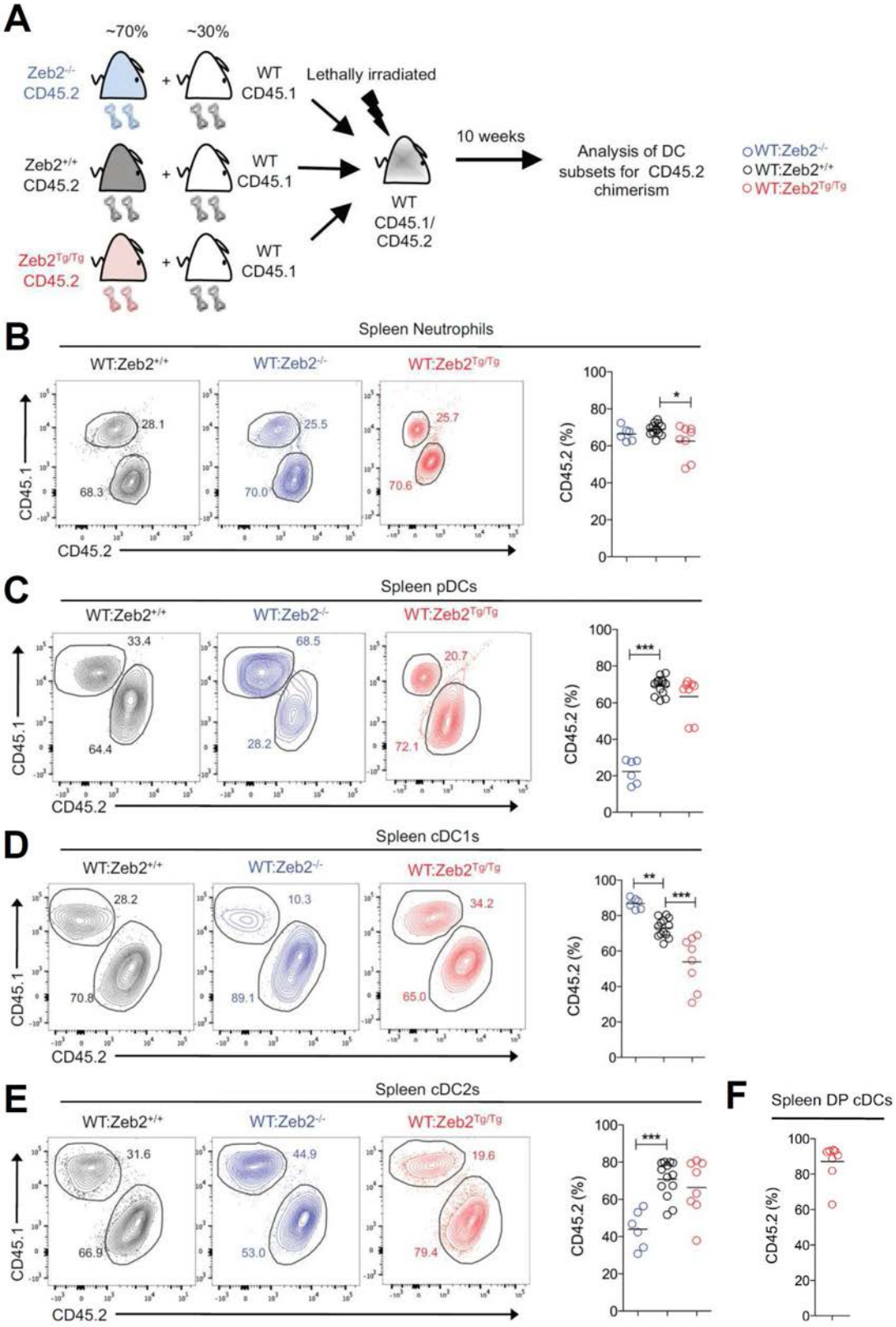

Figure 5 | Zeb2 regulation of splenic cDC subsets is cell intrinsic. (A) Competitive BM chimeric mice were generated by lethally irradiating CD45.1/CD45.2 WT mice and reconstituting with a ~70:30 mix of Zeb2$^{+/+}$, Zeb2$^{-/-}$, or Zeb2$^{Tg/Tg}$ CD45.2 BM and WT CD45.1 BM. (B-E) LEFT: Representative FACS plots showing CD45.1 and CD45.2 staining among splenic neutrophils (B), pDCs (C), cDC1s (D) and cDC2s (E) of indicated chimeras. The numbers represent the proportion of each cell type coming from CD45.1 or CD45.2 BM. RIGHT: Proportions of splenic neutrophils (B) , pDCs (C), cDC1s (D), cDC2s (E), and DP cDCs (F) deriving from CD45.2 donor BM. *, $P < 0.05$; **, $P < 0.01$; ***, $P < 0.001$. Two-way Student's t test.

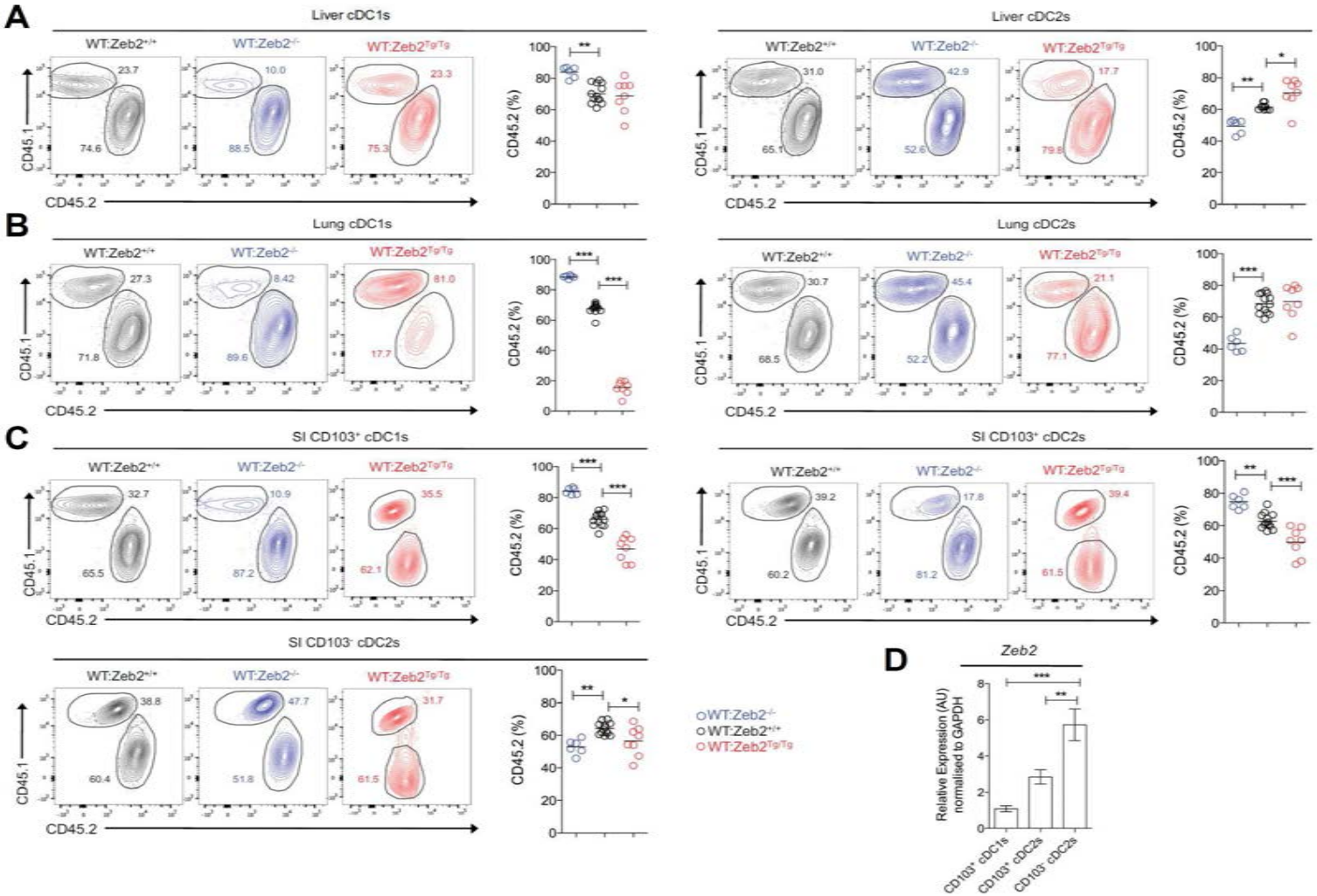

Figure 6 | Zeb2 regulation of cDC subsets is cell intrinsic across tissues. (A - C) Representative FACS plots showing CD45.1 and CD45.2 staining among liver (A) and lung (B) cDC1s and cDC2s and SILP CD103$^+$ cDC1s, CD103$^+$ cDC2s, and CD103$^-$ cDC2s (C) of indicated chimeras. The numbers represent the proportion of each cell type coming from CD45.1 or CD45.2 BM. Proportions of liver (A) and lung (B) cDC1s and cDC2s and SILP CD103$^+$ cDC1s, CD103$^+$ cDC2s, and CD103$^-$ cDC2s (C) deriving from CD45.2 donor BM. Two-way Student's t test. (D) SILP cDCs were FACS-purified from WT mice, and *Zeb2* expression was assessed by RT-qPCR. Results shown are expressed relative to *GAPDH* expression using the $2^{-\Delta\Delta C(t)}$ method with CD103$^+$ cDC1s set to 1. AU, arbitrary units. One-way ANOVA with Bonferroni post-test. Data are pooled from two experiments, with at least n = 6 per group. Error bars represent SEM. AU, arbitrary units. *, P < 0.05; **, P < 0.01; ***, P < 0.001.

and CD103^{+} cDC2s (Figure 6C). This finding in combination with the results in Figure 4 prompted us to examine *Zeb2* expression in the three SILP cDC populations. Fitting with our results, we found that the CD103^{+} cDC2s express significantly less *Zeb2* than their CD103^{-} counterparts, instead expressing similar levels of *Zeb2* to the CD103^{+} cDC1s (Figure 6D).

Zeb2 expression regulates cDC development, not cell survival

Having shown that Zeb2 expression levels skew the prevalence of the cDC subtypes present in multiple tissues, we next sought to determine whether Zeb2 functions during cDC2 development or whether, similar to the previously described cDC2 TFs, it functions in terminally differentiated cDC2s. It has recently been proposed that commitment to the cDC1 and cDC2 lineage is already apparent at the pre-cDC level such that pre-cDCs can be further subdivided into cDC1- and cDC2-committed pre-cDCs on the basis of Ly6C, SiglecH and CD24 expression[15,16]. Thus, we first examined the proportions of these pre-cDCs in the BM of Zeb2$^{-/-}$, Zeb2$^{+/+}$, and Zeb2$^{Tg/Tg}$ mice (Figure 7A and Figure S4). Although no significant differences were observed in any of the populations across the three genotypes, we did notice a trend toward less pre-cDC1s with increasing levels of Zeb2 expression (Figure 7A), consistent with Zeb2 functioning during cDC development. Examination of the pre-cDC subsets in the spleen revealed a similar trend in pre-cDC1s as observed in the BM, in addition to a significant increase in pre-cDC2s with increasing levels of Zeb2 expression (Figure 7B), further pointing toward a role for Zeb2 in controlling cDC2 development. To definitively demonstrate that Zeb2 functions during cDC2 development, we next crossed the recently described late-CD11c^{CRE} mouse, in which the CRE is not active during pre-cDC development but only once the pre-cDCs mature into cDCs[34], with Zeb2$^{fl/fl}$ and R26-Zeb2$^{Tg/Tg}$ mice. Analysis of these mice revealed that the loss of Zeb2 late in cDC development does not affect the prevalence of the cDC subsets, meaning that Zeb2 already regulates cDC development at the pre-cDC stage (Figure 7C). In contrast, the spleens of late-CD11c^{CRE}xR26-Zeb2$^{Tg/Tg}$ showed similar defects as the spleens of CD11c^{CRE}xR26-Zeb2$^{Tg/Tg}$ mice, with a decrease in cDC1s, an increase in cDC2s and the presence of a DP cDC population (Figure 7C). Thus, the addition of Zeb2 in mature cDCs affects the prevalence of the populations in the spleen.

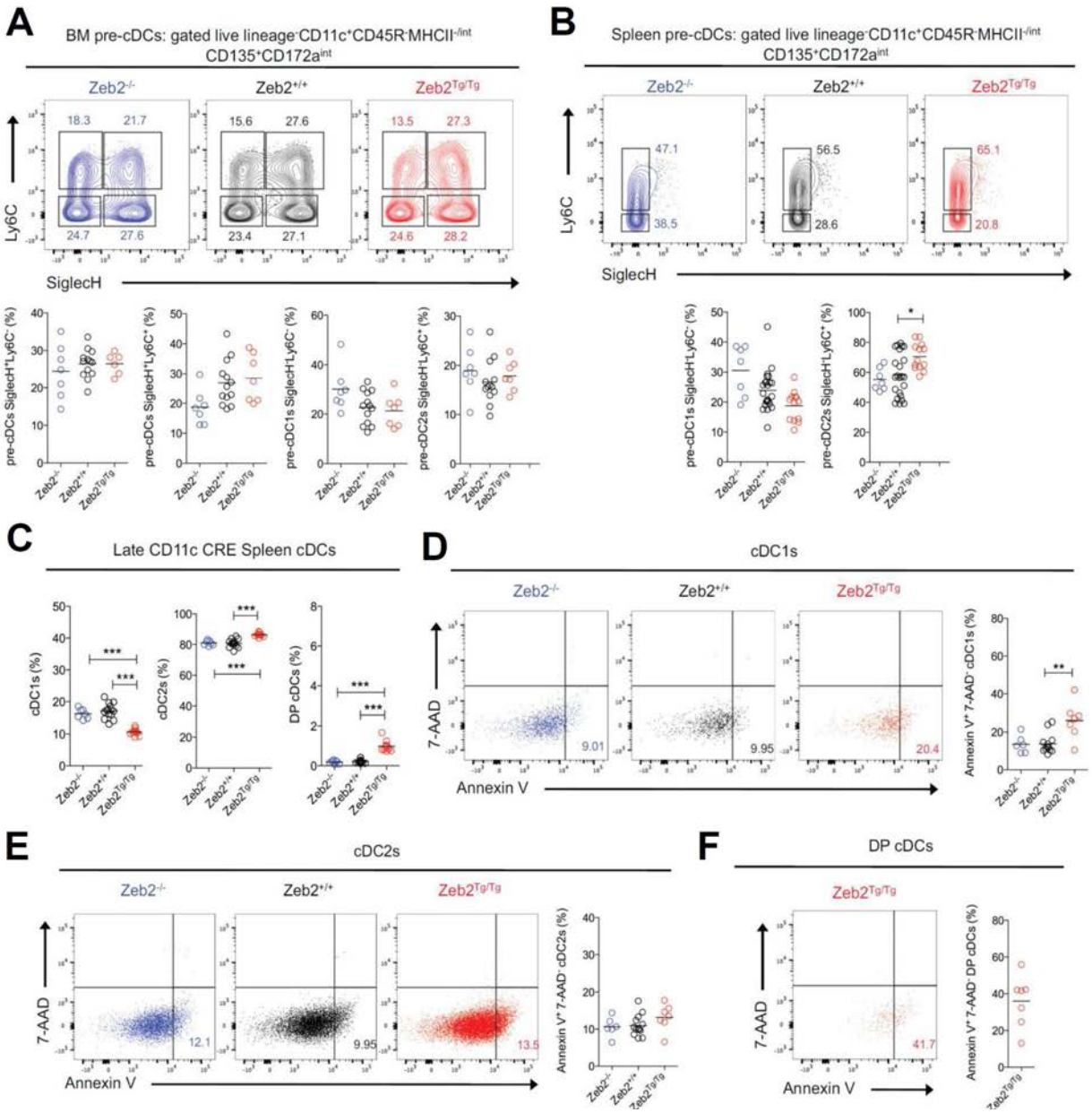

Figure 7 | Zeb2 regulates cDC subset development, not survival. (A) Representative FACS plots showing identification of pre-cDC subsets and proportions of pre-cDC subsets in the BM of indicated mice. Cells were pre-gated as single live lineage$^-$CD11c$^+$CD45R$^-$MHCII$^{-/int}$CD135$^+$SIRPα^{int}. Data are pooled from two experiments, with at least n = 3 per experiment. No significance was detected. (B) Representative FACS plots showing identification of pre-cDC subsets and proportions of pre-cDC subsets in the spleen of indicated mice. Cell were pre-gated as single live lineage$^-$CD11c$^+$CD45R$^-$MHCII$^{-/int}$CD135$^+$SIRPα^{int}. Data are pooled from two experiments, with at least n = 3 per experiment. *, $P < 0.05$ (C) Proportions of cDC subsets as a percentage of total cDCs in the spleen of late-CD11c^{CRE}xZeb2$^{fl/fl}$ (Zeb2$^{-/-}$) and late-CD11c^{CRE}xZeb2$^{Tg/Tg}$ (Zeb2$^{Tg/Tg}$) compared with CRE negative littermate controls (Zeb2$^{+/+}$). Data are pooled from two experiments, with at least n = 3 per experiment. ***, $P < 0.001$ (D-F) Representative FACS plots showing 7-AAD and Annexin V staining and proportions of AnnexinV$^+$7-AAD$^-$ cells in cDC1s (D), cDC2s (E) and DP cDCs (F) . **, $P < 0.01$ (A-F) One-way ANOVA with Bonferroni post-test. (G) Absolute number of recovered Zeb2$^{+/+}$ and Zeb2$^{Tg/Tg}$ cDC1s at indicated time-points following spiking into seed Flt3L BMDC cultures. *, $P < 0.05$; **; $P < 0.01$. Two-way ANOVA with Bonferroni post-test.

To further validate our findings that Zeb2 functions during cDC2 development rather than playing a role in terminally differentiated cDC2s, we examined the survival of cDC subsets across the range of Zeb2 expression levels. Using Annexin V staining we could not detect any differences in the proportion of apoptotic cells (AnnexinV^{+} 7-AAD^{-}) in Zeb2$^{-/-}$ mice (Figure 7D and 7E). There was a slight increase in the proportion of apoptotic cDC1s in Zeb2$^{Tg/Tg}$ mice (Figure 7D). However we could not confirm any increase in cell death when FACS-purified splenic cDC1s were spiked into WT Flt3L BMDC cultures compared with Zeb2$^{+/+}$ cDC1 controls, in fact the opposite trend was observed (Figure 7G). A significant proportion of the splenic DP cDCs from Zeb2$^{Tg/Tg}$ mice were found to be AnnexinV^{+}7-AAD^{-} (Figure 7F), suggesting this atypical population may be apoptotic following their development.

Minimal changes in transcriptomes of mature cDC subsets

Having identified Zeb2 as a regulator of cDC development, we next sought to examine the consequences of differential Zeb2 expression levels in the mature cDCs. To this end, we FACS-purified cDC1s and cDC2s from Zeb2$^{-/-}$, Zeb2$^{+/+}$ and Zeb2$^{Tg/Tg}$ mice and performed RNA-sequencing (RNA-seq) analysis (Figure S2A and S2B, gating strategies). Cluster analysis of this data demonstrated that, fitting with our earlier analysis, the ablation of Zeb2 expression in cDC1s and overexpression of Zeb2 in cDC2s did not have significant effects on the transcriptomes (Figure 8A). To confirm this, we used a visualization method in which each gene is plotted in a graph containing three axes (one axis per genotype) that are placed at a 120° angle, creating a hexagonal triwise plot (Figure 8B). In these hexagons, the direction of a point represents an up-regulation in one or two populations, whereas the distance from the origin represents the magnitude of the up-regulation. Each grid line represents a log2 fold change (FC). Plotting all uniquely annotated genes for cDC1s and cDC2s yielded a profile with most differentially expressed genes in cDC1s either being up-regulated specifically in Zeb2$^{Tg/Tg}$ mice or in both Zeb2$^{-/-}$ and Zeb2$^{+/+}$ mice (Figure 8B). Conversely, in the cDC2s, differentially expressed genes were either up-regulated solely in Zeb2$^{-/-}$ mice or in both Zeb2$^{+/+}$ and Zeb2$^{Tg/Tg}$ mice (Figure 8B), confirming the cluster analysis. Thus, we subsequently focused our analysis on cDC2s from the Zeb2$^{-/-}$ mice and cDC1s from the Zeb2$^{Tg/Tg}$ mice compared with

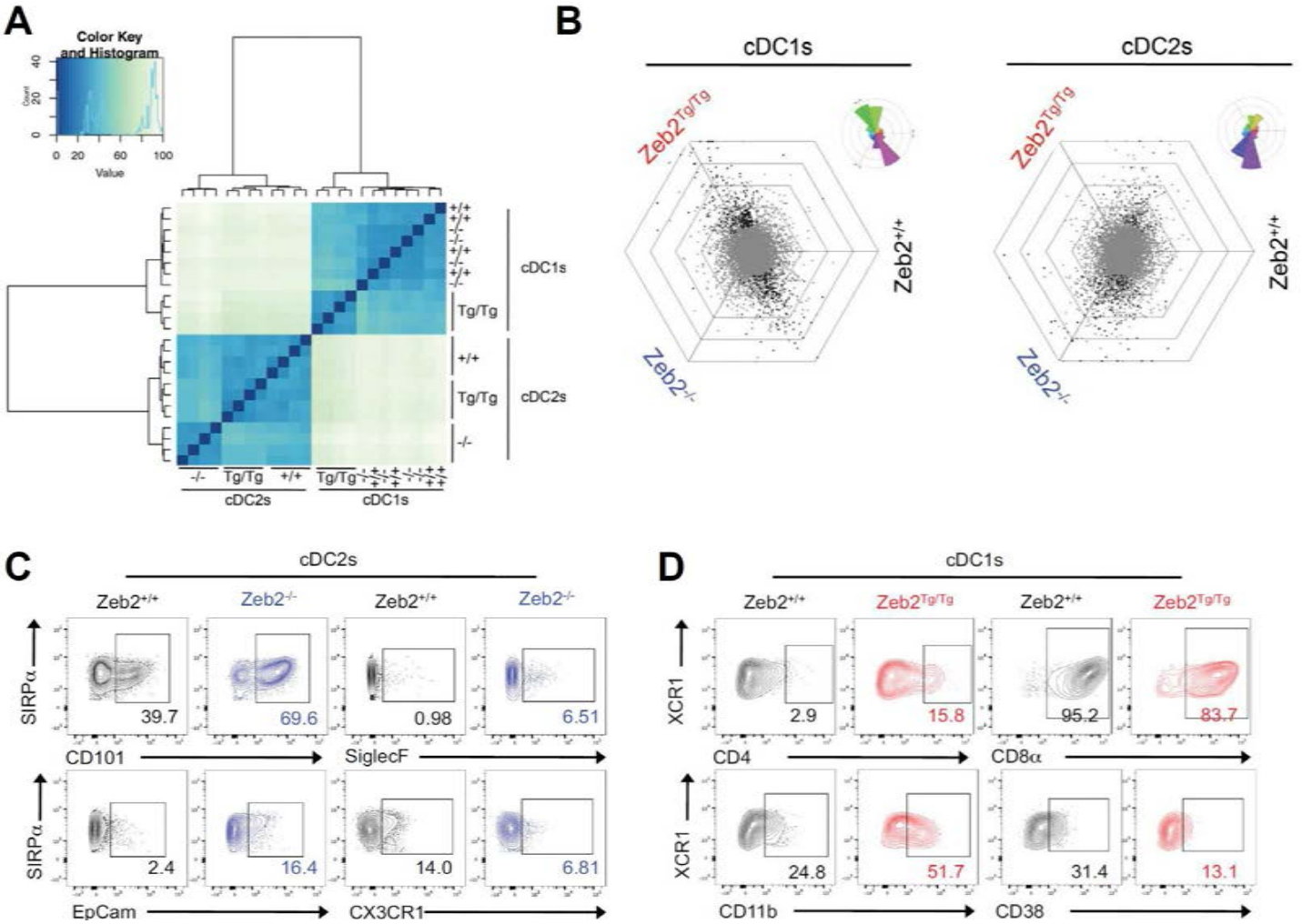

Figure 8 | Altering Zeb2 expression levels affects cDC1 and cDC2 transcriptomes. (A) Cluster analysis of RNA-sequencing data from splenic cDC1s and cDC2s from Zeb2$^{+/+}$, Zeb2$^{-/-}$ and Zeb2$^{Tg/Tg}$ mice. (B) To visualize differential gene expression between Zeb2$^{+/+}$, Zeb2$^{-/-}$ and Zeb2$^{Tg/Tg}$ cDC1s or cDC2s, each gene was plotted in a hexagonal triwise diagram in which the direction of a point represents an up-regulation in one or two populations, whereas the distance from the origin represents the magnitude of this up-regulation. Genes that are ≥ 32-fold differentially expressed are plotted on the outer grid line. Rose diagrams show the percentages of genes in each orientation. Grey and black dots represent respectively non-differentially and statistically significant differentially expressed genes. (C and D) Representative FACS plots showing expression of indicated surface markers in Zeb2$^{-/-}$ and Zeb2$^{+/+}$ cDC2s (C) and in Zeb2$^{+/+}$ and Zeb2$^{Tg/Tg}$ cDC1s (D). Numbers represent the percentage of cDC2s (C) or cDC1s (D) expressing each marker.

their $Zeb2^{+/+}$ counterparts. Applying a stringency level where the adjusted p-value was equal to 0.01 and the log2 FC was less than –1 or greater than 1, we found that 263 genes were differentially expressed in $Zeb2^{Tg/Tg}$ cDC1s (Figure S6A and Table S1), whereas 118 genes were differentially expressed in $Zeb2^{-/-}$ cDC2s (Figure S6B and Table S2). To our surprise, however, most genes were only just over the thresholds, with only a few genes having a log2 FC less than –2 or greater than 2. Examining the list of differentially expressed genes for surface receptors enabled us to validate some of the changes at the protein level by flow cytometry. In $Zeb2^{-/-}$ cDC2s, we were able to confirm changes in CD101, CX3CR1, SiglecF , and epithelial cell adhesion molecule protein (EpCam) expression (Figure 8C). However, some of the differentially expressed genes did not translate into altered protein expression, including CD69 and CCR2 (data not shown). Protein analysis in cDC1s from $Zeb2^{Tg/Tg}$ mice validated changes in CD4, CD8α, CD11b, CD38 (Figure 5D), and CD115 (data not shown), whereas the slight up-regulation of CD101 observed at the mRNA level did not result in increased protein expression (data not shown).

Functional consequences of Zeb2 expression levels

The minimal differences in the transcriptomes of mature cDC subsets upon changes in the level of Zeb2, suggest that once these cDCs develop, they behave normally. To test this hypothesis, we performed IPA analysis on the differentially expressed genes in order to pinpoint cDC functions that are potentially affected upon loss of Zeb2 expression in cDC2s or gain of Zeb2 expression in cDC1s. For both datasets, $Zeb2^{+/+}$ versus $Zeb2^{-/-}$ cDC2s and $Zeb2^{+/+}$ versus $Zeb2^{Tg/Tg}$ cDC1s, there was among others a significant enrichment for the functions Immune Cell Trafficking ($p=1,31 \times 10^{-7}$ for $Zeb2^{+/+}$ versus $Zeb2^{-/-}$ cDC2s; $p=1,35 \times 10^{-18}$ for $Zeb2^{+/+}$ versus $Zeb2^{Tg/Tg}$ cDC1s; Figure S7) and Inflammatory Response ($p=3,21 \times 10^{-7}$ for $Zeb2^{+/+}$ versus $Zeb2^{-/-}$ cDC2s; $p=1,44 \times 10^{-15}$ for $Zeb2^{+/+}$ versus $Zeb2^{Tg/Tg}$ cDC1s; figure S7). As Immune Cell Trafficking includes migration and Inflammatory Response includes antigen presentation by peripheral DCs we looked at these functions in more detail. First we examined if cDC migration was affected by examining the resident and

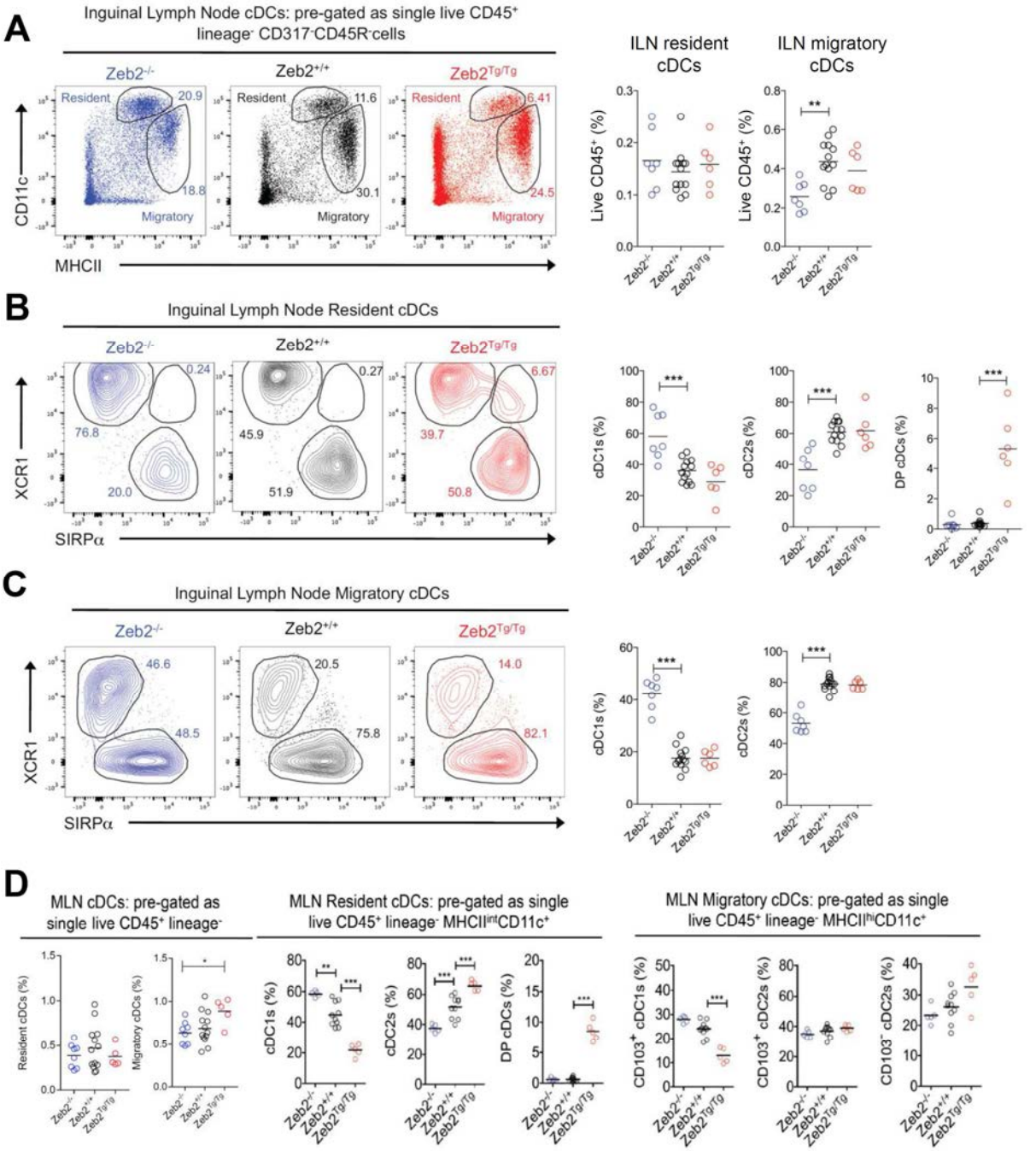

Figure 9 | Zeb2 expression levels regulate cDC migration to LNs. (A) Representative FACS plots showing identification of resident and migratory cDCs and proportions of resident and migratory cDCs in the inguinal lymph nodes (ILNs) of Zeb2$^{-/-}$, Zeb2$^{+/+}$ and Zeb2$^{Tg/Tg}$ mice as a percentage of single live CD45^{+} cells. Data are pooled from two experiments with at least n = 3 per group. **, P < 0.01. One-way ANOVA with Bonferroni post-test. (B,C) Representative FACS plots showing identification of cDC1s and cDC2s amongst resident (B) and migratory (C) cDCs and proportions of cDC1s, cDC2s and DP cDCs as a percentage of total resident (B) and migratory (C) cDCs in the ILNs of Zeb2$^{-/-}$, Zeb2$^{+/+}$ and Zeb2$^{Tg/Tg}$ mice. Data are pooled from two experiments with at least n = 3 per group. ***, P < 0.001. One-way ANOVA with Bonferroni post-test. (D) LEFT panel: proportions of resident and migratory cDCs in the mesenteric lymph node (MLN) of Zeb2$^{-/-}$, Zeb2$^{+/+}$ and Zeb2$^{Tg/Tg}$ mice as a percentage of single live CD45^{+} cells. TWO RIGHT panels: proportion of MLN resident cDC1s, cDC2s and DP cDCs and proportion of MLN migratory CD103^{+} cDC1s, CD103^{+} cDC2s, and CD103^{-} cDC2s as a percentage of, respectively, total resident and migratory cDCs in Zeb2$^{-/-}$, Zeb2$^{+/+}$, and Zeb2$^{Tg/Tg}$ mice. Data are representative of two experiments, with n = 5 per group. *, P < 0.05; **, P < 0.01; ***, P < 0.001. One-way ANOVA with Bonferroni post-test.

migratory cDC populations in the inguinal lymph nodes (ILNs). These populations can be separated on the basis of CD11c and MHCII expression with resident cDCs expressing high levels of CD11c and intermediate levels of MHCII, while migratory cDCs express intermediate levels of CD11c and high levels of MHCII (Figure 9A). While no differences were observed in the proportion of resident cDCs across the three genotypes, we did observe a small but significant decrease in the proportion of migratory cDCs in the $Zeb2^{-/-}$ mice (Figure 9A). Further analysis of the cDC subsets within the resident and migratory gates revealed a similar phenotype to that observed in the spleen and non-lymphoid tissues examined (Figure 9B and 9C). Intriguingly, we did not observe a DP cDC population amongst the $Zeb2^{Tg/Tg}$ migratory cDCs although this population was seen amongst resident cDCs (Figure 9B and 9C). Analysis of cDC populations in the mesenteric LN (MLN) confirmed the results seen in the ILN. A decrease in Zeb2 level is associated with a lower number of migratory cDCs in the MLN (Figure 9D, LEFT panel). Looking into detail to the resident cDC populations, we found a similar trend within the cDC1 and cDC2 populations in $Zeb2^{+/+}$, $Zeb2^{-/-}$, and $Zeb2^{Tg/Tg}$ mice (Figure 9D, MIDDLE panel) as observed in other tissues. Again a DP cDC population was present among the resident cDCs in the $Zeb2^{Tg/Tg}$ mice (Figure 9D, MIDDLE panel). Examination of the migratory cDCs in the MLN (Figure 9D, RIGHT panel) found similar trends to that observed in the SILP (Figure 4D).

As antigen presentation to naive T cells is the main cDC function, we next examined whether $Zeb2^{Tg/Tg}$ cDC1s and $Zeb2^{-/-}$ cDC2s could cross-present antigen to naive $CD8^+$ T cells or present antigen to naive $CD4^+$ T cells respectively. For this we FACS-purified splenic $Zeb2^{+/+}$ and $Zeb2^{Tg/Tg}$ cDC1s and $Zeb2^{+/+}$ and $Zeb2^{-/-}$ cDC2s and cultured them with either OTI ($CD8^+$) or OTII ($CD4^+$) T cells FACS-purified from spleens and LNs of OTI and OTII mice in the presence of purified ovalbumin protein. We did not observe any differences in the ability to cross-present antigen compared with WT controls (Figure 10A-B and 10D-E), as the cDCs were equally capable of inducing T-cell proliferation. Equally we did not observe any differences in the polarisation of proliferating T cells in either case, except for a significant increase in IL-10 production by OTII cells when co-cultured with $Zeb2^{-/-}$ cDC2s (Figure 10C and 10F).

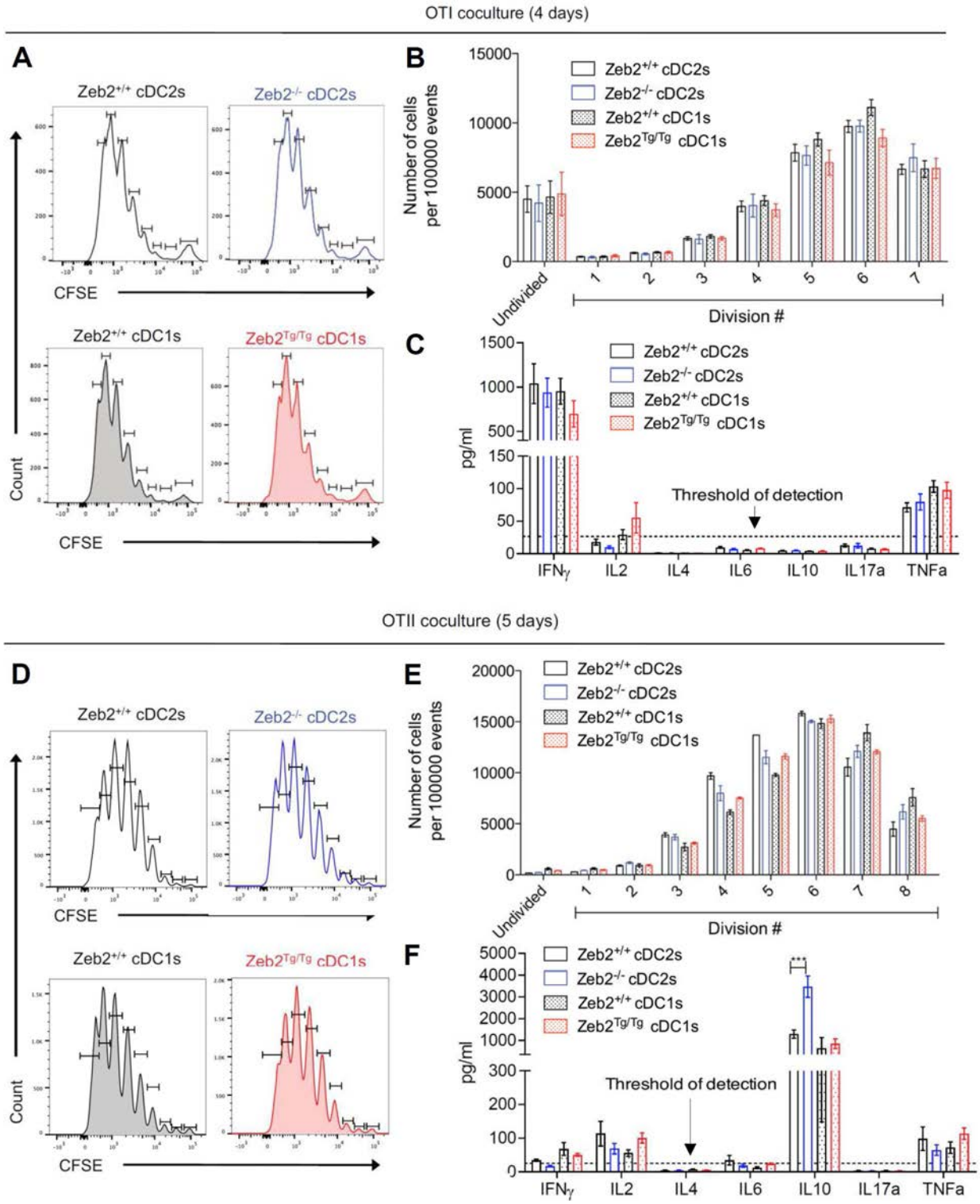

Figure 10 | Zeb2 expression levels do not alter the ability of cDCs to present antigen to T cells. (A and D) Representative histograms showing CFSE dilution on OTI T cells following 4 days of co-culture (A) or on OTII T cells following 5 days of co-culture (D) with $Zeb2^{+/+}$ or $Zeb2^{-/-}$ cDC2s and $Zeb2^{+/+}$ or $Zeb2^{Tg/Tg}$ cDC1s. (B) Proportion of live OTI T cells per 100.000 events per division number following 4 days of co-culture with $Zeb2^{+/+}$ or $Zeb2^{-/-}$ cDC2s and $Zeb2^{+/+}$ or $Zeb2^{Tg/Tg}$ cDC1s. Data are pooled from two experiments with at least n = 5 per group. No significance was detected with two-way ANOVA with Bonferroni post-test. (E) Proportion of live OTII T cells per 100.000 events per division number following 5 days of co-culture with $Zeb2^{+/+}$ or $Zeb2^{-/-}$ cDC2s and $Zeb2^{+/+}$ or $Zeb2^{Tg/Tg}$ cDC1s. Data are from one experiment, representative of two, with at least n = 2 per group. No significance was detected with two-way ANOVA with Bonferroni post-test. (C and F) Cytokines present in co-culture supernatants as measured by cytokine bead array. Data are pooled from two experiments with at least n = 4 per group. Error bars represent SEM. ***, $P < 0.001$. Two-way ANOVA with Bonferroni post-test.

Zeb2 acts as a cDC subset fate switch

Given our findings that Zeb2 functions during development to determine the ratio between the two cDC subsets across a range of mouse tissues, we next sought to investigate whether this is caused by Zeb2 acting as a subset fate switch. To this end, we generated a list of cDC1- and cDC2-associated genes across a range of tissues by examining the transcriptomes of distinct cDC1 and cDC2 subsets available on the Immunological Genome Project Consortium (DC.8+.Sp, DC.8+.MLN, DC.8+.SLN, DC.103+11b-.Lu and DC.103+11b-.SI for cDC1s; and DC.4+.Sp, DC.4+.MLN, DC.4+.SLN and DC.103-11b+24+.Lu for cDC2s). The expression of these genes in cDC1s and cDC2s across the range of Zeb2 expression levels was then examined. This analysis revealed that the $Zeb2^{Tg/Tg}$ cDC1s reduce their expression of some of the cDC1-associated genes including *Alms1, Btla, Cxcr3, Gcsam, Gpr33, Lrrc1, Ly75, Met, Pbx1,* and *Ttc39a* while increasing their expression of some of the cDC2-associated genes including *Apobec1, Clec4a1, Ddx58, Ehf, Itgam, Rtp4,* and *Sirpa* (Figure 11A and 11B). Conversely, $Zeb2^{-/-}$ cDC2s increased their expression of some of the cDC1-associated genes including *Cxcr3, Map4k5, Pbx1, Rnf144b, Snx22, Tmeff1,* and *Ttc39a*, whereas their expression of the cDC2-associated genes, with the exception of *Zeb2* itself, was largely unaffected (Figure 11A and 11B). It seems that the transcriptome of $Zeb2^{-/-}$ cDC2s leans towards a cDC1 transcriptome, while the transcriptome of $Zeb2^{Tg/Tg}$ cDC1s leans towards that of cDC2s. This suggests that Zeb2 could act as a cDC subset fate switch.

With this hypothesis in mind, we sought to focus further on the role of Zeb2 in cDC development. First, we examined how Zeb2 was induced during cDC development by analyzing *Zeb2* expression levels in WT BM-derived cDC subsets after culture of total BM with the canonical cDC growth factors Flt3L or GM-Csf (Csf2). As it has recently been shown that Csf2 BM cultures consist of both monocyte-derived DCs and cDCs[49], we used MHCII, CD115 (Csf1R) and CD26 expression to delineate cDCs and monocyte-derived DCs in these culture systems, concentrating our analysis on the $CD115^{-}CD11c^{+}MHCII^{hi}$ cDCs (Figure S5). Intriguingly, *Zeb2* expression was only induced in cDC2s from the Flt3L cultures (Figure 11C), demonstrating that Zeb2 expression is induced by Flt3L but not by Csf2-signalling.

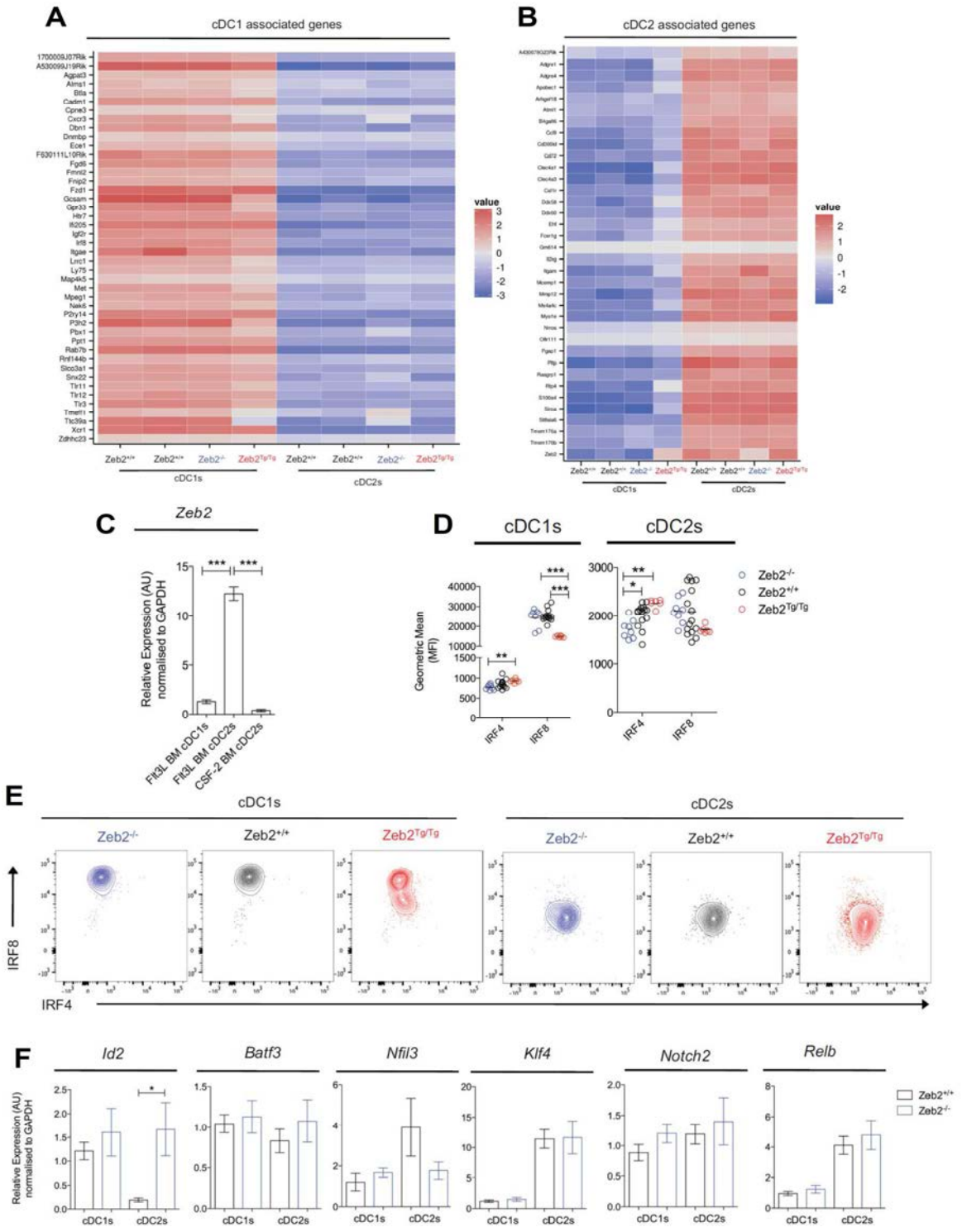

Figure 11 | Zeb2 expression levels dictate cDC subset fate. (A and B) Heat maps showing relative expression of cDC1-(A) and cDC2-(B) associated genes normalized per mean expression of each gene in cDC1s and cDC2s from indicated mice. (C) cDC1s from Flt3L WT BMDC cultures and cDC2s from WT Flt3L and WT Csf2 BMDC cultures were FACS-purified, and *Zeb2* expression was assessed by RT-qPCR. The results are expressed relative to *GAPDH* using the $2^{-\Delta\Delta C(t)}$ method with Flt3L BM cDC1s set to 1. Data are pooled from two experiments, with n = 6 per group. (D) Geometric mean (mean fluorescence intensity [MFI]) of Irf8 and Irf4 expression by splenic cDCs of indicated mice. Data are pooled from two experiments, with at least n = 6 per group. (C and D) One-way ANOVA with Bonferroni post-test. (E) Representative FACS plots showing Irf8 and Irf4 expression by splenic cDC subsets in indicated mice. (F) Splenic cDC1s and cDC2s were FACS-purified from $Zeb2^{+/+}$ or $Zeb2^{-/-}$ mice, and the indicated *TF* expression was assessed by RT-qPCR. The results are expressed relative to *GAPDH* using the $2^{-\Delta\Delta C(t)}$ method with $Zeb2^{+/+}$ cDC1s set to 1. Data are pooled from three experiments, with at least n = 3 per group. Two-way Student's t test. Error bars represent SEM. AU, arbitrary units.*, $P < 0.05$; **, $P < 0.01$; ***, $P < 0.001$.

Having shown that Zeb2 is induced during cDC development, we next investigated the effects of manipulating Zeb2 expression on the other TFs known to function in cDC development and terminal differentiation. Analysis of Irf8 and Irf4 protein expression in the cDCs of $Zeb2^{-/-}$, $Zeb2^{+/+}$ and $Zeb2^{Tg/Tg}$ mice revealed a striking decrease in Irf8 expression in $Zeb2^{Tg/Tg}$ cDC1s that was coupled with a significant increase in Irf4. We also observed a significant decrease in Irf4 expression in $Zeb2^{-/-}$ cDC2s, but this was not correlated with an increase in Irf8 expression (Figure 11D and 11E). Consistent with our earlier findings of an intermediate cDC1/cDC2 phenotype, the DP cDCs in the $Zeb2^{Tg/Tg}$ mice expressed intermediate levels of Irf8 and Irf4 (data not shown). In addition to Irf8 and Irf4, the TFs Id2, Batf3, Nfil3, Relb, Klf4 and Notch2 have all been implicated in cDC development and/or terminal differentiation[19,50,20,22,24,27,47,51,16,28,31,33] . As the expression levels of these TFs cannot be analyzed with flow cytometry, we instead examined their mRNA expression by RT-qPCR in $Zeb2^{-/-}$ cDC1s and cDC2s compared with their Zeb2-sufficient counterparts. Strikingly, we found a significant up-regulation of the cDC1-associated TF *Id2* among the $Zeb2^{-/-}$ cDC2 population (Figure 11F). Consistent with this, we found *Id2* to be differentially expressed in the RNA-sequencing data from $Zeb2^{Tg/Tg}$ cDC1s and $Zeb2^{-/-}$ cDC2s with a log2 FC of –0.6 or 0.6, respectively. We did not detect any other significant changes in the other TFs examined, although there was a trend toward less Nfil3 expression in $Zeb2^{-/-}$ cDC2s (Figure 11F).

Zeb2 regulates DC development by direct repression of Id2

To determine whether Id2 expression was also affected by the loss of Zeb2 early in cDC development, we next examined *Id2* mRNA levels in the cDC1- and cDC2-committed splenic pre-cDC populations. Similar to the results seen in the mature cDC populations, we found an increase in *Id2* expression among the $Zeb2^{-/-}$ pre-cDC2s (Figure 12A), suggesting that Zeb2 may function in cDC2s during development to repress Id2 expression. As Id2 is known to suppress pDC development by antagonizing the E protein TF E2-2[17,18,23,52,53], we also checked *Id2* and *E2-2* expression in the remaining pDCs in the $Zeb2^{-/-}$ mice. As observed for the cDC2s, we found a significant increase in *Id2* expression among the $Zeb2^{-/-}$ pDCs

(Figure 12B), suggesting Zeb2 may regulate both pDC and cDC development through regulation of *Id2* expression. We also detected a small but significant increase in *E2-2* expression in Zeb2$^{-/-}$ pDCs (Figure 12B).

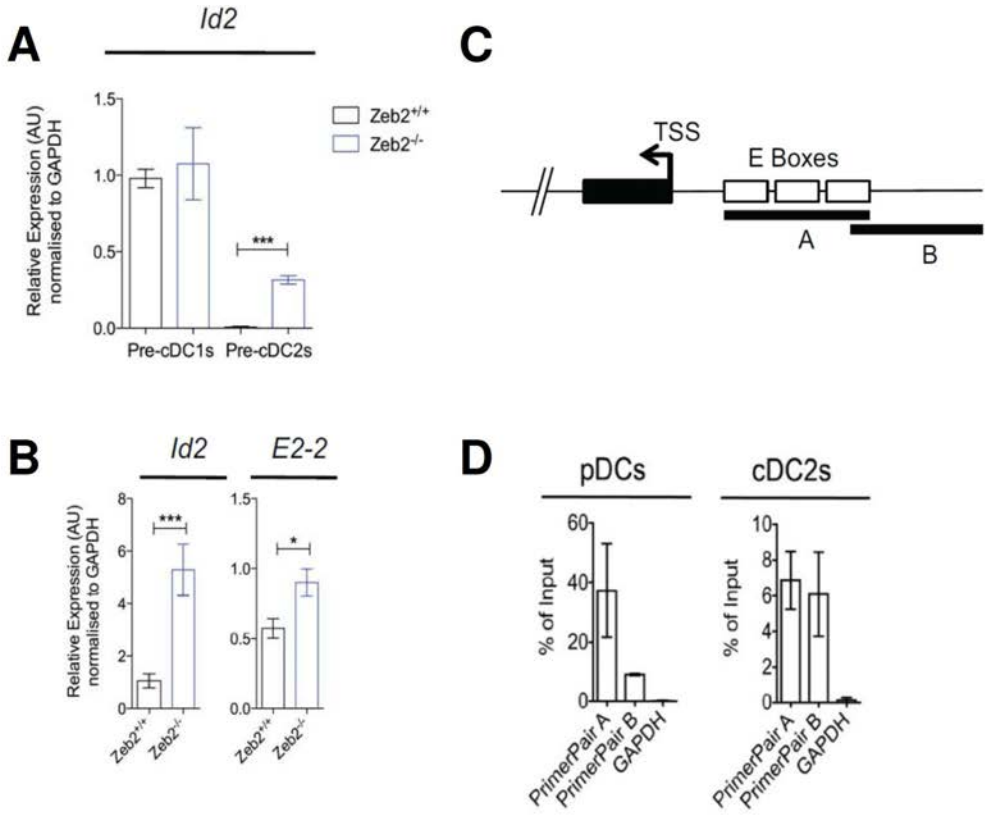

Figure 12 | Zeb2 regulates pDC and cDC development by repressing Id2. (A) Splenic pre-cDC1s and pre-cDC2s were FACS-purified from Zeb2$^{+/+}$ or Zeb2$^{-/-}$ mice and *Id2* expression was assessed by RT-qPCR. The results are expressed relative to *GAPDH* expression using the $2^{-\Delta\Delta C(t)}$ method with Zeb2$^{+/+}$ pre-cDC1s set to 1. Data are pooled from two experiments, with at least n = 2 per group. (B) Splenic pDCs were FACS-purified from Zeb2$^{+/+}$ or Zeb2$^{-/-}$ mice and *Id2* and *E2-2* expression was assessed by RT-qPCR. The results are expressed relative to *GAPDH* expression using the $2^{-\Delta\Delta C(t)}$ method with Zeb2$^{+/+}$ pDCs set to 1. Data are pooled from two experiments, with at least n = 7 per group. (A and B) Two-way Student's t test. Error bars represent SEM. AU, arbitrary units. *, P < 0.05; ***, P < 0.001. (C) Schematic representation of the *Id2* promoter with predicted E-boxes. A and B represent regions amplified by qPCR with primer pair A and primer pair B, respectively. TSS, transcription start site. (D) RT-qPCR analysis on chromatin samples obtained by ChIP performed against the FLAG-tag present on recombinant Zeb2 in splenic pDCs and cDC2s of Zeb2$^{Tg/Tg}$ mice. Data are expressed as the percentage of input. Data are pooled from two independent experiments, with n = 2 per group.

Thus, mechanistically, Zeb2 appears to function during DC development by repressing *Id2* expression, facilitating both pDC and cDC2 development. As Zeb2 is itself a TF, we next examined whether this effect was through direct binding of Zeb2

to the *Id2* promoter region or through an indirect mechanism. *In silico* analyses using PhysBinder[54] or ConTra[55] identified several conserved Zeb binding sites[56] in the *Id2* gene and its surrounding regions in mice and humans (Figure S8). Thus, we next designed two sets of primers to amplify two overlapping regions (A and B) in the *Id2* promoter containing the predicted binding sites (Figure 12C). RT-qPCR was performed on chromatin extracted from splenic pDCs and cDC2s of $Zeb2^{Tg/Tg}$ mice after chromatin immunoprecipitation (ChIP) with an antibody recognizing the FLAG-tag present on Zeb2 in these mice. For both pDCs and cDC2s, we observed a clear enrichment for region A, with ~40% for pDCs and ~6% for cDC2s, whereas region B was amplified with a percentage of enrichment of ~7% and ~5% in pDCs and cDC2s, respectively (Figure 12D). Thus, Zeb2 binds the E-boxes present in the *Id2* promoter, repressing its expression.

1.4 Discussion

TFs have a big influence on the transcriptome of a cell. This governs them with the power to control many cell features, including development, homeostasis and function. To date many TFs have been implicated in development and terminal differentiation of the different DC lineages. For the pDC lineage the most important TF is E2-2. E2-2 not only functions during development, but also maintains the cell fate of the mature pDC[18]. Looking at cDC1 commitment Id2, Batf3 and Irf8 play an essential role, with the last two already determining cell fate from the pre-cDC stage onward[6,16,21–25,29]. On the other hand Irf4, Notch2 and Klf4 are required for terminal differentiation of the cDC2 subset[19,26-31], but the TFs involved in the early commitment of this lineage have not yet been identified. Measuring mRNA levels of TF *Zeb2* along the DC lineage, we saw a low expression in early progenitors followed by an increase specifically in the pDC and cDC2 path from the pre-pDC and pre-cDC2 stage onward. This led us to the hypothesis that Zeb2 could be important in these two DC subsets.

We were able to pinpoint an importance for Zeb2 in the pDC lineage by crossing the $CD11c^{CRE}$ mice with either the $Zeb2^{fl/fl}$ or the R26-$Zeb2^{Tg/Tg}$ mice, generating mice lacking or overexpressing Zeb2 on one or both alleles in $CD11c^{+}$ cells. Loosing *Zeb2* on both alleles in $CD11c^{+}$ cells caused a severe reduction in the pDC population in spleen and blood, with only a very low number of splenic pDCs remaining. These remaining pDCs only show a minor decrease in *Zeb2* mRNA, suggesting these cells were not efficiently targeted by the $CD11c^{CRE}$ line and were able to reach full maturation. Interestingly, loss of only one allele of *Zeb2* had minimal effect on the pDCs, demonstrating that although Zeb2 is a crucial TF for pDC homeostasis, haplo-sufficient expression is able to generate a normal pDC population. Increasing Zeb2 expression on the other hand also had minimal impact on pDC numbers. We hypothesize that this is because pDCs already express high levels of Zeb2 in steady state, and so the moderate increase in Zeb2 expression driven by the Rosa-26 promoter does not provide significant advantage to the cells. Experiments with competitive BM chimeras revealed that the defect in pDCs in the $Zeb2^{-/-}$ mice was cell intrinsic and confirmed that Zeb2 expression is required for pDC homeostasis.

Trying to unravel how Zeb2 is able to control the pDC population, we determined the effect of loss of Zeb2 on the expression levels of two TFs important in pDC development, namely Id2 and E2-2[17,18,23,52]. Despite the small decrease in *Zeb2* mRNA level, the remaining splenic pDCs in Zeb2$^{-/-}$ mice showed a big increase in *Id2* and a smaller increase in *E2-2* mRNA levels. As Id2 antagonizes E2-2 dimerization, and hence its function as a transcriptional regulator[53], it could be that the increased E2-2 expression is an attempt of the Zeb2$^{-/-}$ pDCs to compensate for the increased Id2 levels. ChIP experiments showed that Zeb2 is able to directly bind the E-boxes present in the promoter region of *Id2* and in that way very likely represses *Id2* transcription. This explains why decreased expression of *Zeb2* in Zeb2$^{-/-}$ pDCs is associated with increased *Id2* expression. As Id2 functions during pDC development, and we showed that Zeb2 acts upstream of Id2 and is already highly expressed in pre-pDCs, we can conclude that Zeb2 not only regulates pDC homeostasis as stated before, but also pDC commitment. A cell intrinsic requirement for Zeb2 during pDC development was confirmed by Wu and colleagues[57]. Taken together we propose a model (Figure 14) in which Zeb2 regulates pDC development from the pre-pDC stage onward by directly repressing Id2, allowing the pDC TF E2-2 to bind DNA and induce pDC development.

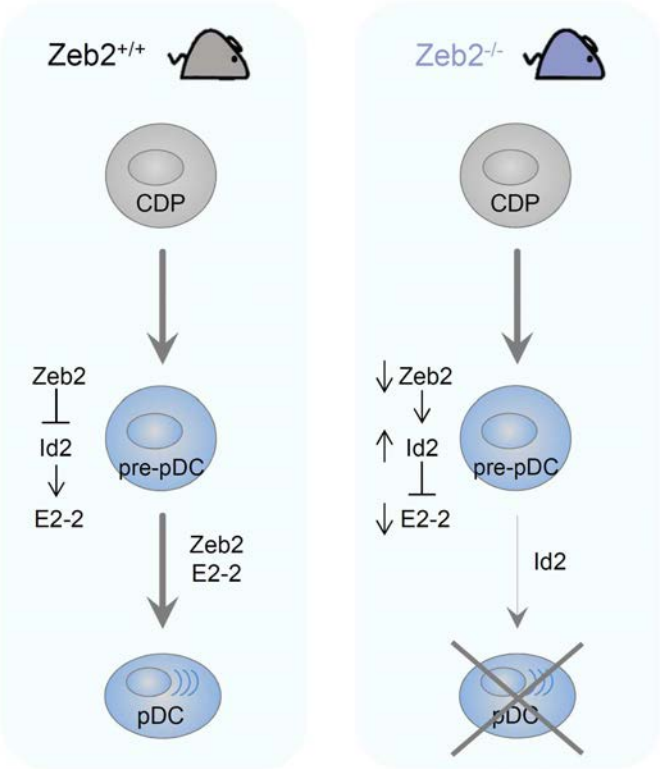

Figure 14 | Proposed model for the action of Zeb2 in pDC development. Zeb2 regulates pDC development from the pre-pDC stage onward by directly repressing Id2, allowing pDC TF E2-2 to induce pDC development.

Fitting with the high mRNA expression data for *Zeb2* in cDC2s, we found that ablation of Zeb2 expression in CD11c$^+$ cells resulted in a cell intrinsic reduction in cDC2s across multiple tissues, demonstrating that Zeb2 is required by cDC2s. This reduction in cDC2s was rather unexpectedly coupled with an increase in cDC1s, which was as well shown to be cell intrinsic. Overexpression of Zeb2 in CD11c$^+$ cells led to a cell intrinsic decrease in cDC1s in all tissues examined, while cDC2s remained unaffected. As hypothesized for the pDCs, we believe that this last finding is because the Rosa-26 promoter does not significantly increase the already high level of Zeb2 in cDC2s. Indeed, qPCR analysis revealed that cDC2s from Zeb2$^{Tg/Tg}$ mice do not express higher *Zeb2* mRNA levels than cDC2s from WT littermate controls. Comparing the different tissues, we found that not all are equally sensitive to the changes in Zeb2 expression. cDCs in the lung for instance appear to be very sensitive, as affecting only one allele of Zeb2 already gave significant differences in the presence of the cDC populations, whereas the cDCs in the liver were not affected by increased expression of Zeb2. This suggests the involvement of some local tissue-imprinting factors.

In the spleen of mice overexpressing Zeb2 in CD11c$^+$ cells we found a new XCR1$^+$SIRPα$^+$ (DP) cDC population and its presence was shown to be cell intrinsic. These DP cDCs were absent in all other tissues examined, except for the inguinal and mesenteric LN. This suggests that either the lymphoid environment is involved or that this is a consequence of the longer half-life of cDCs in lymphoid organs compared to cDCs in peripheral tissues. To our knowledge, such a population has not previously been reported. The intermediate expression of CD24, Irf4 and Irf8 puts forward the idea that the DP cDCs represent an intermediate subset between a cDC1 and a cDC2. This should be further confirmed by performing RNA-seq on this population and comparing the expression profile with that from WT splenic cDC1s and cDC2s. However, a high proportion of those splenic DP cDCs were apoptotic and they were absent from migratory populations in LNs, which led us believe that this intermediate population is dysfunctional.

When looking closer at the different SILP cDC populations, we found that the two cDC2 subsets were not equally affected by changes in Zeb2 expression. CD103$^-$ cDC2s were sensitive to the loss of Zeb2 in a cell intrinsic way, while their CD103$^+$ counterparts were unaffected. Thus SILP CD103$^+$ cDC2s do not require Zeb2 for their generation and, in terms of Zeb2 dependence, these cells are more similar to SILP CD103$^+$ cDC1s. This is not the first example where the CD103$^+$ cDC2s behave similarly to their cDC1 counterparts. Csf2R2b$^{-/-}$ mice, for example, have reduced cDC1 populations in the periphery, but also show a reduction in CD103$^+$ cDC2s in the SI[53,58,59]. Next to this, it has been shown that intestinal CD103$^+$ cDC2s express the typical cDC1 marker CD24[33]. However, there is also substantial evidence that the CD103$^+$ cDC2s represent a unique cDC subset in the gut. For example, the CD103$^+$ cDC2s are the only intestinal cDCs that have been reported to be Notch2 dependent[27], targeted in hu-Langerin diphtheria toxin A mice[60], and affected in mice that express a truncated form of Sirpα[61]. Very recently it was proposed that intestinal CD103$^+$ cDC2s depend on TgfβR-signalling[62] for their development. In addition, CD103$^+$ cDC2s were found to express CD101, SiglecF and Epcam, three markers we showed to be upregulated in splenic Zeb2$^{-/-}$ cDC2s. Additionally, CD103$^+$ cDC2s are dependent on Csf2[58] and we showed that cDC2s from Csf2 BM cultures do not express Zeb2. Furthermore, Zeb2 is known to antagonize Tgfβ-mediated transcription[63]. All of this together suggests that high expression of Zeb2 in CD103$^-$ cDC2s inhibits TgfβR-mediated signalling, whereas the low expression of Zeb2, possibly a consequence of Csf2-signalling, in CD103$^+$ cDC2s allows TgfβR-mediated signalling resulting in the differentiation of this subset and the expression of its typical markers CD101 and SiglecF. Further research is needed to test this hypothesis and further unravel the regulation of intestinal CD103$^+$ cDC2s and the link between intestinal CD103$^-$ and CD103$^+$ cDC2s.

In terms of DC function, it seems that, at least in steady state conditions, the role for Zeb2 is rather limited. The decreased presence of migratory cDCs in Zeb2$^{-/-}$ mice suggests a function for Zeb2 in their capacity to migrate, which was also predicted by the RNA-seq data. As migratory cDCs show a similar trend in cDC1 and cDC2 presence upon altering Zeb2 levels as tissue resident DCs, we believe that the

influence of Zeb2 in migration is the same for the different cDC subsets. The impact on migration could be attributed to the fact that Zeb2 controls the expression of several junctional proteins and hence inhibits cell-cell adhesion[46,64–67]. Zeb2 has been identified before as crucial for the migration of many cell types, including neural crest cells, cortical GABAergic neurons, melanoblasts and many carcinoma cells[36,39,40]. It is likely that also for DC migration Zeb2 behaves in a similar way and that loss of Zeb2 expression leads to increased adhesion to for instance epithelial cells or endothelial cells lining lymph vessels, and thus lowers the ability of DCs to migrate. This hypothesis is supported by the RNA-seq results in which we found an elevated expression of adhesion molecules like *Cldn1*, *Epcam*, *Itgad*, *Cdh17* and *SiglecF* and the down-regulation of migration facilitating *Mmp9* and chemokine related genes (*Cxcr1*, *Ccr2*, *Ackr3* and *Cx3cl1*) upon ablation of Zeb2 in cDC2s. In addition to migration, we also investigated if Zeb2 has an effect on the antigen presenting capacity of cDCs. In conclusion we did not observe any differences in the ability of $Zeb2^{Tg/Tg}$ cDC1s and $Zeb2^{-/-}$ cDC2s to induce naive $CD4^+$ or $CD8^+$ T cell proliferation and polarization in the steady state when compared to their WT counterparts. The only significant difference found, was an increased IL-10 production by $CD4^+$ T cells upon antigen presentation by $Zeb2^{-/-}$ cDC2s. Interestingly, the expression of CD101, for which we found an increased expression on the surface of $Zeb2^{-/-}$ cDC2s, on $CD11c^+$ cells has been associated with increased IL-10 production[68,69]. IL-10 is typically linked with a Treg phenotype and hence the regulation of immune response and self-tolerance[70]. We did not evaluate the presence of Treg cells in $Zeb2^{-/-}$ mice, but in $Zeb2^{-/-}$ cDC2/$CD4^+$ T cell co-cultures we did not find a difference in the presence of $Foxp3^+$ Treg cells (data not shown). Although ablation of Zeb2 decreased the presence of cDC2s, it could be that the remaining ones have an increased ability to prevent auto-immunity or allograft rejection. As so far we only studied steady state conditions and further examination of the functional consequences of altering Zeb2 expression levels during infection and inflammation settings are still required.

To date, we have limited evidence that Zeb2 expression has impact on DC function, but the TF does skew the prevalence of the cDC subtypes. Previously described cDC2 TFs all function in terminally differentiated cDC2s, but here we compiled evidence for Zeb2 functioning during cDC2 development. In the spleen we found an increase in pre-cDC2s with increasing levels of Zeb2, coupled with a decrease in pre-cDC1s pointing toward a role for Zeb2 in controlling cDC2 development. Also, loss of Zeb2 expression in mature DCs did not cause a shift in cDC subset prevalence and we did not find any evidence for a function for Zeb2 in cell survival, supporting the idea that Zeb2 does not operate in terminally differentiated cDCs. Together with the fact that $Zeb2^{-/-}$ cDC2s express cDC1-associated genes and $Zeb2^{Tg/Tg}$ cDC1s express cDC2-associated genes, this led to the hypothesis that Zeb2 acts as a cDC subset fate switch. We suggest that the absence or overexpression of Zeb2 switches the fate of the majority of pre-cDCs, resulting in the development of cDC1s or cDC2s respectively. However, this is not 100% efficient, as some pre-cDCs do become either cDC2s or cDC1s in $Zeb2^{-/-}$ and $Zeb2^{Tg/Tg}$ mice, respectively, and consequently these express some genes typically associated with the alternate subset. A possible explanation for the remaining cDC2s in the $Zeb2^{-/-}$ mice is the existence of different subsets within the cDC2 population. It could be that there is a cDC2 subpopulation that depends on Zeb2 for its development which is no longer present in the $Zeb2^{-/-}$ mice. Whereas the cDC2s that remain do not require Zeb2 for their development, but rather for maintaining a proper cDC2 identity. The partial Zeb2-dependence in cDC2s was independently confirmed by the group of Kenneth Murphy. In their study they suggest that Zeb2 does not control the cDC2 lineage, but rather represses the cDC1 lineage[64]. However, this hypothesis does not explain the cell intrinsic reduction or increase of cDC2s in $Zeb2^{-/-}$ or $Zeb2^{Tg/Tg}$ mice respectively. We believe that Zeb2 acts as a cDC subset fate switch, with its absence skewing the cDCs toward the cDC1 lineage and its overexpression skewing the cDCs toward the cDC2 lineage.

We were able to unravel, at least partially, the mechanism behind this Zeb2 controlled fate switch as well upstream as downstream of the TF. Using both Csf2 and Flt3L supplemented BM-derived DC cultures, we demonstrated that Zeb2 expression is induced by Flt3L, but not by Csf2-signalling. This is consistent with

recent findings that cDC2s, apart from CD103^{+} cDC2s in the small intestine lamina propria, develop normally in mice lacking Csf2[58]. So Zeb2 acts downstream of Flt3L and this is limited to the cDC2 lineage. Further downstream, Zeb2 acts in a similar way as in pDCs. Our ChIP experiments on cDC2s showed that Zeb2 binds to the E-boxes present in the *Id2* promoter which subsequently leads to repression of Id2 expression. In the cDC1 lineage, Zeb2 expression is not induced and hence Id2 is expressed and driving cDC1 commitment.

Collectively our results lead to the model pictured in Figure 15. We propose that in cDC development, Zeb2 functions downstream of Flt3L to regulate commitment toward the cDC2 lineage by repressing Id2. As such, Zeb2 represents the first TF to be described that is involved in the early commitment of pre-cDCs toward the cDC2 lineage.

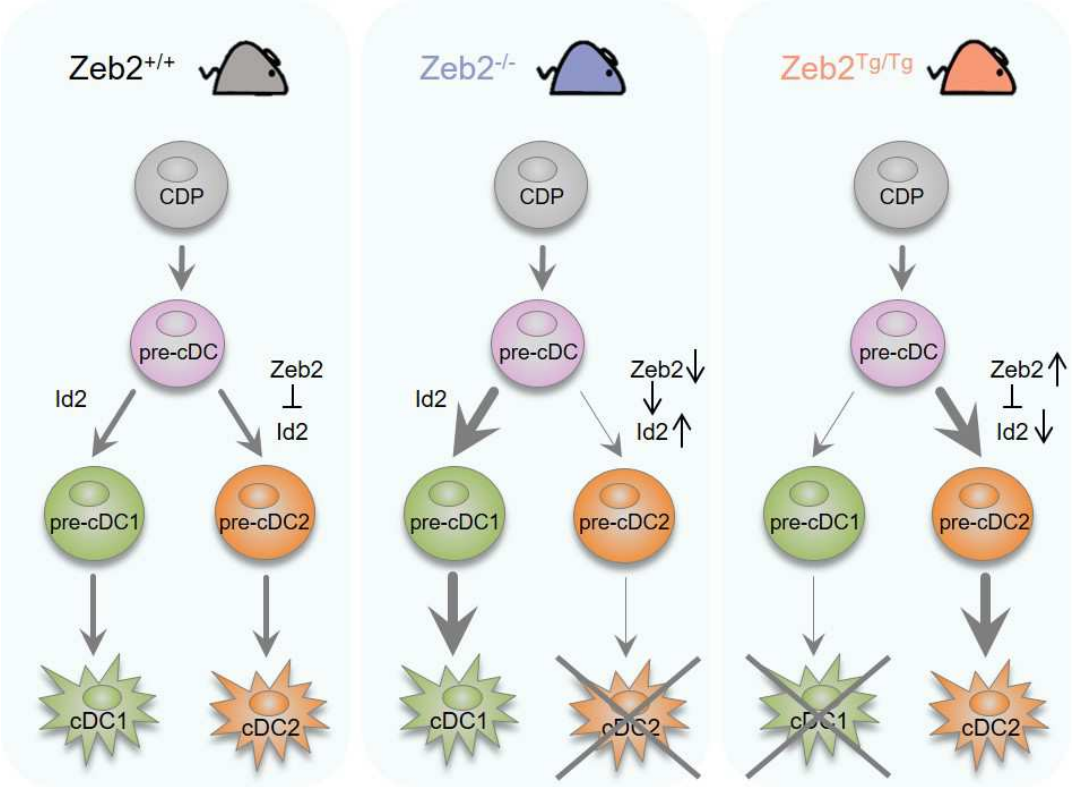

Figure 15 | Proposed model for the action of Zeb2 in cDC development. Zeb2 regulates commitment to the cDC2 lineage by repressing Id2. Hence, loss of Zeb2 expression leads to increased Id2 expression skewing the cDCs toward the cDC1 lineage. On the other hand overexpression of Zeb2 leads to decreased expression of Id2 skewing the cDCs toward the cDC2 lineage.

1.5 Materials and methods

Mice

The generation of $Zeb2^{fl/fl}$ and R26-$Zeb2^{Tg/Tg}$ mice was described previously[45,46]. Mice were backcrossed to a C57BL/6 background for at least seven generations before crossing with the $CD11c^{CRE}$ mice[47] or late-$CD11c^{CRE}$ mice[34]. OTI and OTII mice were purchased from Jackson Laboratories and backcrossed to the $Rag^{-/-}$ background. All mice were bred and maintained at the Vlaams Instituut voor Biotechnologie (Ghent University) under specific pathogen-free conditions and were used between 6 and 12 weeks of age. All experiments were performed in accordance with the ethical committee of the Faculty of Science.

Generation of competitive BM chimeric mice

Competitive BM chimeric mice were generated by lethally irradiating CD45.1/CD45.2 WT mice with a single dose of 8 Gy. 12 hours later mice were reconstituted by intravenous injection of 5 x 10^6 BM cells, which were a ~1:1 mix of CD45.1 WT and CD45.2 $Zeb2^{-/-}$, $Zeb2^{+/+}$ or $Zeb2^{Tg/Tg}$ BM cells. Chimerism was assessed 10 weeks after irradiation in liver, lung, spleen and SI.

Isolation of tissue leukocytes

For the isolation of liver leukocytes, livers were isolated from phosphate buffered saline (PBS)-perfused mice, chopped finely, and incubated for 15–20 min with 1 mg/ml collagenase A (Sigma-Aldrich) and 10 U/ml DNase (Roche) in a shaking water bath at 37°C. Cells were passed through a 70-µm cell strainer. For the isolation of lung, spleen and LN leukocytes, lungs, spleens and LNs were isolated from PBS-perfused mice, chopped finely, and incubated for 30 min with 0.2 mg/ml Liberase TM (Roche) and 10 U/ml DNase (Roche) in a shaking water bath at 37°C. Cells were passed through a 70-µm cell strainer. SILP leukocytes were isolated as described

previously[78]. Briefly, small intestines (SIs) were flushed with PBS or RPMI containing 2% fetal calf serum (FCS) and Peyer's patches were excised. After opening longitudinally and cutting into 0.5 cm segments, they were incubated twice with PBS containing 2mm EDTA (Ethylene-diamine-tetra-acetic acid) in a shaking water bath at 37°C for 20 min. Then the tissue was digested with 1 mg/ml collagenase VIII (Sigma-Aldrich) in a shaking water bath at 37°C for 15 min. Cells were passed through a 40-µm cell strainer. Pre-cDCs were isolated from spleens by gently pressing the spleens through a 70-µm filter (no enzymes) to allow for the detection of SiglecH. BM cells were obtained by flushing femurs and tibias with RPMI. In all instances, except for the SI, red blood cells were lysed with an in house made osmotic lysis buffer (10mM $KHCO_3$, 155 mM NH_4Cl and 0.1 mM EDTA in PBS) before staining for flow cytometric analysis.

BMDC cultures

Total BM was harvested from WT mice, and 2 x 10^6 cells were cultured in RPMI supplemented with Glutamax and Gentamicin in a well of a 6-well plate for 7 days with either 250 ng/ml Flt3L and 10% FCS for Flt3L cultures or 20 ng/ml Csf2 and 5% FCS for Csf2 cultures. Csf2 BMDCs were further supplemented with additional media, FCS and Csf2 at day 3 of culture.

Magnetic pre-enrichment: negative selection of T, B, NK cells and neutrophils

Before FACS-purification of pre-cDCs and cDCs a negative selection for T, B, NK cells and neutrophils was performed on splenic single cell suspensions. For this, cells were first incubated for 20 min with following biotin labelled antibodies; NK1.1 (PK136), CD19 (1D3), CD3e (145-2c11) and Ly6G (1A8). Next, samples were washed and resuspended in cell separation buffer (10mM EDTA and 2% FCS in PBS) in FACS tubes. After incubating with magnetic streptavidin beads (Magnisort; eBioscience) for 10 min at RT, tubes were placed in a magnet for 10 min at room temperature (RT). Supernatant was poured off and tubes were washed with

separation buffer and again left for 10 min at RT in the magnets. Supernatant was poured off and after a second round of magnetic sorting, samples were further processed for FACS.

Flow cytometry and FACS

For flow cytometry, 3–4 x 10^6 cells were stained at 4°C in the dark with antibodies (Table 1). Intracellular staining of Irf4 and Irf8 was performed after fixing and permeabilizing of the cells with a Foxp3 TF-staining buffer set (eBioscience). Data were acquired on a cell analyser (LSRFortessa; BD) and analyzed using FlowJo software (Tree Star). Before FACS-purification of pre-cDCs and cDCs a magnetic pre-enrichment was performed as stated before. Cells were FACS-purified using a flow cytometer (FACSAria II or FACSAria III; BD). After sorting, a purity check was performed for all samples.

Table 1 | Antibodies used for flow cytometry

Antibody	Clone	Antibody	Clone
Fc Block	2.4G2	CD11b	M1/70
Fixable Viability Dye	eBioscience	CD11c	N418
CCR2	475301	CD127	SB/199
CD3e	145-2c11	CD135	A2F10
CD4	RM4-5	CD161	PK136
CD8	53-6.7	CD172a	P84
CD19	1D3	CD317	120g8
CD24	M1-69	CXCR1	SA011F11
CD26	H194-112	Epcam	G8.8
CD38	90	F4/80	BM8
CD45	30-F11	IA-IE	M5/114.15.2
CD45.1	A20	Irf4	M-17
CD45.2	104	Irf8	V3GYWCH
CD45R	RA3-6B2	Ly6C	AL-21
CD64	X54-5/7.1	NK1.1	PK136
CD69	H1.2F3	Sca1	D7
CD101	Moushi101	SiglecF	E50-2440
CD103	2E7	SiglecH	440c
CD115	AFS98	Ter-119	Ter-119
CD117	2B8	Xcr1	ZET

Splenic cDC spiking in Flt3L BMDC cultures

At day 0 a Flt3L BMDC culture was started up as described before from WT CD45.1 mice and 1 x 10^6 cells were seeded in a well of a 24-well plate. At day 4 splenic CD45.2 cDC1s and CD45.2 cDC2s from mice of interest were FACS-purified (as described before) and 6,000 cells per well were spiked into the Flt3L BMDC cultures. Cultures were further supplemented with Flt3L (250 ng/ml) and Csf2 (1 ng/ml). 1, 2, 4 and 6 days after spiking of the splenic cDCs, cells were harvested by roughly pipetting and number of surviving CD45.2 cDCs was assessed by flow cytometry.

Cocultures of cDCs with ovalbumin (OVA) specific OTI or OTII cells

Naive $CD62L^+CD8^+$ (OTI) or $CD4^+$ (OTII) T cells were FACS-purified from the spleen and lymph nodes of $Rag^{-/-}$ OTI or OTII mice. Isolated T cells were incubated with 5 µM CellTrace CFSE (Thermofisher Scientific) for 7 min at 37°C. Splenic cDC1s or cDC2s were FACS-sorted from mice of interest and 10,000 cDCs were cocultured with 50.000 OTI or OTII cells in the presence of 100 µg/ml OVA protein (Worthington). After 4 days for OTI and 5 days for OTII cocultures, culture supernatant was harvested and stored at -20°C for further analyses with a CBA assay. On those same days cells were harvested and CFSE dilution in T cells was assessed by flow cytometry.

CBA assay: BD Cytometric Bead Array (CBA) Mouse Th1/Th2/Th17 Cytokine Kit

To asses concentrations of IFNγ, IL-2, IL-4, IL-6, IL-10, IL-17a and TNFα in supernatant from cDC/T cell cocultures, we performed the CBA Mouse Th1/Th2/Th17 Cytokine Kit from BD (cat. Nr 560485) according to the manufacturer's instructions. Briefly, the following workflow was performed. Preparing cytokine standards, mixing of capture beads, dilution of samples, performing instrument setup, performing the cytokine assay, acquiring data and data analysis. A detailed protocol can be found in the kit manual.

RNA sequencing

25,000 cDC1s or cDC2s from Zeb2$^{-/-}$, Zeb2$^{+/+}$ and Zeb2$^{Tg/Tg}$ mice were FACS-purified into 500 µl of buffer (RLT Plus; QIAGEN) and β-mercaptoethanol. RNA was isolated using an RNeasy Plus micro kit (QIAGEN) and sent to the Vlaams Instituut voor Biotechnologie Nucleomics facility, where the RNA-sequencing was performed using a NextSeq sequencer (Illumina). The pre-processing of the RNA-sequencing data was done by Trimmomatic. The adapters were cut off, and reads were trimmed when the quality dropped below 20. Reads with a length <35 were discarded. All samples passed quality control based on the results of FastQC. Reads were mapped to the mouse reference genome via Tophat2 and counted via HTSeqCount. Samples were subsequently analyzed using R/Bioconductor and the DESeq2 procedure was used to normalize the data.

Gene expression analysis by RT-qPCR

RNA was purified from sorted cells using an RNeasy Plus micro kit (QIAGEN). RNA was reverse transcribed to cDNA with an iScript Advanced cDNA Synthesis kit (Bio-Rad Laboratories). Gene expression was assayed by RT-qPCR using a SensiFast SYBR No-Rox kit (GC Biotech) on a PCR amplification and detection instrument (LightCycler 480; Roche) with the primers listed in Table 2. Gene expression was normalized to *GAPDH*, and the mean relative gene expression was calculated using the $2^{-\Delta\Delta C(t)}$ method.

Table 2 | Primers used for RT-qPCR

Gene	Forward primer	Reverse primer
Batf3	5'-CAGACCCAGAAGGCTGACAAG-3'	5'-CTGCGCAGCACAGAGTTCTC-3'
E2-2	5'-CGAAAAGTTCCTCCGGGTTTG-3'	5'-CGTAGCCGGGCTGATTCAT-3'
GAPDH	5'-GCATGGCCTTCCGTGTTC-3'	5'-TGTCATCATACTTGGCAGGTTTCT-3'
Id2	5'-TCCTGTCCTTGCAGGCATCTGAAT-3'	5'AACGTGTTCTCCTGGTGAAATGGC-3'
Klf4	5'-CGATGAACTGACCAGGCACTAC-3'	5'-CCTCTTCATGTGTAAGGCAAGGTG-3'
Nfil3	5' GAACTCTGCCTTAGCTGAGGT-3'	5- ATTCCCGTTTTCTCCGACACG-3'
Notch2	5'-CCACCTGCCTGGATAAGATCG-3'	5'-CTGCCCGTTGTTCACACAC-3'
RelB	5'-GAATGTCGTCAGGATCTGC-3'	5'-TGGTGGACTTCTTGTCGTAG-3'
Zeb2	5'-GGCAAGGCCTTCAAGTACAA-3'	5'-AAGCGTTTCTTGCAGTTTGG-3'

ChIP and Id2 RT-qPCR

FACS-purified pDC and cDC2 cells from Zeb2$^{Tg/Tg}$ mice were cross-linked with 1% paraformaldehyde in fixation buffer (Active Motif). After nuclei isolation, DNA was fragmented with 25 U micrococcal nuclease for 20 min at 37°C in micrococcal nuclease-digesting buffer (50 mM Tris-HCl, pH 7.6, 1 mM $CaCl_2$, and 0.2% Triton X-100). DNA fragment size (150–500 bp) was confirmed after chromatin preparation in a 1.2% agarose gel. The fragmented chromatin was incubated overnight with 10 µg FLAG-M2 antibody (F3165; Sigma-Aldrich) followed by a pull-down assay using A/G-conjugated agarose beads (EMD Millipore). DNA was purified with an iPure kit (Diagenode) and the quality was measured using a 2100 Bioanalyzer system with a DNA kit (High Sensitivity; Agilent Technologies). RT-qPCR was performed on a Zeb-predicted binding site identified in the Id2 promoter with the following primers: 5′-TACCTGACAAAGAGCTTCCC-3′ and 5′-TTACATACACTGCCCTTGGT-3′ (primer pair A) or 5′-ATGTGGCTGCATCTAGGAA-3′ and 5′-GGGAAGCTCTTTGTCAGGTA-3′ (primer pair B). Primers in the coding sequence of the *GAPDH* gene were used as a control of unspecific binding with the primer pair 5′-TTGAGCTAGGACTGGATAAGCAGG-3′ and 5′-AGTCCGTATTTATAGGAACCCGG-3′. The percentage of enrichment to the input was calculated and shown in a bar graph.

Statistical analysis

Groups were compared with a two-way Student's t test, and multiple-group comparisons were performed using one-way ANOVA followed by a Bonferroni post-test with Prism Software (GraphPad Software). Samples were assumed to be normally distributed with similar variance between groups. No randomization was used to determine experimental groups, and no blinding of the investigator was performed. Group sizes were determined on the basis of previous experience.

Accession numbers

RNA-sequencing data have been deposited in the Gene Expression Omnibus public database under accession no. GSE79903.

1.6 References

1. Gilliet M, Cao W, Liu Y-JJ. Plasmacytoid dendritic cells: sensing nucleic acids in viral infection and autoimmune diseases. *Nature reviews. Immunology*. 2008;8(8):594–606.
2. Swiecki M, Colonna M. The multifaceted biology of plasmacytoid dendritic cells. *Nature reviews. Immunology*. 2015;15(8):471–85.
3. Merad M, Sathe P, Helft J, Miller J, Mortha A. The dendritic cell lineage: ontogeny and function of dendritic cells and their subsets in the steady state and the inflamed setting. *Annu. Rev. Immunol.* 2013;31:563–604.
4. Guilliams M, Ginhoux F, Jakubzick C, et al. Dendritic cells, monocytes and macrophages: a unified nomenclature based on ontogeny. *Nat. Rev. Immunol.* 2014;14(8):571–8.
5. Murphy TL, Grajales-Reyes GE, Wu X, et al. Transcriptional Control of Dendritic Cell Development. *Annu. Rev. Immunol.* 2016;34:93–119.
6. Hildner K, Edelson BT, Purtha WE, et al. Batf3 deficiency reveals a critical role for CD8alpha+ dendritic cells in cytotoxic T cell immunity. *Science*. 2008;322(5904):1097–100.
7. Bachem A, Güttler S, Hartung E, et al. Superior antigen cross-presentation and XCR1 expression define human CD11c+CD141+ cells as homologues of mouse CD8+ dendritic cells. *The Journal of experimental medicine*. 2010;207(6):1273–81.
8. Haniffa M, Shin A, Bigley V, et al. Human tissues contain CD141hi cross-presenting dendritic cells with functional homology to mouse CD103+ nonlymphoid dendritic cells. *Immunity*. 2012;37(1):60–73.
9. Guilliams M, Dutertre C-AA, Scott CL, et al. Unsupervised High-Dimensional Analysis Aligns Dendritic Cells across Tissues and Species. *Immunity*. 2016;45(3):669–684.
10. Naik SH, Sathe P, Park H-YY, et al. Development of plasmacytoid and conventional dendritic cell subtypes from single precursor cells derived in vitro and in vivo. *Nat. Immunol.* 2007;8(11):1217–26.
11. Liu K, Victora GD, Schwickert TA, et al. In vivo analysis of dendritic cell development and homeostasis. *Science*. 2009;324(5925):392–7.
12. Onai N, Obata-Onai A, Schmid MA, et al. Identification of clonogenic common Flt3+M-CSFR+ plasmacytoid and conventional dendritic cell progenitors in mouse bone marrow. *Nature immunology*. 2007;8(11):1207–16.
13. Onai N, Kurabayashi K, Hosoi-Amaike M, et al. A clonogenic progenitor with prominent plasmacytoid dendritic cell developmental potential. *Immunity*. 2013;38(5):943–57.
14. Fogg DK, Sibon C, Miled C, et al. A clonogenic bone marrow progenitor specific for macrophages and dendritic cells. *Science*. 2006;311(5757):83–87.
15. Schlitzer A, Sivakamasundari V, Chen J, et al. Identification of cDC1- and cDC2-committed DC progenitors reveals early lineage priming at the common DC progenitor stage in the bone marrow. *Nat. Immunol.* 2015;16(7):718–28.
16. Grajales-Reyes GE, Iwata A, Albring J, et al. Batf3 maintains autoactivation of Irf8 for commitment of a CD8α(+) conventional DC clonogenic progenitor. *Nat. Immunol.* 2015;16(7):708–17.
17. Cisse B, Caton ML, Lehner M, et al. Transcription factor E2-2 is an essential and specific regulator of plasmacytoid dendritic cell development. *Cell*. 2008;135(1):37–48.
18. Ghosh HS, Cisse B, Bunin A, Lewis KL, Reizis B. Continuous expression of the transcription factor e2-2 maintains the cell fate of mature plasmacytoid dendritic cells. *Immunity*. 2010;33(6):905–16.
19. Tamura T, Tailor P, Yamaoka K, et al. IFN regulatory factor-4 and -8 govern dendritic cell subset development and their functional diversity. *Journal of immunology (Baltimore, Md.: 1950)*. 2005;174(5):2573–81.
20. Tailor P, Tamura T, Morse HC, Ozato K. The BXH2 mutation in IRF8 differentially impairs dendritic cell subset development in the mouse. *Blood*. 2008;
21. Sichien D, Scott CL, Martens L, et al. IRF8 Transcription Factor Controls Survival and Function of Terminally Differentiated Conventional and Plasmacytoid Dendritic Cells, Respectively. *Immunity*. 2016;45(3):626–640.
22. Edelson BT, Bradstreet TR, KC W, et al. Batf3-dependent CD11b(low/-) peripheral dendritic cells are GM-CSF-independent and are not required for Th cell priming after subcutaneous immunization. *PLoS ONE*. 2011;6(10):e25660.
23. Hacker C, Kirsch RD, Ju X-SS, et al. Transcriptional profiling identifies Id2 function in dendritic cell development. *Nat. Immunol.* 2003;4(4):380–6.

24. Jackson JT, Hu Y, Liu R, et al. Id2 expression delineates differential checkpoints in the genetic program of CD8α+ and CD103+ dendritic cell lineages. *EMBO J.* 2011;30(13):2690–704.
25. Kusunoki T, Sugai M, Katakai T, et al. TH2 dominance and defective development of a CD8+ dendritic cell subset in Id2-deficient mice. *J. Allergy Clin. Immunol.* 2003;111(1):136–42.
26. Satpathy AT, Briseño CG, Lee JS, et al. Notch2-dependent classical dendritic cells orchestrate intestinal immunity to attaching-and-effacing bacterial pathogens. *Nat. Immunol.* 2013;14(9):937–48.
27. Lewis KL, Caton ML, Bogunovic M, et al. Notch2 receptor signaling controls functional differentiation of dendritic cells in the spleen and intestine. *Immunity*. 2011;35(5):780–91.
28. Tussiwand R, Everts B, Grajales-Reyes GE, et al. Klf4 expression in conventional dendritic cells is required for T helper 2 cell responses. *Immunity*. 2015;42(5):916–28.
29. Bajaña S, Turner S, Paul J, Ainsua-Enrich E, Kovats S. IRF4 and IRF8 Act in CD11c+ Cells To Regulate Terminal Differentiation of Lung Tissue Dendritic Cells. *J. Immunol.* 2016;196(4):1666–77.
30. Suzuki S, Honma K, Matsuyama T, et al. Critical roles of interferon regulatory factor 4 in CD11bhighCD8alpha- dendritic cell development. *Proc. Natl. Acad. Sci. U.S.A.* 2004;101(24):8981–6.
31. Persson EK, Uronen-Hansson H, Semmrich M, et al. IRF4 transcription-factor-dependent CD103(+)CD11b(+) dendritic cells drive mucosal T helper 17 cell differentiation. *Immunity*. 2013;38(5):958–69.
32. Tamura T, Tailor P, Yamaoka K, et al. IFN regulatory factor-4 and -8 govern dendritic cell subset development and their functional diversity. *J. Immunol.* 2005;174(5):2573–81.
33. Schlitzer A, McGovern N, Teo P, et al. IRF4 Transcription Factor-Dependent CD11b+ Dendritic Cells in Human and Mouse Control Mucosal IL-17 Cytokine Responses. *Immunity*. 2013;38(5):970–983.
34. Williams JW, Tjota MY, Clay BS, et al. Transcription factor IRF4 drives dendritic cells to promote Th2 differentiation. *Nat Commun*. 2013;4:2990.
35. Murphy KM. Transcriptional control of dendritic cell development. *Advances in immunology*. 2013;120:239–67.
36. De Craene B, Berx G. Regulatory networks defining EMT during cancer initiation and progression. *Nat. Rev. Cancer*. 2013;13(2):97–110.
37. Goossens S, Janzen V, Bartunkova S, et al. The EMT regulator Zeb2/Sip1 is essential for murine embryonic hematopoietic stem/progenitor cell differentiation and mobilization. *Blood*. 2011;117(21):5620–30.
38. Li J, Riedt T, Goossens S, et al. The EMT transcription factor Zeb2 controls adult murine hematopoietic differentiation by regulating cytokine signaling. *Blood*. 2017;129(4):460–472.
39. Denecker G, Vandamme N, Akay O, et al. Identification of a ZEB2-MITF-ZEB1 transcriptional network that controls melanogenesis and melanoma progression. *Cell Death Differ.* 2014;21(8):1250–61.
40. Hegarty SV, Sullivan AM, O'Keeffe GW. Zeb2: A multifunctional regulator of nervous system development. *Prog. Neurobiol.* 2015;132:81–95.
41. Van Helden MJ, Goossens S, Daussy C, et al. Terminal NK cell maturation is controlled by concerted actions of T-bet and Zeb2 and is essential for melanoma rejection. *J. Exp. Med.* 2015;212(12):2015–25.
42. Dominguez CX, Amezquita RA, Guan T, et al. The transcription factors ZEB2 and T-bet cooperate to program cytotoxic T cell terminal differentiation in response to LCMV viral infection. *J. Exp. Med.* 2015;212(12):2041–56.
43. Omilusik KD, Best JA, Yu B, et al. Transcriptional repressor ZEB2 promotes terminal differentiation of CD8+ effector and memory T cell populations during infection. *J. Exp. Med.* 2015;212(12):2027–39.
44. Miller JC, Brown BD, Shay T, et al. Deciphering the transcriptional network of the dendritic cell lineage. *Nat. Immunol.* 2012;13(9):888–99.
45. Higashi Y, Maruhashi M, Nelles L, et al. Generation of the floxed allele of the SIP1 (Smad-interacting protein 1) gene for Cre-mediated conditional knockout in the mouse. *Genesis (New York, N.Y. : 2000)*. 2002;32(2):82–4.
46. Tatari MN, De Craene B, Soen B, et al. ZEB2-transgene expression in the epidermis compromises the integrity of the epidermal barrier through the repression of different tight junction proteins. *Cell. Mol. Life Sci.* 2014;71(18):3599–609.
47. Caton ML, Smith-Raska MR, Reizis B. Notch-RBP-J signaling controls the homeostasis of CD8- dendritic cells in the spleen. *The Journal of experimental medicine*. 2007;204(7):1653–64.

48. Scott CL, Bain CC, Wright PB, et al. CCR2(+)CD103(-) intestinal dendritic cells develop from DC-committed precursors and induce interleukin-17 production by T cells. *Mucosal Immunol*. 2015;8(2):327–39.
49. Helft J, Böttcher J, Chakravarty P, et al. GM-CSF Mouse Bone Marrow Cultures Comprise a Heterogeneous Population of CD11c(+)MHCII(+) Macrophages and Dendritic Cells. *Immunity*. 2015;42(6):1197–211.
50. Wu L, D'Amico A, Winkel KD, et al. RelB is essential for the development of myeloid-related CD8alpha- dendritic cells but not of lymphoid-related CD8alpha+ dendritic cells. *Immunity*. 1999;9(6):839–47.
51. Kashiwada M, Pham N-LL, Pewe LL, Harty JT, Rothman PB. NFIL3/E4BP4 is a key transcription factor for CD8α⁺ dendritic cell development. *Blood*. 2011;117(23):6193–7.
52. Spits H, Couwenberg F, Bakker AQ, Weijer K, Uittenbogaart CH. Id2 and Id3 inhibit development of CD34(+) stem cells into predendritic cell (pre-DC)2 but not into pre-DC1. Evidence for a lymphoid origin of pre-DC2. *The Journal of experimental medicine*. 2000;192(12):1775–84.
53. Li HS, Yang CY, Nallaparaju KC, et al. The signal transducers STAT5 and STAT3 control expression of Id2 and E2-2 during dendritic cell development. *Blood*. 2012;120(22):4363–73.
54. Broos S, Soete A, Hooghe B, Moran R. PhysBinder: improving the prediction of transcription factor binding sites by flexible inclusion of biophysical properties. *Nucleic acids.* 2013;41:W531-534.
55. Broos S, Hulpiau P, Galle J, et al. ConTra v2: a tool to identify transcription factor binding sites across species, update 2011. *Nucleic acids research*. 2011;39(suppl_2):W74–W78.
56. Remacle JE, Kraft H, Lerchner W, et al. New mode of DNA binding of multi-zinc finger transcription factors: deltaEF1 family members bind with two hands to two target sites. *The EMBO journal*. 1999;18(18):5073–84.
57. Wu X, Briseño CG, Grajales-Reyes GE, et al. Transcription factor Zeb2 regulates commitment to plasmacytoid dendritic cell and monocyte fate. *Proc. Natl. Acad. Sci. U.S.A.* 2016;113(51):14775–14780.
58. Greter M, Helft J, Chow A, et al. GM-CSF controls nonlymphoid tissue dendritic cell homeostasis but is dispensable for the differentiation of inflammatory dendritic cells. *Immunity*. 2012;36(6):1031–46.
59. Mayer JU, Demiri M, Agace WW, et al. Different populations of CD11b(+) dendritic cells drive Th2 responses in the small intestine and colon. *Nature communications*. 2017;8:15820.
60. Welty NE, Staley C, Ghilardi N, et al. Intestinal lamina propria dendritic cells maintain T cell homeostasis but do not affect commensalism. *The Journal of experimental medicine*. 2013;210(10):2011–24.
61. Scott CL, Tfp ZM, Beckham KS, Douce G, Mowat AM. Signal regulatory protein alpha (SIRPα) regulates the homeostasis of CD103(+) CD11b(+) DCs in the intestinal lamina propria. *Eur. J. Immunol.* 2014;44(12):3658–68.
62. Bain CC, Montgomery J, Scott CL, et al. TGFβR signalling controls CD103+CD11b+ dendritic cell development in the intestine. *Nat Commun*. 2017;8(1):620.
63. Postigo AA. Opposing functions of ZEB proteins in the regulation of the TGFbeta/BMP signaling pathway. *The EMBO journal*. 2003;22(10):2443–52.
64. Comijn J, Berx G, Vermassen P, et al. The two-handed E box binding zinc finger protein SIP1 downregulates E-cadherin and induces invasion. *Molecular cell*. 2001;7(6):1267–78.
65. Vandewalle C, Comijn J, De Craene B, et al. SIP1/ZEB2 induces EMT by repressing genes of different epithelial cell-cell junctions. *Nucleic acids research*. 2005;33(20):6566–78.
66. Shirakihara T, Saitoh M, Miyazono K. Differential regulation of epithelial and mesenchymal markers by deltaEF1 proteins in epithelial mesenchymal transition induced by TGF-beta. *Molecular biology of the cell*. 2007;18(9):3533–44.
67. Eger A, Aigner K, Sonderegger S, et al. DeltaEF1 is a transcriptional repressor of E-cadherin and regulates epithelial plasticity in breast cancer cells. *Oncogene*. 2005;24(14):2375–85.
68. Schey R, Dornhoff H, Baier JL, et al. CD101 inhibits the expansion of colitogenic T cells. *Mucosal Immunol*. 2016;9(5):1205–17.
69. Bouloc A, Bagot M, Delaire S, Bensussan A, Boumsell L. Triggering CD101 molecule on human cutaneous dendritic cells inhibits T cell proliferation via IL-10 production. *Eur. J. Immunol.* 2000;30(11):3132–9.
70. Zhu J, Paul WE. CD4 T cells: fates, functions, and faults. *Blood*. 2008;112(5):1557–69.
71. Cerovic V, Houston SA, Scott CL, et al. Intestinal CD103(-) dendritic cells migrate in lymph and prime effector T cells. *Mucosal immunology*. 2013;6(1):104–13.

1.7 Supplementary figures and tables

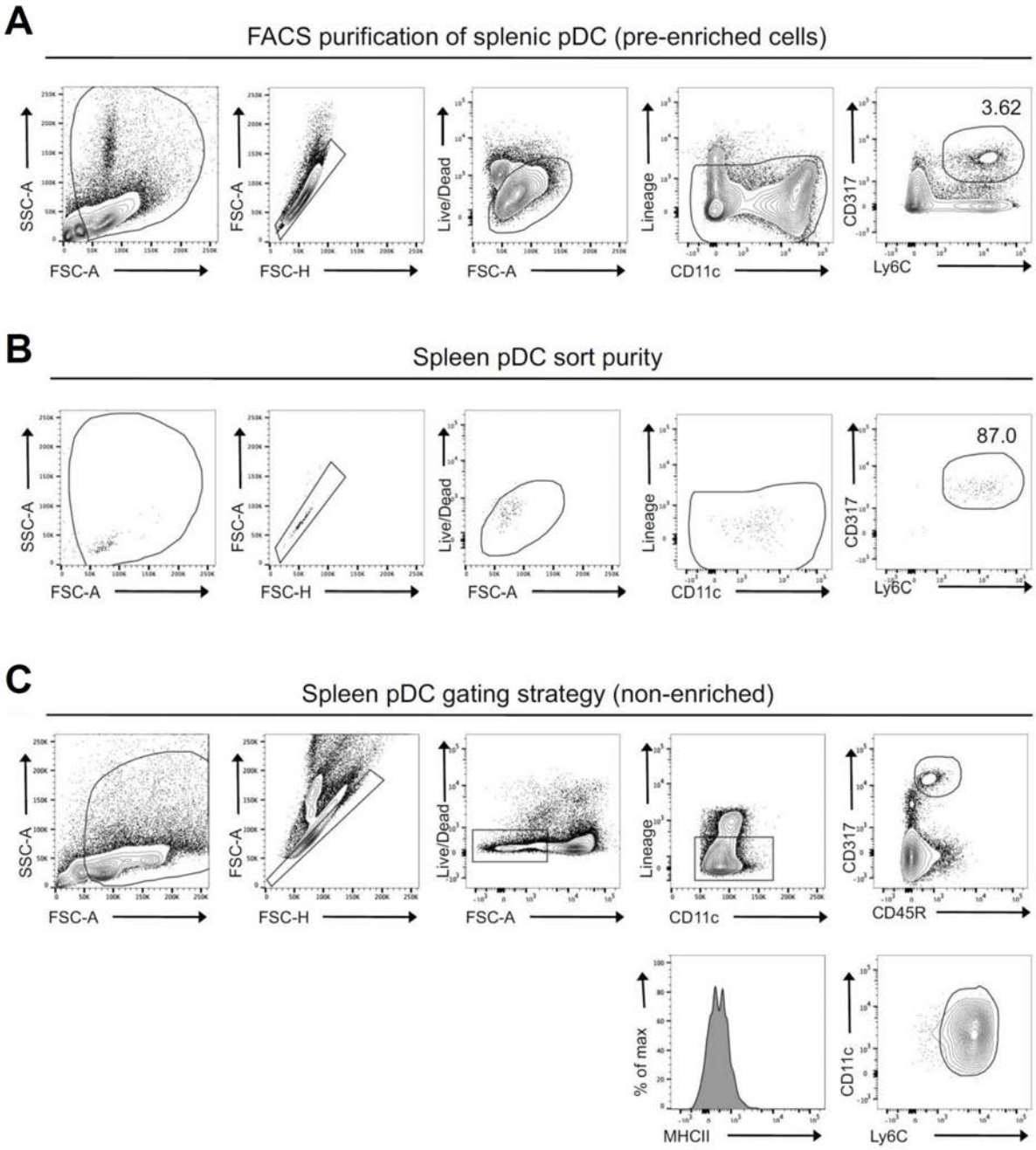

Figure S1 | Splenic pDC gating strategies. (A) Representative FACS plots showing gating strategy for purification of splenic pDCs. The number represent the proportion of pDCs as a percentage of total cells. Samples were pre-enriched using streptavidin negative selection beads (Magnisort; eBioscience). (B) Representative FACS plots showing purity of splenic pDCs after sorting. The number represents the proportion of pDCs as a percentage of total cells. (C) Representative FACS plots showing gating strategy for non-enriched splenic pDCs and CD11c, Ly6C and MHCII expression in splenic pDCs. FSC, forward scatter. SSC, side scatter.

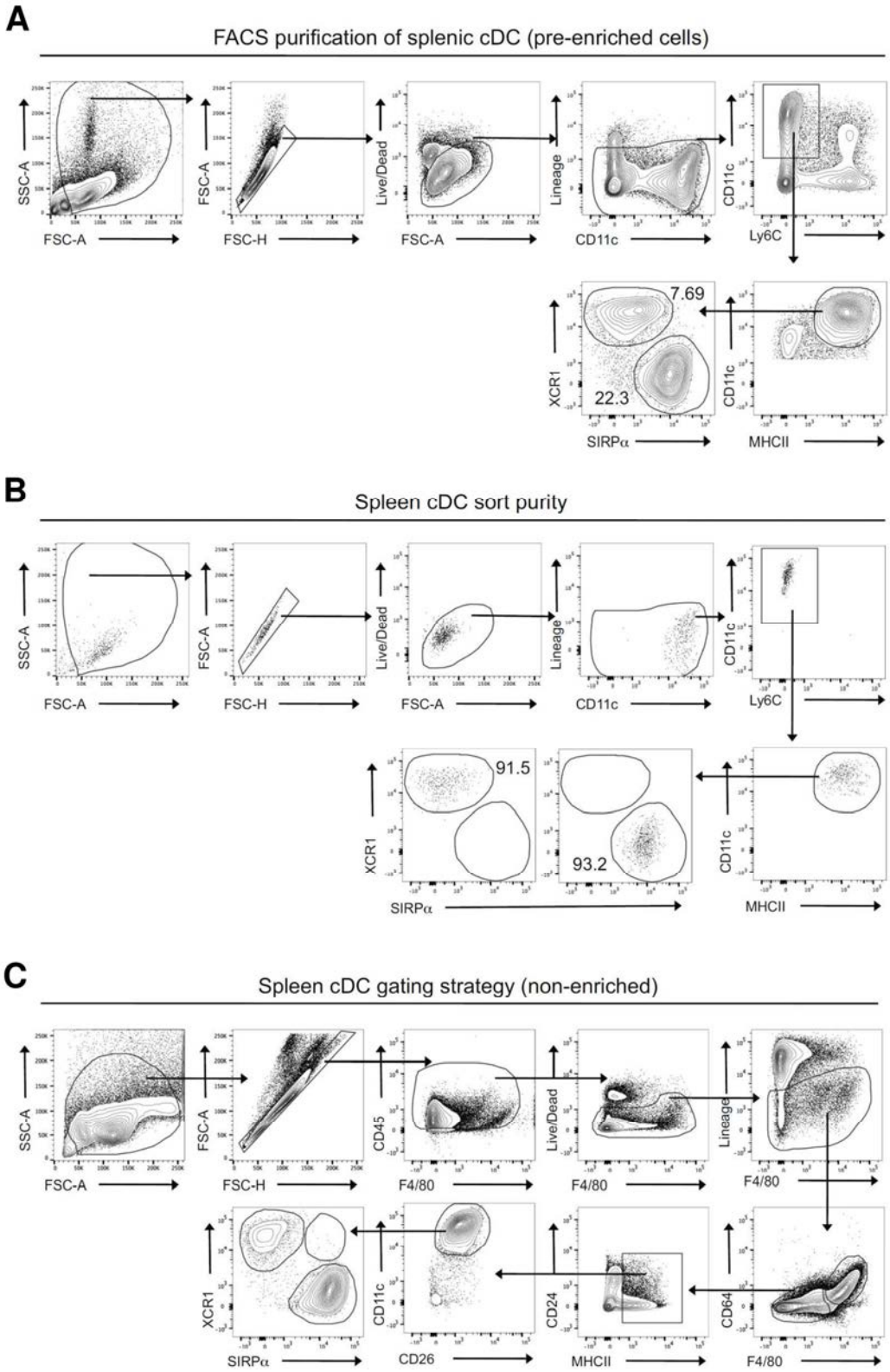

Figure S2 | Splenic cDC gating strategies. (A) Representative FACS plots showing gating strategy for purification of splenic cDC subsets. The numbers represent the proportion of each cDC subset as a percentage of total cells. Samples were pre-enriched using streptavidin negative selection beads (Magnisort; eBioscience). (B) Representative FACS plots showing purity of splenic cDC subsets after sorting. The numbers represent the proportion of each cDC subset as a percentage of total cells. (C) Representative FACS plots showing gating strategy for non-enriched splenic cDC subsets. FSC, forward scatter. SSC, side scatter.

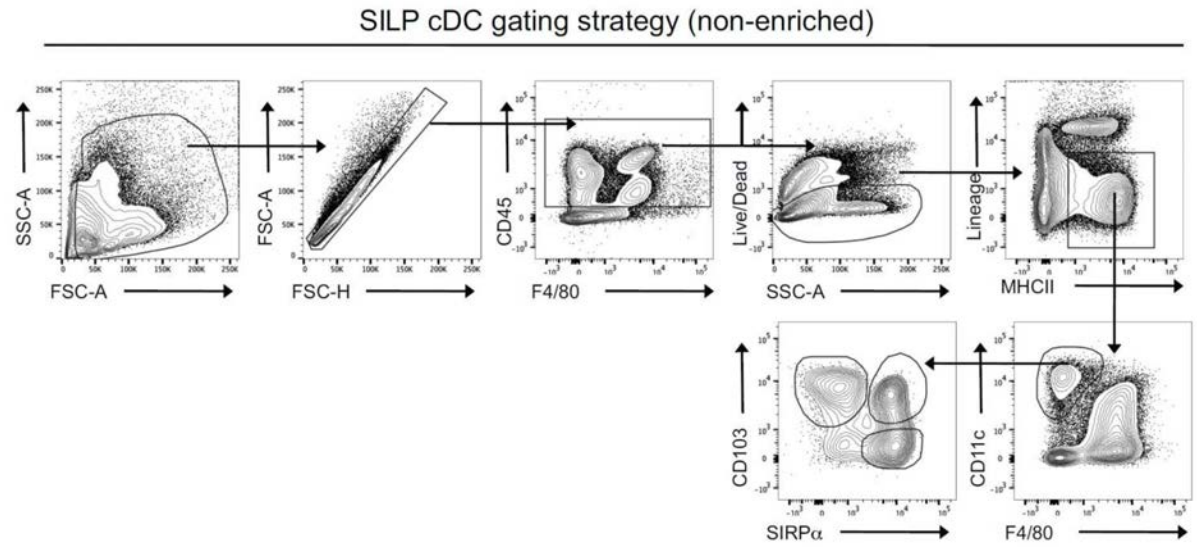

Figure S3 | Gating strategy for SILP cDC subsets. Representative FACS plots showing gating strategy for non-enriched CD103^{+} cDC1s, CD103^{+} cDC2s, and CD103^{-} cDC2s in the SILP. FSC, forward scatter. SSC, side scatter.

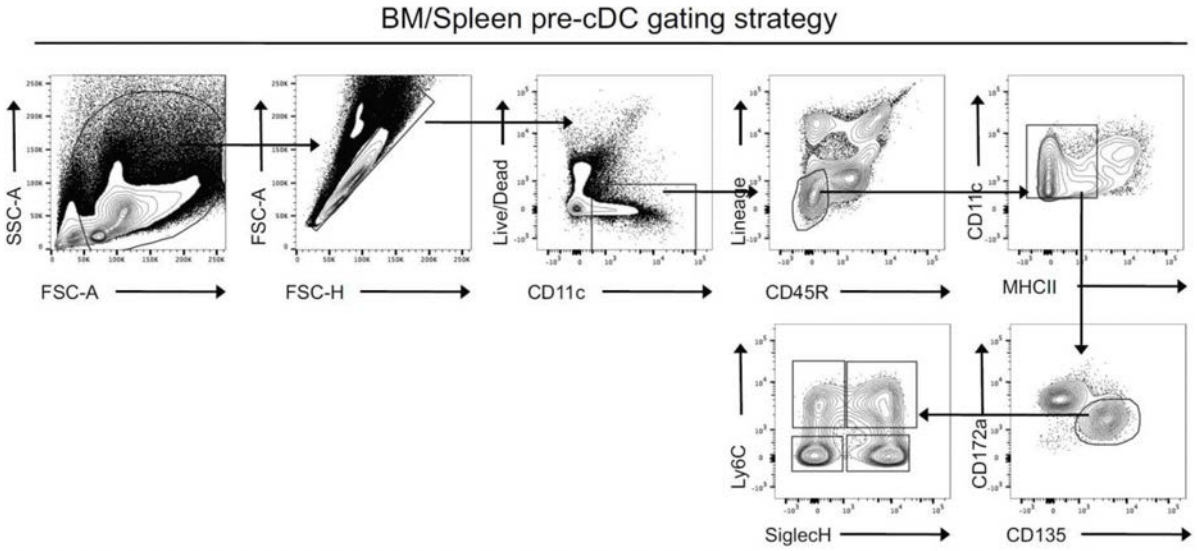

Figure S4 | BM and splenic pre-cDC gating strategy. Representative FACS plots showing gating strategy for identification of pre-cDC subsets in the BM and the spleen. Plots shown are from a BM sample. FSC, forward scatter. SSC, side scatter.

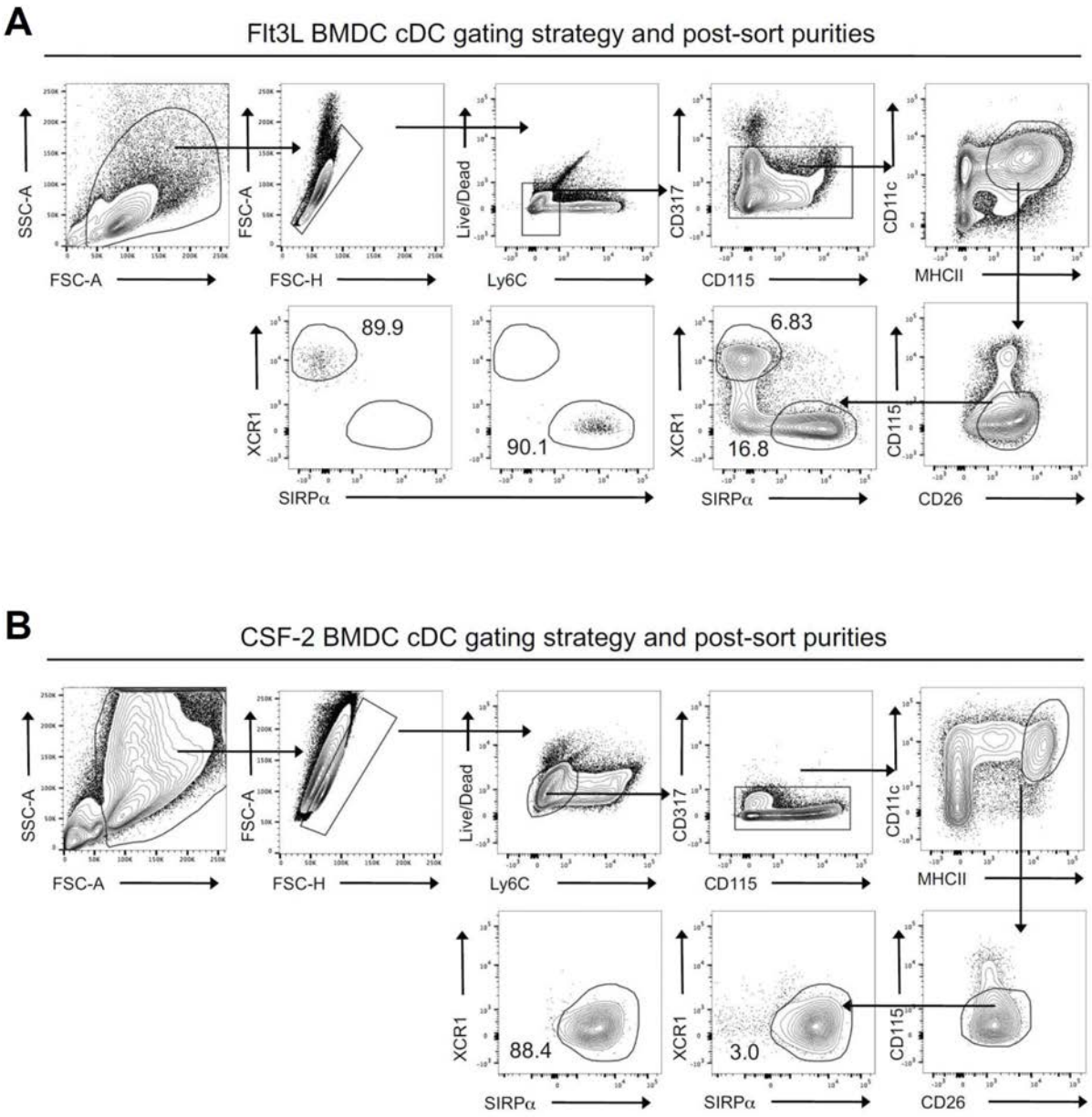

Figure S5 | BMDC gating strategies and post-sort purities. (A en B) Representative FACS plots showing gating strategy and post-sort purities for WT Flt3L BMDC cultures (A) and WT Csf2 BMDC cultures (B). The numbers represent the proportion of indicated cells as a percentage of total cells. FSC, forward scatter. SSC, side scatter.

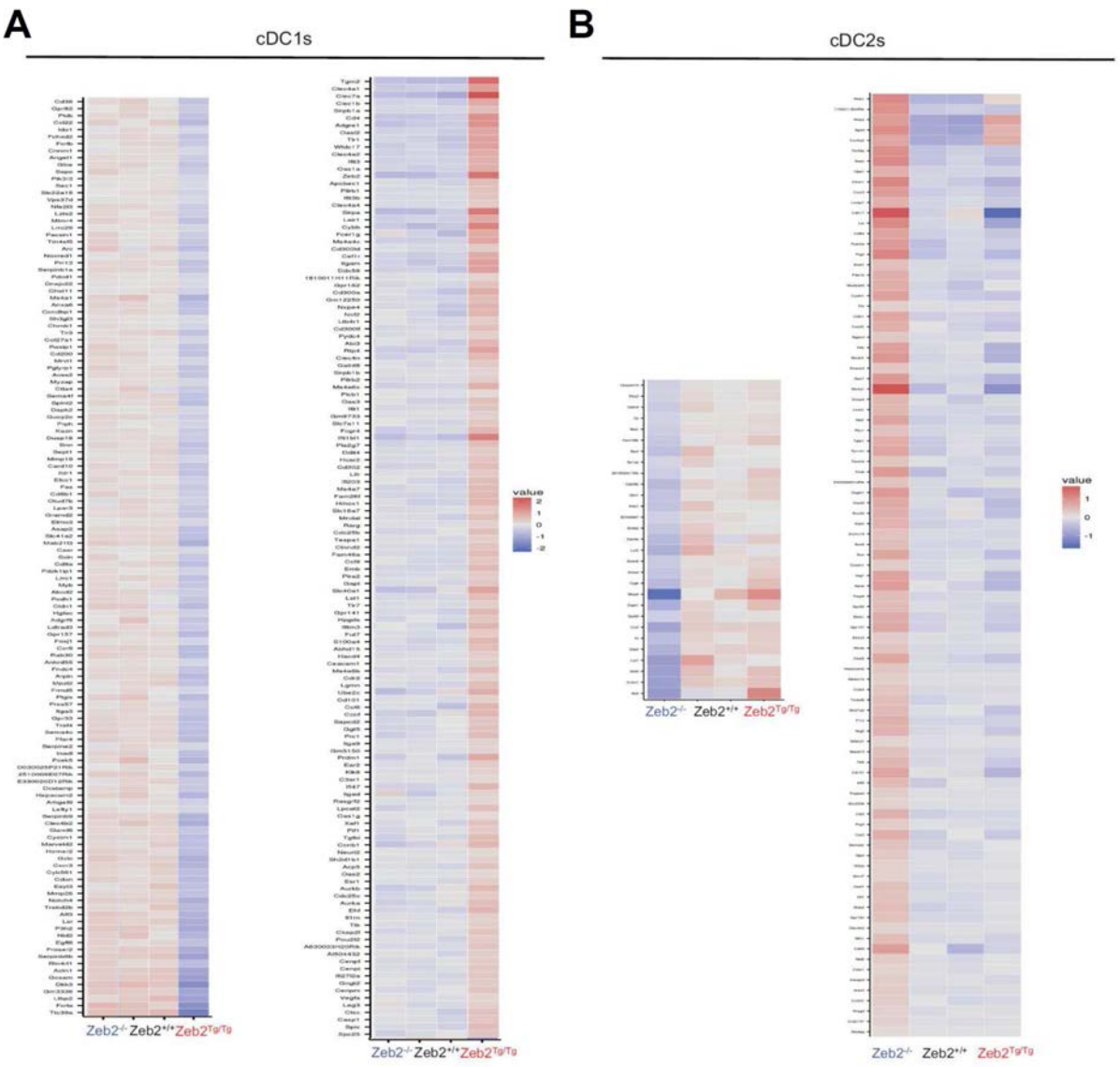

Figure S6 | Zeb2 expression levels control gene expression in cDCs. (A) Heatmap of genes differentially expressed between splenic Zeb2$^{+/+}$and Zeb2$^{Tg/Tg}$ cDC1s shown for splenic Zeb2$^{-/-}$, Zeb2$^{+/+}$ and Zeb2$^{Tg/Tg}$ cDC1s. Genes are listed in Table S1. (B) Heatmap of genes differentially expressed between splenic Zeb2$^{+/+}$and Zeb2$^{-/-}$ cDC2s shown for splenic Zeb2$^{-/-}$, Zeb2$^{+/+}$ and Zeb2$^{Tg/Tg}$ cDC2s. Genes are listed in Table S2.

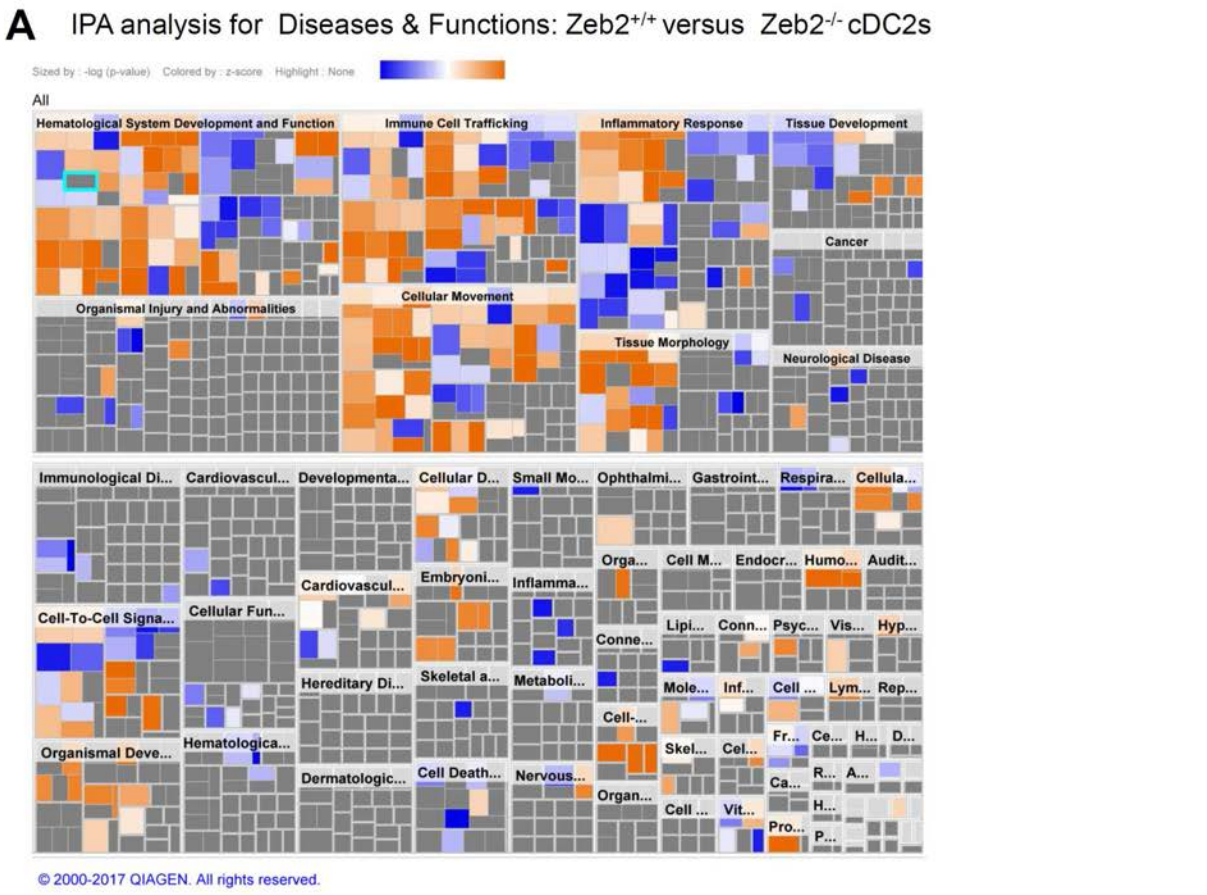

Figure S7 | Functional consequences of Zeb2 expression levels. (A) IPA analysis showing enriched Diseases & Functions in genes differentially expressed between splenic Zeb2$^{+/+}$and Zeb2$^{-/-}$ cDC2s. (B) IPA analysis showing enriched Diseases & Functions in genes differentially expressed between splenic Zeb2$^{+/+}$and Zeb2$^{Tg/Tg}$ cDC1s.

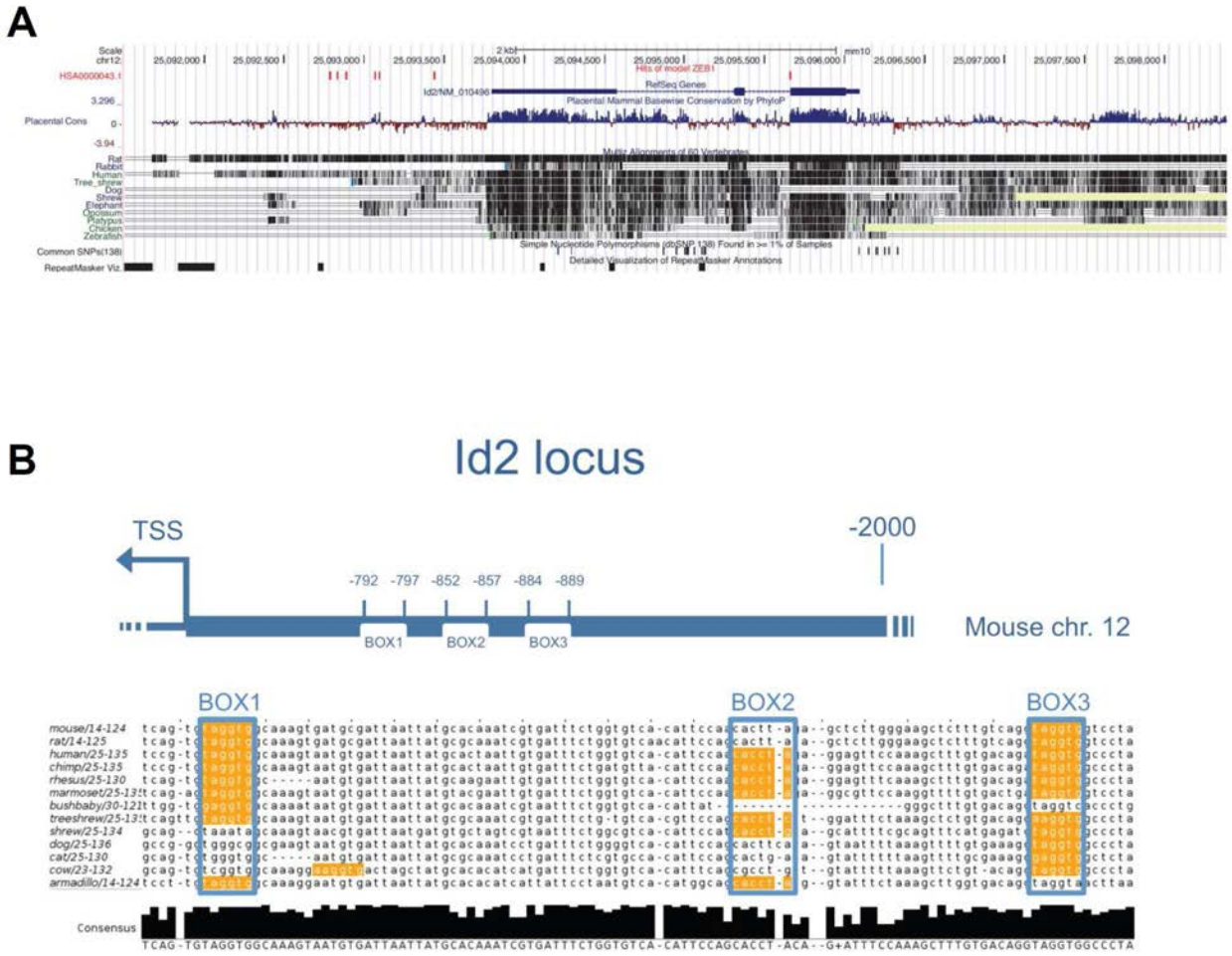

Figure S8 | Predicted Zeb binding sites in *Id2* locus. (A) Physbinder predictions for Zeb1 binding sites in *Id2* locus and surrounding regions. Zeb1 was used as a model for Zeb2, as the binding motifs are conserved between them. The red lines indicate predicted Zeb binding sites. Sequence conservation among other species is also depicted. (B) The top shows a schematic representation of the *Id2* promoter region and ConTra-predicted Zeb E-box binding sites. The bottom shows sequence conservation of these E-boxes across multiple species. TSS, transcription start site. Chr., chromosome.

Table S1 | Differentially expressed genes: Zeb2$^{+/+}$ versus Zeb2$^{Tg/Tg}$ cDC1s

Up-regulated			Down-regulated		
Tgm2	Hcar2	Tgfbi	Cd38	Card10	Slamf6
Clec4a1	Cd302	Ccnb1	Gpr82	Ildr1	Cystm1
Clec7a	Lifr	Neurl2	Pkib	Efcc1	Marveld2
Clec1b	Ifi203	Sh2d1b1	Ccl22	Fas	Homer2
Sirpb1a	Ms4a7	Acp5	Ido1	Cd8b1	Gclc
Cd4	Fam26f	Oas2	Fchsd2	Otud7b	Cxcr3
Adgre1	Hmox1	Esr1	Cnnm1	Lpar3	Cyb561
Oasl2	Slc16a7	Aurkb	Fcrlb	Gramd2	Cdon
Tlr1	Mndal	Cdc25c	Angel1	Elmo3	Esyt3
Wfdc17	Rarg	Aurka	Glce	Asap2	Mmp28
Clec4a2	Cdc25b	Ehf	Sspo	Slc41a2	Notch4
Ifit3	Tespa1	Il1rn	Pik3r3	Mab21l3	Trabd2b
Oas1a	Ctnnd2	Ttk	Sec1	Casr	Aff3
Zeb2	Fam46a	Ckap2l	Slc22a15	Scin	Lsr
Apobec1	Ccl9	Pou2f2	Vps37d	Cd8a	P3h2
Pilrb1	Emb	A630033H20Rik	Nfe2l3	Pdzk1ip1	Nid2
Ifit3b	Pira2	AI504432	Lzts2	Lrrc1	Egfl8
Clec4a4	Gapt	Cenpf	Mtmr4	Myb	Proser2
Sirpa	Slc40a1	Cenpi	Lrrc29	Abcd2	Serpinb6b
Lair1	Lst1	Ifi27l2a	Pacsin1	Pcdh1	Rtn4rl1
Cybb	Tlr7	Gngt2	Tm4sf5	Cldn1	Actn1
Fcer1g	Gpr141	Cenpm	Arc	Hgfac	Gcsam
Ms4a4c	Hpgds	Vegfa	Noxred1	Adgrf5	Dkk3
Cd300ld	Ifitm3	Lag3	Prr13	Ldlrad3	Gm3336
Csf1r	Fut7	Ctsc	Serpinb1a	Gpr157	Ltbp2
Itgam	S100a4	Casp1	Pdcd1	Foxj1	Fcrla
Ddx58	Abhd15	Spic	Dnajc22	Ccr9	Ttc39a
1810011H11Rik	Hacd4	Spc25	Chst11	Rab30	
Gpr162	Ceacam1		Ms4a1	Ankrd55	
Cd300a	Ms4a6b		Anxa6	Fndc4	
Gm12250	Cdr2		Ccndbp1	Arpin	
Nxpe4	Lgmn		Sh3gl3	Mpzl2	
Ncf2	Ube2c		Chrnb1	Frmd5	
Ltb4r1	Cd101		Tlr3	Ptgis	
Cd300lf	Ccl6		Col27a1	Prss57	
Pydc4	Ccnf		Rasip1	Itga3	
Abi3	Sapcd2		Cd200	Gpr33	
Rtp4	Ggt5		Mrvi1	Traf4	
Clec4n	Prc1		Pglyrp1	Sema4c	
Galnt6	Itga9		Acss2	Ffar4	
Sirpb1b	Gm5150		Myzap	Serpine2	
Pilrb2	Prdm1		Ctla4	Inadl	
Ms4a6c	Ear2		Sema4f	Pcsk5	
Plcb1	Klk8		Spint2	D030025P21Rik	
Oas3	C3ar1		Dapk2	2510009E07Rik	
Ifit1	Ifi47		Gucy2c	E330020D12Rik	
Gm9733	Itgad		Prph	Dcstamp	
Slc7a11	Rasgrf2		Kazn	Hepacam2	
Fcgr4	Lpcat2		Dusp18	Arhgef9	
Ifit1bl1	Oas1g		Snn	Lefty1	
Pla2g7	Xaf1		Sept1	Serpinb9	
Ddit4	Pif1		Mmp19	Clec4b2	

Table S2 | Differentially expressed genes: Zeb2$^{+/+}$ versus Zeb2$^{-/-}$ cDC2s

Up-regulated			Down-regulated		
Pclb1	Frk	Snx22	F11r	Clec4b2	Kntc1
1700011B04Rik	Cldn1	Arpin	Nrg2	Slfn1	BC030867
Plcb4	Tmeff1	Zcchc18	Wfdc21	Cd9	Slc9a2
Itgad	Hdc	Snn	Stard10	Nid2	Clec9a
Cox6a2	Siglecf	Sox8	Ttll5	C3ar1	Lyz2
Ttc39a	Rtn4rl1	Cystm1	Cd101	Krtcap3	Smim5
Sspo	Rnase4	Jag1	Aff3	Ackr3	Dmwd
Upp1	Gpc1	Apoe	Pappa2	Cx3cl1	Cygb
Chac1	Dusp4	Paqr9	Gm3336	Rragd	Mmp9
Cxcr3	Ms4a1	Gpr55	Cst3	Ceacam19	Dapk1
Lurap1	Lima1	Efnb1	Prg3	P2ry2	Gpr83
Cdh17	Nid1	Gpr157	Car2	Chtf18	Ccr2
Lsr	Pbx1	Elmo3	Sema4c	Cp	Hr
Cd84	Tgtp1	Oasl2	Gjb2	Ska1	Dab2
Fcer2a	Epcam	Mnda	G0s2	Fam198b	Lyz1
Prg2	Tenm4	Hepacam2	Elovl7	Myof	**Zeb2**
Ecel1	Fcrla	Als2cr12	Oasl1	Slc1a2	Cxcr1
Pde1b	E330020D12Rik	Ccl24	Utf1	2610528A11Rik	Gp2
Slc22a23	Osgin1	Tm4sf5	Strip2	Cd209b	
Cysltr1	Dact3	Slc27a2	Gpr160	Dbn1	

Chapter 2

Loss of Zeb2 in CD11c^{+} cells does not influence the development of hematoproliferative disease in the CD11c^{CRE}xp53$^{fl/fl}$ mouse model

Contributions: Bieke Soen performed all experiments, except for the immunohistochemical stainings (Figure 3 and Figure 5) which were performed by Kelly Lemeire. Bieke Soen performed all data analysis. Joachim Taminau and Gillian Blancke provided technical assistance. Bieke Soen, Steven Goossens, Charlotte Scott and Geert Berx contributed to the conceptualization and discussion of the project and its experiments. Bieke Soen performed the writing of this chapter.

2.1 Abstract

Blastic plasmacytoid dendritic cell neoplasm (BPDCN) is a rare and aggressive disease that is believed to develop from plasmacytoid dendritic cell (pDC) precursors. Currently there is no standardised therapeutic approach and the mean overall survival for patients is 12 to 16 months. A reliable preclinical model for the disease would be helpful to better understand the development of this lymphoma/leukemia subtype and could be used to develop and evaluate improved therapeutic strategies. Based on our finding that Zeb2 is essential for pDC differentiation and ***ZEB2***, as well as ***P53***, are recurrently mutated in BPDCN, we aimed at modelling this disease using our available p53 and Zeb2 loss-of-function mouse models. As the $CD11c^{CRE}$ mouse line allows targeting of the pDC lineage, we intercrossed this CRE line with our conditional Zeb2 and p53 knockout mice to generate $CD11c^{CRE}xp53^{fl/fl}$ and $CD11c^{CRE}xZeb2^{fl/fl}xp53^{fl/fl}$ mice. However, analysis of the cohorts revealed that our novel ***in vivo*** models do not develop BPDCN, but a so far unidentified aggressive proliferative hematopoietic disorder that develops independently of Zeb2.

2.2 Introduction

Blastic plasmacytoid dendritic cell neoplasm (BPDCN), previously referred to as blastic NK-cell lymphoma/leukemia or agranular $CD4^+/CD56^+$ hematodermic neoplasm is currently classified as an 'Acute myeloid leukemia and related neoplasm'[1]. BPDCN occurs mostly in elderly people with a median onset age above 60 years and patients typically show skin lesions and later on involvement of bone marrow, lymph nodes and peripheral blood, including thrombocytopenia and anaemia[2,3]. Additionally, splenomegaly and hepatomegaly can be present at diagnosis[4]. The highly aggressive disease has a poor prognosis, probably due to the fact that the presentation of skin lesions delays diagnosis of this hematopoietic malignancy. BPDCN is believed to derive from pDC precursors[5] and currently the diagnosis of BPDCN is based on the characteristic cytology and immunophenotype of malignant cells co-expressing CD4, CD56, CD123, blood dendritic cell antigens 2 and 4, and CD2AP. Treatment with chemotherapy often leads to relapse and currently chemotherapy followed by allogeneic stem cell transplantation gives the best improvement on survival[2].

In 2014, Menezes ***et al***. performed whole exome sequencing on three BPDCN samples, followed by a targeted next-generation sequencing of 38 selected genes in samples from 25 other BPDCN patients. This revealed that the ***ZEB2*** locus is mutated in 16% of cases. Two frameshift mutations and one mutation causing a single amino acid change were identified[6]. Furthermore, the research team of Mecucci (Perugia University, Italy) found genomic deletions spanning the full ***ZEB2*** locus with a similar frequency as the ***ZEB2*** mutations found by Menezes (personal communication, unpublished). The discovery of these deleterious changes in the ***ZEB2*** locus, together with the finding described in Chapter 1 of the Results section that Zeb2 is important in the development of pDCs[7,8], suggests a possible tumor suppressive role for this transcription factor in BPDCN. In Chapter 1, we used the $CD11c^{CRE}xZeb2^{fl/fl}$ model to investigate the consequences of loss of Zeb2 expression

in pDCs, but ageing of these mice did not lead to disease development. In an attempt to model BPDCN in mice, we hence decided to further cross the $CD11c^{CRE}xZeb2^{fl/fl}$ mice with a CRE-mediated conditional p53 knockout model and reasoned that the added knockout of the tumor suppressor p53 could accelerate the disease. Moreover, ***P53*** was shown to be mutated in 38% of BPDCN cases[9]. If we are able to model this rare neoplasm in mice, this would be beneficial for patients which currently only have a median overall survival of 12 to 16 months[10,11] and for whom no standardized therapeutic approach exists[3]. Indeed, a preclinical mouse model could be used to better understand the disease and for the development of more targeted therapies for BPDCN-patients.

2.3 Results

Breeding setup used to model BPDCN

BPDCN is an aggressive dendritic cell neoplasm believed to be derived from pDC precursors and 16% of cases was shown to have deleterious mutations in the ***ZEB2*** locus. We previously successfully used the CD11c^{CRE}xZeb2$^{fl/fl}$ line to investigate the role of Zeb2 in the pDC lineage[7] (Chapter 1 results section), but upon ageing (until 50 weeks of age) these mice did not develop signs of disease. With the aim to shorten the initiation time for possible disease development, we crossed the model with a CRE-mediated conditional p53 knockout mouse line[12]. The resulting CD11c^{CRE}xZeb2$^{fl/fl}$xp53$^{fl/fl}$ mice will be further referred to as Zeb2$^{-/-}$p53$^{-/-}$ (Figure 1). Two control groups will be used in this study: CD11c^{CRE}xp53$^{fl/fl}$ (Zeb2$^{+/+}$p53$^{-/-}$) mice and CRE^{-} Zeb2$^{fl/fl}$ or Zeb2$^{fl/fl}$p53$^{fl/fl}$ (Zeb2$^{+/+}$p53$^{+/+}$) mice (Figure 1).

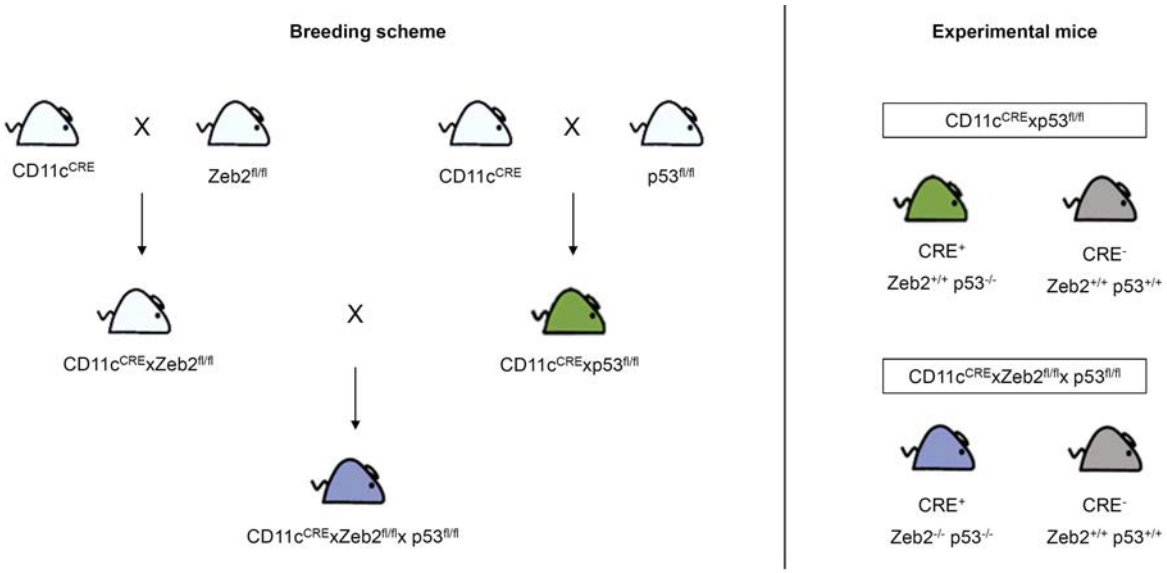

Figure 1 | Breeding scheme and experimental mice in this study. Mice were obtained using the following breeding scheme: first CD11c^{CRE} mice were crossed with either Zeb2$^{fl/fl}$ or p53$^{fl/fl}$ mice. Next the CD11c^{CRE}xZeb2$^{fl/fl}$ mice were further crossed with the CD11c^{CRE}xp53$^{fl/fl}$ mice to generate CD11c^{CRE}xZeb2$^{fl/fl}$xp53$^{fl/fl}$ mice. This resulted in the experimental mouse cohorts used in this study: CRE^{+} CD11c^{CRE}xp53$^{fl/fl}$ mice (Zeb2$^{+/+}$p53$^{-/-}$) with their CRE^{-} control littermates (Zeb2$^{+/+}$p53$^{+/+}$) and CRE^{+} CD11c^{CRE}xZeb2$^{fl/fl}$xp53$^{fl/fl}$ mice (Zeb2$^{-/-}$p53$^{-/-}$) with their CRE^{-} control littermates (Zeb2$^{+/+}$p53$^{+/+}$).

Zeb2$^{-/-}$p53$^{-/-}$ and Zeb2$^{+/+}$p53$^{-/-}$ mice suffer from massive cell infiltration in the liver, splenomegaly and/or enlarged thymus

The health of CD11c^{CRE}xZeb2$^{fl/fl}$xp53$^{fl/fl}$ (Zeb2$^{-/-}$p53$^{-/-}$) and CD11c^{CRE}xp53$^{fl/fl}$ (Zeb2$^{+/+}$p53$^{-/-}$) mice was monitored weekly until a maximum age of 65 weeks. Every week we determined the weight of the mice, palpated them to check for splenomegaly and other growths, and assessed their general well-being (activity, hunched back and breathing). Mice were sacrificed when showing visible signs of disease, such as splenomegaly or breathing problems, or when their weight loss exceeded 15% of their body mass. All CRE^{+} mice, except for one Zeb2$^{+/+}$p53$^{-/-}$ mouse, developed sings of illness with a median onset age of 37 weeks and ranging between 18 and 65 weeks, whereas none of the CRE^{-} mice showed signs of disease. Dissection of the mice immediately revealed apparent problems with different organs. A majority of the sick Zeb2$^{-/-}$p53$^{-/-}$ and Zeb2$^{+/+}$p53$^{-/-}$ mice displayed a massive infiltration of white blood cells in the liver, turning the tissue whitish or yellow and resulting in enlargement of the organ (Figure 2A). Enlargement of the liver was accompanied with a similar discoloration of the spleen and splenomegaly (Figure 2A). When sacrificing mice with breathing problems, we often encountered a heavily enlarged thymus in the chest (Figure 2A). Zeb2$^{-/-}$p53$^{-/-}$ and Zeb2$^{+/+}$p53$^{-/-}$ mice showed a similar distribution of the observed phenotypes with respectively 23.5% and 33.3% of cases showing thymus enlargement, 64.7% and 50% showing cell infiltration in liver and splenomegaly and 11.8% and 16.7% showing cell infiltration in liver, splenomegaly and thymus enlargement (Figure 2B). Next we calculated the ratio of spleen to body mass and found that, normalised to the body weight, diseased Zeb2$^{-/-}$p53$^{-/-}$ and Zeb2$^{+/+}$p53$^{-/-}$ have a significant increase in their spleen weight compared to healthy Zeb2$^{+/+}$p53$^{+/+}$ control mice (Figure 2C). When comparing sick Zeb2$^{-/-}$p53$^{-/-}$ to sick Zeb2$^{+/+}$p53$^{-/-}$ mice, no statistically significant differences could be found in the ratio of spleen to body mass (Figure 2C). At the time of sacrifice, we also collected blood for automated analysis on a Hemavet (Drew Scientific Group) device. In general, we did not find significant differences in the cell numbers per µl blood for white blood cells, red blood cells and platelets (Figure 2D). However, several diseased mice of both groups displayed blood cell numbers outside the normal range. As such, 36.4% of Zeb2$^{-/-}$p53$^{-/-}$ mice had anaemia, whereas 54.5% of

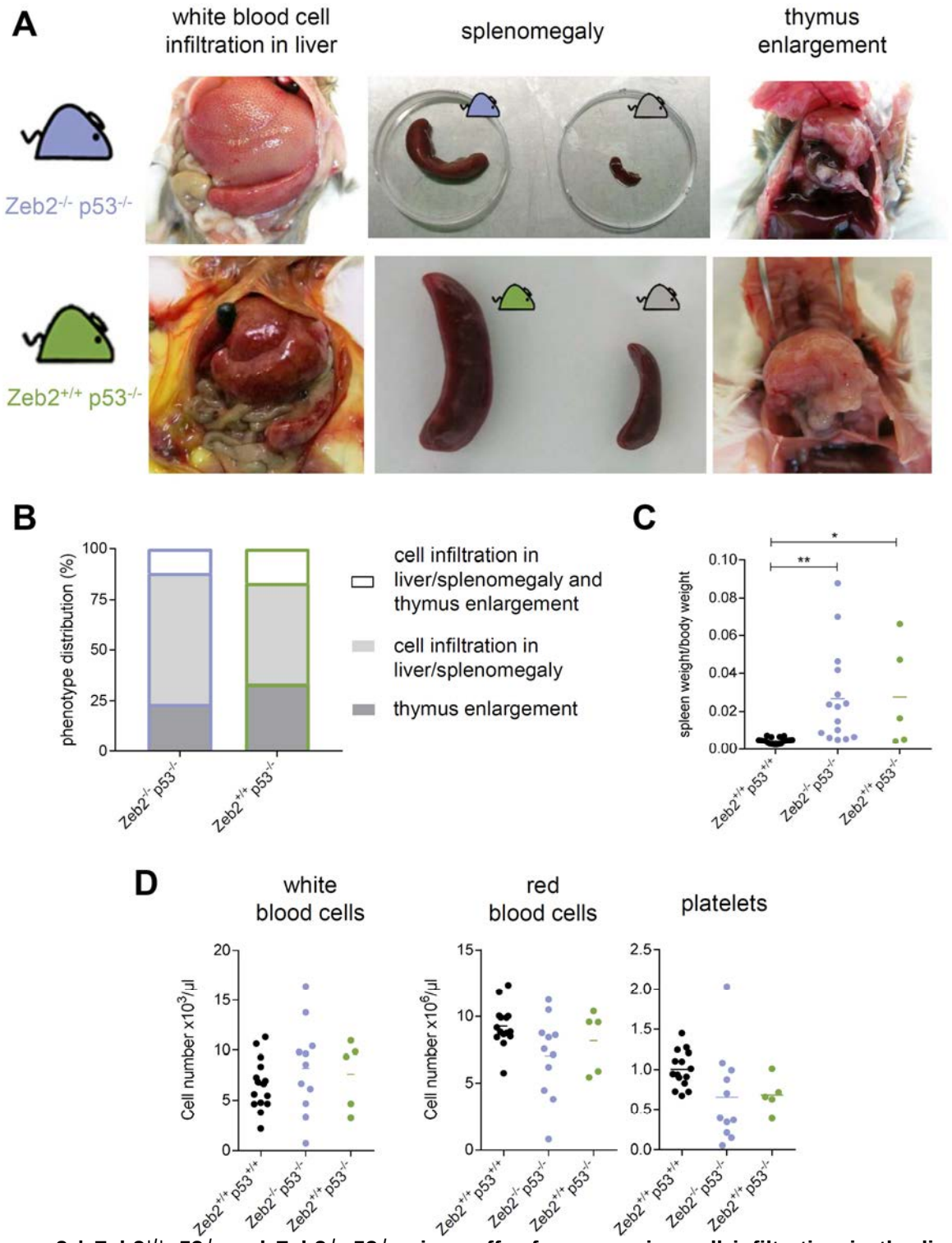

Figure 2 | Zeb2$^{+/+}$p53$^{-/-}$ and Zeb2$^{-/-}$p53$^{-/-}$ mice suffer from massive cell infiltration in the liver, splenomegaly and/or thymus enlargement. (A) Macroscopic pictures showing massive cell infiltration in liver, splenomegaly (affected spleen with blue or green mouse icon next to spleen of CRE^{-} littermate control with grey mouse icon) or enlargement of the thymus in Zeb2$^{+/+}$p53$^{-/-}$ and Zeb2$^{-/-}$p53$^{-/-}$ mice. (B) Distribution of the phenotypes as percentage of total mice in Zeb2$^{-/-}$p53$^{-/-}$ (n=17) and Zeb2$^{+/+}$p53$^{-/-}$ (n=6) mice. (C) Ratio of spleen to body weight for indicated mice. Each dot represents one mouse. *, P < 0.05; **, P< 0.01. One-way ANOVA with Bonferroni post-test. (D) Absolute cell number per µl of blood for white blood cells, red blood cells and platelets determined with Hemavet in Zeb2$^{+/+}$p53$^{+/+}$ (n=15; 40% male, 60% female), Zeb2$^{-/-}$p53$^{-/-}$ mice (n=11; 27% male, 73% female) and Zeb2$^{+/+}$p53$^{-/-}$ mice (n=5; 40% male, 60% female). No significance was found with one-way ANOVA with Bonferroni post-test.

$Zeb2^{-/-}p53^{-/-}$ mice and 20% of $Zeb2^{+/+}p53^{-/-}$ mice suffered from low platelet counts. This reduced numbers of blood cells in diseased mice are suggestive of BM involvement affecting normal hematopoiesis. Indeed, when flushing femurs and tibias from sick mice, we often found the BM to be white/yellow instead of bright red.

$Zeb2^{-/-}p53^{-/-}$ and $Zeb2^{+/+}p53^{-/-}$ mice develop a hematoproliferative disease that does not resemble human BPDCN

Next we performed hematoxylin and eosin (H&E) staining on tissue samples fixed with 4% paraformaldehyde (PFA). This revealed that diseased $Zeb2^{-/-}p53^{-/-}$ and $Zeb2^{+/+}p53^{-/-}$ mice have a disrupted spleen architecture (Figure 3A). The distinction between red and white pulp, which is clearly visible in age-matched $Zeb2^{+/+}p53^{+/+}$ control mice, has disappeared and it seems like the white pulp has expanded (Figure 3A). H&E staining on liver sections of sick $Zeb2^{-/-}p53^{-/-}$ and $Zeb2^{+/+}p53^{-/-}$ mice shows presence of clusters/regions of small basophilic cells low in cytoplasm, next to eosinophilic cytoplasm rich hepatocytes (Figure 3B). In CRE^{-} control liver sections, these clusters are absent. H&E staining on sections of diseased thymi reveals that the architecture of the tissue is disrupted and the distinction between medulla and cortex has disappeared (Figure 3C). In order to find out if the cells present in the affected tissues are proliferating, we stained PFA fixed samples for Ki67. This revealed that the spleen and thymus of $Zeb2^{-/-}p53^{-/-}$ and $Zeb2^{+/+}p53^{-/-}$ mice is indeed full of $Ki67^{+}$ proliferating cells (Figure 3A and 3C). Ki67 staining on liver sections of $Zeb2^{-/-}p53^{-/-}$ and $Zeb2^{+/+}p53^{-/-}$ mice revealed that the infiltrating cell clusters also consist of proliferating cells (Figure 3B). Next, we wondered if the proliferating cells had a hematopoietic origin and thus we opted to stain the liver sections with CD45, as in healthy mice this tissue contains very little hematopoietic cells. Indeed, the cell clusters in the liver of $Zeb2^{-/-}p53^{-/-}$ and $Zeb2^{+/+}p53^{-/-}$ mice are staining positive for CD45 (Figure 3B) and we can conclude that the mice suffer from a hematoproliferative disease.

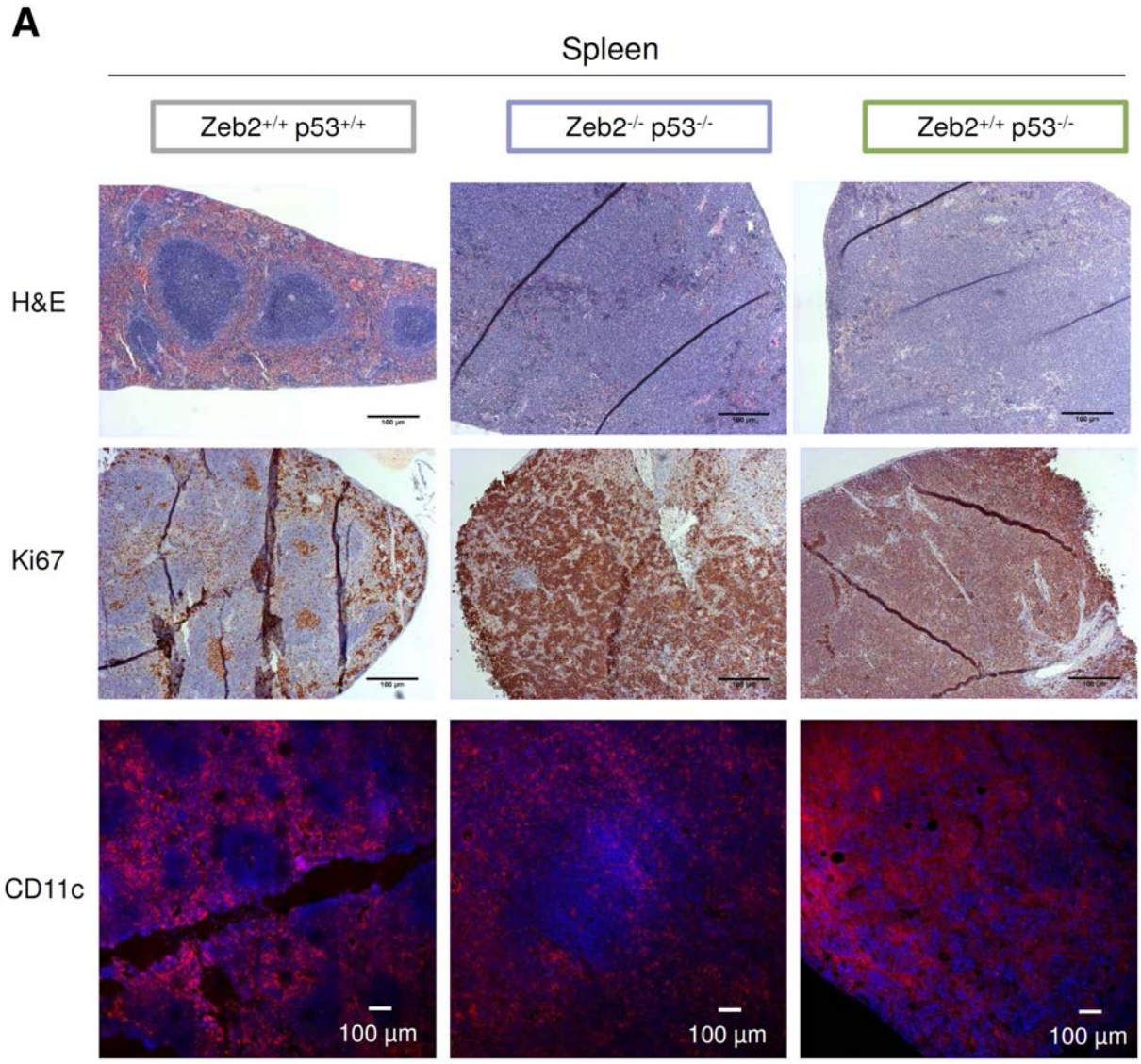

Figure 3 | The spleens of Zeb2$^{-/-}$p53$^{-/-}$ and Zeb2$^{+/+}$p53$^{-/-}$ mice have lost their general architecture. (A) TOP: representative pictures of H&E staining on the spleens of indicated mice. Pictures were taken using a 10x/0.25 objective. Scalebar 100 µm. MIDDLE: representative pictures of immunohistochemical Ki67 staining on the spleens of indicated mice. Pictures were taken using a 10x/0.25 objective. Scalebar 100 µm. BOTTOM: representative pictures of fluorescent CD11c staining on the spleens of indicated mice (blue: DAPI; red: CD11c). Pictures were taken using a 10x/0.4 objective. Scalebar 100 µm.

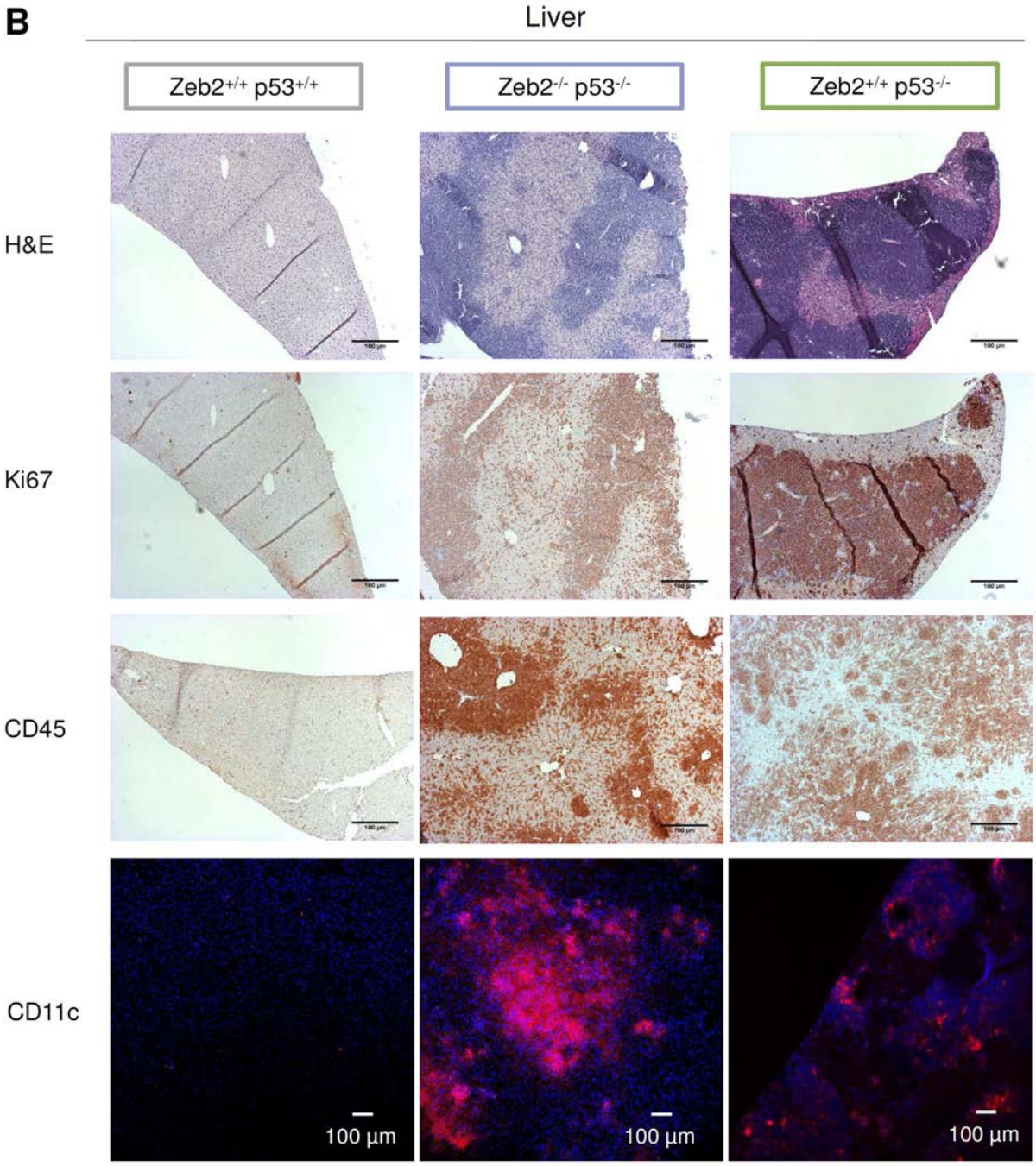

Figure 3 continued | The livers of Zeb2$^{-/-}$p53$^{-/-}$ and Zeb2$^{+/+}$p53$^{-/-}$ mice contain proliferative CD45^{+}CD11c^{+} cells. (B) TOP: representative pictures of H&E staining on the livers of indicated mice. Pictures were taken using a 10x/0.25 objective. Scalebar 100 µm. SECOND ROW: representative pictures of immunohistochemical Ki67 staining on the livers of indicated mice. Pictures were taken using a 10x/0.25 objective. Scalebar 100 µm. THIRD ROW: representative pictures of immunohistochemical CD45 staining on the livers of indicated mice. Pictures were taken using a 10x/0.25 objective. Scalebar 100 µm. BOTTOM: representative pictures of fluorescent CD11c staining on the livers of indicated mice. (blue: DAPI; red: CD11c). Pictures were taken using a 10x/0.4 objective. Scalebar 100 µm.

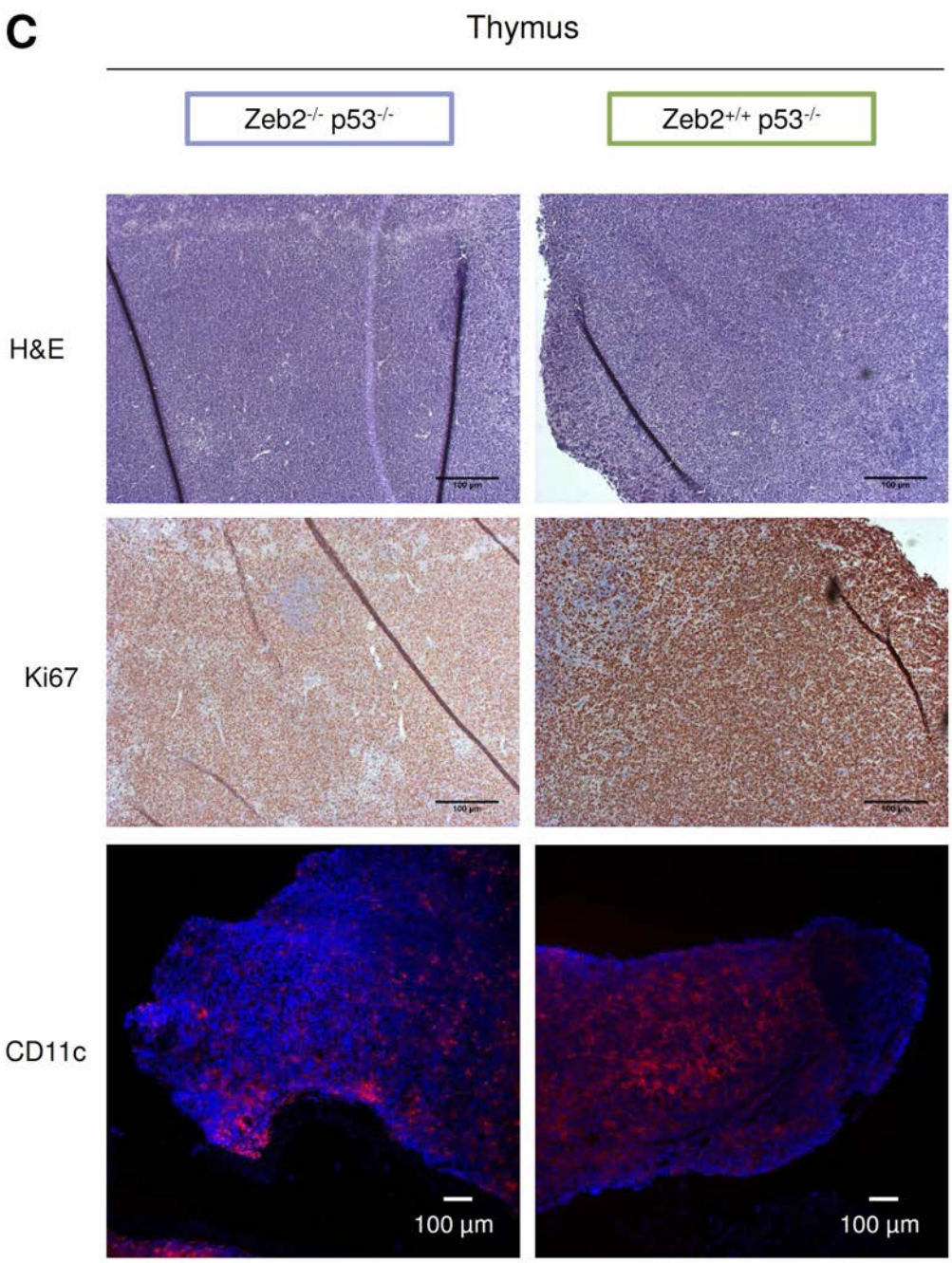

Figure 3 continued | The thymi of Zeb2$^{-/-}$p53$^{-/-}$ and Zeb2$^{+/+}$p53$^{-/-}$ mice contain proliferative CD11c^{+} cells. (C) TOP: representative pictures of H&E staining on the thymi of indicated mice. Pictures were taken using a 10x/0.25 objective. Scalebar 100 µm. MIDDLE: representative pictures on immunohistochemical Ki67 staining on the thymi of indicated mice. Pictures were taken using a 10x/0.25 objective. Scalebar 100 µm. BOTTOM: representative pictures of fluorescent CD11c staining on the thymi of indicated mice. (blue: DAPI; red: CD11c). Pictures were taken using a 10x/0.4 objective. Scalebar 100 µm.

As we mediated knockout of Zeb2 and/or p53 in CD11c$^+$ cells, we wanted to see if the proliferative CD45$^+$ cells still expressed this integrin. In the spleen of sick mice, CD11c was present throughout the tissue, while healthy mice displayed clusters of CD11c$^-$ cells which are typically B and T cell clusters (Figure 3A). CD11c staining on liver sections from Zeb2$^{-/-}$p53$^{-/-}$ and Zeb2$^{+/+}$p53$^{-/-}$ mice again revealed clusters of cells expressing this integrin, while in control Zeb2$^{+/+}$p53$^{+/+}$ mice only very few single CD11c$^+$ cells were found (Figure 3B). In the enlarged thymi of Zeb2$^{-/-}$p53$^{-/-}$ and Zeb2$^{+/+}$p53$^{-/-}$ mice a vast amount of cells expressed CD11c (Figure 3C). Taken together we showed that Zeb2$^{-/-}$p53$^{-/-}$ and Zeb2$^{+/+}$p53$^{-/-}$ mice suffer from a proliferative disorder originating in CD11c expressing hematopoietic cells. Experienced pathologist Prof. Dr. Jo Van Dorpe (Ghent University Hospital) described the cancer as an acute, aggressive, immature and anaplastic hematopoietic malignancy containing a lot of mitotic, but also apoptotic cells.

However, the hematoproliferative disease found in our mouse models does not resemble the human BPDCN that we wanted to mimic, as 73% of patients with BPDCN show the typical skin lesions and patients never suffer from enlargement of the thymus[13]. Additionally, BPDCN cells in human patients typically express CD4 and CD123[4]. Flow cytometric analysis of CD4 and CD123 in affected spleens of diseased mice, did not show significant enrichment of cells expressing CD4 or CD123 compared to spleens from healthy age-matched Zeb2$^{+/+}$p53$^{+/+}$ mice (Figure 4). We also assessed the presence of CD3, CD19 and CD11c on splenic cells of sick Zeb2$^{-/-}$p53$^{-/-}$ and Zeb2$^{+/+}$p53$^{-/-}$ mice, as human BPDCN cells are negative for these surface markers[4]. Although spleens of sick mice were not enriched for CD3 and CD19 expressing cells compared with spleens from Zeb2$^{+/+}$p53$^{+/+}$ mice, we did find a significant increase for CD11c$^+$ cells in spleens from Zeb2$^{-/-}$p53$^{-/-}$ mice (Figure 4). Taken together, analysis of the phenotypes and the expression of surface markers showed that our mouse models develop a hematopoietic proliferative disease that does not resemble human BPDCN.

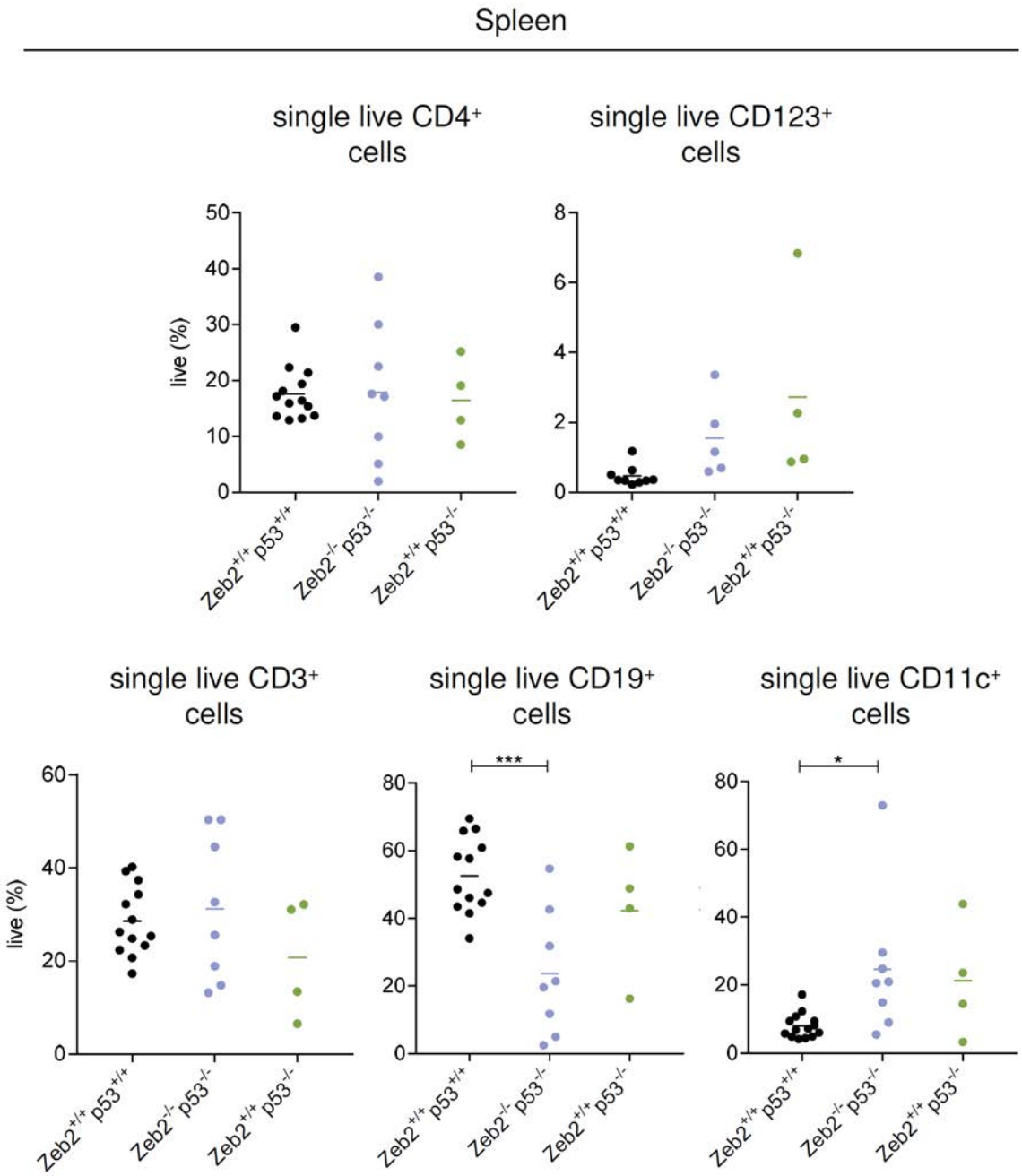

Figure 4 | Cells from diseased spleens of Zeb2$^{-/-}$p53$^{-/-}$ and Zeb$^{+/+}$p53$^{-/-}$ mice do not express typical markers for human BPDCN. Proportion as a percentage of total live cells of singe live CD4^{+}, CD123^{+}, CD3^{+}, CD19^{+} and CD11c^{+} cells in the spleens of Zeb2$^{+/+}$p53$^{+/+}$, Zeb2$^{-/-}$p53$^{-/-}$ and Zeb2$^{+/+}$p53$^{-/-}$ mice. One dot represents one mouse. *, P < 0.05; ***, P < 0.001. One-way ANOVA with Bonferroni post-test.

The hematopoietic malignancy in Zeb2$^{-/-}$p53$^{-/-}$ and Zeb2$^{+/+}$p53$^{-/-}$ mice is independent of Zeb2

Although the proliferative disease in our mice does not mimic human BPDCN, we still wanted to find out if Zeb2 is important in the hematopoietic malignancy that develops in the CD11c^{CRE}xp53$^{fl/fl}$ model. Analysing the Kaplan-Meier curve for percentage disease free mice did not reveal significant differences between Zeb2$^{-/-}$p53$^{-/-}$ and Zeb2$^{+/+}$p53$^{-/-}$ mice, which had an onset age for disease of respectively 37 and 39 weeks (Figure 5A). The similar onset age of disease in Zeb2$^{-/-}$p53$^{-/-}$ and Zeb2$^{+/+}$p53$^{-/-}$ mice, together with the appearance of very similar symptoms (Figure 2), suggests that the hematopoietic malignancy in CD11c^{CRE}xp53$^{fl/fl}$ mice develops independently of Zeb2. To test this hypothesis we performed immunohistochemical staining for Ki67 and Zeb2 on consecutive liver sections of diseased mice. In liver sections from Zeb2$^{-/-}$p53$^{-/-}$ and Zeb2$^{+/+}$p53$^{-/-}$ corresponding regions that stained positive for Ki67, and hence contain proliferating cells, were negative for Zeb2 expression (Figure 5B). This confirmed our hypothesis that the development of the hematopoietic malignancy in CD11c^{CRE}xp53$^{fl/fl}$ mice develops independently of Zeb2 and probably explains why we were unable to identify significant differences between Zeb2$^{-/-}$p53$^{-/-}$ and Zeb2$^{+/+}$p53$^{-/-}$ mice throughout this study.

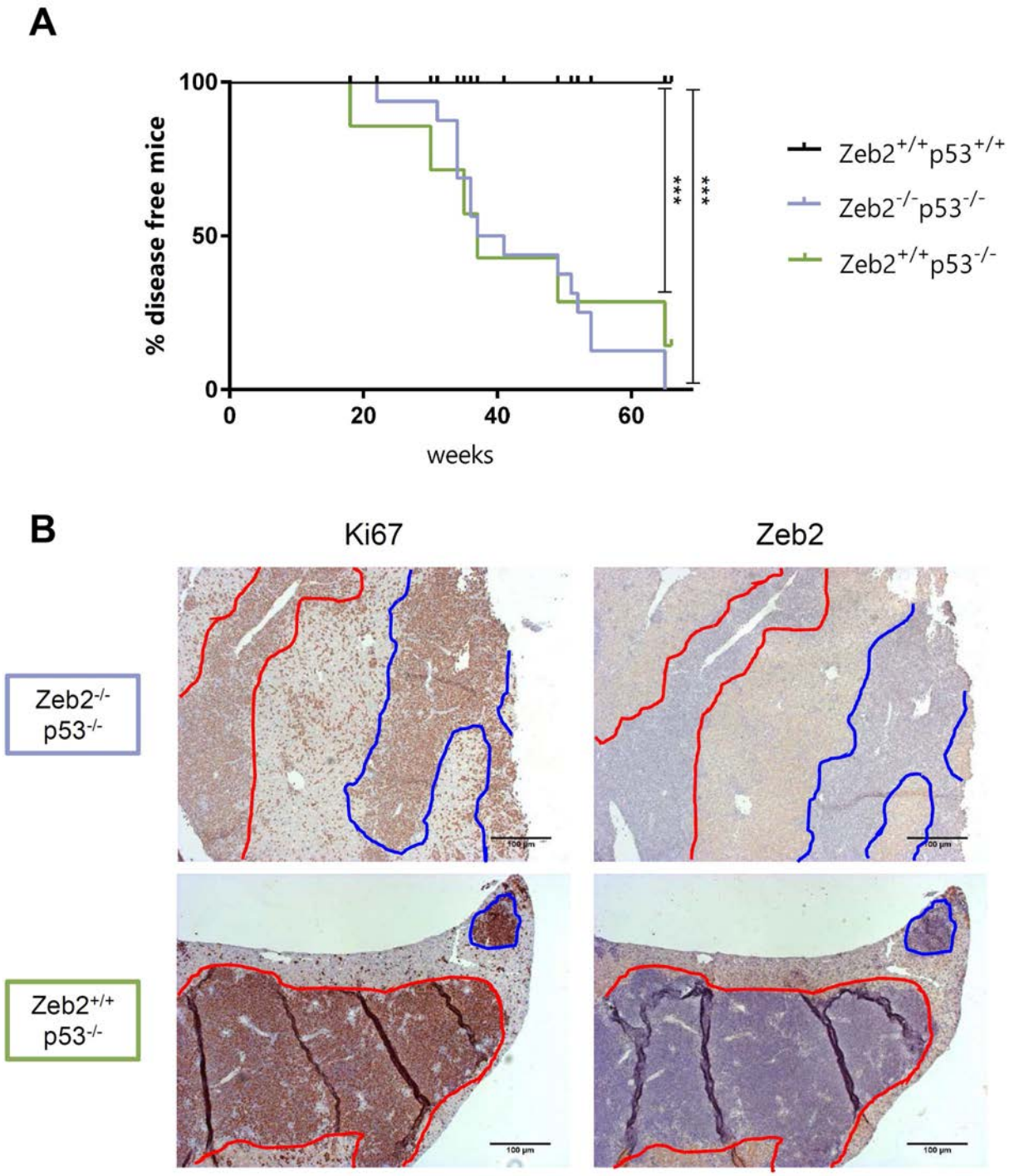

Figure 5 | Development of hematoproliferative disease induced by loss of p53 expression in CD11c$^+$ cells is independent of Zeb2. (A) Kaplan-Meier curve for percentage disease free mice in Zeb2$^{+/+}$p53$^{+/+}$, Zeb2$^{-/-}$p53$^{-/-}$ and Zeb2$^{+/+}$p53$^{-/-}$ mice. ***, P < 0.001. Mantel-Cox test with Bonferroni post-test. (B) Representative pictures of immunohistochemical Ki67 and Zeb2 staining on consecutive liver sections of Zeb2$^{-/-}$p53$^{-/-}$ and Zeb2$^{+/+}$p53$^{-/-}$ mice. Areas indicated with the same colour depict corresponding regions. Pictures were taken using a 10x/0.25 objective. Scalebar 100 µm.

2.4 Discussion

BPDCN is a rare hematopoietic malignancy that is believed to develop from pDC precursors[5]. In 16% of cases deleterious mutations can be found in the ***ZEB2*** gene locus[6]. As we already found a role for Zeb2 in pDC development using the $CD11c^{CRE}xZeb2^{fl/fl}$ model[7], which did not develop disease upon ageing, we aimed at modelling BPDCN in mice by adding loss of the tumor suppressor ***p53***, a gene also frequently mutated in BPDCN[9].

$CD11c^{CRE}xZeb2^{fl/fl}xp53^{fl/fl}$ ($Zeb2^{-/-}p53^{-/-}$) mice and $CD11c^{CRE}xp53^{fl/fl}$ ($Zeb2^{+/+}p53^{-/-}$) mice developed a hematopoietic malignancy which resulted in massive cell infiltration in liver, splenomegaly and/or enlargement of the thymus. Pathological review of the affected tissues suggested that the malignancy is aggressive, acute and likely originates from immature cells. Additionally, several mice suffered from anaemia and thrombocytopenia, suggestive of BM involvement affecting normal hematopoiesis. However, throughout our study we were unable to find differences between $Zeb2^{-/-}p53^{-/-}$ and $Zeb2^{+/+}p53^{-/-}$. Both groups of mice developed similar phenotypes and displayed the same distribution of those phenotypes. Also in terms of disease onset $Zeb2^{-/-}p53^{-/-}$ and $Zeb2^{+/+}p53^{-/-}$ mice behaved similar, with respectively a median onset age of 39 and 37 weeks. Immunohistochemical staining for Zeb2 indeed revealed that in both genotypes, the proliferative cells do not express Zeb2, strongly suggesting that the hematoproliferative disease found in $CD11c^{CRE}xp53^{fl/fl}$ mice develops independently of Zeb2.

The aim of this study was to develop a mouse model for human BPDCN. However, the hematopoietic malignancy that developed in $Zeb2^{-/-}p53^{-/-}$ and $Zeb2^{+/+}p53^{-/-}$ mice did not resemble the human disease. Some typical features of BPDCN, like presence of cutaneous lesions and expression of CD4 and CD123[4], were not found in our mouse models. On the other hand enlargement of the thymus and expression of CD11c by proliferative cells, which was found in $Zeb2^{-/-}p53^{-/-}$ and $Zeb2^{+/+}p53^{-/-}$ mice,

have not been reported in BPDCN patients[14]. We can think of several reasons why the disease in our mouse models does not resemble human BPDCN. First, ***ZEB2*** and ***P53*** are only mutated in respectively 16%[6] and 38%[9] of BPDCN cases and additionally it is not known of these mutations can be considered as driver or passenger mutations for this particular malignancy. Secondly, although deleterious mutations were found in the ***ZEB2*** gene locus of patients, we do not know if these are heterozygous or homozygous. Furthermore, we do not have data on protein expression levels of the transcription factor in human BPDCN cells. It could be that the loss of function mutation in ***ZEB2*** is compensated by enhanced expression of the intact ***ZEB2*** allele or maybe BPDCN cells depend on ZEB2 for their survival, just like AML cells[15]. To test this hypothesis, we could cross the $CD11c^{CRE}xp53^{fl/fl}$ mice with our conditional Rosa26-Zeb2 overexpression model[16] and see if those mice develop BPDCN-like symptoms. Additionally, the $CD11c^{CRE}$ line used does not only target pDCs, but also cDCs, NK cells, T cells, B cells and macrophages (see Results section Chapter 3 Figure 7). Hence it is likely that the tumor suppressor p53 is knocked out in one or more of those cell types and thus the hematopoietic malignancy in the $CD11c^{CRE}xp53^{fl/fl}$ mice does not originate from the pDC lineage. The fact that the $CD11c^{CRE}$ line targets multiple lineages could also explain the manifestation of the disease in different organs across mice, especially the involvement of the thymus in some mice could be explained by the possible targeting of T cells. It was indeed shown before that full knockout of p53 can lead to development of B and T cell malignancies[17] and flow cytometric analysis of the enlarged thymi of several $Zeb2^{-/-}p53^{-/-}$ and $Zeb2^{+/+}p53^{-/-}$ mice showed enrichment for cells expressing the typical B cell marker CD19 or T cell marker CD3 (data not shown). Additionally, extensive flow cytometric analysis of affected splenic, hepatic and thymic tissue did not identify a common immunological marker across sick mice (data not shown). Taken together this suggests that $Zeb2^{-/-}p53^{-/-}$ and $Zeb2^{+/+}p53^{-/-}$ mice may present multiple subtypes of leukemia due to the aspecificity of the $CD11c^{CRE}$ line and hence further attempts for modelling BPDCN in mice would benefit from a CRE-line that specifically targets the pDC lineage.

In conclusion, we were unable to model the human disease BPDCN using $CD11c^{CRE}xZeb2^{fl/fl}xp53^{fl/fl}$ and $CD11c^{CRE}xp53^{fl/fl}$ mice. Nevertheless, the mice did develop an acute, aggressive and immature hematopoietic malignancy that resulted in cell infiltration in the liver, splenomegaly, deficiencies in the blood and/or enlargement of the thymus. Up to date we were not able to identify the specific nature of the hematopoietic malignancy, but we did show that the disease develops independently of Zeb2. We still believe that a preclinical mouse model for BPDCN is necessary to improve targeted therapies for the disease and further research is needed to achieve this goal.

2.5 Materials and methods

Mice

The generation of $Zeb2^{fl/fl}$ and $p53^{fl/fl}$ mice was described previously[12,16]. Mice were crossed with the $CD11c^{CRE}$ mice[18] in order to obtain $CD11c^{CRE}xZeb2^{fl/fl}xp53^{flfl}$ and $CD11c^{CRE}xp53^{fl/fl}$ mice. All mice were bred and maintained at the Vlaams Instituut voor Biotechnologie (Ghent University) under specific pathogen-free conditions and their health was inspected weekly by determining body weight, palpating for splenomegaly and other abnormal growths and assessing general health status (activity, hunched back, breathing). All experiments were performed in accordance with the ethical committee of the Faculty of Science.

Automated blood analysis

20-30 µl of blood was collected from the tail vein of mice into an EDTA coated tube. After mixing of the sample, it was loaded into the Hemavet (Drew Scientific Group) machine for automated blood analysis.

Immunohistochemical staining of paraffin embedded tissue

Tissue from mice euthanized by means of cervical dislocation was washed in PBS and incubated overnight in 4% paraformaldehyde (PFA). Next the tissue was dehydrated, embedded in paraffin and cut into 5 µm sections. For histology, sections were stained with hematoxylin and eosin. For immunohistochemical staining, antigen retrieval was done in citrate buffer and endogenous peroxidase activity was blocked using 3% H_2O_2 in methanol. Next the sections were incubated overnight at 4°C with primary antibody: Zeb2 (Sigma, HPA003456, dilution 1/300), Ki67 (Cell Signaling, 122025, dilution 1/1000) and CD45 (BD Pharmingen, 550539, dilution 1/50). Incubation with a biotin-conjugated secondary antibody (1h, RT) was followed by

streptavidin-HRP based development (substrate development with DAB or AEC). For the staining with Zeb2 antibody, the signal was amplified using the Tyramide Signal Amplification (TSA) kit (Perkin Elmer, Zaventem, Belgium). Finally, slides were counterstained with hematoxylin, dehydrated and mounted with Entellan. Histology and pictures of the stained tissue were taken using an Olympus BX51 Discussion Microscope with a 10x/0.25 objective. Scalebars were added to the pictures using FiJi software.

Immunofluorescent staining of frozen tissue

Freshly isolated tissue was embedded in O.C.T. Compound (Tissue Tek) and snap frozen. 10 µm thick cryosections were obtained and air dried for at least 30 minutes. Next sections were fixed for 2 minutes in a 2% PFA solution. After washing in PBS, sections were stained with directly labelled antibody (CD11c eFluor 660, eBioscience, 50-0114-82, diluted 1/20 in PBT) for 1 hour in the dark at RT. After washing in PBS, sections were incubated with DAPI diluted in PBT for 10 minutes in the dark at RT. Following a last washing step in PBS, sections were mounted with N-propylgallate and imaged with a Leica TCS SP5 confocal microscope using a 10x/0.4 objective. Merging of the pictures and adding of the scalebars was done with FiJi software.

Isolation of splenic cells and flow cytometry

For the isolation of splenic cells, spleens were disected from mice killed with cervical dislocation and gently pressed through a 70-µm filter (no enzymes). Next red blood cells were lysed with ACK Lysing Buffer (Lonza), cells were counted manually and 5×10^6 cells were stained for 45 minutes at 4°C in the dark for flow cytometric analysis (Table 1). Data were acquired on a cell analyser (LSRFortessa; BD) and analyzed using FlowJo software (Tree Star).

Table 1 | Antibodies used for flow cytometry

Antibody	Clone	Antibody	Clone
Fc Block	2.4G2	CD19	1D3
Fixable Viability Dye	eBioscience	CD11c	N418
CD3e	145-2c11	CD123	5B11
CD4	RM4-5		

Statistical analysis

Multiple-group comparisons were performed using one-way ANOVA followed by a Bonferroni post-test with Prism Software (GraphPad Software). Samples were assumed to be normally distributed with similar variance between groups. Analysis of survival curves was performed using Mantel-Cox test with Prism Software, followed by Bonferroni post-test used to calculate adjusted P-values.

2.6 References

1. Vardiman JW, Thiele J, Arber DA, et al. The 2008 revision of the World Health Organization (WHO) classification of myeloid neoplasms and acute leukemia: rationale and important changes. ***Blood***. 2009;114(5):937–51.
2. Laribi K, Denizon N, Besançon A, et al. Blastic Plasmacytoid Dendritic Cell Neoplasm: From Origin of the Cell to Targeted Therapies. ***Biol. Blood Marrow Transplant.*** 2016;22(8):1357–1367.
3. Pagano L, Valentini CG, Grammatico S, Pulsoni A. Blastic plasmacytoid dendritic cell neoplasm: diagnostic criteria and therapeutical approaches. ***Br. J. Haematol.*** 2016;174(2):188–202.
4. Riaz W, Zhang L, Horna P, Sokol L. Blastic Plasmacytoid Dendritic Cell Neoplasm: Update on Molecular Biology, Diagnosis, and Therapy. ***Cancer Control***. 2014;21(4):279–289.
5. Urosevic M, Conrad C, Kamarashev J, et al. CD4+CD56+ hematodermic neoplasms bear a plasmacytoid dendritic cell phenotype. ***Hum Pathol***. 2005;36(9):1020–1024.
6. Menezes J, Acquadro F, Wiseman M, et al. Exome sequencing reveals novel and recurrent mutations with clinical impact in blastic plasmacytoid dendritic cell neoplasm. ***Leukemia***. 2014;28(4):823–9.
7. Scott CL, Soen B, Martens L, et al. The transcription factor Zeb2 regulates development of conventional and plasmacytoid DCs by repressing Id2. ***J. Exp. Med.*** 2016;213(6):897–911.
8. Wu X, Briseño CG, Grajales-Reyes GE, et al. Transcription factor Zeb2 regulates commitment to plasmacytoid dendritic cell and monocyte fate. ***Proc. Natl. Acad. Sci. U.S.A.*** 2016;113(51):14775–14780.
9. Jardin F, Ruminy P, Parmentier F, et al. TET2 and TP53 mutations are frequently observed in blastic plasmacytoid dendritic cell neoplasm. ***Br. J. Haematol.*** 2011;153(3):413–6.
10. Feuillard J, Jacob M-CC, Valensi F, et al. Clinical and biologic features of CD4(+)CD56(+) malignancies. ***Blood***. 2002;99(5):1556–63.
11. Petrella T, Bagot M, Willemze R, et al. Blastic NK-cell lymphomas (agranular CD4+CD56+ hematodermic neoplasms): a review. ***Am. J. Clin. Pathol.*** 2005;123(5):662–75.
12. Jonkers J, Meuwissen R, van der Gulden H, et al. Synergistic tumor suppressor activity of BRCA2 and p53 in a conditional mouse model for breast cancer. ***Nat. Genet.*** 2001;29(4):418–25.
13. Julia F, Dalle S, Duru G, et al. Blastic plasmacytoid dendritic cell neoplasms: clinico-immunohistochemical correlations in a series of 91 patients. ***Am. J. Surg. Pathol.*** 2014;38(5):673–80.
14. Garnache-Ottou F, Feuillard J, Ferrand C, et al. Extended diagnostic criteria for plasmacytoid dendritic cell leukaemia. ***Br. J. Haematol.*** 2009;145(5):624–36.
15. Tsherniak A, Vazquez F, Montgomery PG, et al. Defining a Cancer Dependency Map. ***Cell***. 2017;170(3):564–576.e16.
16. Tatari MN, De Craene B, Soen B, et al. ZEB2-transgene expression in the epidermis compromises the integrity of the epidermal barrier through the repression of different tight junction proteins. ***Cell. Mol. Life Sci.*** 2014;71(18):3599–609.
17. Donehower LA, Harvey M, Slagle BL, et al. Mice deficient for p53 are developmentally normal but susceptible to spontaneous tumours. ***Nature***. 1992;356(6366):215–21.
18. Caton ML, Smith-Raska MR, Reizis B. Notch-RBP-J signaling controls the homeostasis of CD8- dendritic cells in the spleen. ***The Journal of experimental medicine***. 2007;204(7):1653–64.

Chapter 3

Understanding the role of Zeb1 in dendritic cell homeostasis

Contributions: Bieke Soen and Charlotte Scott performed all experiments, except for the immunofluorescent staining (Figure 8) which was performed by Matthias Vanderkerken. Bieke Soen and Charlotte Scott performed all data analysis, except for the bio-informatics analysis shown in Figure 1A and Figure 8A. Joachim Taminau, Gillian Blancke, Sofie De Prijck and Gert Van Isterdael provided technical assistance. Liesbet Martens and Sofie Van Gassen performed the bio-informatics analysis shown in Figure 1A and Figure 8A. Bieke Soen, Charlotte Scott, Bart Lambrecht, Martin Guilliams and Geert Berx contributed to the conceptualization and discussion of the project and its experiments. Bieke Soen performed the writing of this chapter.

3.1 Abstract

Zeb1 is a multi-zinc-finger protein that can act as a transcriptional activator or transcriptional repressor and is best known for its role in epithelial-to-mesenchymal transition during embryogenesis and solid cancer metastasis. Although the function of Zeb1 in the dendritic cell lineage is unknown, its highly homologous family member Zeb2 has been implicated in plasmacytoid and conventional dendritic cell development. Here, we found *Zeb1* to be expressed in cDC1s and cDC2s across most murine tissues. To understand the role of Zeb1 in dendritic cells, we crossed the $CD11c^{CRE}$ mice to the $Zeb1^{fl/fl}$ mice. $CD11c^{CRE}xZeb1^{fl/fl}$ mice had a number of defects within the immune compartment of the spleen, including a reduced population of cDC1s; with the remaining cDC1s having an altered phenotype, and an almost complete lack of splenic macrophages. Additionally, loss of Zeb1 expression specifically in cDC1s also resulted in a reduction of splenic cDC1s and macrophages, together with an increase in CD103 expressing splenic cDC1s. In conclusion, we found that Zeb1 expression in cDC1s is crucial for the homeostasis of splenic mononuclear phagocytes and work is currently ongoing to determine the mechanisms at play.

3.2 Introduction

The transcription factor Zeb1, together with its family member Zeb2, is generally recognized for its role in epithelial-mesenchymal transition (EMT). EMT is a multistep process important during embryonic development and aberrantly activated by tumor cells in order to disseminate and form distant metastasis[1]. Other human diseases that are linked with mutations in the *ZEB1* gene are polymorphous corneal dystrophy type 3 and Fuch's endothelial corneal dystrophy type 6, two conditions characterized by corneal endothelial abnormalities and cloudiness of the cornea[2,3].

In recent years, research performed by us and others revealed that Zeb2 does not solely function as an EMT-TF, but also as a TF crucial for the homeostasis of several lineages of the hematopoietic system. Zeb2 has been shown to play a role in NK cell maturation[4], $CD8^+$ T cell terminal differentiation[5,6] and dendritic cell development[7,8]. For Zeb1 less is known regarding its role in the immune system, but nevertheless a role for Zeb1 in hematopoiesis has been suggested[9,10]. For instance, Zeb1 null mice die perinatally due to skeletal defects and respiratory failure, but were also found to have small hypocellular thymi[11]. Hypocellular thymi were also found in two Zeb1 mutant mice, the Δc-fin mouse and the cellophane mouse, both expressing a truncated Zeb1 lacking the C-terminal zinc finger domain. Moreover, both models display a block in early T cell differentiation[9,10]. In line with this Zeb1 was also found to repress expression of CD4 in T cells by competing with transcriptional activators at the CD4 promoter[12]. Further analysis of the spleen of the cellophane mouse also suggested defects in NK cell and B cell maturation[9]. However, it is unclear if these two Zeb1 mutant models generate truncated forms of Zeb1 that act as dominant negatives or cause loss of function. The recently developed conditional Zeb1 knockout model[13] will be helpful in the validation of these data and is the model we chose for our studies.

As we already identified a role for Zeb2 in the dendritic cell lineage, we were curious if its homolog Zeb1 acts in a similar fashion. Therefore, we crossed the conditional Zeb1 knockout mouse model[13] and the conditional Zeb1 overexpression model (developed in house) with the $CD11c^{CRE}$ line and studied the effects on the DC lineage.

3.3 Results

Zeb1 is expressed in cDC1s and cDC2s across most murine tissues

As we already investigated Zeb2 in DCs, we were curious if its homolog Zeb1 also has a function in the DC lineage. When comparing the expression patterns of *Zeb1* and *Zeb2* mRNA in different murine immune cells, we observed some differences. While *Zeb2* is expressed at relatively high levels in dendritic cell progenitors in the BM and red pulp macrophages (MFs) and NK cells in the spleen, *Zeb1* is expressed at relatively low levels in these populations (Figure 1A). For *Zeb2*, which we and others found to skew cDC development away from the cDC1 lineage[7,8], we see a distinctive pattern of high expression in cDC2s and low expression in cDC1s across different murine tissues (Figure 1A). In contrast, *Zeb1* is lowly expressed across both cDC1s and cDC2s in different murine tissues, with the exception of the liver, where it is not expressed in cDC2s. Additionally, pDCs in the spleen express relatively low levels of *Zeb1* (Figure 1A). As this expression pattern could be suggestive of a role for Zeb1 in the cDC compartment, we crossed the conditional Zeb1 knockout mouse

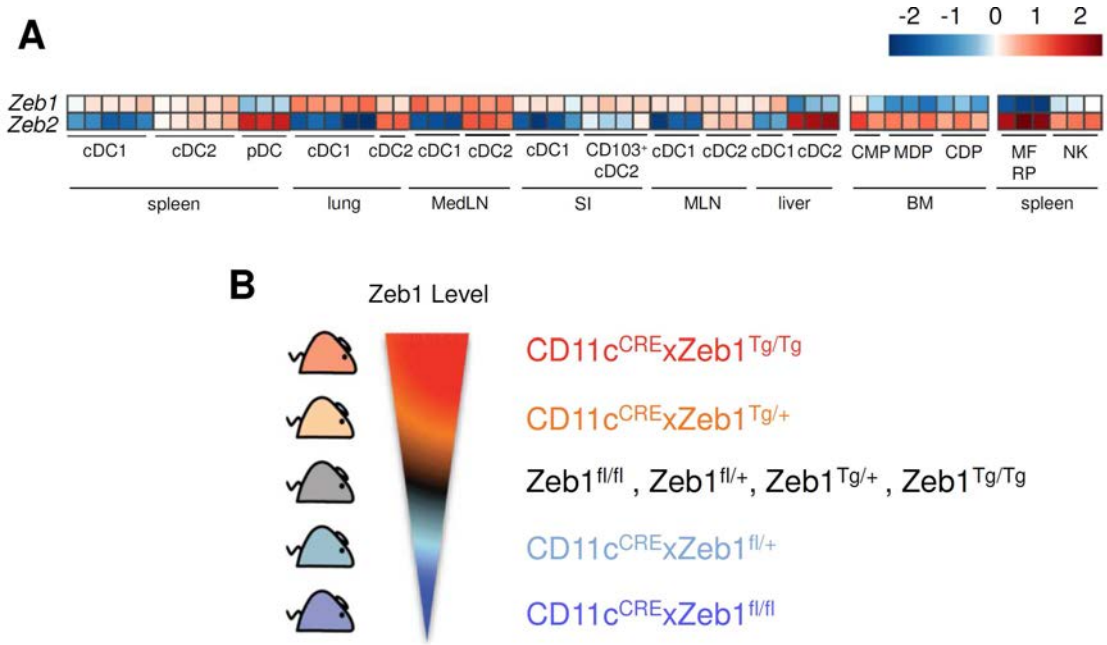

Figure 1 | Expression of *Zeb1* and *Zeb2* in dendritic cells. (A) Heatmap showing relative mRNA expression for *Zeb1* and *Zeb2* in cDC1s, cDC2s and pDCs from the spleen, cDC1s and cDC2s from the lung, mediastinal LN (MedLN), small intestine (SI), mesenteric LN (MLN) and liver, common myeloid progenitors (CMP), monocyte-dendritic cell precursors (MDP) and common dendritic cell precursors (CDP) from the BM and red pulp macrophages (MF RP) and NK cells from the spleen. Data were compiled from the Immgen Consortium. Gene expression was normalized per mean expression of each gene. (B) Schematic showing range of Zeb1 levels and nomenclature of the transgenic mouse lines used in this chapter.

model[13] and the conditional Zeb1 overexpression model (developed in house) with the CD11c^{CRE} line and studied the cDC populations in the resulting mice (Figure 1B).

Splenic cDC1s are reduced in CD11c^{CRE}xZeb1$^{fl/fl}$ mice, while cDC1s in other tissues are unaffected

To investigate the role of Zeb1 in cDCs, we first crossed the conditional Zeb1 knockout mouse[13] to the CD11c^{CRE} line[14] (Figure 1B) and analyzed the lung, liver, small intestine lamina propria (SILP) and spleen for the presence of the different cDC populations (Figure S1, gating strategies). In the lung, SILP and liver no significant differences were observed in terms of proportion or absolute cell number of cDC1s and cDC2s (Figure 2A, B and C; Figure S1B, D and C). When comparing splenic cDCs from CD11c^{CRE}xZeb1$^{fl/fl}$ mice with those from Zeb1$^{fl/fl}$ control littermates, a significant reduction was observed in the cDC1 population both in proportion as well as in absolute cell count (Figure 2D and Figure S1A). Additionally, we found a significant increase in cDC2s as a percentage of total cDCs in the spleens of CD11c^{CRE}xZeb1$^{fl/fl}$ mice. However, no difference was observed in terms of absolute numbers (Figure 2D). The reduction in splenic cDC1s following loss of Zeb1 expression in CD11c^{+} cells was only apparent when both alleles of *Zeb1* were targeted (Figure 2D), suggesting haplo-sufficient expression of Zeb1 is sufficient for normal cDC1 development and/or maintenance.

Splenic cDC1s and cDC2s of CD11c^{CRE}xZeb1$^{fl/fl}$ mice display an altered surface phenotype

Having established that Zeb1 deficiency in CD11c^{+} cells results in a reduction in the cDC1 population, we further looked in detail to the remaining cDCs. To this end, we first assessed the expression of CD103 and CD8α in splenic cDC1s. CD103 or Itgae is typically highly expressed in cDC1s in peripheral tissues, but is typically lacking in splenic cDC1s. CD8α expression follows the opposite trend, with high expression in splenic cDC1s and lower expression in cDC1s from peripheral tissues (with the exception of SILP cDC1s). Assessing protein levels with flow cytometry highlighted

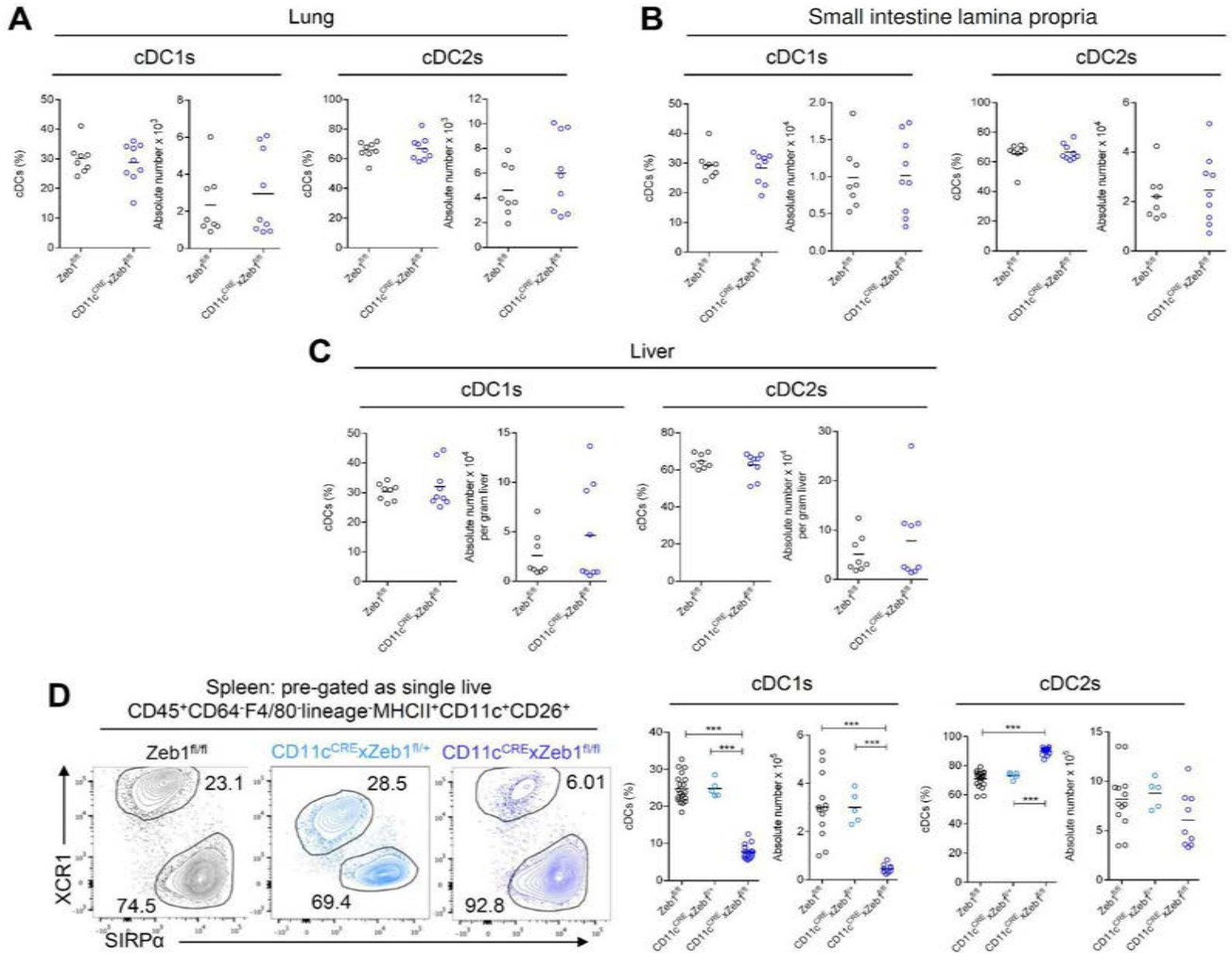

Figure 2 | CD11c^{CRE}xZeb1$^{fl/fl}$ mice show a reduction in splenic cDC1s. (A-C) Proportion as percentage of total cDCs and absolute cell number of cDC1s and cDC2s in the lung (A), SILP (B) and liver (C) of Zeb1$^{fl/fl}$ and CD11c^{CRE}XZeb1$^{fl/fl}$ mice. Data are pooled from two experiments with at least n=7 per group. No significance was found using a two-way Student's t test. (D) Representative FACS plots showing identification of XCR1^{+}SIRPα$^{–}$ cDC1s and XCR1$^{–}$SIRPα^{+} cDC2s in the spleen of indicated mice. Numbers represent the population as a percentage of total cDCs which were pre-gated as single live CD45^{+}CD64^{-}F4/80^{-}lineage^{-}MHCII^{+}CD11c^{+}CD26^{+}. Graphs show proportion as percentage of total cDCs and absolute cell number of cDC1s and cDC2s in the spleen of indicated mice. Data are pooled from two to three experiments with at least n=5 per group. **, P < 0.01; ***, P < 0.001. One-way ANOVA with Bonferroni post-test.

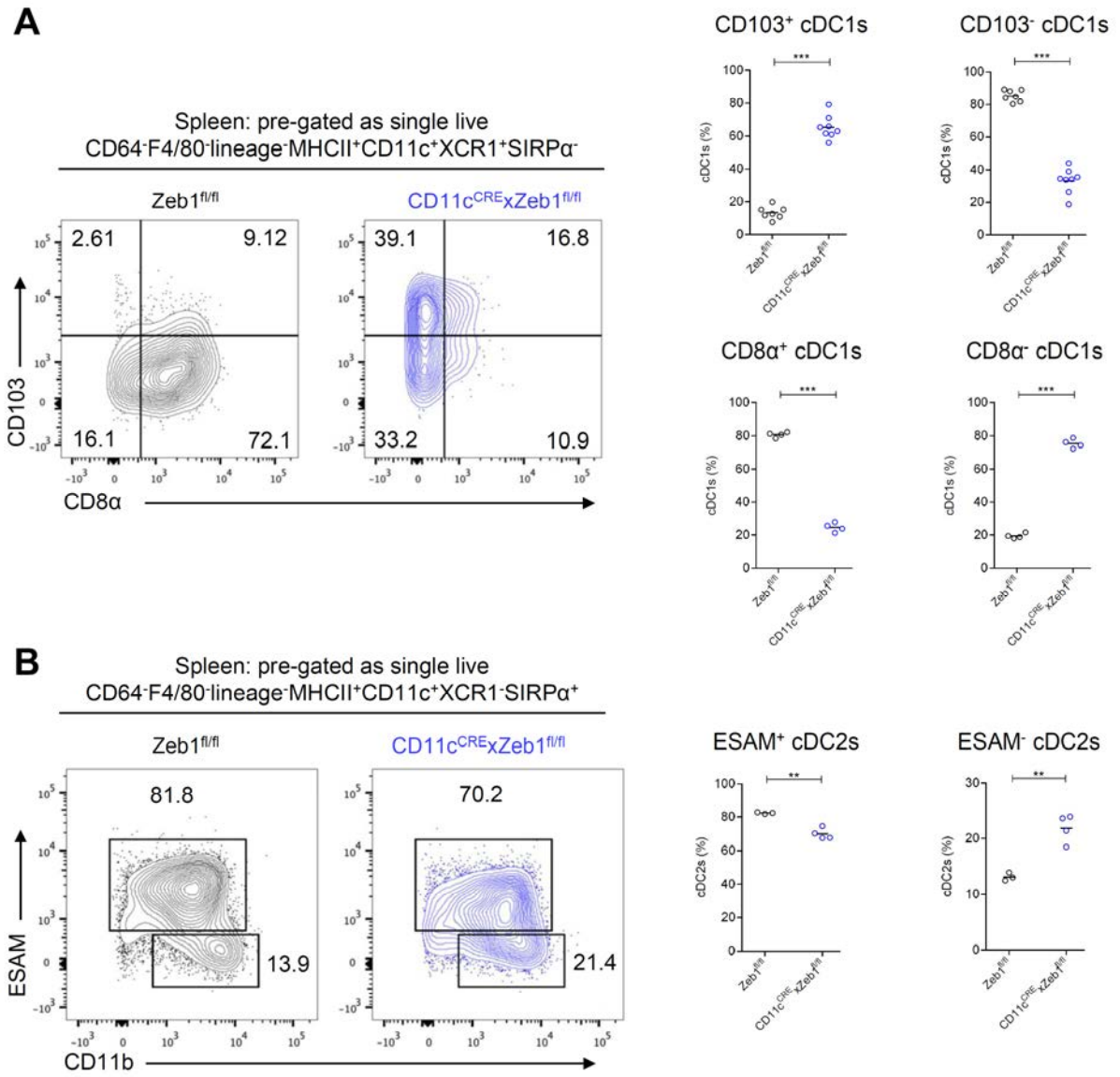

Figure 3 | Splenic cDC1s and cDC2s show a change in surface expression upon loss of Zeb1 in CD11c$^+$ cells. (A) Representative FACS plots showing expression of CD103 and CD8α in splenic cDC1s of Zeb1$^{fl/fl}$ and CD11c^{CRE}xZeb1$^{fl/fl}$ mice. Numbers represent the population as a percentage of total cDC1s which were pre-gated as single live CD64$^-$F4/80$^-$lineage$^-$MHCII$^+$CD11c$^+$XCR1$^+$SIRPα$^-$. Graphs show proportion of indicated population as percentage of total cDC1s. For CD103$^+$ and CD103$^-$ cDC1s data are pooled from two experiments, with at least n=7 per group; for CD8α$^+$ and CD8α$^-$ cDC1s data are from one experiment, with n=4 per group. (B) Representative FACS plots showing expression of ESAM and CD11b in splenic cDC2s of Zeb1$^{fl/fl}$ and CD11c^{CRE}xZeb1$^{fl/fl}$ mice. Numbers represent the population as a percentage of total cDC2s which were pre-gated as single live CD64$^-$F4/80$^-$lineage$^-$MHCII$^+$CD11c$^+$XCR1$^-$SIRPα$^+$. Graphs show proportion of indicated population as percentage of total cDC2s. Data are from one experiment, with at least n=3 per group. (A-B) **, $P < 0.01$; ***, $P < 0.001$. Two-way Student's t test.

that loss of Zeb1 in CD11c^{+} cells causes an upregulation of CD103 surface expression, coupled with a downregulation of CD8α surface expression on splenic cDC1s (Figure 3A). The CD103^{+} fraction of splenic cDC1s increased from 13.27 ± 1.46% in Zeb1$^{fl/fl}$ mice to 65.28 ± 2.50% in CD11c^{CRE}xZeb1$^{fl/fl}$ mice, while the CD8α^{+} fraction decreased from 80.65 ± 0.79% to 24.59 ± 1.36% (Figure 3A). Splenic cDC2s can be divided into two subsets based on ESAM and CD11b expression[15], therefore we examined the expression of ESAM and CD11b in the remaining splenic cDC2s. Knockout of Zeb1 in CD11c^{+} cells caused a loss of definition between ESAM^{+} and ESAM^{-} cDC2s. This led to a significant reduction of the ESAM^{+} fraction of cDC2s, with a decrease from 82.30 ± 0.29% in Zeb1$^{fl/fl}$ mice to 69.98 ± 1.63% in CD11c^{CRE}xZeb1$^{fl/fl}$ mice (Figure 3B). Taken together, it appears that loss of Zeb1 from CD11c expressing cells alters the phenotype of splenic cDCs.

The defect in splenic cDC1s and cDC2s of CD11c^{CRE}xZeb1$^{fl/fl}$ mice is fully observed from 4 weeks of age

Having established the phenotype in adult (6-12 week old) mice, we next wanted to determine if the observed splenic cDC phenotype is present from birth or if it gradually develops with age. For this, we examined CD11c^{CRE}xZeb1$^{fl/fl}$ mice together with their littermate controls at 1 week, 3 weeks and 4 weeks of age. Flow cytometric analysis of splenic cDC1s revealed that their reduction following loss of Zeb1 in CD11c^{+} cells is not present 1 week after birth, but becomes apparent starting from 3 weeks of age (Figure 4A). Next we assessed the presence of CD103 on the surface of splenic cDC1s. Already in 1 week old CD11c^{CRE}xZeb1$^{fl/fl}$ mice we found a significant increase of the CD103^{+} cDC1 subpopulation. The difference with control littermates further increases as the mice become older (Figure 4B and 4C). Surprisingly, a big majority of splenic cDC1s of 1 week old WT mice express CD103 (Figure 4B and 4C). This in contrast to WT adult mice of whom the CD103^{+} fraction of splenic cDC1s is a distinct minority (Figure 3A). It appears that around birth almost all splenic cDC1s express CD103 and this expression is gradually downregulated with age. However, when Zeb1 is not expressed in CD11c^{+} cells this downregulation of

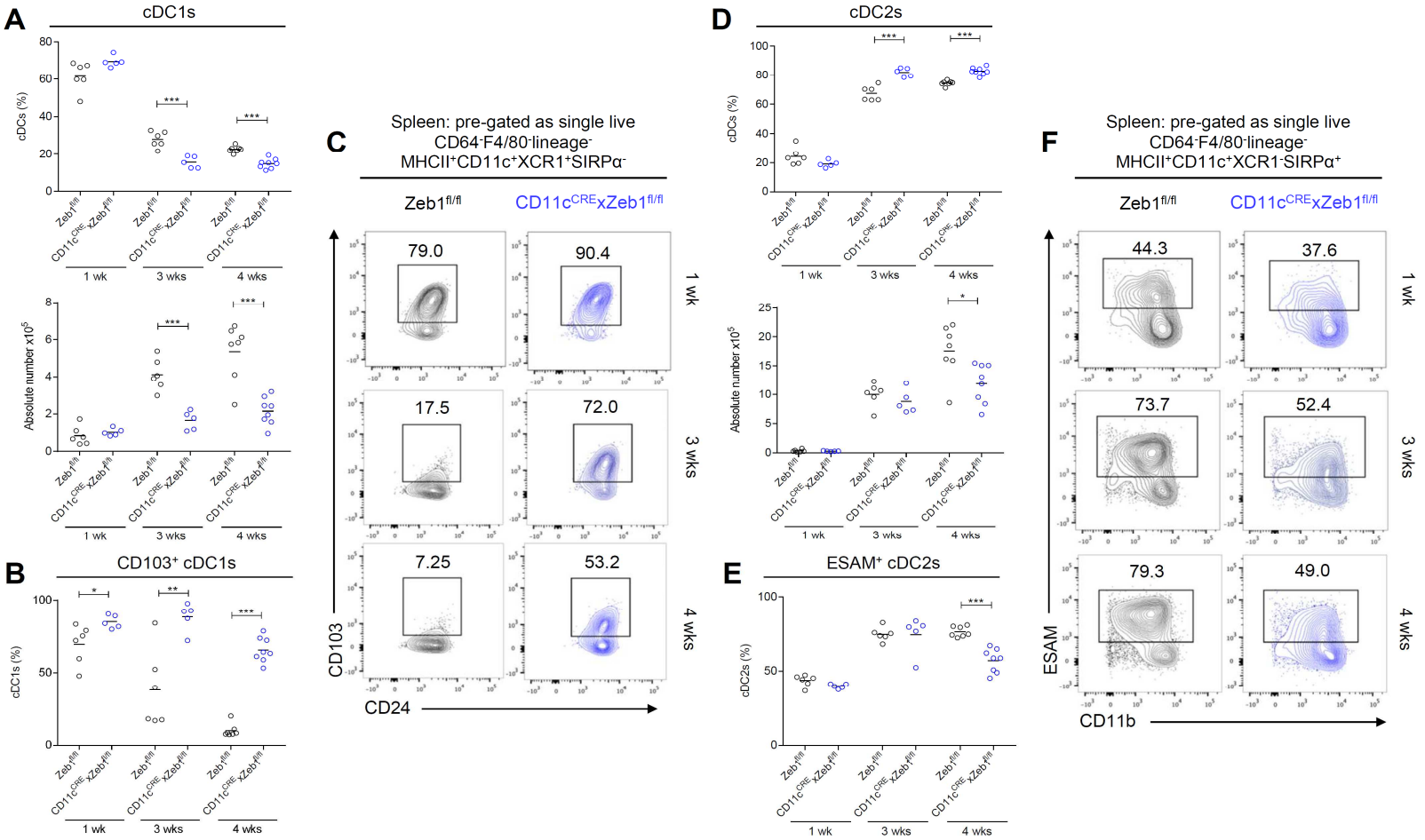

Figure 4 | The defect in splenic cDC1s and cDC2s from CD11c^{CRE}xZeb1$^{fl/fl}$ mice is fully present at 4 weeks of age. (A and D) Proportion as percentage of total cDCs and absolute cell number of cDC1s (A) and cDC2s (D) in the spleen of Zeb1$^{fl/fl}$ and CD11c^{CRE}XZeb1$^{fl/fl}$ mice at 1 week, 3 weeks and 4 weeks of age. (B and E) CD103$^+$ cDC1s as a percentage of total cDC1s (B) and ESAM$^+$ cDC2s as a percentage of total cDC2s (E) in the spleen of Zeb1$^{fl/fl}$ and CD11c^{CRE}XZeb1$^{fl/fl}$ mice at 1 week, 3 weeks and 4 weeks of age. (C and F) Representative FACS plots showing expression of CD103 and CD24 in splenic cDC1s (C) and expression of ESAM and CD11b in splenic cDC2s (F) of Zeb1$^{fl/fl}$ and CD11c^{CRE}xZeb1$^{fl/fl}$ mice at 1 week, 3 weeks and 4 weeks of age. Numbers represent the population as a percentage of total cDC1s which were pre-gated as single live CD64$^-$F4/80$^-$lineage$^-$MHCII$^+$CD11c$^+$XCR$^+$SIRPα$^-$ (C) or as a percentage of total cDC2s which were pre-gated as single live CD64$^-$F4/80$^-$lineage$^-$MHCII$^+$CD11c$^+$XCR1$^-$SIRPα$^+$ (F). (A-F) For 1 week old mice data are from one experiment with at least n=5 per group, for 3 and 4 weeks old mice data are pooled from two experiments with at least n=5 per group. *, P < 0.05; **, P < 0.01; ***, P < 0.001. Two-way Student's t test.

CD103 in splenic cDC1s is decreased (Figure 4 B and 4C). We also investigated how the cDC2 phenotype develops with age. Here we found the increase in splenic cDC2s as a percentage of total cDCs from 3 weeks of age onward (Figure 4D). However, in 4 week old mice this was coupled with a significant reduction in splenic cDC2 cell counts. This is in contrast with adult CD11c^{CRE}xZeb1$^{fl/fl}$ mice, in which we only found a trend towards a decreased absolute number of splenic cDC2s (Figure 2D). Furthermore, the reduction of the ESAM^{+} Notch2-dependent cDC2s is established at 4 weeks of age, but is not significant in younger mice. All in all we can conclude that the reduction and changed surface phenotype of splenic cDC1s and cDC2s in CD11c^{CRE}xZeb1$^{fl/fl}$ mice is present from 4 weeks of age onward, suggesting that the adult tissue environment is needed to provoke the phenotype.

Loss of Zeb1 expression in CD11c^{+} cells has a dominant effect on WT cDC1s

As the CD11c^{CRE} line not only targets cDCs[16], we sought to determine if the effects of Zeb1 knockout in CD11c^{+} cells on splenic cDCs are cell intrinsic or caused by another cell. To this end, we generated competitive BM chimeras, in which CD45.1/CD45.2 WT mice were lethally irradiated and reconstituted with a ~70:30 mix (determined through analysis of splenic neutrophils; Figure 5B and Figure S3) of CD45.2 Zeb1$^{fl/fl}$ or CD11c^{CRE}xZeb1$^{fl/fl}$ BM and CD45.1 WT BM. Eight weeks after reconstitution, the splenic cDC1s and cDC2s were analysed for CD45.2 chimerism (Figure 5A). Although we found that the absolute cell number of total cDC1s is reduced in mice that received the mix with CD11c^{CRE}xZeb1$^{fl/fl}$ BM, the proportion of cDC1s deriving from CD11c^{CRE}xZeb1$^{fl/fl}$ BM was not altered (Figure 5B). Next we analyzed the surface expression of CD103 on splenic cDC1s in the different chimeric mice. When reconstituted with a CD45.2 Zeb1$^{fl/fl}$ / CD45.1 WT BM mix, both cDC1s derived from Zeb1$^{fl/fl}$ mice and WT mice only contained a minority of CD103^{+} cells with an average of 7.13 ± 1.92% for CD45.1 and 6.95 ± 1.63% for CD45.2 cells (Figure 5C). However, reconstitution with the mix containing CD11c^{CRE}xZeb1$^{fl/fl}$ BM did change the expression of CD103 in cDC1s. In these mice on average 46.30 ± 5.21% of cDC1s derived from CD45.2 CD11c^{CRE}xZeb1$^{fl/fl}$ BM were CD103 positive. Surprisingly, an increased fraction (40.95 ± 4.53%) of the cDC1s derived from CD45.1 WT BM also expressed CD103 on their cell surface (Figure 5C). From this

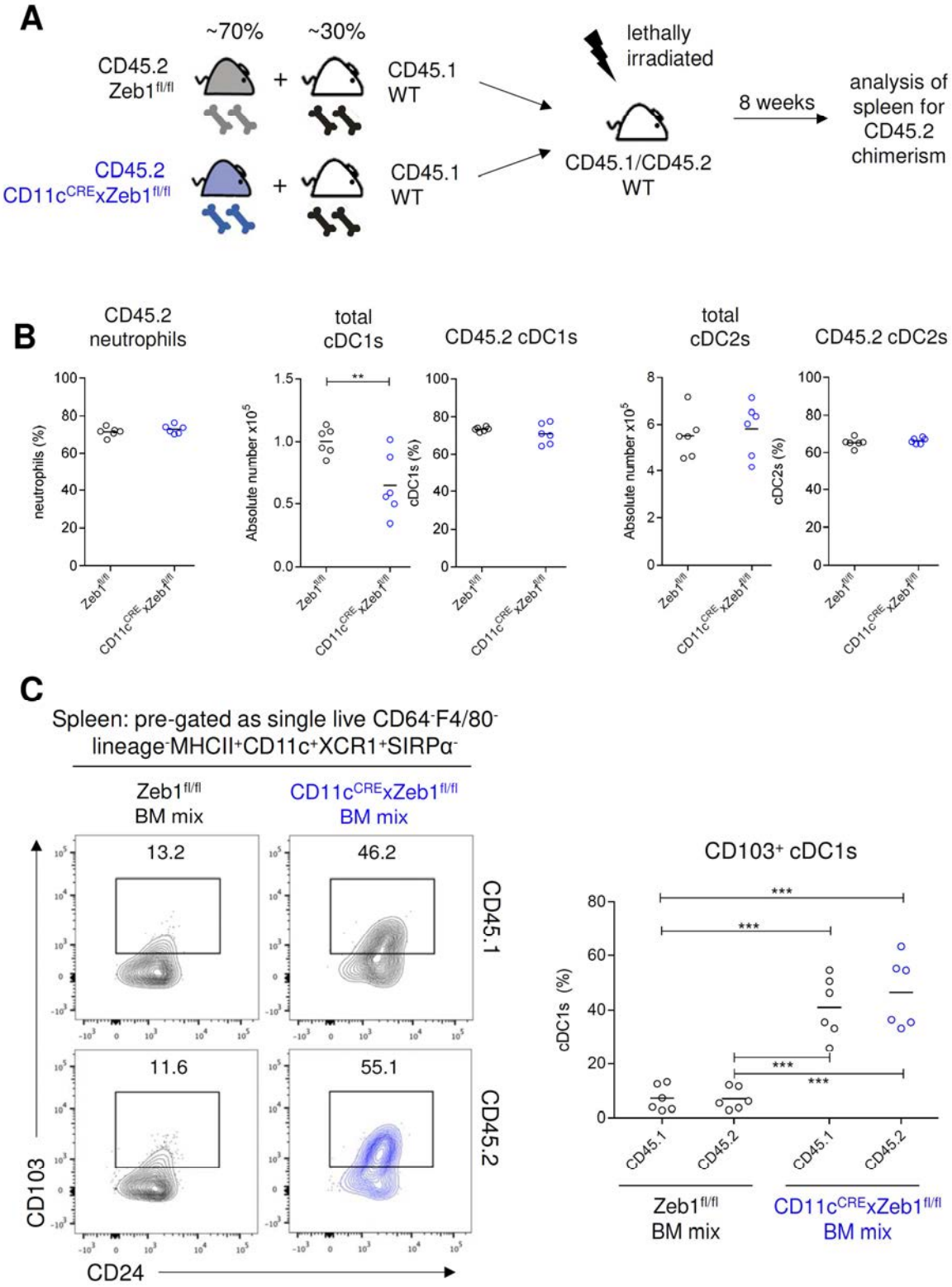

Figure 5 | Loss of Zeb1 expression in CD11c⁺ cells also affects WT cDC1s. (A) Competitive BM chimeric mice were generated by lethally irradiating CD45.1/CD45.2 WT mice and reconstituting with a ~70:30 mix of Zeb1$^{fl/fl}$ or CD11c^{CRE}xZeb1$^{fl/fl}$ CD45.2 BM and WT CD45.1 BM. (B) CD45.2 splenic neutrophils, cDC1s and cDC2s as a percentage of total splenic neutrophils, cDC1s and cDC2s respecitvely. Absolute cell number of splenic cDC1s and cDC2s in chimeric mice. **, P < 0.01. Two-way student's t test. (C) Representative FACS plots showing CD103 and CD24 expression in CD45.1 or CD45.2 splenic cDC1s in chimeric mice. Numbers represent the population as a percentage of total cDC1s. Graph shows CD103⁺ cDC1s as a percentage of total CD45.1 or CD45.2 cDC1s in the spleen of chimeric mice. ***, P < 0.001. One-way ANOVA with Bonferroni post-test. (B and C) Data are pooled from two experiments, with at least n=6 per group.

we can conclude that BM from CD11c^{CRE}xZeb1$^{fl/fl}$ mice (CD45.2) has no competitive advantage or disadvantage over WT BM (CD45.1) to generate cDC1s, but that the lack of Zeb1 in CD11c expressing cells has a dominant effect on all cDC1s, regardless of their Zeb1 expression. As such, the use of competitive BM chimeras does not allow us to determine if the splenic cDC1 defect in CD11c^{CRE}xZeb1$^{fl/fl}$ mice is cell intrinsic or not. With regard to the splenic cDC2s there was no trend towards a decrease in absolute cell numbers when Zeb1 knockout BM was present and the CD45.2^{+} fraction of the cDC2s was not different between mice reconstituted with Zeb1$^{fl/fl}$ and CD11c^{CRE}xZeb1$^{fl/fl}$ BM mix. Again, this means that WT BM and BM from CD11c^{CRE}xZeb1$^{fl/fl}$ mice are equally capable of generating cDC2s. During this experiment however, we did not analyse the expression of ESAM on the splenic cDC2s. Therefore, we do not know if the loss of definition between ESAM^{+} and ESAM^{-} cDC2s in CD11c^{CRE}xZeb1$^{fl/fl}$ mice is cell intrinsic or caused by a dominant factor that can also affect WT cDC2s.

The observed phenotype is caused by loss of Zeb1 in the hematopoietic compartment

Next we wanted to asses if the dominant factor causing the splenic cDC phenotype has a hematopoietic or non-hematopoietic origin. To investigate this, we generated partially protected chimeras, which means that we lethally irradiated CD45.1 WT mice with their spleens protected by a lead skirt. This setup ensures that the non-hematopoietic compartment of the spleen is made up of WT cells and protected from effects of irradiation (Figure 6A). The next day irradiated mice were reconstituted with CD45.2 Zeb1$^{fl/fl}$ or CD45.2 CD11c^{CRE}xZeb1$^{fl/fl}$ BM. As the spleen of the mice was protected during irradiation, we needed to wait for the hematopoietic compartment to change by natural turnover. Therefore, we analysed the spleens of the chimeric mice 8 weeks after reconstitution to confirm chimerism and to determine if the observed splenic cDC phenotype is present (Figure 6A). CD45.2 chimerism in cDC1s, cDC2s and macrophages was calculated as a ratio to the CD45.2 chimerism of the neutrophils in the same sample. Neutrophils showed an average CD45.2:CD45.1 ratio of ~60:40 after reconstitution with both types of BM. For both cDC1s and cDC2s

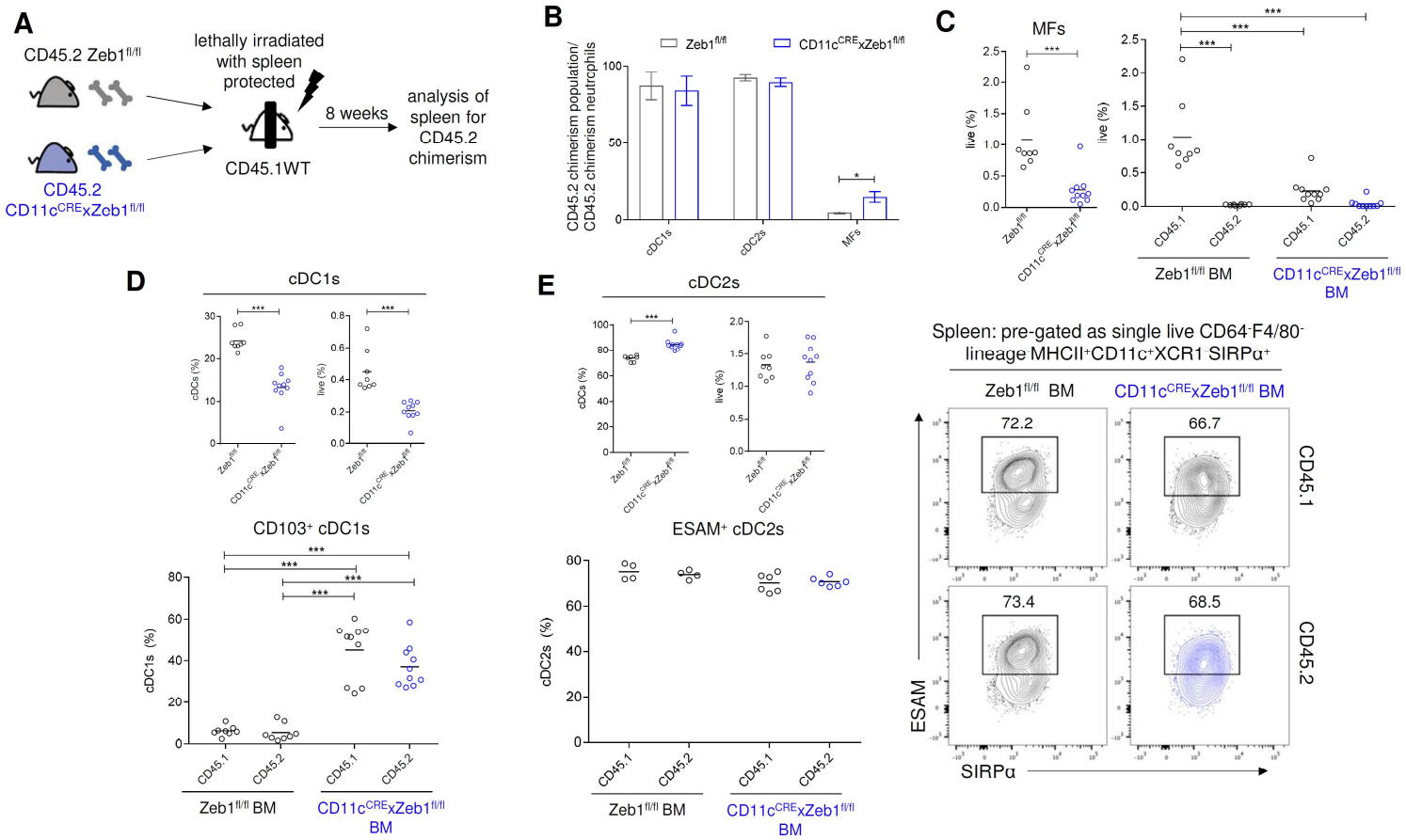

Figure 6 | Loss of Zeb1 in the hematopoietic compartment is causing the observed splenic phenotype. (A) CD45.1 WT mice were lethally irradiated with their spleens protected and reconstituted with CD45.2 Zeb1$^{fl/fl}$ or CD11c^{CRE}xZeb1$^{fl/fl}$ BM. 8 weeks after reconstitution spleens were analysed. (B) Percentage of chimerism after reconstitution with Zeb1$^{fl/fl}$ or CD11c^{CRE}xZeb1$^{fl/fl}$ BM of indicated population represented as the ratio of CD45.2 chimerism in the indicated population to the CD45.2 chimerism in neutrophils. **, P<0.01. Two-way student's t test. (C) Left graph: MFs as percentage of live cells. ***, P<0.001. Two-way student's t test. Right graph: CD45.1 and CD45.2 MFs as percentage of live cells. ***, P<0.001. One-way ANOVA with Bonferroni post-test. (D) Upper graph: cDC1s as percentage of total cDCs and percentage of live cells. ***, P<0.001. Two-way student's t test. Lower graph: CD45.1 and CD45.2 CD103^{+} cDC1s as percentage of total cDC1s. ***, P<0.001. One-way ANOVA with Bonferroni post-test. (E) Upper graph: cDC2s as percentage of total cDCs and percentage of live cells. ***, P<0.001. Two-way student's t test. Lower graph: CD45.1 and CD45.2 ESAM^{+} cDC2s as percentage of total cDC2s. No significance was found with one-way ANOVA with Bonferroni post-test. Representative FACS plots showing ESAM and SIRPα expression in CD45.1 or CD45.2 splenic cDC2s in chimeric mice. Numbers represent the population as a percentage of total cDC2s. (B-E) Data are pooled from two experiments with at least n=8 per group.

there was no significant difference in the percentage of chimerism between mice reconstituted with Zeb1$^{fl/fl}$ or CD11c^{CRE}xZeb1$^{fl/fl}$ BM (Figure 6B). Due to protection of the spleen during irradiation, chimerism in macrophages was low compared with neutrophils. For the macrophages we found a significant increase in CD45.2 chimerism upon reconstitution with CD11c^{CRE}xZeb1$^{fl/fl}$ BM (Figure 6B). This could be explained by the observation that reconstitution with CD11c^{CRE}xZeb1$^{fl/fl}$ BM causes a drastic decrease in the number of macrophages present in the spleen. Surprisingly, this reduced number of macrophages mostly resulted from a non-cell-intrinsic effect on WT CD45.1 macrophages (Figure 6C). This severe decrease of the macrophage population is also observed in the spleen of CD11c^{CRE}xZeb1$^{fl/fl}$ mice (Figure 8D). In our protected chimeras, it is likely that this loss of macrophages is compensated through influx from the CD45.2 BM, leading to a higher percentage of CD45.2 chimerism (Figure 6B). Next we investigated if the observed cDC1 and cDC2 phenotype was also present when using the protected chimera setup. Indeed, reconstitution with CD11c^{CRE}xZeb1$^{fl/fl}$ BM caused a reduction of the cDC1 population (Figure 6D). Again, the remaining cDC1s contained an increased CD103 expressing subpopulation and as observed in the competitive BM chimeras this holds true for both WT CD45.1 cDC1s and Zeb1 knockout CD45.2 cDC1s (Figure 6D). With regards to the cDC2s, reconstitution with CD11c^{CRE}xZeb1$^{fl/fl}$ BM caused an increase in cDC2s when represented as a percentage of total cDCs, but this was not coupled with a difference when expressed as a percentage of live cells (Figure 6E). Although there was no significant decrease in the ESAM^{+} cDC2 fraction, we did notice a loss of definition between the ESAM^{-} and ESAM^{+} subpopulations after reconstitution with CD11c^{CRE}xZeb1$^{fl/fl}$ BM and this for both CD45.1 WT as CD45.2 Zeb1 knockout cDC2s (Figure 6E). The setup used ensured presence of a completely WT non-hematopoietic compartment in the spleen and thus the fact that we find back the originally observed phenotypes demonstrates that the phenotypes are caused by the loss of Zeb1 in a haematopoietic cell. Therefore, we conclude that the splenic cDC phenotype in CD11c^{CRE}xZeb1$^{fl/fl}$ mice is driven by the loss of Zeb1 in an immune cell targeted by the CD11c^{CRE} line.

The CD11c^{CRE} line not only targets cDCs in the spleen

Having established that the loss of Zeb1 in a CD11c expressing hematopoietic cell lies at the origin of the splenic cDC and macrophage phenotype in CD11c^{CRE}xZeb1$^{fl/fl}$ mice, we sought to determine which immune cell could be responsible. To confirm previous findings that the CD11c^{CRE} line targets other immune cells in addition to cDCs[16], we crossed the CRE line with the Rosa-RFP reporter line[17]. Next we analysed the spleen of the resulting mice to determine which cells were tagged with

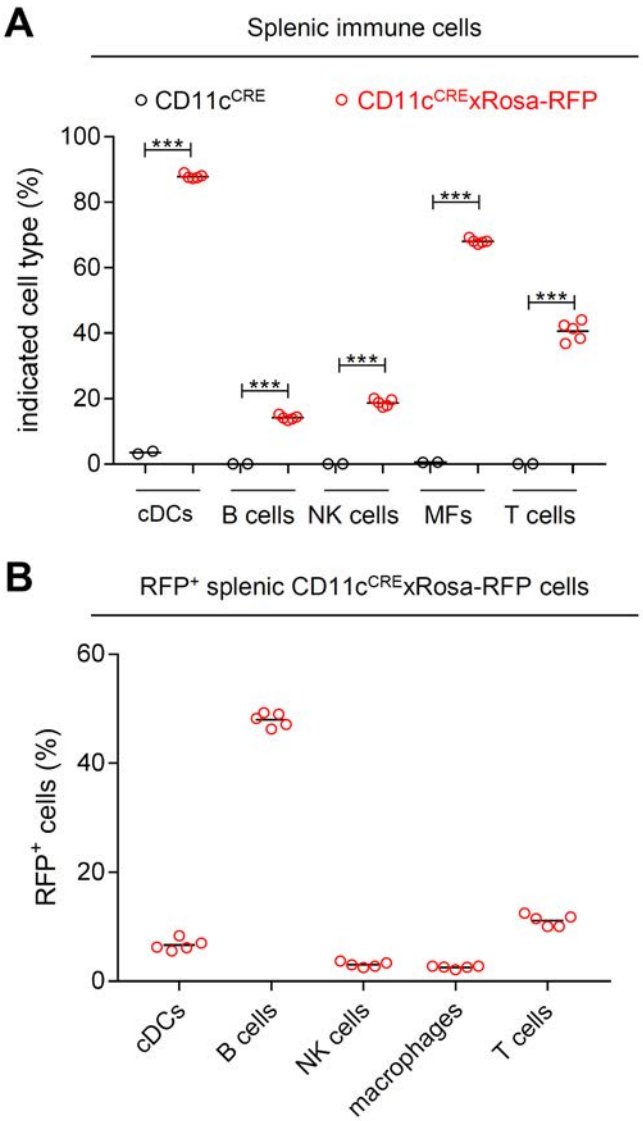

Figure 7 | Off target effects in the spleen of the CD11c^{CRE} mouse line. (A) Graph representing the percentage of indicated cells that show expression of RFP in the spleen of CD11c^{CRE} (black circles) and CD11c^{CRE}xRosa-RFP (red circles) mice. cDCs were pre-gated as single live CD19$^-$CD3$^-$NK1.1$^-$F4/80$^-$CD64$^-$CD11c$^+$MHCII$^+$, B cells as single live CD19$^+$, NK cells as single live CD19$^-$CD3$^-$NK1.1$^+$, macrophages (MFs) as CD19$^-$CD3$^-$NK1.1$^-$F4/80$^+$CD64$^-$ and T cells as single live CD19$^-$CD3$^+$NK1.1$^-$. Data are from one experiment with at least n=2 per group. ***, P < 0.001. Two-way student's t test. (B) Graph representing the proportion of indicated cell type within total RFP$^+$ splenic cells of CD11c^{CRE}xRosa-RFP mice. Data are from one experiment with n=5.

RFP and thus targeted by the CD11c^{CRE} mouse line (Figure S2). This demonstrated that while cDCs were targeted (with an average of 87.90%) also 14.14% of B cells, 18.74% of NK cells, 68.02% of macrophages and 40.60% of T cells expressed RFP and hence are targeted with the CD11c^{CRE} line (Figure 7A). If we than look at all RFP expressing cells in the spleen of CD11c^{CRE}xRosa-RFP mice, we see that only 6.67% of them are the cDCs that we aimed to target. 47.98% of all RFP^{+} cells are B cells, 3.09% are NK cells, 2.26% are macrophages and 11.20% are T cells (Figure 7B). Additionally, it was previously shown that neutrophils and monocytes are also targeted with the CD11c^{CRE} line[16]. As such, it could be that the loss of Zeb1 expression in cDC1s, cDC2s, B cells, NK cells, T cells, macrophages, neutrophils or monocytes causes the splenic cDC phenotype in CD11^{CRE}xZeb1$^{fl/fl}$ mice. Additionally, the loss of Zeb1 could induce cell-intrinsic defects in one of these populations themselves.

Additional effects of loss of Zeb1 in CD11c^{+} cells in the immune system

Having shown that the CD11c^{CRE} line targets other immune cells besides cDCs, we wanted to examine if these cell types were affected in CD11c^{CRE}xZeb1$^{fl/fl}$ mice. To this end, we performed flow cytometry on single cell suspensions from the spleen of CD11c^{CRE}xZeb1$^{fl/fl}$ mice and their control littermates with a mix containing following antibodies: CD11b, CD64, F4/80, NK1.1, Ly6G, CD3, XCR1, Ly6C, MHCII, CD172a (SIRPα), CD19 and CD11c. The obtained data were then processed using the FlowSOM algorithm, which generates a clear overview on how all markers are behaving on all cells without introducing a bias from a subjective manual gating strategy and from only looking at pairwise comparisons[18]. The output of the algorithm is a tree that clusters cells with similar expression of the surface markers in a pie chart, with the size of the pie chart equivalent to the number of cells showing this expression pattern. In the spleen of CD11c^{CRE}xZeb1$^{fl/fl}$ mice we can see that certain cell types have a decreased presence (light blue shadows), while other cell types show an increase in presence (red shadows) compared with the Zeb1$^{fl/fl}$ WT spleens (Figure 8A). This highlights a severe imbalance in the proportions of a number of immune cell subtypes and we next wanted to find out if this also changes the general architecture of the splenic tissue. To examine this, we performed confocal

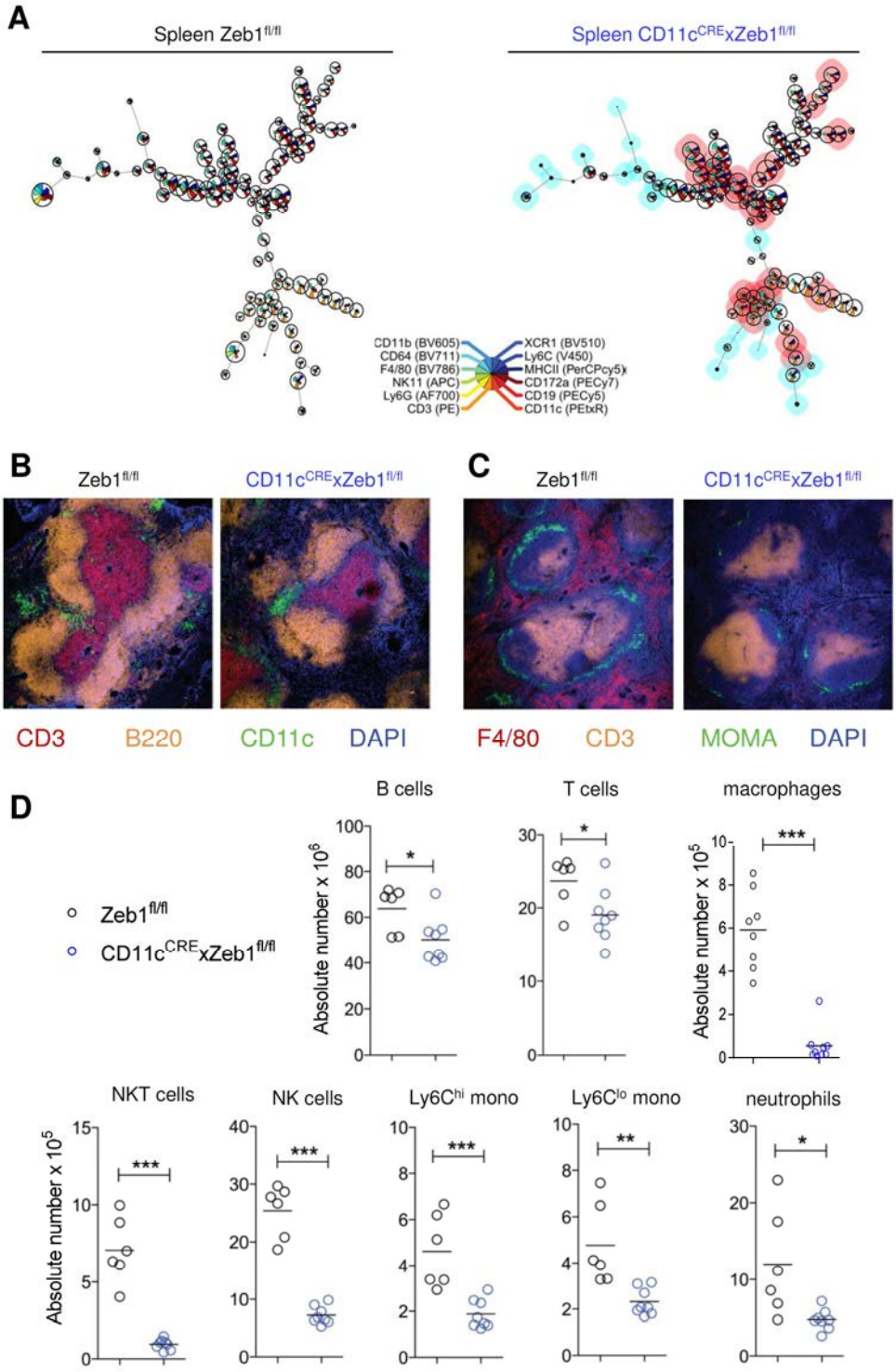

Figure 8 | Additional effects on immune populations in CD11c^{CRE}xZeb1$^{fl/fl}$ spleens. (A) Tree resulting from analysis with the FlowSOM algorithm[18] performed for Zeb1$^{fl/fl}$ and CD11c^{CRE}xZeb1$^{fl/fl}$ spleens. Each pie chart shows expression of the different markers used during flow cytometry (see legend included) and the size of the pie chart is equivalent to the number of cells showing such expression. Bright blue shadows mean reduction in cells and red shadows mean increase in cells when comparing CD11c^{CRE}xZeb1$^{fl/fl}$ splenic cells with those from Zeb1$^{fl/fl}$ littermates.(B) Immunofluerescent staining of spleen sections from Zeb1$^{fl/fl}$ and CD11c^{CRE}xZeb1$^{fl/fl}$ mice with CD3 (red), B220/CD45R (yellow), CD11c (green) and DAPI (blue). (C) Immunofluerescent staining of spleen from Zeb1$^{fl/fl}$ and CD11c^{CRE}xZeb1$^{fl/fl}$ mice with F4/80 (red), CD3 (yellow), MOMA (green) and DAPI (blue). (D) Absolute cell numbers for splenic B cells, T cells, macrophages, NKT cells, NK cells, Ly6C^{hi} monocytes (mono), Ly6C^{lo} monocytes and neutrophils in Zeb1$^{fl/fl}$ (black circles) and CD11c^{CRE}xZeb1$^{fl/fl}$ (blue circles) mice. Data are pooled from two experiments, with at least n=6 per group. *, $P < 0.05$; **, $P < 0.01$; ***, $P < 0.001$. Two-way student's t test.

microscopy on cryosections of the spleens of CD11c^{CRE}xZeb1$^{fl/fl}$ and control littermates with two different antibody combinations. The first antibody mix with CD3, B220 and CD11c allows us to visualize the localization of T cells, B cells and DCs in the spleen respectively. In both spleens from Zeb1$^{fl/fl}$ and CD11c^{CRE}xZeb1$^{fl/fl}$ mice we can clearly distinguish the T cell zone (red) surrounded by B cell follicles (yellow). For both genotypes the dendritic cells (green) are present in the marginal zone (MZ) and the MZ bridging channels (Figure 8B). However, this antibody panel did not allow us to assess the localization of cDC1s and cDC2s or respectively their CD103^{+} and ESAM^{+} subpopulations. Therefore, extra stainings containing XCR1, CD103, SIRPα and ESAM are necessary. The second antibody combination shows the presence of red pulp macrophages (F4/80; red), metallophilic MZ macrophages (MOMA; green) and again the T cell area (CD3; yellow). Although the general cellular layout remains unaffected, this staining reveals an almost complete lack of red pulp macrophages and a reduction in MZ macrophages when Zeb1 expression is absent from CD11c^{+} cells (Figure 8C). Next we manually gated the data from the FlowSOM experiment (Figure S3) to determine in detail what particular immune cells were affected in the spleen from CD11c^{CRE}xZeb1$^{fl/fl}$ mice. This highlighted significant reductions in the absolute cell numbers of B cells, T cells, macrophages, NKT cells, NK cells, Ly6C^{hi} monocytes, Ly6C^{lo} monocytes and neutrophils (Figure 8D and Figure S3). As these cells are targeted by the CD11c^{CRE} line[16] (Figure 7A), these reduced populations could be directly due to the loss of Zeb1 in the cells themselves, but could also be the consequence of a non-cell-intrinsic effect. Moreover, it could be that the loss of one of these populations is the cause of the cDC phenotype. Despite this reductions in cell numbers of all these different types of immune cells, we did not find a difference in spleen weight (data not shown) and general architecture of the spleen (Figure 8B and 8C). Nevertheless, the absence of red pulp macrophages seen on cryosections of CD11c^{CRE}xZeb1$^{fl/fl}$ mice (Figure 8C), was confirmed by flow cytometry for which enzymatic digestion only isolated red pulp macrophages and not MZ macrophages (Figure 8D). Moreover, this loss of red pulp macrophages was previously observed in the protected chimeras, in which we determined that this was caused by a dominant factor that also affected wild type red pulp macrophages.

NK cells do not drive the splenic cDC phenotype in CD11c^{CRE}xZeb1$^{fl/fl}$ mice

We next wanted to determine which of the immune cells may be causing the observed effects in CD11c^{CRE}xZeb1$^{fl/fl}$ mice. To this end we crossed the Zeb1$^{fl/fl}$ mice to a number of different CRE lines that were available in house. First we crossed the conditional Zeb1 knockout mouse with the NK cell specific NKp46^{CRE} line containing an internal ribosome entry site (IRES) followed by an *iCRE* gene in the 3' end of the *NKp46* gene. Flow cytometric analysis of the spleen revealed that loss of Zeb1 in NK cells causes a small but significant reduction in absolute NK cell numbers (Figure 9 and Figure S3). To explore if the splenic phenotype of the CD11c^{CRE}xZeb1$^{fl/fl}$ mice is repeated in the NKp46^{CRE}xZeb1$^{fl/fl}$ cross, the presence of MFs, cDC1s and cDC2s was assessed. Differences in the number or phenotype of these three cell populations were however not observed in this model (Figure 9A). From the findings in NKp46^{CRE}xZeb1$^{fl/fl}$ mice we can conclude two things. First, the reduction in NK cell numbers in the spleen of CD11c^{CRE}xZeb1$^{fl/fl}$ mice is likely, at least in part, cell intrinsic. Secondly, the defect in cDCs and macrophages in CD11c^{CRE}xZeb1$^{fl/fl}$ mice is not driven by the loss of Zeb1 in NK cells.

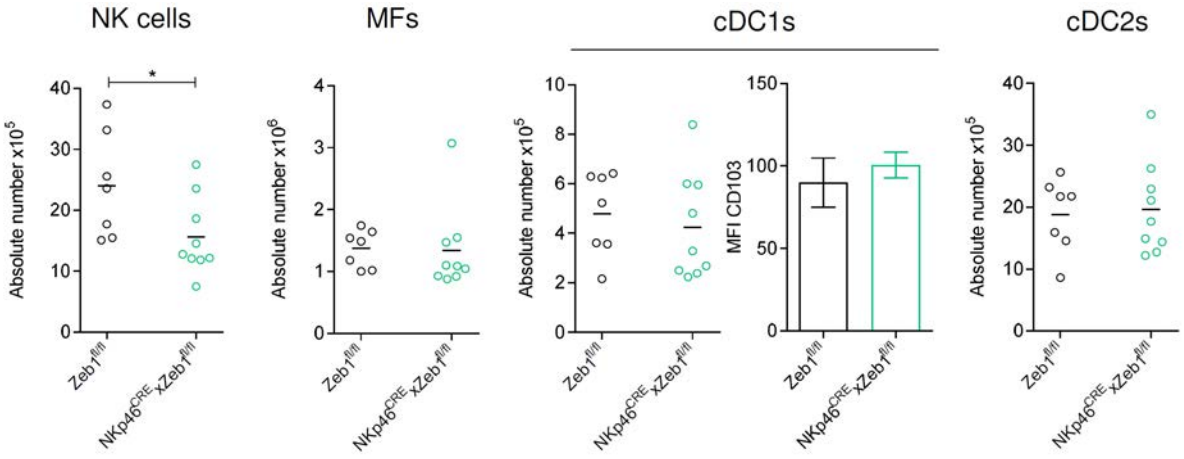

Figure 9 | Loss of Zeb1 in NK cells is not the cause of the observed cDC and MF phenotype. (A) Dot plots showing absolute cell numbers of NK cells, macrophages (MFs), cDC1s and cDC2s in the spleen of Zeb1$^{fl/fl}$ and NKp46^{CRE}xZeb1$^{fl/fl}$ mice. Bar graph showing mean fluorescence intensity (MFI; geometric mean) of CD103 for splenic cDC1s of Zeb1$^{fl/fl}$ and NKp46^{CRE}xZeb1$^{fl/fl}$ mice. Data are pooled from two experiments with at least n=7 per group. *, P<0.05. Two-way student's t test.

The observed phenotype is caused by the loss of Zeb1 in cDC1s

Next we wanted to determine if the effects seen in the CD11c^{CRE}xZeb1$^{fl/fl}$ mice are caused by the loss of Zeb1 in cDCs. Therefore we wanted to determine if we could use the Zbtb46^{CRE} line, which has previously been reported to specifically target cDCs within the hematopoietic compartment[19,20]. Therefore, we crossed the Zbtb46^{CRE} line to the Rosa-RFP reporter mice and assessed the expression of RFP in splenic immune cells. This revealed that cDC1s and cDC2s are indeed targeted, but rather inefficiently, with respectively 68.72 ± 1.11% and 47.93 ± 0.60% cells

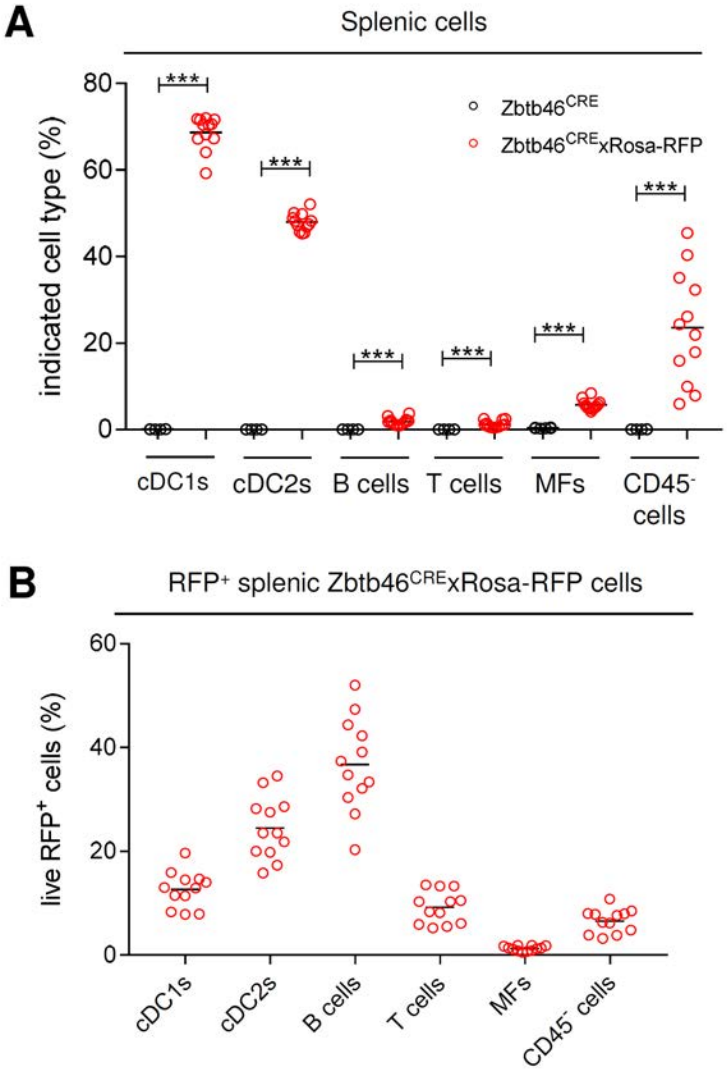

Figure 10 | Off target effects in the spleen of the Zbtb46^{CRE} mouse. (A) Graph representing the percentage of indicated cells that show expression of RFP in the spleen of Zbtb46^{CRE} (black circles) and Zbtb46^{CRE}xRosa-RFP (red circles) mice. ***, P < 0.001. Two-way student's t test. (B) Graph representing the proportion of indicated cell type within total RFP^{+} splenic cells of Zbtb46^{CRE}xRosa-RFP mice. Data or pooled from two experiments with at least n=6 per group.

expressing RFP (Figure 10A and Figure S4). However, we found that also 1.90 ± 0.24% of B cells, 1.00 ± 0.22% of T cells and 5.97 ± 0.34% of macrophages expressed RFP and are thus targeted with the Zbtb46^{CRE} line (Figure 10A). Additionally, 23.57 ± 3.71% of splenic CD45^{-} cells expressed RFP. If we than consider all RFP-expressing cells in the spleen of Zbtb46^{CRE}xRosa-RFP mice, we see that only 12.64% and 24.48% of them are cDC1s and cDC2s respectively, while 34.73% are B cells, 9.21% are T cells, 1.27% are macrophages and 6.59% are CD45^{-} cells (Figure 10B).

Due to the off target effects and the inefficient targeting of the cDCs, we decided not to use the Zbtb46^{CRE} line and further search for more specific CRE lines. This led us to the new XCR1^{CRE} line (generated by Bernard Malissen at the Centre d'Immunophenomique, Marseille, France) containing an IRES followed by the i*CRE-recombinase* gene at the 3' end of the *Xcr1* gene and developed to target cDC1s.

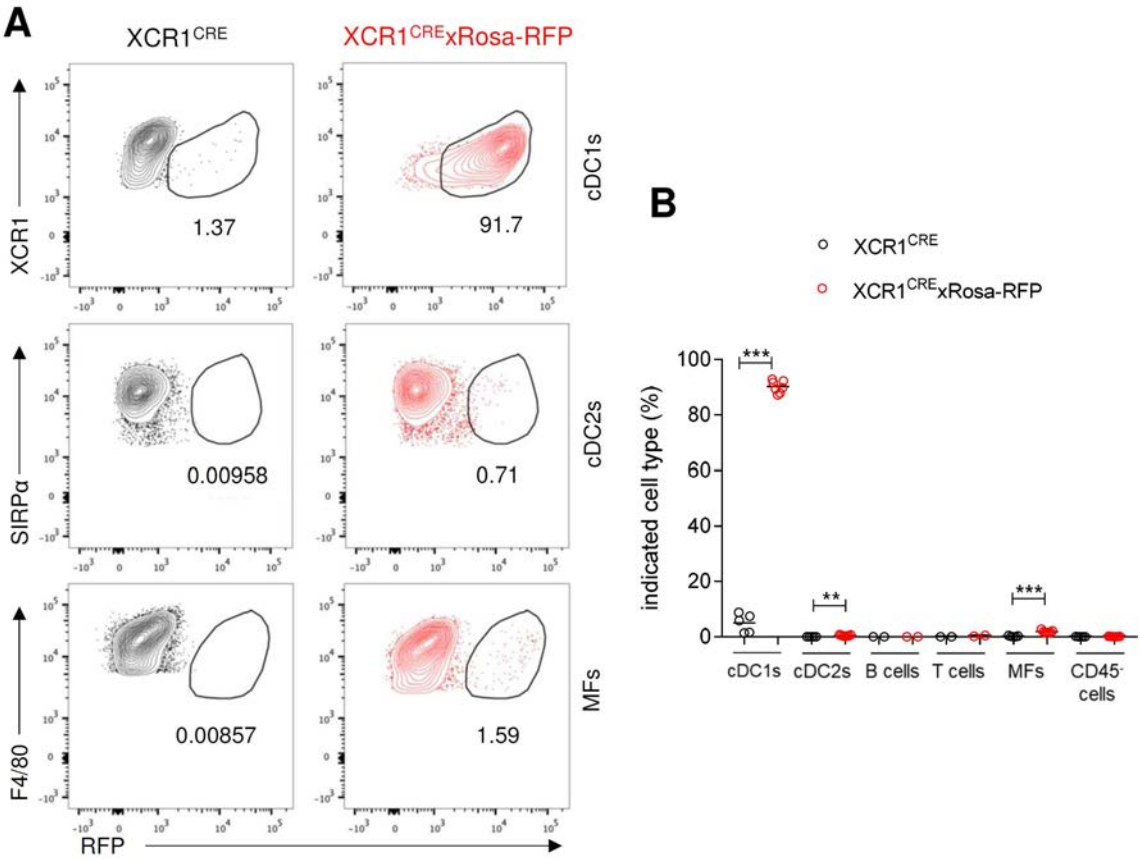

Figure 11 | The XCR1^{CRE} mouse line specifically and efficiently targets splenic cDC1s. (A) Representative FACS plots showing expression of RFP and XCR1 in cDC1s, RFP and SIRPα in cDC2s and RFP and F4/80 in macrophages (MFs) in the spleen of XCR1^{CRE} and XCR1^{CRE}xRosa-RFP mice. (B) Graph representing the percentage of indicated cells that show expression of RFP in the spleen of XCR1^{CRE} (black circles) and XCR1^{CRE}xRosa-RFP (red circles) mice. **, P < 0.01; ***, P < 0.001. Two-way student's t test. For cDC1s, cDC2s, MFs and CD45^{-} cells data or pooled from two experiments with at least n=5 per group. For B cells and T cells data ar from one experiment with n=2 per group.

As this is a new mouse model, we first checked the expression of RFP in XCR1^{CRE}xRosa-RFP mice, to determine if the cDC1 population is specifically and efficiently targeted. RFP was expressed in 90.17 ± 0.83% of splenic cDC1s, confirming that the new XCR1^{CRE} line efficiently targets cDC1s. Additionally, only a minority of splenic cDC2s (0.46 ± 0.09%), B cells (0.03 ± 0.02%), T cells (0.33 ± 0.12%), macrophages (1.84 ± 0.16%) and CD45^{-} cells (0.09 ± 0.03%) was targeted with the XCR1^{CRE} line (Figure 11A and 11B and Figure S4).

Having shown that the XCR1^{CRE} line specifically and efficiently targets cDC1s, we next analysed the presence and surface phenotype of cDC1s and cDC2s and the presence of macrophages in the spleen of XCR1^{CRE}xZeb1$^{fl/fl}$ mice. As observed in CD11c^{CRE}xZeb1$^{fl/fl}$ mice, we found a reduction in the splenic macrophage population upon knockout of Zeb1 in cDC1s (Figure 12A). With regard to the cDC1 population in the spleen, we again found a decrease in both proportion and absolute cell number (Figure 12B). Furthermore, the remaining cDC1s in the spleen of XCR1^{CRE}xZeb1$^{fl/fl}$ mice expressed increased levels of CD103 and decreased levels of CD8α (Figure 12C). Looking to the splenic cDC2s, we again found the definition between ESAM^{+} and ESAM^{-} cDC2s to be lost upon lack of Zeb1 expression in cDC1s, resulting in a decreased proportion of ESAM^{+} cDC2s (Figure 12D). Analogous to the CD11c^{CRE}xZeb1$^{fl/fl}$ model, analysis of cDC populations in the lung and liver of XCR1^{CRE}xZeb1$^{fl/fl}$ did not reveal any significant changes despite the fact that we efficiently targeted cDC1s in these tissues (data not shown). Given the finding that the XCR1^{CRE} line specifically and efficiently targets the cDC1s (Figure 11) and the presence of the splenic phenotype in the XCR1^{CRE}xZeb1$^{fl/fl}$ mice, we conclude that loss of Zeb1 in cDC1s causes a defect not only in splenic cDC1s, but also in splenic cDC2s and macrophages. Work is ongoing to determine the mechanisms at play.

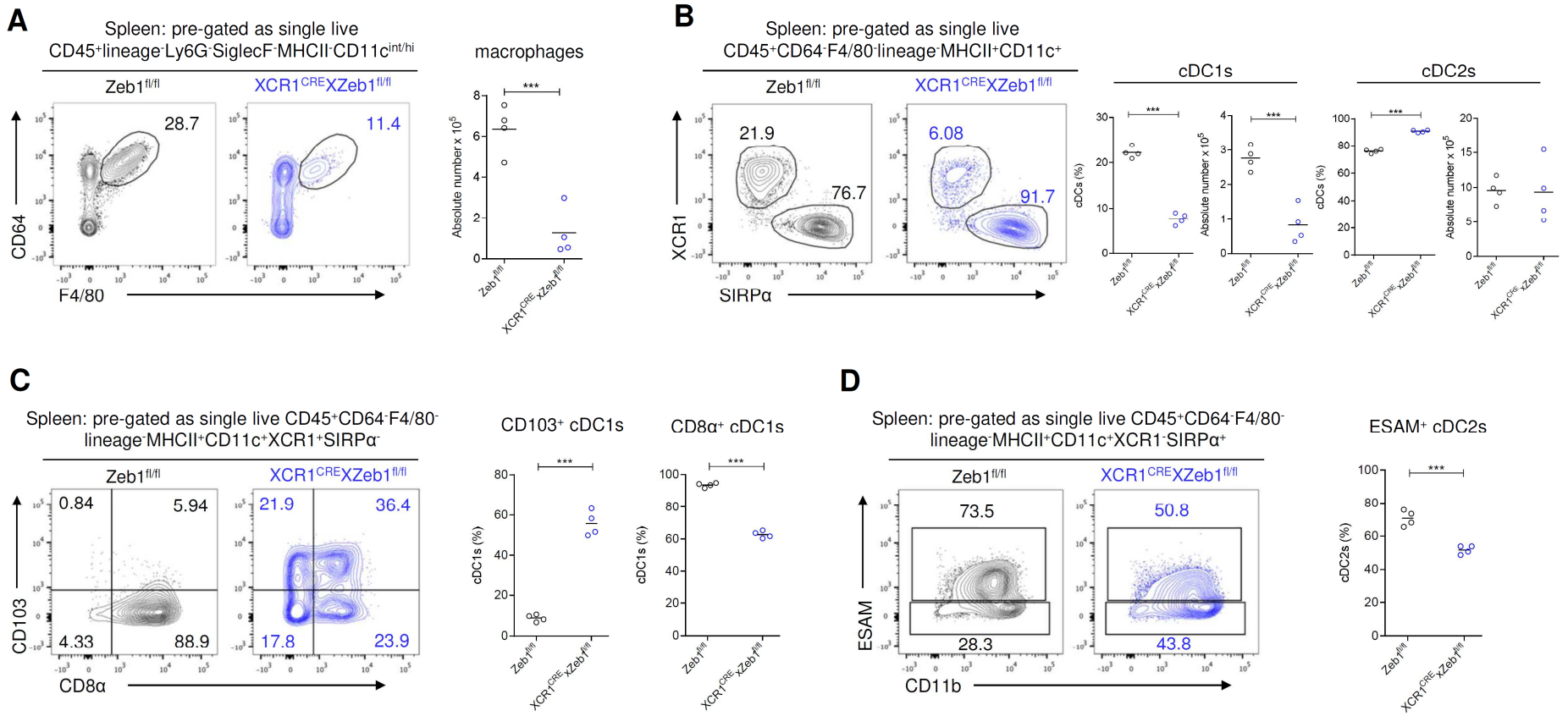

Figure 12 | Loss of Zeb1 in cDC1s causes a defect in splenic cDC1s, cDC2s and macrophages. (A) Representative FACS plots showing identification of CD64^{+}F4/80^{+} macrophages in the spleen of Zeb1$^{fl/fl}$ and XCR1^{CRE}xZeb1$^{fl/fl}$ mice. Numbers represent the population as a percentage of total CD45^{+}lineage^{-}Ly6G^{-}SiglecF^{-}MHCII^{-}CD11c$^{int/hi}$ cells. Graph shows absolute cell number of macrophages in the spleen of Zeb1$^{fl/fl}$ and XCR1^{CRE}xZeb1$^{fl/fl}$ mice. (B) Representative FACS plots showing identification of XCR1^{+}SIRPα^{-} cDC1s and XCR1^{-}SIRPα^{+} cDC2s in the spleen of Zeb1$^{fl/fl}$ and XCR1^{CRE}xZeb1$^{fl/fl}$ mice. Numbers represent the population as a percentage of total cDCs. Graphs show proportion as percentage of total cDCs and absolute cell number of cDC1s and cDC2s in the spleen of Zeb1$^{fl/fl}$ and XCR1^{CRE}xZeb1$^{fl/fl}$ mice. (C) Representative FACS plots showing expression of CD103 and CD8α in cDC1s in the spleen of Zeb1$^{fl/fl}$ and XCR1^{CRE}xZeb1$^{fl/fl}$ mice. Numbers represent the population as a percentage of total cDC1s. Graphs show proportion of indicated population as percentage of total cDC1s. (D) Representative FACS plots showing expression of ESAM and CD11b in cDC2s in the spleen of Zeb1$^{fl/fl}$ and XCR1^{CRE}xZeb1$^{fl/fl}$ mice. Numbers represent the population as a percentage of total cDC2s. Graphs show proportion of ESAM^{+} cDC2s as percentage of total cDC2s. (A-D) . Data are from one experiment with n=4 per group. ***, P < 0.001. Two-way Student's t test.

Overexpression of Zeb1 in CD11c^{+} cells leads to a decrease in cDC1s in the lung

After discovering and thoroughly analysing the severe phenotype in the spleen of CD11c^{CRE}xZeb1$^{fl/fl}$ mice, we wondered what the consequences were of overexpressing Zeb1 in cDCs. As the XCR1^{CRE} line only targets cDC1s (Figure 11) and the Zbtb46^{CRE} line (Figure 10) displays as many off target effects as the CD11c^{CRE} line, we first opted to cross the Zeb1 overexpression model with the CD11c^{CRE} line. Next, we performed flow cytometry on the lung, spleen, SILP and liver of CD11c^{CRE}xZeb1$^{Tg/Tg}$ mice to determine the presence of cDC1s and cDC2s. In the lung we found a vast reduction in both the proportion and the absolute cell number of cDC1s (Figure 13A). Additionally, lung cDC2s showed a significant increase when represented as a percentage of total cDCs, but this was not coupled with a difference in the absolute cell number of this population (Figure 13A). Analysis of the spleen revealed again a significant reduction in the proportion of cDC1s, but this reduction was not seen in terms of absolute cell number (Figure 13C). In the SILP and the liver of CD11c^{CRE}xZeb1$^{Tg/Tg}$ mice no significant differences in the presence of cDC1s or cDC2s were observed (Figure 13D and E).

cDC1s in the lung of CD11c^{CRE}xZeb1$^{Tg/Tg}$ mice display an altered surface expression of CD103

Having established that overexpression of Zeb1 in CD11c^{+} cells leads to a reduction in pulmonary cDC1s, we decided to further focus on this population. As we already knew that the loss of Zeb1 in splenic cDC1s led to a change in the surface expression of CD103 and CD8α on these cells, we also investigated the surface expression of these two proteins in the remaining cDC1s in the lung of CD11c^{CRE}xZeb1$^{Tg/Tg}$ mice. While the expression of CD8α on the remaining cDC1s in the lung did not change, the CD103^{+} proportion of pulmonary cDC1s decreased from 91.99 ± 1.55% in Zeb1$^{Tg/Tg}$ mice to 69.16 ± 3.77% in CD11c^{CRE}xZeb1$^{Tg/Tg}$ mice, suggesting a role for Zeb1 in the regulation of CD103 expression (Figure 13B).

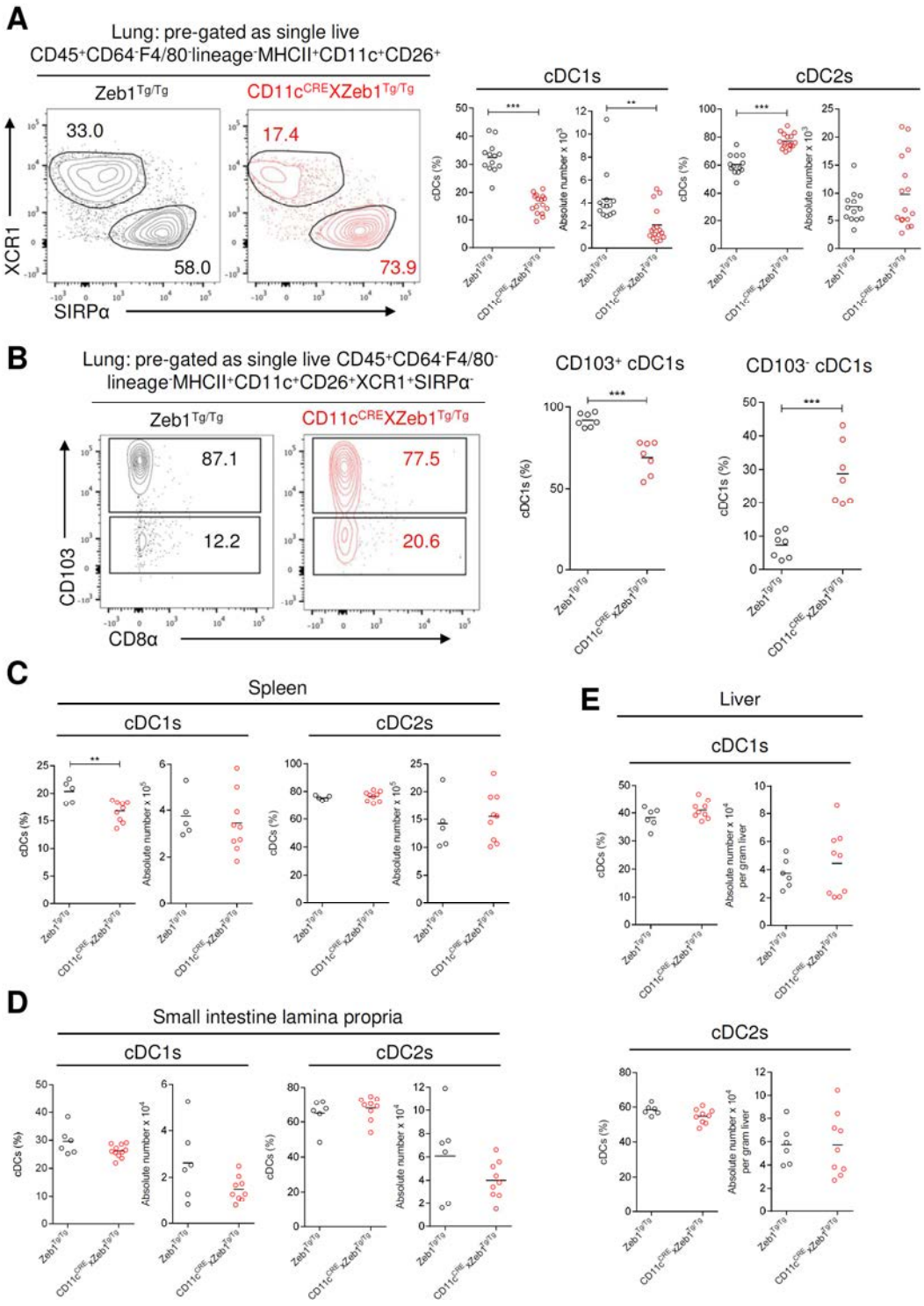

Figure 13 | CD11c^{CRE}xZeb1$^{Tg/Tg}$ mice show a reduction in pulmonary cDC1s, with the remaining ones displaying an altered CD103 expression. (A) Representative FACS plots showing identification of XCR1$^+$SIRPα$^-$ cDC1s and XCR1$^-$SIRPα$^+$ cDC2s in the lung of Zeb1$^{Tg/Tg}$ and CD11c^{CRE}xZeb1$^{Tg/Tg}$ mice. Numbers represent the population as a percentage of total cDCs which were pre-gated as single live CD45$^+$CD64$^-$F4/80$^-$ lineage$^-$MHCII$^+$CD11c$^+$CD26$^+$. Graphs show proportion as percentage of total cDCs and absolute cell number of cDC1s and cDC2s in the lung. (B) Representative FACS plots showing expression of CD103 and CD8α in cDC1s in the lung of Zeb1$^{Tg/Tg}$ and CD11c^{CRE}xZeb1$^{Tg/Tg}$ mice. Numbers represent the population as a percentage of total cDC1s which were pre-gated as single live CD64$^-$F4/80$^-$lineage$^-$MHCII$^+$CD11c$^+$CD26$^+$XCR1$^+$SIRPα$^-$. Graphs show proportion of indicated population as percentage of total cDC1s. (C-E) Proportion as percentage of total cDCs and absolute cell number of cDC1s and cDC2s in the spleen (C), SILP (D) and liver (E) of Zeb1$^{Tg/Tg}$ and CD11c^{CRE}xZeb1$^{Tg/Tg}$ mice. Data are pooled from two to four experiments with at least n=5 per group. **, $P < 0.01$; ***, $P < 0.001$. Two-way Student's t test.

The decrease of pulmonary cDC1s and the altered CD103 surface expression on the remaining pulmonary cDC1s in CD11c^{CRE}xZeb1$^{Tg/Tg}$ mice is cell intrinsic

Next we sought to determine if the defects seen in the cDC1 population in the lung of CD11c^{CRE}xZeb1$^{Tg/Tg}$ mice were cell intrinsic or caused by additional targets of the CD11c^{CRE} line. To this end we again generated competitive BM chimeras for which we lethally irradiated CD45.1/CD45.2 WT mice and reconstituted them with a ~70:30 mix (as determined from the analysis of neutrophils in the lung) of CD45.2 Zeb1$^{Tg/Tg}$ or CD11c^{CRE}xZeb1$^{Tg/Tg}$ BM and CD45.1 WT BM (Figure 14A). Reconstitution with the BM mix containing CD11c^{CRE}xZeb1$^{Tg/Tg}$ BM did not result in a reduction of total lung cDC1s. However, analysis of the chimerism revealed that most of these cells were originating from CD45.1 WT BM (Figure 14B). On the other hand, WT and CD11c^{CRE}xZeb1$^{Tg/Tg}$ BM were equally capable of generating cDC2s in the lung (Figure 14B). Further looking into detail to the cDC1 population in the lung of the competitive chimeras, we found that when mice were reconstituted with a BM mix containing CD11c^{CRE}xZeb1$^{Tg/Tg}$ BM the proportion of CD103^{+} cDC1s is reduced (Figure 14C). However, unlike what we had seen in the spleen of competitive chimeras generated with CD11c^{CRE}xZeb1$^{fl/fl}$ BM, this reduction of the CD103 expressing cDC1s was only shown for cDC1s differentiating from CD45.2 Zeb1 overexpressing BM and not for cDC1s developing from CD45.1 WT BM (Figure 14C). In conclusion the results from the competitive BM chimeras reveal that the effects observed within pulmonary cDC1s in mice overexpressing Zeb1 in CD11c^{+} cells are cell intrinsic. Nevertheless, further research is needed to determine if the decrease in the cDC1 population in the lung is due to a defect in their development or cell death resulting from the overexpression of Zeb1 in fully differentiated cells.

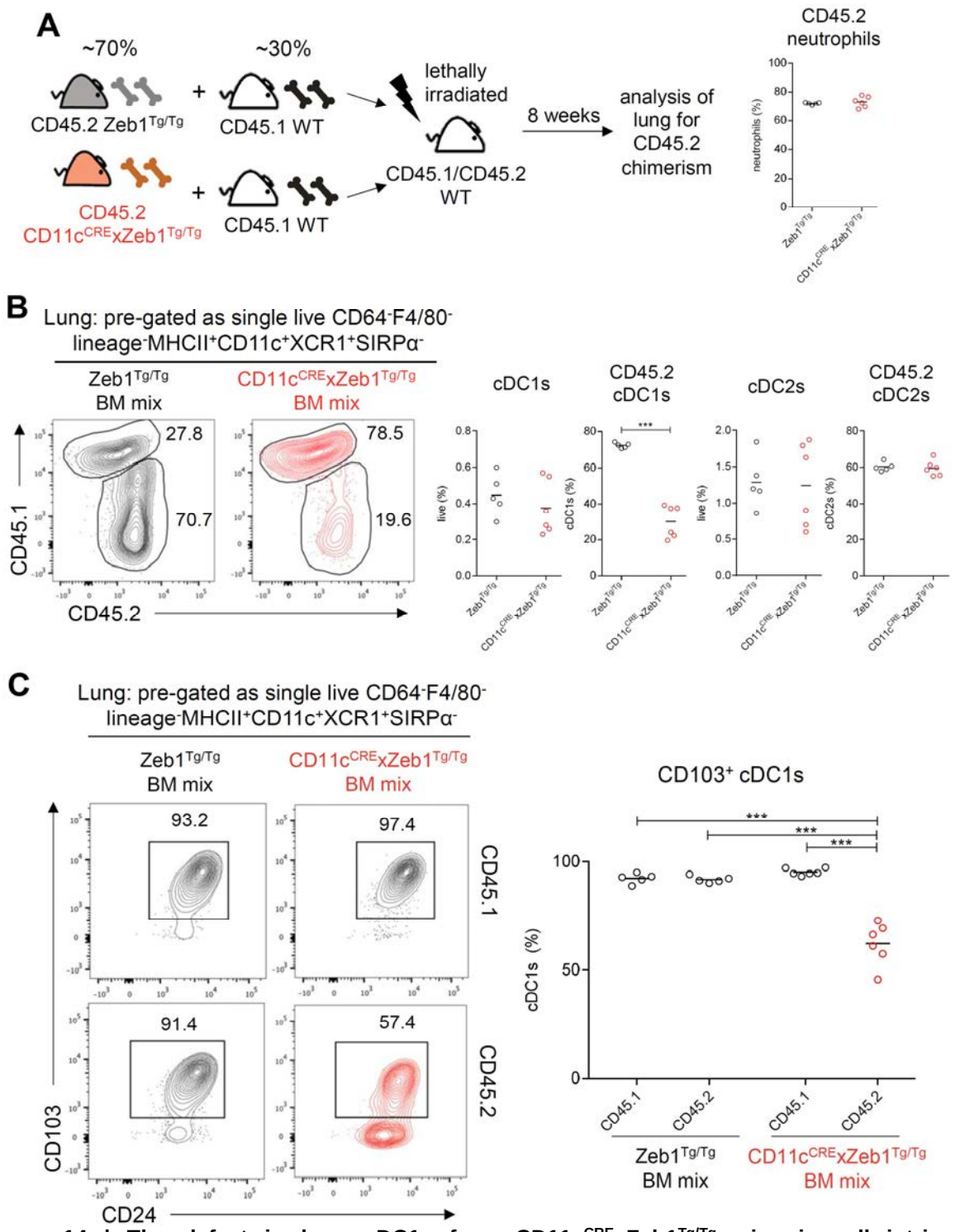

Figure 14 | The defect in lung cDC1s from CD11c^{CRE}xZeb1$^{Tg/Tg}$ mice is cell intrinsic. (A) Competitive BM chimeric mice were generated by lethally irradiating CD45.1/CD45.2 WT mice and reconsituting with a ~70:30 mix of Zeb1$^{Tg/Tg}$ or CD11c^{CRE}xZeb1$^{Tg/Tg}$ CD45.2 BM and WT CD45.1 BM. Graph represents CD45.2 lung neutrophils as a percentage of total lung neutrophils. No significance was found using two-way student's t test. (B) Representative FACS plots showing CD45.1 and CD45.2 expression on cDC1s in the lung of chimeric mice. Graphs show cDC1s and cDC2s as a percentage of live cells and CD45.2 cDC1s and CD45.2 cDC2s as a percentage of respectively total cDC1s and total cDC2s in chimeric mice. ***, $P < 0.001$. Two-way student's t test. (C) Representative FACS plots showing CD103 and CD24 expression in CD45.1 or CD45.2 cDC1s in the lung of chimeric mice. Numbers represent the population as a percentage of total CD45.1 or CD45.2 cDC1s. Graph shows CD103^{+} cDC1s as a percentage of total CD45.1 or CD45.2 cDC1s in the lung of chimeric mice. ***, $P < 0.001$. One-way ANOVA with Bonferroni post-test. Data are pooled from two experiments, with at least n=5 per group.

3.4 Discussion

Having established a role for Zeb2 in dendritic cell development[7], we wondered if its family member Zeb1 also had a function in the dendritic cell lineage. Analysis of publically available expression data revealed that *Zeb1* is expressed in both cDC1s and cDC2s across murine tissues. The loss of Zeb1 expression specifically in cDC1s, using the newly generated XCR1^{CRE} line, resulted in a reduction of splenic cDC1s and red pulp macrophages, together with an increase in CD103 expressing splenic cDC1s and a loss of definition between ESAM^{+} and ESAM^{-} splenic cDC2s. Furthermore, CD11c^{CRE}xZeb1$^{fl/fl}$ mice displayed the same splenic phenotype as XCR1^{CRE}xZeb1$^{fl/fl}$ mice and additionally we found a reduced number of splenic B cells, T cells, NKT cells, NK cells, Ly6C^{hi} monocytes, Ly6C^{lo} monocytes, neutrophils and marginal zone macrophages. On the other hand, overexpression of Zeb1 in cDCs led to a cell intrinsic loss of pulmonary cDC1s, with the remaining ones showing a decreased expression of CD103.

The defects in the Zeb1 knockout and Zeb1 overexpression models used in this study were restricted to one tissue, respectively the spleen and the lung. With regards to the CD11c^{CRE}xZeb1$^{fl/fl}$ and XCR1^{CRE}xZeb1$^{fl/fl}$ mice, we hypothesize that the difference in tissue architecture and environment between the spleen and the other peripheral tissues examined (lung, liver and SILP) is at the base of the tissue-specificity of the phenotype, similar to the recently proposed theory on the niche being the dominant factor conferring macrophage identity[21]. First, in most peripheral tissues WT cDC1s typically express CD103 on their surface and lack expression of CD8α, while in the spleen cDC1s express CD8α and lack CD103 expression. However, loss of Zeb1 expression in cDC1s, caused the splenic cDC1s to display a surface expression of both proteins that is typical for peripheral cDC1s, with increased CD103 and decreased CD8α expression. Furthermore, we found that the loss of Zeb1 in cDC1s not only affected the cDC1 population in the spleen, but also led to a decrease in ESAM expressing cDC2s and red pulp macrophages. Indeed, the presence of ESAM^{hi} cDC2s is restricted to the spleen[15] and for tissue-resident macrophages it was shown that their gene expression and function is highly tissue-specific[22–24]. Additionally, in the spleen many different types of immune cells are in

close contact to each other, which is not the case in the peripheral tissues. This could explain why the loss of Zeb1 in cDC1s also affects other cell types, a phenomenon that was not found in the peripheral organs investigated. On the other hand the cDC1 defect in $CD11c^{CRE}xZeb1^{Tg/Tg}$ mice was restricted to the lung and was shown to be cell intrinsic. Although the expression of *Zeb1* at mRNA level seems to be similar in the cDC1s of the examined tissues (Figure 1A), we do not know if this holds true for the protein level of Zeb1. Perhaps Zeb1 is not expressed or expressed at lower levels in pulmonary cDC1s, compared to splenic, intestinal and hepatic cDC1s and as such the overexpression of Zeb1 is only problematic in pulmonary cDC1s. In order to test this hypothesis, we should perform flow cytometry analysis including an intra-cellular staining for Zeb1. Unfortunately, so far we were unable to find a good antibody to perform this experiment.

Next to the defect in both cDC populations, the spleen of $CD11c^{CRE}xZeb1^{fl/fl}$ mice also displayed reduced numbers of macrophages, B cells, T cells, NKT cells, NK cells, $Ly6C^{hi}$ monocytes, $Ly6C^{lo}$ monocytes and neutrophils. Crossing the $CD11c^{CRE}$ line with the Rosa-RFP reporter line showed us that CRE recombinase activity is not only present in cDCs, but also in macrophages, T cells, B cells and NK cells. Additionally, it was previously shown that neutrophils and monocytes are also targeted with the $CD11c^{CRE}$ line[16]. So the loss of Zeb1 in either of these cell types targeted with the $CD11c^{CRE}$ line could cause a cell intrinsic defect in the cell itself, but could also be the cause of the defects in other cell types of the spleen. Using $NKp46^{CRE}xZeb1^{fl/fl}$ mice we found that the reduction of splenic NK cells is at least partly cell intrinsic to the loss of Zeb1. Additionally, the experiments with the competitive and the protected BM chimeras revealed that loss of Zeb1 in $CD11c^{+}$ cells has a dominant effect on all cDC1s, cDC2s and macrophages, regardless of their Zeb1 expression. To determine this dominant effect we have sent RNA from splenic $CD103^{+}$ WT cDC1s, $ESAM^{+}$ WT cDC2s and $ESAM^{-}$ WT cDC2s from the protected BM chimeras that received $CD11c^{CRE}xZeb1^{fl/fl}$ BM for RNA-sequencing and are currently waiting for the results. Furthermore, the analysis of the $XCR1^{CRE}xZeb1^{fl/fl}$ mice showed us that loss of Zeb1 expression specifically in cDC1s not only affects cDC1s, but also cDC2s and macrophages. However, for splenic B cells, T cells, NKT cells, monocytes and neutrophils it remains unclear if their reduced numbers are cell intrinsic or not. All of these findings raise the question if we

have to reconsider other DC research that is based on the CD11c^{CRE} line and the Zbtb46^{CRE} line, as for this last model we also identified considerable off target effects. Inclusion of BM chimeras that show a cell intrinsic effect adds more credibility to the results. However, a lot of publications using CD11c^{CRE} and Zbtb46^{CRE} do not use BM chimeras and hence we should be careful in interpreting them. The use of other CRE lines which are truly specific, such as the XCR1^{CRE} line, could be a solution in the future.

The expression of the integrin Itgae or CD103 on the surface of cDC1s is directly regulated by Csf2[25,26], however the role of CD103 on cDC1s is unclear. In intraepithelial lymphocytes (IELs), mostly T cells, CD103 expression was shown to be induced by Tgfβ1[27–29], which is expressed by many cell types including epithelial cells[30,31]. E-cadherin, mostly expressed by epithelial cells, is the main ligand for the integrin CD103[32]. This interaction between CD103 on IELs and E-cadherin on epithelial cells could explain why CD103 was shown to be important in the retention of IELs in the mucosal epithelium of the gut[32,33], the oral mucosa[34] and skin epidermis[34,35]. As the expression of CD103 on cDC1s is mostly found in peripheral organs, it could be that in the periphery the same CD103-E-cadherin interaction ensures the retention of cDC1s in the epithelium, where they scan for antigen. In the spleen on the other hand, we found that wild type cDC1s do not express CD103, probably because in lymphoid organs they do not need to be in the epithelium. Indeed, at steady-state cDC1s are present in the T cell zone of the spleen, where they cross-present antigen to CD8^{+} T cells[36]. With this theory in mind, one could hypothesize that aberrant expression of CD103 on splenic cDC1s caused by the loss of Zeb1 expression, results in incorrect localisation of cDC1s in the spleen. Additionally, as CD8α^{+} cDC1s are normally located in the T cell areas and CD8α^{-} cDC2s in the marginal zone[36], the decreased expression of CD8α could also cause mislocalisation of the Zeb1-deficient cDC1s. Incorrect localisation of cDC1s in the spleen could subsequently cause an imbalance in the splenic micro-environment leading to cell death of ESAM-expressing cDC2s and red pulp macrophages. To test this hypothesis, we should determine the localisation of cDC1s in the spleen of WT and XCR1^{CRE}xZeb1$^{fl/fl}$ mice. This could for instance be done with confocal microscopy on tissue sections stained with anti-XCR1 and anti-CD103 antibodies. However, evidence against the CD103-associated localisation hypothesis is that

almost all splenic cDC1s from adult WT C57BL/6 mice purchased at Janvier were CD103^{+}. This in contrast to adult C57BL/6 mice bred in our animal house, in which splenic cDC1s are almost all CD103^{-}. Hence, we can state that CD103 expression on splenic cDC1s is different from animal facility to animal facility, a phenomenon that could be caused by differences in microbiome. Strikingly, we found that the observed splenic phenotype in CD11c^{CRE}xZeb1$^{fl/fl}$ mice, including the defective downregulation of CD103 on cDC1s, is established around weaning, which is typically associated with alterations in gut microbiota[37]. Maybe the loss of cDC1s, due to the loss of Zeb1 expression, causes a shift in the microbiome which subsequently affects the presence of macrophages and the phenotype of cDC2s. Further research, using for instance antibiotic treatments or experiments in a germfree facility, is needed to test this hypothesis.

To date, we confirmed that the expression of Zeb1 in splenic cDC1s is essential to maintain homeostasis of mononuclear phagocytes in the spleen. Our current working hypothesis is as follows: loss of Zeb1 in cDC1s inhibits or induces the release of a factor in the splenic environment that is either essential or detrimental to the survival of other immune cells in the niche (Figure 15). To test this hypothesis the new XCR1^{CRE}xZeb1$^{fl/fl}$ model, in which Zeb1 is knocked out specifically in cDC1s, will be a

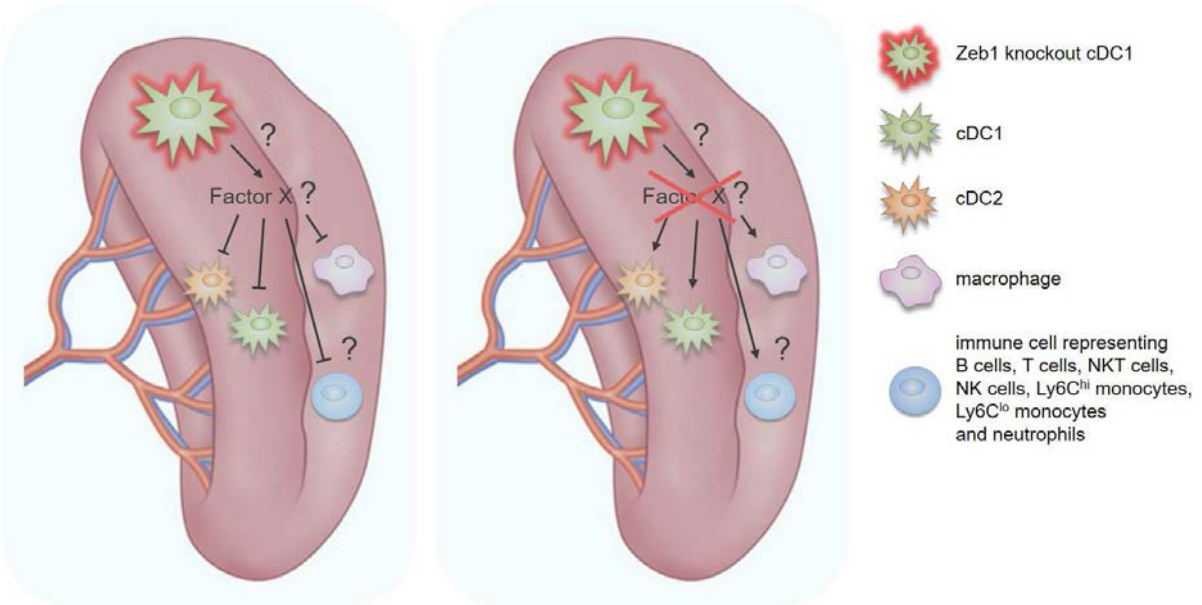

Figure 15 | Working hypothesis on the role of Zeb1 in splenic cDC1s. We hypothesise that loss of Zeb1 expression in splenic cDC1s leads to the release or the lack of a dominant factor in the splenic environment, which subsequently leads to a defect in different types of immune cells including the mononuclear phagocytes.

very helpful tool. First we need to repeat the FlowSom phenotyping experiment in these mice to confirm if the defects in B cells, T cells, NKT cells, NK cells, Ly6C^{hi} monocytes, Ly6C^{lo} monocytes and neutrophils seen in the CD11c^{CRE} model are also observed in the XCR1^{CRE} model. Comparing the phenotypes of the XCR1^{CRE} model to the phenotypes of the CD11c^{CRE} model will reveal what part of the phenotype in the CD11c^{CRE} model was a consequence of the off target loss of Zeb1 in immune cells other than cDC1s. Finally, we would like to identify the unknown factor of which we believe that its aberrant expression or lack of expression by cDC1s causes this imbalance in the splenic environment. To this end we would like to FACS-purify cDC1s from the spleen of XCR1^{CRE}xZeb1$^{fl/fl}$ mice and control littermates and isolate their RNA for RNA-sequencing. We hope that the final experiments proposed here will be sufficient to fill the gaps in our current working model (Figure 15).

Additionally it would be interesting to use the XCR1^{CRE}xZeb1$^{fl/fl}$ model in functional studies. First we would like to test the cross-presentation capacities of the remaining splenic cDC1s *in vitro* by setting up coculture experiments with OTI cells in the presence of purified ovalbumin protein. Furthermore, we would like to challenge the functioning of Zeb1-deficient splenic cDC1s *in vivo*. To this end we could infect XCR1^{CRE}xZeb1$^{fl/fl}$ mice with the intracellular bacterium *Listeria monocytogenes*, as it was shown that splenic cDC1s mediate T cell priming and induce differentiation of naive CD8^{+} T cells into pathogen-specific protective memory cells[38]. Interestingly, we have created a mouse model that almost completely lacks red pulp macrophages, which are mostly functioning as scavengers for ageing and dying red blood cells, but also possess several mechanisms to protect against blood-borne pathogens[39]. For instance, red pulp macrophages limit uptake of iron by *E. coli* through the release of lipocalin-2[40] and they express the natural resistance associated macrophage protein-1 (NRAMP1) in their phagosomes which facilitates protection against intraphagosomal pathogens like *Mycobacterium bovis, Leishmania donovani* and *Salmonella typhimurium*[41]. As our XCR1^{CRE}xZeb1$^{fl/fl}$ model is deficient for red pulp macrophages, it would be interesting to challenge the mice with *Salmonella typhimurium*, for which in house a protocol is running, and follow the course of disease in the affected spleen. However, when analysing and interpreting results of *in vivo* challenges in XCR1^{CRE}xZeb1$^{fl/fl}$ mice, we need to keep in mind that the mice have defects in cDC1s, cDC2s and red pulp macrophages and thus we need to be

careful in assigning the results to the correct cell type. Moreover, if further phenotyping reveals that the additional defects in the splenic immune compartment observed in the CD11c^{CRE}xZeb1$^{fl/fl}$ are repeated in the XCR1^{CRE}xZeb1$^{fl/fl}$ model, the proposed *in vivo* challenges would not provide useful information and will not be performed.

Finally, the project on the overexpression of Zeb1 in dendritic cells needs further research. Due to time restrictions, we only performed a general phenotyping of dendritic cells in different tissues of the CD11c^{CRE}xZeb1$^{Tg/Tg}$ mice and this revealed that overexpression of Zeb1 in CD11c^{+} cells leads to a decrease of cDC1s in the lung. Next to that we found that among the remaining lung cDC1s an decreased fraction of them expresses CD103 on their surface. Experiments with competitive BM chimeras revealed the defect in cDC1s to be cell intrinsic and thus cDC1s derived from CD11c^{CRE}xZeb1$^{Tg/Tg}$ lose the competition with their WT counterparts in becoming cDC1s. These findings bring up some other questions. Why is the phenotype restricted to the lung? Does the loss of CD103 expression on cDC1s in the lung change their location, their ability to migrate or their antigen presenting capacities? How does Zeb1 regulate the expression of CD103 on the surface of pulmonary cDC1s? Is the decrease in the cDC1 population in the lung caused by a defect in their development or by cell death of mature cDC1s? Work is ongoing to answer all these questions and to determine the mechanisms at play.

3.5 Materials and methods

Immgen data processing

Gene expression data were downloaded from the Immgen database (GSE15907). After merging expression values of all samples, data was normalized within arrays (probeset summarization, background correction and log2-transofrmation) and between arrays (quantile normalization) using the Robust Multi-array Average (RMA) procedure in R. Only probesets that mapped uniquely to one gene were kept, and for each gene the probeset with the highest expression level was kept.

Mice

The generation of $Zeb1^{fl/fl}$ was described previously[13]. The Rosa26-$Zeb1^{Tg/Tg}$ mice were created in-house and contain a loxP flanked stop-cassette followed by the *Zeb1* gene in the Rosa26 locus. Mice were backcrossed to a C57BL/6 background for at least seven generations before crossing with the $CD11c^{CRE}$ line[14], the $NKp46^{CRE}$ line[42] or the $XCR1^{CRE}$ line (generated by Bernard Malissen at the Centre d'Immunophenomique, Marseille, France). $CD11c^{CRE}$, $XCR1^{CRE}$ and $Zbtb46^{CRE}$ mice[19] were also crossed with the Rosa-RFP reporter mouse[17]. All mice were bred and maintained at the VIB-UGent center for inflammation research (IRC) under specific pathogen-free conditions and were used between 6 and 12 weeks of age, unless stated differently. All experiments were performed in accordance with the ethical committee of the Faculty of Science.

Isolation of tissue leukocytes

For the isolation of liver leukocytes, livers were isolated from PBS-perfused mice, chopped finely, and incubated for 15–20 min with 1 mg/ml collagenase A (Sigma-Aldrich) and 10 U/ml DNase (Roche) in a shaking water bath at 37°C. Cells were passed through a 70-µm cell strainer. For the isolation of lung and spleen leukocytes, lungs and spleens were isolated from PBS-perfused mice, chopped finely, and

incubated for 30 min with 0.2 mg/ml Liberase TM (Roche) and 10 U/ml DNase (Roche) in a shaking water bath at 37°C. Cells were passed through a 70-µm cell strainer. SILP leukocytes were isolated as described previously[43]. Briefly, small intestines were flushed with PBS or RPMI containing 2% FCS and Peyer's patches were excised. After opening longitudinally and cutting into 0.5 cm segments, they were incubated twice with PBS containing 2mm EDTA in a shaking water bath at 37°C for 20 min. Then the tissue was digested with 1 mg/ml collagenase VIII (Sigma-Aldric) in a shaking water bath for 15 min. Cells were passed through a 40-µm cell strainer. In all instances, except for the SI, red blood cells were lysed with an in house made osmotic lysis buffer (10mM $KHCO_3$, 155 mM NH_4Cl and 0.1 mM EDTA in PBS) before staining for flow cytometric analysis.

Flow cytometry

For flow cytometry, 3–4 x 10^6 cells were stained at 4°C in the dark with antibodies (Table 1). Data were acquired on a cell analyser (LSRFortessa; BD) and analyzed using FlowJo software (Tree Star).

Table 1 | Antibodies used for flow cytometry

Antibody	Clone	Antibody	Clone
Fc Block	2.4G2	CD103	2E7
Fixable Viability Dye	eBioscience	CD11b	M1/70
CD3e	145-2c11	CD11c	N418
CD4	RM4-5	CD172a	P84
CD8α	53-6.7	ESAM	1G8
CD19	1D3	F4/80	BM8
CD24	M1-69	IA-IE	M5/114.15.2
CD26	H194-112	Ly6C	AL-21
CD45	30-F11	Ly6G	1A8
CD45.1	A20	NK1.1	PK136
CD45.2	104	SiglecF	E50-2440
CD45R/B220	RA3-6B2	Ter-119	Ter-119
CD64	X54-5/7.1	XCR1	ZET

Generation of competitive BM chimeric mice

Competitive BM chimeric mice were generated by lethally irradiating CD45.1/CD45.2 WT mice with a single dose of 8 Gy. 12 hours later mice were reconstituted by intravenous injection of 5 x 10^6 BM cells, which were a ~1:1 mix of CD45.1 WT and CD45.2 $Zeb1^{fl/fl}$, $Zeb1^{Tg/Tg}$, $CD11c^{CRE}xZeb1^{fl/fl}$ or $CD11c^{Cre}xZeb1^{Tg/Tg}$ BM cells. Chimerism was assessed 8 weeks after irradiation in spleen or lung.

Generation of partially protected chimeras

6 week-old WT CD45.1 mice were anaesthetized by intraperitoneal administration of Ketamine (150 mg/kg) and Xylazine (10 mg/kg). Spleens were protected with a 3-cm-thick lead cover before mice were lethally irradiated with 8Gy. Once recovered from the anaesthesia, mice were reconstituted by intravenous administration of 10 x 10^6 BM cells from congenic CD45.2 $Zeb1^{fl/fl}$ or $CD11c^{CRE}xZeb1^{fl/fl}$ mice. 8 weeks after irradiation chimerism in the spleen was assessed by flow cytometry.

Analysis with FlowSOM algorithm

First data was manually pre-gated as single live cells using FlowJo. Next the data was compensated and transformed using the logicleTransform() function in R. Then, the clustering algorithm was trained on an aggregated random sampling, taking 333334 cells from each of the samples, resulting in 4 million cells in total. 12 markers and a ten-by-ten grid were used for clustering, resulting in hundred clusters. Each of the cleaned up files were mapped onto the discovered clusters, to define their cell distribution. The results were visualized with the node size representative of the mean cluster frequency of all samples from each group. Finally, the cluster frequencies were compared between the two groups ($Zeb1^{fl/fl}$ and $CD11c^{CRE}xZeb1^{fl/fl}$) using a Wilcox test and those clustered with a p-value lower than 0.5 were selected as significant. The cluster was given a light blue shadow when significantly decreased in $CD11c^{CRE}xZeb1^{fl/fl}$ mice and a red shadow when significantly increased.

Immunofluorescent staining of tissue sections

Freshly isolated spleens were embedded in O.C.T. Compound (Tissue Tek) and snap frozen. 10 µm thick cryosections were obtained and air dried for at least 30 minutes. Next sections were fixed for 2 minutes in a 2% PFA solution. After washing in PBS, sections were stained with directly labelled antibodies diluted in PBT (CD3; 145-2c11, B220; RA3-6B2, CD11c; N418, F4/80; BM8, CD169; MOMA-1) for 1 hour in the dark at RT. After washing in PBS, sections were next incubated with DAPI diluted in PBT for 10 minutes in the dark at RT. Following a last washing step in PBS, sections were mounted with N-propylgallate and imaged with a Zeiss LSM 780 confocal microscope.

Statistical analysis

Groups were compared with a two-way Student's t test, and multiple-group comparisons were performed using one-way ANOVA followed by a Bonferroni post-test with Prism Software (GraphPad Software). Samples were assumed to be normally distributed with similar variance between groups. No randomization was used to determine experimental groups, and no blinding of the investigator was performed. Group sizes were determined on the basis of previous experience.

3.6 References

1. De Craene B, Berx G. Regulatory networks defining EMT during cancer initiation and progression. *Nat. Rev. Cancer*. 2013;13(2):97–110.
2. Chung D-WDW, Frausto RF, Ann LB, Jang MS, Aldave AJ. Functional impact of ZEB1 mutations associated with posterior polymorphous and Fuchs' endothelial corneal dystrophies. *Invest. Ophthalmol. Vis. Sci.* 2014;55(10):6159–66.
3. Aldave AJ, Ann LB, Frausto RF, et al. Classification of posterior polymorphous corneal dystrophy as a corneal ectatic disorder following confirmation of associated significant corneal steepening. *JAMA Ophthalmol*. 2013;131(12):1583–90.
4. Van Helden MJ, Goossens S, Daussy C, et al. Terminal NK cell maturation is controlled by concerted actions of T-bet and Zeb2 and is essential for melanoma rejection. *J. Exp. Med.* 2015;212(12):2015–25.
5. Omilusik KD, Best JA, Yu B, et al. Transcriptional repressor ZEB2 promotes terminal differentiation of CD8+ effector and memory T cell populations during infection. *J. Exp. Med.* 2015;212(12):2027–39.
6. Dominguez CX, Amezquita RA, Guan T, et al. The transcription factors ZEB2 and T-bet cooperate to program cytotoxic T cell terminal differentiation in response to LCMV viral infection. *J. Exp. Med.* 2015;212(12):2041–56.
7. Scott CL, Soen B, Martens L, et al. The transcription factor Zeb2 regulates development of conventional and plasmacytoid DCs by repressing Id2. *J. Exp. Med.* 2016;213(6):897–911.
8. Wu X, Briseño CG, Grajales-Reyes GE, et al. Transcription factor Zeb2 regulates commitment to plasmacytoid dendritic cell and monocyte fate. *Proc. Natl. Acad. Sci. U.S.A.* 2016;113(51):14775–14780.
9. Arnold CN, Pirie E, Dosenovic P, et al. A forward genetic screen reveals roles for Nfkbid, Zeb1, and Ruvbl2 in humoral immunity. *Proc. Natl. Acad. Sci. U.S.A.* 2012;109(31):12286–93.
10. Higashi Y, Moribe H, Takagi T, et al. Impairment of T cell development in deltaEF1 mutant mice. *J. Exp. Med.* 1997;185(8):1467–79.
11. Takagi T, Moribe H, Kondoh H, Higashi Y. DeltaEF1, a zinc finger and homeodomain transcription factor, is required for skeleton patterning in multiple lineages. *Development*. 1998;125(1):21–31.
12. Brabletz T, Jung A, Hlubek F, et al. Negative regulation of CD4 expression in T cells by the transcriptional repressor ZEB. *Int. Immunol.* 1999;11(10):1701–8.
13. Brabletz S, Lasierra Losada M, Schmalhofer O, et al. Generation and characterization of mice for conditional inactivation of Zeb1. *Genesis*. 2017;55(4):
14. Caton ML, Smith-Raska MR, Reizis B. Notch-RBP-J signaling controls the homeostasis of CD8- dendritic cells in the spleen. *The Journal of experimental medicine*. 2007;204(7):1653–64.
15. Lewis KL, Caton ML, Bogunovic M, et al. Notch2 receptor signaling controls functional differentiation of dendritic cells in the spleen and intestine. *Immunity*. 2011;35(5):780–91.
16. Abram CL, Roberge GL, Hu Y, Lowell CA. Comparative analysis of the efficiency and specificity of myeloid-Cre deleting strains using ROSA-EYFP reporter mice. *J. Immunol. Methods*. 2014;408:89–100.
17. Luche H, Weber O, Nageswara Rao T, Blum C, Fehling HJ. Faithful activation of an extra-bright red fluorescent protein in "knock-in" Cre-reporter mice ideally suited for lineage tracing studies. *Eur. J. Immunol.* 2007;37(1):43–53.
18. Gassen S, Callebaut B, Helden M, et al. FlowSOM: Using self□organizing maps for visualization and interpretation of cytometry data. *Cytom Part A*. 2015;87(7):636–645.
19. Loschko J, Schreiber HA, Rieke GJ, et al. Absence of MHC class II on cDCs results in microbial-dependent intestinal inflammation. *J. Exp. Med.* 2016;213(4):517–34.
20. Loschko J, Rieke GJ, Schreiber HA, et al. Inducible targeting of cDCs and their subsets in vivo. *J. Immunol. Methods*. 2016;434:32–8.
21. Guilliams M, Scott CL. Does niche competition determine the origin of tissue-resident macrophages? *Nat. Rev. Immunol.* 2017;17(7):451–460.
22. Gautier EL, Shay T, Miller J, et al. Gene-expression profiles and transcriptional regulatory pathways that underlie the identity and diversity of mouse tissue macrophages. *Nat. Immunol.* 2012;13(11):1118–28.

23. Heinz S, Benner C, Spann N, et al. Simple combinations of lineage-determining transcription factors prime cis-regulatory elements required for macrophage and B cell identities. *Mol. Cell*. 2010;38(4):576–89.
24. Gosselin D, Link VM, Romanoski CE, et al. Environment drives selection and function of enhancers controlling tissue-specific macrophage identities. *Cell*. 2014;159(6):1327–40.
25. Edelson BT, Bradstreet TR, KC W, et al. Batf3-dependent CD11b(low/-) peripheral dendritic cells are GM-CSF-independent and are not required for Th cell priming after subcutaneous immunization. *PLoS ONE*. 2011;6(10):e25660.
26. Zhan Y, Carrington EM, van Nieuwenhuijze A, et al. GM-CSF increases cross-presentation and CD103 expression by mouse CD8$^+$ spleen dendritic cells. *Eur. J. Immunol.* 2011;41(9):2585–95.
27. Parker CM, Cepek KL, Russell GJ, et al. A family of beta 7 integrins on human mucosal lymphocytes. *Proc. Natl. Acad. Sci. U.S.A.* 1992;89(5):1924–8.
28. Braun A, Schlickum S, Dewert N, Schön M, Schön MP. Integrin αE (CD103) is induced but plays no pathogenic role in psoriasiform skin lesions of TGFβ1 transgenic mice. *Exp. Dermatol.* 2016;25(4):311–3.
29. Kilshaw PJ, Murant SJ. Expression and regulation of beta 7(beta p) integrins on mouse lymphocytes: relevance to the mucosal immune system. *Eur. J. Immunol.* 1991;21(10):2591–7.
30. Denney L, Byrne AJ, Shea TJ, et al. Pulmonary Epithelial Cell-Derived Cytokine TGF-β1 Is a Critical Cofactor for Enhanced Innate Lymphoid Cell Function. *Immunity*. 2015;43(5):945–58.
31. Barnard JA, Warwick GJ, Gold LI. Localization of transforming growth factor beta isoforms in the normal murine small intestine and colon. *Gastroenterology*. 1993;105(1):67–73.
32. Cepek KL, Shaw SK, Parker CM, et al. Adhesion between epithelial cells and T lymphocytes mediated by E-cadherin and the alpha E beta 7 integrin. *Nature*. 1994;372(6502):190–3.
33. Shaw SK, Hermanowski-Vosatka A, Shibahara T, et al. Migration of intestinal intraepithelial lymphocytes into a polarized epithelial monolayer. *Am. J. Physiol.* 1998;275(3 Pt 1):G584–91.
34. Brown DW, Furness J, Speight PM, et al. Mechanisms of binding of cutaneous lymphocyte-associated antigen-positive and alphaebeta7-positive lymphocytes to oral and skin keratinocytes. *Immunology*. 1999;98(1):9–15.
35. Pauls K, Schön M, Kubitza RC, et al. Role of integrin alphaE(CD103)beta7 for tissue-specific epidermal localization of CD8+ T lymphocytes. *J. Invest. Dermatol.* 2001;117(3):569–75.
36. Hey YY, O'Neill HC. Murine spleen contains a diversity of myeloid and dendritic cells distinct in antigen presenting function. *J. Cell. Mol. Med.* 2012;16(11):2611–9.
37. Rothe M, Blaut M. Evolution of the gut microbiota and the influence of diet. *Benef Microbes*. 2013;4(1):31–7.
38. Campisi L, Soudja SM, Cazareth J, et al. Splenic CD8α$^+$ dendritic cells undergo rapid programming by cytosolic bacteria and inflammation to induce protective CD8$^+$ T-cell memory. *Eur. J. Immunol.* 2011;41(6):1594–605.
39. Borges da Silva H, Fonseca R, Pereira RM, et al. Splenic Macrophage Subsets and Their Function during Blood-Borne Infections. *Front Immunol*. 2015;6:480.
40. Flo TH, Smith KD, Sato S, et al. Lipocalin 2 mediates an innate immune response to bacterial infection by sequestrating iron. *Nature*. 2004;432(7019):917–21.
41. Vidal S, Tremblay ML, Govoni G, et al. The Ity/Lsh/Bcg locus: natural resistance to infection with intracellular parasites is abrogated by disruption of the Nramp1 gene. *J. Exp. Med.* 1995;182(3):655–66.
42. Narni-Mancinelli E, Chaix J, Fenis A, et al. Fate mapping analysis of lymphoid cells expressing the NKp46 cell surface receptor. *Proc. Natl. Acad. Sci. U.S.A.* 2011;108(45):18324–9.
43. Cerovic V, Houston SA, Scott CL, et al. Intestinal CD103(-) dendritic cells migrate in lymph and prime effector T cells. *Mucosal immunology*. 2013;6(1):104–13.

3.7 Supplementary figures

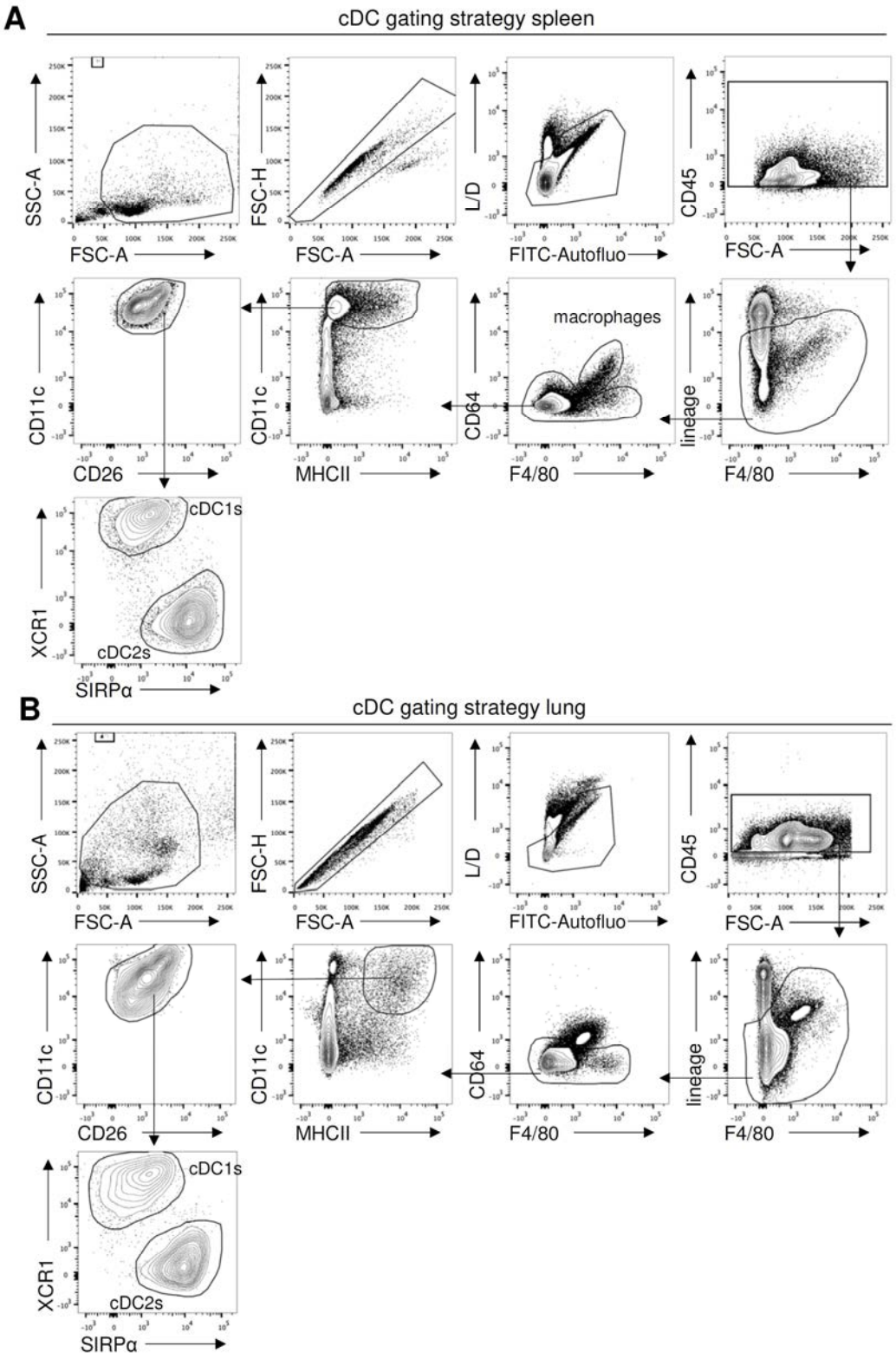

Figure S1 | cDC gating strategy for different organs. (A) Representative FACS plots showing gating strategy for macrophages, cDC1s and cDC2s in the spleen. (B) Representative FACS plots showing gating strategy for cDC1s and cDC2s in the lung. FSC, forward scatter. SSC, side scatter. L/D, live/dead. Autofluo, autofluorescence.

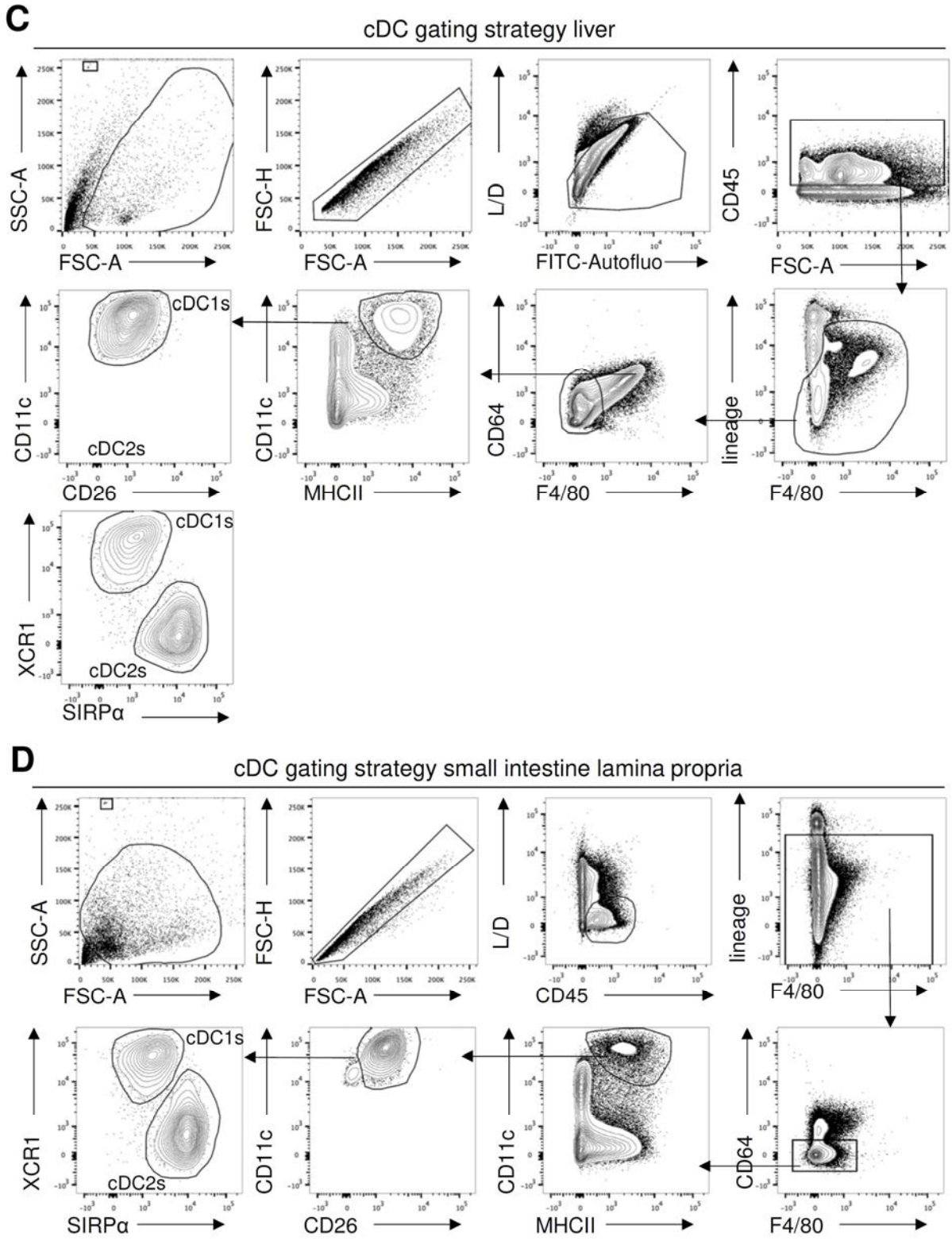

Figure S1 continued | cDC gating strategy for different organs. (C) Representative FACS plots showing gating strategy for cDC1s and cDC2s in the liver. (D) Representative FACS plots showing gating strategy for cDC1s and cDC2s in the small intestine lamina propria. FSC, forward scatter. SSC, side scatter. L/D, live/dead. Autofluo, autofluorescence.

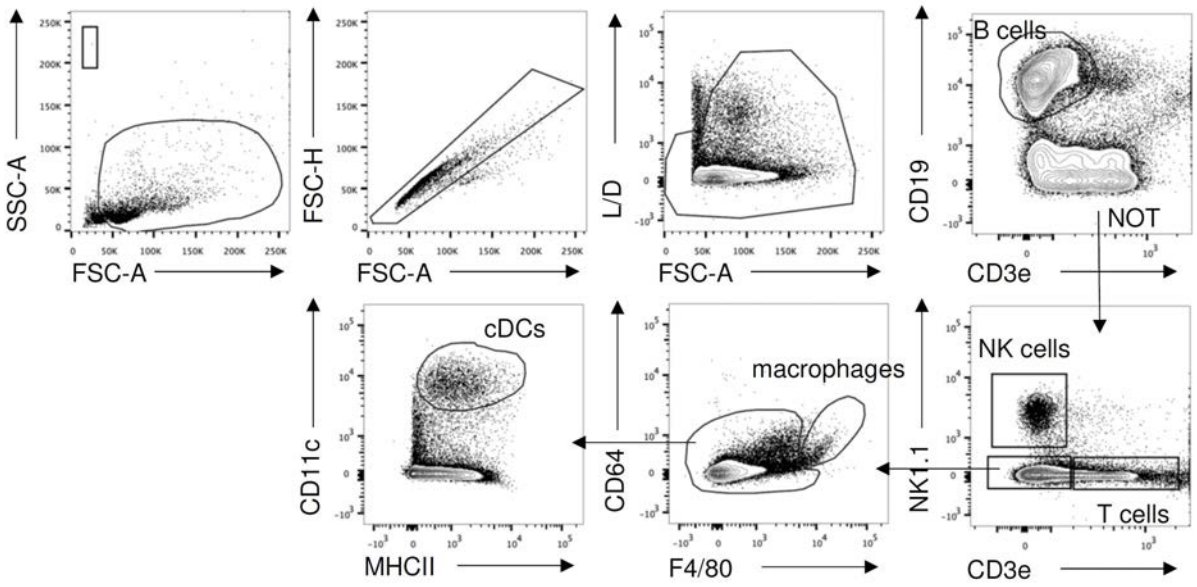

Figure S2 | Gating strategy to identify splenic B cells, NK cells, T cells, macrophages and cDCs as performed in CD11c^{CRE}xRosa-RFP mice. Representative FACS plots showing gating strategy for B cells, NK cells, T cells, macrophages and cDCs as performed in the spleen of CD11c^{CRE}xRosa-RFP mice. FSC, forward scatter. SSC, side scatter. L/D, live/dead.

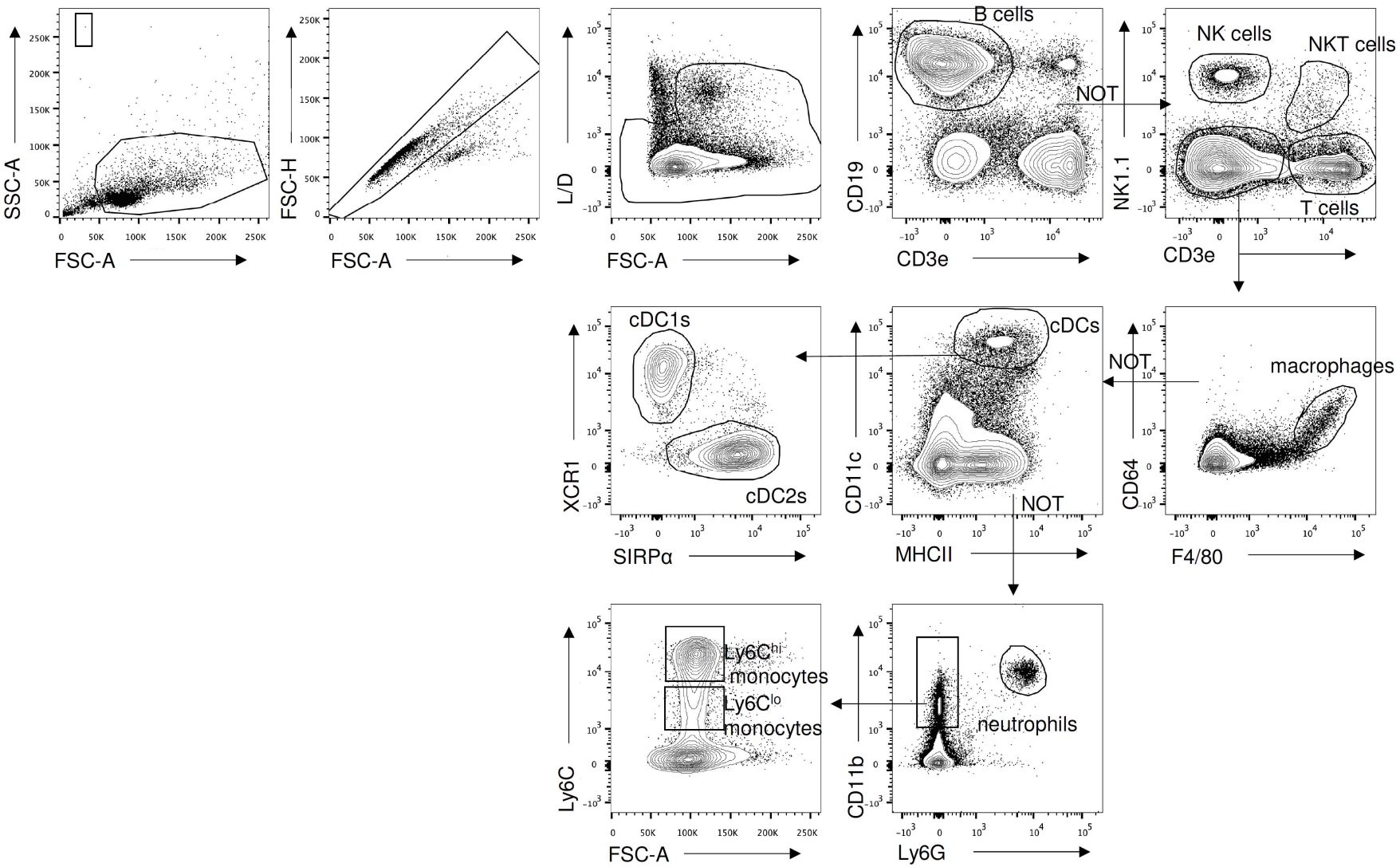

Figure S3 | Gating strategy to identify splenic B cells, NK cells, NKT cells, T cells, macrophages, cDC1s, cDC2s, neutrophils, Ly6C^{hi} and Ly6C^{lo} monocytes. Representative FACS plots showing gating strategy to identify splenic B cells, NK cells, NKT cells, T cells, macrophages, cDC1s, cDC2s, neutrophils, Ly6C^{hi} and Ly6C^{lo} monocytes. FSC, forward scatter. SSC, side scatter. L/D, live/dead.

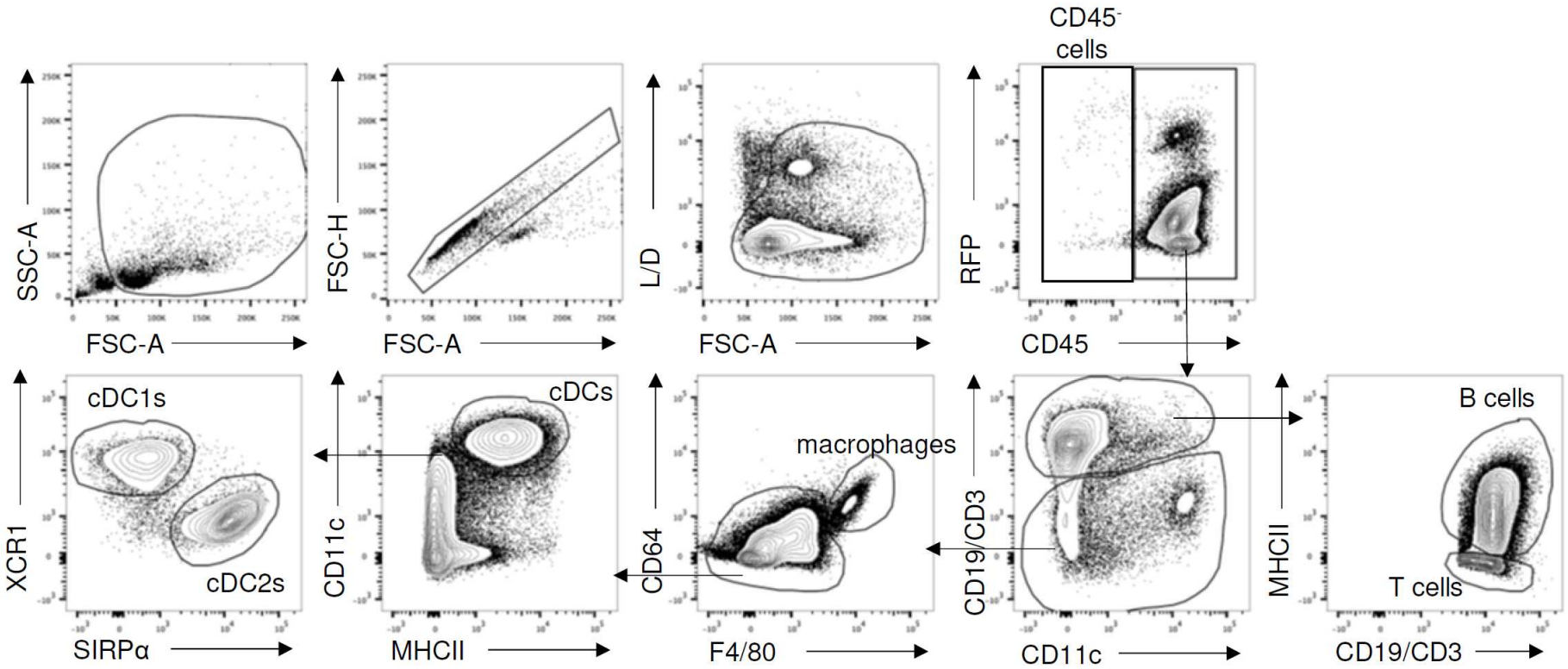

Figure S4 | Gating strategy to identify splenic B cells, T cells, macrophages, cDC1s, cDC2s and CD45$^-$ cells as performed in Zbtb46^{CRE}xRosa-RFP mice and XCR1^{CRE}xRosa-RFP mice. Representative FACS plots showing gating strategy for B cells, T cells, macrophages, cDC1s, cDC2s and CD45$^-$ cells as performed in the spleen of Zbtb46^{CRE}xRosa-RFP mice and XCR1^{CRE}xRosa-RFP mice. FSC, forward scatter. SSC, side scatter. L/D, live/dead.

Chapter 4

Zeb2 is essential for macrophage survival

Contributions: Bieke Soen performed and analyzed experiments shown in Figures 1B-D, 2, 3 and 4. Bieke Soen and Charlotte Scott performed and analyzed experiments shown in Figures 5, 6 and 7. Joachim Taminau, Gillian Blancke and Gert Van Isterdael provided technical assistance. Liesbet Martens performed the bio-informatics analysis shown in Figure 1A. Bieke Soen, Charlotte Scott, Martin Guilliams and Geert Berx contributed to the conceptualization and discussion of the project and its experiments. Bieke Soen performed the writing of this chapter.

4.1 Abstract

Depending on the tissue, macrophages develop either from yolk-sac macrophages, fetal liver monocytes or bone marrow monocytes. In most tissues resident macrophages are able to maintain their pool through local proliferation, however in some tissues macrophages require constant replenishment from adult blood monocytes to sustain their numbers. Despite the limited set of progenitors, gene expression among tissue-resident macrophages is highly heterogeneous. It was suggested that factors in the local environment induce the expression of tissue-specific TFs, like Gata6 in peritoneal macrophages and Pparγ in alveolar macrophages. These tissue-specific TFs probably cooperate with the chromatin remodelling TF Pu.1, which is required for the development of all macrophages. This cooperation could explain the tissue-specific gene expression in macrophages. Except for Pu.1, so far no TFs were described to govern development or maintenance of the whole macrophage lineage. Here we identified that high expression of the TF *Zeb2* is a conserved feature across tissue-resident macrophages. Moreover, the removal of Zeb2 from fully differentiated macrophages in lung, spleen, colon and liver results in an altered macrophage phenotype and eventually in their disappearance.

4.2 Introduction

Macrophages were first described in 1883 as phagocytic cells with importance in host defense and elimination of dying cells[1,2]. For a long time it was believed that all tissue-resident macrophages arise from adult blood monocytes after migration into the tissue and are continuously replenished through this influx[3,4]. Now we know that in mice most tissue-resident macrophages develop alongside the tissue during embryogenesis from yolk-sac macrophages or fetal liver monocytes and are able to self-maintain in the adult tissue[5,6]. In some tissues, like the skin dermis, heart and intestine, macrophages first develop from yolk-sac macrophages or fetal liver monocytes and are then gradually replaced by blood monocytes[7–10]. Despite being derived from a limited number of progenitors (yolk-sac macrophages, fetal liver monocytes and blood monocytes), gene expression among tissue-resident macrophages is immensely heterogeneous[11,12]. This implies that macrophages are highly influenced by the micro-environment in which they reside[13]. It has been suggested that tissue-specific factors induce secondary TFs in local macrophages and that these cooperate with the more general macrophage TF Pu.1[14,15]. With the help of Pu.1, tissue-specific secondary TFs can influence the chromatin landscape and hence gene expression[12,14,15]. However, apart from Pu.1 so far no TF has been identified to control all tissue-resident macrophages. As Zeb proteins are also able to change the chromatin landscape and gene expression and we showed a role for Zebs in DCs, we wondered if they could also function in macrophage development and homeostasis. When looking at publically available expression data for *Zeb1* and *Zeb2* in different tissue-resident macrophages, we noticed that *Zeb1* mRNA levels are rather low in the macrophage lineage, while *Zeb2* mRNA levels are high compared to splenic DCs (Figure 1A). In light of this, we further investigated if Zeb2 played a role across different tissue macrophages. For this we combined *in vitro* work using different macrophage cell lines with *in vivo* experiments. For this last part, we crossed our conditional Zeb2 knockout model with three different CRE lines, namely *Lyz2*^{CRE} (referred to as LysM^{CRE}) , *Itgax*^{CRE} (referred to as CD11c^{CRE}) and the newly generated *Clec4f*^{CRE} (referred to as KC^{CRE}).

4.3 Results

High expression of *Zeb2* and low expression of *Zeb1* in murine tissue-resident macrophages and murine macrophage cell lines

To determine the possibility of a role for Zeb proteins in macrophages (MFs), we first investigated the mRNA expression levels in different murine tissue-resident macrophages and macrophage cell lines. For this we looked at *Zeb* expression levels in different FACS-purified murine macrophage populations (Kupffer cells, alveolar macrophages, splenic red pulp macrophages, peritoneal macrophages, microglia and small intestinal macrophages) and compared this with classical (Ly6C^{hi}) and non-classical (Ly6C^{lo}) BM monocytes and other immune cell populations isolated from the spleen (B cells; follicular, germinal center and marginal zone, T cells; naive CD4^{+} and naive CD8^{+}, cDC1s and cDC2s) and neutrophils isolated from the blood. Data were compiled from previously published studies performed by the Immgen Consortium[11,16–19] and published by the group of Prof. Guilliams[20,21] (Figure 1A, Scott *et al.* (under review, Addendum p.252)). Compared to splenic DCs, we see a low expression of *Zeb1*, but a high expression of *Zeb2* in Kupffer cells (KCs), alveolar MFs (AMs), microglia (MG), splenic red pulp MFs (RP), peritoneal MFs (PT) and small intestinal MFs (SI). Both Ly6C^{hi} and Ly6C^{lo} BM monocytes (Mo) show a rather low expression of *Zeb2* compared to the different tissue-resident MFs (Figure 1A). The same holds true for the different murine cell lines analyzed (Table 1 Materials and methods). C3H-Hej, C3H-Hen, MH-S, P388D1 and Raw264-7 can be considered as macrophage cell lines, while WEHI3 are cultured monocytes. From the different cell lines RNA was extracted and RT-qPCR was performed to determine the relative mRNA expression levels of *Zeb1* and *Zeb2*. As for the publically available data the levels of *Zeb2* are mostly higher in the macrophage cultures compared to the WEHI3 monocytes. *Zeb1* shows the opposite trend with the highest expression in the WEHI3 monocytic line (Figure 1B). Based on the Immgen data and the RT-qPCR results from the cell lines, we hypothesized Zeb2 to be generally important in the macrophage lineage.

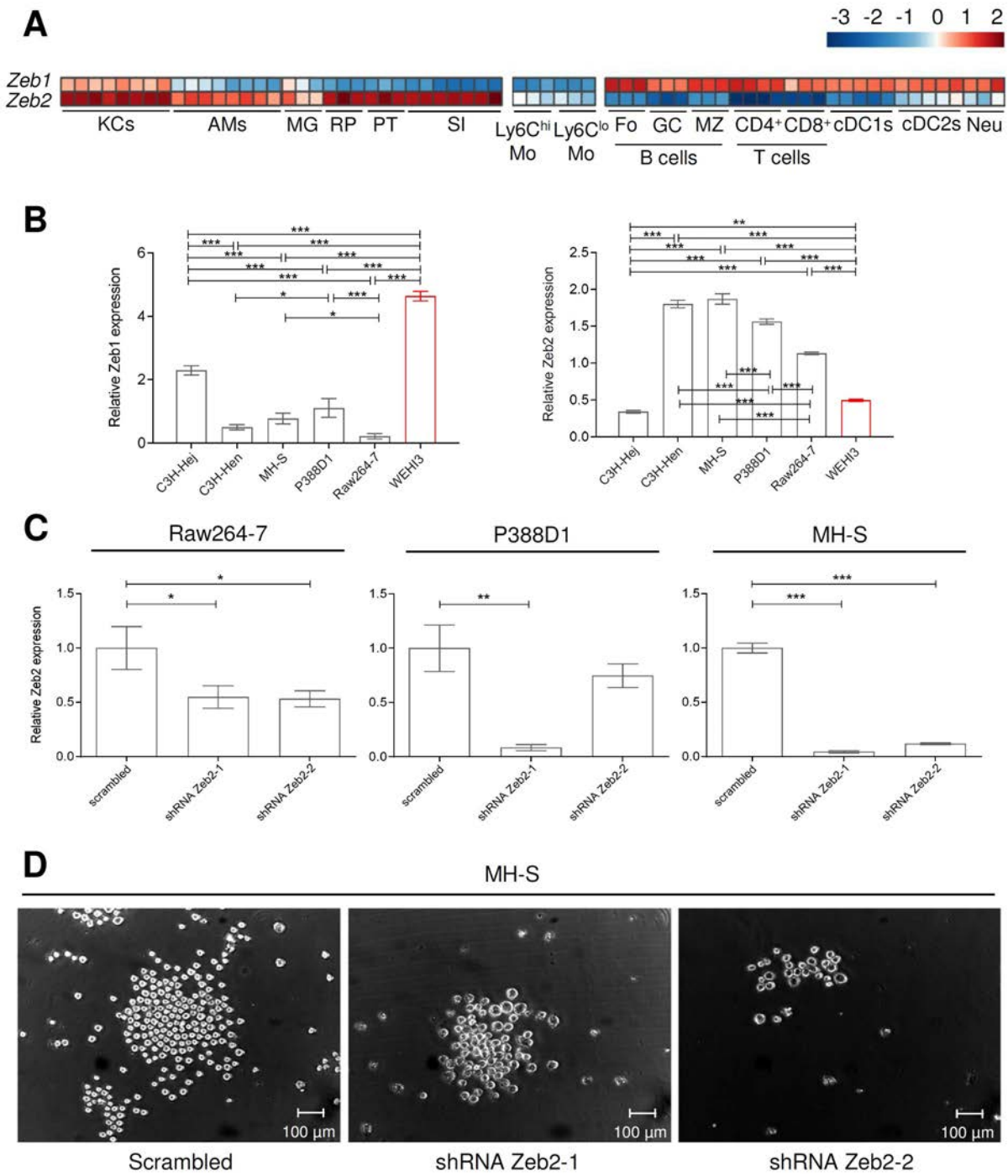

Figure 1 | Knockdown of Zeb2 in murine macrophage cell lines affects cell survival. (A) Heatmap showing *Zeb1* and *Zeb2* expression in murine tissue-resident MFs and other immune cells including splenic B cells, naive T cells, cDC1s, cDC2s and blood neutrophils and Ly6C^{hi} and Ly6C^{lo} BM monocytes. Data are from microarray analyses performed either in house or by the Immgen consortium. Gene expression was normalized per mean expression of each gene. (B) Relative *Zeb1* and *Zeb2* mRNA expression in different murien MF (black) and monocyte (red) cell lines. Results (mean and SD of three technical replicates) shown are expressed relative to *Calm2* and *Eef1a1* expression using qbase$^+$ software with the average expression across samples set to 1. *, P < 0.05; **, P < 0.01; ***, P < 0.001. One-way ANOVA with Bonferroni post-test. (C) Relative *Zeb2* mRNA expression after transduction with a scrambled or two Zeb2 shRNA constructs in indicated MF cell lines. Results (mean and SD of three technical replicates) shown are expressed relative to *Calm2* and *Eef1a1* expression using qbase$^+$ software with the scrambled construct set to 1. *P < 0.05; **P < 0.01; ***, P < 0.001. Two-way student's t test was used to compare the scrambled to the Zeb2 shRNA constructs. (D) Pictures of the MH-S cell line 7 days after transduction with either a scrambled or a Zeb2 knockdown shRNA (shRNA Zeb2-1 and shRNA Zeb2-2). Scalebar 100 µm.

Knockdown of Zeb2 in murine macrophage cell lines results in cell death

To investigate the role of Zeb2 in MF homeostasis, we first utilised the murine macrophage cell lines Raw264-7, P388D1 and MH-S as those lines are often used and most easy to transduce. The three cell lines were transduced with constitutive lentiviral vectors containing either a scrambled non-targeting shRNA or a shRNA targeting the *Zeb2* mRNA (shRNA Zeb2-1 and shRNA Zeb2-2). Shortly after transduction we extracted RNA to confirm a knockdown for *Zeb2* through RT-qPCR. For all three cell lines we were able to confirm a decreased *Zeb2* mRNA expression for both Zeb2 knockdown constructs when compared to the scrambled construct (Figure 1C). The efficiency of knockdown varied between ~95% with shRNA Zeb2-1 in MH-S cells and ~25% with shRNA Zeb2-2 in P388D1 cells. Despite the varying knockdown efficiency, decreased levels of *Zeb2* had a massive effect on the macrophage cell lines. Shortly after transduction with shRNA against *Zeb2* the cells started to die and it was impossible to further passage the cells, while cells transduced with the scrambled non-targeting shRNA could be further kept in culture (Figure 1D). This *in vitro* findings strongly suggest a dependency for Zeb2 in macrophage survival and hence we next aimed to investigate if this finding holds true *in vivo*.

BM derived macrophages from LysM^{CRE}xZeb2$^{fl/fl}$ mice have an increased population of Ly6C^{+} cells

To investigate the role of Zeb2 in macrophages *in vivo*, we first crossed the conditional Zeb2 knockout mouse model[22] with the LysM^{CRE} line[23] in order to achieve loss of Zeb2 in monocytes, mature macrophages and neutrophils[24]. Hence, the resulting LysM^{CRE}xZeb2$^{fl/fl}$ mice should allow us to investigate the consequences of loss of Zeb2 expression across different tissue-resident macrophages. As we suspected Zeb2 to play a role in maturation or survival of macrophages, we first cultured whole BM of LysM^{CRE}xZeb2$^{fl/fl}$ mice and Zeb2$^{fl/fl}$ control mice supplemented with Csf1 (M-Csf). After 3 days of culturing a subtle difference in number of differentiated cells could be seen in the culture plates, with a trend towards a

decrease in number of cells in plates with Zeb2 KO BM (Figure 2A). Although this did not result in a significant difference in cell counts on day 7 of culturing, there was a trend towards lower cell numbers in LysM^{CRE}xZeb2$^{fl/fl}$ BM cultures compared with cultures from control littermates (Figure 2B). On the 7th day of culturing, cells were harvested and stained for flow cytometry with antibodies against different macrophage and monocyte markers (Ccr2, Ly6C, CD11b, CD11c, CD64 and F4/80). All markers except Ly6C were expressed at comparable levels between Zeb2 KO and WT BM (Figure 2C). Upon further investigation we found a significant increase in Ly6C^{+}CD64^{+} cells, coupled with a significant decrease in Ly6C^{-}CD64^{+} cells in cultures derived from LysM^{CRE}xZeb2$^{fl/fl}$ BM (Figure 2C).

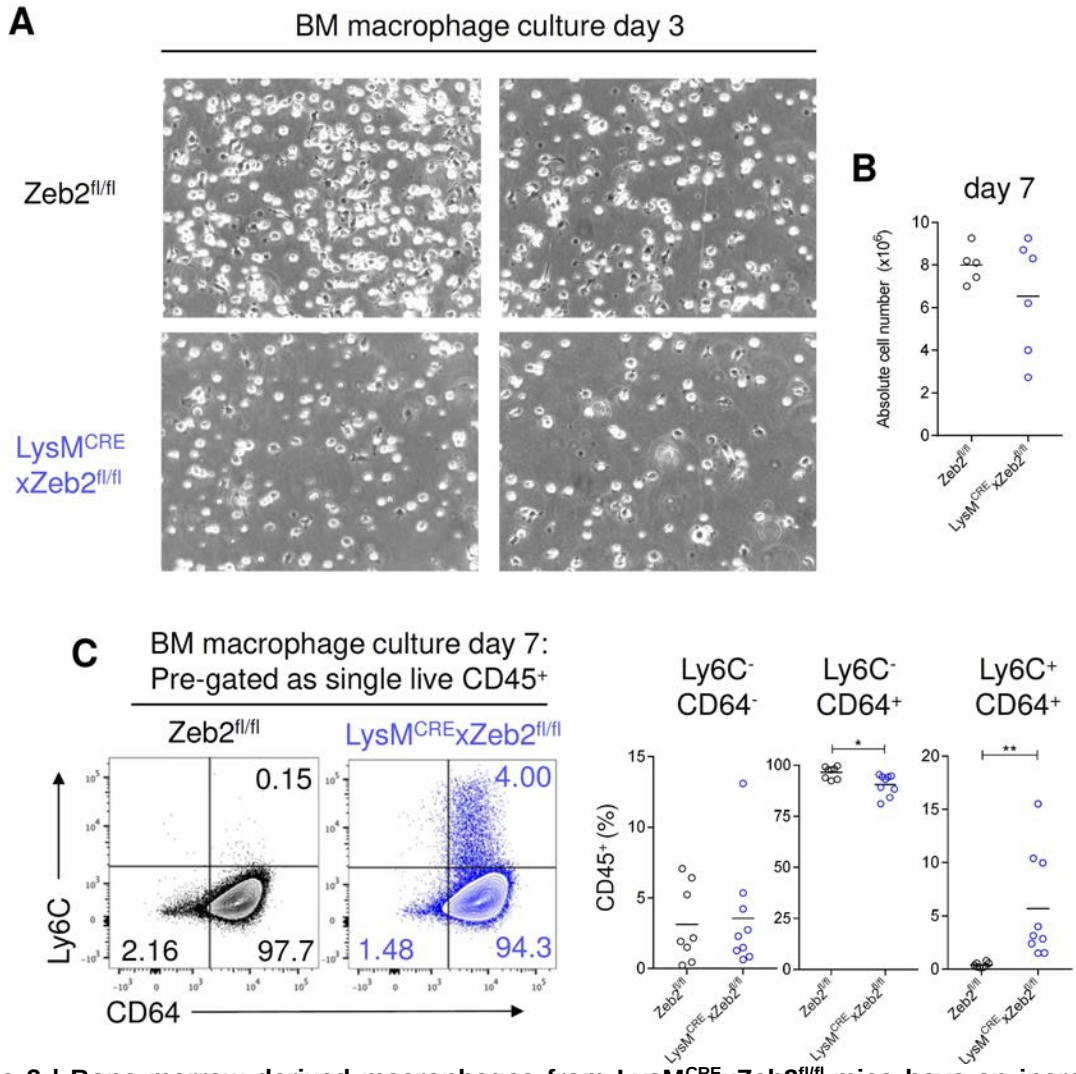

Figure 2 | Bone marrow derived macrophages from LysM^{CRE}xZeb2$^{fl/fl}$ mice have an increased Ly6C^{+} subpopulation. (A) Pictures showing BM derived macrophage cultures after 3 days of culturing supplemented with Csf1 for Zeb2$^{fl/fl}$ and LysM^{CRE}xZeb2$^{fl/fl}$ whole BM. (B) Cell counts from one 10 cm dish on day 7 of Csf1 BM cultures from Zeb2$^{fl/fl}$ and LysM^{CRE}xZeb2$^{fl/fl}$ mice. (C) Representative FACS plots showing Ly6C and CD64 expression on BM derived macrophages after 7 days of culturing for Zeb2$^{fl/fl}$ and LysM^{CRE}xZeb2$^{fl/fl}$ BM. The numbers represent the proportion of each population as percentage of live CD45^{+} cells. Graphs represent the percentage of cells as frequency of total live CD45^{+} cells. *, P < 0.05; **, P < 0.01. Two-way student's t test.

LysM^{CRE}xZeb2$^{fl/fl}$ mice do not show a reduction in colon or liver resident macrophages

Having shown a small increase in Ly6C expression in *ex vivo* cultured macrophages from LysM^{CRE}xZeb2$^{fl/fl}$ mice, we next aimed to investigate the presence of tissue-resident macrophages in these mice. We decided to dissect the liver and colon of the mice and determine the presence of monocytes and macrophages with flow cytometry (Figure S1 and S2), because in the colon macrophages typically develop from blood monocytes, while in the liver Kupffer cells are derived from embryonic origin. When looking at Kupffer cells, Ly6C^{hi} monocytes and neutrophils, we could not detect statistically significant differences in the presence of these populations in the liver of LysM^{CRE}xZeb2$^{fl/fl}$ compared to their WT littermate controls (Figure 3A and B and Figure S1). Next we analyzed the colon lamina propria for MFs, monocytes and transitioning monocytes, which are monocytes maturing into MFs. Also in this organ we were unable to find statistical differences when comparing LysM^{CRE}xZeb2$^{fl/fl}$ mice with WT littermate controls (Figure 3C and D and Figure S2).

BM derived macrophages from LysM^{CRE}xZeb2$^{fl/fl}$ mice reveal an inefficient CRE recombinase activity

Despite the small difference found during *ex vivo* differentiation of LysM^{CRE}xZeb2$^{fl/fl}$ BM, we were unable to find differences in monocyte or macrophage populations *in vivo*. However, the LysM^{CRE} line was reported before to be inefficient[24] and we suspected that this was also the case in our LysM^{CRE}xZeb2$^{fl/fl}$ mice. In order to test this hypothesis, we sorted the Ly6C^{-}CD64^{+} and Ly6C^{+}CD64^{+} fractions from the 7 day old BM cultures, extracted genomic DNA and performed a PCR designed to specifically detect if CRE excision took place. This PCR only generates a 288 bp long fragment when the seventh exon of Zeb2 was actually excised by CRE recombinase activity, while lack of loxP sites (CRE^{-} cells) or lack of excision in CRE^{+} cells does not generate a PCR-product. The results show a clear enrichment of PCR-product for the Ly6C^{+}CD64^{+} sorted fraction from LysM^{CRE}xZeb2$^{fl/fl}$ BM when comparing with the Ly6C^{-}CD64^{+} fraction sorted from the same BM culture (Figure 4). This would suggest

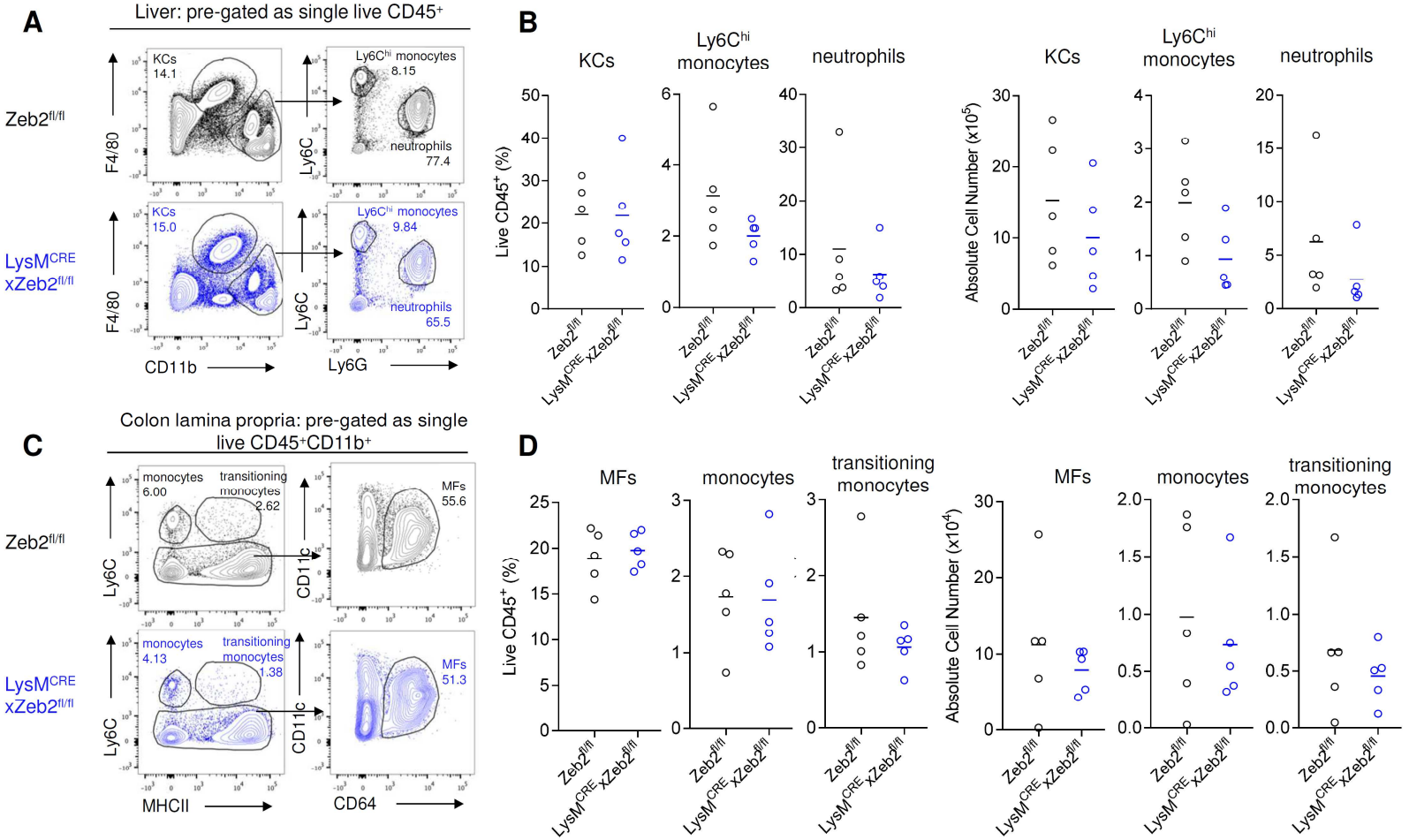

Figure 3 | LysM^{CRE}xZeb2$^{fl/fl}$ mice do not show reduction in colon or liver resident MFs. (A) Representative FACS plots showing identification of F4/80$^+$ KCs, Ly6C^{hi} monocytes and Ly6G$^+$ neutrophils in the liver of Zeb2$^{fl/fl}$ and LysM^{CRE}xZeb2$^{fl/fl}$ mice. For KCs the number represents the proportion of live CD45$^+$ cells and for monocytes and neutrophils the proportion of live CD45$^+$CD11b$^+$ cells. (B) Proportion as a percentage of live CD45$^+$ cells and absolute cell number of indicated cell type in liver of indicated mice. Data are pooled from two experiments, with n=5 per group. (C) Representative FACS plots showing identification of Ly6C$^+$ monocytes, Ly6C$^+$MHCII$^+$ transitioning monocytes and F4/80$^+$ MFs in the colon lamina propria of Zeb2$^{fl/fl}$ and LysM^{CRE}xZeb2$^{fl/fl}$ mice. For monocytes and transitioning monocytes the number represents the proportion of live CD45$^+$CD11b$^+$ cells and for MFs the proportion of live CD45$^+$CD11b$^+$Ly6C$^-$ cells. (D) Proportion as a percentage of live CD45$^+$ cells and absolute cell number of indicated cell type in colon lamina propria of indicated mice. Data are pooled from two experiments, with n=5 per group. (B and D) No statistical significance detected with two-way student's t test.

that the immature Ly6C^{+} monocytic fraction is enriched for cells with an actual KO for Zeb2, while the more mature Ly6C^{-}CD64^{+} macrophage fraction contains more cells which have retained intact *Zeb2* alleles. This last finding could be due to an inefficient CRE recombinase activity, potentially combined with loss of cells that have efficiently floxed out the seventh exon of Zeb2. Having found evidence fitting our hypothesis of inefficient CRE excision in the LysM^{CRE}xZeb2$^{fl/fl}$ model, we decided to explore the use of hopefully more efficient CRE lines to further investigate the role of Zeb2 in macrophages.

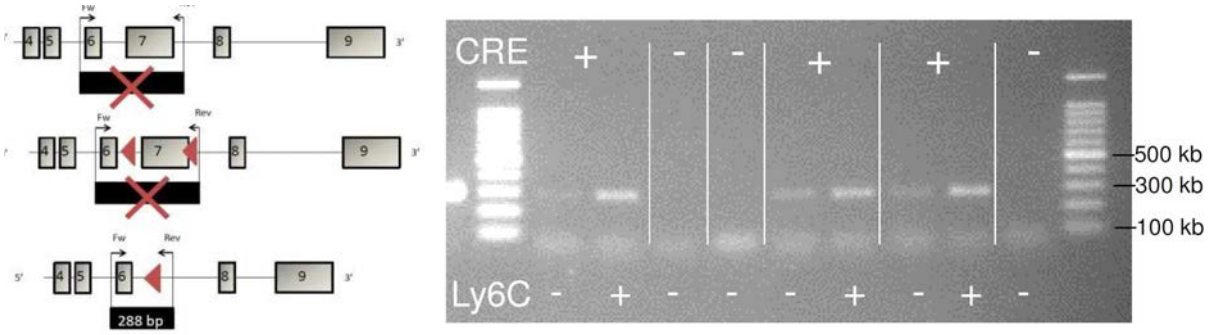

Figure 4 | Inefficient CRE recombinase activity in LysM^{CRE}xZeb2$^{fl/fl}$ mice. Schematic representation and result of PCR used to determine CRE excision of the 7th exon of *Zeb2*. Grey blocks represent the exons of *Zeb2*, arrows represent primers, red triangles represent loxP sites, red crosses represent lack of PCR-product. Samples loaded on the gel were fractions (Ly6C^{-}CD64^{+} and Ly6C^{+}CD64^{+}) sorted from CRE^{-} (Zeb2$^{fl/fl}$) and CRE^{+} (LysM^{CRE}xZeb2$^{fl/fl}$) BM derived macrophages after 7 days of culturing.

The KC^{CRE} mouse line efficiently targets Kupffer cells

In search for more efficient and specific CRE lines to target tissue-resident macrophages, we opted to first focus on Kupffer cells in the liver. Recently it was shown that the C-type lectin, Clec4F, is exclusively expressed by murine KCs[20]. Therefore, the lab of Prof. Guilliams with which we closely collaborated, generated the KC^{CRE} mice by introducing an internal ribosome entry site (IRES) and *CRE recombinase* into the 3' untranslated region of the *Clec4f* gene. To validate if the newly generated CRE line efficiently targets KCs, we crossed it with the Rosa-RFP reporter line[18]. We next isolated the liver and performed flow cytometry to check for RFP-expression among KCs. This revealed that 88.35 ± 1.54% of F4/80^{+}CD64^{+} Clec4F^{+}Tim4^{+} KCs express RFP and can thus be efficiently targeted with the new KC^{CRE} mouse line (Figure 5A and Figure S3).

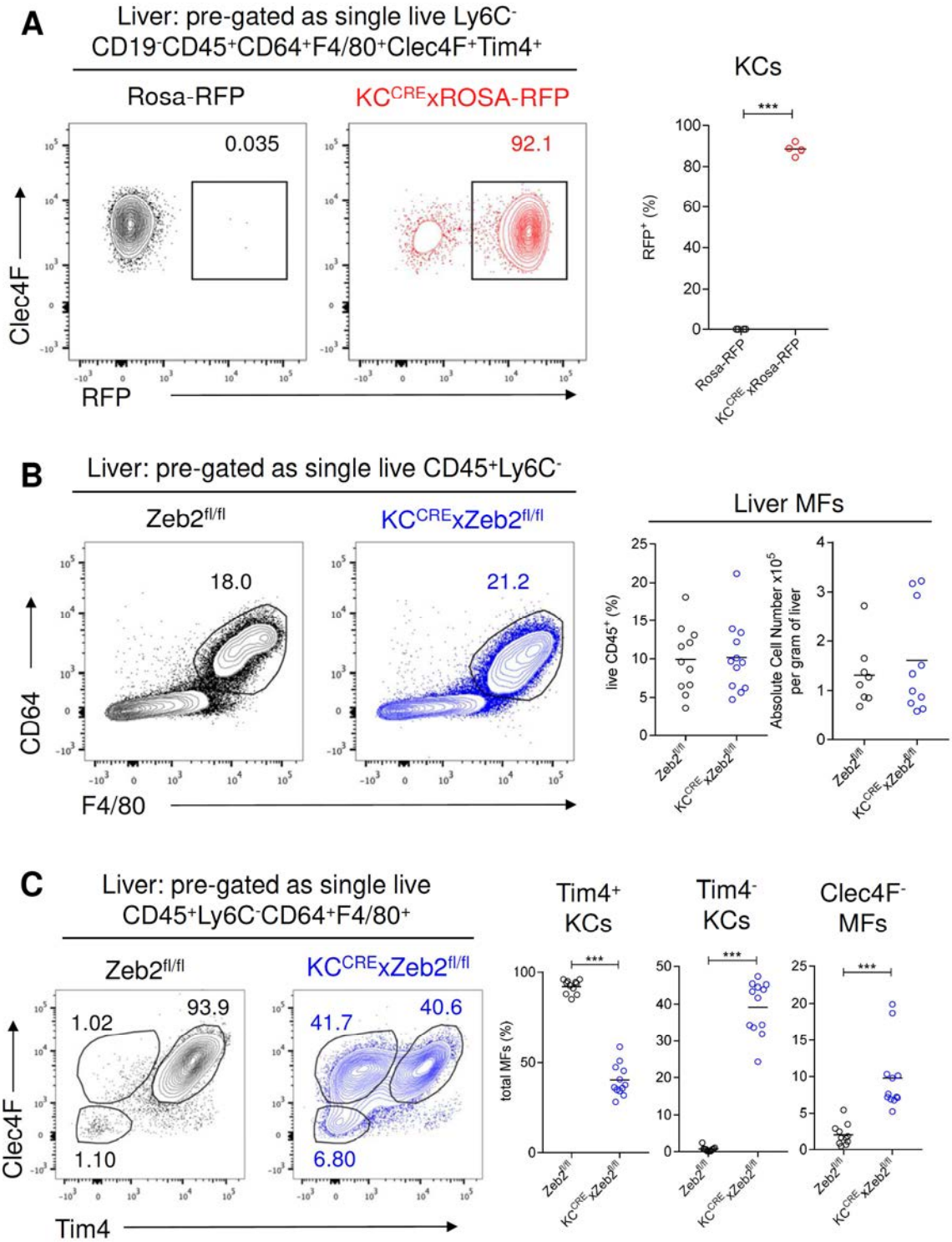

Figure 5 | KCs of KC^{CRE}xZeb2$^{fl/fl}$ mice have an altered phenotype. (A) Representative FACS plots showing RFP expression in KCs from Rosa-RFP and KC^{CRE}xRosa-RFP mice. Numbers represent the proportion of RFP$^+$ cells as a percentage of total KCs. Data are from one experiment with n=4 per group. (B) Representative FACS plots showing the presence of liver MFs in Zeb2$^{fl/fl}$ and KC^{CRE}xZeb2$^{fl/fl}$ mice. Numbers represent hepatic MFs as percentage of live CD45$^+$ cells. Graphs show proportion as a percentage of live CD45$^+$ cells and absolute cell number per g liver of MFs in the liver of indicated mice. For percentage of live CD45$^+$ data are pooled from three experiments, with at least n=11 per group; for absolute cell numbers data are pooled from two experiments, with at least n=8 per group. (C) Representative FACS plots showing Clec4F and Tim4 expression in hepatic MFs of Zeb2$^{fl/fl}$ and KC^{CRE}xZeb2$^{fl/fl}$ mice. Numbers represent the proportion of each subpopulation as percentage of total liver MFs. Graphs show proportion as a percentage of total liver MFs for indicated cell types. Data are pooled from two experiments, with at least n=11 per group.(A-C) ***, P < 0.001. Two-way student's t test.

Loss of Zeb2 in KCs alters their phenotype

We next analysed the presence of MFs in the liver of $KC^{CRE}xZeb2^{fl/fl}$ mice. To our surprise we did not find significant differences in either the proportion or absolute cell number when comparing total liver $F4/80^{+}CD64^{+}$ MFs of $KC^{CRE}xZeb2^{fl/fl}$ mice with those of their control littermates (Figure 5B and Figure S3). However, since our initial analysis in the $LysM^{CRE}xZeb2^{fl/fl}$ mice, two additional markers had been identified to be expressed on KCs, namely Clec4F and Tim4[14,20]. Thus, here we also examined expression of these markers. Importantly, this highlighted that while in $Zeb2^{fl/fl}$ mice nearly all hepatic MFs are $Clec4F^{+}Tim4^{+}$ KCs, the livers of $KC^{CRE}xZeb2^{fl/fl}$ mice had a significant reduction in $Clec4F^{+}Tim4^{+}$ KCs coupled with a significant increase in both $Clec4F^{+}Tim4^{-}$ KCs and $Clec4F^{-}Tim4^{-}$ MFs (Figure 5C). This resembles what has previously been published on KC-DTR mice. In this model administration of diphtheria toxin leads to depletion of liver-resident Kupffer cells. This creates niche availability and subsequent engraftment from circulating monocytes in the liver[20]. Engrafted monocytes then differentiate into $Clec4F^{-}$ MFs, which further differentiate into $Tim4^{-}$ KCs to finally become long-lived self-renewing $Tim4^{+}$ KCs[20]. Hence, the presence of $Tim4^{-}Clec4F^{-}$ monocyte-derived MFs and $Tim4^{-}Clec4F^{+}$ KCs in the liver of $KC^{CRE}xZeb2^{fl/fl}$ mice suggests that self-renewing KCs die and are subsequently replaced by monocyte-derived cells.

AMs, splenic MFs and colonic MFs are reduced in $CD11c^{CRE}xZeb2^{fl/fl}$ mice

Having shown a role for Zeb2 in KC homeostasis, we wanted to see if this also holds true for other tissue-resident macrophages. As alveolar macrophages (AMs) express high levels of CD11c, we wondered if we could use the $CD11c^{CRE}$ line[25] to target these tissue-resident macrophages. We therefore crossed the $CD11c^{CRE}$ line with the Rosa-RFP reporter mouse line[26], and checked for RFP expression in macrophages in the lung. We found that lung MFs are efficiently targeted with the $CD11c^{CRE}$ line, as on average 91.24% of lung MFs express RFP in the $CD11c^{CRE}$xRosa-RFP mice (Figure 6A). Additionally, we have previously shown that splenic macrophages can be targeted with the $CD11c^{CRE}$ mouse model (see Chapter 3 of Results section). We

determined that 68.02 ± 0.33% of macrophages are RFP$^+$ in the spleen of CD11c^{CRE}xRosa-RFP mice (Figure 6B). Furthermore, it has previously been reported that colonic macrophages express CD11c and can be targeted with the CD11c^{CRE} line[27]. Knowing this, we decided to have a closer look at alveolar, splenic and colonic macrophages in the CD11c^{CRE}xZeb2$^{fl/fl}$ model, which was previously used to investigate Zeb2 in dendritic cells (see Chapter 1 of Results section).

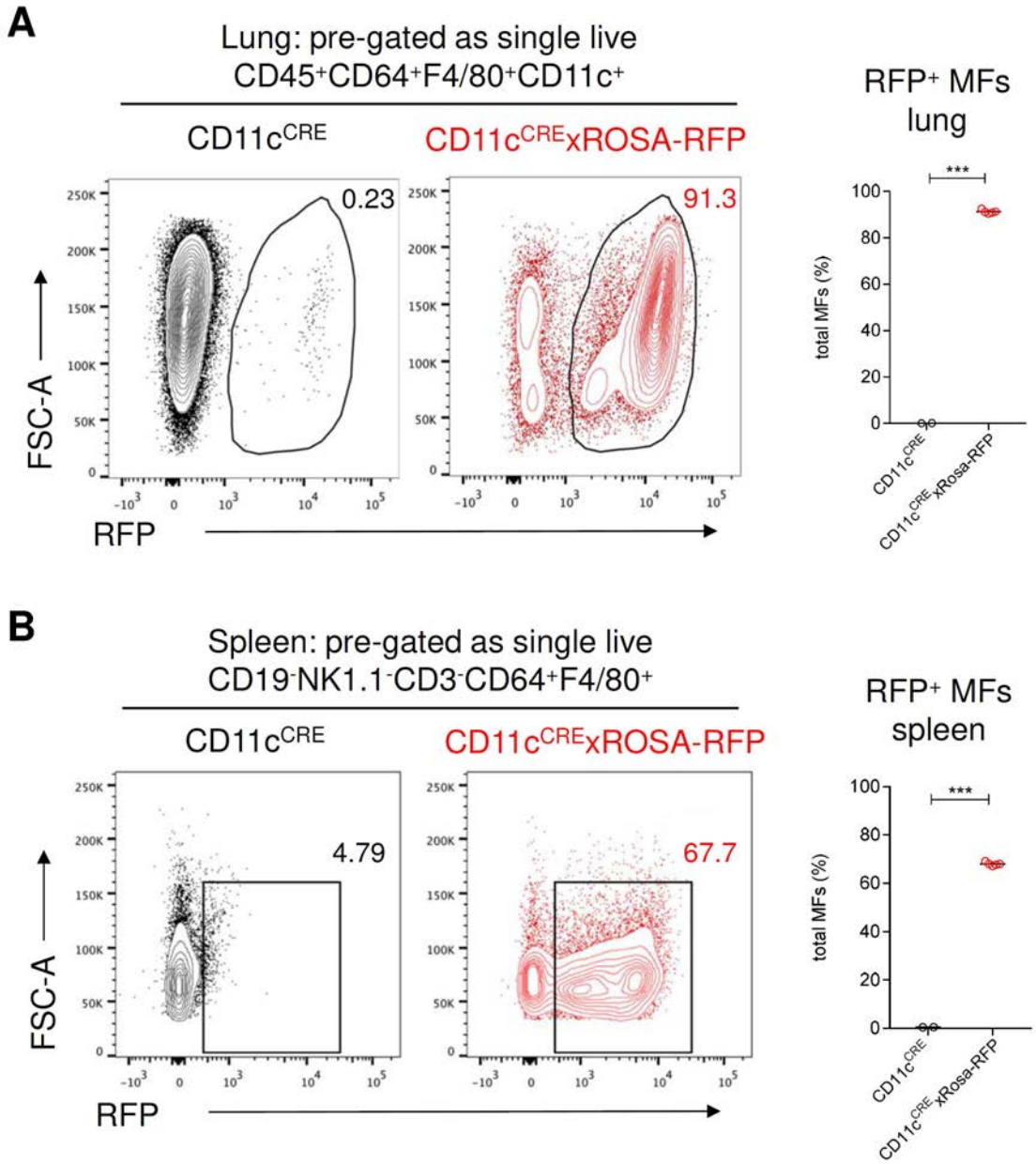

Figure 6 | CD11c^{CRE} mice can be used to efficiently target pulmonary MFs and splenic MFs. (A) Representative FACS plots showing RFP expression in MFs in the lung of CD11c^{CRE} and CD11c^{CRE}xRosa-RFP mice. Numbers represent the proportion of RFP$^+$ cells as a percentage of total lung MFs. Data are from one experiment with at least n=2 per group. (B) Representative FACS plots showing RFP expression in splenic MFs from CD11c^{CRE} and CD11c^{CRE}xRosa-RFP mice. Numbers represent the proportion of RFP$^+$ cells as a percentage of total splenic MFs. Data are from one experiment with at least n=2 per group. ***, P < 0.001. Two-way student's t test.

Using flow cytometric analysis we first examined the lungs of $CD11c^{CRE}xZeb2^{fl/fl}$ mice. This revealed a reduction in total $CD64^{+}F4/80^{+}CD11c^{+}SiglecF^{+}$ AMs upon loss of Zeb2 (Figure 7A and Figure S4). When represented as frequency of live $CD45^{+}$ cells AMs have a mean presence of 4.08 ± 0.68% in $CD11c^{CRE}xZeb2^{fl/fl}$ lungs, compared to a mean presence of 7.78 ± 1.75% in lungs from control littermates (Figure 7A). This reduction is also observed in terms of absolute cell number (Figure 7A). Moreover, examination of the remaining AMs in $CD11c^{CRE}xZeb2^{fl/fl}$ mice, revealed ~45% of AMs to express CD11b, while in control littermates only ~1% of AMs expressed this integrin (Figure 7B). We next performed the same analysis in the spleen of $CD11c^{CRE}xZeb2^{fl/fl}$ mice. Although no significant difference could be established when presented as a percentage of live $CD45^{+}$ cells, we did find a significant difference in absolute cell number of splenic MFs (Figure 7C and Figure S5). Splenic MF cell numbers decreased from 7.52×10^5 to 4.44×10^5 (Figure 7C). Simultaneously we again verified the expression of CD11b and this revealed that also splenic MFs gain expression of CD11b upon loss of Zeb2 expression. Here we found that among total splenic MFs of $CD11c^{CRE}xZeb2^{fl/fl}$ mice 21.26 ± 1.39% expressed CD11b, compared to 1.51 ± 0.13% in control $Zeb2^{fl/fl}$ mice (Figure 7D). For both AMs and splenic MFs, the increased CD11b surface expression was shown to be highly significant (Figure 7B and D). Although we did not find differences in the presence of colonic macrophages in the $LysM^{CRE}xZeb2^{fl/fl}$ mice, we repeated the analysis in the more efficient $CD11c^{CRE}xZeb2^{fl/fl}$ model. This revealed a significant increase in transitioning monocytes when represented as a percentage of live $CD45^{+}$ cells. However, this increase was not significant when calculated as an absolute cell number (Figure 7E and Figure S6). Nevertheless, loss of Zeb2 in colonic macrophages did result in a decrease of both proportion and absolute cell number of this population (Figure 7E). Colonic MF numbers decreased from 3.47×10^5 in $Zeb2^{fl/fl}$ mice to 1.70×10^5 in $CD11c^{CRE}xZeb2^{fl/fl}$ mice. All together we showed that $CD11c^{CRE}xZeb2^{fl/fl}$ mice have a reduced number of alveolar, splenic and colonic MFs and the remaining alveolar and splenic MFs have an increased fraction of CD11b expressing cells.

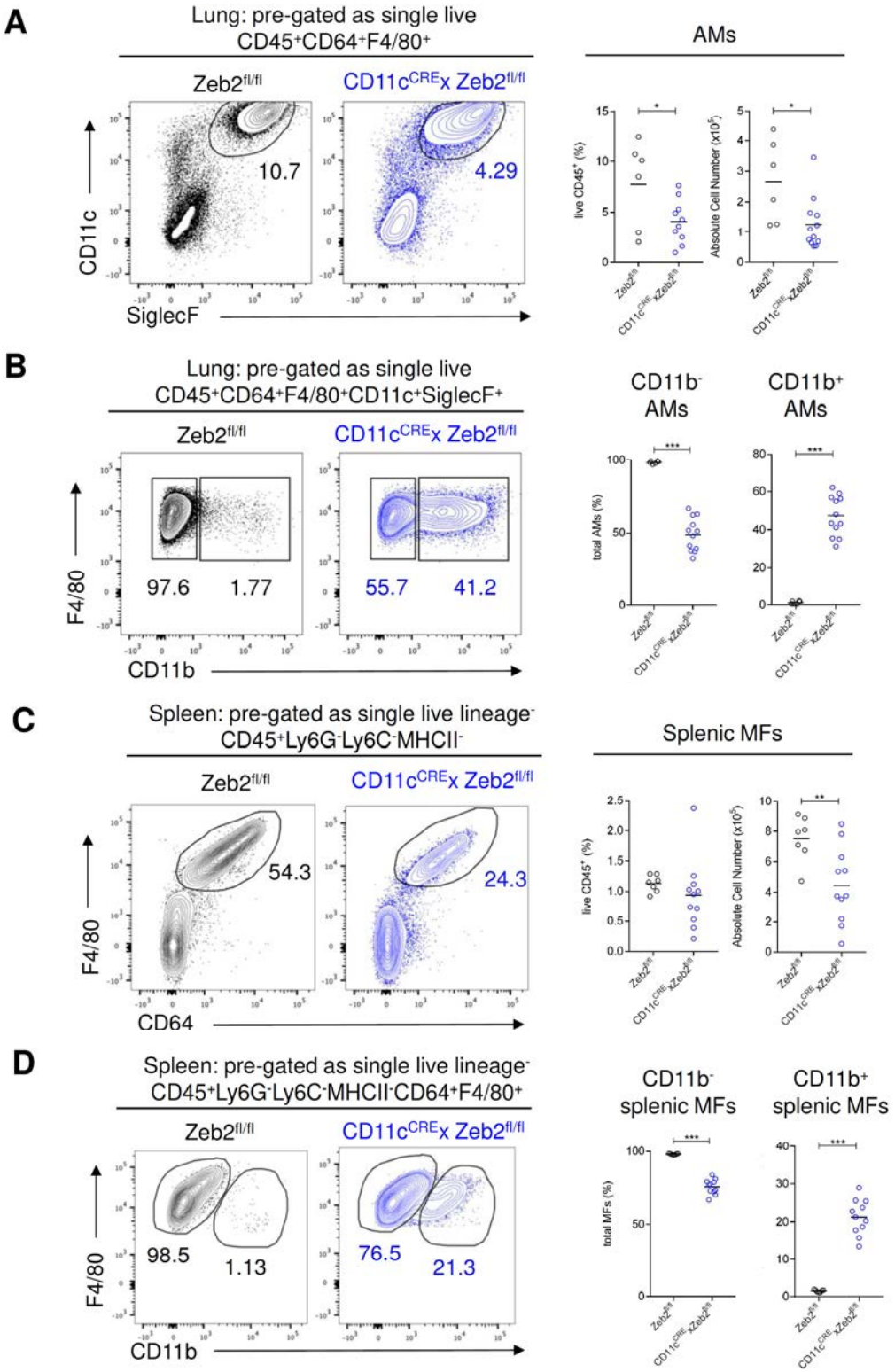

Figure 7 | In CD11c^{CRE}xZeb2$^{fl/fl}$ mice AMs and splenic MFs have a reduced number and gain expression of CD11b. (A and C) Representative FACS plots showing the presence of AMs (A) and splenic MFs (C) in Zeb2$^{fl/fl}$ and CD11c^{CRE}xZeb2$^{fl/fl}$ mice. Numbers represent AMs (A) or splenic MFs (C) as frequency of live CD45$^+$ cells. Graphs show proportion as a percentage of live CD45$^+$ cells and absolute cell number of AMs in the lung (A) and MFs in the spleen (C) of indicated mice. (B and D) Representative FACS plots showing CD11b expression in AMs (B) and splenic MFs (D) of Zeb2$^{fl/fl}$ and CD11c^{CRE}xZeb2$^{fl/fl}$ mice. Numbers represent the proportion of CD11b$^-$ and CD11b$^+$ AMs as frequency of total AMs (B) or the proportion of CD11b$^-$ and CD11b$^+$ splenic MFs as frequency of total splenic MFs (D). Graphs show proportion as a percentage of total AMs (B) or total splenic MFs (D) for indicated cell types. Data are pooled from two experiments, with at least n=6 per group. *P < 0.05; **, P < 0.01; ***, P < 0.001. Two-way student's t test.

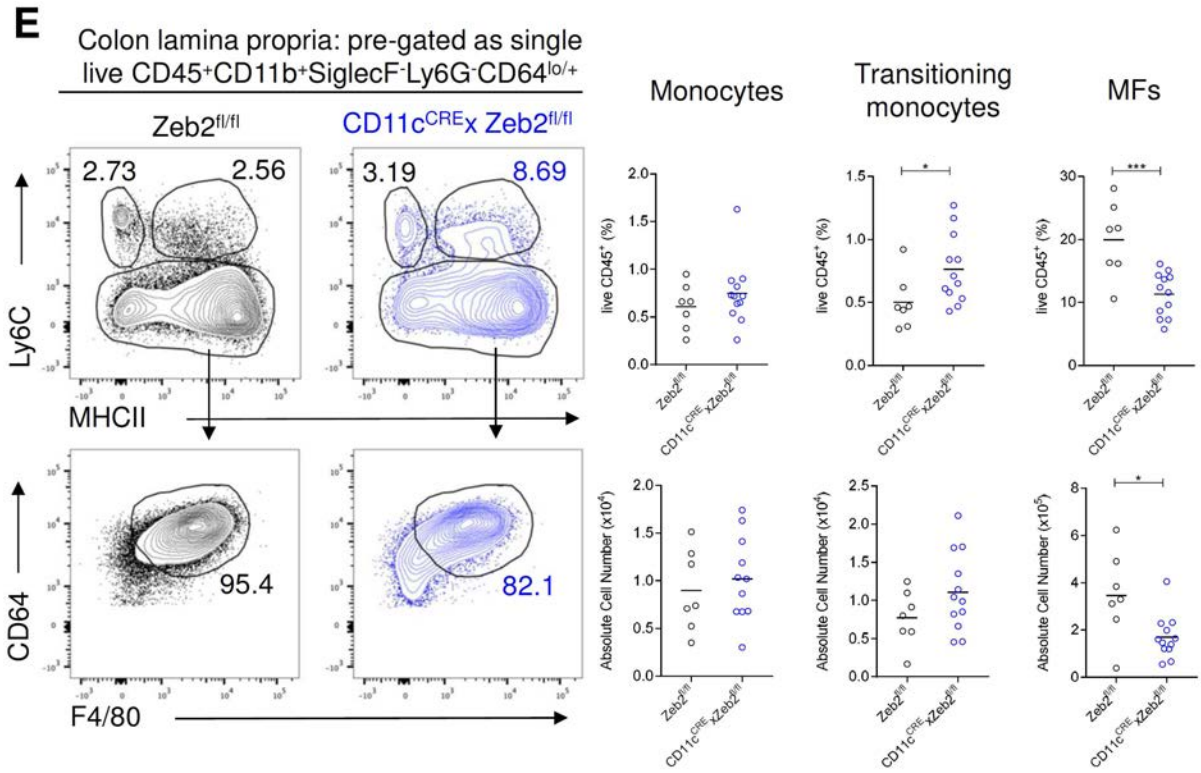

Figure 7 continued | Colonic MFs are reduced in CD11c^{CRE}xZeb2$^{fl/fl}$ mice. (E) Representative FACS plots showing identification of Ly6C^{+}MHCII^{-} monocytes, Ly6C^{+}MHCII^{+} transitioning monocytes and Ly6C^{-}CD64^{+}F4/80^{+} MFs in the colon lamina propria of Zeb2$^{fl/fl}$ and CD11c^{CRE}xZeb2$^{fl/fl}$ mice. For monocytes and transitioning monocytes the number represents the proportion of live CD45^{+}CD11b^{+}SiglecF^{-}Ly6G^{-}CD64$^{lo/+}$ cells and for MFs the proportion of CD45^{+}CD11b^{+}SiglecF^{-}Ly6G^{-}CD64$^{lo/+}$Ly6C^{-} cells. Graphs represent proportion as a percentage of live CD45^{+} cells and absolute cell number of indicated cell type in colon lamina propria of indicated mice. Data are pooled from two experiments with at least n=7 per group. *, P < 0.05; ***, P < 0.001. Two-way student's t test.

4.4 Discussion

First, we looked at the publically available expression data for *Zeb2* mRNA in different tissue-resident macrophages and found that high expression of *Zeb2* is conserved across all macrophages considered. Moreover, further analysis performed outside of this thesis confirmed Zeb2 to be one of the 67 core macrophage genes (Scott *et al.* (under review); Addendum p.252). As described earlier in this thesis, we already found a definite role for Zeb2 in cDC2 development. Comparing expression levels, it is evident that *Zeb2* is expressed at higher levels in macrophages than in cDC2s. This, together with the finding that *Zeb2* mRNA levels are higher in macrophages than in monocytes, led to the hypothesis that Zeb2 could function in macrophage homeostasis.

To investigate this, we started *in vitro* with several murine macrophage cell lines and one murine monocytic cell line. Also here, we found that *Zeb2* is expressed at higher levels in the macrophage cell lines compared with the monocytic line. Next, we tried to knockdown Zeb2 expression in three macrophage lines through transduction with constitutive shRNA constructs. Shortly after transduction we were able to confirm a significant knockdown of *Zeb2* mRNA levels. However, we were unable to further passage the macrophage lines that were transduced with both Zeb2 knockdown constructs, while the lines transduced with a non-targeting scrambled shRNA could be passaged, suggesting that loss of Zeb2 may affect macrophage survival. When using other vectors expressing GFP together with a Zeb2-targeting shRNA, similar problems were encountered (data not shown). Additionally, after FACS-purifying GFP^+ cells, the cultures were unable to further proliferate when transduced with Zeb2-targeting shRNA vectors, while the GFP^+ cells sorted from cultures transduced with the scrambled construct could be further passaged. From this we concluded that, at least *in vitro*, macrophages depend on Zeb2 for their survival and/or proliferation. We next wanted to see if this held true for different tissue-resident macrophages *in vivo*.

Initially, we crossed our conditional Zeb2 knockout mouse model with the LysM^{CRE} line which was reported to target neutrophils, monocytes and mature macrophages[24]. Analysis of BM derived macrophages revealed that seven day old Csf1 cultures from LysM^{CRE}xZeb2$^{fl/fl}$ mice have an increased population of Ly6C^{+} cells compared with cultures from littermate controls. Despite this promising result *ex vivo*, we were unable to confirm a role for Zeb2 in macrophages *in vivo* when analysing the liver and colon of LysM^{CRE}xZeb2$^{fl/fl}$ mice. However, a PCR for detecting CRE recombinase activity performed on FACS-purified Ly6C^{+} and Ly6C^{-} cells from seven day old Csf1 cultures of LysM^{CRE}xZeb2$^{fl/fl}$ BM, demonstrated that the LysM^{CRE} line is rather inefficient. Previously, Abram and colleagues also reported that the LysM^{CRE} line only targets around 40% of splenic macrophages and peripheral blood monocytes[24]. Because of the inefficiency found in the LysM^{CRE} line, we sought other CRE lines that are more efficient at targeting specific tissue-resident macrophages. With the newly generated KC^{CRE}, which contains the *CRE recombinase* gene in the 3' untranslated region of the KC specific *Clec4f* gene[20] (Scott *et al.* (under review); Addendum p.252), we were able to target around 88% of KCs. As we and others[24,27] showed that the CD11c^{CRE} line targets tissue-resident macrophages in the lung, spleen and colon, we opted to use this CRE line to investigate the role of Zeb2 in alveolar, splenic and colonic macrophages. Both *Clec4F* and *CD11c* are expressed in late stages of macrophage development[20,28], and thus both CRE lines are considered to only target fully mature MFs.

To our surprise, livers from KC^{CRE}xZeb2$^{fl/fl}$ mice did not show a difference in general MF numbers. Nevertheless, looking more in detail to hepatic MFs with surface markers Tim4 and Clec4F we did find interesting changes. Liver MFs of the KC^{CRE}xZeb2$^{fl/fl}$ mice show a significant reduction of fully mature Tim4^{+}Clec4F^{+} KCs, which was coupled with a remarkable increase in Tim4^{-} KCs and Tim4^{-}Clec4F^{-} MFs. A very similar phenotype was reported before by Scott *et al*. in the KC-DTR mice. In this mouse model administration of diphtheria toxin results in loss of long-lived KCs, after which they get replaced by monocyte derived cells. Their development starts as Tim4^{-}Clec4F^{-} MFs, further differentiating into Tim4^{-}Clec4F^{+} KCs and finally maturing fully in long-lived self-renewing Tim4^{+}Clec4F^{+} KCs[20]. The presence of both Tim4^{-}

populations and the reduction in mature KCs in $KC^{CRE}xZeb2^{fl/fl}$ suggests that Zeb2 knockout KCs die and are continuously replaced from the BM, a hypothesis that was confirmed by Scott *et al.* (Scott *et al.* (under review); Addendum p.252). As the KC^{CRE} line acts late in development, KCs from $KC^{CRE}xZeb2^{fl/fl}$ mice are able to develop normally and only flox out *Zeb2* following expression of *Clec4f* upon full maturation. This continuous cycle of death of mature KCs resulting from loss of Zeb2 followed by replacement from infiltrating monocytes, explains why we don't see a reduction of total MF numbers in the liver of $KC^{CRE}xZeb2^{fl/fl}$ mice. It could be that this cycle was also present in the liver of $LysM^{CRE}xZeb2^{fl/fl}$ mice, but due to the lack of Clec4F and Tim4 in the $LysM^{CRE}$ analysis we were unable to pick up on this. Moreover, work performed outside the scope of this thesis revealed that KCs in the $KC^{CRE}xZeb2^{fl/fl}$ model contained both cells with homozygous ($Zeb2^{-/-}$) and heterozygous ($Zeb2^{+/-}$) loss of Zeb2 and with time $Zeb2^{-/-}$ KCs are outcompeted through local proliferation of more fit $Zeb2^{-/+}$ KCs (Scott *et al.* (under review); Addendum p.252). Keeping in mind the inefficiency of the $LysM^{CRE}$ model, it is likely that in the $LysM^{CRE}xZeb2^{fl/fl}$ mice there exists a fraction of KCs that have retained one or two intact alleles of *Zeb2*. Based on our knowledge from the $KC^{CRE}xZeb2^{fl/fl}$ model, we would hypothesize that in $LysM^{CRE}xZeb2^{fl/fl}$ mice KCs that are truly Zeb2 knockout do die, but get replaced through proliferation of Zeb2-sufficient macrophages. This would again explain the lack of phenotype in the liver of $LysM^{CRE}xZeb2^{fl/fl}$ mice.

To investigate if Zeb2 also plays a role in survival of tissue-resident macrophages other than KCs, we next made use of our $CD11c^{CRE}xZeb2^{fl/fl}$ model which allows us to generate loss of Zeb2 expression in mature MFs of the lung, spleen and colon. Doing so, we detected a significant reduction in absolute cell number of alveolar, splenic and colonic macrophages. As this reduction was found in steady state, it suggests that all three MF populations depend on Zeb2 for their survival. One could ask, why there are still mature macrophages present in the tissue. We believe that, as in the $LysM^{CRE}$ and KC^{CRE} models, Zeb2 expressing macrophages are still present and proliferate locally to fill the available niche. Further examination, performed outside of this thesis, confirmed that $Zeb2^{+/-}$ AMs are indeed present in the lung of

CD11c^{CRE}xZeb2$^{fl/fl}$ mice and that these Zeb2-sufficient AMs in time refill the niche through local proliferation (Scott *et al.* (under review); Addendum p.252).

Another interesting finding is that more than half of the remaining alveolar MFs and around one fifth of the remaining splenic MFs of CD11c^{CRE}xZeb2$^{fl/fl}$ mice displayed surface expression of the phagocytic receptor CD11b. It has been shown that during AM development CD11b expression is initially high, but later on downregulated upon full maturation of the MF an this independent of its origin (yolk sac MF, fetal liver monocyte or adult BM monocyte)[21,28]. Based on this, we hypothesized that the presence of CD11b^{+} AMs in the lung of CD11c^{CRE}XZeb2$^{fl/fl}$ mice is due to input from the BM and this influx is required to maintain AM numbers. However, follow-up experiments using partially protected BM chimeras revealed that there is no significant contribution from the BM to replace AMs that have died due to loss of Zeb2 expression (Scott *et al.* (under review); Addendum p.252). The replacement of KCs, but lack (or minor) replacement of AMs by BM derived cells, is in line we the niche hypothesis from Guilliams and Scott[13]. They proposed that the highly controlled regulation of a full niche inhibits monocytes to differentiate into macrophages and monocyte-to-macrophage differentiation only takes place in an available and accessible niche. Applying this niche hypothesis, only the liver macrophage niche is accessible for circulating monocytes as KCs reside in the bloodstream of the liver sinusoids. The niche for AMs is unaccessible for circulating progenitors due to the presence of the lung epithelial barrier between the bloodstream and the alveolar space.

In conclusion, we showed here that high expression of transcription factor *Zeb2* is a general feature of the macrophage lineage. Furthermore loss of Zeb2 in mature macrophages leads to their disappearance, suggesting cell death, and changes in their surface phenotype. So we can speculate that Zeb2 is required to maintain terminally differentiated macrophages. The next question is how Zeb2 functions to maintain the macrophage lineage and the answer to this was found outside the work of this thesis. Scott *et al.* demonstrated that Zeb2 is crucial in preserving the tissue-specific identity of macrophages through regulation of tissue-specific macrophage

TFs, such as Lxrα in KCs and potentially Cebpβ in AMs (Scott *et al.* (under review); Addendum p.252). How Zeb2 is able to regulate the expression of the tissue-specific macrophage TFs remains to be elucidated. Another question that remains unanswered is if Zeb2, next to its role in mature macrophages, also functions during macrophage development. It was suggested before that Zeb2 is required for commitment to the monocyte lineage[29], but the CRE lines used in this chapter did not allow us to assess the role of Zeb2 in early macrophage development. A more general CRE line, for instance based on the pre-macrophage expression profile from Mass *et al.*, targeting MF development at an earlier time point, would help us to resolve this last question.

4.5 Materials and methods

Immgen data processing

Gene expression data used were from the Immgen database (GSE15907), other publically available microarray data sets deposited to NCBI GEO under accession no. GSE75225 and GSE76999 and unpublished in house generated data. After merging expression values of all samples, data was normalized within arrays (probeset summarization, background correction and log2-transformation) and between arrays (quantile normalization) using the Robust Multi-array Average (RMA) procedure in R. Only probesets that mapped uniquely to one gene were kept, and for each gene the probeset with the highest expression level was kept.

Cell lines

The following macrophage and monocytic cell lines present in the department were used: C3H-Hej, C3H-Hen, P388D1, MH-S, WEHI3 and Raw264-7. Details on these cell lines can be found in Table 1. C3H-Hej and C3H-Hen cells were cultured in RPMI supplemented with 10% FCS. MH-S cells were cultured in RPMI supplemented with 10% FCS, glutamine and β-mercaptoethanol. Raw264-7 wells were cultured in DMEM supplemented with 10% FCS and glutamine. P388D1 and WEHI3 cells were cultured in RPMI supplemented with 10% FCS, glutamine, Na-Pyruvate and β-mercaptoethanol.

Table 1 | Murine cell lines used for *in vitro* work

Cell line	Cell type	Source
C3H-Hej (=GG2EE)	Macrophage	Isolated from C3H/HeJ mice. Immortalization achieved by infection with J2 recombinant retrovirus.
C3H-Hen (=INF-3A)	Myelomonocyte	Derived from bone marrow of C3H/HeN (H-2k) mice. Immortalization was performed by infection with J2 recombinant retrovirus.
P388D1	Monocyte/ macrophage	Established in 1975 from the ascites of a DBA/2 mouse with a lymphoid neoplasm.
MH-S	Alveolar macrophage	Derived in 1989 by SV40 transformation of an adherent cell-enriched population of mouse alveolar macrophages.
WEHI3	Monocyte	Derived from monocytes of a murine leukemia model in 1976.
Raw264-7	Macrophage	Established from a tumor induced by Abelson murine leukemia virus.

Lentiviral transduction

First the appropriate plasmid mixes were concentrated with a sodium acetate/ethanol precipitation. For this the following ratio of plasmids was used: a 2/2/1 ratio of shRNA-plasmid / pCMVdeltaR839-packaging-plasmid / pMD2.G-packaging-plasmid. The three shRNA-plasmids used are the TRC1 version from Sigma's MISSION®RNAi and have a pLKO.1-puro backbone. The control scrambled plasmid contains a sequence that does not target any mammalian genes known (SHC002), the two Zeb2 shRNA's target the coding sequence of Zeb2 (shRNA Zeb2-1 = TRCN0000013530; shRNA Zeb2-2 = TRCN0000070887). Next Hek293T cells were transfected with a calcium phosphate transfection protocol, virus was harvested on day 2 and day 3 after transfection and was immediately used to transduce cells of interest. Transduced cells were cultured with puromycin to perform a negative selection for non-transduced cells.

Gene expression analysis by RT-qPCR

RNA was purified from cell lines using TRIsure (Bioline, GC Biotech) according to the manufacturers guidelines. RNA was reverse transcribed to cDNA with an iScript Advanced cDNA Synthesis kit (Bio-Rad Laboratories). Gene expression was assayed by real-time qPCR using a SensiFast SYBR No-Rox kit (GC Biotech) on a PCR amplification and detection instrument (LightCycler 480; Roche) with the primers listed in Table 2. Gene expression was normalized to the reference genes Calm2 and Eef1a1 and relative gene expression was calculated using qbase$^+$ software (Biogazelle).

Table 2 | Primers used for RT-qPCR

Gene	Forward primer	Reverse primer
Calm2	5'-TTTGCCTCAAAATCCATTCCA-3'	5'-GCAGAGCAACCATTGGGTAAA-3'
Eef1a1	5'-TCGCCTTGGACGTTCTTTT-3'	5'-GTGGACTTGCCGGAATCTAC-3'
Zeb1	5'-TTGCGTGTCAGGCATGGAT-3'	5'-GAAAACGGCTGTGAACCAAAA-3'
Zeb2	5'-GGCAAGGCCTTCAAGTACAA-3'	5'-AAGCGTTTCTTGCAGTTTGG-3'

Mice

The generation of Zeb2$^{fl/fl}$ mice was described previously[22]. Mice were backcrossed to a C57BL/6 background for at least seven generations before crossing with the CD11c^{CRE} mice[25], LysM^{CRE} mice[23] and KC^{CRE} mice (B6-Clec4ftm3Ciphe; developed in the Centre d'Immunophenomique, Marseille, France). CD11c^{CRE} mice and KC^{CRE} mice were also crossed with the Rosa-RFP reporter mouse[26]. All mice were used on a C57Bl/6 background between 6 and 12 weeks of age. All mice were bred and maintained at the IRC (Ghent University) under specific pathogen free conditions. All animals were randomly allocated to experimental groups and littermate controls were used in all experiments. All experiments were performed in accordance with the ethical committee of the Faculty of Science.

Cultures of BM derived macrophages

Total BM was harvested from mice, red blood cells were lysed with ACK lysing buffer (Biowhittaker) and 15-20 x 10^6 cells were cultured in RPMI supplemented with Glutamax, non-essential amino acids and penicillin/streptomycin in a 10 cm petri dish for 7 days with 20ng/ml Csf1. On day 3 of cultivation cells were passaged by gently loosening them with a cell scraper.

Isolation of tissue leukocytes

For the isolation of liver leukocytes, livers were isolated from PBS-perfused mice, chopped finely and subjected to GentleMACs dissociation and incubated for 20 min with 1 mg/ml Collagenase A (Sigma) and 10U/ml DNase (Roche) in a shaking water bath at 37°C. Following a second round of GentleMACs dissociation, single cell suspensions were filtered over a 100-µm filter. For the isolation of lung and spleen leukocytes, lungs and spleens were isolated from PBS-perfused mice, chopped finely, and incubated for 30 min with 0.2 mg/ml Liberase TM (Roche) and 10 U/ml DNase (Roche) in a shaking water bath at 37°C. Cells were passed through a 70-µm cell strainer. For the isolation of colonic lamina propria leukocytes, colons were flushed with RPMI containing 2% FCS. After opening longitudinally and cutting into 0.5 cm segments, they were incubated twice with PBS containing 2mm EDTA in a shaking water bath at 37°C for 15 minutes (first incubation round) and 30 minutes (second incubation round). Then the tissue was digested with 1 mg/ml Dispase II (Gibco), 30 µg/ml DNAse (Roche), 0.75 mg/ml Collagenase D (Roche) and 0.425 mg/ml Collagenase V (Sigma) in a shaking water bath for 30 to 45 min. Cells were passed through a 40-µm cell strainer. In all instances, except for the colon, red blood cells were lysed with an in house made osmotic lysis buffer (10mM $KHCO_3$, 155 mM NH_4Cl and 0.1 mM EDTA in PBS) before staining for flow cytometric analysis.

Flow cytometry and FACS

For flow cytometry, 3–4 x 10^6 cells were stained at 4°C in the dark with antibodies (Table 3) and analysed with a Fortessa (BD Biosciences) and FlowJo software (TreeStar). In case of FACS-purification, cells were FACS-purified using a flow cytometer (FACSAria II or FACSAria III; BD). After sorting, a purity check was performed for all samples.

Table 3 | Antibodies used for flow cytometry

Antibody	Clone	Antibody	Clone
Fc Block	2.4G2	CD11c	N418
Fixable Viability Dye	eBioscience	Clec4F	AF2784
7-AAD	BD Pharmingen	F4/80	BM8
CCR2	475301	IA-IE	M5/114.15.2
CD3e	145-2c11	Ly6C	AL-21
CD19	1D3	Ly6G	1A8
CD45	30-F11	NK1.1	PK136
CD64	X54-5/7.1	SiglecF	E50-2440
CD11b	M1/70	Tim4	RMT4-54

Statistical analysis

Groups were compared with a two-way Student's t test using Prism Software (GraphPad Software). Samples were assumed to be normally distributed with similar variance between groups. No randomization was used to determine experimental groups, and no blinding of the investigator was performed. Group sizes were determined on the basis of previous experience.

4.6 References

1. Merien F. A Journey with Elie Metchnikoff: From Innate Cell Mechanisms in Infectious Diseases to Quantum Biology. *Frontiers Public Heal*. 2016;4:125.
2. METSCHNIKOFF E. Memoirs: Researches on the Intracellular Digestion of Invertebrates. *Journal of Cell Science*. 1884;2(93):89–111.
3. Van Furth R, Cohn ZA. The origin and kinetics of mononuclear phagocytes. *J. Exp. Med.* 1968;128(3):415–35.
4. Van Furth R, Diesselhoff-Den Dulk MM. The kinetics of promonocytes and monocytes in the bone marrow. *J. Exp. Med.* 1970;132(4):813–28.
5. Yona S, Kim K-WW, Wolf Y, et al. Fate mapping reveals origins and dynamics of monocytes and tissue macrophages under homeostasis. *Immunity*. 2013;38(1):79–91.
6. Ginhoux F, Guilliams M. Tissue-Resident Macrophage Ontogeny and Homeostasis. *Immunity*. 2016;44(3):439–449.
7. Tamoutounour S, Guilliams M, Montanana Sanchis F, et al. Origins and functional specialization of macrophages and of conventional and monocyte-derived dendritic cells in mouse skin. *Immunity*. 2013;39(5):925–38.
8. Epelman S, Lavine KJ, Beaudin AE, et al. Embryonic and adult-derived resident cardiac macrophages are maintained through distinct mechanisms at steady state and during inflammation. *Immunity*. 2014;40(1):91–104.
9. Molawi K, Wolf Y, Kandalla PK, et al. Progressive replacement of embryo-derived cardiac macrophages with age. *J. Exp. Med.* 2014;211(11):2151–8.
10. Bain CC, Bravo-Blas A, Scott CL, et al. Constant replenishment from circulating monocytes maintains the macrophage pool in the intestine of adult mice. *Nat. Immunol.* 2014;15(10):929–937.
11. Gautier EL, Shay T, Miller J, et al. Gene-expression profiles and transcriptional regulatory pathways that underlie the identity and diversity of mouse tissue macrophages. *Nat. Immunol.* 2012;13(11):1118–28.
12. Heinz S, Benner C, Spann N, et al. Simple combinations of lineage-determining transcription factors prime cis-regulatory elements required for macrophage and B cell identities. *Mol. Cell*. 2010;38(4):576–89.
13. Guilliams M, Scott CL. Does niche competition determine the origin of tissue-resident macrophages? *Nat. Rev. Immunol.* 2017;17(7):451–460.
14. Lavin Y, Winter D, Blecher-Gonen R, et al. Tissue-resident macrophage enhancer landscapes are shaped by the local microenvironment. *Cell*. 2014;159(6):1312–26.
15. Gosselin D, Link VM, Romanoski CE, et al. Environment drives selection and function of enhancers controlling tissue-specific macrophage identities. *Cell*. 2014;159(6):1327–40.
16. Ericson JA, Duffau P, Yasuda K, et al. Gene expression during the generation and activation of mouse neutrophils: implication of novel functional and regulatory pathways. *PLoS ONE*. 2014;9(10):e108553.
17. Heng TS, Painter MW. The Immunological Genome Project: networks of gene expression in immune cells. *Nat. Immunol.* 2008;9(10):1091–4.
18. Miller JC, Brown BD, Shay T, et al. Deciphering the transcriptional network of the dendritic cell lineage. *Nat. Immunol.* 2012;13(9):888–99.
19. Painter MW, Davis S, Hardy RR, Mathis D, Benoist C. Transcriptomes of the B and T lineages compared by multiplatform microarray profiling. *J. Immunol.* 2011;186(5):3047–57.
20. Scott CL, Zheng F, De Baetselier P, et al. Bone marrow-derived monocytes give rise to self-renewing and fully differentiated Kupffer cells. *Nat Commun*. 2016;7:10321.
21. Van de Laar L, Saelens W, De Prijck S, et al. Yolk Sac Macrophages, Fetal Liver, and Adult Monocytes Can Colonize an Empty Niche and Develop into Functional Tissue-Resident Macrophages. *Immunity*. 2016;44(4):755–68.
22. Higashi Y, Maruhashi M, Nelles L, et al. Generation of the floxed allele of the SIP1 (Smad-interacting protein 1) gene for Cre-mediated conditional knockout in the mouse. *Genesis*. 2002;32(2):82–84.
23. Clausen BE, Burkhardt C, Reith W, Renkawitz R, Förster I. Conditional gene targeting in macrophages and granulocytes using LysMcre mice. *Transgenic Res.* 1999;8(4):265–77.

24. Abram CL, Roberge GL, Hu Y, Lowell CA. Comparative analysis of the efficiency and specificity of myeloid-Cre deleting strains using ROSA-EYFP reporter mice. *J. Immunol. Methods*. 2014;408:89–100.
25. Caton ML, Smith-Raska MR, Reizis B. Notch-RBP-J signaling controls the homeostasis of CD8- dendritic cells in the spleen. *The Journal of experimental medicine*. 2007;204(7):1653–64.
26. Luche H, Weber O, Nageswara Rao T, Blum C, Fehling HJ. Faithful activation of an extra-bright red fluorescent protein in "knock-in" Cre-reporter mice ideally suited for lineage tracing studies. *Eur. J. Immunol.* 2007;37(1):43–53.
27. Schridde A, Bain CC, Mayer JU, et al. Tissue-specific differentiation of colonic macrophages requires TGFβ receptor-mediated signaling. *Mucosal Immunol*. 2017;10(6):1387–1399.
28. Guilliams M, De Kleer I, Henri S, et al. Alveolar macrophages develop from fetal monocytes that differentiate into long-lived cells in the first week of life via GM-CSF. *J. Exp. Med.* 2013;210(10):1977–92.
29. Wu X, Briseño C, Grajales-Reyes G, et al. Transcription factor Zeb2 regulates commitment to plasmacytoid dendritic cell and monocyte fate. *Proc National Acad Sci*. 2016;113(51):14775–14780.

4.7 Supplementary figures

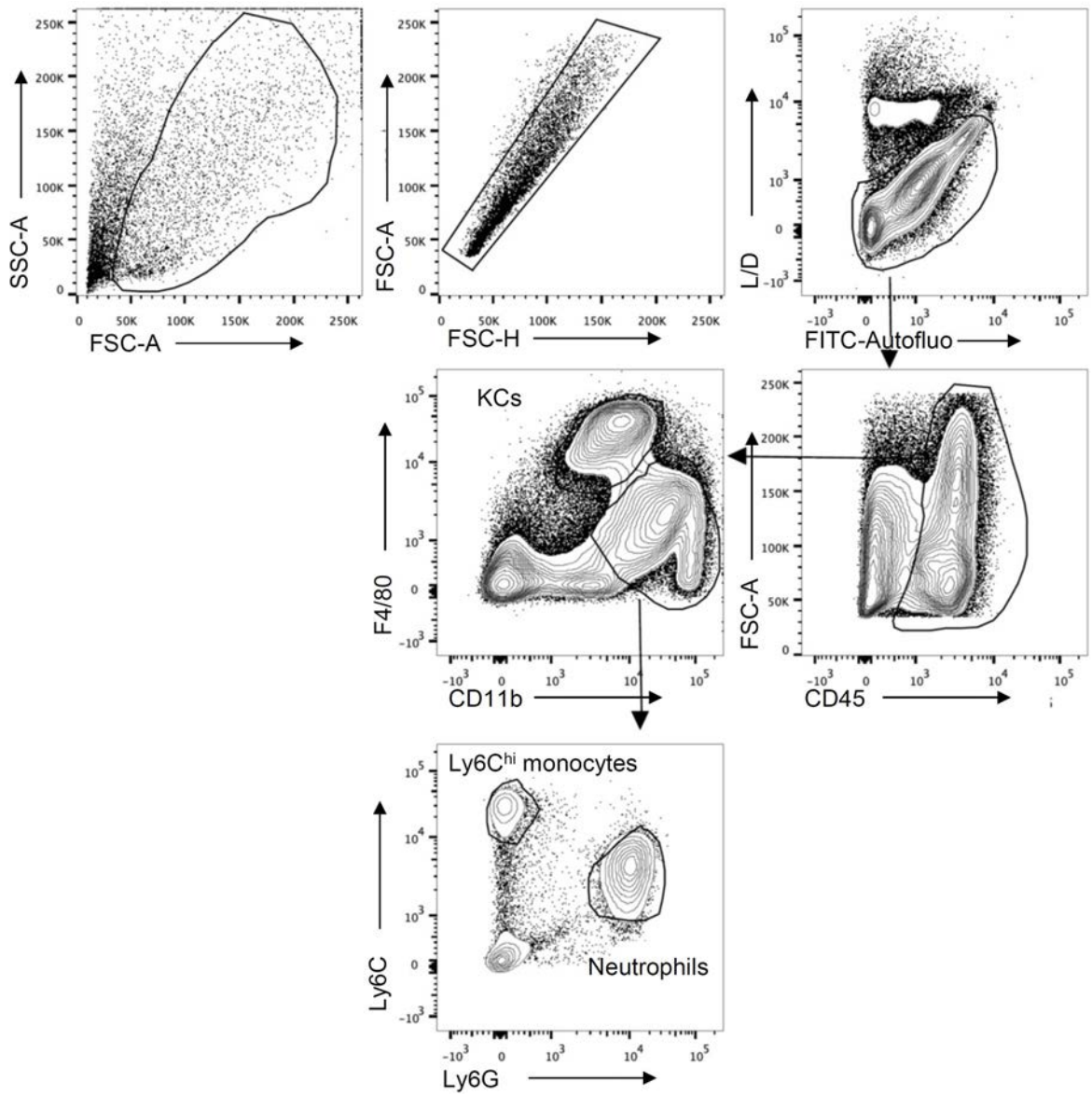

Figure S1 | Gating strategy for liver KCs, Ly6C^{hi} monocytes and neutrophils as performed in the LysM^{CRE}xZeb2$^{fl/fl}$ mouse model. Representative FACS plots showing gating strategy for KCs, Ly6C^{hi} monocytes and neutrophils in the liver. FSC, forward scatter. SSC, side scatter. Autofluo, autofluorescence. L/D, live/dead.

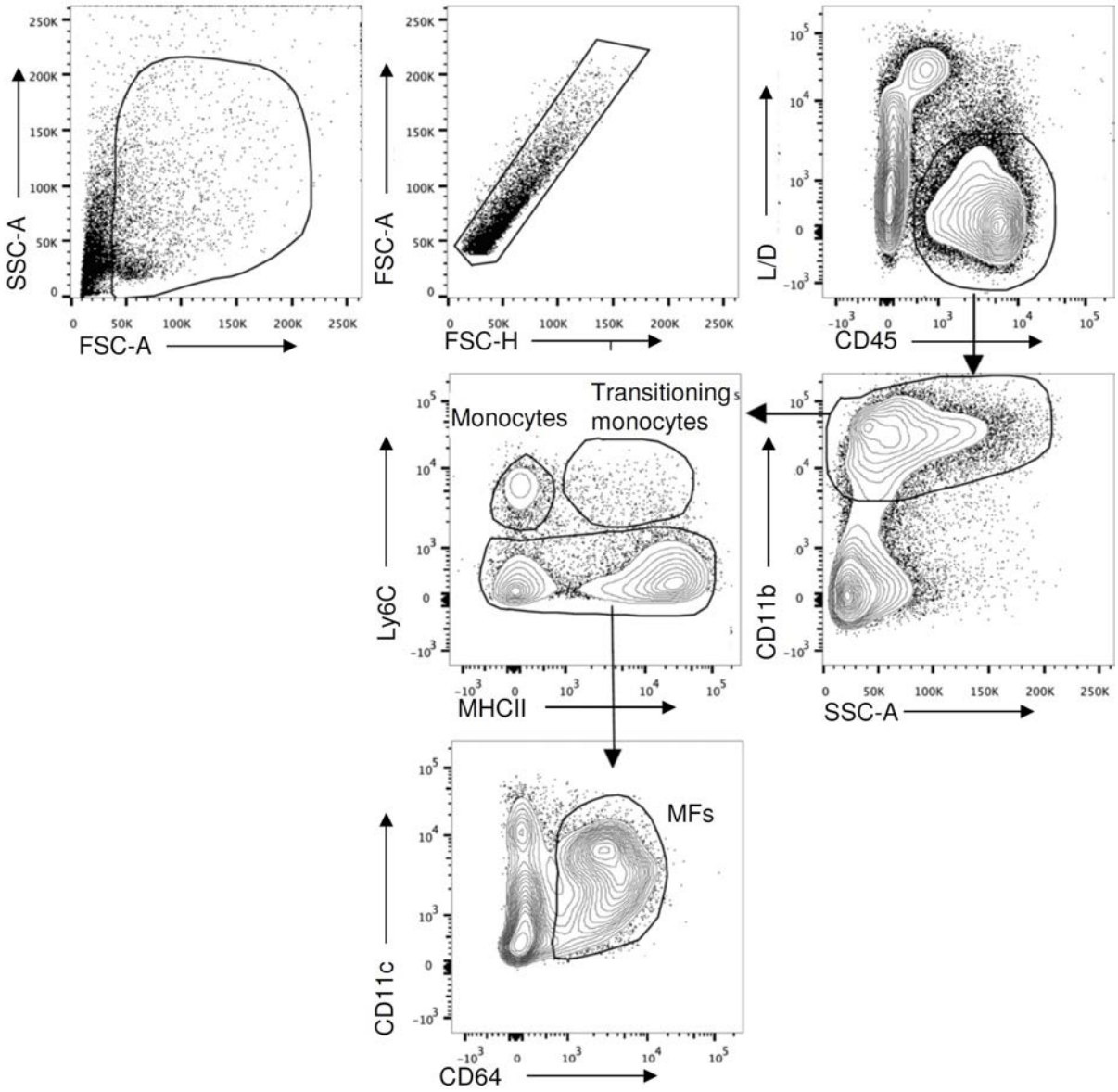

Figure S2 | Gating strategy for colon lamina propria monocytes, transitioning monocytes and MFs as performed in the LysM^{CRE}xZeb2$^{fl/fl}$ mouse model. Representative FACS plots showing gating strategy for monocytes, transitioning monocytes and MFs in the lamina propria of the colon. FSC, forward scatter. SSC, side scatter. L/D, live/dead.

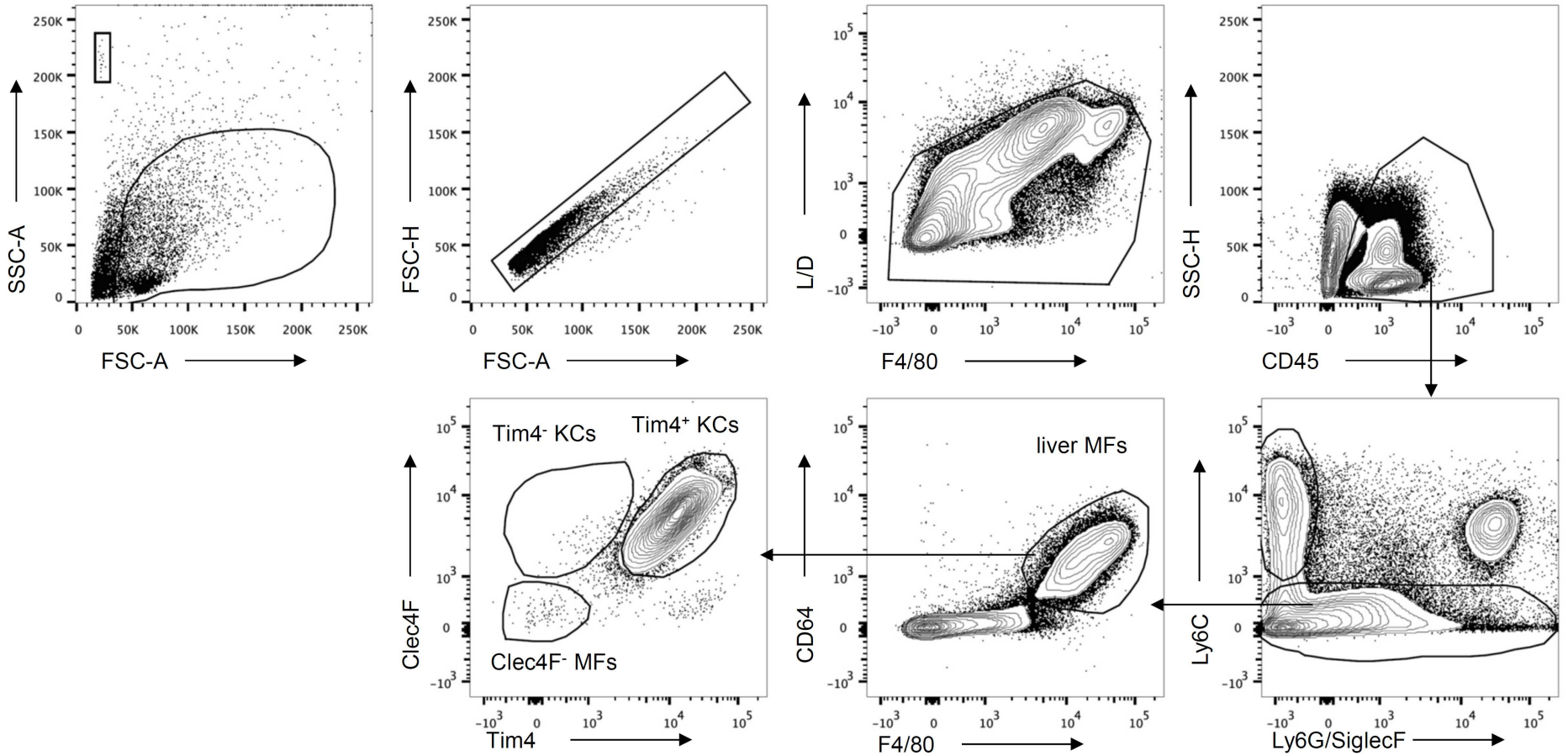

Figure S3 | Gating strategy for liver KCs as performed in the KC^{CRE}xZeb2$^{fl/fl}$ mouse model. Representative FACS plots showing gating strategy for Tim4^{-} KCs, Tim4^{+} KCs and Clec4F^{-} MFs in liver. FSC, forward scatter. SSC, side scatter. L/D, live/dead.

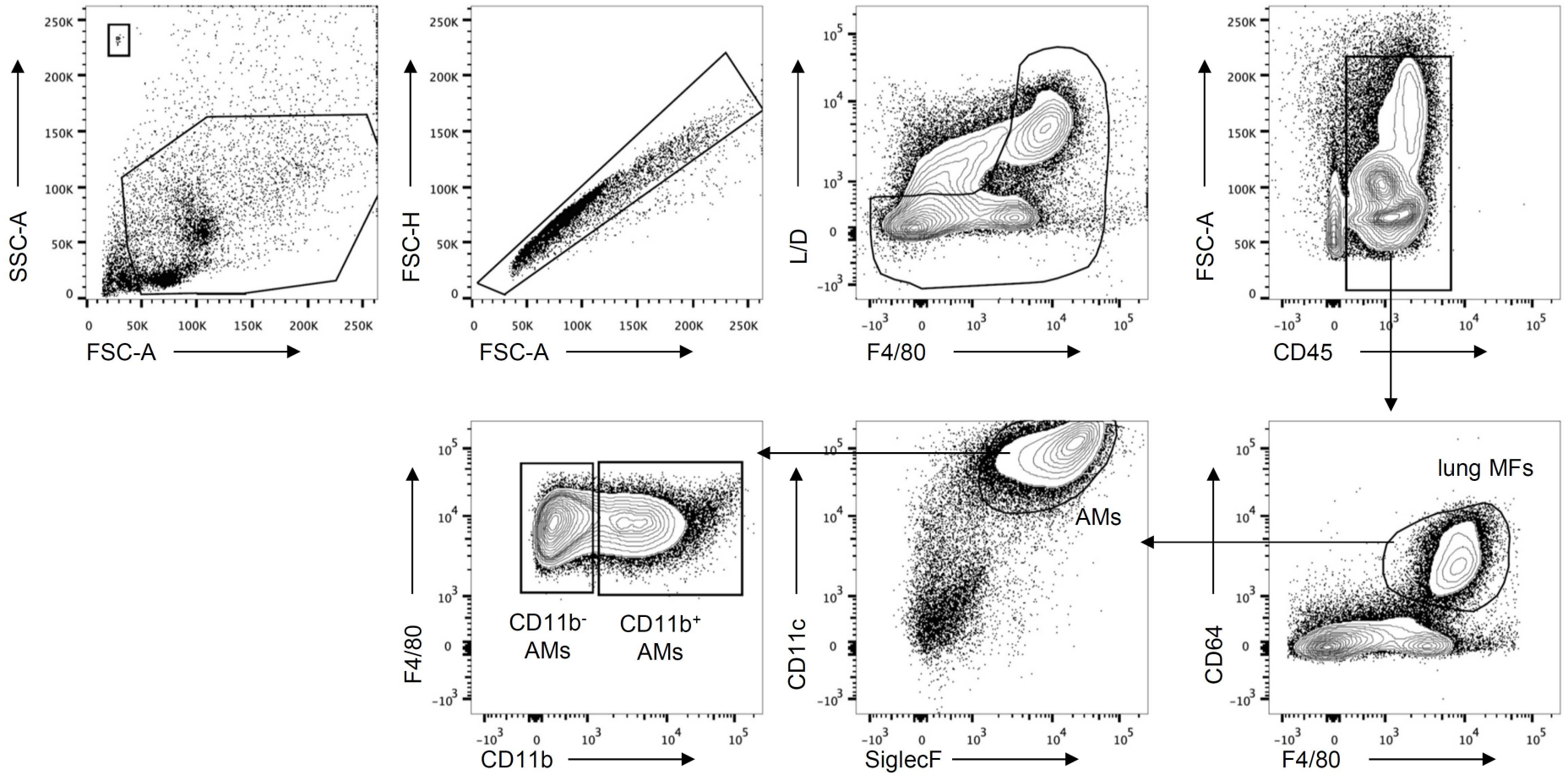

Figure S4 | Gating strategy for alveolar macrophages as performed in the CD11c^{CRE}xZeb2$^{fl/fl}$ mouse model. Representative FACS plots showing gating strategy for alveolar macrophages in the lung. FSC, forward scatter. SSC, side scatter. L/D, live/dead.

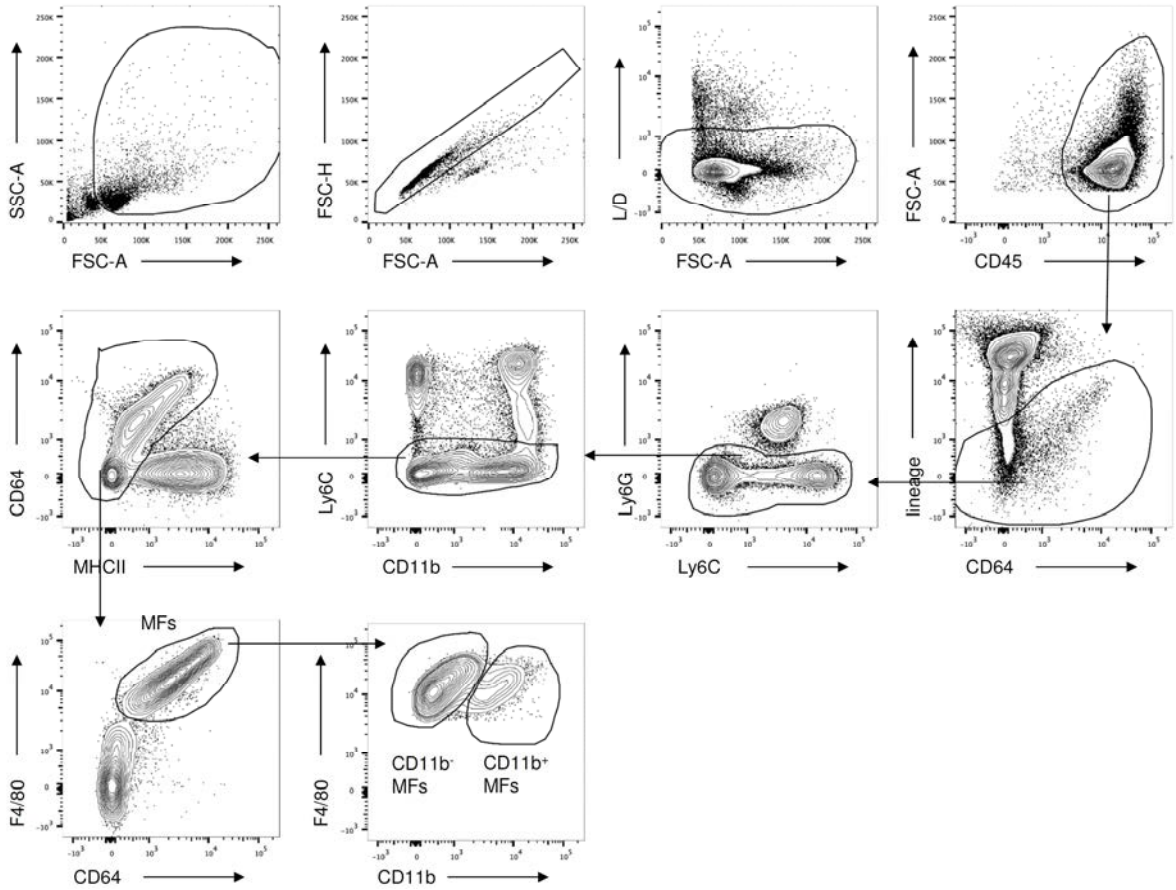

Figure S5 | Gating strategy for splenic macrophages as performed in the CD11c^{CRE}xZeb2$^{fl/fl}$ mouse model. Representative FACS plots showing gating strategy for macrophages in the spleen. FSC, forward scatter. SSC, side scatter. L/D, live/dead.

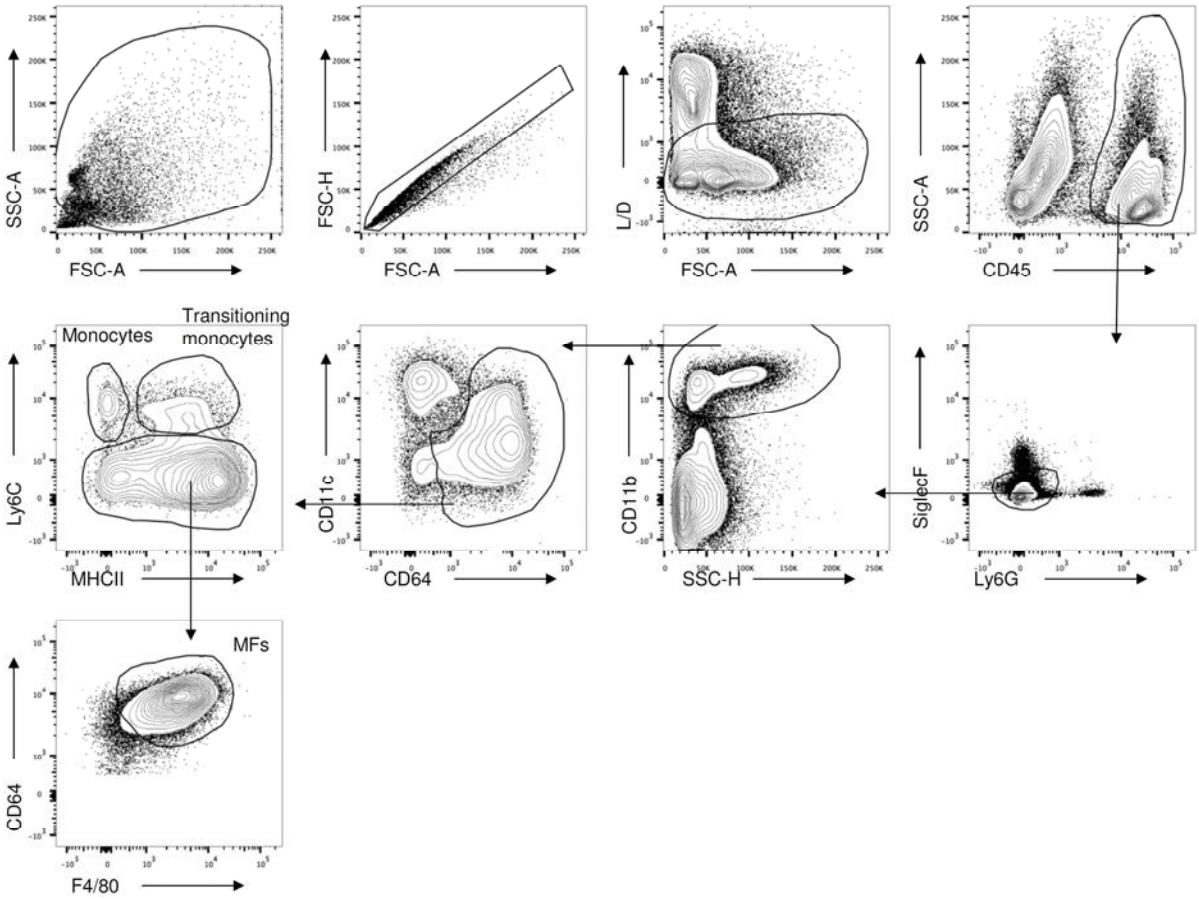

Figure S6 | Gating strategy for colon lamina propria monocytes, transitioning monocytes and macrophages as performed in the CD11c^{CRE}xZeb2$^{fl/fl}$ mouse model. Representative FACS plots showing gating strategy for monocytes, transitioning monocytes and macrophages in the colon lamina propria. FSC, forward scatter. SSC, side scatter. L/D, live/dead.

Part 4
General discussion and future perspectives

Throughout this PhD thesis we have shown that Zeb1 and Zeb2 are master regulators of mononuclear phagocyte development and homeostasis. For the dendritic cell lineage we found that Zeb2 regulates development of conventional and plasmacytoid DCs, whereas Zeb1 in cDC1s is important for the homeostasis of splenic cDCs and macrophages. Furthermore, we showed that Zeb2 is important for the survival of macrophages across multiple murine tissues. Finally, based on recurrent mutations in the *ZEB2* locus in blastic plasmacytoid dendritic cell neoplasm (BPDCN), we attempted to model this rare malignant disease in mice. However, the mice developed a hematoproliferative disease that did not resemble BPDCN. Although the results were discussed at the end of each chapter, some remaining questions and future perspectives will be further addressed in this section. Additionally, we would like to introduce some general concepts on the role of Zeb proteins in the hematopoietic system and the consequences of this for cancer therapy development.

Remaining questions and future perspectives

What about the remaining pDCs and cDC2s in CD11c^{CRE}xZeb2$^{fl/fl}$ mice?

During the course of the first results chapter we have shown that Zeb2 regulates commitment of the cDC2 and the pDC lineage. However, in CD11c^{CRE}xZeb2$^{fl/fl}$ mice we still find a residual pool of both pDCs and cDC2s. Such a partial reduction in cDC2s in CD11c^{CRE}xZeb2$^{fl/fl}$ mice was independently reported by the group of Kenneth Murphy[1]. The remaining pDCs and cDC2s suggest that a Zeb2-dependent and a Zeb2-independent subset could exist within both DC populations. However, we could not identify specific surface markers for the subsets of pDCs and cDC2s requiring Zeb2. Although showing a similar partial reduction in cDC2s using inducible CRE systems such as the Mx1^{CRE}, Murphy and colleagues proposed that Zeb2 does not control the cDC2 lineage. They suggest that Zeb2 rather represses the development of the cDC1 lineage[1]. However, this hypothesis does not explain the cell intrinsic nature of the reduction in cDC2s in these mice.

Another hypothesis regarding the remaining pDCs and cDC2s in CD11c^{CRE}xZeb2$^{fl/fl}$ mice is that in these cells one intact allele of Zeb2 may be present. Indeed, follow-up experiments outside the scope of this thesis considering the role of Zeb2 in macrophages revealed that in CD11c^{CRE}xZeb2$^{fl/fl}$ mice Zeb2$^{-/+}$ alveolar macrophages are present (Scott *et al.* (under review); Addendum p.252) and thus this could also be the case for other cells targeted in this mouse model. Additionally, haplo-sufficiency of Zeb2 in the residual populations would also explain why we only see minimal differences regarding gene expression, migration and antigen presentation. Therefore we would like to FACS-purify the residual populations, extract genomic DNA and perform a PCR designed to specifically detect if CRE excision took place. Additionally, PrimeFlow RNA Assay, a flow cytometry technique that detects the presence of specific RNAs in the cell, was used successfully to show the presence of Zeb2$^{-/+}$ macrophages and hence we would like to use this method to answer the question if the remaining pDCs and cDC2s in CD11c^{CRE}xZeb2$^{fl/fl}$ mice are indeed heterozygous for the loss of Zeb2. This question could also be answered by using single cell RNA-sequencing.

What about Zeb2 and epigenetic regulation?

In Chapter 1 of the results section, we found that Zeb2 regulates pDC and cDC development by directly repressing Id2. However, we think that this is only a part of the mechanism downstream of Zeb2 and we believe that known interactions of Zeb2 with epigenetic modifiers, such as nucleosome remodeling complex Nurd or lysine demethylase Kdm1a, may also play a role[2–4]. Preliminary data (not shown) suggest that the loss of Zeb2 in cDC2s is correlated with a shift from repressive to active histone marks at the promoter regions of around 930 genes. In the future, we will further link these data to the RNA-sequencing data obtained in Chapter 1 in order to find out which genes change their mRNA expression following the identified epigenetic switch. Finally, it would be ideal if we could trace back which gene promoters are epigenetically controlled following binding of Zeb2 by using ChIP-seq. However, a ChIP-grade Zeb2-antibody is currently not available and thus we will first need to generate ChIP-grade Zeb2-antibodies or invest in developing a mouse model expressing tagged Zeb2 protein from the endogenous *Zeb2* promoter using CRISPaint technology[5].

The role of Zeb proteins in cDCs and macrophages during infection

In the discussion part of Chapter 1 and Chapter 3, we proposed to further investigate the functional consequences of altering Zeb2 and Zeb1 expression in dendritic cells during infection and inflammation settings. However, as we showed in the course of this thesis that CD11c^{CRE}xZeb2$^{fl/fl}$ mice also have reduced macrophage populations in several tissues and we found defects in multiple lineages of the splenic immune compartment of CD11c^{CRE}xZeb1$^{fl/fl}$ mice, interpreting results of infection models in these mice will be very complicated and likely not conclusive. Furthermore, as we hypothesize that the remaining pDCs, cDC2s and macrophages in CD11c^{CRE}xZeb2$^{fl/fl}$ mice could have a haplo-sufficient expression of Zeb2, this adds another layer of complexity. One possible solution is the use of the newly developed XCR1^{CRE} line (Chapter 3). XCR1^{CRE}xZeb1$^{fl/fl}$ mice would indeed allow us to investigate the functional consequences of altered expression of Zeb1 specifically in cDC1s. However, also with this model caution is needed, as we showed in Chapter 3 that the loss of Zeb1 in cDC1s also affects cDC2s and macrophages. As Zeb2 is mainly expressed in pDCs and cDC2s, it would be interesting to cross our CRE-mediated conditional loss of Zeb2 line with a pDC and cDC2 specific CRE line. This would allow us to specifically investigate the role of Zeb2 in pDCs and cDC2s during infection, without the additional effects in CD11c expressing non DCs. Unfortunately, such CRE lines do not exist and currently there are no pDC or cDC2 specific genes known that can be used to develop such mouse models.

With regard to investigating the role of Zeb proteins in macrophages during inflammatory settings, we again cannot use the CD11c^{CRE} line, as to many different immune cell lineages are targeted with this mouse model. Furthermore, Scott *et al.* (under review; Addendum p.252) showed that the Fcgr1^{CRE} line, generated by the lab of Bernard Malissen and containing an *iCRE recombinase* in the 3' untranslated region of the *Fcrgr1* gene, efficiently targets macrophages across murine tissues. However, like the CD11c^{CRE} line a number of other immune cells are also targeted (although minimally) and thus using this CRE line to investigate the role of Zeb proteins during infection in macrophages, would again generate results that are difficult to interpret. In contrast, we have shown that the KC^{CRE} line specifically and efficiently targets Kupffer cells. Hence, we could use KC^{CRE}xZeb2$^{fl/fl}$ mice to determine the function of the

transcription factor in Kupffer cells during for instance acetaminophen-induced liver injury[6] or high-fat-diet-induced non-alcoholic steatohepatitis[7].

ZEBs in mononuclear phagocytes: translation to the human field

Throughout this PhD thesis we have shown a role for both Zeb proteins in the homeostasis and development of mononuclear phagocytes in mice. However, if we want to be in the position to manipulate or therapeutically target dendritic cells and macrophages in different human diseases, such as infections, auto-immunity or cancer, it will be crucial to confirm our findings in the human field. Currently, little is known on the expression patterns of ZEB1 and ZEB2 in human mature DCs or tissue-resident macrophages. The difficult access to human tissue and the fact that DCs are rare cells, makes it challenging to research the human aspects. Nevertheless, one study reporting on gene expression in human blood-derived, splenic and thymic DCs, found *ZEB1* to be upregulated in cDC1s compared to cDC2s and pDCs, whereas *ZEB2* was shown to be upregulated in cDC2s and pDCs compared to cDC1s[8]. At least at the mRNA level, this confirms our findings in mice.

One option to check if our conclusions on Zeb2 in DCs and macrophages are valid in human, would be to assess the presence of pDCs, cDC1s, cDC2s and macrophages in Mowat-Wilson syndrome patients. However, as these patients are heterozygous for the loss of ZEB2 and heterozygous loss of Zeb2 in mice did not yield significant changes, at least regarding the numbers of DCs or macrophages, negative results would not be conclusive. Currently, collaborators are looking into immune cells in the blood of Mowat-Wilson syndrome patients, but this approach has its limitations, as DCs in the blood are not mature and macrophages are only present in tissues. If we would have access to BM from Mowat-Wilson syndrome patients, we could culture the BM with FLT3L and determine if the different DC populations are able to develop and function properly. This BM could also be cultured with CSF1 in order to determine if macrophages from Mowat-Wilson syndrome patients develop normally, are able to survive and perform their function.

How to proceed in the search for a preclinical mouse model for BPDCN?

The main goal of Chapter 2 was to develop a clinical mouse model for the human disease blastic plasmacytoid dendritic cell neoplasm (BPDCN). Based on recurrent mutations in the *ZEB2* and *P53* loci and the suggestion that the proliferative disease develops in the pDC lineage[9], we opted to use $CD11c^{CRE}xp53^{fl/fl}$ and $CD11c^{CRE}xZeb2^{fl/fl}xp53^{fl/fl}$ mice. Although mice of both genotypes developed the same hematopoietic malignancy, the disease did not resemble human BPDCN. We can think of several reasons to explain this dissimilarity. First, it could be that the severe phenotype induced by the loss of p53 in CD11c expressing cells, does not allow the possible development of a BPDCN-like disease upon additional loss of Zeb2 expression. Furthermore, we do not know if the *ZEB2* and *P53* mutations that are found in BPDCN-patients are present on only one or on both alleles. If only one allele is affected, this would mean that intact ZEB2 and P53 protein are still present and functional. Therefore, we would like to obtain samples from BPDCN patients, which could be achieved in collaboration with the research team of Prof. Mecucci at the University of Perugia in Italy, and perform immunohistochemical stainings to assess the presence of both proteins. However, absence of the proteins in BPDCN-cells does not necessarily mean that the deleterious mutations in the *ZEB2* and/or *P53* loci are driver mutations, but we chose these genes because they are our genes of expertise and we showed a role for Zeb2 in the pDC lineage. Maybe targeting other genes that are recurrently mutated in BPDCN, such as *Tet2* and *Asxl1*[9], whether or not in combination with *Zeb2*, will be more effective to come to a preclinical model for the disease. Not only the choice of genes, but also the choice of CRE line can possibly explain why we were unable to model BPDCN. We used the $CD11c^{CRE}$ line because it efficiently targets pDCs in mice, but through the course of this thesis, we confirmed that this CRE line also targets multiple other hematopoietic lineages. Therefore, we believe that the search for a clinically relevant mouse model for BPDCN would benefit from a CRE line that specifically targets the pDC lineage. Unfortunately, such a CRE line does not exist at this time and currently there are no pDC specific genes known that can be used to develop such a mouse model.

General concepts

Zebs, Tgfβ and Csf2

During the course of this PhD thesis, multiple findings hinted to a link between Zeb proteins, Tgfβ-signaling and Csf2. When investigating the role of Zeb2 in dendritic cell development in Chapter 1 of the results section, we came across the first hint, which was the differential expression of Zeb2 in $CD103^-$ and $CD103^+$ cDC2s in the small intestine lamina propria. Very recently it was suggested that the $CD103^+$ cDC2s develop from their $CD103^-$ counterparts and that this process is regulated through TgfβR-mediated signaling[10], and it is already known for a long time that Zeb2 is able to inhibit Tgfβ-induced transcription[11]. Additionally, $CD103^+$ cDC2s are dependent on Csf2[12] and we showed that cDC2s from Csf2 BM cultures do not express Zeb2. Furthermore, $CD103^+$ cDC2s express CD101, SiglecF and Epcam, while their $CD103^-$ counterparts do not[10]. Remarkably, we showed that these three markers were also upregulated on the surface of splenic Zeb2-deficient cDC2s. Moreover, follow-up experiments on Chapter 4 outside the scope of this thesis, revealed that Zeb2-deficient Kupffer cells aberrantly express SiglecF on their surface, while Zeb2-deficient alveolar macrophages aberrantly display surface-expression of CD101 and Epcam (Scott *et al.* (under review); Addendum p.252), suggesting a common mechanism in cDC2s and macrophages. In Chapter 3 the increased expression of CD103 on the surface of Zeb1-deficient splenic cDC1s and the cell intrinsic decreased expression of CD103 on pulmonary cDC1s in $CD11c^{CRE}xZeb1^{Tg/Tg}$ mice forms another link with Csf2, as it has been suggested that Csf2 induces the expression of CD103 on cDC1s[13]. Taken together this led to the hypothesis that a general mechanism may be at play in cDCs and macrophages in which TgfβR-mediated signaling leads to the phosphorylation of R-Smads. Subsequently, Zeb proteins are able to interact with those activated R- Smads and as such inhibit TgfβR-mediated transcription of a set of genes, including *CD101*, *SiglecF*, *Epcam* and *CD103* (Figure 1, left panel). However, reduced expression of Zebs as a consequence of Csf2-signaling or targeted gene deletion counteracts Zeb-mediated inhibition of Tgfβ-mediated transcription, leading to the expression of *CD101*, *SiglecF*, *Epcam* and *CD103* (Figure 1, right panel). Further experiments are necessary to validate this hypothesis and to determine the differences in this model for cDC1s, cDC2s and macrophages. Provided that the $XCR1^{CRE}$ line is

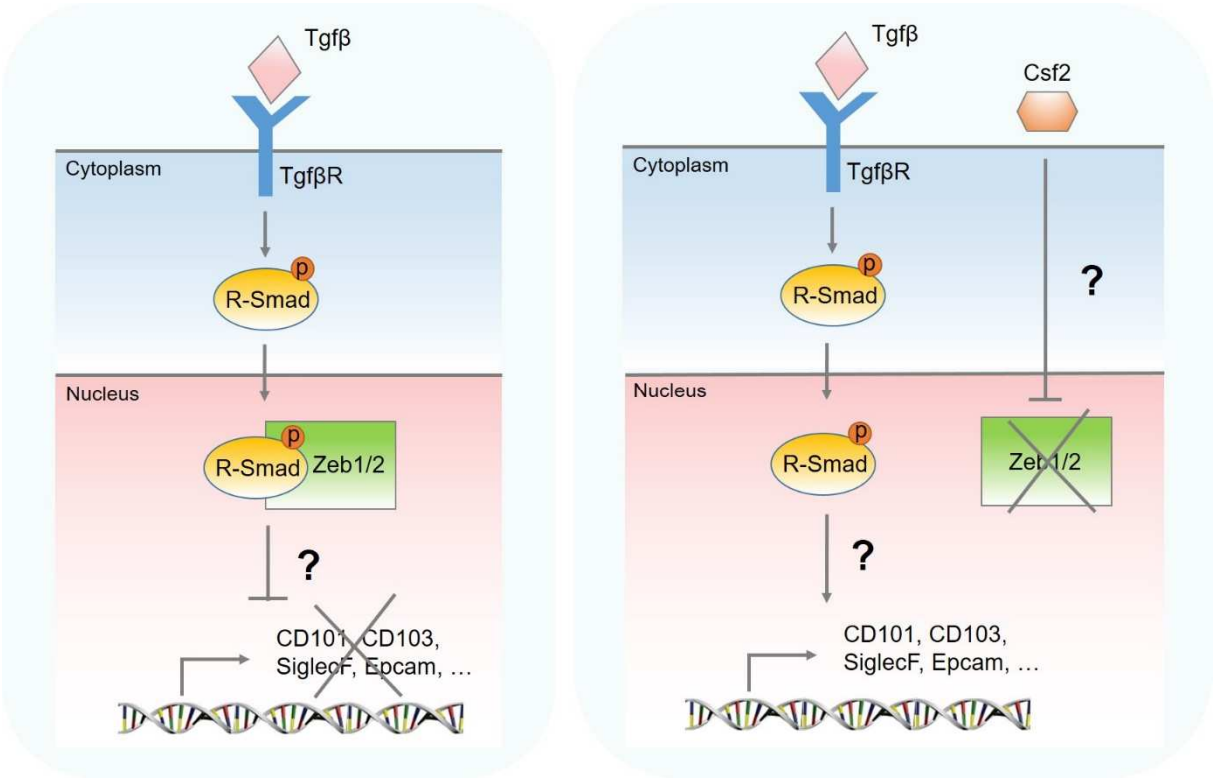

Figure 1 | Hypothesis for the action of Zeb proteins in mononuclear phagocytes. LEFT PANEL: TgfβR-mediated signaling leads to the phosphorylation of R-Smads and subsequently Zeb proteins are able to interact with those activated R-Smads and as such inhibit TgfβR-mediated transcription of a set of genes, including *CD101*, *CD103*, *SiglecF* and *Epcam*. RIGHT PANEL: reduced expression of Zebs as a consequence of Csf2-signaling or targeted gene deletion counteracts Zeb-mediated inhibition of Tgfβ-mediated transcription, leading to the expression of *CD101*, *SiglecF*, *Epcam* and *CD103*.

functional in *in vitro* settings, we could for instance culture BM from XCR1^{CRE}xZeb1$^{Tg/Tg}$ mice in the presence of Flt3L and Csf2 and determine if the generation of CD103^{+} cDC1s is decreased. On the other hand, we could culture BM from XCR1^{CRE}xZeb1$^{fl/fl}$ mice in the presence of Flt3L and determine if CD103^{+} cDC1s can be generated in the absence of Csf2 and if possible assess their surface expression of CD101, SiglecF and Epcam. Furthermore, we could add Tgfβ into Flt3L WT BM cultures with the aim of generating CD103^{+} cDC2s and verify if the addition of Csf2 or the use of tamoxifen-inducible Zeb2 KO BM from Rosa26$^{CRE\text{-}ERT2}$xZeb2$^{fl/fl}$ mice would increase their production. Additionally, we could add Csf2 in differentiated Csf1 BM-derived macrophage cultures and determine the expression of CD101, Epcam, SiglecF and Zeb2.

Oscillation of Zeb proteins during hematopoietic differentiation

Based on the observed complementary expression patterns of *Zeb1* and *Zeb2* mRNAs during embryonic development and the aggravated phenotypes in mice combining loss-of-function of Zeb1 and Zeb2, it was suggested that Zeb transcription factors may have partly overlapping, compensatory functions[14]. In line with this, expression of *Zeb1* and *Zeb2* is mostly mutually exclusive during murine hematopoietic differentiation, except in the hematopoietic stem and multipotent progenitor cell compartment, where *Zeb1* and *Zeb2* are co-expressed at moderate levels (Figure 3 of General introduction p.11). Further along the pathway of differentiation several cell fate decision points are characterized with switching levels of *Zeb1* and *Zeb2* mRNA. For instance, following the multipotent progenitor (MPP) stage, cells either commit to the lymphoid lineage with high expression of Zeb1 and low expression of Zeb2 in the common lymphoid progenitor (CLP) or to the myeloid lineage with high expression of Zeb2 and low expression of Zeb1 in the common myeloid progenitor (CMP) (Figure 2 , upper panel). When looking at T cell differentiation, counter-oscillating levels of both mRNAs are observed along the entire differentiation pathway (Figure 2, upper panel). Furthermore, DC differentiation is also characterized by oscillating levels of *Zeb2*, however in the DC lineage this is not coupled with counter-oscillation of *Zeb1* levels (Figure 2, lower panel). Remarkably, most of the hematopoietic differentiation defects seen in the Zeb1/2 loss- or gain-of-function mouse models occur exactly at the cell fate decision checkpoints (Figure 2). As such, loss of Zeb2 early in development leads to the accumulation of non-committed progenitors and a decrease in fully matured functional blood cells[15,16] (Figure 2, upper panel). In line with the increasing levels during the DN to DP transition in T cell development, Zeb1 mutant mouse models are suffering from a block in T cell differentiation precisely at that point[17,18] (Figure 2, upper panel). Furthermore, the activation of $CD8^+$ T cells, which is characterized by high expression of Zeb2, is impaired in Zeb2 loss-of-function models[19,20] (Figure 2, upper panel). Inactivation of Zeb2 in the hematopoietic system also resulted in problems in the myeloid lineage, such as the inability to commit to the monocyte lineage coupled with an increased commitment to the granulocyte lineage[1,16] (Figure 2, lower panel). Finally, we and others showed that in line with the high expression of Zeb2 in pDCs and cDC2s, loss of Zeb2 in dendritic cells leads to a defect in pDC and cDC2 development[1,21] (Figure 2, lower panel).

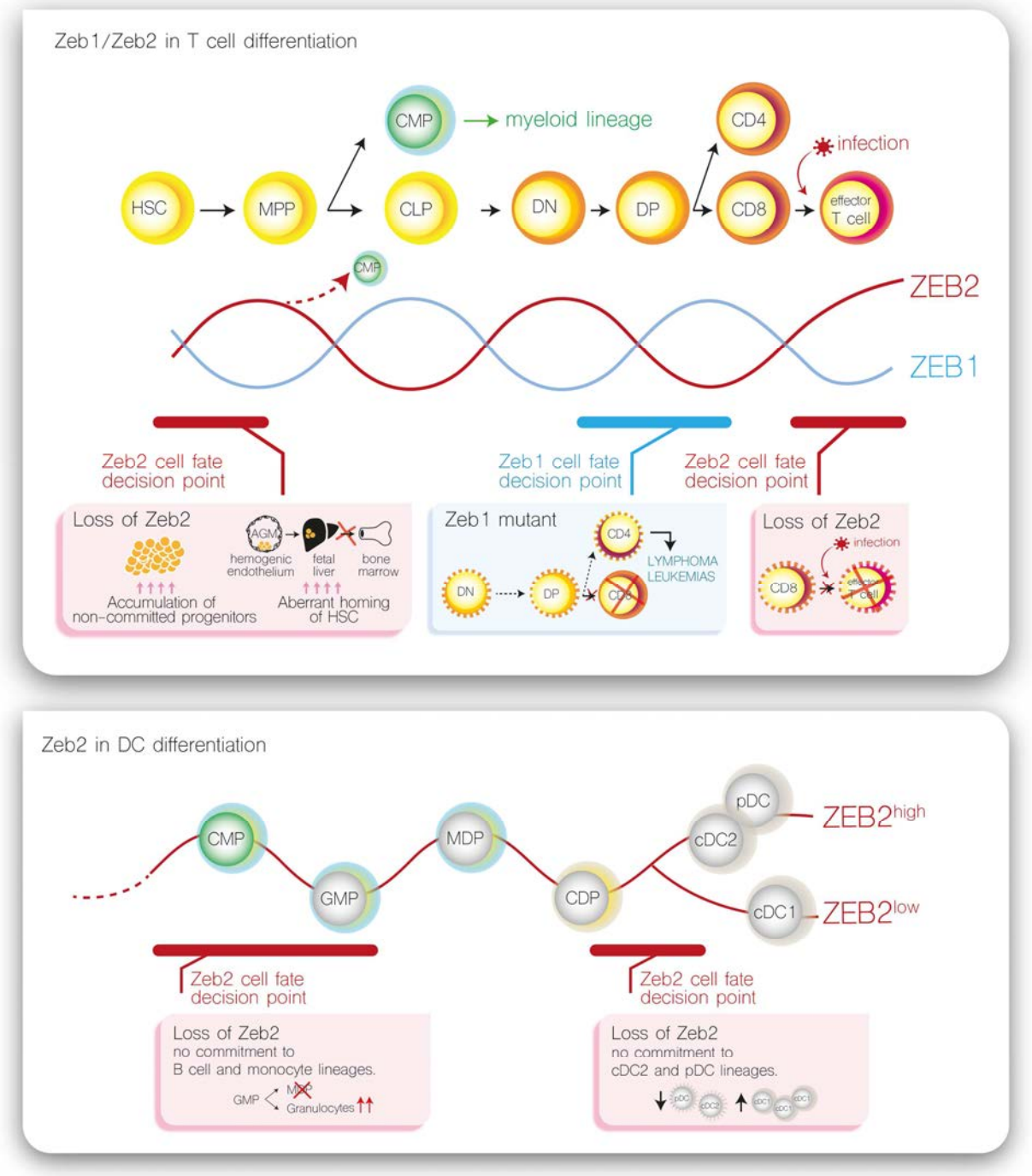

Figure 2 | Examples of *Zeb* expression switching as a molecular driver of important cell fate decision checkpoints during hematopoietic differentiation. The figure is based on expression data available via http://servers.binf.ku.dk/bloodspot/ and shows micro-array data from murine samples. UPPER PANEL: Counter-oscillating expression levels of *Zeb1* and *Zeb2* during T cell differentiation with indications of known differentiation defects in Zeb1 and Zeb2 loss-of-function mouse models. LOWER PANEL: Oscillating *Zeb2* expression levels during dendritic cell differentiation with indications of known differentiation defects in Zeb2 loss-of-function mouse models.

Based on these observations, one could hypothesize that oscillations of Zeb levels may control hematopoietic differentiation. At this point, the molecular mechanisms that control such a *Zeb* mRNA switching remain largely unexplored. However, negative feedback mechanisms via the miRNA-200 family might partially explain these Zeb1/2 oscillations. Indeed, miRNA-200 family members are able to inhibit expression of Zeb proteins at the post-transcriptional level by binding to highly conserved target sites in their 3' untranslated region. In addition, Zebs are also able to transcriptionally repress the miRNA-200 family, suggesting a negative feedback loop that can fuel this Zeb1/2 switching[22,23]. As such, the miRNA-200 family is involved in a counterregulatory network in which Zeb2 drives terminal differentiation of $CD8^+$ T cells, while Zeb1 is involved in maturation and survival of memory $CD8^+$ T cells[24]. Interestingly, also in non-hematopoietic cell lineages, including the melanocytes, a similar oscillation between *Zeb1/2* mRNAs has been described[25,26]. Of note, this concept has also been suggested for other protein families, including the Gata2/Gata1 switch as an important driver of molecular development[27]. In the future, we would like to investigate the importance of and the mechanism behind *Zeb* oscillations in hematopoietic differentiation, starting with determining the levels of the miR-200 family members in the different dendritic cell subtypes.

Consequences for targeting Zeb proteins in cancer

Initially, Zeb proteins were mainly studied as EMT inducing transcription factors that endow epithelial cancer cells with the capacity to disseminate from the primary tumor site, coupled with the gain of stem cell properties and features for therapy resistance. Although EMT is not a hallmark of hematologic malignancies, there is extensive evidence that ZEBs also play an important role in initiation and progression of different subtypes of lymphomas and leukemias. Depending on the lineage of origin of these malignancies, ZEB1 and ZEB2 can both act as oncogenes or tumor suppressors. These often contradictory, synergistic and/or complementary functions of ZEBs in lymphoma/leukemia may be, at least in part, explained by their very pleiotropic functions (cellular adhesion and mobilization/homing, stem cell properties, development and immune regulation) at various stages during hematopoiesis. Additionally, the intricate functioning of ZEB proteins in hematopoietic malignancies may also be influenced by their complex oscillating expression profile, in combination

with the presence or absence of cell-context dependent co-factors and downstream targets. This complexity raises the question if it would be feasible to therapeutically target ZEBs in the context of leukemia. Additionally, as metastasis is the major cause of death in cancer patients, we could also consider targeting ZEBs in solid cancers as a preventative treatment to avoid dissemination from the primary tumor. However, next to the inherent difficulty of targeting transcription factors, the main concern for therapeutic inhibition or reactivation of ZEB proteins might reside in the possible side effects. Indeed, previous work and the results in this thesis show that Zeb1 and Zeb2 have physiological functions throughout the body, including control of the immune system, where they safeguard development and functioning of different immune cell types. Interfering with this could not only disturb response to pathogens, but could also interrupt tumor immunosurveillance. To prevent these important side effects, specific pathways acting downstream of Zebs such as their interaction with cancer specific co-activators, co-repressors and chromatin remodeling complexes or their competition for DNA binding with other E-box binding transcription factors, could be targeted. More research will be required to dissect the mode of action of ZEB1 and ZEB2 in solid tumor cells, leukemic cells and non-transformed immune cells which may open the avenue to less toxic and more specific therapies for hematologic malignancies and solid cancers.

References

1. Wu X, Briseño CG, Grajales-Reyes GE, et al. Transcription factor Zeb2 regulates commitment to plasmacytoid dendritic cell and monocyte fate. *Proc. Natl. Acad. Sci. U.S.A.* 2016;113(51):14775–14780.
2. Verstappen G, van Grunsven LA, Michiels C, et al. Atypical Mowat-Wilson patient confirms the importance of the novel association between ZFHX1B/SIP1 and NuRD corepressor complex. *Human molecular genetics*. 2008;17(8):1175–83.
3. Wu LM, Wang J, Conidi A, et al. Zeb2 recruits HDAC-NuRD to inhibit Notch and controls Schwann cell differentiation and remyelination. *Nature neuroscience*. 2016;19(8):1060–72.
4. Goossens S, Peirs S, Van Loocke W, et al. Oncogenic ZEB2 activation drives sensitivity toward KDM1A inhibition in T-cell acute lymphoblastic leukemia. *Blood*. 2017;129(8):981–990.
5. Schmid-Burgk JL, Höning K, Ebert TS, Hornung V. CRISPaint allows modular base-specific gene tagging using a ligase-4-dependent mechanism. *Nat Commun*. 2016;7:12338.
6. Ramachandran A, Jaeschke H. Mechanisms of acetaminophen hepatotoxicity and their translation to the human pathophysiology. *J Clin Transl Res*. 2017;3(Suppl 1):157–169.
7. Leroux A, Ferrere G, Godie V, et al. Toxic lipids stored by Kupffer cells correlates with their pro-inflammatory phenotype at an early stage of steatohepatitis. *J. Hepatol.* 2012;57(1):141–9.
8. Heidkamp GF, Sander J, Lehmann CHKH, et al. Human lymphoid organ dendritic cell identity is predominantly dictated by ontogeny, not tissue microenvironment. *Sci Immunol*. 2016;1(6):
9. Menezes J, Acquadro F, Wiseman M, et al. Exome sequencing reveals novel and recurrent mutations with clinical impact in blastic plasmacytoid dendritic cell neoplasm. *Leukemia*. 2014;28(4):823–9.
10. Bain CC, Montgomery J, Scott CL, et al. TGFβR signalling controls CD103+CD11b+ dendritic cell development in the intestine. *Nat Commun*. 2017;8(1):620.
11. Postigo AA. Opposing functions of ZEB proteins in the regulation of the TGFbeta/BMP signaling pathway. *The EMBO journal*. 2003;22(10):2443–52.
12. Greter M, Helft J, Chow A, et al. GM-CSF controls nonlymphoid tissue dendritic cell homeostasis but is dispensable for the differentiation of inflammatory dendritic cells. *Immunity*. 2012;36(6):1031–46.
13. Edelson BT, Bradstreet TR, KC W, et al. Batf3-dependent CD11b(low/-) peripheral dendritic cells are GM-CSF-independent and are not required for Th cell priming after subcutaneous immunization. *PLoS ONE*. 2011;6(10):e25660.
14. Miyoshi T, Maruhashi M, Van De Putte T, et al. Complementary expression pattern of Zfhx1 genes Sip1 and deltaEF1 in the mouse embryo and their genetic interaction revealed by compound mutants. *Dev. Dyn.* 2006;235(7):1941–52.
15. Goossens S, Janzen V, Bartunkova S, et al. The EMT regulator Zeb2/Sip1 is essential for murine embryonic hematopoietic stem/progenitor cell differentiation and mobilization. *Blood*. 2011;117(21):5620–30.
16. Li J, Riedt T, Goossens S, et al. The EMT transcription factor Zeb2 controls adult murine hematopoietic differentiation by regulating cytokine signaling. *Blood*. 2017;129(4):460–472.
17. Higashi Y, Moribe H, Takagi T, et al. Impairment of T cell development in deltaEF1 mutant mice. *J. Exp. Med.* 1997;185(8):1467–79.
18. Arnold CN, Pirie E, Dosenovic P, et al. A forward genetic screen reveals roles for Nfkbid, Zeb1, and Ruvbl2 in humoral immunity. *Proc. Natl. Acad. Sci. U.S.A.* 2012;109(31):12286–93.
19. Omilusik KD, Best JA, Yu B, et al. Transcriptional repressor ZEB2 promotes terminal differentiation of CD8+ effector and memory T cell populations during infection. *J. Exp. Med.* 2015;212(12):2027–39.
20. Dominguez CX, Amezquita RA, Guan T, et al. The transcription factors ZEB2 and T-bet cooperate to program cytotoxic T cell terminal differentiation in response to LCMV viral infection. *J. Exp. Med.* 2015;212(12):2041–56.
21. Scott CL, Soen B, Martens L, et al. The transcription factor Zeb2 regulates development of conventional and plasmacytoid DCs by repressing Id2. *J. Exp. Med.* 2016;213(6):897–911.
22. Hill L, Browne G, Tulchinsky E. ZEB/miR-200 feedback loop: at the crossroads of signal transduction in cancer. *Int. J. Cancer*. 2013;132(4):745–54.
23. Brabletz S, Brabletz T. The ZEB/miR-200 feedback loop--a motor of cellular plasticity in development and cancer? *EMBO Rep.* 2010;11(9):670–7.
24. Guan T, Dominguez CX, Amezquita RA, et al. ZEB1, ZEB2, and the miR-200 family form a counterregulatory network to regulate CD8+T cell fates. *J. Exp. Med.* 2018;215(4):1153–1168.
25. Vandamme N, Berx G. Melanoma cells revive an embryonic transcriptional network to dictate phenotypic heterogeneity. *Front Oncol*. 2014;4:352.
26. Denecker G, Vandamme N, Akay O, et al. Identification of a ZEB2-MITF-ZEB1 transcriptional network that controls melanogenesis and melanoma progression. *Cell Death Differ.* 2014;21(8):1250–61.
27. Bresnick EH, Lee H-YY, Fujiwara T, Johnson KD, Keles S. GATA switches as developmental drivers. *J. Biol. Chem.* 2010;285(41):31087–93.

Part 5
Addendum

Accepted manuscripts

HemaSphere
Powered by EHA

EHA EUROPEAN HEMATOLOGY ASSOCIATION

Review Article
OPEN ACCESS

ZEB Proteins in Leukemia: Friends, Foes, or Friendly Foes?

Bieke Soen[1,2], Niels Vandamme[1,2], Geert Berx[1,2], Jürg Schwaller[3], Pieter Van Vlierberghe[2,4], Steven Goossens[1,2,4]

Correspondence: Steven Goossens (e-mail: Steven.Goossens@ugent.be).

Abstract

ZEB1 and ZEB2 play pivotal roles in solid cancer metastasis by allowing cancer cells to invade and disseminate through the transcriptional regulation of epithelial-to-mesenchymal transition. ZEB expression is also associated with the acquisition of cancer stem cell properties and therapy resistance. Consequently, expression levels of ZEB1/2 and of their direct target genes are widely seen as reliable prognostic markers for solid tumor aggressiveness and cancer patient outcome.

Recent loss-of-function mouse models demonstrated that both ZEBs are also essential hematopoietic transcription factors governing blood lineage commitment and fidelity. Interestingly, both gain- and loss-of-function mutations have been reported in multiple hematological malignancies. Combined with emerging functional studies, these data suggest that ZEB1 and ZEB2 can act as tumor suppressors and/or oncogenes in blood borne malignancies, depending on the cellular context. Here, we review these novel insights and discuss how balanced expression of ZEB proteins may be essential to safeguard the functionality of the immune system and prevent leukemia.

ZEB1 and ZEB2: 2 structurally related E-box-binding transcription factors

The ZEB (Zinc finger E-box-binding homeobox) protein family of transcription factors was discovered in *Drosophila melanogaster* and consists of 2 structurally conserved multidomain proteins, ZEB1 (originally called ZFHX1A, TCF8, or δEF1) and ZEB2 (originally called ZFHX1B or SIP1).[1,2] Both ZEBs contain an amino-terminal (NZF) and carboxy-terminal zinc finger cluster (CZF), which enables them to bind regulatory DNA sequences in their target promoters. Each zinc finger cluster binds an independent 5′-CANNTG-3′ motif, which overlaps with the core of an E2-box sequence,[3–5] a binding site for transcription factors of the basic helix-loop-helix (bHLH) family. ZEBs can repress target gene transcription through the recruitment of the CtBP corepressor complex via their CtBP interaction domain (CID).[6] Additional conserved domains were documented by which ZEBs can recruit other transcriptional complexes to their target promoters. For instance, the amino-terminus of both ZEBs can bind the Nucleosome Remodeling and Deacetylase complex (NuRD, also known as the Mi-2 complex).[7,8] Also, a SMAD Binding Domain (SBD) is located between the NZF and the central homeobox domain.[4] Although this SBD is highly conserved and both ZEBs can directly interact with SMADs, they may have an opposite downstream effect[9]: ZEB1 synergizes with SMAD proteins to activate SMAD-mediated transcription, while ZEB2 seems to inhibit SMAD-mediated transcription. It is believed that this opposite effect is regulated by the differential recruitment of ZEB1/2-specific coactivators/repressors, which may be tissue-specifically expressed. Initially, the N-terminal region of ZEB1, but not ZEB2, was documented to interact with p300 and P/CAF. This differential recruitment of P/CAF may switch ZEB1 from a repressor to an activator through the displacement of CtBP1 from the CID.[9,10] Later, others demonstrated that, depending on the experimental context, ZEB2 and ZEB1 are equally potent to bind p300 and P/CAF.[11] This suggests that other mechanisms/cofactors are contributing to the differential ZEB1/2-specific effects on SMAD-mediated transcription.

Based on the extensive and continuously growing list of interaction partners and putative downstream targets, one can expect that ZEBs have very pleiotropic functions, which largely depend on the cellular context. Indeed, the chromatin status and the presence/absence of tissue-specific interaction partners strongly influence their role as a transcriptional repressor/

Funding: Our work is supported by the Research Foundation Flanders (FWO, 1504317N), Special Research Fund Ghent University (BOF24Y2017002001), the Worldwide Cancer Research (16-1157), Stand Up To Cancer (Kom op tegen Kanker, Flanders), the Swiss Bridge Foundation, the Swiss National Science Foundation (31003A_149714/1), and the Swiss Cancer League (KFS-3019-08-2012).

Disclosure: The authors have indicated they have no potential conflicts of interest to disclose.

[1]*Department for Biomedical Molecular Biology, Ghent University, Ghent, Belgium*
[2]*Cancer Research Institute Ghent, Ghent, Belgium*
[3]*Department of Biomedicine, University Children's Hospital, University of Basel, Basel, Switzerland*
[4]*Department of Pediatrics and Genetics, Center for Medical Genetics, Ghent University, Ghent, Belgium*

HemaSphere (2018) Vol:No
Received: 17 January 2018 / Received in final form: 9 April 2018 / Accepted: 11 April 2018
Citation: Soen B, Vandamme N, Berx G, Schwaller J, Van Vlierberghe P, Goossens S. ZEB Proteins in Leukemia: Friends, Foes or Friendly Foes? *HemaSphere*, 2018;00:00. http://dx.doi.org/10.1097/HS9.0000000000000043

Published May 16, 2016

JEM

Brief Definitive Report

The transcription factor Zeb2 regulates development of conventional and plasmacytoid DCs by repressing Id2

Charlotte L. Scott,[1,4,5*] Bieke Soen,[2,5*] Liesbet Martens,[3,4] Nicolas Skrypek,[2,5] Wouter Saelens,[3,4] Joachim Taminau,[2,5] Gillian Blancke,[2,5] Gert Van Isterdael,[1,4] Danny Huylebroeck,[6,7] Jody Haigh,[9] Yvan Saeys,[3,4] Martin Guilliams,[1,5] Bart N. Lambrecht,[1,4,8**] and Geert Berx[2,5**]

[1]Laboratory of Immunoregulation and Mucosal Immunology, [2]Unit of Molecular and Cellular Oncology, and [3]Data Mining and Modeling for Biomedicine, Inflammation Research Center, Vlaams Instituut voor Biotechnologie, 9052 Ghent, Belgium
[4]Department of Respiratory Medicine and [5]Department of Biomedical Molecular Biology, Ghent University, 9000 Ghent, Belgium
[6]Laboratory of Molecular Biology (Celgen), Department of Development and Regeneration, Katholieke Universiteit Leuven, 3000 Leuven, Belgium
[7]Department of Cell Biology and [8]Department of Pulmonary Medicine, Erasmus University Medical Center, 3015 GE Rotterdam, Netherlands
[9]Mammalian Functional Genetics Laboratory, Division of Blood Cancers, Australian Centre for Blood Diseases, Monash University, Melbourne, Victoria 3800, Australia

Plasmacytoid dendritic cells (DCs [pDCs]) develop from pre-pDCs, whereas two lineages of conventional DCs (cDCs; cDC1s and cDC2s) develop from lineage-committed pre-cDCs. Several transcription factors (TFs) have been implicated in regulating the development of pDCs (E2-2 and Id2) and cDC1s (Irf8, Id2, and Batf3); however, those required for the early commitment of pre-cDCs toward the cDC2 lineage are unknown. Here, we identify the TF zinc finger E box–binding homeobox 2 (Zeb2) to play a crucial role in regulating DC development. Zeb2 was expressed from the pre-pDC and pre-cDC stage onward and highly expressed in mature pDCs and cDC2s. Mice conditionally lacking *Zeb2* in CD11c$^+$ cells had a cell-intrinsic reduction in pDCs and cDC2s, coupled with an increase in cDC1s. Conversely, mice in which CD11c$^+$ cells overexpressed *Zeb2* displayed a reduction in cDC1s. This was accompanied by altered expression of Id2, which was up-regulated in cDC2s and pDCs from conditional knockout mice. Zeb2 chromatin immunoprecipitation analysis revealed Id2 to be a direct target of Zeb2. Thus, we conclude that Zeb2 regulates commitment to both the cDC2 and pDC lineages through repression of Id2.

DCs reside in almost all tissues in the body, where they function as immune sentinels. DCs can be subdivided into two main groups: plasmacytoid DCs (pDCs), which are specialized in the production of type I interferons to elicit an antiviral immune response (Swiecki and Colonna, 2015), and conventional DCs (cDCs), which are professional antigen-presenting cells. cDCs form the crucial link between the innate and adaptive arms of the immune system by sampling local antigens and subsequently migrating to their draining LNs, where they initiate appropriate responses from T cells (Merad et al., 2013). cDCs exist in two main subtypes, which were recently termed cDC1s and cDC2s (Guilliams et al., 2014). cDC1s, expressing XCR1 and usually CD103 and/or CD8α, are functionally specialized in cross-presentation of antigens to CD8$^+$ T cells (Hildner et al., 2008; Bachem et al., 2010; Haniffa et al., 2012). cDC2s express CD172a (signal regulatory protein α [SIRPα]) and usually CD11b or CD4 and are functionally specialized in the presentation of antigens to CD4$^+$ T cells (Merad et al., 2013).

DCs develop in the BM through a series of differentiation intermediates, each with a further degree of commitment to a specific lineage, that see the common myeloid progenitor (CMP) become a macrophage–DC progenitor (MDP) and then a common DC progenitor (CDP), with the penultimate step of differentiation resulting in generation of the pre-pDC and pre-cDCs (Naik et al., 2007; Liu et al., 2009; Merad et al., 2013; Onai et al., 2013). Furthermore, it has recently been shown that pre-cDCs can be further subdivided into pre-cDC1s and pre-cDC2s, which are committed to the cDC1 and cDC2 lineages, respectively (Grajales-Reyes et al., 2015; Schlitzer et al., 2015). Pre-pDCs develop into pDCs in the BM, which then migrate out to the periphery, whereas the pre-cDC subsets first migrate to the periphery and then undergo their final differentiation into cDCs (Liu et al., 2009; Onai et al., 2013; Schlitzer et al., 2015). The development of pDCs, cDC1s, and cDC2s requires the concerted action of several lineage-determining transcription factors (TFs). The main TF involved in pDC development and maintenance is the basic helix–loop–helix E protein E2-2 (Cisse et al., 2008; Ghosh et al., 2010), whereas cDC1s require Irf8, Batf3, and

*C.L. Scott and B. Soen contributed equally to this paper.

**B.N. Lambrecht and G. Berx contributed equally to this paper.

Correspondence to Bart N. Lambrecht: bart.lambrecht@irc.vib-ugent.be; or Geert Berx: Geert.Berx@irc.vib-ugent.be

Abbreviations used: cDC, conventional DC; CDP, common DC progenitor; ChIP, chromatin immunoprecipitation; CMP, common myeloid progenitor; DP, double positive; FC, fold change; LP, lamina propria; MDP, macrophage–DC progenitor; MLN, mesenteric LN; pDC, plasmacytoid DC; qPCR, quantitative PCR; SI, small intestine; SIRPα, signal regulatory protein α; TF, transcription factor.

The Rockefeller University Press $30.00
J. Exp. Med. 2016 Vol. 213 No. 6 897–911
www.jem.org/cgi/doi/10.1084/jem.20151715

Supplemental Material can be found at:
http://jem.rupress.org/content/suppl/2016/05/11/jem.20151715.DC1.html

Cell. Mol. Life Sci. (2014) 71:3599–3609
DOI 10.1007/s00018-014-1589-0

Cellular and Molecular Life Sciences

RESEARCH ARTICLE

ZEB2-transgene expression in the epidermis compromises the integrity of the epidermal barrier through the repression of different tight junction proteins

Marianthi N. Tatari · Bram De Craene · Bieke Soen · Joachim Taminau · Petra Vermassen · Steven Goossens · Katharina Haigh · Silvia Cazzola · Jo Lambert · Danny Huylebroeck · Jody J. Haigh · Geert Berx

Received: 2 October 2013 / Revised: 26 January 2014 / Accepted: 13 February 2014 / Published online: 27 February 2014

Abstract Epithelial homeostasis within the epidermis is maintained by means of multiple cell–cell adhesion complexes such as adherens junctions, tight junctions, gap junctions, and desmosomes. These complexes co-operate in the formation and the regulation of the epidermal barrier. Disruption of the epidermal barrier through the deregulation of the above complexes is the cause behind a number of skin disorders such as psoriasis, dermatitis, keratosis, and others. During epithelial-to-mesenchymal transition (EMT), epithelial cells lose their adhesive capacities and gain mesenchymal properties. ZEB transcription factors are key inducers of EMT. In order to gain a better understanding of the functional role of ZEB2 in epidermal homeostasis, we generated a mouse model with conditional overexpression of *Zeb2* in the epidermis. Our analysis revealed that *Zeb2* expression in the epidermis leads to hyperproliferation due to the combined downregulation of different tight junction proteins compromising the epidermal barrier. Using two epidermis-specific in vivo models and in vitro promoter assays, we identified occludin as a new Zeb2 target gene. Immunohistological analysis performed on human skin biopsies covering various pathogeneses revealed ZEB2 expression in the epidermis of pemphigus vulgaris. Collectively, our data support the notion for a potential role of ZEB2 in intracellular signaling of this disease.

Keywords EMT · ZEB2 · Tight junctions · Skin

Electronic supplementary material The online version of this article (doi:10.1007/s00018-014-1589-0) contains supplementary material, which is available to authorized users.

M. N. Tatari · B. De Craene · B. Soen · J. Taminau · P. Vermassen · G. Berx (✉)
Unit of Molecular and Cellular Oncology, Inflammation Research Center, VIB, Technologiepark 927, 9052 Ghent (Zwijnaarde), Belgium
e-mail: geert.berx@irc.vib-ugent.be

M. N. Tatari · B. De Craene · B. Soen · J. Taminau · P. Vermassen · S. Goossens · K. Haigh · J. J. Haigh · G. Berx
Department of Biomedical Molecular Biology, Ghent University, 9052 Ghent, Belgium

S. Goossens · K. Haigh · J. J. Haigh
Unit of Vascular Cell Biology, Inflammation Research Center, VIB, 9052 Ghent, Belgium

S. Cazzola · D. Huylebroeck
Laboratory of Molecular Biology (Celgen), Department of Development and Regeneration, Faculty of Medicine, Research Unit Embryo and Stem Cells, University of Leuven (KU Leuven), 3000 Leuven, Belgium

J. Lambert
Department of Dermatology 2K4, Ghent University Hospital, De Pintelaan 185, 9000 Ghent, Belgium

Introduction

The two major cell types forming the metazoan body, epithelial and mesenchymal cells, differ both morphologically and functionally. Epithelial cells are characterized by apical-basal polarization and by the close contact they maintain with neighboring cells through adherens junctions, tight junctions, desmosomes and gap junctions, creating a rigid three-dimensional structure that can support organ function [1]. In contrast, mesenchymal cells show anterior-posterior polarization and no durable adhesive properties, forming irregular structures without a uniform composition or density. The main distinctive feature of mesenchymal cells is their ability to actively migrate as individual cells [2].

Cells can switch between the epithelial and mesenchymal types through a process called epithelial-to-mesenchymal

EV-TRACK: transparent reporting and centralizing knowledge in extracellular vesicle research

EV-TRACK Consortium*

We argue that the field of extracellular vesicle (EV) biology needs more transparent reporting to facilitate interpretation and replication of experiments. To achieve this, we describe EV-TRACK, a crowdsourcing knowledgebase (http://evtrack.org) that centralizes EV biology and methodology with the goal of stimulating authors, reviewers, editors and funders to put experimental guidelines into practice.

EVs have emerged as having important (patho)physiological roles, and as such they have been the focus of intense study over the past decade[1–4]. Despite substantial progress, the complexity and challenges associated with EV research remain considerable[5]. EVs released from different cell types (and even from a single cell type) are heterogeneous in size and in protein, nucleic acid and lipid content[6–9]. The isolation of EV populations is frequently complicated by the presence of contaminants with comparable features[10,11]. Different isolation methods enrich for single or multiple EV subtypes with diverse composition and variable purity, thus identifying method-dependent EV content and function[6–11]. Each detection and characterization method has its own accuracy and precision in measuring EVs[12,13]. Still, functional studies on EVs vastly outnumber those focusing on EV biology and methodology (**Supplementary Fig. 1**).

In EV research, as in any field, the implementation of different methods requires validated controls and adequate reporting of experimental parameters. Failure to follow these principles can result in data that are difficult to interpret and reproduce[14]. Similar to minimal information checklists in other fields[15–17], the International Society for Extracellular Vesicles (ISEV) introduced minimal informations for studies on EVs (MISEV) guidelines[18,19]. Nevertheless, EV research is unfolding at a rate that impedes widespread adoption of these guidelines.

We convened an international consortium to develop the EV-TRACK knowledgebase, which records experimental parameters of EV-related studies. EV-TRACK implements a bottom-up community consensus approach and encourages researchers to upload published and unpublished experiments and provide feedback. It is a unique resource that was developed to (i) create an informed dialog among researchers about relevant experimental parameters, (ii) improve the rigor and interpretation of experiments studying EVs, and (iii) record the evolution of EV research. The final goal of the EV-TRACK consortium is to facilitate standardization of EV research through increased systematic reporting on EV biology and methodology.

Creation of the EV-TRACK knowledgebase

Currently, the EV-TRACK knowledgebase comprises methodological specifications of 1,226 EV-related articles published in 2010–2015 (**Supplementary Fig. 2**). Publications that included multiple sample types or isolation methods were separated into multiple entries, resulting in 1,742 experiments (**Supplementary Methods**). For each experiment, we completed a checklist of 115 parameters—based partially on the MISEV guidelines[19]—relating to sample type, preanalytical variables, isolation protocol and characterization method (**Supplementary Table 1**). Data were curated before inclusion in the knowledgebase, which can be accessed freely at http://evtrack.org.

Figure 1 | The seven enabling features of the EV-TRACK platform.

EV research practices

To assess current practices in EV experiments, we performed an in-depth analysis of the data in the EV-TRACK knowledgebase. This revealed widespread heterogeneity in EV isolation methods and inconsistent implementation and reporting of important experimental parameters, including isolation methods and characterization of EV size, composition and purity (**Supplementary Fig. 3**).

The 1,742 experiments that are recorded in EV-TRACK report 190 unique isolation methods and 1,038 unique protocols to retrieve EVs from biofluids (**Supplementary Tables 2** and **3**). Differential ultracentrifugation (dUC) is the most popular method (45% of all experiments), but with variable parameters selected by researchers, even for experiments handling a similar sample type. For cell culture supernatant ($n = 813$ experiments using dUC), 218 unique combinations of centrifugation steps and final pelleting times are recorded, along with a

*A full list of authors and affiliations appears at the end of the paper. e-mail: an.hendrix@ugent.be

Z

Zinc Finger E-Box-Binding Homeobox 2

Özden Akay[1,2,3], Kenneth Bruneel[1,2,3], Bieke Soen[1,2,3], Eva De Smedt[1,2,3], Niels Vandamme[1,2,3] and Geert Berx[1,2,3]
[1]Molecular and Cellular Oncology Lab, Inflammation Research Center, VIB, Ghent, Belgium
[2]Department for Biomedical Molecular Biology, Ghent University, Ghent, Belgium
[3]Cancer Research Institute Ghent (CRIG), Ghent, Belgium

Synonyms

Danio rerio: Zeb2b, sip1b, zfhx1b; *Homo sapiens*: SIP1, SIP-1, SMADIP1, ZFHX1B; *Mus musculus*: Zeb2, Zfx1b, Zfhx1b; *Xenopus tropicalis*: XSip1

Historical Background

Zinc finger E-box-binding homeobox 2 (ZEB2) is a zinc finger and homeodomain transcription factor. ZEB2 was identified as a protein binding to the MH2 domain of different Smad proteins involved in BMP- and TGF-ß pathways (Verschueren et al. 1999). Initial studies correlating ZEB2 and E-cadherin downregulation in carcinomas were followed by a significant amount of research linking ZEB2 and epithelial-to-mesenchymal transition (EMT) during tumor progression (Comijn et al. 2001). Together with its paralog ZEB1, ZEB2 belongs to the Zeb family of transcription factors characterized by two zinc finger clusters separated by a homeodomain. During evolution, the duplication of the ancestral ZEB gene and diversification of ZEB2 from ZEB1 coincide with the onset of neural crest development and specification.

Physiological Functions of ZEB2

During embryonic development studies in several model organisms such as mouse, chick, and *Xenopus*, ZEB2 mRNA can be detected from gastrula stage onward with persisting expression during the early neurula stage in the neural tube, neural crest, and retina (Hegarty et al. 2015). Later, ZEB2 expression is predominantly found in pre-migratory and migratory neural crest cells. The expression patterns in neuronal tissues and neural crest derivatives are well documented, and ZEB2 deficiencies are commonly associated with neuropathies in mouse and human. In many adult tissues, ZEB2 expression can be found back during physiological conditions in several E-cadherin-negative tissues from the central nervous system, melanocytes, various muscle types, fibroblasts, and specific hematopoietic lineages (Katoh and Katoh 2009; Vandewalle et al. 2009; Sanchez-Tillo et al. 2011; Gheldof et al. 2012).

S. Choi (ed.), *Encyclopedia of Signaling Molecules*,
DOI 10.1007/978-1-4614-6438-9_101944-1

Z

ZEB1 (Zinc Finger E-Box Binding Homeobox 1)

Eva De Smedt[1,2,3], Kenneth Bruneel[1,2,3], Bieke Soen[1,2,3], Özden Akay[1,2,3], Niels Vandamme[1,2,3] and Geert Berx[1,2,3]
[1]Molecular and Cellular Oncology Lab, Inflammation Research Center, VIB, Ghent, Belgium
[2]Department for Biomedical Molecular Biology, Ghent University, Ghent, Belgium
[3]Cancer Research Institute Ghent (CRIG), Ghent, Belgium

Synonyms

Danio rerio: Kheper
Drosophila melanogaster: Zfh-1
Gallus gallus domesticus: δEF1
Homo sapiens: NIL-2-A; AREB6; ZEB; TCF-8
Mesocricetus auratus: BZP
Mus musculus: ZFHX1A
Rattus norvegicus: MEB1; ZFHEP
Xenopus laevis: XdEF1

Historical Background

Zinc finger E-box binding homeobox 1 (ZEB1) is a zinc finger and homeodomain transcription factor playing a key role in epithelial-to-mesenchymal transition (EMT) during embryogenesis by controlling cell behavior and cell adhesion. ZEB1 has also been extensively studied in the context of tumor progression as many cancer types reactivate embryonic EMT programs to promote metastasis. Besides EMT-related programs in embryonic and pathological contexts, ZEB1 plays a key role during differentiation of a wide variety of cell types. ZEB1 was first reported in 1991 as δEF1, a transcriptional repressor of the δ1-crystalline enhancer in chicken during lens development (Funahashi et al. 1991). Independently, ZEB1 was described as NIL-2-A, a transcriptional repressor of human IL-2 in activated T cells (Williams et al. 1991). In 1994, the first full-length cDNA clone of ZEB1, designated as ZEB, was cloned from a HeLa cancer cell line cDNA library, and "ZEB" was identified as repressor of the immunoglobulin heavy chain in B cells (Genetta et al. 1994). Together with its paralog ZEB2, ZEB1 belongs to the ZEB family of transcription factors characterized by two zinc finger clusters separated by a homeodomain. During evolution, the duplication of the ancestral ZEB gene and diversification of ZEB1 from ZEB2 coincides with the onset of neural crest development and specification (Gheldof et al. 2012). ZEB2 is expressed in the neural crest and ZEB2-null embryos die after failure of neural crest development and delamination. In contrast, ZEB1 is mainly expressed in neural crest derivatives and ZEB1-null animals suffer from major skeletal defects and die perinatally. Although evolutionary

S. Choi (ed.), *Encyclopedia of Signaling Molecules*,
DOI 10.1007/978-1-4614-6438-9_101943-1

Manuscript under review

ZEB2 is required to maintain the tissue-specific identities of macrophages

Charlotte L. Scott[1,2,3,*,#], Wouter T'Jonck[1,2,#], Liesbet Martens[2,4], Helena Todorov[2,4], Dorine Sichien[1,2], Bieke Soen[2,5], Johnny Bonnardel[1,2], Sofie De Prijck[1,2], Niels Vandamme[2,5], Robrecht Cannoodt[2,4], Wouter Saelens[2,4] , Bavo Vanneste[1,2], Wendy Toussaint[6,7], Pieter De Bleser[2,4], Nozomi Takahashi[2,8], Peter Vandenabeele[2,8], Sandrine Henri[9] , Clare Pridans[9], David A. Hume[10], Bart N. Lambrecht[6,7], Patrick De Baetselier[12,13], Simon WF Milling[3], Jo A. Van Ginderachter[12,13], Bernard Malissen[9,14], Geert Berx[2,5], Alain Beschin[12,13,#], Yvan Saeys[4,15,#] and Martin Guilliams[1,2,16,*, #].

1 Laboratory of Myeloid Cell Ontogeny and Functional Specialization, VIB Center for Inflammation Research, Technologiepark 927, Ghent, Belgium.
2 Department of Biomedical Molecular Biology, Ghent University, Ghent, Belgium.
3 Institute of Infection, Immunity and Inflammation, College of Medical, Veterinary and Life Sciences, University of Glasgow, Glasgow, UK.
4 Data Mining and Modeling for Biomedicine, VIB Center for Inflammation Research, Technologiepark 927, Ghent, Belgium.
5 Molecular and Cellular Oncology Lab, VIB Center for Inflammation Research, Technologiepark 927, Ghent, Belgium.
6 Laboratory of Mucosal Immunology and Immunoregulation, VIB Center for Inflammation Research, Technologiepark 927, Ghent, Belgium.
7 Department of Respiratory Medicine, Ghent University, Ghent, Belgium.
8 Laboratory of Molecular Signaling and Cell Death, VIB Center for Inflammation Research, Technologiepark 927, Belgium.
9 Centre d'Immunologie de Marseille-Luminy, Aix Marseille Université, INSERM, CNRS 13288 Marseille, France
10 MRC Centre for Inflammation Research, University of Edinburgh, The Queen's Medical Research Institute, Edinburgh, UK
11 Mater Research-University of Queensland, Translational Research Institute, 37 Kent St, Woolloongabba, Qld 4102, Australia
12 Myeloid Cell Immunology Lab, VIB Center for Inflammation Research, Brussels, Belgium.
13 Laboratory of Cellular and Molecular Immunology, Vrije Universiteit Brussel, Brussels, Belgium.
14 Centre d'Immunophénomique, Aix Marseille Université, INSERM, CNRS, 13288 Marseille, France.
15 Department of Applied Mathematics, Computer Science and Statistics, Ghent University, Ghent, Belgium.
16 Lead Contact
# These authors contributed equally to this work.
*Correspondence :martin.guilliams@irc.vib-ugent.be(MG);charlotte.scott@irc.vib-ugent.be (CLS)

Running Title: ZEB2 preserves tissue-specific identities of macrophages

Non-standard abbreviations:
Mac: Macrophage
KC: Kupffer cell
AM: Alveolar Mac
MG: Microglia
RP: Splenic Red Pulp Mac
PT: Peritoneal Mac
BM: Bone Marrow
cDC: Conventional Dendritic Cell
EMT: Epithelial-Mesenchymal Transition
GMP: Granulocyte-Macrophage progenitor
TF: Transcription Factor

Keywords: Macrophage, Transcription Factor, ZEB2, LXRα, Kupffer Cell, Alveolar Macrophage, Splenic Macrophage, Colon Macrophage Lineage, Microglia, Transcriptional Regulation, Survival, *Clec4f*^{CRE}, Fcgr1^{CRE}.

Highlights

- The transcription factor ZEB2 is highly expressed across the macrophage lineage.
- ZEB2 preserves the tissue-specific identities of macrophages across tissues.
- ZEB2 deficient macrophages are outcompeted by WT counterparts.
- ZEB2 maintains LXRα, which is crucial for Kupffer cell identity.

eTOC Blurb

ZEB2 forms part of the core signature of macrophages across tissues. Scott *et al.* demonstrate that ZEB2 is critical for maintaining the tissue identities of macrophages, with loss of ZEB2 resulting in tissue-specific changes in the transcriptomes of different macrophage populations and the subsequent disappearance of these cells. In KCs, ZEB2 was found to maintain LXRα expression, loss of which is sufficient to reproduce the loss of KC identity and KC disappearance.

SUMMARY

Heterogeneity between different macrophage populations has become a defining feature of this lineage. However, the conserved factors defining macrophages remain largely unknown. The transcription factor ZEB2 is best described for its role in epithelial to mesenchymal transition, however its role within the immune system is now being elucidated. We show here that *Zeb2* expression is a conserved feature of macrophages. Using *Clec4f*^{CRE}, *Itgax*^{CRE} and *Fcgr1*^{CRE} mice to target five different macrophage populations, we found that loss of ZEB2 results in macrophage disappearance from the tissues, coupled with their subsequent replenishment from bone-marrow precursors in open niches. Mechanistically, we found that ZEB2 functions to maintain the tissue-specific identities of macrophages. In Kupffer cells, ZEB2 achieved this by regulating expression of the transcription factor LXRα, removal of which recapitulated the loss of Kupffer cell identity and disappearance. Thus, ZEB2 expression is required in macrophages to preserve their tissue-specific identities.

INTRODUCTION

Macrophages (macs) were first described over a century ago as cells essential for host defense. In recent years, the macrophage field has undergone a conceptual revolution. Two main findings have arisen from this; firstly it is now clear that, in mouse models, these cells typically arise during embryogenesis from either yolk-sac macs or fetal liver monocytes and in most tissues then self-maintain throughout life (Bain *et al*., 2014; Ginhoux and Guilliams, 2016; Gomez Perdiguero *et al*., 2015; Guilliams *et al*., 2013; Hashimoto *et al.,* 2013; Hoeffel *et al*., 2015; Yona *et al*., 2013). In a selection of tissues including the heart, gut and the dermis this self-maintenance is abrogated resulting in the continual replenishment of these macs from bone marrow (BM) monocytes (Bain *et al*., 2013; Epelman *et al*., 2014; Molawi *et al*., 2014; Tamoutounour *et al*., 2013). Importantly however, life-span cannot be inferred from mac origin as BM monocytes can differentiate into *bona-fide* long-lived self-renewing macs as has been shown in the liver (Scott *et al*., 2016b) and the alveolar space (van de Laar *et al*., 2016). Secondly, it is now evident that macs across different organs of the body are highly heterogeneous, with each mac population having its own unique transcriptional and chromatin landscape (Gautier *et a*l., 2012; Gosselin *et al*., 2014; Lavin *et al*., 2014; Mass *et al.,* 2016; Scott *et al*., 2016b; T'Jonck *et al*., 2018). This heterogeneity is present despite the fact that all mac populations arise from a limited number of progenitor types, indicating a substantial role for the local mac niche in driving mac phenotypes (Guilliams and Scott, 2017). Mac heterogeneity is also thought to underlie the contribution of macs to tissue homeostasis, as macs have been shown to perform different 'accessory functions' in their specific tissues of residence (Okabe and Medzhitov, 2016). For example, alveolar macs (AMs) in the alveolar space play a role in lipid metabolism preventing the buildup of excess surfactant proteins (Remmerie and Scott, 2018). Research has recently been focused on understanding the heterogeneity of macs from one tissue to another, but it remains largely unknown if macs also require some conserved factors for their macrophage identity, irrespective of their tissue of residence. While high expression of the transcription factor (TF) PU.1 (Monticelli and Natoli,

2017) and dependence on signaling through the CSF1R either via CSF1 (Gow *et al*., 2014; Hume *et al*., 1988; Tagliani *et al*., 2011) or, in the case of microglia and Langerhans cells, via IL-34 (Wang *et al*., 2012) are characteristic features of the mac lineage, not much else is known regarding additional conserved TFs that drive and maintain this entire lineage of myeloid cells. Zinc finger E box binding homeobox 2 (ZEB2, SIP1, ZFXH1B) is a TF best known for its role in epithelial to mesenchymal transition (EMT) and mesenchymal to epithelial transition (MET), in which epithelial cells lose their cellular identity and are converted into mesenchymal cells and *vice versa* (Comijn *et al*., 2001; Vandewalle *et al*., 2005). EMT/MET transitions are crucial in embryonic development, wound healing and cancer (De Craene and Berx, 2013). Mice lacking *Zeb2* are embryonic lethal (Higashi *et al*., 2002; Van de Putte *et al*., 2003), while patients with heterozygous abnormalities in *Zeb2* expression often develop Hirschsprung's disease and Mowat-Wilson syndrome (Vandewalle *et al*., 2009). In addition to EMT/MET, ZEB2 has been implicated in development of the nervous system (Hegarty *et al*., 2015) and mouse melanocyte differentiation (Denecker *et al*., 2014). In the immune system, it has recently been reported that ZEB2 functions to regulate NK cell maturation (van Helden *et al*., 2015), the terminal differentiation of $CD8^+$ effector T cells (Dominguez *et al*., 2015; Omilusik *et al*., 2015) and we and others have reported a role for ZEB2 in the differentiation and development of pDCs and cDC2s (Scott *et al*., 2016a; Sichien *et al*., 2017; Wu *et al*., 2016). Additionally, ZEB2 has been suggested to play a role in controlling the fate of the Granulocyte-Macrophage progenitor (GMP) with mice lacking ZEB2 ($Mx1^{CRE}$x$Zeb2^{fl/fl}$) having reduced numbers of $Ly6C^{hi}$ monocytes but concomitantly increased neutrophil development (Wu *et al*., 2016). Here, we examined *Zeb2* expression in a variety of mac populations and show that high expression of *Zeb2* is a conserved feature of the mac lineage. Furthermore, through the generation of Kupffer Cell specific CRE ($Clec4f^{CRE}$) mice and $Fcgr1^{CRE}$ mice and the use of $Itgax^{CRE}$ mice, we found that loss of ZEB2 in five different macs resulted in the loss of their tissue identities and their subsequent disappearance. More specifically, we found that ZEB2 functions to maintain KC identity, at least in part, by regulating expression of the TF LXRα (*Nr1h3*).

RESULTS

Zeb2 expression is conserved across the macrophage lineage

Although recent work has demonstrated that macs represent a highly heterogeneous lineage (Gautier *et al*., 2012; Lavin *et al*., 2014; Scott *et al*., 2016b), we sought here to identify TFs conserved across the mac lineage. To this end, we compiled data from previously published studies performed by the Immgen Consortium (Ericson *et al*., 2014; Gautier *et al*., 2012; Heng *et al*., 2008; Miller *et al*., 2012; Painter *et al*., 2011), our previously published studies (Scott *et al*., 2016b; van de Laar *et al*., 2016) and data generated during this study, thus including additional mac populations not previously included in similar analyses. This comparison yielded a list of 67 core mac genes (Figure S1A). Included in this list are genes previously ascribed to the mac lineage including *Fcgr1, Mertk* and *Cd14* (Gautier *et al*., 2012; Guilliams *et al*., 2016). Interestingly, the TF *Zeb2* was also included in this list of core mac genes. While this TF has also recently been identified as a core gene in pre-macs (Mass *et al*., 2016), its precise role within the mac lineage has not yet been investigated. Thus, here we next sought to examine this.

Loss of ZEB2 in KCs and AMs results in an altered phenotype

Given that $Zeb2^{-/-}$ mice are embryonic lethal (Higashi *et al*., 2002; Van de Putte *et al*., 2003) we utilized CRE-LOX systems to specifically remove *Zeb2* expression from different mac subsets. Based on *Zeb2* expression levels (Figure S1A), we first examined the effects of ZEB2 loss in KCs (higher *Zeb2*) and AMs (lower *Zeb2*). Having recently shown that the C-type lectin, CLEC4F, is exclusively expressed by murine KCs (Scott *et al.,* 2016b) and because KCs are poorly targeted by other available CREs, we generated $Clec4f^{CRE}$ mice by introducing an internal ribosome entry site (IRES) and iCRE recombinase (Shimshek *et al*., 2002) into the 3' untranslated region of the *Clec4f* gene. Crossing these mice to the Rosa26-lox-stop-lox-RFP

reporter line revealed 4.81±3.83% of total live liver cells expressed RFP (Figure S1B). Further analysis of these mice revealed that the majority were CD64$^+$F4/80$^+$CLEC4F$^+$TIM4$^+$ KCs with 89.14±3.31% of KCs expressing RFP (Figure S1C-E). However, a minor population of B cells, despite lacking expression of CLEC4F, were also found to express RFP, accounting for 2.34±0.15% of total B cells (Figure S1C-E). Analysis of RFP-expressing cells across tissues in these mice revealed a minor population of B cells in all tissues expressing RFP (Figure S1B). Despite this minor contamination, we concluded that thes mice represent a good model to efficiently target KCs and thus we crossed them to Zeb2$^{fl/fl}$ mice to study the consequences of deleting ZEB2 in KCs. Interestingly, analysis of the mac compartment in the liver of *Clec4f*^{CRE}x*Zeb2*$^{fl/fl}$ mice revealed that although there was no significant difference in the absolute number of total CD64$^+$F4/80$^+$ hepatic macs compared with Zeb2$^{fl/fl}$ littermate controls (Figure 1A), there was a difference in their surface phenotype, with *Clec4f*^{CRE}x*Zeb2*$^{fl/fl}$ mice having a reduced populations of Clec4F$^+$Tim4$^+$ KCs and increased populations of Clec4F$^+$Tim4$^-$ KCs and Clec4F$^-$Tim4$^-$ macs (Figure 1A). This suggests that ZEB2 may be important for KCs and also highlights the importance of examining tissue-specific macrophage markers.

As ZEB2 appears to play a role in KCs, we next examined if it also was required by AMs. To remove ZEB2 from AMs, we made use of *Itgax*^{CRE} mice, which efficiently target AMs alongside a number of other CD11c-expressing cells (Durai and Murphy, 2016). By crossing the *Itgax*^{CRE} mice to Rosa26-lox-stop-lox-RFP reporters we first confirmed that AMs are efficiently targeted (92.32±2.35%) in these mice (Figure S1F). Subsequent analysis of the total AM population in *Itgax*^{CRE}x*Zeb2*$^{fl/fl}$ and *Zeb2*$^{fl/fl}$ littermate controls (defined as F4/80$^+$CD64$^+$CD11c$^+$SiglecF$^+$) revealed a slight but significant reduction in AMs (Figure 1B). In addition, the loss of ZEB2 from CD11c-expressing cells also significantly altered the surface phenotype of the remaining AMs with a significant proportion expressing CD11b in the absence of ZEB2 (Figure 1B).

Presence of ZEB2$^{+/-}$ cells in the lung and the liver

To understand how *Zeb2* expression was affecting mac numbers and phenotype, we performed single cell RNA sequencing analysis (SC-RNA-Seq) on total KCs (Clec4F$^+$CD64$^+$F4/80$^+$) and total AMs (CD64$^+$F4/80$^+$SiglecF$^+$CD11c$^+$) from *Clec4f*^{CRE}x*Zeb2*$^{fl/fl}$ or *Itgax*^{CRE}x*Zeb2*$^{fl/fl}$ mice compared with *Zeb2*$^{fl/fl}$ littermate controls. Following pre-processing of the data using the Marioni pipeline (Lun *et al.*, 2016), poor quality (low UMI counts, high mitochondrial genes), contaminating (doublets) and actively proliferating cells were excluded (Figure S1G) and t-SNE plots with both CRE$^-$ and CRE$^+$ cells combined for KCs and AMs were generated (Figure 1C,D). Interestingly, this revealed the presence of multiple populations of CRE$^+$ cells in both the KCs and AMs. To begin to assess what these distinct populations were, we initially grouped thes clusters into groups based on their genotype. For the KCs, this led to the identification of 1 group of CRE$^-$ cells (consisting of clusters 0,2,4,7, herein referred to as group 0) and 3 distinct groups of CRE$^+$ cells (cluster 6=group 1, cluster 5=group 2 and clusters 1+3=group3) (Figure 1C). For the AMs, we identified 1 group of CRE$^-$ cells (Group 0) consisting of clusters 0,2,5,8, one group of mixed CRE$^-$ and CRE$^+$ cells (Group 1= cluster 6), and three groups of CRE$^+$ cells (group 2=cluster 3, group 3=clusters 1+4 and group 4=cluster 7) (Figure 1D). Next, we examined *Zeb2* expression between the groups. However, as the Zeb2$^{fl/fl}$ construction generates a truncated form of the mRNA lacking the 7th exon but possessing the same 3' end, it is not possible to determine which cells express full-length mRNA and which cells expressed the floxed mRNA with the 3' Assay from 10X Genomics. As such, we were unable to conclude based on *Zeb2* expression if these cells had all efficiently deleted *Zeb2*. Instead, a group of CRE$^+$ cells appeared to have increased its expression of *Zeb2* in each organ (Figure 1E,F). Thus, we next sought to find markers that could distinguish the different CRE$^+$ populations by flow cytometry, to enable their further analysis. To this end, we next determined the DE genes between these groups. For the KCs, this generated a list of 224 DE genes for Group 0, 180 for Group 1, 534 for Group 2 and 693 for Group 3 (Figure 1G & Table S1) and identified SiglecF and CD20 (*Ms4a1*) to be markers that could potentially be used to distinguish between the groups of CRE$^+$ cells (Figure 1E). For the AMs, this analysis identified 821 DE genes in Group 0, 312 for Group 1, 230 for Group 2, 929 for Group 3 and 883 in Group

4 (Figure 1H & Table S2) and identified CD326 (*Epcam*) and CD10 as two markers which could distinguish between the groups of CRE^{+} cells (Figure 1F).
Having identified potential markers, we next examined expression of these by flow cytometry. While not expressed by KCs from littermate *Zeb2*$^{fl/fl}$ mice, SiglecF and CD20 were found to be expressed by a proportion of KCs in *Clec4f*^{CRE}xZeb2$^{fl/fl}$ mice at 6 weeks of age (Figure 2A). qRT-PCR analysis for *Zeb2* in SiglecF^{+}, SiglecF^{-}Tim4^{+} and SiglecF^{-}Tim4^{-} KCs (corresponding to Group 3, Group 1 and Group 2, respectively) revealed that SiglecF^{+} KCs had efficiently deleted *Zeb2*; while SiglecF^{-} cells maintained expression of *Zeb2* at levels comparable with KCs isolated from Zeb2$^{fl/fl}$ control mice, irrespective of Tim 4 expression (Figure 2B and data not shown). Similarly, analysis of EpCam and CD101 expression in AMs from *Itgax*^{CRE}x*Zeb2*$^{fl/fl}$ mice identified two populations, those expressing EpCam and CD101 and those negative for both markers, with only the latter population being observed in AMs from Zeb2$^{fl/fl}$ mice (Figure 2C). Again, qRT-PCR analysis determined that only the EpCam^{+}CD101^{+} AMs had efficiently deleted *Zeb2* (Figure 2D). As there is no good antibody to detect ZEB2 by flow cytometry, we made use of the prime flow assay which measure *Zeb2* mRNA expression by flow cytometry to confirm the qRT-PCR analysis at the single cell level. This confirmed our findings that SiglecF^{+} KCs and EpCam^{+} AMs had all efficiently deleted *Zeb2* (Figure 2E,F). Genomic PCR on the distinct populations of KCs and AMs identified the SiglecF^{-} KCs and EpCam^{-} AMs as being heterozygous for the *Zeb2* deletion (Figure S2A,B), indicating that for an unknown reason, these cells are able to preserve one copy of *Zeb2*. Returning to the SC-RNA-Seq analysis, we could then identify Group 0 in each tissue to be *Zeb2*$^{+/+}$ macs from the CRE^{-} mice and Group 3 in each tissue to represent *bona fide Zeb2*$^{-/-}$ macs from the CRE^{+} mice. Interestingly, Group 3 was the population in each tissue expressing higher levels of *Zeb2* according to the SC-RNA-Seq data, suggesting that a feedback mechanism may be in place in the *Zeb2*$^{-/-}$ macs, where these cells attempt to increase the expression of the truncated *Zeb2* mRNA. As we have recently shown that Tim4 expression on KCs correlates with the time these cells have spent in the tissue (Scott et al., 2016b), we next defined Group 1 KCs which lacked expression of *Siglecf* and expressed *Timd4* as long-lived *Zeb2*$^{+/-}$ KCs, while Group 2 KCs which lacked expression of *Siglecf* and *Timd4*, but which expressed *Cx3cr1* and *Ccr2* wer defined as Zeb2$^{+/-}$ putative moKCs that had recently entered the tissue. In the AMs, the minor population Group 1 contains both CRE^{-} Zeb2$^{+/+}$ and some CRE^{+} *Zeb2*$^{+/-}$ cells. Analysis of the DE genes by IPA suggested that this minor population had an oxidative stress & unfolded protein response signature, which caused them to fall in a separate cluster (data not shown). Group 2 were identified as *Zeb2*$^{+/-}$ cells lacking expression of *Epcam* and *Cd101* and the minor Group 4 were (alongside the main Group 3) also identified as Zeb2$^{-/-}$ cells expressing *Epcam* and *Cd101*. Analysis of the DE genes between Groups 3 and 4 found that these cells clustered separately from the Group 3 *Zeb2*$^{-/-}$ cells due to their increased expression of MHCII pathway associated genes (Figure 1H). This suggests that these may represent cells that arise from monocytes, as increased MHCII expression has been reported on monocyte-derived AMs (van de Laar *et al*., 2016).

ZEB2$^{+/-}$ macrophages outcompete their Zeb2$^{-/-}$ counterparts with time

Having identified a *Zeb2*$^{+/-}$ of macs amongst both the AMs and KCs in the CRE^{+} mice, we next sought to investigate the maintenance of this population with age. We hypothesized that if *Zeb2* expression was critical for macs, then one would expect that the *Zeb2*$^{+/-}$ population would outcompete the *Zeb2*$^{-/-}$ population with time. Thus, we tracked the presence of the SiglecF^{+}CD20^{int}*Zeb2*$^{-/-}$ KC and CD101^{+}EpCam^{+}*Zeb2*$^{-/-}$ AM populations at 6 and 12 weeks of age. We found that both *Zeb2*$^{-/-}$ KCs (Figure 2A) and *Zeb2*$^{-/-}$ AMs (Figure 2C) were significantly reduced at 12 weeks of age. This reduction in SiglecF^{+} KCs between 6 and 12 weeks of age was confirmed by confocal microscopy (Figure S2C). Moreover, distinct islands of Clec4F^{+}Tim4^{+}SiglecF^{-} and Clec4F^{+}Tim4^{-}SiglecF^{-} KCs were observed at both time-points but were increased in size at 12 weeks. This implies that proliferation of *Zeb2*$^{+/-}$ KCs may represent a mechanism by which these cells expand with age. To investigate if this was occurring, we examined expression of the cell proliferation marker Ki-67 by the different KC populations in

Clec4f^{CRE}x*Zeb2*$^{fl/fl}$ mice. This analysis showed that while *Zeb2*$^{+/+}$ KCs in littermate controls proliferated at a low level (2.71±1.92%), SiglecF^{-} *Zeb2*$^{+/-}$ KCs from *Clec4f*^{CRE}x*Zeb2*$^{fl/fl}$ mice proliferated at significantly higher levels (13.27±5.47%). Conversely, *Zeb2*$^{-/-}$ SiglecF^{+} KCs from *Clec4f*^{CRE}x*Zeb2*$^{fl/fl}$ mice were restricted in their ability to proliferate, being only 4.83±1.88% Ki-67^{+} (Figure S2D,E). We next examined if this also occurred in the lung. Also here, Ki-67 staining revealed that *Zeb2*$^{-/-}$ EpCam^{+} AMs did not proliferate to any great extent (2.36±0.86%), while their *Zeb2*$^{+/-}$ EpCam^{-} counterparts in *Itgax*^{CRE}x*Zeb2*$^{fl/fl}$ proliferated at significantly increased rates (10.40±0.83%) compared with EpCam^{-} Zeb2$^{+/+}$ AMs in littermate controls (4.40±1.26%) (Figure S2F,G). Given this reduced proliferation by *Zeb2*$^{-/-}$ macs, we next sought to determine if this was due to a defect in their ability to proliferate. To this end, we administered CSF-1Fc or PBS to *Clec4f*^{CRE}x*Zeb2*$^{fl/fl}$ mice, a procedure that has been described to induce KC proliferation (Gow *et al*., 2014). *Zeb2*$^{-/-}$ KCs proliferated efficiently in response to CSF-1 (Figure S2H) indicating that loss of *Zeb2* does not block the proliferative capacity of macs, but rather may be required for their maintenance.

Loss of *Zeb2* leads to macrophage disappearance

To examine the idea that loss of *Zeb2* induces macrophage disappearance, we generated BM chimeras in which CD45.1^{+} mice were irradiated and reconstituted with congenic CD45.2^{+} Rosa-26$^{CRE-ERT2}$x*Zeb2*$^{fl/fl}$ BM. Chimeras were made to prevent death of the animals due to *Zeb2* loss in non-hematopoietic cells. Six weeks post reconstitution, mice were administered tamoxifen for 5 days by oral gavage to induce CRE-mediated loss of *Zeb2*. KCs and AMs were then examined 2, 6, 20, 34 and 48 days after the last dose of tamoxifen and expression of CD101 and EpCam (Lung AMs) or SiglecF and CD20 (Liver KCs) in donor-derived CD45.2 cells were assessed (Figure 2G). Controls included both CD45.2 cells from control mice that were not treated with tamoxifen and host CD45.1^{+} WT cells from mice treated with tamoxifen (pooled in Figure 2H,I). In the liver, 12.27±3.88% of donor-derived KCs expressed SiglecF and CD20 2 days post the last dose of tamoxifen and this rose modestly to 15.27±5.55% at day 6. 20 days post the last dose of tamoxifen, SiglecF^{+}CD20^{+} KCs could no longer be detected in the liver implying that the *Zeb2*$^{-/-}$ KCs had disappeared (Figure 2H). This disappearance of *Zeb2*$^{-/-}$ KCs was confirmed by PrimeFlow assay, as by day 20 all *Zeb2*$^{-/-}$ KCs were lost (Figure S2I). In the lung, two days post administration of tamoxifen 26.1±4.23% of CD45.2 donor AMs expressed CD101 and EpCam. This further increased to a maximum of 56.4±2.02% six days post the last dose of tamoxifen. At the later time points examined this dropped to 44.7±7.88% at day 20, 21.22±5.19% at day 34 and 10.78±3.25% at day 48 (Figure 2I). This disappearance of *Zeb2*$^{-/-}$ AMs was also confirmed using the PrimeFlow assay (Figure S2J). Taken together, these results demonstrate that ZEB2 is strictly required for the continued presence of macrophages in tissues and suggest that loss of ZEB2 may result in impaired mac maintenance.

Loss of *Zeb2* from KCs but not AMs, results in their replenishment from BM

As *Zeb2*$^{-/-}$ KCs and AMs were lost with time and as our SC-RNA-Seq data suggested ther may be monocyte-derived macs within both the KC pool (Group 2, Figure 1C,G) and AM populations (Group 4, Figure 1D, H), we next investigated if the *Zeb2*$^{-/-}$ macs were being replenished from the BM or if mac numbers were maintained solely by local proliferation of *Zeb2*$^{+/-}$ counterparts. To examine this, we generated partially-protected chimeras, in which *Clec4f*^{CRE}X*Zeb2*$^{fl/fl}$, *Itgax*^{CRE}X*Zeb2*$^{fl/fl}$ or Zeb2$^{fl/fl}$ littermate controls were irradiated with their livers or lungs protected to avoid any radiation damage and reconstituted with congenic CD45.1 WT BM (Figure 3A). Four weeks later, we examined the proportion of CD45.1^{+} cells within the blood monocytes and KCs in the liver (defined as Clec4F^{+}) or AMs in the lung (defined as CD11c^{+}SigleF^{+}). As the mice were partially protected from irradiation, the animals were between 30-50% chimeric (calculated by examining chimerism in blood Ly6C^{hi} monocytes). Comparison of the chimerism between the blood monocytes and liver KCs found that KCs were chimeric and thus a significant fraction of cells were of BM origin (Figure 3B). However, lung AMs displayed very low levels of chimerism (Figure 3C), suggesting that there is little contribution of the BM to the AM pool, fitting with our niche hypothesis where BM

monocytes would not be able to gain significant access to the lung in adult mice due to the epithelial barrier (Guilliams and Scott, 2017). To further investigate how *Zeb2*$^{-/-}$ macs were being lost and replaced by *Zeb2*$^{+/-}$ counterparts, we next questioned whether the macs wer eddying in the absence of ZEB2. Thus, we examined expression of a number of genes associated with distinct cell death pathways in our SC-RNA-Seq analysis. While a number of these genes were either not expressed or their expression was not altered in *Zeb2*$^{-/-}$ macs, we did observe that *RipK3*, *Il1a* and *Il1b* were upregulated in Zeb2$^{-/-}$ KCs and AMs, suggesting that the loss of *Zeb2* may result in mac death by necroptosis (Figure 3D,E). Moreover, we evaluated the expression of RIPK3 and phosphorylated MLKL (pMLKL) by cells recovered from bronchioalveolar lavage fluid from our inducible *Zeb2* conditional KO chimeras 27 days post the last dose of tamoxifen and compared them to chimeras which received corn oil as a control. Total cells from BAL fluid were used to prevent induction of cell death during the extensive enzymatic digestions required to isolate macs from tissues. This analysis revealed a trend (p=0.06) towards increased pMLKL (Figure 3F). Taken together, our results demonstrate that ZEB2 is critical for the maintenance of KCs and AMS, with *Zeb2*$^{-/-}$ macs being lost from the tissue with time. Furthermore, it suggests that *Zeb2*$^{-/-}$ macs may be lost through necroptotic cell death.

Zeb2 controls tissue specific identity of lung and liver macrophages

Having identified the distinct populations of KCs and AMs present in our conditional KO mice, we next sought to use the SC-RNA-Seq data to determine the mechanism through which loss of *Zeb2* induces the disappearance of macs from tissues. As loss of Zeb2 affects both KCs and AMs, we first looked for the DE genes that were conserved between both mac populations. However, this demonstrated that the majority of DE genes were unique to either the KC (459 DE genes) or AM (701 DE genes) population (Figure 3G). As the gene expression profiles of different tissue macs have been shown to be highly heterogeneous and ZEB2 is known for its role in altering cellular identities in EMT/MET, we next hypothesized that ZEB2 may control the tissue-specific identities of the different mac populations, with its loss rendering the macs less suited to their tissue of residence resulting in their subsequent loss. To examine this, we investigated how the core KC and AM transcriptional profile changed in the absence of ZEB2. However, as additional mac populations have been sequenced since the core profiles of these two macs were first described (Gautier *et al*., 2012; Scot *et al*., 2016b), we first redefined these profiles. To achieve this, we compared the transcriptional profile of AMs, KCs, microglia, peritoneal macs, colonic macs and splenic red pulp macs (Lavin *et al*., 2014) and identified the genes specific to the KCs and AMs (Figure S3). As ther was significant overlap between the transcriptional profiles of KCs and splenic macs, splenic macs were excluded when defining the core profile of KCs and *vice versa*. Furthermore, as these core lists were defined on the basis of bulk RNA seq, which are at risk of containing genes from contaminating cells, we performed an additional control whereby to be considered as a core gene, it must be expressed in at least 20% of our Zeb2$^{fl/fl}$ KCs and AMs profiled by SC-RNA-Seq (Figure S3). This was required because previously reported core macrophage gene lists (Gautier *et al*., 2012; Lavin *et al*., 2014; Scott *et al*., 2016b) contained genes expressed by contaminating cells, for example , a number of endothelial cell genes were included in the previously reported KC core list (Lynch *et al*., 2018). We next compared how expression of the top core genes were altered upon loss of ZEB2 and found that there were significant changes to the core profiles of both mac populations with 60% of the KC tissue-specific genes and 72% of the AM tissue-specific genes affected by the loss of *Zeb2* (Figure 3H, I, highlighted genes are the genes significantly altered by *Zeb2* loss), suggesting ZEB2 may play a role in maintaining the tissue-specific identities of these macs.

Loss of KC identity in absence of ZEB2 is in part due to the loss of LXRα

We next aimed to examine the mechanism through which Zeb2 could control mac tissue-specific identities. For this, we chose to focus on the KCs for which we have the most specific CRE line. The tissue-specific identity of macs has been proposed to be controlled by a small set of tissue-specific TFs (Gautier *et al*., 2012; Gosselin *et al*., 2014; Lavin *et al*., 2014; Mass

et al., 2016; Scott *et al*, 2016b; T'Jonck *et al*. 2018). Interestingly, *Nr1h3* (encoding LXRα) a TF proposed to be required for KC identity (Mass *et al*., 2016) was among the list of DE core KC identity gens in KCs lacking *Zeb2* (Figure 3H). Thus, we hypothesized, that ZEB2 may control KC identity by regulating LXRα expression. LXRα was previously reported to be dispensable for KC development and survival, but this conclusion was based solely on F4/80 and CD68 expression (A-Gonzalez et al., 2013). Therefore, we decided to revisit the effects of loss of *Nr1h3* on KCs. We crossed *Nr1h3*$^{fl/fl}$ mice with *Clec4f*^{CRE} mice generating *Clec4f*^{CRE}xNr1h3$^{fl/fl}$ mice. Analysis of these mice confirmed, as in mice lacking *Zeb2*, and as previously reported (A-Gonzalez *et al*., 2013), that the loss of *Nr1h3* did not significantly affect the proportion or absolute number of total hepatic CD64^{+}F4/80^{+} macs (Figure 4A). However, as for the loss of *Zeb2*, it did dramatically alter the proportions of cells expressing Clec4F and Tim4 (Figure 4B), again highlighting the need for tissue-specific markers when examining macs. As observed with loss of *Zeb2*, protected chimeras demonstrated that in the absence of *Nr1h3*, KCs were being replaced from a BM source (Figure 4C). As these data fit with the idea that ZEB2 may function to control KC identity through maintaining LXRα expression, we next sought to determine whether the effect of *Zeb2* loss on the KCs transcriptome may reflect loss of LXRα dependent genes. Thus, we performed SC-RNA-Seq of KCs from *Clec4f*^{CRE}x*Nr1h3*$^{fl/fl}$ mice and *Nr1h3*$^{fl/fl}$ littermate controls. Following the same pre-processing analysis as used for the ZEB2 single cell data (Figure S1G), we identified 2 main groups of KCs in the t-SNE plot of CRE^{-} and CRE^{+} cells. Group 0 consisted of *Nr1h3*$^{+/+}$ KCs from the CRE^{-} mice and group 1 consisted of with *Nr1h3*$^{-/-}$ KCs from the CRE^{+} mice (Figure 4D). Mice lacking only one copy of LXRα in their KCs (*Clec4f*^{CRE}x*Nr1h3*$^{fl/+}$) did not display a similar phenotype to *Clec4f*^{CRE}x*Nr1h3*$^{fl/fl}$ mice, suggesting no obvious effect of *Nr1h3* haploinsufficiency on KCs (Figure S4A). Analysis of the DE genes between *Nr1h3*$^{+/+}$ KCs and *Nr1h3*$^{-/-}$ KCs identified 451 DE genes (Figure 4E and Table S3). In accordance with our hypothesis many of thes DE gens were also core KC genes including *Cdh5*, *Pcolce2*, *Kcna2*, *C6* and *Il18bp* (Figure 3H) and were similarly lost upon loss of *Zeb2* (Figure 4E). Moreover, we were able to confirm this downregulation in both *Zeb2*$^{-/-}$ and *Nr1h3*$^{-/-}$ KCs either at the protein level by flow cytometry (CD55; Figure 4F,G) or at the mRNA level by qRT-PCR (Figure S4B,C). As loss of ZEB2 and LXRα led to replacement of the KC pool from the BM, we noticed that a number of the DE genes were also related to origin of the KCs. To remove any DE genes associated with mac origin and hence only examine DE genes resulting from the loss of LXRα or ZEB2, we used our previously published data (Scott et al., 2016b) and identified any DE genes (adj. P value <0.05, Log FC <-1, >1) between moKCs from KC-DTR mice 15 days post treatment with DT and embryonic KCs (Figure S4D). Comparison of the overlap between the remaining non-origin related DE genes associated with the *Zeb2*$^{-/-}$ and *Nr1h3*$^{-/-}$ KCs identified that 203 of the 435 DE genes in *Nr1h3*$^{-/-}$ KCs were conserved in both datasets (Figure 4H), including many of the liver-specific core KC genes. Crucially, while there is a significant overlap between the two genotypes, this is not 100%, indicating that loss of LXRα is not solely responsible for all the DE genes identified in Zeb2$^{-/-}$ KCs. Nonetheless, loss of LXRα is sufficient to recapitulate the loss of KC identity and the disappearance and subsequent replenishment of KCs by BM cells observed in *Clec4f*^{CRE}x*Zeb2*$^{fl/fl}$ mice. Taken together these data demonstrate that ZEB2 controls KC identity and their continued presence in the tissue at least in part by regulating LXRα expression and as such highlights a previously unappreciated role for LXRα in KC biology.

We have recently shown that the phosphatidylserine receptor TIM4 can act as a marker of long-lived KCs, as KCs do not acquire expression of this receptor immediately upon differentiation from BM monocytes (Scott *et al*., 2016b). Rather monocyte-derived KCs (moKCs) acquire TIM4 expression very slowly (Scott *et al*., 2016b) with a small proportion of moKCs remaining TIM4$^-$ 120 days post DT administration in a *Clec4f*-DTR mouse (Figure 2A). As adult *Clec4f*^{CRE}xZeb2$^{fl/fl}$ mice contain many CLEC4F$^+$TIM4$^-$ KCs and CLEC4F$^-$TIM4$^-$ macs this suggests that there may be an accumulation of moKCs, possibly due to continuous death of KCs in the absence of ZEB2. To mimic such a scenario, we crossed *Clec4f*^{CRE} mice to Rosa-DTA mice in which terminally-differentiated KCs express diphtheria toxin and subsequently die. *Clec4f*^{CRE}xRosa-DTA$^{Tg/+}$ mice exhibit a similar pattern of CLEC4F and TIM4 expression amongst total liver macs as observed with the loss of ZEB2 (Figure 2B). As KCs are continuously dying and being replaced in the DTA model, we reasoned that the presence of TIM4- KCs in *Clec4f*^{CRE}xZeb2$^{fl/fl}$ mice could indicate a similar continuous cycling of the KCs in the absence of ZEB2. Additionally, low level chimerism was observed at this early time-point amongst the TIM4$^+$ KCs (Figure 2C), indicating that some KCs of BM origin were persisting in the liver and acquiring TIM4 expression. Taken together, these results suggest that KCs can no longer self-maintain in the absence of ZEB2, and thus require input from the BM to maintain the KC pool. We have previously reported that all mac progenitors (yolk-sac macs, fetal liver monocytes and BM monocytes) initially upregulate CD11b expression during the initial stages of differentiation into AMs (van de Laar *et al*., 2016). As we had also observed an increase in CD11b expression in ZEB2-deficient AMs, we hypothesized that the AM population in *Itgax*^{CRE}xZeb2$^{fl/fl}$ mice may also require input from BM to maintain its numbers. To examine this, we used the same chimera approach as above, only this time protecting the lung. Comparison of the chimerism between the blood monocytes and lung AMs found that almost none of the CD11b$^+$ nor CD11b$^-$ AMs were chimeric thus demonstrating that these cells were not primarily of BM origin but rather that the CD11b$^+$ AMs arise predominantly from the original embryonically derived AM population (Figure 2D).

ZEB2 functions across the mac lineage to maintain the tissue-specific identities

Having shown that ZEB2 is required by KCs and AMs to maintain tissue-specific identities and that Zeb2 is expressed across the entire mac lineage, we next aimed to investigate if this was a requirement across the mac lineage. To examine the role of ZEB2 in additional mac populations including splenic macs, microglia and colonic macs we used the *Fcgr1*^{CRE} line recently generated by the lab of Bernard Malissen. These mice were generated by introducing an IRES, iCRE recombinase (Shimshek *et al*., 2002), a 2A cleaved sequence and a fluorescent reporter known as mTFP1 (Ai et al., 2006) into the 3' untranslated region of the *Fcgr1* gene. Crossing this line to the Rosa26-lox-stop-lox-RFP reporter line revealed that all these macs were efficiently targeted; splenic macs (92.03±2.43%), colonic macs (92.47±1.41%) and microglia (98.93±0.39%) (Figure S5A-D). Notably, however, a number of other immune cells are also targeted in these mice across tissues. For example, in the spleen this includes some penetrance in CD64$^-$ B cells, T cells, cDC1s and cDC2s (Figure S5A).

Analysis of the *Fcgr1*^{CRE}x*Zeb2*$^{fl/fl}$ mice revealed that while ther was no significant change in the proportion or number of the total splenic mac population defined as Lin$^-$CD64$^+$F4/80$^+$ (Figure 5A), there was a significant population of thes macs which gained expression of CD11b in the absence of *Zeb2* (Figure 5A). In addition, we observe a significant reduction in absolute number of microglia (Figure 5B) and *Zeb2*$^{-/-}$ microglia were found to upregulate their expression of CD11c (Figure 5B). To examine if ZEB2 also functions in the maintenance of BM monocyte-derived macs, we next examined if ZEB2 was also required in colonic macs which are constantly replaced by BM monocytes during adulthood along a trajectory dubbed the 'monocyte-waterfall' (Bain *et al*., 2014; 2013; Tamoutounour *et al*., 2012). Analysis of the monocyte-waterfall in *Fcgr1*^{CRE}x*Zeb2*$^{fl/fl}$ mice identified a significant reduction in the number of mature colonic macs alongside a significant increase in the proportion and number of Ly6C$^+$MHCII$^+$ transitioning monocytes (Figure 5C). To determine if these changes in phenotype and number reflected changes in the tissue-specific identities of these macs, we next performed SC-RNA-Seq analysis on splenic macs, microglia and colonic macs from

Zeb2$^{fl/fl}$ and *Fcgr1*^{CRE}x*Zeb2*$^{fl/fl}$ mice. Following the same pre-processing as described for the KCs and AMs (Figure S1G), we used expression of *Zeb2*, *Ms4a1*, *Siglecf*, *Cd101* or *Epcam* (the markers used to identify *Zeb2*$^{-/-}$ macs in the lung and liver) to identify *Zeb2*$^{-/-}$ macs in the spleen, brain and colon (Figure 6). Note that, as was observed for the lung and liver, the *Zeb2*$^{-/-}$ macs in the spleen, brain and colon expressed higher levels of *Zeb2*, again suggesting a feedback mechanism in the *Zeb2*$^{-/-}$ macs as these cells seem to increase the expression of the truncated *Zeb2* mRNA (Figure 6). We identified 3 main groups of cells in the splenic macs (Group 0; *Zeb2*$^{+/+}$ macs from the CRE^{-} mice, Group1; presumably *Zeb2*$^{+/-}$ macs from the CRE^{+} mice clustering close to the *Zeb2*$^{+/+}$ macs from the CRE^{-} mice and Group 2; *Zeb2*$^{-/-}$ macs from the CRE^{+} mice clustering separately and expressing higher levels of *Zeb2*, *Siglecf* and *Epcam*) (Figure 6A). In addition, we identified 2 groups of cells in the microglia (Group 0; *Zeb2*$^{+/+}$ macs from the CRE^{-} mice and Group 1; *Zeb2*$^{-/-}$ macs from the CRE^{+} mice expressing higher *Zeb2*, *Siglecf* and *Cd101*) (Figure 6B). All microglia from the CRE^{+} mice clustered together and uniformly expressed higher *Zeb2*, *Siglecf* and *Cd101*, suggesting no presence of *Zeb2*$^{+/-}$ microglia in the brain. While we performed the SC-RNA-Seq analysis on total colonic macs (Figure 6C), we found these could be divided into two main groups of cells, those expressing high levels of *Cd74* (coding for the MHCII-associated invariant chain), *H2-Aa*, *H2-Eb1* and *Itgax* (coding for CD11c) and those expressing low levels of *Cd74* (Figure 6C). As all the Zeb2$^{-/-}$ cells (identified by higher *Zeb2*, *Ms4a1* and *SiglecF*) expressed high levels of *Cd74* (Figure 6D) and as the gene expression profiles of the *Cd74*^{hi} and *Cd74*^{lo} *Zeb2*$^{+/+}$ subsets of colonic macs from CRE^{-} mice were distinct (Figure S6), we chose to focus our analysis on the comparison between *Cd74*^{hi} *Zeb2*$^{+/+}$ macs and *Cd74*^{hi} *Zeb2*$^{-/-}$ macs (Figure 6D). An additional reason is that previous studies have also focused on *CD74*^{hi} intestinal macs (Lavin *et al*., 2014; Zigmond *et al*., 2012). Within *CD74*^{hi} macs, we identified 2 main groups of cells (Group 0; containing a mix of *Zeb2*$^{+/+}$ macs from the CRE^{-} mice and presumably *Zeb2*$^{+/-}$ macs from the CRE^{+} mice clustering together, and Group 1; containing *Zeb2*$^{-/-}$ macs from the CRE^{+} mice expressing higher *Zeb2*, *Ms4a1* and *SiglecF*) (Figure 6D).

To examine if the core profiles of these macs had been altered by the loss of *Zeb2*, we next determined the core profiles of these macs as described above using data from Lavin *et al*. (Lavin., 2014) (Figure S7A-C). Again, due to the overlap between liver KCs and splenic macs, KCs were excluded from the comparison when defining the core profile of splenic macs. Having defined the core profiles, we next examined the expression of these genes in *Zeb2*$^{-/-}$ macs in each tissue. As for the liver and lung, this revealed that the core profiles of the different macs were significantly altered in the absence of *Zeb2* with a significant number of core genes being altered in the *Zeb2*$^{-/-}$ mac (60% in splenic macs and microglia and 76% in colonic macs; highlighted genes in Figure 7A-C). Examples of significantly DE identity genes include *Vcam1* and *Hmox1* in the splenic macs, *Sparc* and *Hexb* in the microglia and *Apol7c* and *Ms4a7* in the colonic macs (Figure 7A-C). Consistent with the data from the liver and lung (Figure 2G-I), *Zeb2*$^{-/-}$ splenic macs were also found to disappear with time in mice in which Zeb2 loss was induced by tamoxifen administration (Figure S7D,E). The brain and colon were unfortunately not assessed but the conserved effects in the liver, lung and spleen strongly suggests that loss of *Zeb2* induces mac disappearance across tissues.

To further confirm that the loss of ZEB2 results in tissue-specific changes, we next examined the overlap between the DE genes in the 5 tissues (Tables S1,2,4,5 & 6). Generation of a single t-SNE file containing all *Zeb2*$^{+/+}$ and *Zeb2*$^{-/-}$ macs from the 5 tissues studied (Figure 7D) demonstrated that loss of Zeb2 did not direct the cells from each tissue along a single component in the tSNE graph, suggesting the changes were predominantly tissue-specific. In support of this, we found that the majority of DE genes were specifically altered in only one of the 5 tissues (Figure 7E) and only 32 DE genes were shared by all tissues (Figure 7E,F). Taken together, these data highlight that loss of *Zeb2* has a striking tissue-specific effect on mac identity.

DISCUSSION

TFs are at the core of lineage specification and commitment through regulation of gene expression. TFs can function at various stages in a cell, during development and/or in the maintenance of the terminally-differentiated cells as well as in controlling specific cellular functions. While a number of TFs have recently been identified in specific mac populations including ID3 in KCs (Mass *et al*., 2016), PPARγ in AMs (Schneider *et al*., 2014) and GATA6 in peritoneal macs (Lavin *et al*., 2014; Okabe and Medzhitov, 2014), the TFs governing the entire mac lineage remain to be fully investigated. One TF required for the development of the mac lineage is PU.1 which interacts with a number of other TFs, including members of the Fos-Jun AP1 family (Dahl *et al*., 2003; Monticelli and Natoli, 2017; Rojo *et al*., 2017). Here we report that ZEB2 is highly expressed in macs across tissues, including the lung, liver, spleen, intestine and brain. In addition, *Zeb2* has been reported to already be expressed in the embryonic pre-mac precursors (Mass *et al*., 2016). Our data indicate that ZEB2 is required to maintain the cellular identity of macrophages with is loss leading to disappearance of the macrophages from all tissues studied. Therefore, just as ZEB2 controls cell identity in EMT/MET (Comijn *et al*., 2001; De Craene and Berx, 2013; Vandewalle *et al*.,2005), it is essential for the maintenance of the mac identity across tissues.

SC-RNA-Seq analysis of the different mac populations revealed that ZEB2 was often not efficiently deleted in all macs using the two distinct CRE models we employed, with *Zeb2*$^{-/-}$ and *Zeb2*$^{+/-}$ populations being observed in all tissues except for the brain. The mechanism by which some *Zeb2*$^{+/-}$ macs can retain one unfloxed *Zeb2* allele remains unclear and requires further investigation. *Zeb2*$^{-/-}$ macs were distinguished from *Zeb2*$^{+/-}$ counterparts within the same mouse on the basis of their phenotype. KCs expressed SiglecF and CD20 (encoded by *Ms4a1*) following loss of ZEB2, while AMs expressed CD101 and EpCam. Interestingly, these markers, although not conserved between all the mac populations studied here, were conserved in a number of the populations (*Siglecf*; Liver, Brain, Spleen and Colon, *Cd101*; Brain, Lung, *Ms4a1*; Liver, Spleen and Colon, *Epcam*; Lung and Colon) and with ZEB2-deficient cDC2s (Scott *et al*., 2016a) suggesting that ZEB2 expression may be linked with the repression of a set of surface receptors. SiglecF and CD101 expression has recently been reported on CD103^{+} cDC2s in the small intestine (Bain *et al*., 2017). Remarkably, this subset of cDC2s exists independently of ZEB2 expression (Scott *et al*., 2016a; Sichien *et al*., 2017) further suggesting that expression of these markers is repressed by ZEB2. However, it was not through these markers that we first determined an effect of loss of ZEB2 expression in KCs and AMs. Rather, we noted a loss of Tim4 expression in Clec4F^{+} KCs and an increase in Clec4F^{-} macs within total F4/80^{+}CD64^{+} hepatic macs, an increase in CD11b expression in AMs and splenic macs, an increase in CD11c in microglia and an increased turnover rate of macs in the colon. This highlights the importance of looking at the tissue-specific mac markers and not just F4/80 or CD64 when examining different mac populations.

In terms of understanding mac ontogeny we recently proposed the mac niche hypothesis, whereby the local mac niche would determine if any given progenitor could engraft and develop into a mac or not (Guilliams and Scott, 2017). We suggested that niche availability and niche accessibility would be the two main factors determining mac ontogeny. Loss of ZEB2 within mature macs induces macrophage disappearance, which creates niche availability. We found that these lost macs are replaced (in part) by cells of BM origin (likely BM monocytes) in the liver, but not significantly in the lung. It is worth noting, however, that we do see a small population of MHCII-expressing AMs in the SC-RNA-Seq analysis and found few BM-derived cells in the chimeras, indicating that a minor fraction of AMs could be replaced by monocytes. This major replacement of KCs but minor replacement of AMs is in line with our niche hypothesis (Guilliams and Scott, 2017) as only the liver mac niches are accessible to progenitors circulating in the blood as liver KCs reside in the bloodstream of the liver sinusoids while the alveolar mac niches are not easily accessible due to the presence of the lung epithelial barrier. Importantly, however, we only see a small reduction in total AM cell number following loss of ZEB2 despite there being very limited replenishment from the BM. This is because the *Zeb2*$^{+/-}$ AMs present are sufficient to refill the niche with time through local

proliferation. Proliferation of *Zeb2*$^{+/-}$ macs also contributes to mac maintenance in the liver. The dual mechanism of replacement in the liver via both BM precursors and local proliferation is consistent with our previous study whereby partial depletion of KCs using the *Clec4f*-DTR mice led to reconstitution of the mac pool via the same two mechanisms (Scott *et al*., 2016b).This highlights the crucial requirement for ZEB2 within the mac lineage as *Zeb2*$^{-/-}$ macs are outcompeted from the mac niche, regardless of the repopulation mechanism.

How does ZEB2 function to maintain the mac lineage? As loss of CSF1R expression has been proposed to be the mechanism behind the failure of *Zeb2*$^{-/-}$ GMPs to commit to the monocyte lineage (Wu *et al*., 2016), one possible hypothesis is that ZEB2 may control mac survival by regulating CSF1R signaling. Consistent with this, CSF1R signaling is absolutely required for KC, microglia, colonic mac and splenic mac but not AM survival (MacDonald *et al*., 2010) and a small downregulation of CSF1R within the *Zeb2*$^{-/-}$ KCs, microglia and colonic macs but not splenic macs or AMs was detected (Tables S1,2,6,7 & 8). However, as *Zeb2*$^{-/-}$ KCs responded to administration of CSF1Fc this implies that CSF1R signaling is still functional in these macs. Rather, we propose that loss of ZEB2 leads to significant alterations in tissue-specific identities of these cells. In KCs, loss of *Zeb2* leads to loss of *Nr1h3* suggesting that one mechanism of action of ZEB2 is to maintain the expression of TFs driving the tissue-specific identities of the different mac populations. We found that loss of LXRα in KCs recapitulated the main traits of *Zeb2*$^{-/-}$ KCs with loss of liver-specific identity and disappearance from the liver, suggesting that downregulation of LXRα is at least in part responsible for the phenotype of *Zeb2*$^{-/-}$ KCs. The mechanisms underlying the control of tissue-specific identities by *Zeb2* in other organs remain to be investigated, but the loss of the TF *Cebpb* in the *Zeb2*$^{-/-}$ AMs (Figure 1G), a TF recently reported to be essential for AMs (Cain *et al*., 2013), suggests that loss of *Zeb2* may also induce the loss of tissue-specific identity by loss of tissue-specific TFs in other macs but this remains to be investigated.

In conclusion, our study highlights that high levels of *Zeb2* expression is a defining characteristic of the mac lineage. ZEB2 is crucial for the maintenance of macs, with its absence leading to dramatic changes in their transcriptional profiles, including loss of roughly 60% of their tissue-specific identities potentially through the decreased expression of tissue-specific TFs, as demonstrated for LXRα in KCs. This loss of identity inevitably results in macrophage disappearance, possibly due to death by necroptosis, identifying ZEB2 as a crucial TF in macrophage biology and LXRα as a master TF in KCs.

AUTHOR CONTRIBUTIONS

Conceptualization: CLS and MG; Methodology: CLS, MG, JB, LM, RC, HT, NT, PDBl, WS, YS; Formal Analysis: CLS, WT, HT, DS, JB, BS, PDBl and LM; Investigation: CLS, WT, DS, JB, BV, SH, BM, SDP, NV, BS and LM; Resources: MG, ABe, BM, JVG, PDBa, GB, DH, CP, NT, PV, BNL and YS; Writing: CLS and MG; Supervision: MG, GB, SWFM and YS.

ACKNOWLEDGEMENTS

We would like to thank Karl Vergote, Gillian Blanke and Joachim Taminau for help with genotyping the various mouse lines used in this study, Gert Van Isterdael from the Flow Cytometry Core Facility for assistance and Professor Allan Mowat for critical reading of the manuscript. This study benefitted from data assembled by the Immgen Consortium. We would also like to thank VIB TechWatch for supporting the 10x genomics installation. We thank F. Fiore, A. Adda-Benatia and F. Danjan for construction of the *Fcgr1-IRES-iCre-TEAL* mice and Anna Baranska for her preliminary characterization of the *FcgR1*^{CRE} line (data not shown). This work was supported by PHENOMIN and European Research Council (FP7/2007–2013 grant n° 322465) to BM, CLS is supported by a Marie Curie Intra-European Fellowship as part of Horizon 2020 and a Sir Henry Wellcome Postdoctoral Fellowship. JB is supported by an FWO Postdoctoral fellowship. BS is supported by an FWO PhD fellowship. SWFM is supported by the Medical Research Council and Arthritis UK. GB's laboratory is supported by the FWO, GOA-Ghent University, and the Belgian Federation for the Study Against Cancer. YS's lab is

supported by the FWO and YS is a Marylou Ingram Scholar. MG's lab is supported by the FWO and an ERC Consolidator grant.

CONFLICTS OF INTEREST

The authors declare no conflict of interest.

REFERENCES

A-Gonzalez, N., Guillen, J.A., Gallardo, G., Diaz, M., la Rosa, de, J.V., Hernandez, I.H., Casanova-Acebes, M., opez, F., Tabraue, C., Beceiro, S., Hong, C., Lara, P.C., Andujar, M., Arai, S., Miyazaki, T., Li, S., Corbí, A.L., ontonoz, P., Hidalgo, A., Castrillo, A., 2013. The nuclear receptor LXRα controls the functional specialization of splenic macrophages. Nat Immunol 14, 831–839. doi:10.1038/ni.2622

Ai, H.-W., Henderson, J.N., Remington, S.J., Campbell, R.E., 2006. Directed evolution of a monomeric, bright and photostable version of Clavularia cyan fluorescent protein: structural characterization and applications in fluorescence imaging. Biochem J 400, 531–540. doi:10.1042/BJ20060874

Bain, C.C., Bravo-Blas, A., Scott, C.L., Gomez Perdiguero, E., Geissmann, F., Henri, S., Malissen, B., Osborne, L.C., Artis, D., Mowat, A.M., 2014. Constant replenishment from circulating monocytes maintains the macrophage pool in the intestine of adult mice. Nat Immunol. doi:10.1038/ni.2967

Bain, C.C., Montgomery, J., Scott, C.L., Kel, J.M., Girard-Madoux, M.J.H., Martens, L., Zangerle-Murray, T.F.P., Ober-Blöbaum, J., Lindenbergh-Kortleve, D., Samsom, J.N., Henri, S., Lawrence, T., Saeys, Y., Malissen, B., Dalod, M., Clausen, B.E., Mowat, A.M., 2017. TGFβR signalling controls CD103(+)CD11b(+) dendritic cell development in the intestine. Nat Commun 8, 620. doi:10.1038/s41467-017-00658-6

Bain, C.C., Scott, C.L., Uronen-Hansson, H., Gudjonsson, S., Jansson, O., Grip, O., Guilliams, M., Malissen, B., Agace, W.W., Mowat, A.M., 2013. Resident and proinflammatory macrophages in the colon represent alternative context-dependent fates of the same Ly6Chi monocyte precursors. Mucosal immunology 6, 498–510. doi:10.1038/mi.2012.89

Broos, S., Soete, A., Hooghe, B., Moran, R., van Roy, F., De Bleser, P., 2013. PhysBinder: Improving the prediction of transcription factor binding sites by flexible inclusion of biophysical properties. Nucleic Acids Res. 41, W531–4. doi:10.1093/nar/gkt288

Cain, D.W., O'Koren, E.G., Kan, M.J., Womble, M., Sempowski, G.D., Hopper, K., Gunn, M.D., Kelsoe, G., 2013. Identification of a tissue-specific, C/EBPβ-dependent pathway of differentiation for murine peritoneal macrophages. The Journal of Immunology 191, 4665–4675. doi:10.4049/jimmunol.1300581

Cannoodt, R., Saelens, W., Sichien, D., Tavernier, S., Janssens, S., Guilliams, M., Lambrecht, B.N., De Preter, K., Saeys, Y., 2016. SCORPIUS improves trajectory inference and identifies novel modules in dendritic cell development. doi:10.1101/079509

Caton, M.L., Smith-Raska, M.R., Reizis, B., 2007. Notch-RBP-J signaling controls the homeostasis of CD8- dendritic cells in the spleen. J Exp Med 204, 1653–1664. doi:10.1084/jem.20062648

Comijn, J., Berx, G., Vermassen, P., Verschueren, K., van Grunsven, L., Bruyneel, E., Mareel, M., Huylebroeck, D., van Roy, F., 2001. The two-handed E box binding zinc finger protein SIP1 downregulates E-cadherin and induces invasion. Mol Cell 7, 1267–1278.

Dahl, R., Walsh, J.C., Lancki, D., Laslo, P., Iyer, S.R., Singh, H., Simon, M.C., 2003. Regulation of macrophage and neutrophil cell fates by the PU.1:C/EBPalpha ratio and granulocyte colony-stimulating factor. Nature Immunology 4, 1029–1036. doi:10.1038/ni973

De Craene, B., Berx, G., 2013. Regulatory networks defining EMT during cancer initiation and progression. Nat. Rev. Cancer 13, 97–110. doi:10.1038/nrc3447

Denecker, G., Vandamme, N., Akay, O., Koludrovic, D., Taminau, J., Lemeire, K., Gheldof, A., De Craene, B., Van Gele, M., Brochez, L., Udupi, G.M., Rafferty, M., Balint, B., Gallagher, W.M., Ghanem, G., Huylebroeck, D., Haigh, J., van den Oord, J., Larue, L., Davidson, I., Marine, J.-C., Berx, G., 2014. Identification of a ZEB2-MITF-ZEB1 transcriptional network that controls melanogenesis and melanoma progression. Cell Death Differ. 21, 1250–1261. doi:10.1038/cdd.2014.44

Dominguez, C.X., Amezquita, R.A., Guan, T., Marshall, H.D., Joshi, N.S., Kleinstein, S.H., Kaech, S.M., 2015. The transcription factors ZEB2 and T-bet cooperate to program cytotoxic T cell terminal differentiation in response to LCMV viral infection. J Exp Med 212, jem.20150186–2056. doi:10.1084/jem.20150186

Durai, V., Murphy, K.M., 2016. Functions of Murine Dendritic Cells. Immunity 45, 719–736. doi:10.1016/j.immuni.2016.10.010

Epelman, S., Lavine, K.J., Beaudin, A.E., Sojka, D.K., Carrero, J.A., Calderon, B., Brija, T., Gautier, E.L., Ivanov, S., Satpathy, A.T., Schilling, J.D., Schwendener, R., Sergin, I., Razani, B., Forsberg, E.C., Yokoyama, W.M., Unanue, E.R., Colonna, M., Randolph, G.J., Mann, D.L., 2014. Embryonic and Adult-Derived Resident Cardiac Macrophages Are Maintained through Distinct Mechanisms at Steady State and during Inflammation. Immunity 40, 91–104. doi:10.1016/j.immuni.2013.11.019

Ericson, J.A., Duffau, P., Yasuda, K., Ortiz-Lopez, A., Rothamel, K., Rifkin, I.R., Monach, P.A., ImmGen Consortium, 2014. Gene expression during the generation and activation of mouse neutrophils: implication of novel functional and regulatory pathways. PLoS ONE 9, e108553. doi:10.1371/journal.pone.0108553

Gautier, E.L., Shay, T., Miller, J., Greter, M., Jakubzick, C., Ivanov, S., Helft, J., Chow, A., Elpek, K.G., Gordonov, S., Mazloom, A.R., Ma'ayan, A., Chua, W.-J., Hansen, T.H., Turley, S.J., Merad, M., Randolph, G.J., Immunological Genome Consortium, 2012. Gene-expression profiles and transcriptional regulatory pathways that underlie the identity and diversity of mouse tissue macrophages. Nat Immunol 13, 1118–1128.doi:10.1038/ni.2419

Ginhoux, F., Guilliams, M., 2016. Tissue-Resident Macrophage Ontogeny and Homeostasis. Immunity 44, 439–449. doi:10.1016/j.immuni.2016.02.024 Gomez Perdiguero, E., Klapproth, K., Schulz, C., Busch, K., Azzoni, E., Crozet, L., Garner, H., Trouillet, C., de Bruijn, M.F., Geissmann, F., Rodewald, H.-R., 2015. Tissue-resident macrophages originate from yolk-sac-derived erythro-myeloid progenitors. Nature 518, 547–551. doi:10.1038/nature13989
Gosselin, D., Link, V.M., Romanoski, C.E., Fonseca, G.J., Eichenfield, D.Z., Spann, N.J., Stender, J.D., Chun, H.B., Garner, H., Geissmann, F., Glass, C.K., 2014. Environment drives selection and function of enhancers controlling tissue-specific macrophage identities. Cell 159, 1327–1340. doi:10.1016/j.cell.2014.11.023
Gow, D.J., Sauter, K.A., Pridans, C., Moffat, L., Sehgal, A., Stutchfield, B.M., Raza, S., Beard, P.M., Tsai, Y.-T., Bainbridge, G., Boner, P.L., Fici, G., Garcia-Tapia, D., Martin, R.A., Oliphant, T., Shelly, J.A., Tiwari, R., Wilson, T.L., Smith, L.B., Mabbott, N.A., Hume, D.A., 2014. Characterisation of a novel Fc conjugate of macrophage colonystimulating factor. Mol. Ther. 22, 1580–1592. doi:10.1038/mt.2014.112
Guilliams, M., De Kleer, I., Henri, S., Post, S., Vanhoutte, L., De Prijck, S., Deswarte, K., Malissen, B., Hammad, H., Lambrecht, B.N., 2013. Alveolar macrophages develop from fetal monocytes that differentiate into long-lived cells in the first week of life via GM-CSF. Journal of Experimental Medicine 210, 1977–1992. doi:10.1084/jem.20131199
Guilliams, M., Dutertre, C.-A., Scott, C.L., McGovern, N., Sichien, D., Chakarov, S., Van Gassen, S., Chen, J., Poidinger, M., De Prijck, S., Tavernier, S.J., Low, I., Irac, S.E., Mattar, C.N., Sumatoh, H.R., Low, G.H.L., Chung, T.J.K., Chan, D.K.H., Tan, K.K., Hon, T.L.K., Fossum, E., Bogen, B., Choolani, M., Chan, J.K.Y., Larbi, A., Luche, H., Henri, S., Saeys, Y., Newell, E.W., Lambrecht, B.N., Malissen, B., Ginhoux, F., 2016. Unsupervised High-Dimensional Analysis Aligns Dendritic Cells across Tissues and Species. Immunity 45, 669–684. doi:10.1016/j.immuni.2016.08.015
Guilliams, M., Scott, C.L., 2017. Does niche competition determine the origin of tissue-resident macrophages? Nat Rev Immunol 128, 415. doi:10.1038/nri.2017.42
Hashimoto, D., Chow, A., Noizat, C., Teo, P., Beasley, M.B., Leboeuf, M., Becker, C.D., See, P., Price, J., Lucas, D., Greter, M., Mortha, A., Boyer, S.W., Forsberg, E.C., Tanaka, M., van Rooijen, N., García-Sastre, A., Stanley, E.R., Ginhoux, F., Frenette, P.S., Merad, M., 2013. Tissue-resident macrophages self-maintain locally throughout adult life with minimal contribution from circulating monocytes. Immunity 38, 792–804. doi:10.1016/j.immuni.2013.04.004
Hegarty, S.V., Sullivan, A.M., O'Keeffe, G.W., 2015. Zeb2: A multifunctional regulator of nervous system development. Prog. Neurobiol. 132, 81–95.doi:10.1016/j.pneurobio.2015.07.001
Heng, T.S.P., Painter, M.W., Immunological Genome Project Consortium, 2008. The Immunological Genome Project: networks of gene expression in immune cells. Nat Immunol 9, 1091–1094. doi:10.1038/ni1008-1091
Higashi, Y., Maruhashi, M., Nelles, L., Van de Putte, T., Verschueren, K., Miyoshi, T., Yoshimoto, A., Kondoh, H., Huylebroeck, D., 2002. Generation of the floxed allele of the SIP1 (Smad-interacting protein 1) gene for Cre-mediated conditional knockout in the mouse. Genesis 32, 82–84.
Hoeffel, G., Chen, J., Lavin, Y., Low, D., Almeida, F.F., See, P., Beaudin, A.E., Lum, J., Low, I., Forsberg, E.C., Poidinger, M., Zolezzi, F., Larbi, A., Ng, L.G., Chan, J.K.Y., Greter, M., Becher, B., Samokhvalov, I.M., Merad, M., Ginhoux, F., 2015. C-myb(+) erythromyeloid progenitor-derived fetal monocytes give rise to adult tissue-resident macrophages. Immunity 42, 665–678. doi:10.1016/j.immuni.2015.03.011
Hume, D.A., Pavli, P., Donahue, R.E., Fidler, I.J., 1988. The effect of human recombinant macrophage colony-stimulating factor (CSF-1) on the murine mononuclear phagocyte system in vivo. J Immunol 141, 3405–3409.
Kranz, A., Fu, J., Duerschke, K., Weidlich, S., Naumann, R., Stewart, A.F., Anastassiadis, K., 2010. An improved Flp deleter mouse in C57Bl/6 based on Flpo recombinase. Genesis 48, 512–520. doi:10.1002/dvg.20641
Lavin, Y., Winter, D., Blecher-Gonen, R., David, E., Keren-Shaul, H., Merad, M., Jung, S., Amit, I., 2014. Tissue-resident macrophage enhancer landscapes are shaped by the local microenvironment. Cell 159, 1312–1326. doi:10.1016/j.cell.2014.11.018
Luche, H., Weber, O., Nageswara Rao, T., Blum, C., Fehling, H.J., 2007. Faithful activation of an extra-bright red fluorescent protein in “knock-in” Cre-reporter mice ideally suited for lineage tracing studies. Eur J Immunol 37, 43–53. doi:10.1002/eji.200636745
Lun, A.T.L., McCarthy, D.J., Marioni, J.C., 2016. A step-by-step workflow for low-level analysis of single-cell RNA-seq data with Bioconductor. F1000Res 5, 2122.doi:10.12688/f1000research.9501.2
Lynch, R.W., Hawley, C.A., Pellicoro, A., Bain, C.C., Iredale, J.P., Jenkins, S.J., 2018. An efficient method to isolate Kupffer cells eliminating endothelial cell contamination and selective bias. J. Leukoc. Biol. 95, 2157. doi:10.1002/JLB.1TA0517-169R
MacDonald, K.P.A., Palmer, J.S., Cronau, S., Seppanen, E., Olver, S., Raffelt, N.C., Kuns, R., Pettit, A.R., Clouston, A., Wainwright, B., Branstetter, D., Smith, J., Paxton, R.J., Cerretti, D.P., Bonham, L., Hill, G.R., Hume, D.A., 2010. An antibody against the colonystimulating factor 1 receptor depletes the resident subset of monocytes and tissue- and tumor-associated macrophages but does not inhibit inflammation. Blood 116, 3955–3963. doi:10.1182/blood-2010-02-266296
Mass, E., Ballesteros, I., Farlik, M., Halbritter, F., Günther, P., Crozet, L., Jacome-Galarza, C.E., Händler, K., Klughammer, J., Kobayashi, Y., Gomez Perdiguero, E., Schultze, J.L., Beyer, M., Bock, C., Geissmann, F., 2016. Specification of tissue-resident macrophages during organogenesis. Science 353, aaf4238–aaf4238. doi:10.1126/science.aaf4238
Miller, J.C., Brown, B.D., Shay, T., Gautier, E.L., Jojic, V., Cohain, A., Pandey, G., Leboeuf, M., Elpek, K.G., Helft, J., Hashimoto, D., Chow, A., Price, J., Greter, M., Bogunovic, M., Bellemare-Pelletier, A., Frenette, P.S., Randolph, G.J., Turley, S.J., Merad, M., Immunological Genome Consortium, 2012. Deciphering the transcriptional network of

the dendritic cell lineage. Nat Immunol 13, 888–899. doi:10.1038/ni.2370
Molawi, K., Wolf, Y., Kandalla, P.K., Favret, J., Hagemeyer, N., Frenzel, K., Pinto, A.R., Klapproth, K., Henri, S., Malissen, B., Rodewald, H.-R., Rosenthal, N.A., Bajénoff, M., Prinz, M., Jung, S., Sieweke, M.H., 2014. Progressive replacement of embryo-derived cardiac macrophages with age. Journal of Experimental Medicine 211, 2151–2158. doi:10.1084/jem.20140639
Monticelli, S., Natoli, G., 2017. Transcriptional determination and functional specificity of myeloid cells: making sense of diversity. Nat Rev Immunol 44, 439. doi:10.1038/nri.2017.51
Okabe, Y., Medzhitov, R., 2016. Tissue biology perspective on macrophages. Nat Immunol 17, 9–17. doi:10.1038/ni.3320
Okabe, Y., Medzhitov, R., 2014. Tissue-specific signals control reversible program of localization and functional polarization of macrophages. Cell 157, 832–844.doi:10.1016/j.cell.2014.04.016
Omilusik, K.D., Best, J.A., Yu, B., Goossens, S., Weidemann, A., Nguyen, J.V., Seuntjens, E., Stryjewska, A., Zweier, C., Roychoudhuri, R., Gattinoni, L., Bird, L.M., Higashi, Y., Kondoh, H., Huylebroeck, D., Haigh, J., Goldrath, A.W., 2015. Transcriptional repressor ZEB2 promotes terminal differentiation of CD8+ effector and memory T cell populations during infection. J Exp Med.
Painter, M.W., Davis, S., Hardy, R.R., Mathis, D., Benoist, C., Immunological Genome Project Consortium, 2011. Transcriptomes of the B and T lineages compared by multiplatform microarray profiling. The Journal of Immunology 186, 3047–3057.doi:10.4049/jimmunol.1002695
Pettitt, S.J., Liang, Q., Rairdan, X.Y., Moran, J.L., Prosser, H.M., Beier, D.R., Lloyd, K.C., Bradley, A., Skarnes, W.C., 2009. Agouti C57BL/6N embryonic stem cells for mouse genetic resources. Nat. Methods 6, 493–495. doi:10.1038/nmeth.1342
Remmerie, A., Scott, C.L., 2018. Macrophages and Lipid Metabolism. Cell Immunol. doi:10.1016/j.cellimm.2018.01.020
Rojo, R., Pridans, C., Langlais, D., Hume, D.A., 2017. Transcriptional mechanisms that control expression of the macrophage colony-stimulating factor receptor locus. Clin. Sci. 131, 2161–2182. doi:10.1042/CS20170238
Schneider, C., Nobs, S.P., Kurrer, M., Rehrauer, H., Thiele, C., Kopf, M., 2014. Induction of the nuclear receptor PPAR-[gamma] by the cytokine GM-CSF is critical for the differentiation of fetal monocytes into alveolar macrophages. Nature Immunology 15, 1026–1037. doi:10.1038/ni.3005
Scott, C.L., Bain, C.C., Wright, P.B., Sichien, D., Kotarsky, K., Persson, E.K., Luda, K., Guilliams, M., Lambrecht, B.N., Agace, W.W., Milling, S.W., Mowat, A.M., 2014. CCR2(+)CD103(-) intestinal dendritic cells develop from DC-committed precursors and induce interleukin-17 production by T cells. Mucosal immunology 8, 327–339. doi:10.1038/mi.2014.70
Scott, C.L., Soen, B., Martens, L., Skrypek, N., Saelens, W., Taminau, J., Blancke, G., Van Isterdael, G., Huylebroeck, D., Haigh, J., Saeys, Y., Guilliams, M., Lambrecht, B.N., Berx, G., 2016a. The transcription factor Zeb2 regulates development of conventional and plasmacytoid DCs by repressing Id2. Journal of Experimental Medicine 213, 897–911. doi:10.1084/jem.20151715
Scott, C.L., Zheng, F., De Baetselier, P., Martens, L., Saeys, Y., De Prijck, S., Lippens, S., Abels, C., Schoonooghe, S., Raes, G., Devoogdt, N., Lambrecht, B.N., Beschin, A., Guilliams, M., 2016b. Bone marrow-derived monocytes give rise to self-renewing and fully differentiated Kupffer cells. Nat Commun 7, 10321. doi:10.1038/ncomms10321
Shimshek, D.R., Kim, J., Hübner, M.R., Spergel, D.J., Buchholz, F., Casanova, E., Stewart, A.F., Seeburg, P.H., Sprengel, R., 2002. Codon-improved Cre recombinase (iCre) expression in the mouse. Genesis 32, 19–26. doi:10.1002/gene.10023
Sichien, D., Lambrecht, B.N., Guilliams, M., Scott, C.L., 2017. Development of conventional dendritic cells: from common bone marrow progenitors to multiple subsets in peripheral tissues. Mucosal immunology 10, 831 EP –. doi:10.1038/mi.2017.8
T'Jonck, W., Guilliams, M., Bonnardel, J., 2018. Niche signals and transcription factors involved in tissue-resident macrophage development. Cell Immunol. doi:10.1016/j.cellimm.2018.02.005
Tagliani, E., Shi, C., Nancy, P., Tay, C.-S., Pamer, E.G., Erlebacher, A., 2011. Coordinate regulation of tissue macrophage and dendritic cell population dynamics by CSF-1. Journal of Experimental Medicine 208, 1901–1916. doi:10.1084/jem.20110866
Tamoutounour, S., Guilliams, M., Montanana Sanchis, F., Liu, H., Terhorst, D., Malosse, C., Pollet, E., Ardouin, L., Luche, H., Sanchez, C., Dalod, M., Malissen, B., Henri, S., 2013. Origins and functional specialization of macrophages and of conventional and monocyte-derived dendritic cells in mouse skin. Immunity 39, 925–938. doi:10.1016/j.immuni.2013.10.004
Tamoutounour, S., Henri, S., Lelouard, H., de Bovis, B., de Haar, C., van der Woude, C.J., Woltman, A.M., Reyal, Y., Bonnet, D., Sichien, D., Bain, C.C., Mcl Mowat, A., Reis E Sousa, C., Poulin, L.F., Malissen, B., Guilliams, M., 2012. CD64 distinguishes macrophages from dendritic cells in the gut and reveals the Th1-inducing role of mesenteric lymph node macrophages during colitis. Eur J Immunol. doi:10.1002/eji.201242847
van de Laar, L., Saelens, W., De Prijck, S., Martens, L., Scott, C.L., Van Isterdael, G., Hoffmann, E., Beyaert, R., Saeys, Y., Lambrecht, B.N., Guilliams, M., 2016. Yolk Sac Macrophages, Fetal Liver, and Adult Monocytes Can Colonize an Empty Niche and Develop into Functional Tissue-Resident Macrophages. Immunity 44, 755–768. doi:10.1016/j.immuni.2016.02.017
Van de Putte, T., Maruhashi, M., Francis, A., Nelles, L., Kondoh, H., Huylebroeck, D., Higashi, Y., 2003. Mice lacking ZFHX1B, the gene that codes for Smad-interacting protein-1, reveal a role for multiple neural crest cell defects in the etiology of Hirschsprung disease-mental retardation syndrome. Am. J. Hum. Genet. 72, 465–470. doi:10.1086/346092

van Helden, M.J., Goossens, S., Daussy, C., Mathieu, A.-L., Faure, F., Marçais, A., Vandamme, N., Farla, N., Mayol, K., Viel, S., Degouve, S., Debien, E., Seuntjens, E., Conidi, A., Chaix, J., Mangeot, P., de Bernard, S., Buffat, L., Haigh, J.J., Huylebroeck, D., Lambrecht, B.N., Berx, G., Walzer, T., 2015. Terminal NK cell maturation is controlled by concerted actions of T-bet and Zeb2 and is essential for melanoma rejection. Journal of Experimental Medicine 212, 2015–2025. doi:10.1084/jem.20150809
Vandewalle, C., Comijn, J., De Craene, B., Vermassen, P., Bruyneel, E., Andersen, H., Tulchinsky, E., van Roy, F., Berx, G., 2005. SIP1/ZEB2 induces EMT by repressing genes of different epithelial cell-cell junctions. Nucleic Acids Res. 33, 6566–6578.doi:10.1093/nar/gki965
Vandewalle, C., van Roy, F., Berx, G., 2009. The role of the ZEB family of transcription factors in development and disease. Cell Mol Life Sci 66, 773–787. doi:10.1007/s00018-008-8465-8
Ventura, A., Kirsch, D.G., McLaughlin, M.E., Tuveson, D.A., Grimm, J., Lintault, L., Newman, J., Reczek, E.E., Weissleder, R., Jacks, T., 2007. Restoration of p53 function leads to tumour regression in vivo. Nature 445, 661-665. doi:10.1038/nature05541
Wang, Y., Szretter, K.J., Vermi, W., Gilfillan, S., Rossini, C., Cella, M., Barrow, A.D., Diamond, M.S., Colonna, M., 2012. IL-34 is a tissue-restricted ligand of CSF1R required for the development of Langerhans cells and microglia. Nat Immunol 13, 753–760.doi:10.1038/ni.2360
Wu, X., Briseño, C.G., Grajales-Reyes, G.E., Haldar, M., Iwata, A., Kretzer, N.M., KC, W., Tussiwand, R., Higashi, Y., Murphy, T.L., Murphy, K.M., 2016. Transcription factor Zeb2 regulates commitment to plasmacytoid dendritic cell and monocyte fate. Proceedings of the National Academy of Sciences 113, 14775–14780. doi:10.1073/pnas.1611408114
Yona, S., Kim, K.-W., Wolf, Y., Mildner, A., Varol, D., Breker, M., Strauss-Ayali, D., Viukov, S., Guilliams, M., Misharin, A., Hume, D.A., Perlman, H., Malissen, B., Zelzer, E., Jung, S., 2013. Fate mapping reveals origins and dynamics of monocytes and tissue macrophages under homeostasis. Immunity 38, 79–91. doi:10.1016/j.immuni.2012.12.001
Zhang, Y., Breevoort, S.R., Angdisen, J., Fu, M., Schmidt, D.R., Holmstrom, S.R., Kliewer, S.A., Mangelsdorf, D.J., Schulman, I.G., 2012. Liver LXRα expression is crucial for whole body cholesterol homeostasis and reverse cholesterol transport in mice. J Clin Invest 122, 1688–1699. doi:10.1172/JCI59817
Zigmond, E., Varol, C., Farache, J., Elmaliah, E., Satpathy, A.T., Friedlander, G., Mack, M., Shpigel, N., Boneca, I.G., Murphy, K.M., Shakhar, G., Halpern, Z., Jung, S., 2012.Ly6C(hi) Monocytes in the Inflamed Colon Give Rise to Proinflammatory Effector Cells and Migratory Antigen-Presenting Cells. Immunity 37, 1076–1090. doi:10.1016/j.immuni.2012.08.026

FIGURE LEGENDS

Figure 1: ZEB2 controls mac number and surface phenotype.

(A) Expression of CD64 and F4/80 by live CD45$^+$Ly6G$^-$Ly6C$^-$ liver cells and Clec4F and Tim4 by total liver macs in *Clec4f*^{CRE}x*Zeb2*$^{fl/fl}$ and *Zeb2*$^{fl/fl}$ mice. Absolute number of liver macs (CD64$^+$F4/80$^+$) per gram of liver and % of total macs expressing Clec4F and Tim4. Data are pooled from 4 experiments with n=11-13 per group. ***p<0.001 Student's t test. (B) Expression of SiglecF, F4/80 and CD11b by live CD45$^+$CD64$^+$CD11c$^+$ Lung macs in *Itgax*^{CRE}x*Zeb2*$^{fl/fl}$ and *Zeb2*$^{fl/fl}$ mice. AMs (CD64$^+$F4/80$^+$CD11c$^+$SiglecF$^+$) as a % of total live CD45$^+$ cells, absolute number and % of CD11b$^+$ and CD11b$^-$ AMs in *Itgax*^{CRE}x*Zeb2*$^{fl/fl}$ or *Zeb2*$^{fl/fl}$ mice. Data are pooled from 2 experiments with n=7-8 per group. *p<0.05, ***p<0.001 Student's t test. (C) t-SNE plot of SC-RNA-Seq data following preprocessing of KCs sorted as Clec4F$^+$ from *Clec4f*^{CRE}x*Zeb2*$^{fl/fl}$ or *Zeb2*$^{fl/fl}$ mice, showing clusters of KCs, assigned groups and CRE$^-$ (Red) and CRE$^+$ (Teal) overlay. (D) t-SNE plot of SC-RNA-Seq data following preprocessing of AMs sorted as SiglecF$^+$CD11c$^+$ from *Itgax*^{CRE}x*Zeb2*$^{fl/fl}$ or *Zeb2*$^{fl/fl}$ mice, showing clusters of AMs, assigned groups and CRE$^-$ (Red) and CRE$^+$ (Teal) overlay. (E) tSNE plots showing expression of *Zeb2*, *Siglecf* and *Ms4a1* in aggregated KC SC-RNA-Seq data. (F) tSNE plots showing expression of *Zeb2*, *Epcam* and *Cd101* in aggregated AM SC-RNA-Seq data. (G,H) Top DE genes per group based on Log Fold Change per group of KCs (G) or AMs (H).

Figure 2: ZEB2-/- macs are lost with time

(A) Expression and % of SiglecF and CD20 by Clec4F$^+$ KCs at 6 and 12 weeks of age compared with *Zeb2*$^{fl/fl}$ controls. Data are pooled from 1-2 experiments with n=7-10 per group. ***p<0.001 One way ANOVA with Bonferroni post-test. (B) Relative expression of *Zeb2* mRNA normalized to β-actin as determined by qPCR of FACS-purified SiglecF$^+$ and SiglecF$^-$ KCs compared with CRE$^-$ control KCs. Data are pooled from 1 experiment with n=5-7 per group. ***p<0.001 One way ANOVA with Bonferroni post-test. (C) Expression and % of EpCam and CD101 by AMs at 6 and 12 weeks of age compared with *Zeb2*$^{fl/fl}$ controls. Data are pooled from 1-2 experiments with n=5-11 per group. ***p<0.001 One way ANOVA with Bonferroni post-test. (D) Relative expression of *Zeb2* mRNA normalized to β-actin as determined by qPCR of FACS-purified EpCam$^+$ and EpCam$^-$ AMs compared with CRE$^-$ control AMs. Data are pooled from 1 experiment with n=5-7 per group. ***p<0.001 One way ANOVA with Bonferroni post-test. (E) Expression of *Zeb2* mRNA (determined by primeflow assay) and SiglecF in KCs from Zeb2$^{fl/fl}$ and *Clec4f*^{CRE}xZeb2$^{fl/fl}$ mice compared with label probe only control (no primer). Data are

representative of 1 experiment with n=5-6 per group. (F) Expression of *Zeb2* mRNA (determined by primeflow assay) and EpCam in AMs from Zeb2$^{fl/fl}$ and *Itgax*^{CRE}xZeb2$^{fl/fl}$ mice compared with label probe only control (no primer). Data are representative of 1 experiment with n=4-5 per group. (G) Schematic of experimental set up. (H) % SiglecF^{+}CD20^{int} KCs amongst total CD45.2^{+} KCs at indicated time points (days) post the last dose of tamoxifen. Data are pooled from 2 experiments with n= 4-7 per time-point. ***p<0.001, One way ANOVA with Bonferroni post-test comparing each time point with the previous time point. (I) % CD101^{+}EpCam^{+} AMs amongst total CD45.2^{+} AMs at indicated time points (days) post the last dose of tamoxifen. Data are pooled from 2 experiments with n= 4-7 per time-point. ***p<0.001, One way ANOVA with Bonferroni post-test comparing each time point to the previous time point. In all panels, controls are pooled from donor macs from mice not administered tamoxifen and host macs from mice administered tamoxifen.

Figure 3: ZEB2 controls tissue identity of KCs and AMs

(A) Schematic of experimental set up. (B) Expression of CD45.1 (donor) and Tim4 in total Clec4F^{+} KCs in *Clec4f*^{CRE}x*Zeb2*$^{fl/fl}$ chimeras. % total chimerism of KCs in Zeb2$^{fl/fl}$ and *Clec4f*^{CRE}x*Zeb2*$^{fl/fl}$ mice 4 weeks post irradiation shown as a ratio over the chimerism in blood Ly6C^{hi} monocytes in the same mouse. Data are pooled from 2 experiments with n=6-10 per group.***p<0.001 Student's t-test. (C) Expression of CD45.1 (donor) and CD45.2 (host) in total lung AMs in *Itgax*^{CRE}x*Zeb2*$^{fl/fl}$ mice. % total chimerism of AMs in *Zeb2*$^{fl/fl}$ and *Itgax*^{CRE}x*Zeb2*$^{fl/fl}$ mice 4 weeks post irradiation shown as a ratio over the chimerism in blood Ly6C^{hi} monocytes in the same mouse. Data are pooled from 2 experiments with n=5-8 per group. NS; non-significant. Student's t-test. (D,E) Heatmap of expression of cell death-associated genes per group of KCs (D) or AMs (E) from SC-RNA-Seq data. (F) Representative western blots for RIPK3, pMLKL and Tubulin expression by total BAL cells isolated from CD45.1 mice that were irradiated (8gy) and reconstituted with Rosa-26$^{CRE-ERT2}$x*Zeb2*$^{fl/fl}$ BM. 33 weeks post reconstitution, mice were fed 5mg tamoxifen or corn oil as a control for 5 days. 27 days after the last dose of tamoxifen or corn oil, mice were sacrificed and BAL fluid isolated. BAL fluid from 3-4 mice was pooled per replicate and 150,000 cells were used per lane. Ratio of band intensity was calculated using ImageJ. Data are pooled from 2 experiments with n=6-8 per group. Student's t-test was used to calculate indicated p values. (G) Venn diagram showing DE genes specific to *Zeb2*$^{-/-}$ KCs (Group 3), *Zeb2*$^{-/-}$ AMs (Group 3) or shared between both mac populations. (H,I) Heatmap showing expression of top core genes across KC (H) or AM (I) groups from SC-RNA-Seq analysis. Highlighted genes are significantly differentially expressed.

Figure 4: Loss of LXRα from KCs recapitulates main features of ZEB2-/- KCs

(A) Expression of CD64 and F4/80 by live CD45^{+}Ly6G^{-}Ly6C^{-} liver cells in *Clec4f*^{CRE}x*Nr1h3*$^{fl/fl}$ and *Nr1h3*$^{fl/fl}$ mice. Liver macs (CD64^{+}F4/80^{+}) as a % of total live CD45^{+} cells and absolute number per gram of liver. Data are pooled from 2 experiments with n=12 per group. (B) Expression of Clec4F and Tim4 by total liver macs in *Clec4f*^{CRE}x*Nr1h3*$^{fl/fl}$ and *Nr1h3*$^{fl/fl}$ mice and % of total macs expressing Clec4F and Tim4. Data are pooled from 2 experiments with n=12 per group. ***p<0.001 Student's t test. (C) % total chimerism of total Clec4F^{+} KCs in *Nr1h3*$^{fl/fl}$ and *Clec4f*^{CRE}x*Nr1h3*$^{fl/fl}$ mice 4 weeks post irradiation shown as a ratio over the chimerism in blood Ly6C^{hi} monocytes in the same mouse. Data are pooled from 2 experiments with n=6-8 per group. ***p<0.001; Student's t-test. (D) t-SNE plot of SC-RNA-Seq data from KCs sorted as Clec4F^{+} from *Clec4f*^{CRE}x*Nr1h3*$^{fl/fl}$ and *Nr1h3*$^{fl/fl}$ mice, showing clusters of KCs, assigned groups and CRE^{-} (Red) and CRE^{+} (Teal) overlay. (E) Heatmaps showing top DE genes (15 downregulated, 15 upregulated) based on LogFC in KCs with loss of LXRα and expression of the top 15 down and upregulated genes in LXRα$^{-/-}$ KCs by the indicated groups of KCs from *Zeb2*$^{fl/fl}$ and *Clec4f*^{CRE}x*Zeb2*$^{fl/fl}$ mice. (F,G) Histogram and MFI of CD55 protein expression as measured by flow cytometry in (F) Zeb2$^{+/+}$ (*Zeb2*$^{fl/fl}$), SiglecF^{+} Zeb2$^{-/-}$ KCs and SiglecF^{-} Zeb2$^{+/-}$ KCs from *Clec4f*^{CRE}x*Zeb2*$^{fl/fl}$ mice and (G) Nr1h3$^{+/+}$ (*Nr1h3*$^{fl/fl}$) and Nr1h3$^{-/-}$ KCs from *Clec4f*^{CRE}x*Nr1h3*$^{fl/fl}$ mice. (H) Venn diagram showing DE genes specific to *Zeb2*$^{-/-}$ KCs, *Nr1h3*$^{-/-}$ KCs or shared between both mac populations.

Figure 5: Loss of ZEB2 affects mac phenotype and/or number across tissues

(A) Expression of CD64, F4/80 and CD11b by live CD45^{+}Ly6G^{-}CD64^{+}Ly6C^{-}MHCII^{-} splenic macs in *Fcgr1*^{CRE}x*Zeb2*$^{fl/fl}$ and *Zeb2*$^{fl/fl}$ mice. Splenic macs as a % of total live CD45^{+} cells, absolute number and % of CD11b^{+} and CD11b^{-} splenic macs in *Fcgr1*^{CRE}x*Zeb2*$^{fl/fl}$ or *Zeb2*$^{fl/fl}$ mice. Data are pooled from 2 experiments with n=8-11 per group. ***p<0.001 Student's t test. (B) Expression of CD64, F4/80, CD11c and CD11b by live CD45^{int} microglia in *Fcgr1*^{CRE}x*Zeb2*$^{fl/fl}$ and *Zeb2*$^{fl/fl}$ mice. Microglia as a % of total live CD45^{+} cells, absolute number and % of CD11c^{+} and CD11c^{-} microglia in *Fcgr1*^{CRE}x*Zeb2*$^{fl/fl}$ or *Zeb2*$^{fl/fl}$ mice. Data are pooled from 2 experiments with n=8-11 per group. **p,0.01, ***p<0.001 Student's t test. (C) Expression of Ly6C and MHCII (monocyte waterfall) by live CD45^{+}CD11b^{+}Ly6G^{-}SiglecF^{-} non cDCs in *Fcgr1*^{CRE}x*Zeb2*$^{fl/fl}$ and *Zeb2*$^{fl/fl}$ mice. % of liver CD45^{+} and absolute number of Ly6C^{+}MHCII^{-}, Ly6C^{+}MHCII^{+} and Ly6C^{-} Macs in *Fcgr1*^{CRE}x*Zeb2*$^{fl/fl}$ or *Zeb2*$^{fl/fl}$ mice. Data are pooled from 2 experiments with n=8-11 per group. *p<0.05, **p<0.01, ***p<0.001 Student's t test.

Figure 6: Loss of *Zeb2* results in altered transcriptome across mac lineage
(A,B) t-SNE plot of SC-RNA-Seq data from splenic macs (A) and microglia (B) sorted from *Fcgr1*^{CRE}x*Zeb2*$^{fl/fl}$ and *Zeb2*$^{fl/fl}$ mice, showing clusters of macs, assigned groups and CRE^{-} (Red) and CRE^{+} (Teal) overlay and expression of indicated genes. (C) t-SNE plot of SC-RNASeq data from total colonic macs from *Fcgr1*^{CRE}x*Zeb2*$^{fl/fl}$ and *Zeb2*$^{fl/fl}$ mice, showing clusters of macs and *Cd74, Itgax, H2-Aa and H2-Eb1* expression. (D) t-SNE plot of SC-RNA-Seq data from *Cd74*^{hi} colonic macs from *Fcgr1*^{CRE}x*Zeb2*$^{fl/fl}$ and *Zeb2*$^{fl/fl}$ mice, showing clusters of macs, assigned groups and CRE^{-} (Red) and CRE^{+} (Teal) overlay and expression of indicated genes

Figure 7: Loss of ZEB2 results in loss of mac tissue-specific identity across tissues
(A-C) Heatmap showing expression of top core splenic mac (A), microglia (B) or Cd74^{hi} colonic mac (C) genes across indicated groups from SC-RNA-Seq analysis of macs isolated from that tissue. Highlighted genes are significantly differentially expressed. (D) t-SNE showing all macs sequenced by SC-RNA-Seq from the indicated 5 tissues. Zeb2$^{-/-}$ macs are shown in bold color, ZEB2$^{+/+}$ or Zeb2$^{+/-}$ macs are shown in faded color. Open circles represent cells arising from CRE^{-} mice while filled circles are those isolated from CRE^{+} mice (*Fcgr1*^{CRE}, *Itgax*^{CRE} or *Clec4f*^{CRE}). (E) Venn Diagram detailing conservation or specificity of DE genes across and between all 5 tissue mac populations in the absence of *Zeb2*. (F) Heatmap showing 32 DE genes conserved across all 5 tissue mac populations.

STAR METHODS

CONTACT FOR REAGENT AND RESOURCE SHARING

Further information and requests for resources and reagents should be directed to and will be fulfilled by the lead contact, Martin Guilliams (martin.guilliams@irc.vib-ugent.be).

EXPERIMENTAL MODEL AND SUBJECT DETAILS

In vivo animal studies: The following mice were used in this study; Zeb2$^{fl/fl}$ (Higashi et al., 2002), LXRα$^{fl/fl}$, *Itgax*^{CRE} (Caton et al., 2007), Rosa-RFP (Luche et al., 2007), Rosa-26$^{CRE-ERT2}$(Ventura *et al*., 2007), *Clec4f*^{CRE} (B6-*Clec4f*tm3Ciphe; were developed by the Centre d'Immunophenomique, Marseille, France) and *Fcgr1*^{CRE} (B6-Fcgr1tm3Ciphe; generated by Bernard Malissen). All mice were used on a C57Bl/6 background and a mix of male and female mice were used for each experiment. Mice were used between 6 and 8 weeks of age unless otherwise stated. All mice were bred and maintained at the VIB (Ghent University) under specific pathogen free conditions. All animals were randomly allocated to experimental groups and littermate controls were used in all experiments. All experiments were performed in accordance with the ethical committee of the Faculty of Science of the VIB.
Construction of Clec4f-IRES-iCRE mice: Using ET recombination, an IRES-iCRE-loxP-Cre-NeoR-loxP cassette was introduced in the 3' untranslated region of the *Clec4f* gene, downstream of the stop codon. JM8.F6 C57BL/6N ES cells (Pettitt et al., 2009) were electroporated with the targeting vector. After selection in G418, ES cell clones were screened for proper homologous recombination by Southern blot. A neomycin-specific probe was used to ensure that adventitious non-homologous recombination events had not occurred in the selected ES clones. Properly recombined ES cells were injected into FVB blastocysts. Germline transmission led to the self-excision of the loxP-Cre-NeoR-loxP cassette in male germinal cells. The resulting *Clec4f-IRES-iCRE* allele (official name B6-*Clec4f*m2Ciphe, called here *Clec4fCRE)* was identified by PCR of tail DNA. The primers: sense 5'-GATTCCCCTTCAGACCCTGAAT-3', sense 5'-TGATGAACTACATCAGAACCTGG-3' and antisense 5'-TATTGAGGGCTTATCTGGGC-3' amplify a 496 bp band in case of the wild-type *Clec4f* allele and a 304 bp band in the case of the *Clec4f-IRES-iCre* allele.
Construction of Fcgr1-IRES-iCRE-2A-TEAL mice: Using ET recombination, an IRES-iCRE-2A-TEAL-frt-neoR-frt cassette was introduced in the 3' untranslated region of the *Fcgr1* gene, downstream of the stop codon. The targeting construct was abutted to a cassette coding for the diphtheria toxin fragment A, and linearized with Pme1. JM8.F6 C57BL/6N ES cells (Pettitt *et al*., 2009) were electroporated with the targeting vector. After selection in G418, ES cell clones were screened for proper homologous recombination by Southern blot. A neomycin-specific probe was used to ensure that adventitious non-homologous recombination events had not occurred in the selected ES clones. Properly recombined ES cells were injected into

FVB blastocysts. Upon germline transmission, mice were then crossed to mice expressing the site-specific recombinase FLP (Kranz *et al*., 2010) to delete the frt-flanked neoR cassette. The resulting *Fcgr1-IRES-iCRETEAL* floxed allele (official name B6-*Fcgr1*tm2Ciphe, called here *Fcgr1*^{CRE}) was identified by PCR of tail DNA. The primers: sense 5'-CCCTTCCTCCCAGTGACAGTACTG-3', sense 5'-GACGGCATGGACGAGCTGTACA-3' and antisense 5'-TGAACCCATCCACCCTGTGAG-3' amplify a 402 bp band in case of the wild-type *Fcgr1* allele and a 464 bp band in the case of the *Fcgr1-IRES-iCre-TEAL* allele.

METHOD DETAILS

Isolation of tissue leukocytes: For the isolation of liver leukocytes, livers were isolated from PBS-perfused mice, chopped finely and subjected to GentleMACS dissociation and incubated for 20 min with 1 mg/ml Collagenase A (Sigma) and 10U/ml DNase (Roche) in a shaking water bath at 37°C. Following a second round of GentleMACS dissociation, single cell suspensions were filtered over a 100um filter. For the isolation of lung, brain and spleen leukocytes, lungs, brains, kidneys and spleens were isolated from PBS-perfused mice finely chopped and incubated for 30 min with 0.2 mg/ml Liberase TM (Roche) and 10 U/ml DNase (Roche) in a shaking water bath at 37 °C. Single cell suspensions from brain were then subjected to a 100:40 percoll gradient (Sigma) to isolate leukocytes. Colonic intestinal lamina propria leukocytes were isolated as described previously (Bain *et al*., 2013; Scott *et al*., 2014).

Generation of BM chimeras: Partially-protected: 6 week-old *Clec4f*^{CRE}x*Zeb2*$^{fl/fl}$, *Itgax*^{CRE}x*Zeb2*$^{fl/fl}$ or *Zeb2*$^{fl/fl}$ littermate controls (CD45.2) were anaesthetized by intraperitoneal administration of Ketamine (150 mg/kg) and Xylazine (10 mg/kg). Livers were protected with a 3-cm-thick lead cover before mice were lethally irradiated with 8Gy. Once recovered from the anesthesia, mice were reconstituted by intravenous administration of 10x10^6 BM cells from congenic CD45.1 or CD45.1/CD45.2 BM from wild-type mice. 4 weeks after irradiation chimerism in the blood and liver or lung was assessed by flow cytometry. Non-protected: 6-8 week old CD45.1 or CD45.1/CD45.2 WT mice were lethally irradiated with 8Gy. Mice were reconstituted with 2-3X10^6 BM cells from gender-matched *Zeb2*$^{fl/fl}$ or Rosa-26$^{CRE\text{-}ERT2}$x*Zeb2*$^{fl/fl}$ (CD45.2) mice. 7-8 weeks post irradiation mice were fed 5mg tamoxifen by oral gavage daily for 5 days before being sacrificed at the indicated time-points after the final dose.

Flow Cytometry: Cells (0.5–5x10^6) were stained with appropriate antibodies at 4 °C in the dark for 30-45 mins and were analyzed with a Fortessa (BD Biosciences) and FlowJo software (TreeStar). KCs/AMs were sorted using an ARIA II or ARIA III (BD, Biosciences). The full list of antibodies used can be found in the Key Resource Table. Primeflow assay (Thermo Fischer) 40 for *Zeb2* expression was performed in 96-well U bottom plates according to the manufacturer's instructions using commercially available Zeb2 primers (Thermo Fischer).

Bulk RNA Sequencing: 25,000 Clec4F$^+$Tim4$^+$ KCs from *Zeb2*$^{fl/fl}$ or *Clec4F*^{CRE}x*Zeb2*$^{fl/fl}$ were FACS-purified into 500µl of RLT plus buffer (QIAGEN) and β-mercaptoethanol. RNA was isolated using a RNeasy Plus micro kit (QIAGEN) and sent to the VIB Nucleomics facility, where the RNA sequencing was performed using a NextSeq sequencer (Illumina). The pre-processing of the RNA sequencing data was done by Trimmomatic. The adapters were cut and reads were trimmed when the quality dropped below 20. Reads with a length <35 were discarded. All samples passed quality control based on the results of FastQC. Reads were mapped to the mouse reference genome via Tophat2 and counted via HTSeqCount. Samples were subsequently analyzed using R/Bioconductor, and the limma (voom) procedure was used to normalize the data.

Single Cell RNA Sequencing: Sorting and RNA isolation: 60000 Clec4F$^+$CD64$^+$F4/80$^+$CD45$^+$ live cells from livers of *Clec4f*^{CRE}x*Zeb2*$^{fl/fl}$ and *Zeb2*$^{fl/fl}$ littermate controls, 60000 CD11c$^+$SiglecF$^+$F4/80$^+$CD64$^+$CD45$^+$ live cells from lungs of *Itgax*^{CRE}x*Zeb2*$^{fl/fl}$ and *Zeb2*$^{fl/fl}$ littermate controls, 20000 CD45^{in}tF4/80$^+$CD64$^+$ live cells from brains of *Fcgr1*^{CRE}x*Zeb2*$^{fl/fl}$ and *Zeb2*$^{fl/fl}$ littermate controls, 60000 CD45$^+$Ly6C$^-$Ly6G$^-$SiglecF$^-$CD64$^+$F4/80$^+$ live cells from colons of *Fcgr1*^{CRE}x*Zeb2*$^{fl/fl}$ and *Zeb2*$^{fl/fl}$ littermate controls and 60000 CD45$^+$Ly6C$^-$Ly6G$^-$SiglecF$^-$CD64$^+$F4/80$^+$ live cells from spleens of *Fcgr1*^{CRE}x*Zeb2*$^{fl/fl}$ and *Zeb2*$^{fl/fl}$ littermate controls were FACS-purified. Cells were sorted into PBS 0.04% BSA, spun down and resuspended in PBS/0.04%BSA at an estimated final concentration of 1000 cells/µl. Cellular suspensions

(target recovery of 6000 cells) were loaded on a GemCode Single-Cell Instrument (10x Genomics, Pleasanton, CA, USA) to generate single-cell Gel Bead-in- EMulsion (GEMs). Single-cell RNA-Seq libraries were prepared using GemCode Single-Cell 3'Gel Bead and Library Kit (10x Genomics) according to the manufacturer's instructions. Briefly, GEM-RT was performed in 96-deep well reaction module: 55°C for 45min, 85°C for 5 min; end at 4°C. After RT, GEMs were broken down and the cDNA was cleaned up with DynaBeads MyOne Silane Beads (Thermo Fisher Scientific, 37002D) and SPRIselect Reagent Kit (SPRI; Beckman Coulter; B23318). cDNA was amplified with 96-Deep Well Reaction Module: 98 °C for 3 min; cycled 12 times : 98°C for 15s, 67°C for 20 s, and 72°C for 1 min; 72°C for 1 min; end at 4°C. Amplified cDNA product was cleaned up with SPRIselect Reagent Kit prior to enzymatic fragmentation. Indexed sequencing libraries were generated using the reagents in the GemCode Single-Cell 3' Library Kit with the following intermediates: (1) end repair; (2) A-tailing; (3) adapter ligation; (4) post-ligation SPRIselect cleanup and (5) sample index PCR. Pre-fragmentation and post-sample index PCR samples were analysed using the Agilent 2100 Bioanalyzer.

RNA sequencing analysis: Sequencing libraries were loaded on an Illumina NextSeq500 (KCs, AMs) or HiSeq (microglia, splenic macs, colonis macs) with sequencing settings following recommendations of 10X Genomics (26/8/0/98 - 2.1pM loading concentration). Sequencing was performed at the VIB Nucleomics Core (VIB, Leuven). The demultiplexing of the raw data was done by the 10x's CellRanger software (version 2.0.0 (KCs, AMs) or version 2.0.2 (microglia, splenic macs, colonic macs); cellranger mkfastq which wraps Illumina's bcl2fastq). The reads obtained from the demultiplexing were used as the input for 'cellranger count' (10x's CellRanger software) which align the reads to the mouse reference genome (mm10) using STAR and collapses to unique molecular identifier (UMI) counts. The result is a large digital expression matrix with cell barcodes as rows and gene identities as columns. The aggregation of the Cre^- and Cre^+ samples was done using 'cellranger aggr' (10x's CellRanger software). Preprocessing data: Preprocessing of the data was done by the scran and scater R package according to workflow proposed by the Marioni lab (Lun *et al.*, 2016). Outlier cells were identified based on 3 metrics (library size, number of expressed genes and mitochondrial proportion) and cells were tagged as outliers when they were 3 median absolute deviation (MADs) away from the median value of each metric across all cells. Low-abundance genes were removed using the 'calcAverage' function and the proposed workflow. The raw counts were normalised and log2 transformed by first calculating "size factors" that represent the extent to which counts should be scaled in each library. Detecting highly variable genes, finding clusters and creating tSNE plots was done using the Seurat pipeline. Marker genes per identified subpopulation were found using the findMarker function of the Seurat pipeline. Additional low quality (low UMI counts, high % of mitochondrial genes), contaminating (potential doublets) and actively proliferating cells were also removed from the analysis (Figure S1G).

Gene expression analysis by real-time RT-PCR: RNA was purified from 10000-25000 sorted cells using an RNeasy Plus micro kit (QIAGEN). RNA was reverse transcribed to cDNA with an iScript Advanced cDNA Synthesis kit (Bio-Rad Laboratories). Gene expression was assayed by real-time RT-PCR using a SensiFast SYBR NoRox kit (GC Biotech) on a PCR amplification and detection instrument (LightCycler 480; Roche) with the primers listed in the Key Resource Table. Gene expression was normalized to β-actin, and the mean relative gene expression was calculated using the $2^{-\Delta\Delta C(t)}$ method.

Confocal Microscopy: 2-3mm slices of livers were fixed by immersion in Antigen fix (Diapath) for 1h, washed in PBS, infused overnight in 30% sucrose and frozen in Tissue-Tek OCT compound (Sakura Finetek) for cryostat sectioning. After permeabilization with 0.5% saponin and unspecific binding site blocking with 2% bovine serum albumin, 1% fetal calf serum and 1% donkey serum for 30 minutes, 14µm–thick cryostat tissue sections were labeled overnight at 4°C with primary antibodies followed by incubation for 1 hour at room temperature with secondary antibodies. When two rat antibodies were used on the same section, the directly conjugated rat antibody was incubated for 1h after blocking with a donkey anti-rat secondary antibody with 1% rat serum for 30 minutes. Slices were mounted on ProLong Diamond

(Thermo fisher scientific) and imaged with a Zeiss LSM 780 confocal microscope (Carl Zeiss, Oberkochen, Germany). Images were analyzed using ImageJ software.
PCR analysis of Zeb2 deletion: 25000 cells of required phenotype and genotype were FACS-purified from livers and lungs of *Clec4f*^{CRE}xZeb2$^{fl/fl}$ and *Itgax*^{CRE}xZeb2$^{fl/fl}$ mice respectively. DNA was extracted by boiling the cells at 95C in 50µl 50mM NaOH for 20minutes. After boiling 5µl 1.5M Tris pH8.8 was added to the cells. 1 or 0.2µl pf extracted DNA was added to a PCR reaction containing primer pairs (Zeb2 PCR) listed in the key resource table and Allin Red Taq polymerase (HighQu). PCR protocol was as follows: 95C 1min, 40 cycles of 95C 15secs, 62C 15secs, 72C 30secs and a 5min incubation at 72C. PCR products were resolved on a 2% agarose gel.

QUANTIFICATION AND STATISTICAL ANALYSIS

In all experiments, data are presented as mean ± SEM unless stated otherwise. Statistical tests were selected based on appropriate assumptions with respect to data distribution and variance characteristics. Student's t test (two-tailed) was used for the statistical analysis of differences between two groups. One-way ANOVA with Bonferroni post-test was used for the statistical analysis of differences between more than two groups. Statistical significance was defined as $p < 0.05$. Sample sizes were chosen according to standard guidelines. Number of animals is indicated as ''n.'' Of note, sizes of the tested animal groups were also dictated by availability of the transgenic strains and litter sizes, allowing littermate controls. Pre-established exclusion criteria are based on IACUC guidelines. The investigator was not blinded to the mouse group allocation.

DATA AND SOFTWARE AVAILABILITY

All RNA-sequencing data have been deposited in the Gene Expression Omnibus publicdatabase under accession no. XXXX.

KEY RESOURCES TABLE

REAGENT or RESOURCE	SOURCE	IDENTIFIER
Antibodies		
CD64 – BV711	Biolegend	139311
F4/80 - Biotin	eBioscience	13-4801-85
CD11c – PE-eFluor 610	eBioscience	61-0114-82
CD11b – PE-Cy7	BD Biosciences	552850
CD11b – Horizon V450	BD Biosciences	560455
Clec4F - Unconjugated	R & D Systems	AF2784
SiglecF - PE	BD Biosciences	552126
SiglecF – BUV395	BD Biosciences	740280
SiglecF – Unconjugated	BD Biosciences	552125
Ly6G - FITC	BD Biosciences	551460
Ly6G - PE	BD Biosciences	551461
Ly6G - APC	BD Biosciences	560599
CD26 - FITC	BD Biosciences	559652
CD45 – BV510	Biolegend	103138
MHCII – AF700	eBioscience	56-5321-82
Tim4 – PerCP-eFluor710	eBioscience	46-5866-82
Tim4 – AF647	Biolegend	130008
Tim4 - PE	eBioscience	12-5866-82
Ly6C – eFluor450	eBioscience	48-5932-82
Ly6C - FITC	BD Biosciences	553104
CD20 - PE	eBioscience	12-0203-82
CD101 - PE	eBioscience	12-1011-82
CD326 (EpCam) – PE-Cy7	Biolegend	118216
RFP – Unconjugated	Rockland	600-401-379
F4/80 - Unconjugated	ABD Pharmingen Serotec	MCA497R
CD55 – PE	Biolegend	131803
F4/80 – BV786	Biolegend	123141
Chemicals, Peptides, and Recombinant Proteins		
BV605 – Streptavidin	BD Biosciences	563260
Donkey Anti-Goat IgG – AF647	Thermo Fischer	A-21447
Donkey Anti-Goat IgG – AF488	Thermo Fischer	A-11055
DAPI	Invitrogen	D1306
Donkey Anti-Rat Cy3	Jackson Immunoresearch	712-166-153
Donkey Anti-Rabbit - AF647	Invitrogen	A21247
Tamoxifen	Sigma-Aldrich	T5648-1G
Corn Oil	Sigma-Aldrich	C8267-500ML
Sensifast SYBR no Rox mix	Bioline	BIO-98020
Saponin	Sigma-Aldrich	4521
Donkey Serum	Abcam	ab7475
Rat Serum	Sigma Aldrich	R9759
FoxP3 Transcription factor staining buffer kit	eBioscience	00-5523-00
Critical Commercial Assays		
PrimeFlow RNA Assay	Thermo Fischer	88-18005-210
Zeb2 probes Type 1 for PrimeFlow	Thermo Fischer	PF-210
RNeasy Micro Plus kit	QIAGEN	74034
Sensifast cDNA synthesis kit	Bioline	BIO-65054
Allin Red Taq	HighQu	HQ.HSM0305
CSF1fc	David Hume/Clare Pridans	(Gow et al., 2014)

Deposited Data		
RAW and analyzed data	GEO	GSXXXX
Experimental Models: Organisms/Strains		
Mouse: Zeb2$^{fl/fl}$	Huylebroeck Lab	(Higashi et al., 2002)
Mouse: *Clec4f*^{CRE}	CIPHE, Marseille, France	This study
Mouse: *Itgax*^{CRE}	Jackson Laboratories	Stock No: 008068
Mouse: Rosa-RFP	Malissen Lab	(Luche et al., 2007)
Mouse: Rosa-26$^{CRE-ERT2}$	Jackson Laboratories	Stock No: 008463
Mouse CD45.1	Harlan	Stock: B6.SJL-PtprcaPep3b/BoyJ
Mouse Fcgr1^{CRE}	Bernard Malissen, Marseille, France	This study
Mouse LXRα$^{fl/fl}$	Institut de la Souris, GIE, France	(A-Gonzalez et al., 2013)
Oligonucleotides		
β-Actin qPCR FWD:		GCTTCTAGGCGGACTGTTACTGA
β-Actin qPCR REV:		GCCATGCCAATGTTGTCTCTTAT
Zeb2 qPCR FWD:		CCAGAGGAAACAAGGATTTCAG
Zeb2 qPCR REV:		AGGCCTGACATGTAGTCTTGTG
AZeb2 common (Flox or deletion) PCR		GGGGTCTCCACAGAGTTGAT
Zeb2 deletion PCR		TGTTTGTTTTGGAGACCGGA
Zeb2 flox PCR		CTTGCAGTTTGGGCATTCGT
Nr1h3 qPCR FWD		CAAGGGAGCACGCTATGTCTG
Nr1h3 qPCR REV		GGACACCGAAGTGGCTTGAG
Cd5l qPCR FWD		GAGGACACATGGATGGAATGT
Cd5l qPCR REV		ACCCTTGTGTAGCACCTCCA
Apoc1 qPCR FWD		TCCTGTCCTGATTGTGGTCGT
Apoc1 qPCR REV		CCAAAGTGTTCCCAAACTCCTT
Cdh5 qPCR FWD		CACTGCTTTGGGAGCCTTC
Cdh5 qPCR REV		GGGGCAGCGATTCATTTTTC
Software and Algorithms		
GraphPad Prism 6	GraphPad Software, Inc., California	
FlowJo 10.2	TreeStar, FlowJo LLC, Ashland, Oregon	
Image J	NIH, Bethesda, Maryland	

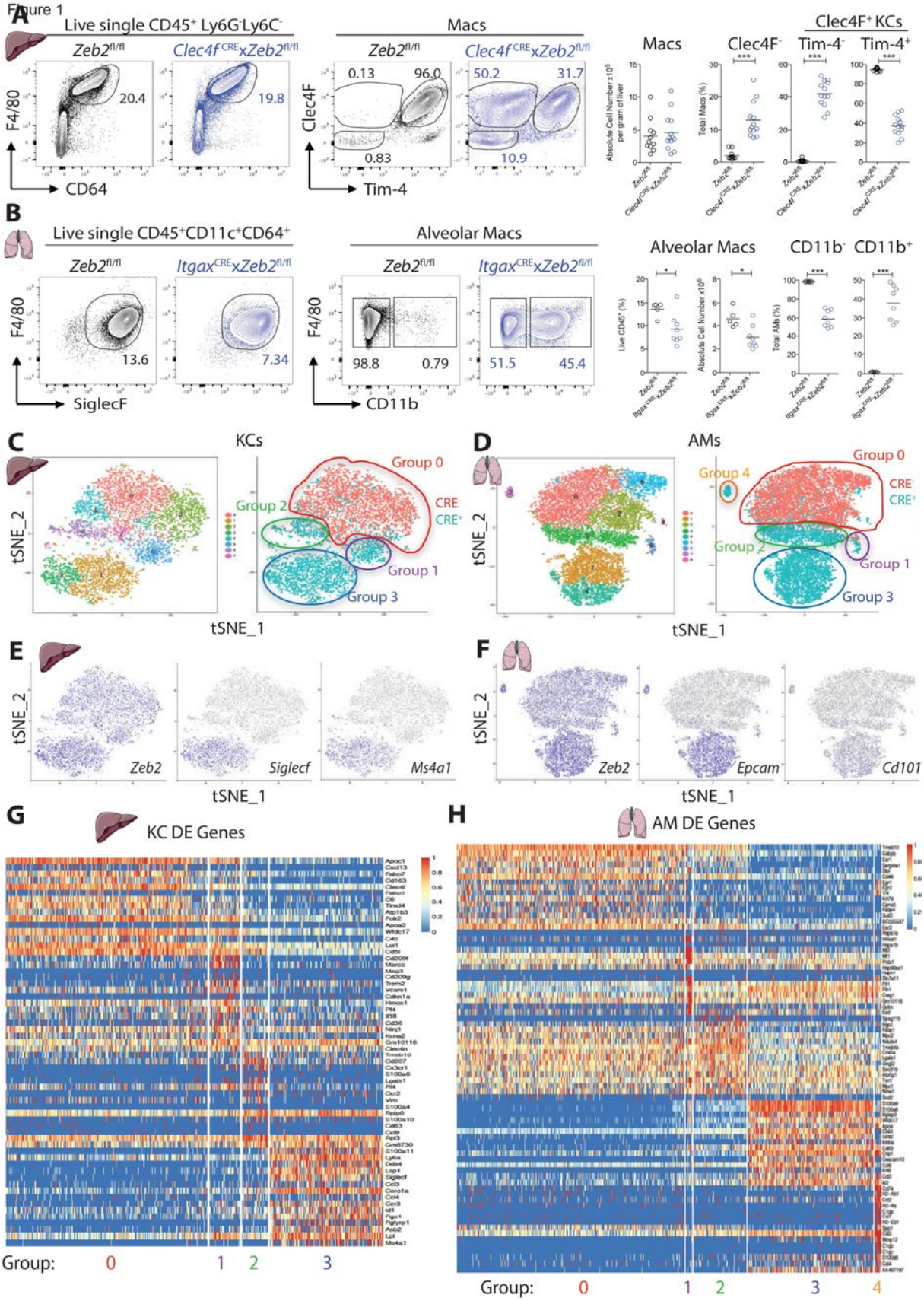
A
Live single CD45+ Ly6G-Ly6C-
Zeb2fl/fl
Clec4fCRExZeb2fl/fl
F4/80
CD64
20.4
19.8
Macs
Clec4F
Tim-4
0.13
96.0
0.83
50.2
31.7
10.9
Clec4F+ KCs
Macs
Clec4F-
Tim-4-
Tim-4+
B
Live single CD45+CD11c+CD64+
ItgaxCRExZeb2fl/fl
SiglecF
13.6
7.34
Alveolar Macs
CD11b
98.8
0.79
51.5
45.4
CD11b-
CD11b+
C
KCs
tSNE_2
tSNE_1
Group 0
Group 2
Group 1
Group 3
CRE-
CRE+
D
AMs
Group 4
E
Zeb2
Siglecf
Ms4a1
F
Epcam
Cd101
G
KC DE Genes
Group:
H
AM DE Genes

Figure 2

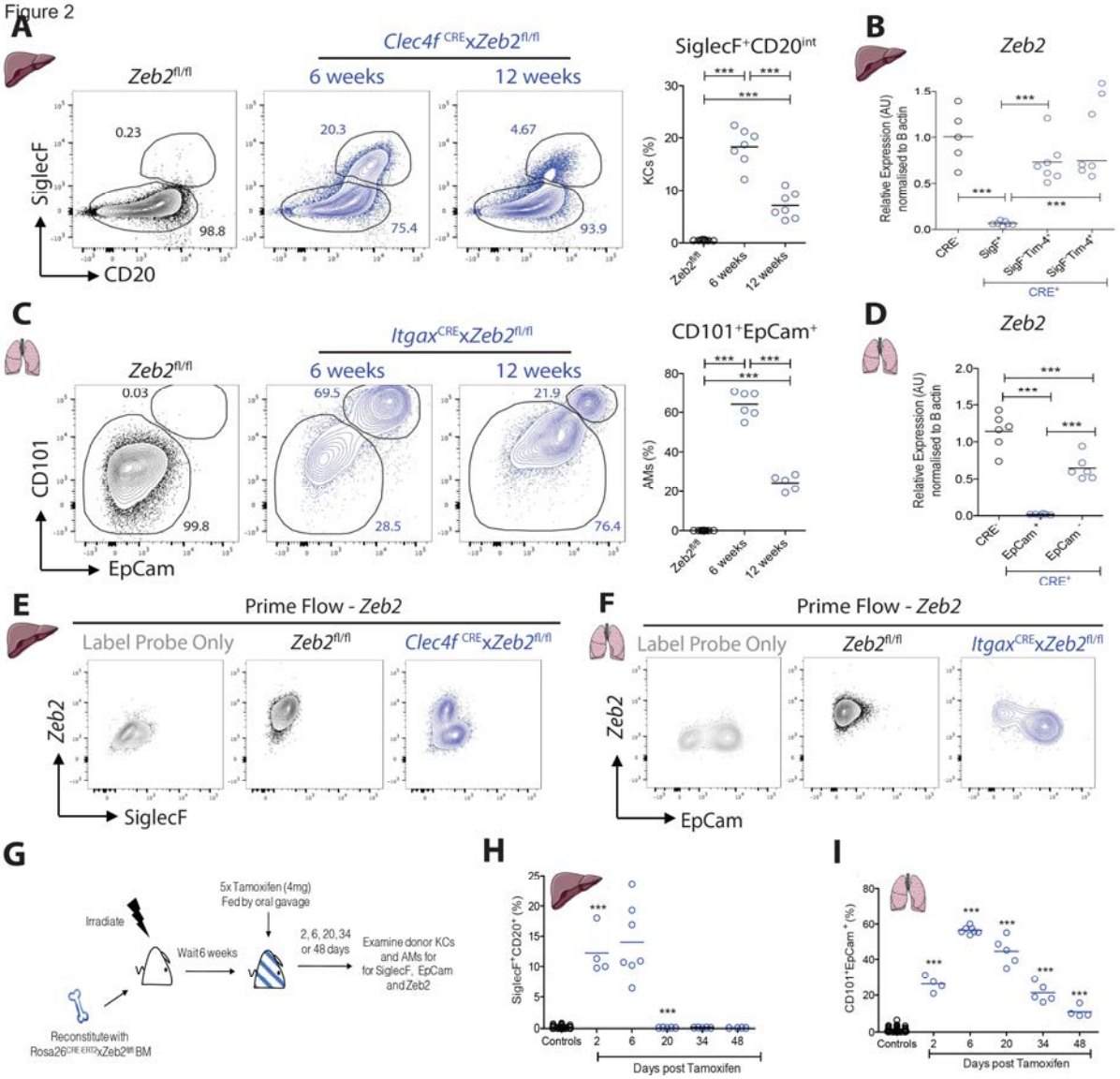
A
Clec4f CRE xZeb2 fl/fl
Zeb2 fl/fl
6 weeks
12 weeks
SiglecF
CD20
0.23
98.8
20.3
75.4
4.67
93.9
SiglecF+CD20int
KCs (%)
Zeb2fl/fl
6 weeks
12 weeks
B
Zeb2
Relative Expression (AU) normalised to B actin
CRE-
SigF+
SigF-Tim-4+
SigF-Tim-4-
CRE+
C
Itgax CRE xZeb2 fl/fl
Zeb2 fl/fl
6 weeks
12 weeks
CD101
EpCam
0.03
99.8
69.5
28.5
21.9
76.4
CD101+EpCam+
AMs (%)
Zeb2fl/fl
6 weeks
12 weeks
D
Zeb2
Relative Expression (AU) normalised to B actin
CRE-
EpCam+
EpCam-
CRE+
E
Prime Flow - Zeb2
Label Probe Only
Zeb2 fl/fl
Clec4f CRE xZeb2 fl/fl
Zeb2
SiglecF
F
Prime Flow - Zeb2
Label Probe Only
Zeb2 fl/fl
Itgax CRE xZeb2 fl/fl
Zeb2
EpCam
G
Irradiate
5x Tamoxifen (4mg) Fed by oral gavage
Wait 6 weeks
2, 6, 20, 34 or 48 days
Examine donor KCs and AMs for for SiglecF, EpCam and Zeb2
Reconstitute with Rosa26CRE-ERTxZeb2fl/fl BM
H
SiglecF+CD20+ (%)
Controls
2
6
20
34
48
Days post Tamoxifen
I
CD101+EpCam+ (%)
Controls
2
6
20
34
48
Days post Tamoxifen

Figure 3

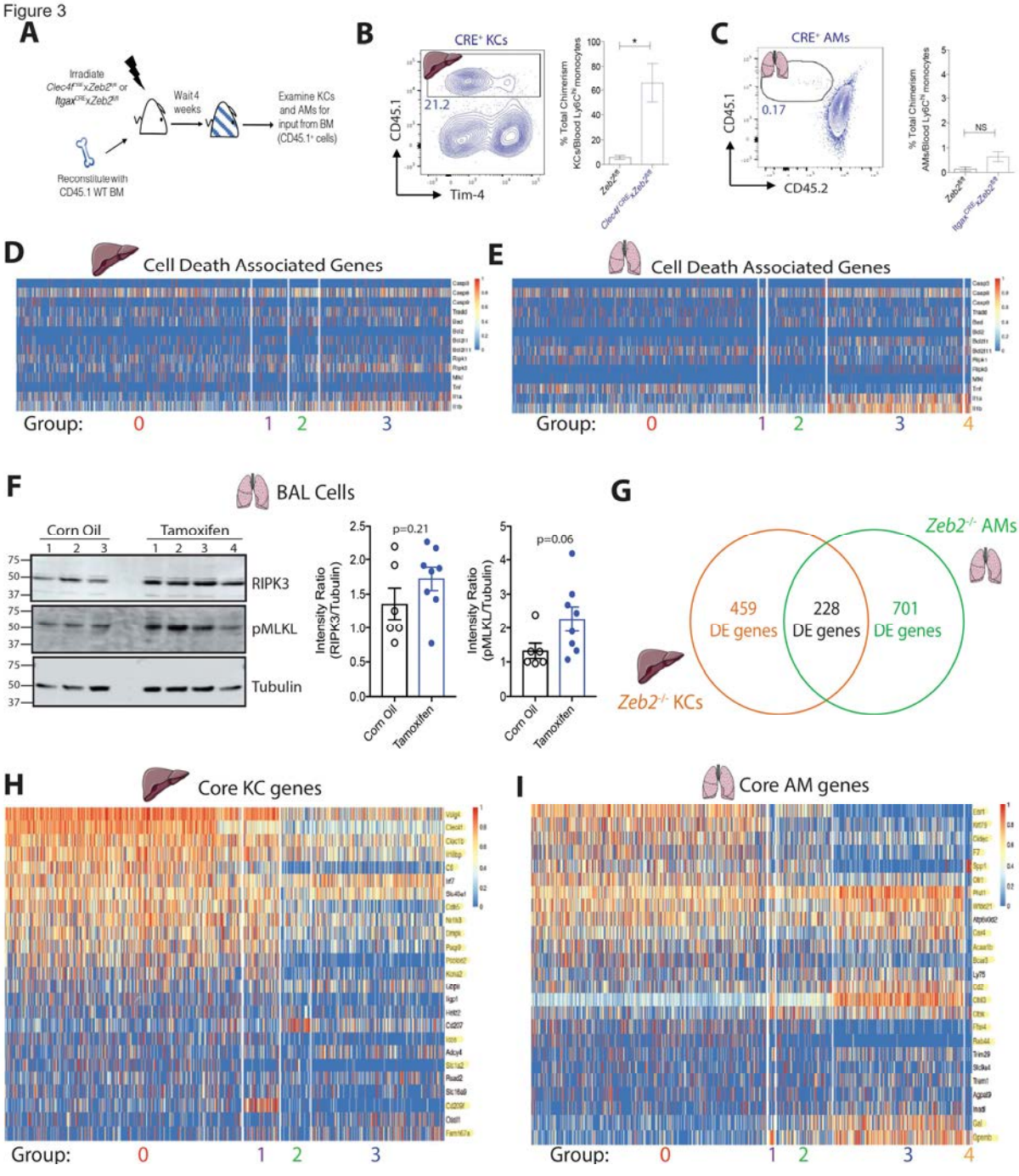
A
Irradiate
Clec4f^cre xZeb2^fl or
Itgax^cre xZeb2^fl
Wait 4 weeks
Examine KCs and AMs for input from BM (CD45.1+ cells)
Reconstitute with CD45.1 WT BM
B
CRE+ KCs
21.2
CD45.1
Tim-4
% Total Chimerism KCs/Blood Ly6C^hi monocytes
Zeb2^fl/fl
Clec4f^cre xZeb2^fl/fl
C
CRE+ AMs
0.17
CD45.1
CD45.2
% Total Chimerism AMs/Blood Ly6C^hi monocytes
NS
Zeb2^fl/fl
Itgax^cre xZeb2^fl/fl
D
Cell Death Associated Genes
Group: 0 1 2 3
E
Cell Death Associated Genes
Group: 0 1 2 3 4
F
BAL Cells
Corn Oil
Tamoxifen
RIPK3
pMLKL
Tubulin
Intensity Ratio (RIPK3/Tubulin)
p=0.21
Intensity Ratio (pMLKL/Tubulin)
p=0.06
Corn Oil
Tamoxifen
G
Zeb2^-/- AMs
459 DE genes
228 DE genes
701 DE genes
Zeb2^-/- KCs
H
Core KC genes
Group: 0 1 2 3
I
Core AM genes
Group: 0 1 2 3 4

Figure 4

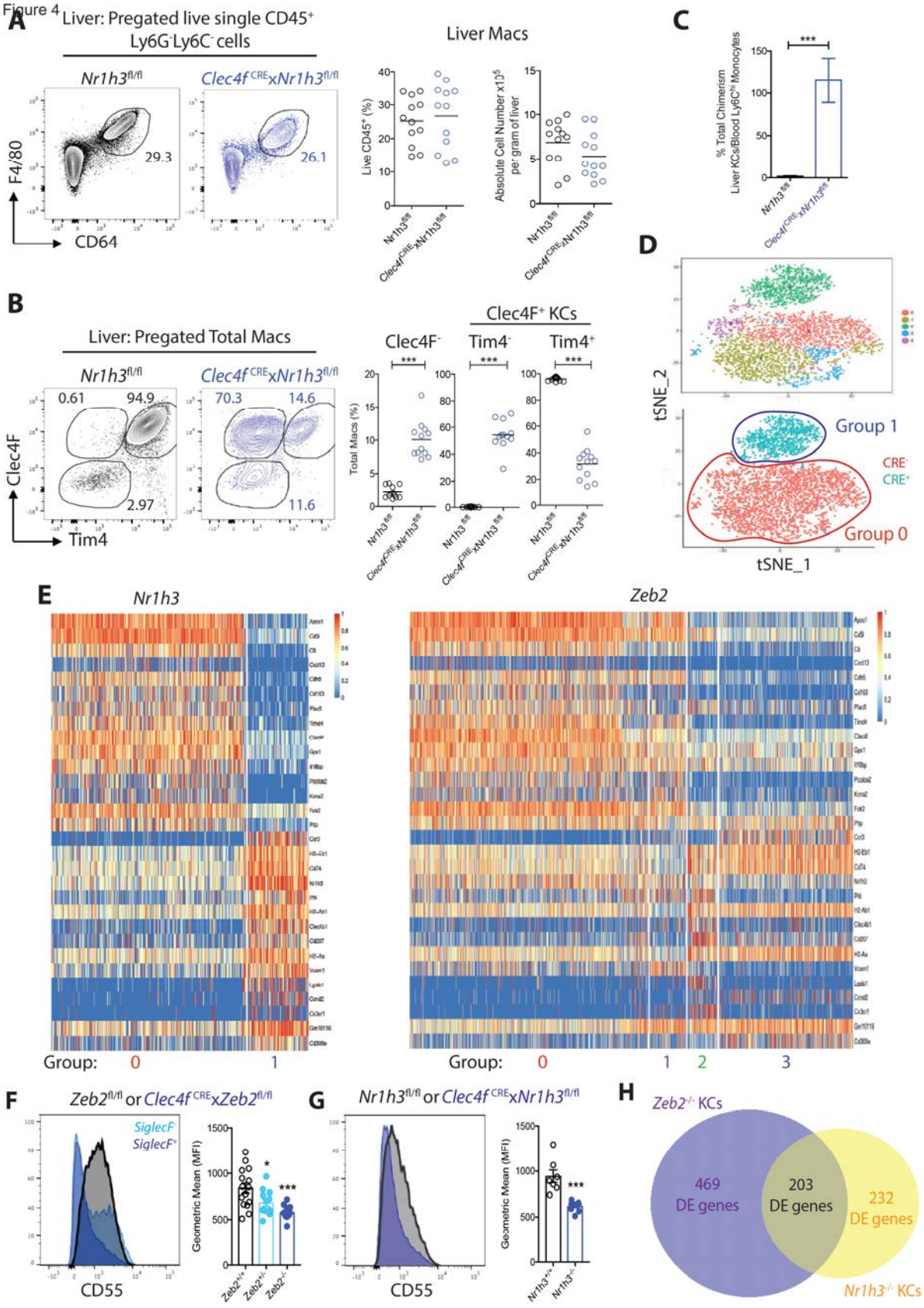
A
Liver: Pregated live single CD45+ Ly6G-Ly6C- cells
Nr1h3fl/fl
Clec4fCRExNr1h3fl/fl
F4/80
CD64
29.3
26.1
Liver Macs
Live CD45+ (%)
Absolute Cell Number x10^5 per gram of liver
B
Liver: Pregated Total Macs
Clec4F
Tim4
0.61
94.9
2.97
70.3
14.6
11.6
Clec4F+ KCs
Clec4F-
Tim4-
Tim4+
Total Macs (%)
C
% Total Chimerism Liver KCs/Blood Ly6Chi Monocytes
***
D
tSNE_2
tSNE_1
Group 1
Group 0
CRE-
CRE+
E
Nr1h3
Zeb2
Group: 0 1
Group: 0 1 2 3
F
Zeb2fl/fl or Clec4fCRExZeb2fl/fl
SiglecF-
SiglecF+
CD55
Geometric Mean (MFI)
G
Nr1h3fl/fl or Clec4fCRExNr1h3fl/fl
CD55
Geometric Mean (MFI)
H
Zeb2-/- KCs
469 DE genes
203 DE genes
232 DE genes
Nr1h3-/- KCs

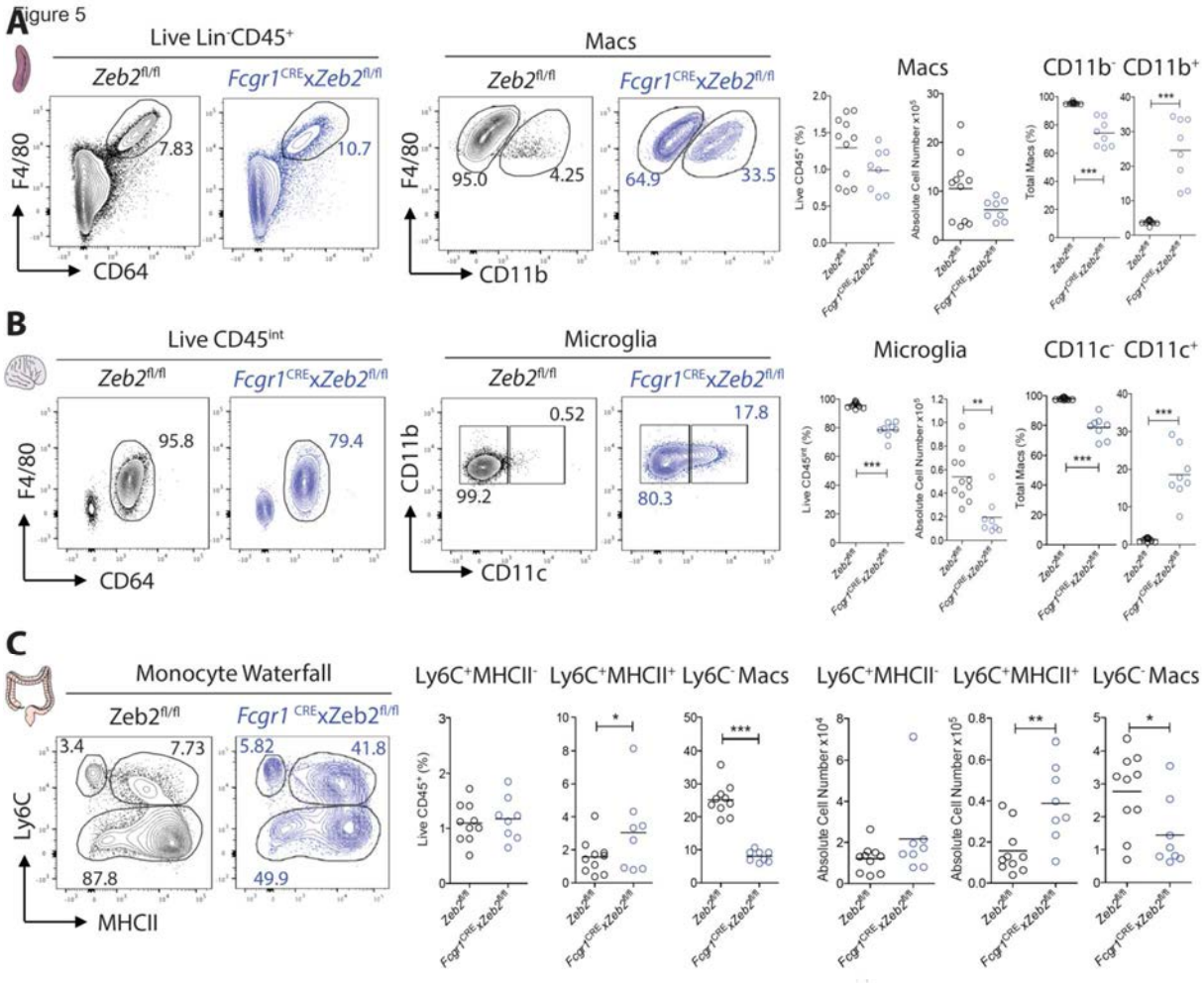
Figure 5
A
Live Lin-CD45+
Zeb2fl/fl
Fcgr1CRExZeb2fl/fl
F4/80
CD64
7.83
10.7
Macs
CD11b
95.0
4.25
64.9
33.5
Live CD45+ (%)
Absolute Cell Number x10^5
CD11b- CD11b+
Total Macs (%)
B
Live CD45int
Microglia
CD11c
95.8
79.4
0.52
99.2
17.8
80.3
Live CD45int (%)
CD11c- CD11c+
C
Monocyte Waterfall
Ly6C
MHCII
3.4
7.73
87.8
5.82
41.8
49.9
Ly6C+MHCII-
Ly6C+MHCII+
Ly6C- Macs
Absolute Cell Number x10^4

Figure 6

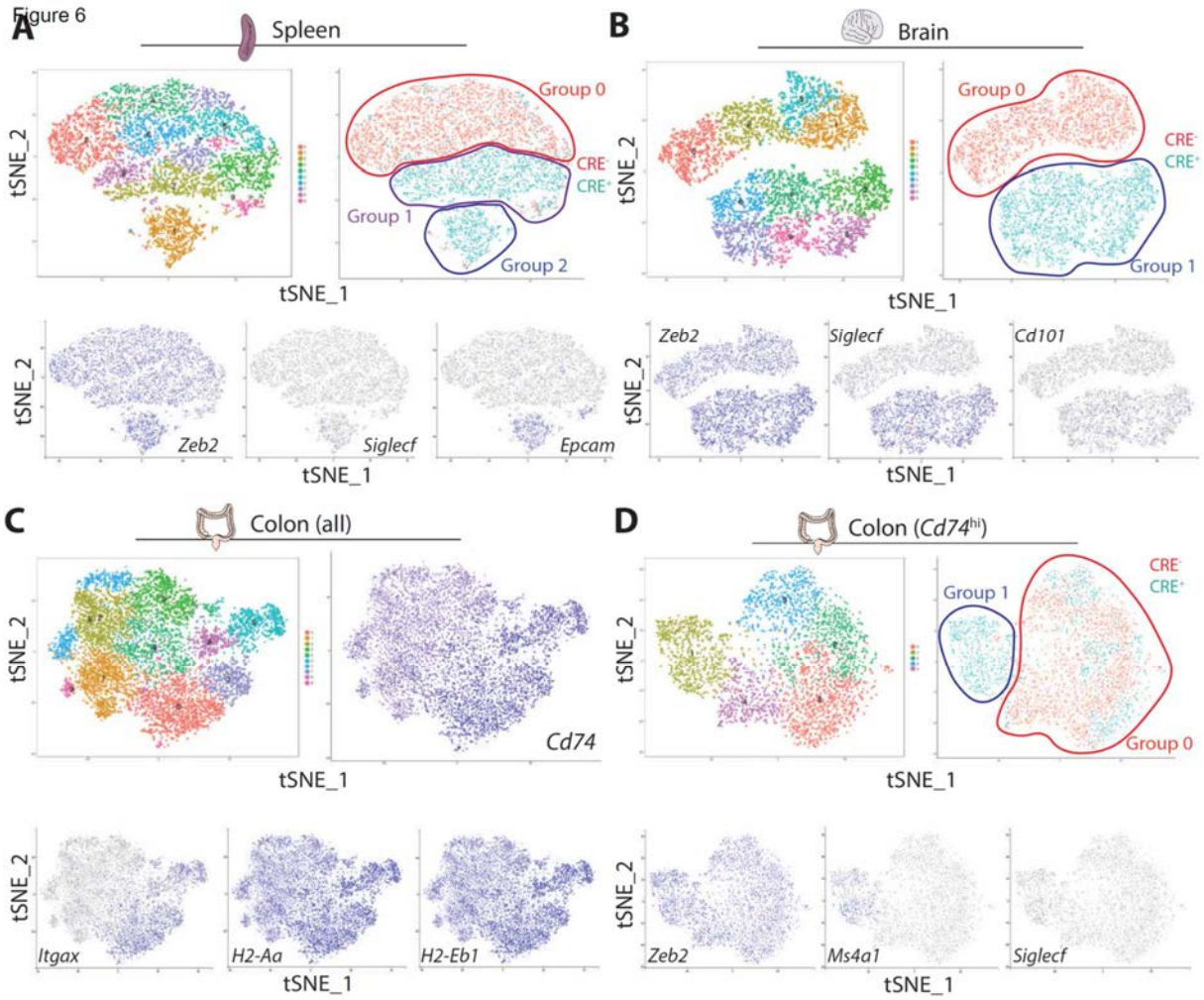
A
Spleen
tSNE_2
tSNE_1
Group 0
CRE-
CRE+
Group 1
Group 2
Zeb2
Siglecf
Epcam
B
Brain
Group 0
CRE-
CRE+
Group 1
Zeb2
Siglecf
Cd101
C
Colon (all)
Cd74
Itgax
H2-Aa
H2-Eb1
D
Colon (Cd74hi)
Group 1
CRE-
CRE+
Group 0
Zeb2
Ms4a1
Siglecf

Figure 7

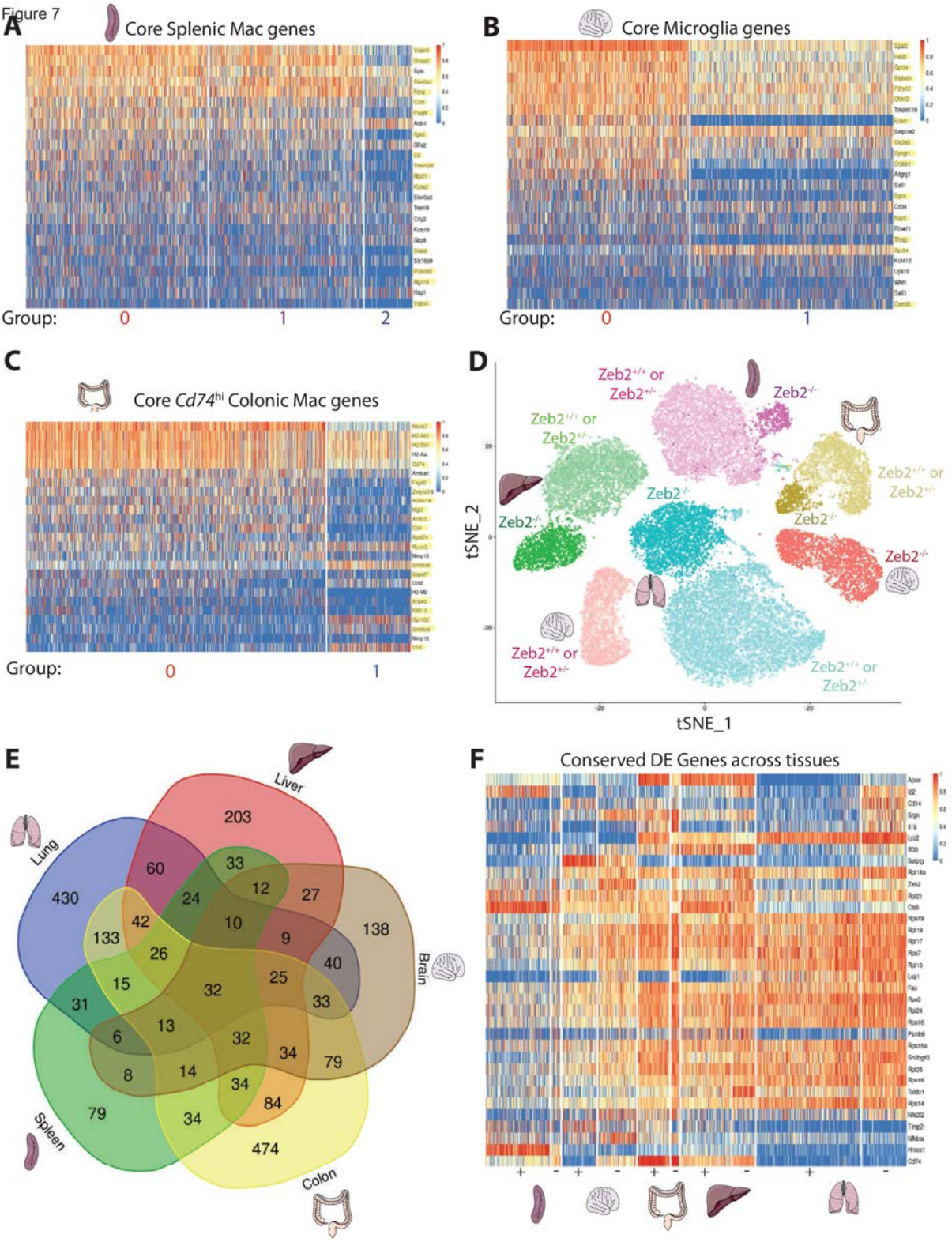
A
Core Splenic Mac genes
Group: 0 1 2
B
Core Microglia genes
Group: 0 1
C
Core Cd74hi Colonic Mac genes
Group: 0 1
D
Zeb2+/+ or Zeb2+/-
Zeb2-/-
tSNE_2
tSNE_1
E
Liver
Lung
Brain
Spleen
Colon
203
60
33
12
27
430
24
42
10
9
138
133
26
40
15
32
25
33
31
13
6
32
34
79
8
14
34
84
79
34
474
F
Conserved DE Genes across tissues

Figure S1; Related to Figure 1: Zeb2 expression, validation of CRE lines and SC-RNA-Seq analysis pipeline.

(A) Heatmap showing relative expression of genes (normalized per mean expression of each gene identified to be shared among tissue resident macs and lacking from other immune cells including splenic B cells, naïve T cells, cDC1s, cDC2s and blood neutrophils. Data are from microarray analyses performed either in house or by the Immgen consortium. (B) % of RFP-expressing cells in indicated tissues of *Clec4f*^{CRE}xRosa-RFP$^{+/-}$ (CRE^{+}) and Rosa-RFP$^{+/-}$ (CRE^{-}) mice. Data are pooled from 2-3 experiments with n=8-16 per group. **p<0.01, ***p<0.001 Student's t test. (C) Expression of CLEC4F, RFP and DAPI by confocal microscopy in liver of *Clec4f*^{CRE}xRosa-RFP$^{+/-}$ mice. Data are representative of 2 experiments with n=9. (D) % of KCs (CLEC4F^{+}TIM4^{+}CD64^{+}F4/80^{+}) and B cells (CD19^{+}MHCII^{+}) expressing RFP in *Clec4f*^{CRE}xRosa-RFP$^{+/-}$ mice (CRE^{+}) and Rosa-RFP$^{+/-}$ mice (CRE^{-}) and expression of CLEC4F and RFP by KCs (red) and B cells (grey) in the liver of *Clec4f*^{CRE}xRosa-RFP+/- mice. Data are pooled from 3 (KCs) or 1(B cells) experiment(s) with n=4-16 per group. ***p<0.001 Student's t test. (E) Expression of CD64, F4/80, CLEC4F, TIM4, CD19 and MHCII on RFP+ cells in the liver of *Clec4f*^{CRE}xRosa-RFP$^{+/-}$ mice. Data are representative of 3 experiments with n=12-16 per group. (F) Expression of RFP by CD11c^{+}CD64^{+}F4/80^{+}SiglecF^{+} AMs and % of AMs expressing RFP in *Itgax*^{CRE}xRosaRFP$^{+/-}$ (CRE^{+}) and Rosa-RFP$^{+/-}$ (CRE^{-}) mice. Data are pooled from 2 experiments with n=5-9 per group. ***p<0.001 Student's t test. (G) Pipeline followed for analysis of SC-RNA-Seq data.

Figure S2; Related to Figure 2: Presence of Zeb2+/- macs in liver and lung of conditional KO mice

(A,B) 2% Agarose gel showing results of genomic PCR for Zeb2 flox and Zeb2 deletion band in indicated mac populations from (A) *Clec4f*^{CRE}x*Zeb2*$^{fl/fl}$ and (B) *Itgax*^{CRE}x*Zeb2*$^{fl/fl}$ mice compared with *Zeb2*$^{fl/fl}$ littermate controls. All samples are run in duplicate. For the PCR reaction 1µl DNA loaded was in the first well of each sample and 0.2µl DNA was loaded in the second well. (C) Expression of Clec4F, Tim4, SiglecF and DAPI by confocal microscopy in liver of *Clec4f*^{CRE}x*Zeb2*$^{fl/fl}$ mice at 6 and 12 weeks of age compared with *Zeb2*$^{fl/fl}$ livers. Data are representative of 1 experiment with n=2 per group. (D,E) Expression of F4/80 and Ki-67 by indicated KC populations. Data are pooled from 2 experiments with n=8-14 per group. ***p<0.001, One way ANOVA with Bonferroni post-test (F,G) Expression of EpCam and Ki-67 by indicated AM populations. Data are pooled from 2 experiments with n=4-9 per group. ***p<0.001, One way ANOVA with Bonferroni post-test. (H) Absolute number of KCs in *Zeb2*$^{fl/fl}$ (CRE^{-}) and Clec4f^{CRE}xZeb2$^{fl/fl}$ (CRE^{+}) mice which received 1mg/kg CSF1Fc subcutaneously for 4 days or PBS as a control before being sacrificed on day 6. (I) *Zeb2* mRNA expression (PrimeFlow) and SiglecF expression in CD45.2 donor KCs (blue) and CD45.1 host KCs (black) at indicated time-points. (J) *Zeb2* mRNA expression (PrimeFlow) and CD101 expression in CD45.2 donor AMs (blue) and CD45.1 host AMs (black) at indicated time-points.

Figure S3; related to Figure 3: Core KC and AM transcriptional profiles redefined

(A,B) Heatmap showing expression of core KC (A) or AM (B) genes by KCs, colon macs (LiMacs), AMs (Lung), Microglia, peritoneal macs and splenic macs. Data was previously published by (Lavin *et al*., 2014) and downloaded from the NCBI for this analysis.

Figure S4; related to Figure 4: Loss of LXRα from KCs mimics main features of loss of ZEB2

(A) Expression of Clec4F and Tim4 by total liver macs in *Clec4f*^{CRE}x*Nr1h3*$^{fl/+}$ and *Nr1h3*$^{fl/+}$ mice and % of total macs expressing Clec4F and Tim4. Data are pooled from 2 experiments with n=6-7 per group. *p<0.05, ***p<0.001 Student's t test. (B) Relative mRNA expression of indicated genes normalized to β-actin as determined by qPCR of FACS-purified KCs from *Zeb2*$^{fl/fl}$ mice (*Zeb2*$^{+/+}$), SiglecF^{-} KCs (*Zeb2*$^{+/-}$) and SiglecF^{+} KCs (*Zeb2*$^{-/-}$) from *Clec4f*^{CRE}x*Zeb2*$^{fl/fl}$. Data are pooled from 2 experiments with n=8 per group. *p<0.05, ***p<0.001 One way ANOVA with Bonferroni post-test. (C) Relative mRNA expression of indicated genes normalized to β-actin as determined by qPCR of FACS-purified KCs from *Nr1h3*$^{fl/fl}$ mice (*Nr1h3*$^{+/+}$) or *Clec4f*^{CRE}x*Nr1h3*$^{fl/fl}$ mice (*Nr1h3*$^{-/-}$). Data are pooled from 2 experiments with n=8 per group. ***p<0.001 Student's t-test. (D) Table of DE genes (adj. p value 0.05, log FC <1 or >1) between embryonic KCs and monocyte derived (moKCs) from KC-DTR mice 15 days post administration of DT(Scott et al., 2016).

Figure S5; related to Figure 5: Fcgr1CRE validation.

(A) Expression of RFP by indicated splenic immune cell populations including B cells, T cells, Neutrophils, Eosinophils and cDC1s and cDC2s (cDC subsets; defined on the basis of CD11b expression) in *Fcgr1*^{CRE}xRosa-RFP$^{+/-}$ mice compared with Rosa-RFP$^{+/-}$ littermate controls. Data are pooled from 2 experiments with n= 6-9 per group. Students t test. ***p<0.001. (B) Expression of RFP by CD64^{+}F4/80^{+}Lin^{-}MHCII^{-} splenic macs and % of splenic macs expressing RFP in *Fcgr1*^{CRE}xRosaRFP$^{+/-}$ (CRE^{+}) and Rosa-RFP$^{+/-}$ (CRE^{-}) mice. Data are pooled from 2 experiments with n=6-9 per group. ***p<0.001 Student's t test. (C) Expression of RFP and MHCII by colonic macs in *Fcgr1*^{CRE}xRosa-RFP$^{+/-}$

mice compared with Rosa-RFP$^{+/-}$ littermate controls. Data are pooled from 2 experiments with n= 6-9 per group. Students t test. ***p<0.001. (D) Expression of RFP and CD45 by microglia in *Fcgr1*^{CRE}xRosa-RFP$^{+/-}$ mice compared with Rosa-RFP$^{+/-}$ littermate controls. Data are pooled from 2 experiments with n= 6-9 per group. Students t test. ***p<0.001.

Figure S6; related to Figure 6: Core Transcriptomic profile of Cd74lo colonic macs

Heatmap showing expression of core *Cd74*^{lo} colonic mac genes. Heatmap was created by comparing SC-RNA-Seq data from *Cd74*^{lo} colonic macs with *Cd74*^{hi} colonic macs, KC, AMs, microglia and splenic macs.

Figure S7; related to Figure 7: Core transcriptomic profiles of splenic macs, microglia and colonic *Cd74*^{hi} macs redefined and loss of *Zeb2*$^{-/-}$ splenic macs with time

(A-C) Heatmap showing expression of core splenic mac (A), microglia (B) or colonic *Cd74*^{hi} mac (C) genes by KCs, colonic macs, AMs, microglia, peritoneal macs and splenic macs. Data was previously published by (Lavin *et al*., 2014) and downloaded from the NCBI and filtered based on SC-RNA-Seq data to remove contaminating genes. (D) % CD11b^{+}CD20^{+} splenic macs amongst total CD45.2^{+} splenic macs at indicated time points (days) post the last dose of tamoxifen. Data are pooled from 2 experiments with n= 4-7 per time-point. ***p<0.001, One way ANOVA with Bonferroni post-test comparing each time point with the previous time point. (E) *Zeb2* mRNA expression (PrimeFlow) and CD11b expression in CD45.2 donor Splenic macs (blue) and CD45.1 host splenic macs (black) at indicated time-points.

Supplemental Figure 1

Click here to download Supplemental Text and Figures Figure S1.pdf

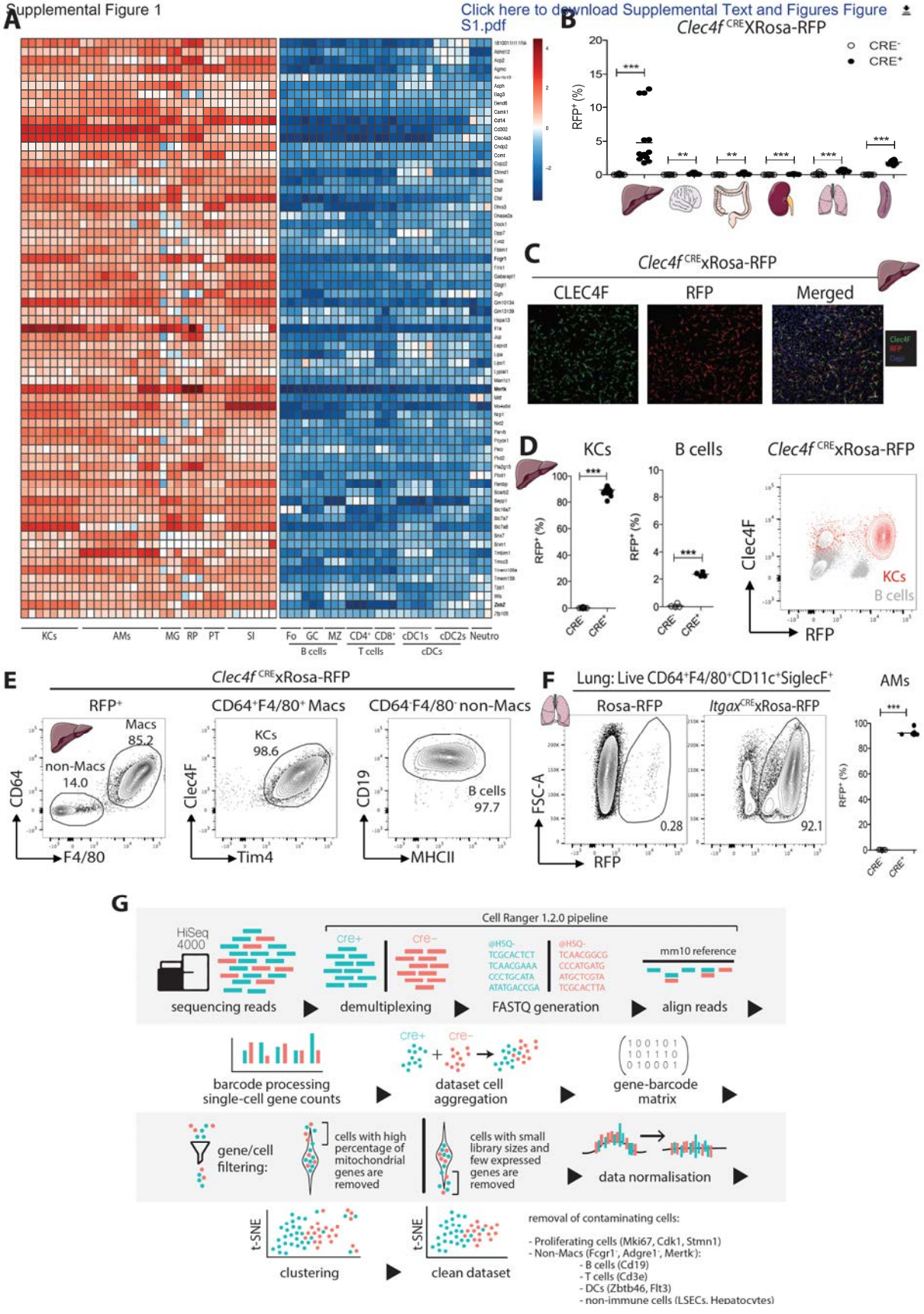

Supplemental Figure 2

Click here to download Supplemental Text and Figures Figure S2.pdf

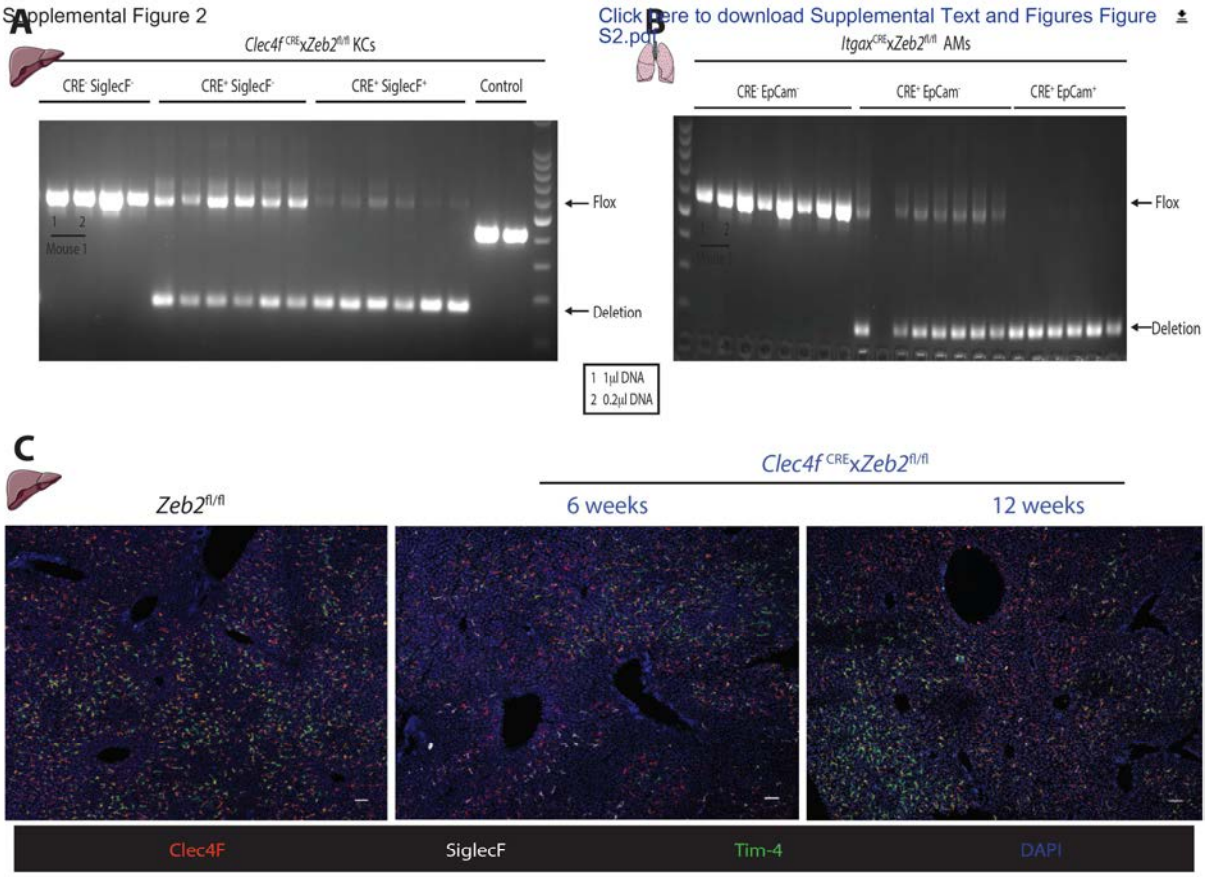

Supplemental Figure 3

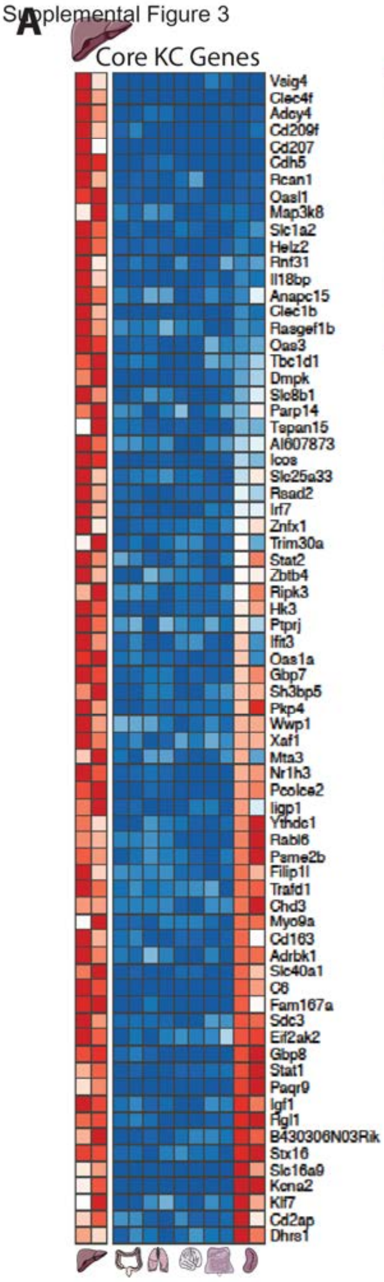

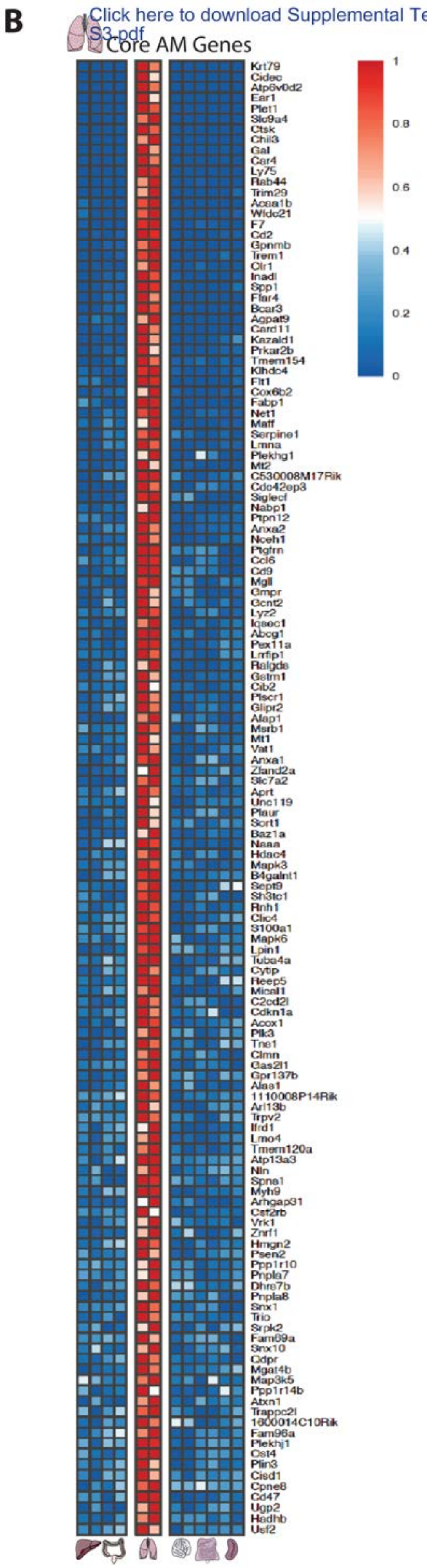

Supplemental Figure 4

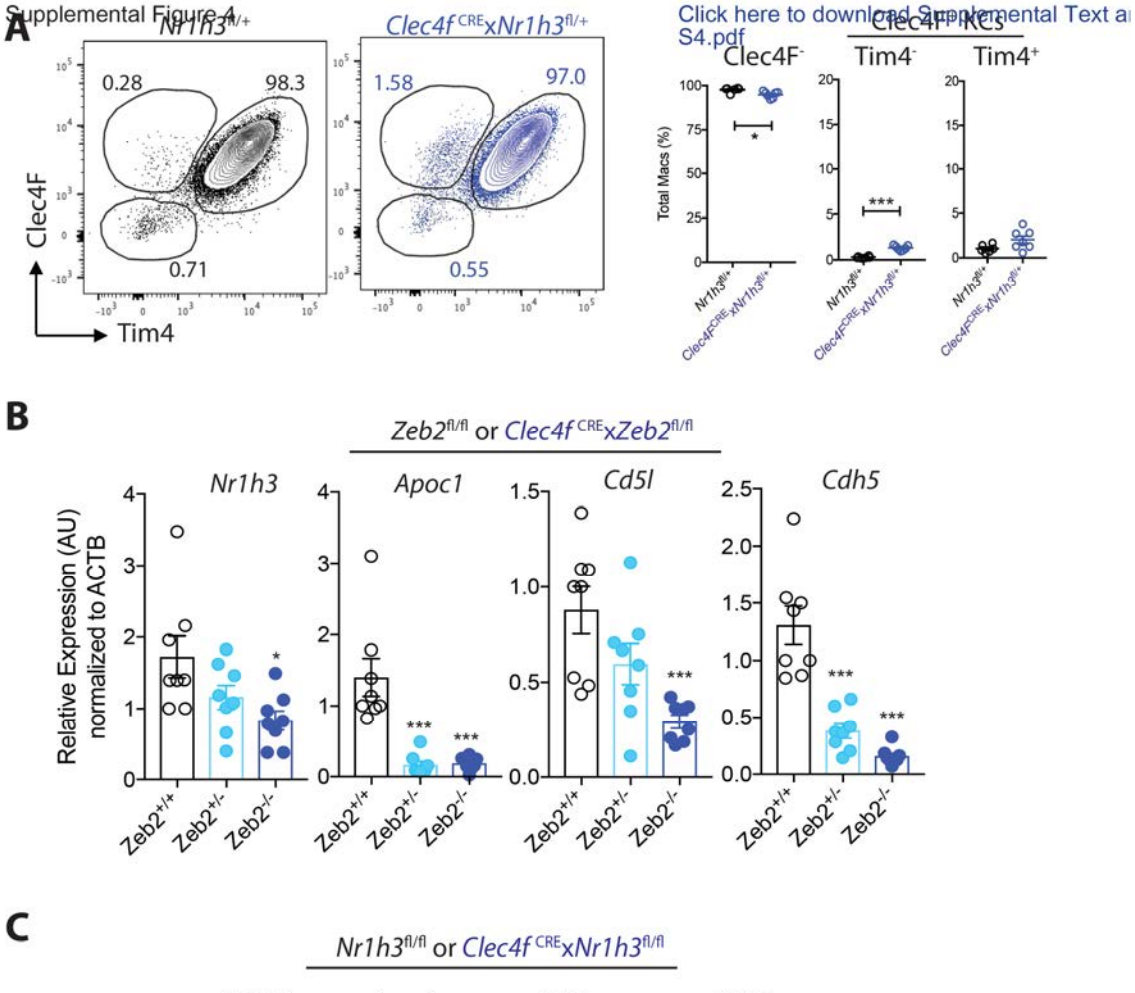

Click here to download Supplemental Text and S4.pdf

D

moKC genes
(DE genes between WT and moKCs D15 Adj P value 0.05, Log FC <1 or >1)

Ccr2	Prelid2	mt-Tm	Cd163	Ccdc109b
Cx3cr1	Tceal1	C6	Slc27a6	Cd207
Ccr3	Hyal4	C4b	Colec12	Anpep
Tspan32	Kitl	Kcnj16	Xlr	Cpne8
Ccr1	Ecm1	Fam84a	Sdc2	Stk39
Ptgs2	Ryk	Raver2	Bmpr1a	Apoc1
Lphn3	Btbd11	Stard13	Timd4	Marco
Clec4b1	Enpp2	n-R5s89	Cd209f	Cfh
Ifi44	Klhl13	3830403N18	Cxcl13	Mcts2

Supplemental Figure 5

Click here to download Supplemental Text and Figures Figure S5.pdf

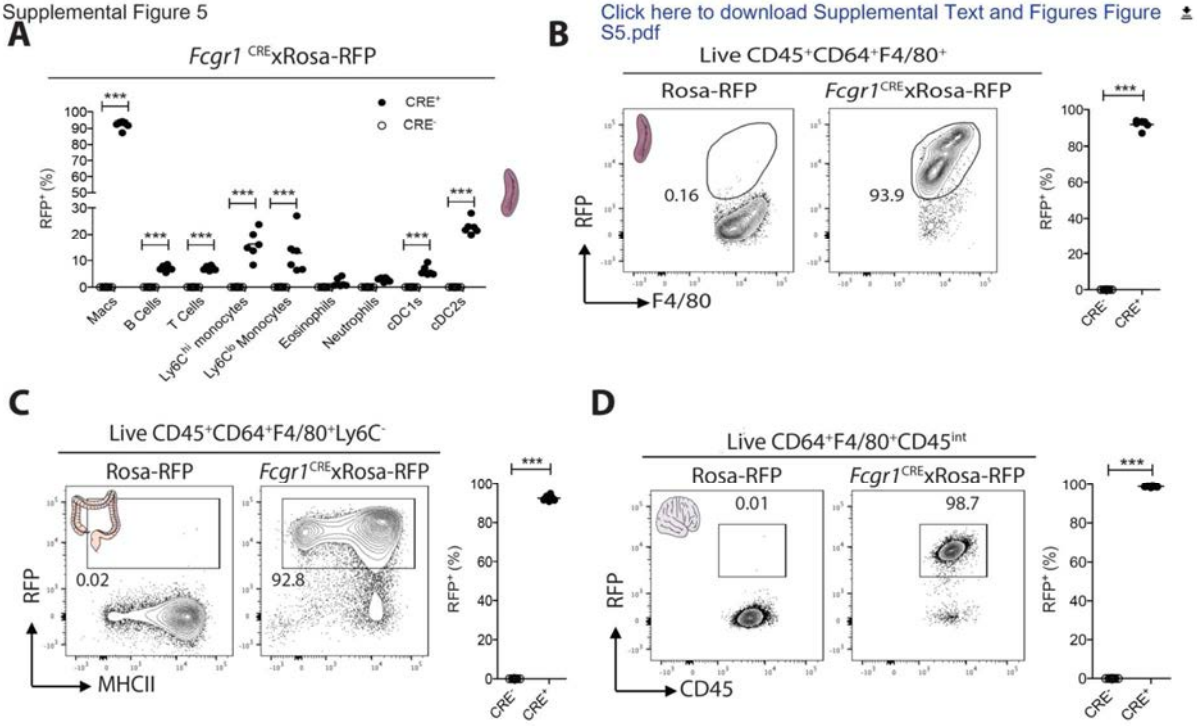

Supplemental Figure 6

Click here to dowr
S6.pdf

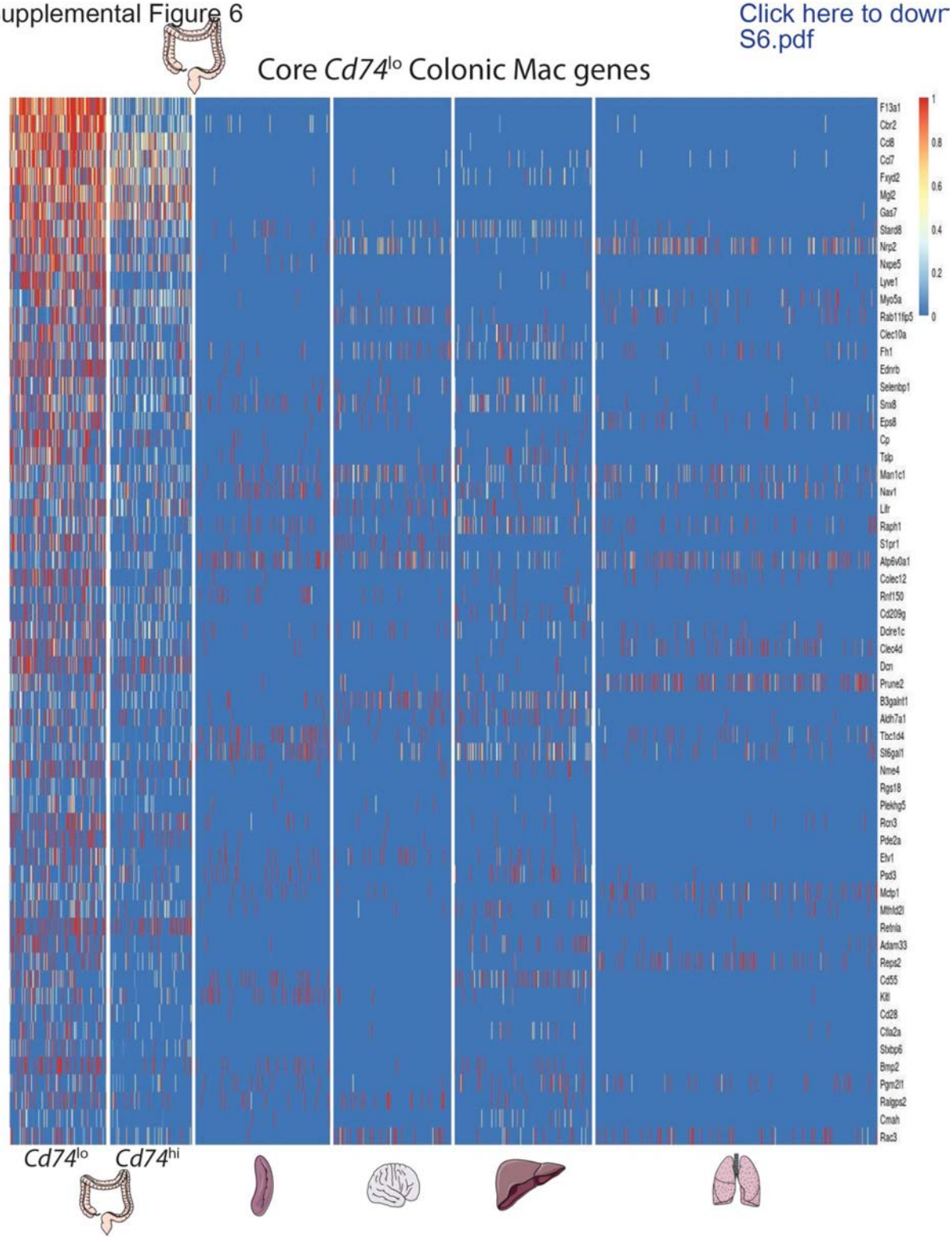

Supplemental Figure 7

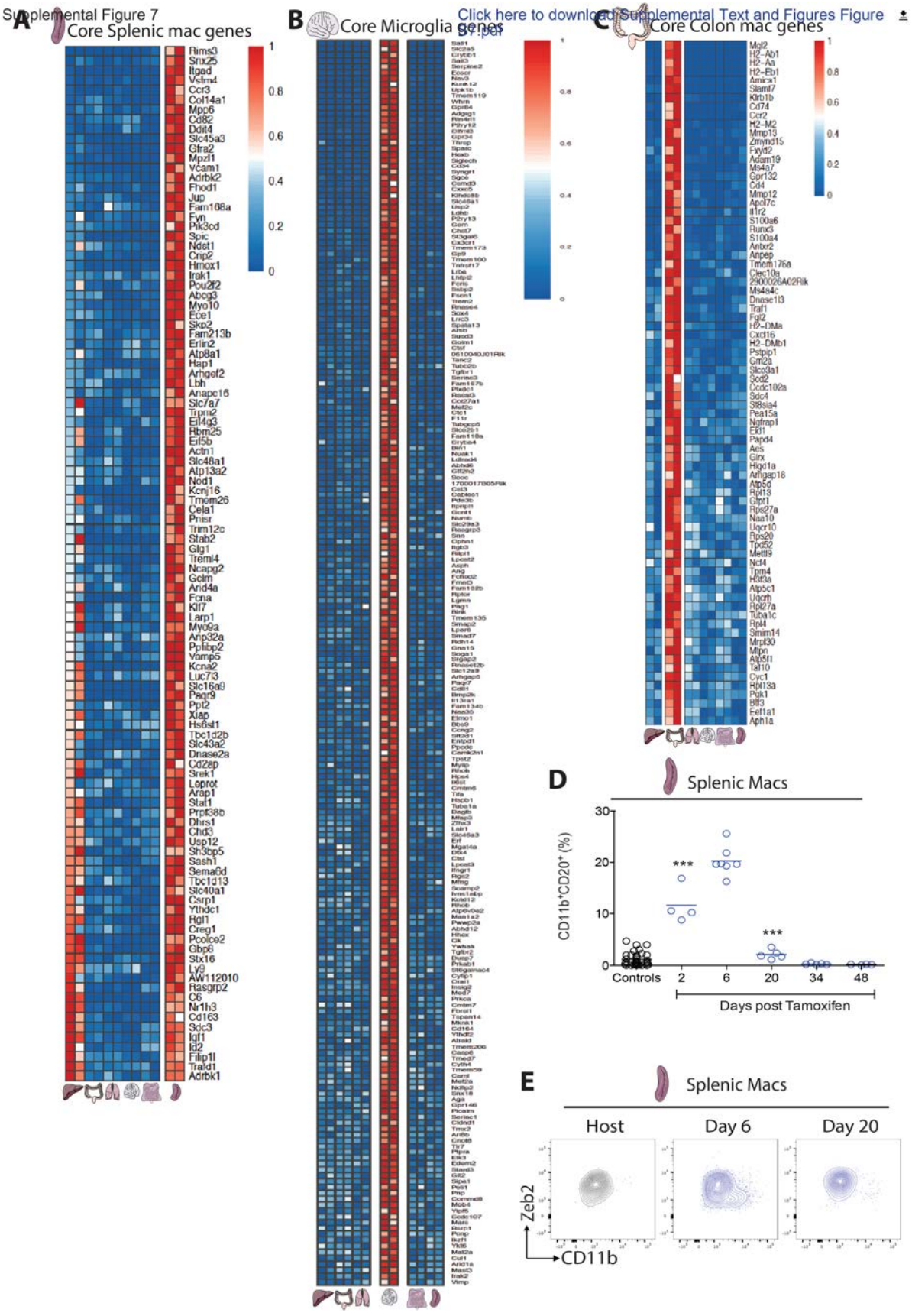

Part 6
Curriculum Vitae

Curriculum Vitae | Bieke Soen

°1989, November 10th
Roeselare, Belgium
biekesoen@hotmail.com

Work experience and education

2012-current	***PhD in Science, Biotechnology*** 'Zeb1 and Zeb2 : master regulators of mononuclear phagocyte development and homeostasis' Promotors: Prof. Dr. G. Berx - Prof. Dr. C. Scott Molecular and Cellular Oncology Lab Department of Biomedical Molecular Biology, Ghent University Cancer Research Institute Ghent VIB-UGent Inflammation Research Center PhD Fellowship - Research Foundation Flanders (FWO)
2012-2013	***Laboratory animal science (FELASA Cat. C)*** Ghent University
2011-2012	***Master Thesis in Bioscience Engineering - Biotechnology*** 'Research to the innate immune response of human macrophages to ***Chlamydia psittaci'***
2007-2012	***Master in Bioscience Engineering - Biotechnology*** Faculty of Bioscience Engineering, Ghent University
2001-2007	***Science - Mathematics*** Klein Seminarie, Roeselare, Belgium

Training and Workshops

C1 Training Single Cell RNA Sequencing Fluidigm ~ VIB-BITS Training 'Hands-on introduction to ChIP-Seq analysis' ~ VIB-BITS Training 'Introduction to NGS data analysis' ~ VIB-BITS 'Custom IPA training' ~ VIB-BIC Basic Image Processing and Analysis ~ Effective Oral Presentations (Jean-Luc Doumont) ~ CLC Workbench Training

Academic activities

Supervisor thesis student Master II (1 year, Matthias Dierick)
Supervisor project Master I (6 weeks, Sven Jonckheere)
Supervisor practical course: 'Mouse models of cancer'
Responsible PCR-room (2013-2018)

Accepted manuscripts

Scott CL, **Soen B**, Martens L, Skrypek N, Saelens W, Taminau J, Blancke G, van Isterdael G, Huylebroeck D, Haigh J, Saeys Y, Guilliams M, Lambrecht BN, Berx G. The transcription factor Zeb2 regulates development of conventional and plasmacytoid DCs by repressing Id2. J Exp Medicine. 2016; 213(6):897–911.

Marianthi N, De Craene B, **Soen B**, Taminau J, Vermassen P, Goossens S, Haigh K, Cazzola S, Lambert J, Huylebroeck D, Haigh J, Berx G. ZEB2-transgene Expression in the Epidermis Compromises the Integrity of the Epidermal Barrier through the repression of Different Tight Junction Proteins. Cell Moll Life Sci. 2014; 71(18):3599-609.

Soen B, Vandamme N, Berx G, Schwaller J, Van Vlierberghe P, Goossens S. ZEB proteins in leukemia: friends, foes or friendly foes? Hemasphere. 2018.

Akay Ö, Bruneel K, **Soen B**, De Smedt E, Vandamme N, Berx G. Zinc Finger E-Box-Binding Homeobox 2. Encyclopedia of Signaling Molecules. 2017; Chapter No: 101944-1.

De Smedt E, Bruneel K, **Soen B**, Akay Ö, Vandamme N, Berx G. ZEB1 (Zinc Finger E-Box Binding Homeobox 1). Encyclopedia of Signaling Molecules. 2017; Chapter No: 101943-1.

Van Deun J, Mestdagh P, Agostinis P, (...), Berx G, (...), **Soen B**, (…), De Wever O, Vandesompele J, Hendrix A. EV-TRACK: transparent reporting and centralizing knowledge in extracellular vesicle research. Nature Methods. 2017; 14(3):228-232.

Manuscript under review

Scott CL, T'Jonck W, Martens L, Todorov H, Sichien D, **Soen B,** Bonnardel J, De Prijck S, Vandamme N, Cannoodt R, Saelens W, Vanneste B, Toussaint W, De Bleser P, Takahashi N, Vandenabeele P, Henri S, Pridans C, Hume D, Lambrect B, De Baetselier P, Milling SWF, Van Ginderachter J, Malissen B, Berx G, Beschin A, Saeys Y, Guilliams M. Zeb2 is required to maintain the tissue-specific identities of macrophages. Immunity.

Manuscript in preparation

Skrypek N, **Soen B**, Tatari M, De Craene B, Taminau J, Blancke G, Vandamme N, Berx G. Zeb2 overexpression in basal cells, along with p53 inactivation, accelerates the development of skin carcinosarcoma.

Conference attendance

- 'Disease Models and Cancer Program', DMBR workshop, Ghent, 2013
- 'From Science to Treatment Innovation in Cancer', Brussels, 2014
- Oncopoint Research Seminar, Ghent, 2014, 2015 and 2016
- BACR Annual Meeting, 2014 and 2015
- 'Tumour microenvironment and signalling', EMBO|EMBL Symposium, Heidelberg, Germany, 2014
- 'Molecular Mechanisms of Inflammation', IRC-FWO Symposium, Ghent, 2015
- 'Cell Adhesion and Communication', BSCDB Autumn Meeting, Ghent, 2016
- 'Innate immunity & lymphoid homeostasis symposium', IRC Symposium, Ghent, 2016
- 'Light on the dark side of the genome', f-TALES, Ghent, 2016
- 'Macrophage Biology in the Single-Cell Era', VIB Conference, Ghent, 2017

Oral presentations

'Role of EMT transcription factors in skin epidermis', Oncopoint Research Seminar, Ghent, 2015.

'The transcription factor Zeb2 regulates development of conventional and plasmacytoid DCs by repressing Id2', IRC Pre-doc Symposium, Ghent, 2016.

'The transcription factor Zeb2 regulates development of conventional and plasmacytoid DCs by repressing Id2', IRC Hot Science - cool talks, Ghent, 2016.

Poster presentation

'The transcription factor Zeb2 regulates development of conventional and plasmacytoid DCs by repressing Id2', BSCDB Autumn Meeting, Ghent, 2016

Part 7
Acknowledgements
Dankwoord

Dankwoord

“If I have seen further, it is by standing on the shoulders of Giants.”

Isaac Newton

Bij het lezen van deze quote voelde ik de grapjes rond mijn kleine gestalte al in de lucht hangen. Maar wat ik hier eigenlijk mee wil vertellen, is dat ik dit boek nooit had kunnen schrijven zonder de hulp van heel wat fantastische mensen.

Even terug naar het begin van mijn doctoraat. Geert, ik weet nog dat je tijdens mijn eerste jaar eens tegen me zei: ‘Met je studies heb je al bewezen dat je slim bent, maar je moet nog bewijzen dat je ook een goede onderzoekster bent’. Ik hoop dat ik je de voorbije zes jaar heb kunnen overtuigen dat dit misschien wel het geval is? Bedankt Geert voor het vertrouwen en de steun. Je hebt van mij een kritische wetenschapster gemaakt die durft opkomen voor haar mening. Daarnaast wil ik je ook bedanken voor het begrip tijdens mijn zwangerschap. Nogal zenuwachtig kwam ik je bureau binnen om het nieuws te vertellen en ik zie jou nog altijd met je beide handen naar je hoofd grijpen en achteroverleunen in je stoel. Maar ondanks de initiële shock, wenste je me proficiat en konden we al snel tot een overeenkomst komen over aangepast werk. Op die manier kon ik mama worden, zonder dat de voortgang in mijn onderzoek werd onderbroken.

Dear Charlie, thank you for adopting the ‘girl from the cancer lab’ and introducing her into the complex world of immunology. You always patiently answered my questions and guided me in both practical as cognitive work. During the Zeb1 project, there were a few months during which every experiment we came up with gave unexpected results, which was quite frustrating. But you always managed to keep up the spirit and think of a solution to tackle the problem. You are an inspiration for young female scientists and I believe a great carrier is coming your way. It was an honor to work by your side and become your first graduated PhD student.

A sincere thank you goes to all the members of my Examination Committee for reading and providing feedback to improve my PhD dissertation. Thanks as well to all the people from the core facilities in our department. Gert en Kim, dank u wel voor de altijd vlotte flow cytometry en FACS service. Bedankt ook aan de mensen van het animalarium en alle dierenverzorgers. Aangezien mijn thesis volledig rust op experimenten met muizen, zijn jullie een belangrijke schakel geweest. Kelly, merci voor de kleuringen doorheen de jaren en de vele leuke babbeltjes. Je bent iemand die altijd vraagt hoe het gaat en dat apprecieer ik enorm.

Lieve collega UGBe'tjes. Als geen ander weten jullie dat onderzoek bij momenten nogal frustrerend kan verlopen, maar ondanks dit is de sfeer in onze groep altijd uitmuntend. Er wordt gelachen, onnozel gedaan en gezeverd op een manier die ik ten zeerste kan appreciëren. Maar ook als er eens serieus moet gebabbeld worden of er eens iets van mijn hart moet, staan jullie altijd klaar met een luisterend oor. Jullie hebben gezorgd voor heel wat hartverwarmende en hilarische momenten die me altijd zullen bijblijven en die van jullie niet alleen supercollega's maken, maar ook fantastische vrienden. Bubbeltjesplastiek op mijn stoel, Gillian en Morgane die komen babysitten zodat ik een avondje op stap kan met Eva, motiverende prentjes op mijn bureau, hoe mijn computer telkens Bieke Soen corrigeert naar Blikje Soep, het vieren van de 2-0 Eva-Mendel, Disney-prinsessen, housewarmings, gegrimeerd als skelet in het midden van de nacht naar huis rijden, …

Steven, met jou was het altijd leerrijk discussiëren over wetenschappelijk problemen. Bedankt voor de vlotte samenwerking doorheen de jaren en merci om deel uit te maken van mijn examencommissie. Tim Pieters, die in mijn hoofd soms wordt verward met Pieter Timmers, jij bent de koning van de gevatte woordspelingen die me altijd weer aan het lachen brengen. Nicolas, thank you for taking on the 'eartumour' project and the elaborate discussions on this subject. Your support on this matter gave me the freedom to focus on my immunology projects. Bram, jouw begeleiding tijdens de eerste jaren van mijn doctoraat hebben me vooral werkethos bijgebracht. Het woordje 'opnieuw' is vele malen gevallen en heeft mijn doorzettingsvermogen gesterkt, waarvoor ik je wil bedanken. Jannick, merci voor de vele aangename carpoolritjes. Ondanks het ongeloof van vele collega's, konden wij wel een serieus gesprek voeren

met elkaar. Lieve Natalie, merci voor je goed humeur en je sprankelend gezelschap. Je had altijd tijd voor een babbeltje en was altijd bereid om te luisteren of een handje te helpen.

Gillian en Joachim, jullie staan altijd klaar om te helpen, wij hebben het maar te vragen en jullie brengen het in orde. Bedankt voor alle praktische hulp de voorbije jaren en nog een extra merci voor alle klusjes die ik tijdens mijn zwangerschap niet zelf mocht uitvoeren. Sara, wij hebben misschien niet veel samengewerkt, maar toch was je altijd bereid om te helpen. Özden, you were a perfect companion to go through the struggles of starting a PhD and taking the necessary courses. Sven, ik heb nooit veel vertrouwen gehad in mijn educatieve capaciteiten. Toch ben jij intussen van master 1 student onder mijn begeleiding geëvolueerd tot doctoraatsstudent in onze groep. Kenneth of 'Knet', bedankt voor de vele discussies over de West-Vlaamse woordenschat. Het was altijd aangenaam beginnen aan een nieuwe week op maandagmorgen met jouw vraag hoe mijn weekend was geweest. 'Neleken', jij bent zo één van die personen waar het direct mee klikt. We kennen elkaar nog niet zolang, maar hebben toch al heel wat met elkaar kunnen delen, zoals onze zwangerschap en het mama worden. Ik wens je nog veel geluk in de wetenschap en de kliniek, je zal dit fantastisch doen. Nielske, jij en ik, dat was 'Manten en Kalle'. Wie nu juist Manten is en wie Kalle, daar zijn we nooit over uit geraakt. Merci voor de deugddoende pauzekes samen en het af en toe luisteren naar mijn geklaag. Ook bedankt voor de 'bubbelkesplastiek', het onnozel doen, organiseren van feestjes en ontwerpen van mijn cover.

Eva'tje, omdat je toch wel een speciaal plekje hebt veroverd in mijn hart, krijg jij een aparte alinea in dit dankwoord. Jouw positivisme heeft mij door een aantal moeilijke momenten gehaald. Als je weer eens op één van je lange reizen vertrok, liet je een briefje achter om mij te motiveren en het gemis van jouw energie naast mij te compenseren. Merci voor jouw hilarische pogingen tot het vervoegen van het West-Vlaamse werkwoord 'ja' en intussen heb ik dankzij jou het woord 'gekreft' toegevoegd aan mijn woordenschat. Ik vond het zo jammer dat ik je trouwfeest heb gemist, maar als je graag eens zou hebben dat jouw stoel wordt bekleed met 'bubbeltjesplastiek', dan regel ik dat!

Bedankt aan al mijn vrienden om mijn gedachten te helpen verzetten en me even het werk te doen vergeten. Af en toe ontstressen met jullie was nodig om er dan weer keihard tegenaan te gaan. Cel en genners, met jullie sarcastische opmerkingen over de ‘medemens’ is het altijd lachen geblazen. Merci FFF-maatjes en alle andere muzikale vrienden voor het samen musiceren. Lieselot en Dieter, bedankt om ons te overtuigen echte petanquers te worden en samen met Annelies en Bram te zorgen voor ontspannende etentjes.

Mama en papa, van jullie heb ik altijd alle vrijheid en steun gekregen om te doen waar ik van droomde. Jullie hadden er soms meer vertrouwen in dan ikzelf dat ik het tot een goed einde zou brengen. En jullie hadden gelijk, ik ben ingenieur, doctor, muzikant en mama geworden. Merci voor alle hulp doorheen de jaren en af en toe de bemoedigende woorden ‘Da komt ollamaole wel in orde!’. Dikke merci ook aan mijn zus Maaike en schoonbroer Dieter, broer Jelle en schoonzus Milissa, mijn schoonouders en alle andere Eggermontjes. Jullie staan altijd paraat om te helpen en hebben al die tijd voor mij gesupporterd. Dank u wel!

Aäron, liefste Bollie, ik ben nu dan misschien doctor in de wetenschappen, maar jij verdient de titel ‘doctor in het echtgenootschap’. Ik weet dat ik niet altijd de meest aangename persoon ben als ik onder stress sta. Ik kan dan nogal eens kortaf zijn en veel klagen, maar desondanks ben jij er altijd om mij te kalmeren en terug te doen lachen. Merci Bolleke om al die jaren mijn steun en toeverlaat te zijn. Je mag me nu eindelijk aanspreken en voorstellen als Dr. Ir. Soen  . Lieve kleine Raben, ook jij verdiend een woordje van dank. Jij was altijd een motivatie om snel te beginnen aan mijn werk en het tempo hoog te houden, om dan ’s avonds beloond te worden met jouw stralend lachende gezichtje!


Tès geweun e prente.
Happy Birthday Little One
Hiauw!
Blijven gaan mama !!
Angel piggy
Veel Geluk
Just

Thank you!!!